Studies on the biology of an ectoparasitic digenean, transversotrema patialense (soparkar), with special reference to the developmental stages.

Bundy, D. A. P

UNIVERSITY OF LONDON, KING'S COLLEGE

STUDIES ON THE BIOLOGY OF AN ECTOPARASITIC DIGENEAN, Transversotrema patialense (SOPARKAR), WITH SPECIAL REFERENCE TO THE DEVELOPMENTAL STAGES.

By DONALD ALFRED PAYNE BUNDY

Thesis submitted for the degree of
Doctor of Philosophy in the Faculty
of Science of the University of London.

1979

FRONTISPIECE

The swimming cercaria of Transversotrema patialense.

This plate is a composite of six sequential swimming positions, 3 msec. apart, superimposed to reveal the complexity of the relative motion of the cercarial components. The six positions are shown separately in Plate 48.

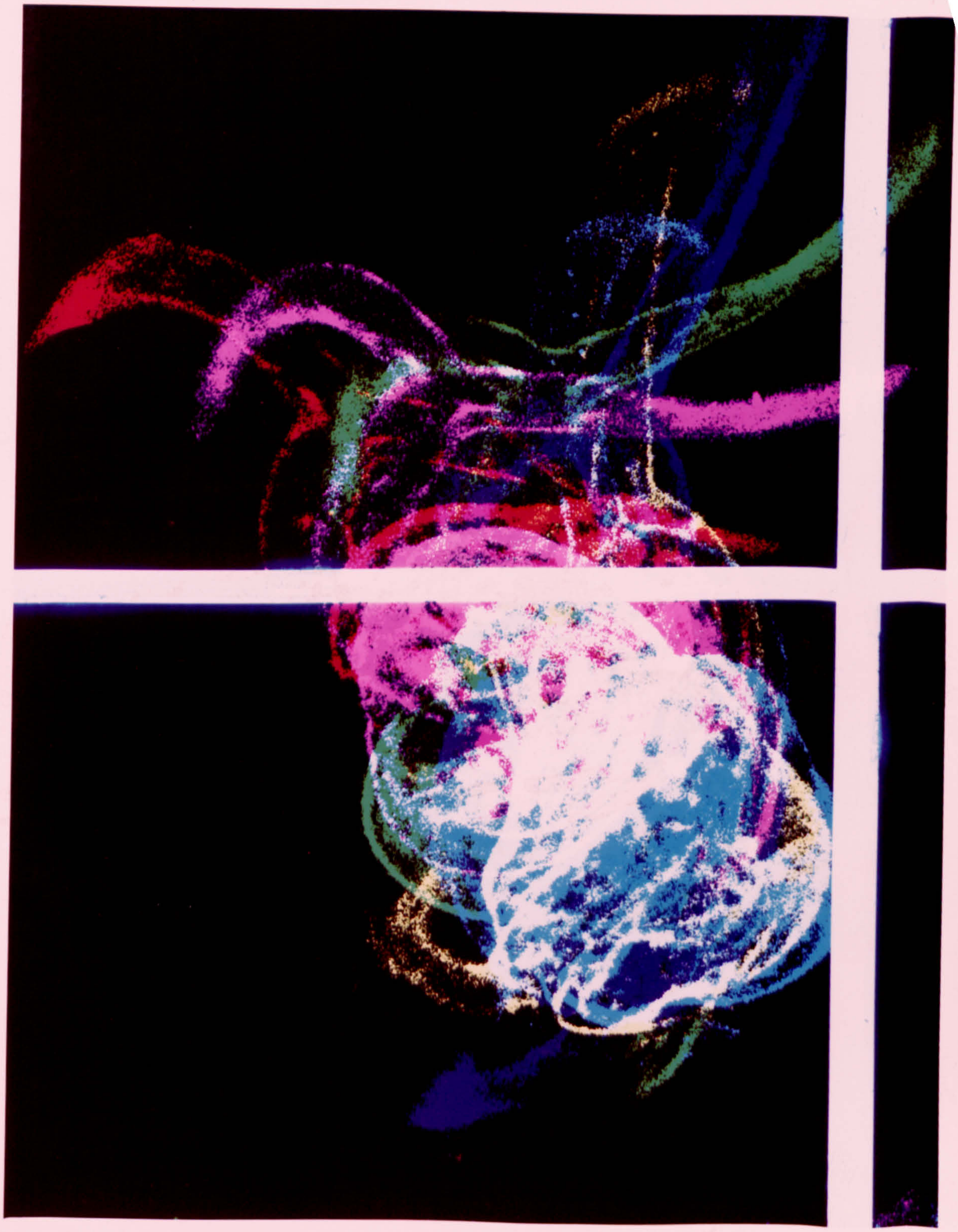

Studies on the Biology of an Ectoparasitic Digenean, *Transversotrema patialense* (Soparkar), with special reference to the Developmental Stages

By Donald Alfred Payne Bundy

ABSTRACT

Morphological changes during egg, intramolluscan and cercarial development have been examined qualitatively and quantitatively in an attempt to gain some insight into the biology of the developmental stages of *Transversotrema patialense*. An investigation of the effects of exogenous factors on this developmental process attempted to quantify the constraints imposed by the abiotic environment.

An analysis of egg capsule morphometrics illustrated the inadequacie of this characteristic in separating species of *Transversotrema*.

The developmental fate of the egg capsule contents and the influence of temperature are described. The rate of egg development was temperature dependent over the range 15-30°C, and outside this range no development occurred. The times taken to attain arbitrary stages of miracidial morphogenesis had the same proportional relationships to to the total developmental period, independent of developmental temperature.

An examination of the effect of photoperiod on hatching indicated the presence of endogenous control mechanisms. Eggs maintained in a 12/12h D/L cycle hatched around the mid-point of the light period. This circadian rhythmicity was not abolished by incubation in a constant light regime.

The ultrastructure of the hatched miracidium is described with special reference to the epithelial cells, ridge layer and protonephridial system.

At 25°C the miracidial population exhibited an age-dependent death rate. The instantaneous death rate increased as an exponential function of time.

After the miracidia penetrate and infect the intermediate host, *Melanoides tuberculata*, the frequency distributions of different redial and cercarial size categories altered during development.

Intramolluscan rediae produced cercariae which emerged approximately 130 days after infection. The ultrastructure of the two developmental stages and the adult worm on the definitive host, *Brachydanio rerio*, are described. Particular attention was paid to the structure, steric relationships and mode of formation of the tegument. The effects of absolute age and somatic growth on spine distribution and dimensions in cercariae and adults have been investigated and these results discussed in the light of past use of spine dimensions in taxonomy.

Infection of the definitive host required active swimming. Cercarial swimming has been quantitatively described using high-speed cinematographic techniques. The hydrodynamic consequences of swimming as a means of propulsion in small aquatic organisms are discussed.

ACKNOWLEDGEMENTS

I would like to express my sincere gratitude to my supervisor, Dr. P.J. Whitfield and to Dr. R.M. Anderson and Dr. M.E.J. Holwill who provided guidance and help throughout this study, and to all the other academic and technical staff who have assisted me.

This study was carried out during the tenure of a Research Studentship provided by the Science Research Council.

CONTENTS

		Page
Abstract		i
Contents		iii
Index to Figures		x
Index to Tables		xiv
Section 1.	General Introduction	1
Section 2.	General Materials and Methods	8
2.1	Water conditioning	9
2.2	Maintenance of the intermediate host	9
2.3	Stimulation of cercarial emergence	9
2.4	Infection and maintenance of the definitive host	10
2.5	Anaesthetisation of host fish and removal of adult flukes	10
2.6	Collection of fluke eggs	11
2.7	Snail dissection to obtain intramolluscan larvae	13
2.8	Electron microscopy	13
Section 3.	Egg Morphometrics	17
3.1	Introduction	18
3.2	Materials and Methods	19
3.3	Results	23
3.4	Discussion	29
Section 4.	Qualitative Aspects of Egg Development	37
4.1	Introduction	38
4.2	Materials and Methods	38
4.2.1	Effect of differing culture conditions on the visibility of egg contents through the capsule wall	38

		Page
4.2.2	Egg capsule surface ultrastructure	39
4.2.3	Effect of collection techniques on egg viability	39
4.2.4	Effect of culture techniques on egg viability	40
4.2.5	Effect of single fluke infections on egg viability	40
4.3	Results	41
4.3.1	Effect of differing culture conditions on the visibility of egg contents through the egg capsule wall	41
4.3.2	Egg capsule surface ultrastructure	44
4.3.3	Effect of collection techniques on egg viability	46
4.3.4	Effect of culture techniques on egg viability	46
4.3.5	Effect of single fluke infections on egg viability	48
4.4	Discussion	48
Section 5.	Quantitative Aspects of Egg Development	55
5.1	Introduction	56
5.2	Materials and Methods	56
5.2.1	Effect of temperature on egg development and viability	56
5.2.2	Effect of storage at 10°C on subsequent egg viability at 25°C	57
5.2.3	Effect of illumination period on egg development	57
5.3	Results	57
5.3.1	Effect of temperature on egg development and viability	57
5.3.2	Effect of storage at 10°C on subsequent egg viability at 25°C	74
5.3.3	Effect of illumination period on egg development	77
5.4	Discussion	78

	Page
Section 6. Egg Hatching	90
6.1 Introduction	91
6.2 Materials and Methods	91
6.2.1 Effect of alternating light and dark periods on the temporal distribution of hatching at 30°C	91
6.2.2 Effect of mechanical stimulation on the temporal distribution of hatching	93
6.2.3 Effect of temperature on the temporal distribution of hatching	93
6.2.4 Effect of constant illumination on the temporal distribution of hatching	94
6.2.5 Effect of constant darkness on egg hatching and development	94
6.3 Results	95
6.3.1 Effect of alternating light and dark periods on the temporal distribution of hatching	95
6.3.2 Effect of mechanical stimulation on the temporal distribution of hatching	95
6.3.3 Effect of temperature on the temporal distribution of hatching	100
6.3.4 Effect of constant light on the temporal distribution of hatching	100
6.3.5 Effect of constant darkness on egg hatching and development	104
6.4 Discussion	105
Section 7. Miracidial Survival	116
7.1 Introduction	117
7.2 Materials and Methods	117
7.3 Results	118
7.4 Discussion	122

	Page
Section 8. Miracidial Ultrastructure	125
8.1 Introduction	126
8.2 Materials and Methods	127
8.3 Results	127
8.3.1 The miracidial body wall and associated structures	127
8.3.2 The protonephridial system	139
8.4 Discussion	142
Section 9. Intramolluscan Development	153
9.1 Introduction	154
9.2 Materials and Methods	154
9.2.1 Early development	154
9.2.2 Time course of development of intramolluscan stages	155
9.2.3 Period of development of infection	159
9.3 Results	160
9.3.1 Early development	160
9.3.2 Time course of the development of intramolluscan stages	160
9.3.2a Observations at known intervals during the development of the intramolluscan larval stages	160
9.3.2b Location of intramolluscan larval stages	161
9.3.2c Time course of development of intramolluscan rediae and cercariae	163
9.3.2d Infra-redial larvae	170
9.3.3 The period of development of infection	177
9.3.4 Effects of infection on the molluscan host	185
9.4 Discussion	186

	Page
Section 10. Cercarial Development	198
10.1 Introduction	199
10.2 Materials and Methods	199
10.3 Results	200
10.3.1 General	200
10.3.2 Structure of the body surface during development from intramolluscan cercaria to adult	203
10.3.3 The digestive tract	209
10.3.4 Protonephridia	211
10.3.5 Vitelline cells	211
10.3.6 Sensory structures	212
10.3.7 Sperm development	212
10.4 Discussion	213
10.4.1 General	213
10.4.2 The body surface	214
10.4.3 The digestive tract	221
10.4.4 Protonephridia	223
10.4.5 Vitelline cells	223
10.4.6 Sensory structures	224
Section 11. Spine Morphology	227
11.1 Introduction	228
11.2 Materials and Methods	229
11.2.1 Preparation for microscopy	229
11.2.2 Spine growth	230
11.2.3 Spine density	230
11.2.4 Number of spine rows	232
11.2.5 Spine number	232
11.2.6 Fluke growth	232

	Page
11.3 Results	233
11.3.1 General distribution of spines	233
11.3.2 Spine and related tegumental ultrastructure	234
11.3.3 Fluke - host interface	239
11.3.4 Spine growth	240
11.3.5 Spine density	242
11.3.6 Number of spine rows	242
11.3.7 Spine number	244
11.3.8 Fluke growth	244
11.4 Discussion	247
11.4.1 The structure and composition of tegumental spines	248
11.4.2 Tegumental spine formation	251
11.4.3 Growth of tegumental spines	255
11.4.4 The fluke - host interface	258
11.4.5 Spines as a taxonomic feature	259
Section 12. Cercarial Locomotion	265
12.1 Introduction	266
12.2 Materials and Methods	267
12.2.1 Cine and microflash photography	267
12.2.2 Estimation of cercarial density	270
12.3 Results	271
12.3.1 General structure of the cercaria	271
12.3.2 Phases of cercarial behaviour	271
12.3.3 Quantitative description of cercarial swimming	275
12.3.4 Cercarial density	294
12.3.5 Reynolds number for cercarial swimming	294
12.3.6 Viscous effects on the dropping cercaria	295

	Page
12.4 Discussion	299
12.4.1 Hydrodynamic aspects of dropping behaviour	299
12.4.2 Hydrodynamic aspects of swimming behaviour	301
Section 13. General Discussion	312
References	317
List of Plates	358
Plates	360
List of Appendices	409
Appendices	410

Index to Figures

		Page
1.1	The life cycle of <u>Transversotrema patialense</u>	4
2.1	Vertical section through fish breeding trap used to collect fluke eggs	12
3.1	Diagrammatic representation of egg size parameters	21
3.2	The effect of fluke age on egg width and length	24
3.3	Size-frequency of egg length dimension	26
3.4	Range of egg sizes in described species of the Family Transversotrematidae	35
4.1	Superifical sculpturing of the capsule of digenean eggs	42
4.2	Developmental stages of the eggs of <u>T. patialense</u>	45
5.1	Proportion of eggs in Developmental stages and categories	59
5.2	Proportion of eggs developing, moribund and disoperculate with increasing age	62
5.3	Schematic representation of the possible fates of developing eggs	63
5.4	Instantaneous rate of loss per egg per day from the developing egg population	65
5.5	Effect of temperature on the period required to attain the mid-stage points	69
5.6	Egg development rate and thermal constant	73
5.7	Q_{10} and period of development	75
5.8	The period of development of the eggs of different digenean species	89

		Page
6.1	Percentage of eggs hatching during any hourly period, 12/12h D/L, 30°C	97
6.2	Percentage of eggs hatching during one hour periods at different times of day	98
6.3	Percentage of eggs hatching per day post egg collection	99
6.4	Percentage of eggs hatching during any hourly period, 12/12h D/L, 25°C	102
7.1	Mortality rate and survival of miracidia	121
8.1	Schematic diagram of the miracidium of *T. patialense*	128
8.2	The body wall of the miracidium of *T. patialense*	130
8.3	Median longitudinal section of epithelial cell locomotory cilium	133
8.4	Superifical sensory endings of the miracidium of *T. patialense*	135
8.5	Schematic representation of protonephridial tubule convolution of *T. patialense* miracidium	141
9.1	Mean number of cercariae and rediae per snail at different times during the development of intramolluscan infection	166
9.2	Mean proportion of rediae per snail in different size classes of rediae	167
9.3	Mean proportion of cercariae per snail in different size classes of cercariae	169
9.4	Mean number of cercariae per snail in different size classes of cercariae	171

		Page
9.5	Frequency distribution of intra-redial rediae	176
9.6	Frequency distribution of intra-redial cercariae	179
9.7	Effect of redial size on the number of intra-redial larvae	181
9.8	Effect of redial size on the type of intraredial contents	183
9.9	Schematic representation of intra-molluscan cycle	188
10.1	Structure of the adult of Transversotrema patialense	204
10.2	Size relationships during growth from newly emerged intraredial cercaria to adult fluke	205
10.3	The structure of the body surface during development from newly emerged intraredial cercaria to adult fluke	206
11.1	Schematic representation of the position of spine rows on the dorsal and ventral surface of adult flukes	231
11.2	The structure of the spine and related body wall of cercariae and adults	236
11.3	Spine growth from 0 to 21 days after attachment	241
11.4	Relationship between spine density and fluke surface area	243
11.5	The same symmetrical pattern described for different repeating units	261
11.6	Description of the plane lattice of digenean spine distribution	263
12.1	Arrangement of photographic apparatus	268

		Page
12.2	Cercaria in extended and reflexed configuration	273
12.3	Tracings of sequential orientation of reflexed body region during swimming sequence A.	277
12.4	Conventional description of relative angles during swimming	279
12.5	Angles subtended by cercarial components to trajectory of whole organism	280
12.6	Motion of exposed tail stem and furcae relative to conceptually constrained body region	281
12.7	Conventional angles relative to exposed tail stem and furcae	283
12.8	Angle subtended by exposed tail stem to antero-posterior axis of reflexed body region	284
12.9	Angles subtended by right and left furcae to exposed tail stem	287
12.10	Angle between furcae	288
12.11	Orientation of the left furca during a recovery stroke	290
12.12	Orientation of furca during recovery and effective stroke	291
12.13	Simultaneous orientation of right and left furcae during a propulsive cycle	293

Index to Tables

		Page
1.1	Regional records of the family Transversotrematidae	3
3.1	The effect of fluke age on egg size	25
3.2	The relationship between vitelline cell number and egg capsule size for four species of digeneans	32
3.3	Recorded egg dimensions of species within the family Transversotrematidae	34
4.1	Stages in egg development	46
4.2	Effect of collection technique on eggs	47
4.3	Effect of antibiotics on eggs	47
5.1	Proportional egg development at 10°C	58
5.2	Age in days of eggs at mid-stage of developmental stages 0-4 for the temperature range 10-35°C	70
5.3	Parameters of the exponential model fitted to time to mid-stage against temperature experimental data for developmental stages 1, 2, 3 and 4	70
5.4	Proportion of developmental period, relative to age at mid-point of stage 4, spent in attaining the mid-point of stages 0, 1, 2 and 3	72
5.5	Effect of temperature on egg development	76
5.6	Proportional development under different light regimes at 25°C	77
5.7	Effect of temperature on egg development for three digenean species	79
5.8	Egg development period for different species of Digenea	88

		Page
6.1	Temporal distribution of egg hatching at 30°C, 12/12h L/D	96
6.2	Temporal distribution of egg hatching at 25°C, 12/12h L/D	101
6.3	Temporal distribution of egg hatching at 30°C, 12/12h L/L	103
6.4	Effect of light on development and hatching of eggs at 30°C	104
7.1	Survival and mortality parameters of the miracidium at 25°C	120
9.1	Use of regression to determine overall cercarial length from body length measurements	158
9.2	Experimental parameters of snail dissections	162
9.3	Numbers and proportions of rediae per snail at different stages of infection	164
9.4	Numbers and proportions of cercariae per snail at different stages of infection	168
9.5	Intraredial contents at different stages of infection	172
9.6	Mean number of intraredial larvae per redia at different stages of infection	174
9.7	Frequency distribution of intraredial rediae, numbers per redia at different stages of infection	175
9.8	Frequency distribution of intraredial cercariae, numbers per redia at different stages of infection	178
9.9	Effect of redial size on the number of intraredial larvae	180

		Page
9.10	Effect of redial size on the type of intraredial contents	182
9.11	Age of infection in days PPI at which members of a population of 15 snails first emitted cercariae	184
11.1	Change in mean spine dimensions with fluke age	240
11.2	Change in mean spine density with fluke age	242
11.3	Effect of fluke age on the mean number of spine rows	242
11.4	Estimated spine number from LM observation of fluke ventral surface	245
11.5	Change in fluke surface area with fluke age	246
11.6	Indirect estimate of total spine number on the surface of flukes of known age	247
12.1	Velocity of movement of the furca during the effective stroke	296
12.2	Terminal velocity of dropping cercaria determined by experimental and theoretical means	298
12.3	Relationship between cercarial swimming velocity and cercarial size	310

SECTION 1:

GENERAL INTRODUCTION

1. General Introduction

The Family Transversotrematidae Yamaguti, 1953 has a trans-equatorial distribution in tropical and subtropical regions (Table 1.1). Only two genera are included: Prototransversotrema Angel, 1969 and Transversotrema Witenberg, 1944. The former genus is represented by a single species, the marine P. steeri Angel, 1969 while the latter genus comprises seven species only two of which are found in marine habitats: T. haasi Witenberg, 1944 and T. licinum Manter, 1970. The present investigation concerns the fresh-water species T. patialense (Soparkar, 1924).

T. patialense has the distinction of being the first transversotrematid to be described. In 1924 Soparkar recorded the presence of Cercaria patialensis within the cerithiacean mollusc Melanoides tuberculata (Müller). Despite further observations of the cercaria the adult was not described until 1964 when Crusz, Ratnayake and Sathananthan discovered specimens living beneath the scales of two species of fresh-water fishes.

The life cycle of T. patialense has been described in outline (Figure 1.1). The adult fluke lives ectoparasitically beneath the scales of fresh-water fishes. There appears to be little host specificity at this stage, the adults having been recorded from six different natural host species (Crusz and Sathananthan, 1960; Roa and Ganapati, 1967; Murty and Rao, 1968; Sim, 1972) and eighteen different experimental host species (Rao and Ganapati, 1967; Sim, 1972; Whitfield and Wells, 1973).

Eggs emerging from the adult fluke drop from the host surface and develop to release a free living miracidial stage (Sim, 1972). The miracidium infects a molluscan host and transforms to a mother

TABLE 1.1

Regional Records of the Family Transversotrematidae

Species	Location	Source
Transversotrema patialense (Soparkar, 1924)	India	: Soparkar, 1924; Anantaraman, 1948; Rao and Ganapati, 1967; Murty and Rao, 1968
	Sri Lanka	: Crusz, 1956; Crusz, Ratnayake and Sathananthan, 1964; Crusz and Sathananthan, 1960
	Malaysia	: Sim, 1972; Betterton, 1977
	Zaire	: Brien, 1954
T. soparkari (Pandey, 1971)	India	: Pandey 1971; Pande and Shukla, 1972
T. chackai (Mohandas, 1973)	India	: Nadakal, Mohandas and Sonderaraman, 1969; Mohandas, 1973
T. koliensis (Olivier, 1947)	Solomon Islands	: Olivier, 1947
T. laruei (Velasquez, 1958)	Philippines	: Velasquez, 1958 and 1961
T. hagsi (Witenberg, 1944)	Red Sea	: Witenberg, 1944; Overstreet, 1977
	Philippines	: Velasquez, 1975
T. licinum (Manter, 1970)	Australia	: Manter, 1965 and 1970
Prototransversotrema steeri (Angel, 1969)	Australia	: Angel, 1969

Figure 1.1: The life cycle of Transversotrema patialense.

Surface of tropical freshwater fish (Brachydanio rerio).

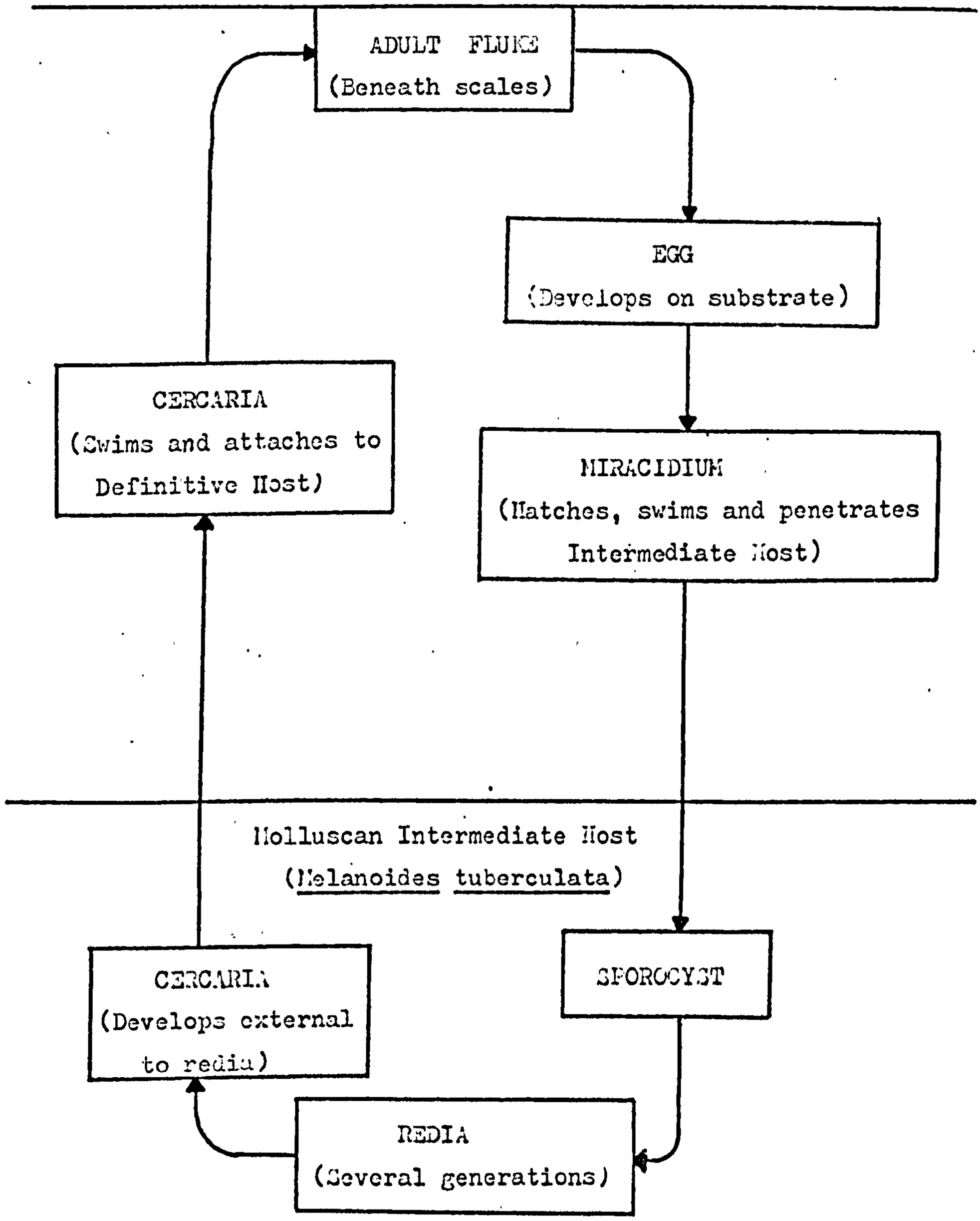

sporocyst within the muscular foot tissues of the host. In Malaysia, Sri Lanka and India the intermediate host was Melanoides tuberculata while the single African record of the parasite identified the host as M. anomala (Brien, 1954).

One or more redial generations develop within the digestive gland of the intermediate host (Soparkar, 1924). Cercariae develop initially within the rediae but emerge at a relatively early stage to continue development free within the digestive gland (Sim, 1972).

Mature cercariae emerge from the molluscan host with fully developed reproductive organs (Soparkar, 1924). The cercariae swim actively in the water column until they encounter a suitable piscine host. They then attach to the host surface, lose their tails and take up position beneath the scales to complete development to the adult (Rao and Ganapati, 1967).

The ectoparasitic habit of the adult fluke permits non-destructive assessment of parasite burdens by superficial observation of anaesthetised fish. This degree of accessibility is almost unique among the digeneans and has prompted the utilization of transversotrematids as the experimental subjects of several investigations of adult fluke biology. There have been a number of recent investigations into the population dynamics of adult T. patialense and into the cercarial-adult transformation (Whitfield, Anderson and Moloney, 1975; Anderson, 1976; Anderson, Whitfield and Mills, 1977; Mills, 1977).

Other developmental stages of the parasite, however, have received relatively little attention. Of these the more accessible cercarial stage has attracted most interest, with investigations into cercarial population survival characteristics, activity

patterns and attachment behaviour (Anderson and Whitfield, 1975; Whitfield, Anderson and Bundy, 1977; Whitfield et al., 1975). Aspects of the egg and intramolluscan stages have been almost entirely neglected, the only published investigation being a preliminary description of egg and intramolluscan development (Sim, 1972). The investigations presented here attempt to improve understanding of these larval stages by providing information on the development of T. patialense from the newly released unembryonated egg, through the ontogeny of the miracidium and intramolluscan development to the release of the infective cercaria. In addition the locomotion of the cercaria is discussed.

The maintenance of the life cycle is intrinsically a continuous process in any self-sustaining parasite population. The ensuing report discusses aspects of this process from the time of emergence of the egg to the time the cercaria-adult transformation occurs at reinfection of the definitive host. To avoid too unwieldy a presentation each separate topic is considered within a separate section. Each topic is introduced and discussed in relation to the broader aspects of digenean biology. To simplify this treatment a general materials and methods section (Section 2) describes those techniques utilised commonly throughout this investigation but specific techniques are presented within the section to which they relate.

The experimental manipulability of the adult and free swimming cercarial populations of T. patialense means that the potential exists for an unusually detailed understanding of the biology and population dynamics of this digenean. As has been noted above, a considerable start has been made in describing the developmental

biology and population processes of the adult generation (i.e. cercariae and adults). For any comprehensive analysis of the life cycle to be possible, however, the more inaccessible egg and intra-molluscan phases of the life history need to be subjected to the same depth of analysis as the mature cercariae and adults.

The general aim of the work reported here is to provide information on the ultrastructure, developmental biology, reproductive biology and behaviour of the less understood developmental stages. Such information on all aspects of the life cycle is a necessary prerequisite for precise and efficient design of experiments for elucidation of the population dynamics of the parasite. It is hoped that this contribution, in conjunction with previous studies on mature cercariae and adults, will provide the bases for a significant advance in the interpretation of the population biology of <u>T. patialense</u>.

SECTION 2:

GENERAL MATERIALS AND METHODS

2. General Materials and Methods

2.1 Water Conditioning

In order to standardise conditions all experiments involving the maintenance of parasites or hosts were conducted using "conditioned" water. To produce constant supplies of this, a 50 l container was filled with tap water at 24°C and a population of guppies (Poecilia reticulata) was introduced. After a month the water was considered suitable for use, although not more than 20 l were removed and replaced with tap water within any subsequent one month period.

2.2 Maintenance of the Intermediate Host

Populations of Melanoides tuberculata were maintained in 13 l tanks of conditioned water at 25°C. The base of the tank was covered to a depth of 3 cm with gravel to provide a suitable substrate for these melaiid burrowing snails. Excess food was provided in the form of proprietory fish food (Vit-a-min, King British Aquarium Accesories Co. Ltd.) and dried lettuce. The snails also appeared to feed on natural growths of the filamentous green alga Cladophora sp.

2.3 Stimulation of Cercarial Emergence

The emergence of cercariae was stimulated by a reduction in light intensity following the procedure of Anderson and Whitfield (1975). Snails were placed in the dark for one hour in a crystalising dish containing conditioned water at 24°C. Emergent cercariae were then visible under incident light against a dark back-ground and could be removed using a pasteur pipette.

2.4 Infection and Maintenance of the Definitive Host

The definitive host fish, the Zebra Danio (Brachydanio rerio), was infected by exposure to newly emerged cercariae. The cyprinid was placed in a 500 ml crystalising dish of conditioned water containing the required number of cercariae and left for one hour. Immediately before exposure the fish was fed proprietory fish food to satiation in order to minimise and standardise as far as possible the predation of parasites.

Time zero of infection was taken to be the mid-point of the exposure period ± half the exposure period.

Populations of fish were maintained in aerated 13 l tanks at 24°C in a 12/12 h dark/light regime and provided with proprietory fish food.

2.5 Anaesthetisation of Host Fish and Removal of Adult Flukes

Adult flukes were removed from infected fish after anaesthetisation. The anaesthetic MS 222 (Sandoz) is believed to be specific for poikilothermic vertebrates and at the concentrations and durations of exposure used has no obvious effects on T. patialense (Whitfield et al., 1975). Infected fish were placed in petri dishes containing a 1:10,000 w/v solution of MS 222 and observed under 20 x magnification. A hook-shaped tungsten wire mounted in a needle clamp was then used to sweep the flukes from beneath the scales. No apparent physical damage was caused to parasite or host by this procedure.

2.6 Collection of Fluke Eggs

Infected fish were maintained in the upper chamber of a fish breeding trap (Figure 2.1). Eggs dropped from the fish surface and passed into the lower chamber through a slotted partition which separated the two chambers and prevented the fish from ingesting more than a very small proportion of the fluke eggs.

After a known period the fish and partition were removed and the trap contents filtered through a 36μm Endicot sieve. The residue was washed off the sieve with a minimum volume of water and filtered under slight vacuum onto Whatman GF/A microfibre filter discs (pore size 2μm) in 15 ml Millipore filter funnels.

Moistened filter discs were observed under 40 x magnification while the eggs were pipetted individually into 5 ml crystalising dishes of water using fine bore (300μm diameter) pipettes.

The eggs were then pipetted individually for a second time, on this occasion into 25 ml sample tubes of water. The tubes were sealed and agitated for ten minutes on a rotary suspension mixer. After allowing the eggs to sediment 20 ml of water was removed and a further 20 ml of clean water substituted. The eggs were then agitated for a further ten minutes.

After this procedure the egg surface was relatively free of adherent mucus, particles of fish faeces and other detritus. Similarly, the water, due to minimal transfer and maximal dilution, contained few of the rotifers, ciliates and bacteria normally associated with fish conditioned water.

Figure 2.1: Vertical section through fish breeding trap used to collect fluke eggs (see text).

1: fish maintenance chamber

2: slot in partition

3: egg collection chamber.

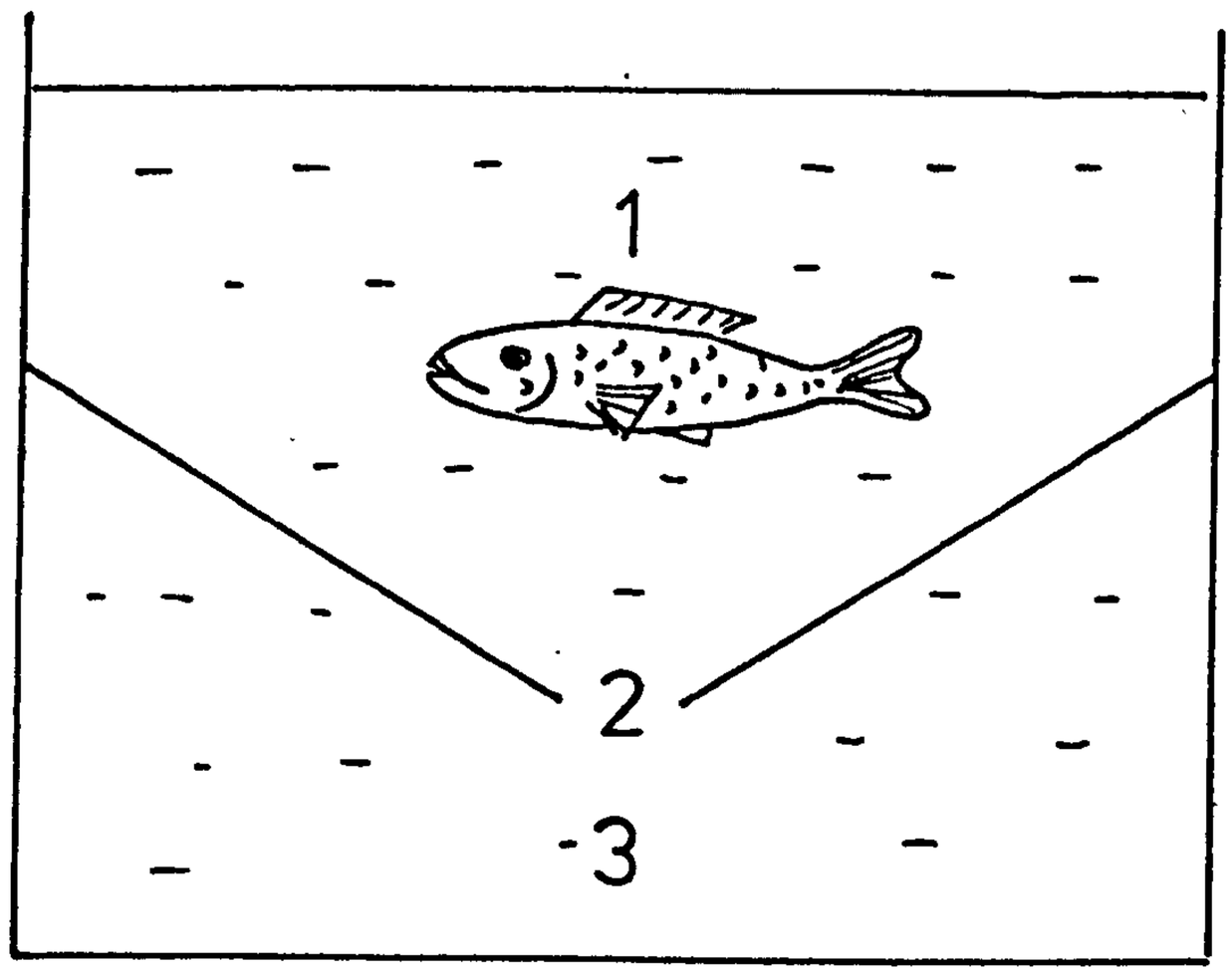
1
2
3

2.7 Snail Dissection to Obtain Intramolluscan Larvae

Removal of intramolluscan larval stages required dissection of the snail host. A standardised procedure was adopted:

a) Using fine scissors the shell was cut along the outside of the whorls towards the apex and the soft body tissues withdrawn from the shell.

b) The body of the snail was immersed in 0.66 M Sorensen's Phosphate buffer at pH 7.38 (80 ml $^{M}/_{15}$ dibasic sodium phosphate with 20 ml $^{M}/_{15}$ potassium acid phosphate).

c) The body was divided into three sections: the basal region comprising the foot, brood pouch and mantle cavity; the mid-region comprising the heart, stomach and style sac; and the apical region comprising the digestive gland and ovary.

d) Each section was isolated in separate drops of phosphate buffer and teased apart using fine needles.

e) Larval stages were removed using a mouth pipette mounted with fine-bore pipettes of 600μm or 300μm diameter depending on larval dimensions.

2.8 Electron Microscopy

Both scanning electron microscopy (S.E.M.) and transmission electron microscopy (T.E.M.) were used in the present investigations. The preliminary stages of double fixation and dehydration were common to both techniques:

a) Primary aldehyde fixation. Two hours in 2.5% glutaraldehyde solution in cacodylate buffer at 4°C.

90 ml	0.05 M	Sodium cacodylate
10 ml	25%	Glutaraldehyde
6 g		Sucrose

b) Cacodylate buffer rinse. pH 7.2.

100 ml	0.05 M	Sodium cacodylate
12 g		Sucrose

c) Post fixation. One hour in 1% osmium tetroxide cacodylate buffer at 4°C.

10 ml	0.05 M	Sodium cacodylate
0.1 g		Osmium tetroxide crystals
0.9 g		Sucrose

d) Cacodylate buffer rinse.

e) Dehydration. Alcohol series 50, 70, 90 and 100% ethanol. Two changes of 50% and 100%, ten minutes per solution.

Subsequent treatments of material differed for S.E.M. and T.E.M.

Scanning Electron Microscopy: After double fixation and dehydration the material was transferred through two changes of Analar acetone. In a Polaron E3000 critical point drying unit the acetone was replaced with liquid carbon dioxide and the material dried. Small specimens were then mounted on self-adhesive stubs while larger specimens were attached to the stubs with high conductivity paint (Silver Dag). A 40 nm gold coating was then applied using a Polaron E5000 diode sputter system.

Prepared specimens were observed using a Cambridge Stereoscan S4-10.

Transmission Electron Microscopy: After double fixation and dehydration the material was transferred through two changes of propylene oxide.

The TAAB embedding material used had the following components:

5 ml TAAB resin.

4.5 ml Dodecenylsuccinic anhydride (DDSA)

0.5 ml Methyl nadic anhydride (MNA)

0.2 ml 2,4,6 tri-(Dimethylaminomethyl) phenol (DMP-30).

DDSA and MNA are differential resin hardeners, their relative proportions determining the final consistency of the resin block. DMP-30 is an accelerator.

The following embedding sequence was utilised once the material was in propylene oxide:

a) TAAB resin mix added 1:1 and incubated at 60°C for 30 mins.

b) TAAB resin mix added 1:3 and incubated at 60°C for 30 mins.

c) Material transferred to pure TAAB resin mix and incubated at 60°C for 3 mins.

d) Material blocked out and incubated at 60°C for 24h.

The blocks were trimmed and then sectioned using glass or diamond knives with either a Porter Blum MT2-B or LKB MK.III ultramicrotome. Silver sections approximately 60 nm thick were floated off and flattened with chloroform/xylene vapour.

Sections were picked up on dilute hydrochloric acid etched copper grids and stained using the following procedure.

Uranyl acetate for 10 min. at 60°C.

Redistilled water wash.

Lead citrate, prepared using the high pH technique of Reynolds (1963), at room temperature.

The sections were then viewed using an AEI EM6B transmission electron microscope.

Section 3:

Egg Morphometrics

3. Egg Morphometrics

3.1 Introduction

In Transversotrema patialense the egg is the initial unit in the transmission of infection from the piscine definitive host to the molluscan intermediate host. The newly emerged egg must contain sufficient nutrients to support the embryogenesis and subsequent swimming and infective activities of the non-feeding miracidial stage.

In many organisms nutrients occupy the greater proportion of the contents of newly formed eggs, and hence egg size is a function of the amount of nutrient contained. An exchange between Vance (1973a, 1973b and 1974) and Underwood (1974) developed the concept of a relationship between egg size (assumed equivalent to nutrient availability) and reproductive strategy in ovigerous organisms. Steele (1977) and Strathman (1977) have reviewed this concept and demonstrated a relationship between egg size and such features of larval nutrient requirement as longevity and size at metamorphosis in certain taxa of crustaceans, molluscs, tunicates, polychaetes, amphibians and birds.

The subsequent investigation attempts to determine the proportion of the egg of T. patialense which is occupied by nutrients, in the form of vitelline cells, and hence to discover to what extent egg size is a function of nutrient content in this species.

Digenean egg size is additionally of interest because of its frequent use as a taxonomic feature. To have any value in the taxonomic separation of species a dimensional character such as

egg size must be species specific and of known variability (Hsu and Hsu, 1958; Nelson, Teesdale and Highton, 1962). The present investigation seeks to determine for T. patialense the age dependency and population variability of egg dimensions, and to examine the value of egg size as a taxonomic criterion in the Family Transversotrematidae.

3.2 Materials and Methods

a) The effect of fluke age on egg size

A population of twenty B. rerio were infected with cercariae, using the technique described in Section 2.4, so that approximately twenty flukes attached to each fish. The fish were maintained in 13 l tanks at 24°C and fed excess food.

The infection exposure period was from 11.30-12.00 hours and hence noon was considered time zero for fluke age.

After two days egg collections were made every night until a single collection yielded 30 or more eggs. Collections were made from fish which had been held in breeding traps overnight from noon on one day to noon the next. The time of the egg collection was then taken to be 24.00 hours ± 12h.

Collections were made subsequently at weekly intervals until egg production again fell below 30 eggs per collection.

The eggs from each collection were cleaned (Section 2.6) and pipetted onto a microscope slide and covered with a vaseline supported coverslip. The first thirty eggs encountered when scanning the slide were measured using a micrometer eye-piece,

and the length of the egg (L) and its width at the widest point (Bmax) were determined (Figure 3.1).

These data were used to determine the mean width and length of eggs produced by flukes of known age.

The sample size of 30 eggs was selected on the following basis. The requirement in this investigation was that the sample mean ($\bar{x}$) approximated the population mean (μ), that is for flukes at a particular age the mean egg dimensions determined from measurement of a sample of eggs approximates the value obtained if the eggs of all flukes at that age could be measured. The accuracy of this approximation is, therefore, a function of the number of eggs measured, or the sample size.

In the present investigation the required level of accuracy was arbitrarily selected: the sample mean should have a 95% probability of falling within $\pm$ 3μm of the population mean; $\mu = \bar{x} \pm 3\ \mu m$ ($p = 0.95$). That is to say the 95% confidence limits of the sample mean should not exceed $\pm$ 3μm.

The 95% confidence limits are given by $s/\sqrt{n} \times 1.96$ where s is the sample standard deviation and n the sample size. Hence for 3μm confidence limits the standard error of the sample is 3/1.96 or 1.5306, the square of which is an estimate of population variance $\sigma^2 = 2.3427$.

Sample variance is a function of population variance and sample size according to the relationship:

$$s^2 = \sigma^2/n$$

Figure 3.1: Diagrammatic representation of egg size parameter.

L = Egg length

Bmax = Egg maximum width

B = Egg width at $^{L}/2$

H = Distance of Bmax from nearest end

t = Thickness of egg capsule wall.

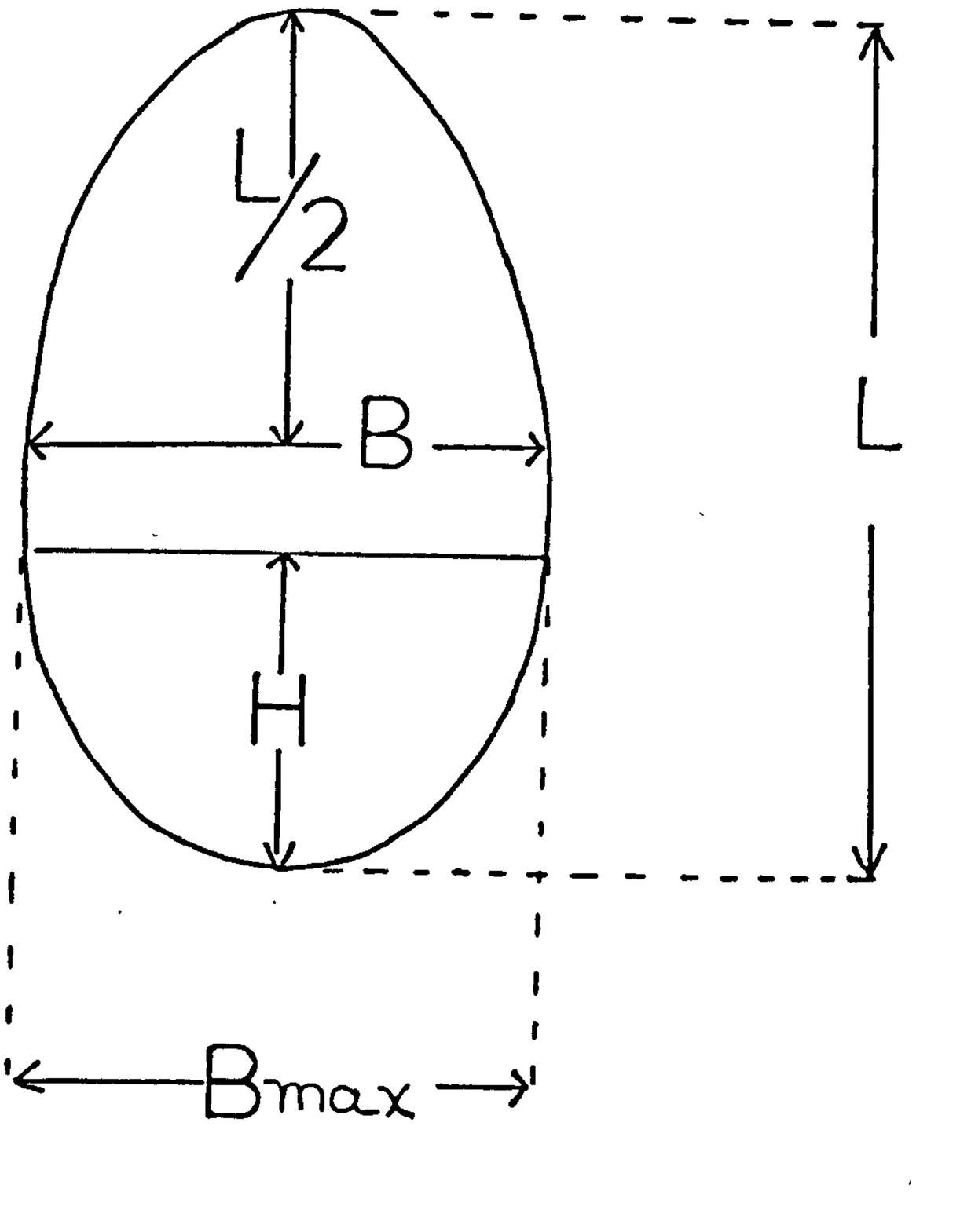
L/2
B
L
H
Bmax

where s^2 = sample variance, σ^2 = population variance and n is the sample size. Hence:

$$n = s^2/\sigma^2 = s^2/2.3427$$

Using this formula the sample size giving the required degree of accuracy may be estimated from known values of sample variance. In the present investigation four sample size estimates were obtained and these indicated that a sample mean determined from a sample size greater than 26.42 would have a 95% probability of falling within $\pm 3\mu$m of the population mean. In practice a slightly larger sample size of 30 eggs was utilised.

b) Population variation in egg dimensions

A population of 40 fish infected with a mixed age population of flukes was held in maintenance tanks at 24°C. Egg collections from these fish were cleaned (Section 2.6) and mounted under vaseline supported coverslips. Every egg collected was measured for length and maximum width. This procedure was repeated until a total of 750 pairs of egg dimensions had been obtained.

These data were analysed to determine the distribution of length measurements, and the mean width and length.

c) Egg volume

Twenty eggs were collected from a population of B. rerio infected with a mixed age population of flukes. The eggs were mounted beneath vaseline supported coverslips. Using an eyepiece micrometer the diameters of the zygote and six different vitelline cells were determined for each egg. Each

cell was measured twice, the second measurement normal to the first, and the mean of these two measurements taken as the true diameter.

The eggs were then photographed using a Zeiss Ultraphot and the 5" x 4" negatives (TRI-X PAN film) enlarged to A4 prints. An accurate magnification factor was obtained by similarly photographing a stage micrometer.

Five parameters of each egg were measured from the photographic enlargements: length (L); width at half length (B); maximum width (Bmax); distance of Bmax from nearest end (H); and thickness of egg capsule wall (t) (see Figure 3.1). From the dimensions it was possible to estimate mean values for: total egg volume, internal egg volume, volume of capsule material, volume of zygote, vitelline cell volume and interstitial volume.

3.3 Results

a) The effect of fluke age on egg size

The results are shown in Table 3.1 and Figure 3.2. Each point on Figure 3.2 represents the mean egg length or width at a particular fluke age in days post-infection (P.I.). The points were fitted with 95% confidence limits. Days 5.5 and 61.5 (P.I.) were the first and last days respectively that more than 30 eggs were collected.

An analysis of variance test was applied to the data to determine the variation in egg capsule dimensions with the factor fluke age. The resulting F values relate to the

Figure 3.2: The effect of fluke age on egg width and length.

Data points fitted with 95% confidence limits.

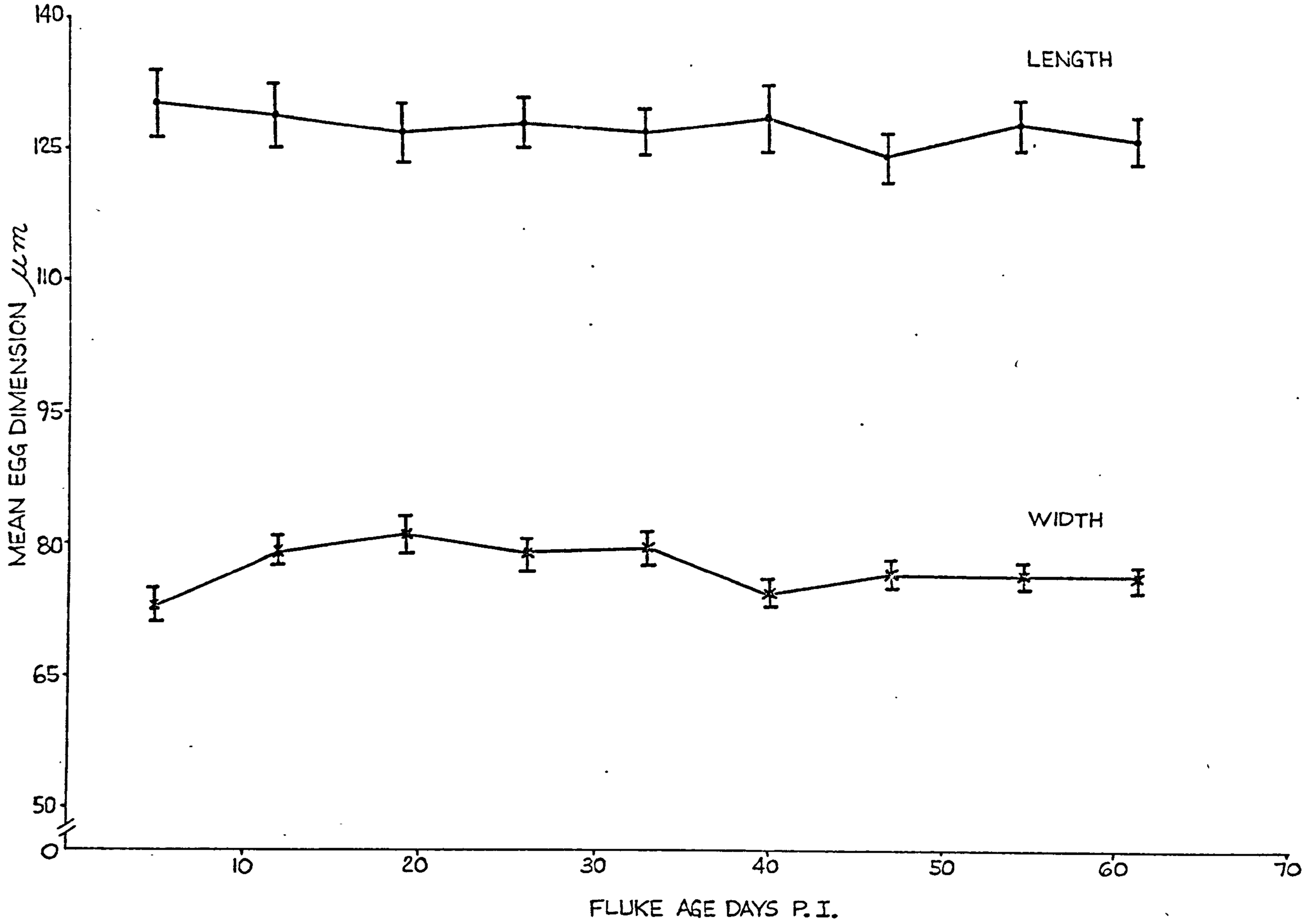
140
125
110
95
80
65
50
0
MEAN EGG DIMENSION μm
LENGTH
WIDTH
10
20
30
40
50
60
70
FLUKE AGE DAYS P. I.

factor fluke age.

Egg capsule length: $P(F = 2.18) < 0.05 > 0.025$; D.F. 8;261.

Egg capsule width: $P(F = 9.57) < 0.01$; D.F. 8;261.

Hence at the 2.5% level egg capsule width changed significantly with fluke age while egg capsule length did not.

TABLE 3.1

The effect of fluke age on egg size

FLUKE AGE (DAYS P.I.)	MEAN EGG DIMENSION ± 95% CONFIDENCE LIMITS (n = 30)	
	LENGTH μm	WIDTH μm
5.5	130.37 ± 2.81	72.77 ± 2.04
12.5	129.32 ± 2.70	79.27 ± 2.25
19.5	127.22 ± 2.52	81.48 ± 2.77
26.5	128.44 ± 2.24	78.76 ± 1.82
33.5	127.17 ± 1.80	80.31 ± 1.70
40.5	129.55 ± 2.47	74.86 ± 1.17
47.5	124.84 ± 2.09	76.76 ± 0.90
54.5	128.25 ± 1.93	76.60 ± 1.02
61.5	126.32 ± 1.98	76.02 ± 1.06

b) Population variation in egg dimensions

Because of the lack of age dependency of egg length, as shown above, the egg length data from flukes of all ages could be considered together. A frequency histogram of egg length (n = 750) is shown in Figure 3.3. The data were fitted with a theoretical normal distribution curve approximated from the data using the method of Hastings (1955). The computer program used to determine the theoretical values was adapted from that

Figure 3.3: Size-frequency distribution of egg length dimension. The observed data is shown as a histogram and fitted with a predicted normal distribution (see text).

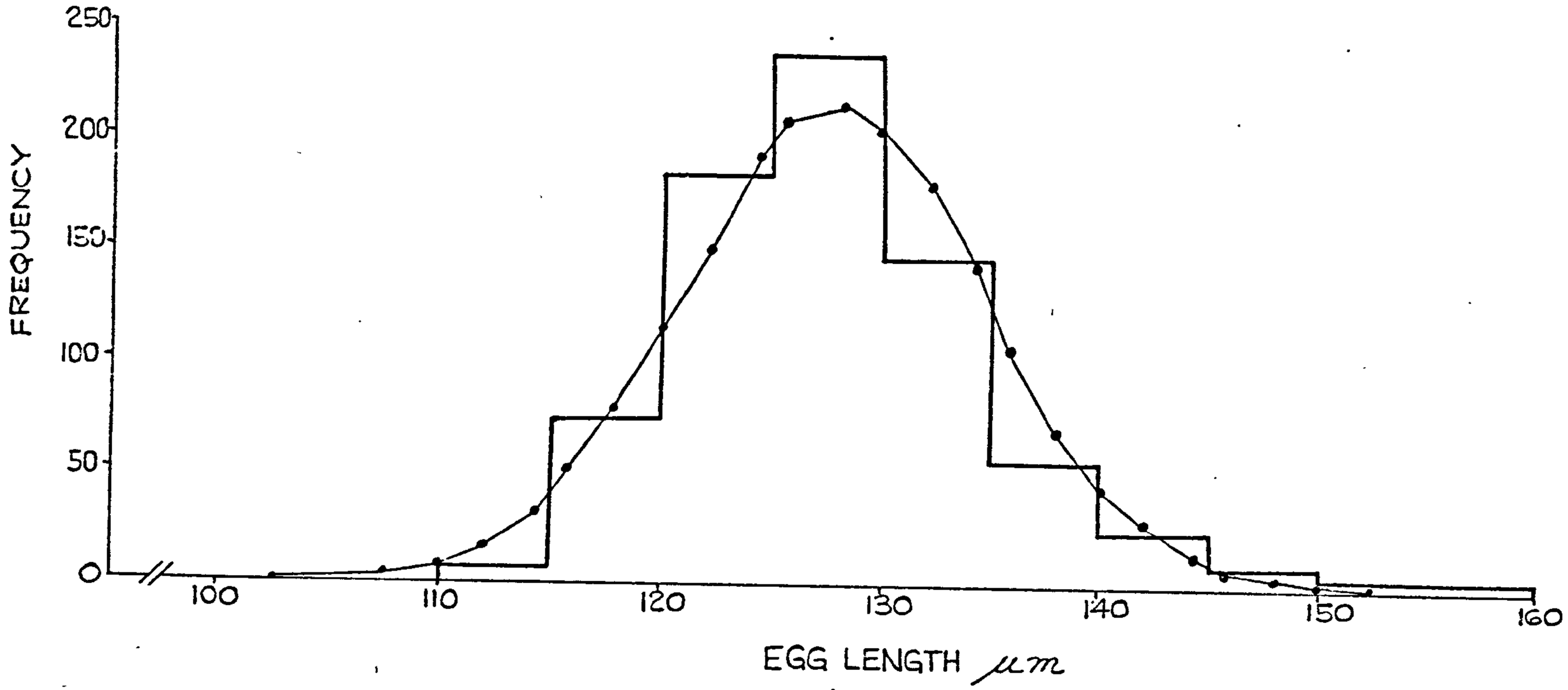
250
200
150
100
50
0
FREQUENCY
100
110
120
130
140
150
160
EGG LENGTH μm

of Davies (1971).

The significance of these results was estimated using a Chi-squared test, strengthened by the modifications suggested by Yates (1934) and Cochran (1954). It should be noted that because the approximation used to derive the theoretical curve relies on estimates of both the population and sample means the degrees of freedom are given by the number of classes minus two. The results of the test was P(Chi-squared = 7.214) >0.05: D.F.5.

The distribution of length measurements does not depart significantly from normal.

c) Egg volume

The volume of an asymmetric egg may be estimated from four linear dimensions using a technique adapted by Tatum (1975) from Preston (1974).

The following constants must first be estimated:

$$C_1 = \sqrt{2(Bmax/B-1)}$$

$$SIN\,\Theta_m = 1 - 2H/L$$

$$C_2 = ((SIN\,\Theta_m - C_1)/2)/C_1$$

where Bmax, B, H and L are egg dimensions shown in Figure 3.1.

The egg volume may then be determined from:

$$Volume = (\pi L\, Bmax^2)/6.\ (1+2/5C_2 - 4/5C_1^2 + 3/35C_2^2)$$

For the egg of T. patialense the mean egg volume from twenty individual volume estimates was $344 \pm 13.9 \times 10^3 \mu m^3$. This is an estimate of the total volume, ± 95% confidence limits, and includes the volume of the egg capsule.

For an encapsulated egg the internal volume is less than the external volume by an amount proportional to the volume of the capsule. Capsule volume, as a percentage of external volume, is given by:

$$600 \times t/d \ \%$$

where t = thickness of capsule wall, and d = average external diameter = $\sqrt[3]{LB^2}$

Using the mean values: L = 127.8μm (n = 750); B = 76.8μm (n = 750); and t = 1.77 (n = 20): the internal volume was found to be 11.67% less than the external volume.

Hence the volume of the egg capsule was 40.14 x $10^3 \mu m^3$ and the internal egg volume 303.85 x $10^3 \mu m^3$.

The mean volume of the spherical vitelline cells and zygotes was calculated directly from the mean diameter values. The zygote had a mean diameter of 25.4μm (n = 20) and the volume was 8.58 x $10^3 \mu m^3$. The vitelline cells had a mean diameter of 14.00μm (n = 160) and the volume was 1.44 x $10^3 \mu m^3$.

Empirical techniques have demonstrated that when small spheres are packed in a manner so that they do not become distorted there is approximately 39% space or "voidage" between the spheres (see Section 3.4). If the vitelline cells of the egg of T. patialense are considered to act in a similar manner then the volume of vitelline material may be estimated by subtraction:

volume of vitelline material = internal volume of egg - [volume of zygote + 0.39 (internal volume of egg)] .

= 176.77 x $10^3 \mu m^3$.

The relative proportions of the components of internal egg volume are therefore: Zygote 2.8%, vitelline material 58.2%, and intercellular space 39%.

The volume of vitelline material present is commensurate with the presence of 123 vitelline cells of diameter 14μm. Unfortunately, it was not possible to confirm this estimate by direct counting of vitelline cells. This was due to two factors. Firstly, the opacity of the capsule wall (see Section 4.) prevented delineation of all vitelline cell margins. It was, therefore, not possible to accurately define individual cells. Secondly, due to their large number the vitelline cells overlapped so that under microscopic examination several layers of cells appeared to be present. Nomarsky interference optics were used in an attempt to avoid this problem. This optical system has a very shallow depth of field so that image appears to lie in a single plane. By focusing on a plane lying in the medium long axis of the egg more than 60 vitelline cells could generally be discerned. Focusing immediately above or below this plane revealed the presence of futher cells but due to their overlapping and irregular arrangement it was not possible to determine which cells had already been counted and hence no accurate assessment of numbers could be achieved by this method.

3.4 Discussion

The qualitative observation that vitelline material is the main component of digenean eggs was confirmed quantitatively for T. patialense. The volume of the freshly shed egg contents consisted

of approximately 3% zygote, 60% vitelline material and the remainder interstitial fluid.

It must be stressed that these results were arrived at by a series of approximations, the technical difficulties of direct solution being insurmountable in the time and with the techniques available. The indirect means employed involved two major assumptions.

Firstly, the shape of the egg capsule was assumed to be only slightly asymmetric. This assumption greatly simplifies the volume calculations (Preston, 1974; Tatum, 1975).

Secondly, it was assumed that the vitelline cells were packed in a chance manner and that their marginal voids were insignificantly small. This assumption requires some explanation. The vitelline cells may be considered as undistorted monometric, or identically sized, spheres enclosed within a large container. Spaces (voids) would then arise between the spheres and between the spheres and the container wall (marginal voids). The volume of the marginal voids is extremely difficult to estimate and is a function of the relative sizes of the spheres and container (Fraser, 1935). With small spheres in a large container the marginal voids become infinitesimally small and the size relationship of vitelline cells to the egg capsule of T. patialense was assumed to come into this category. The volume between the spheres (voidage or porosity) can be determined by geometrical principles and ranges from 26-47% from the "loosest" to the "tightest" form of packing (Grafton and Fraser, 1935). In natural situations, however, uniform packing is rare, a more usual situation being chance packing, "those fortuitous combinations of

systematic colonies with intervening or surrounding haphazard or actually orderless zones" (Grafton and Fraser, 1935). Empirical findings show that such arrangements have a voidage of 37-44%, 35-43% or 37-38% (Fraser, 1935; Grafton and Fraser, 1935; Crisp and Williams, 1971). The vitelline cells were assumed packed in a chance manner within the egg capsule of T. patialense, and the voidage volume or volume of interstitial material estimated at 39%.

The results presented here suggest, on proportional considerations alone, that the size of the egg of T. patialense is predominantly a function of the quantity of enclosed nutrients. Whether this relationship applies throughout the Digenea cannot be conclusively determined without accurate volume estimates for other species. However, assuming relative constancy of vitelline cell dimensions, some indication of the wider applicability of this relationship can be obtained by comparing enclosed vitelline cell number to egg capsule size (Table 3.2). While no precise conclusions may be drawn from such incomplete data there is an apparent trend for large eggs to contain more vitelline cells.

The length of the egg capsules of T. patialense was shown to be independent of fluke age over the range 5.5 to 61.5 days P.I. Egg capsule width, however, changed significantly with age over this range. Examination of the data reveals that the minimum mean width, on day 5.5 P.I., differs from the maximum mean width, on day 19.5 P.I., by only 10.7%. This indicates that egg capsule width changes in absolute terms only slightly with fluke age.

Andersen and Halvorsen (1978) have also demonstrated age dependency in helminth egg dimensions. Three species of Diphyllobothrium

were examined in the hamster and arctic fox. D. ditremum eggs showed no age dependency, D. dendriticum eggs showed width age dependency in the hamster only, with a variation of 4.6% between maximum and minimum width, and D. latum eggs exhibited length (4.7-8.3%) and width (8.0-12.1%) age dependency in the hamster only.

TABLE 3.2

Relationship between vitelline cell number and egg capsule size for four species of digeneans

SPECIES	No. VITELLINE CELLS	CAPSULE SIZE LENGTH x WIDTH μm	SOURCE
Clonorchis sinensis	5-7	28 x 16	Ujne, 1936
Halipegus eccentricus	6-7	65 x 26	Guilford, 1961
Fasciola hepatica	20-30	137 x 80	Stephenson, 1947
Transversotrema patialense	100+	128 x 77	Present study

Too few examples have been studied with sufficient quantitative rigour to allow firm conclusions, but an apparent implication of the above results might be that the width dimension of helminth eggs is a more variable feature than the length dimension, and that in both cases the proportional change is small. On this basis it appears that the relative age independence of the length dimension makes it a more reliable parameter for taxonomic use.

There is a general consensus of opinion that digenean egg size is determined by the dimensions of the ootype and uterus (Smyth and Clegg, 1959). The results presented here demonstrate that egg length in T. patialense is independent of fluke age over the range 5.5-61.5 days, a period during which somatic growth of the adult fluke occurs (Section 11). These results suggest the reproductive

tracts involved in oogenesis may have a differential growth rate, the ootype and uterus maintaining constant dimensions during the somatic growth of the fluke. In T. patialense this differential growth rate would not need to be particularly marked due to the limited somatic growth of the adult. It would be interesting to determine whether a differential growth rate in species exhibiting a considerable increase in somatic growth, such as the fasciolids and strigeids, is also sufficient to maintain an egg length independent of fluke age and size.

Table 3.3 and Figure 3.4 illustrate the reported egg dimensions of supposed species within the Family Transversotrematidae. The marine species Prototransversotrema steeri, T. licinum and T. haasi show clear differences from the other reported species. The dimension ranges of the remaining four species overlap with each other and with the results of the present investigation. On the basis of these recorded results, therefore, it is impossible to separate the species on egg size alone. Indeed it is not even possible to compare these results statistically as in no case were the sample variance and number of observations recorded in earlier reports.

This investigation reveals two important considerations in the use of egg dimensions as taxonomic criteria. Firstly, egg capsule length is apparently a more reliable characteristic than width since length is normally distributed and relatively independent of fluke age. Secondly, it is necessary to be more precise in recording egg dimensions than is current in the literature. An unqualified mean or range is useless for comparative purposes unless the species considered exhibit considerable

TABLE 3.3 Reported egg dimensions of species within the Family Transversotrematidae

SPECIES	EGG DIMENSIONS: RANGE (MEAN) μm		SOURCE
	LENGTH	WIDTH	
1) Transversotrema patialense	112-158 (128)	60-104 (77)	Present study
2) " "	104-176	56-88	Crusz et al., 1964
3) T. soparkari	140-176	68-109	Pande and Shukla, 1972
4) T. chackai	125-160	50-75	Mohandas, 1973
5) T. laruei	125-150 (137.5)	46-81 (63.5)	Velasquez, 1961
6) T. haasi	90	70	Witenberg, 1944
7) T. licinum	84-112	30-55	Manter, 1970
8) Prototransversotrema steeri	84-116 (99)	45-60 (51)	Angel, 1969

Figure 3.4: Range of egg sizes in described species of the Family Transversotrematidae (see Table 3.4).

1) Transversotrema patialense (Present study)
2) T. patialense (Crusz et al., 1964)
3) T. soparkari (Pande and Shukla, 1972)
4) T. chackai (Mohandas, 1973)
5) T. laruei (Velasquez, 1961)
6) T. haasi (Witenberg, 1944)
7) T. licinum (Manter, 1970)
8) Prototransversotrema steeri (Angel, 1969)

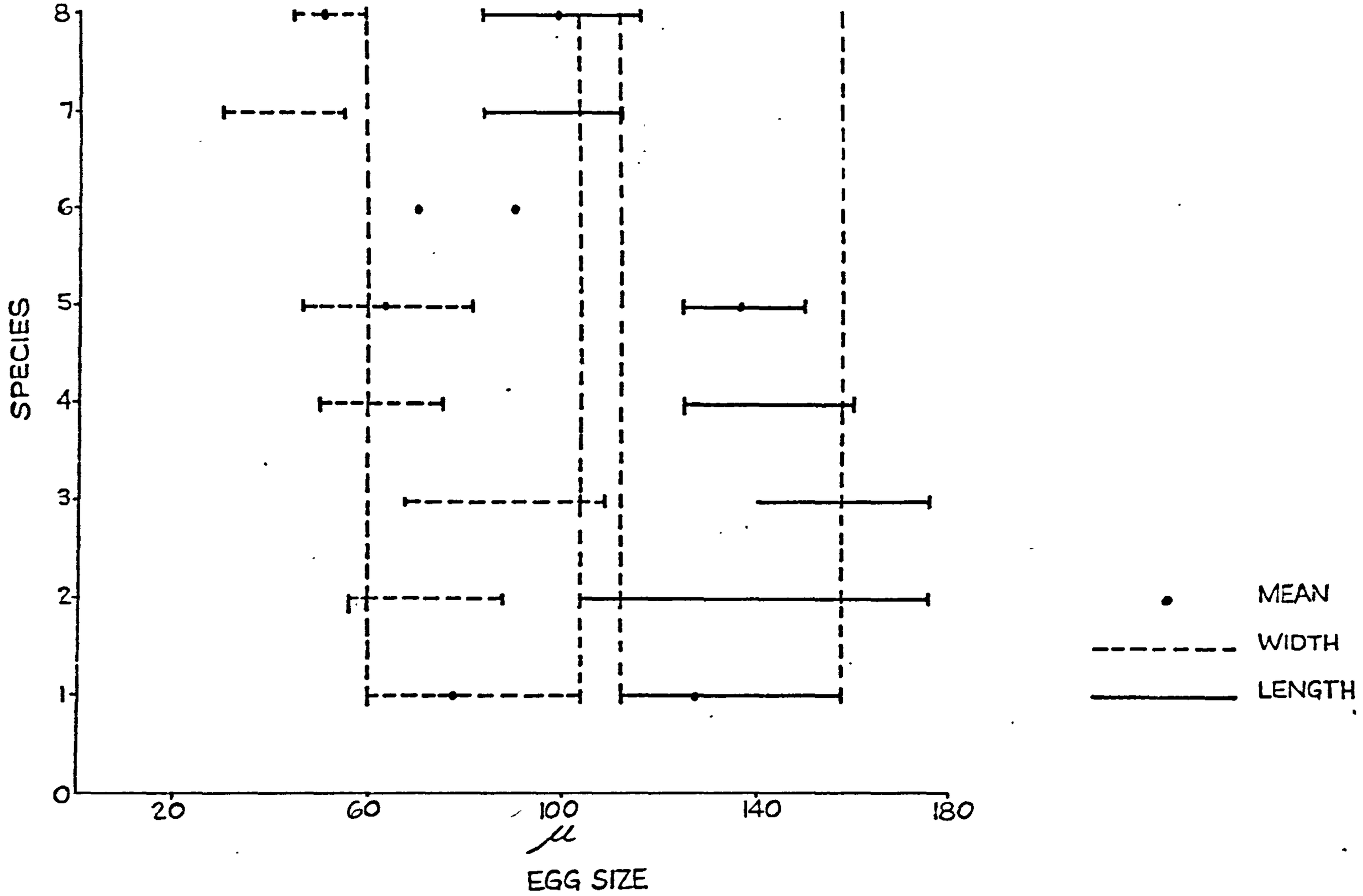
SPECIES
8
7
6
5
4
3
2
1
0
20
60
100
140
180
μ
EGG SIZE
MEAN
WIDTH
LENGTH

differences in egg dimensions. If the mean, variance and number of observations were stated for each species described then it would be possible, using simple statistical techniques, to determine the precise probability that a series of egg measurements resembled those of one or another species.

Section 4:

Qualitative Aspects of Egg Development

4. Qualitative Aspects of Egg Development

4.1 Introduction

The eggs of T. patialense develop once they have left the adult fluke (Sim, 1972). This development presumably occurs on the aquatic substrate where the eggs are exposed to variations in such exogenous factors as temperature and illumination. If the results presented in this thesis are to have any validy as a contribution to understanding the population characteristics of larval development it is essential that the influence of these exogenous factors on egg development is described in quantitative detail. A pre-requisite for any such quantitative approach is an understanding of the basic features of the biology of egg development.

The results reported in this section involve a qualitative description of egg development and a comparison of the experimental usefulness of different egg culture techniques. These investigations form an essential preliminary to the quantitative analyses of egg development recorded in Section 5.

4.2 Materials and Methods

4.2.1 Effect of differing culture conditions on the visibility of egg contents through the egg capsule wall

Eggs were collected and cleaned using the techniques described in Section 2.6. The eggs were then resuspended in three changes of autoclaved conditioned water. All procedures were carried out in a laminar flow cabinet (type HLF/H, SLEE Co. Ltd.). The eggs were then incubated in 25 ml pre-sterilized specimen vials con-

taining 15 ml of one of two culture media. One culture medium consisted of autoclaved conditioned water and the other of autoclaved conditioned water containing 100 units/ml of penicillin/streptomycin (Flow Laboratories).

The eggs were incubated at 25°C in a 12/12h D/L regime, aliquots of eggs being removed at daily intervals to assess development. Eggs were examined in their culture medium under vaseline supported cover-slips using a Zeiss RA microscope adapted with Nomarsky interference optics.

4.2.2 Egg capsule surface ultrastructure

Eggs were collected and cleaned, using the techniques described in Section 2.6, before preparing for S.E.M. and T.E.M. using the procedures described in Section 2.8.

4.2.3 Effect of collection techniques on egg viability

Eggs were collected from infected fish maintained in breeding traps overnight (Section 2.6). The eggs were suspended in the water from the breeding traps by gentle agitation and then the suspension was poured into two separate vessels. By this means two samples from the same population were available for separate treatment.

Treatment 1, Filtration. The eggs were filtered from the suspension using a metal sieve and then filtered under vacuum onto glass-fibre filter pads (Section 2.6).

Treatment 2, Sedimentation. The eggs were resuspended and the sample poured into a 3 litre Baermann funnel and allowed to settle for 30 minutes. The contents of the funnel collecting

tube were run off into a 100 ml crystalising dish and the eggs allowed to sediment.

Eggs from both treatments were pipetted onto slides and examined under vaseline supported cover-slips. The condition of the first 200 eggs encountered from each treatment was recorded.

4.2.4 Effect of culture techniques on egg viability

Eggs were collected and cleaned (Section 2.6). One group of eggs was incubated in autoclaved conditioned water and another group in autoclaved conditioned water containing penicillin/ streptomycin. The preparative procedures were as described in Section 4.2.1. The eggs were incubated at 25°C, 12/12h D/L.

On day 9 post collection (P.C.) an aliquot of 100 eggs was removed from each culture medium and examined microscopically.

This procedure was followed for five populations of eggs.

4.2.5 Effect of single fluke infections on egg viability

A single newly emerged cercaria (Section 2.3) was placed in a petri dish with a single uninfected Brachydanio rerio. After nine fish had been exposed to a single infection in this manner they were returned to their maintenance tank.

After one hour the fish were examined under anaesthetic (Section 2.5) and the presence of a single parasite confirmed. The fish were then returned to the maintenance tank.

At 10 and 20 days post infection (P.I.) eggs were collected from the fish and incubated at 30°C. After 7 days incubation the egg contents were examined microscopically.

At 11 and 21 days P.I. eggs were collected from the fish and examined immediately.

At 12 and 22 days P.I. the fish were anaesthetised and the presence of a single fluke per fish confirmed.

4.3 Results

4.3.1 Effect of differing culture conditions on the visibility of egg contents through the egg capsule wall

The contents of eggs incubated in media without antibiotics were not generally discernable by approximately 12 days P.C. at 25°C. Throughout this period the egg capsule became increasingly opaque due to a superficial film, possibly of bacterial origin.

The presence of antibiotics in the culture medium reduced the growth of the obscuring film and permitted observation of miracidial morphogenesis through the egg capsule wall. The following observations were made on eggs incubated in media containing antibiotics.

The newly emerged egg consisted of a tanned capsule containing a zygote surrounded by spherical vitelline cells (Figure 4.1.0). Each vitelline cell contained a nucleus and numerous granular inclusions.

As development proceeded the zygote divided to produce two similarly sized cells, the cleavage plane lying approximately normal to the long axis of the egg. It was not possible to distinguish the two cells on the basis of size or nuclear infrastructure.

Figure 4.1: Superficial sculpturing of the capsule of digenean eggs.

a) Thread-like extensions of T. patialense (b, boss; e, extension).

b) Apical villosities of Cryptocotyle lingua (Krupa, 1974).

c) Minute spines of Schistosoma spp. (Hockley, 1968).

a)

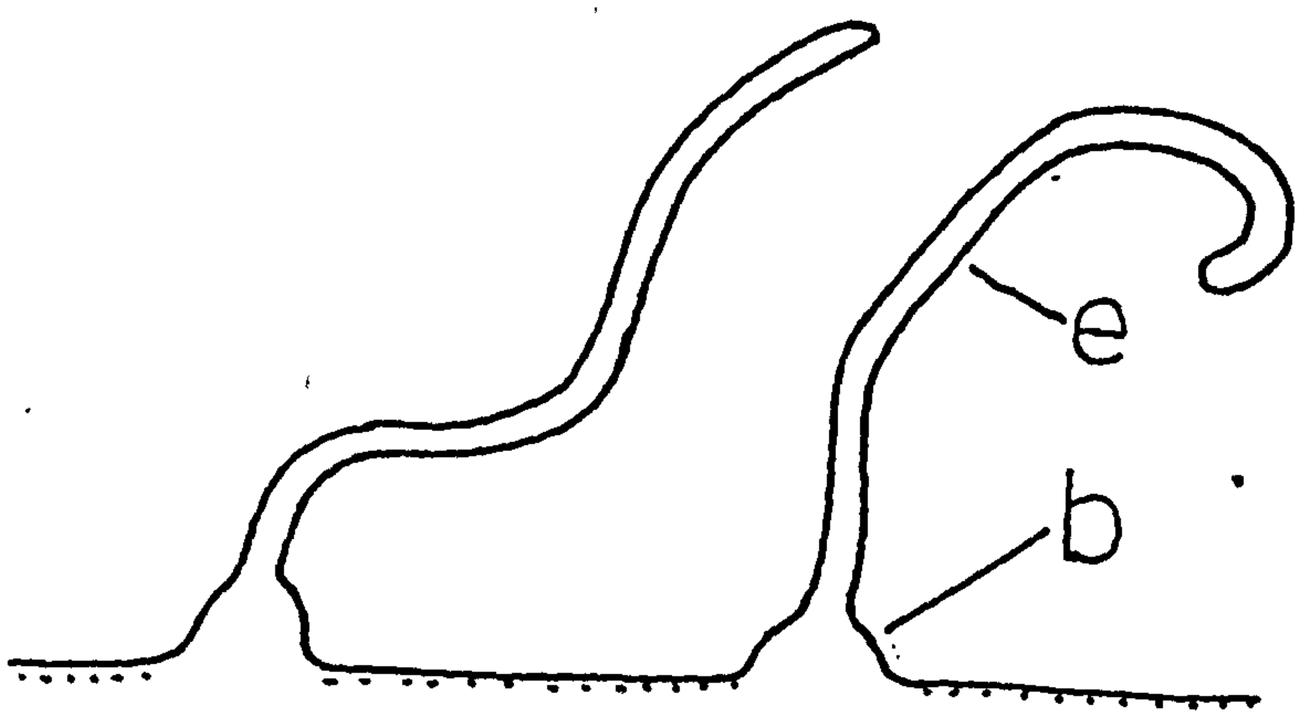

b)

c)

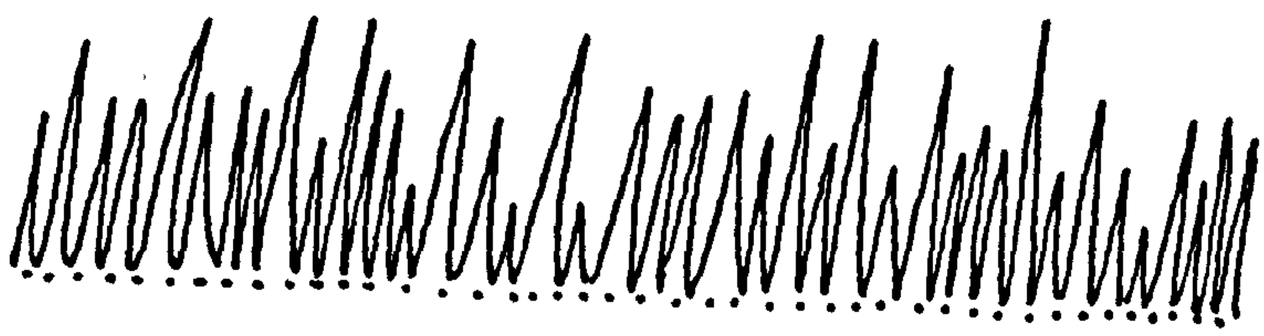

Division to the four-cell (Figure 4.2.1) and 8-cell stage then occurred. Due to the increasing number of cells subsequent divisions could not be accurately followed.

At approximately the thirty-cell stage the pattern of vitelline cells changed abruptly. The vitelline cells became swollen and closely apposed to each other so that the cells had an angular instead of spherical outline (Figure 4.2.2). The closely applied membranes of these cells were refractile so that the embryo was surrounded by a refractile rind, effectively preventing observation of embryonic development.

At a later stage in egg development the refractile rind of vitelline cells began to dissassemble and coalesce. The resulting units of vitelline material were very variable in size and shape. The undistorted outline of these units indicated that they were not closely applied to each other.

The embryo became more readily observable at this stage. Black pigment granules condensed in the regions predestined to become the miracidial ocelli (Figure 4.2.3).

By the time the vitelline material was reduced to two ovoid refractile bodies the miracidium was apparently fully formed within the egg capsule (Figure 4.2.4). The miracidium contained a pair of active flame cells and itself moved actively within the capsule. In the terminal stages before hatching the cilia surrounding the miracidium became active.

Hatching itself was not observed microscopically. No operculum was discernable in the capsule of developing eggs, but after hatching

a terminal operculum was either entirely detached from the capsule or attached at one point and hinged back. The capsule apparently contained only the ovoid refractile bodies which were greatly increased in volume and entirely filled the capsule lumen.

It was apparent from these observations of egg development that unambiguous, non-overlapping stages could be arbitrarily assigned to sections of the developmental sequence. Developmental stages were defined as shown in Table 4.1.

Eggs which were not developing could be similarly assigned to two categories. Firstly, moribund (M) eggs in which the contents of the capsule were amorphous. Secondly, dis-operculate (D) eggs in which the operculum was displaced.

4.3.2 Egg capusle surface ultrastructure

Scanning electron micrographs revealed that the entire surface of the egg capsule has a "felted" appearance due to the presence of numerous thread-like extensions (Plate 1). The extensions are present at a density of approximately $1\,\mu m^{-2}$ which is equivalent to approximately 26,000 over the whole egg surface (for an egg of length $128\,\mu m$ and width $77\,\mu m$ the surface area is $26{,}138\,\mu m^2$, mean egg dimensions from Section 3). Using higher magnifications of both S.E.M. and T.E.M. the structure of each extension could be clearly distinguished (Plates 1 and 11; and Figure 4.1). Each extension arises from a protuberant "boss" approximately $0.4\,\mu m$ in diameter. The extensions are cylindrical with an average diameter of $0.12\,\mu m$ and length of $3\,\mu m$.

Despite attempts to clean the egg bacteria and other material was observed trapped among the extensions against the capsule surface (Plate 1c).

Figure 4.2: Developmental stages of the egg of T. patialense

Stage 0: Newly shed, zygote uncleaved and vitelline cells spherical.

Stage 1: Zygote cleaved (embryo at 4-cell stage), vitelline cells spherical.

Stage 2: Developing embryo surrounded by refractile rind of vitelline cells.

Stage 3: Vitelline cells coalesced and pigment granules condensed in embryonic ocelli.

Stage 4: Mature miracidium within capsule.

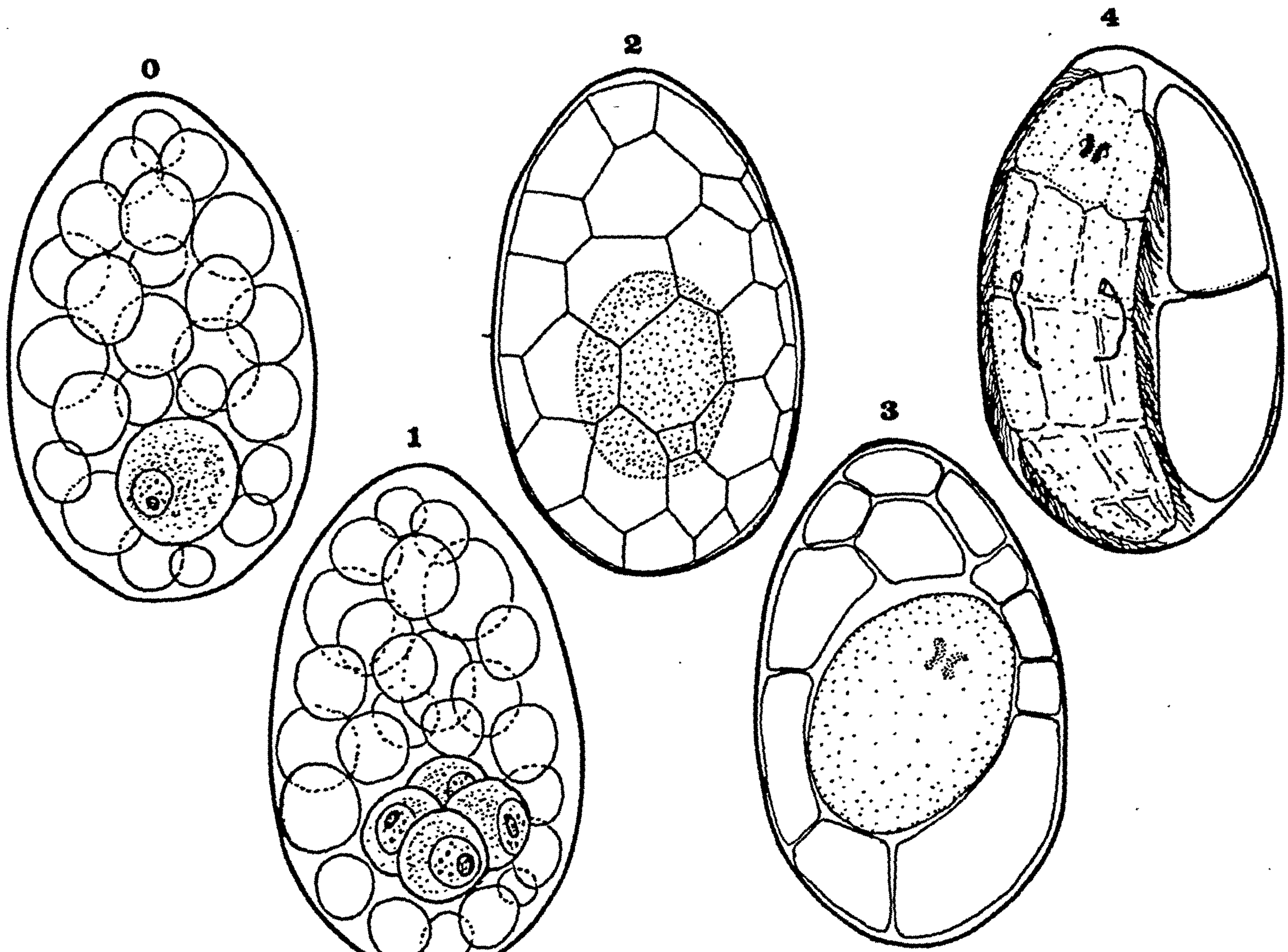
0
1
2
3
4
2n

TABLE 4.1 Stages in egg development

STAGE	CHARACTERISTICS
0	Zygote uncleaved (Figure 4.1.0)
1	Zygote cleaved, vitelline cells spherical (Figure 4.1.1)
2	Refractile rind of vitelline cells, no pigment visible in embryonic ocelli (Figure 4.1.2)
3	Pigment condensed in embryonic ocelli, no cilia or flame cells present in embryo (Figure 4.1.3)
4	Miracidium with cilia and flame cells, vitelline material in two ovoid bodies (Figure 4.1.4)

4.3.3 Effect of collection techniques on egg viability

The condition of the eggs immediately after collection by two different treatments is shown in Table 4.2.

The similarity of the two results suggests that overt damage to the egg capsule is not a result of the filtration technique. It is probable that a proportion of eggs were damaged before collection.

4.3.4 Effect of culture techniques on egg viability

The results are shown in Table 4.3. Since the eggs were examined on day 9 P.C. it was still possible to discern the egg contents through the capsule wall. The proportions of eggs at the different developmental stages were similar whether or not antibiotics were utilised. This suggests that antibiotics do not affect the viability or rate of development of the eggs.

TABLE 4.2 Effect of collection technique on eggs

TECHNIQUE	PROPORTION (n=200)			
	INTACT	DAMAGED	DIS-OPERCULATE	MORIBUND
Filtration	0.80	0.11	0.06	0.03
Sedimentation	0.76	0.15	0.05	0.04

TABLE 4.3 Effect of antibiotics (5 replicates of n=100)

Expressed as proportions in: Stages 0-4, dis-operculate (D) and moribund (M)

MEDIA	MEAN PROPORTION						
	0	1	2	3	4	D	M
WITH ANTIBIOTICS	0.02	0.04	0.59	0	0	0.09	0.26
WITHOUT ANTIBIOTICS	0.02	0.03	0.61	0	0	0.10	0.24

4.3.5 Effect of single fluke infections on egg viability

All 9 fish utilised in this experiment were infected with a single fluke throughout the experimental period.

On days 10 and 20 P.I., a total of 6 and 8 eggs were collected from the fish. After incubation at 30°C for 7 days all eggs were classified as moribund.

On days 11 and 21 P.I., a total of 8 and 7 eggs were collected. In two eggs the contents appeared characteristic of Stage 0 except that no nucleolus was present in the supposed zygote. All other eggs were classified as moribund.

A single fluke on a host does not, therefore, appear capable of producing viable eggs. Mircroscopical examination of the individual flukes indicated no superficial morphological differences from adults in multiple infections.

4.4 Discussion

The results show that observations on egg development and miracidial morphogenesis may be hindered by the opacity of the capsule. This problem may be avoided by the use of antibiotics in the culture medium, this addition having no apparent effects on egg development.

It may be concluded from the sucess of antibiotics in preventing the development of a superficial film on the capsule that the opacity is due to the growth of bacterial colonies. This conclusion appears to be supported by the observation that bacteria and detritus are retained against the surface of the capsule, even after cleaning, by the superficial extensions.

It should be noted that the effect of the superficial film on egg viability has not been demonstrated. This layer, supposedly comprised of bacteria and detrites, may not in fact affect egg development but for experimental analyses of egg development by direct observation its prevention is essential.

The external sculpturing of the egg capsule of T. patialense that apparently retains the superficial layer differs from that previously described in the platyhelminths. The "apical villosities" described by Krupa (1974) on the capsule of Cryptocotyle lingua were simple surface elevations (Figure 4.2b). Species of the genus Schistosoma have been taxonomically separated on the basis of the position of individual large spines on the egg. These species, however, also carry arrays of minute spines only observable under T.E.M. or S.E.M. (Figure 4.2c). These show specific size variation:

S. mansoni, length (L) = 0.28 μm, width (W) = 0.03–0.1 μm;

S. haematobium, L = 0.2 μm, W = 0.03–0.1 μm; and

S. japonicum, L = 0.05 μm, W = 0.02 μm (Hockley, 1968; Schnitzer, Sodeman, Sodeman and Durkee, 1971).

S. haematobium may additionally be separated from the other two species on spine morphology as its spines are rounded at the tip while those of the others are sharply pointed. This feature is probably not the result of abrasion as suggested by Hockley (1968) since it was observable in utero (Schnitzer et al., 1971).

The egg capsule of Fasciola hepatica is smooth, no general external sculpturing is apparent under T.E.M. or S.E.M. (Wilson, 1967a; Koie, Christensen and Nansen, 1976).

The capsule of Clonorchis sinensis is "etched" with irregular markings visible under LM, the capsule otherwise appearing smooth (Komiya, 1966).

Information is sparse concerning the sculpturing of egg surfaces in the Cestoda. 3μm spines have been described on the egg surface of the caryophylleid Khawia iowensis and the anoplocephalid genus Monoecocestus (Calentine and Ulmer, 1961; Freeman, 1949). In neither case, however, is the origin of the embryonic envelopes fully understood and hence analogy with the digenean capsule may be unjustified. The outer coat of Hymenolepis diminuta eggs has been extensively studied using S.E.M. and T.E.M. and is composed of globular units fused to an amorphous matrix (Pence, 1970; Rybicka, 1972; Lethbridge, 1976). The mucopolysaccharide or mucoprotein composition of this layer militates against any simple comparison with digenean capsules (Smyth and Clegg, 1959; Rybicka, 1966; Pence, 1970). The egg capsules of pseudophyllideans have similar origins to those of digeneans. In several species of Diphyllobothriids the egg capsule is "pitted", the surface bearing irregularly distributed concavities (Hilliard, 1960; Rybicka, 1966).

The function of capsule sculpturing is obscure. Hockley (1968) suggested that the spines of Schistosoma may achieve positional maintenance, enhanced area for enzymatic secretion, or entrapment and localisation of egg secretions; views recapitulated with reservations by Schnitzer et al. (1971). Krupa (1974) postulated a mechanical function for the apical villosities of Cryptocotyle lingua eggs, suggesting that they entwined with flaps of the uterine wall and so assisted egg movement along the uterus.

These hypotheses are unsatisfactory in a number of ways, not the least being the difficulties inherent in postulating such gross mechanical functions for structures on the diminutive scale of the sculpturing. An alternative hypothesis is that the sculpturing arises as an incidental consequence of physical constraints imposed upon capsule formation. More specifically, that the final topography of the egg capsule is a consequence of incidental moulding effects at the capsule-reproductive tract interface.

The newly formed capsule of digenean eggs is plastic, gradually hardening due to quinone-tanning or some other mechanism (Smyth and Clegg, 1959; Madhavi, 1966 and 1968; Wilson, 1967a; Nollen, 1971; Ramalingam, 1973). It is suggested that some feature of the ootype or uterus influences the form of the capsule surface during the initial plastic condition.

Unfortunately, there are as yet no clear indications as to which features of the reproductive tract of T. patialense exert an influence on the formation of the capsule extensions. In particular two aspects of this sculpturing requires explanation. Firstly, what regions of the reproductive tract function as moulds? It would apparently require long thin tubular invaginations to mould the cylindrical extensions. The lumen of a gland cell is a possible candidate except that it would require 26,000 gland cells to mould all the extensions on the egg. Secondly, how is the sculpturing applied evenly over the whole capsule surface? Since the egg capsule is formed within a tubular reproductive tract it would be expected that however tightly the tract closed about the egg the terminal portions of the capsule would not be subject to any moulding in-

fluence. Improved comprehension of the origins of the capsule sculpturing must await more precise understanding of the ultra-structure of the regions involved in capsule formation.

A second feature of the capsules that has significance for the present experimental design is their apparent fragility. Attempts to collect eggs by the less stressful technique of sedimentation produced a similar proportion of damaged capsules to the separation of eggs by filtration. This result implies that the capsules are damaged before they are collected. A possible reason for this is that the fish are able to ingest fluke eggs, despite the precaution of the use of breeding traps to separate the fish from the eggs, and crack the capsules during passage through the cyprinid grinding pharynx. Due to the constancy of the damaged proportion, eggs in this state were omitted from all subsequent analyses.

Inspection of the results of the experiment on egg collection techniques reveals that dis-operculate and moribund eggs are present in initial collections. Additionally, some of the intact eggs present in the initial collections were at an advanced stage of development - while most eggs were at developmental stage 0 a very few eggs were at stages 2, 3 or 4. The presence of dis-operculate, moribund and precocious eggs in initial collections may be a consequence of the fluke's location beneath the scales of its piscine host. The genital atrium of the fluke is anteriorly situated (Section 10) and hence unless the fluke turns round or moves out from under the scale the egg would emerge into the thick layer of mucus beneath the scale. Eggs have been observed retained on the host in this manner. Such eggs may then develop, hatch or

become moribund before falling from the fish surface with sloughed mucus and so appear in egg collections which otherwise contain only newly emerged eggs.

Perhaps the most significant result in terms of its effect on egg viability and development was that obtained from the examination of single fluke infections. A single fluke on a host is apparently unable to produce viable eggs. This suggests that reciprocal copulation with another individual is a prerequisite for fertilization and further that accessibility of partners and copulation frequency may have important consequences for the proportion of fertile eggs produced. In order, therefore, to reduce the variability in the proportion of fertile eggs produced an experiment designed to investigate egg development should utilise large numbers of flukes per fish, hopefully increasing the probability of between-fluke contacts to the point where potentially all flukes could achieve cross fertilization and hence maximal egg fertility.

The significance of copulation to egg production and viability in hermaphrodite flukes has received scant attention in the literature.

Three possible consequences of single fluke infections have been reported. Firstly, the fluke failed to develop to a normal adult and did not produce eggs - Paragonimus kellicotti (Sogandares-Bernal, 1966). Secondly, the fluke failed to develop to a normal adult and produced eggs which were not viable - Philophthalmus sp. (Fried, 1962). Thirdly, the fluke developed to a normal adult and produced viable eggs - Echinostoma revoltum, E. malayanum, Zygocotyle lunata and Philophthalmus megalurus (Beaver, 1937;

Lie, 1965; Bacha, 1966; Nollen, 1968).

To these three results may now be added a fourth. In T. patialense an apparently normal ovigerous adult developed but the resulting eggs were not viable.

This series of investigations has established guidelines for the design of experiments for subsequent quantitative analyses of egg development in T. patialense. Such experiments should utilise eggs from heavily infected hosts, the eggs being collected by relatively simple filtration procedures. Provided the eggs are then incubated in sterile media containing antibiotics the proportional development of the eggs may be examined throughout the period of development by the use of defined developmental stages based on the morphology of the egg contents.

Section 5:

Quantitative Aspects of Egg Development

5. Quantitative Aspects of Egg Development

5.1 Introduction

In the previous section aspects of the biology of Transversotrema patialense eggs were described with emphasis on their relevance to the experimental design of a quantitative analysis of egg development. In particular it was demonstrated that the continuous sequence of development from zygote to mature miracidium could be arbitrarily divided into unambiguous stages on the basis of the appearance of the egg contents. In the present section this basic method of appraising egg developmental status is utilised in an examination of the effect of exogenous factors on rate parameters of egg development. In particular the effects of temperature and photoperiod are discussed.

5.2 Materials and Methods

5.2.1 Effect of temperature on egg development and viability

Eggs were collected and cleaned as described in Section 2.6. Vials of eggs were prepared for culture (Section 4.2) and incubated over a range of temperatures from 10-35°C at 5°C intervals in a 12/12h dark/light illumination regime.

At each of the six experimental temperatures three replicate egg collections were incubated and at intervals in days P.C. aliquots of 20+ eggs were examined from each. The intervals between examination periods were different for the different incubation temperatures: 35°C, 30°C and 25°C examined every 2 days; 20°C every 3 days;

15°C every 12 days; and 10°C at irregular intervals of approximately 30 days.

For each aliquot the proportion of eggs at each of the developmental stages was determined by microscopical examination. Eggs with torn capsules were excluded from these results.

5.2.2 Effect of storage at 10°C on subsequent egg viability at 25°C

4 vials of eggs were prepared for culture (Section 4.2) and incubated at 10°C. Two vials were removed at 4 weeks P.C. and again at 16 weeks P.C. and brought to a temperature of 25°C in steps of 5°C/24h. After 14 days at 25°C the eggs were examined.

5.2.3 Effect of illumination period on egg development

Eggs were prepared for culture (Section 4.2) and incubated at 25°C in an incubator providing 12/12h dark/light (D/L) or permanent illumination (L/L). Vials of eggs were also incubated at 25°C with the vial made light-tight by surrounding them in aluminium foil to provide permanent dark conditions (D/D).

After 14 days an aliquot of egg was removed from vials under each of the light conditions and the proportion at the different developmental stages determined for 20 eggs from each aliquot.

5.3 Results

5.3.1 Effect of temperature on egg development and viability

The proportion of eggs dis-operculate, moribund and at each of the developmental stages 0-4 was determined over the temperature range 10-35°C at 5°C intervals. Each proportion represents the mean of 3 replicates of 20 eggs each. The results for the different

temperatures are presented as follows: 10°C, Table 5.1; 15°C, Figure 5.1a; 20°C, Figure 5.1b; 25°C, Figure 5.1c; 30°C, Figure 5.1d; 35°C, Figure 5.1e. The data are recorded in Appendix 1.

TABLE 5.1

Proportional egg development at 10°C (n = 60)

TIME OF OBSERVATION DAYS P.C.	MEAN PROPORTION OF EGGS AT DEVELOPMENTAL STAGES						
	0	1	2	3	4	D	M
0	0.95	0	0	0	0	0.05	0
35	0.88	0	0	0	0	0.02	0.16
84	0.49	0	0	0	0	0.05	0.46
112	0.40	0	0	0	0	0.17	0.43

Development occurred at all temperatures over the range 15-30°C. The pattern of development was broadly similar at all temperatures within this range and hence the Figures representing these temperatures may be considered together. The abscissa in each case is the time axis expressed in days P.C. Ordinates of proportion are presented for each of the developmental stages 0, 1, 2, 3 and 4 and for the non-developmental categories moribund (M) and dis-operculate (D). Each histogram bar represents the proportion of eggs in a particular condition on a specific day P.C. when the eggs were examined, hence the width of the bar varies with the time scale. This proportion was determined by taking the mean of three aliquots of 20 eggs from separate populations.

As eggs developed the population of eggs changed its developmental state and moved partially from one stage to the next. In

Figure 5.1: Proportion of eggs in Developmental Stages 0, 1, 2, 3 and 4, and Developmental Categories Moribund (M) and Disoperculate (D), (see Text). Proportions shown for temperatures:
a) 15°C b) 20°C c) 25°C d) 30°C e) 35°C.

a)

PROPORTION

0 1.0 0.5 0

1 0.5 0

2 0.5 0

3 0.5 0

4 0.5 0

D 0.5 0

M 0.5 0

0 12 24 36 48 60 72 84 96 108 120 132 144 156

AGE (DAYS)

15°C

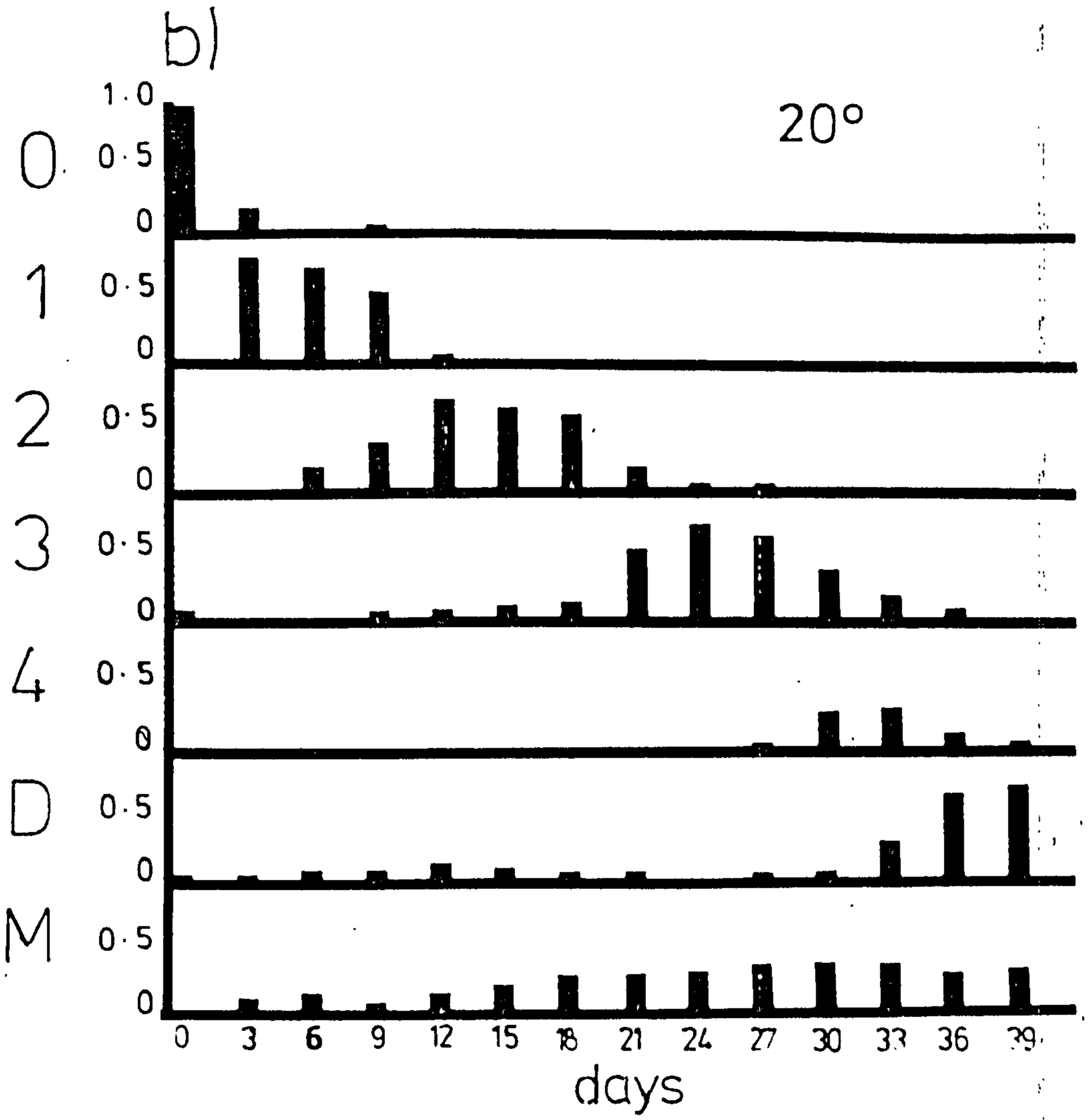
b)
20°
1·0
0·5
0
0
1
2
3
4
D
M
0·5
0 3 6 9 12 15 18 21 24 27 30 33 36 39
days
c)
25°
1·0
0·5
0
0 2 4 6 8 10 12 14 16 18 20 22 24
days

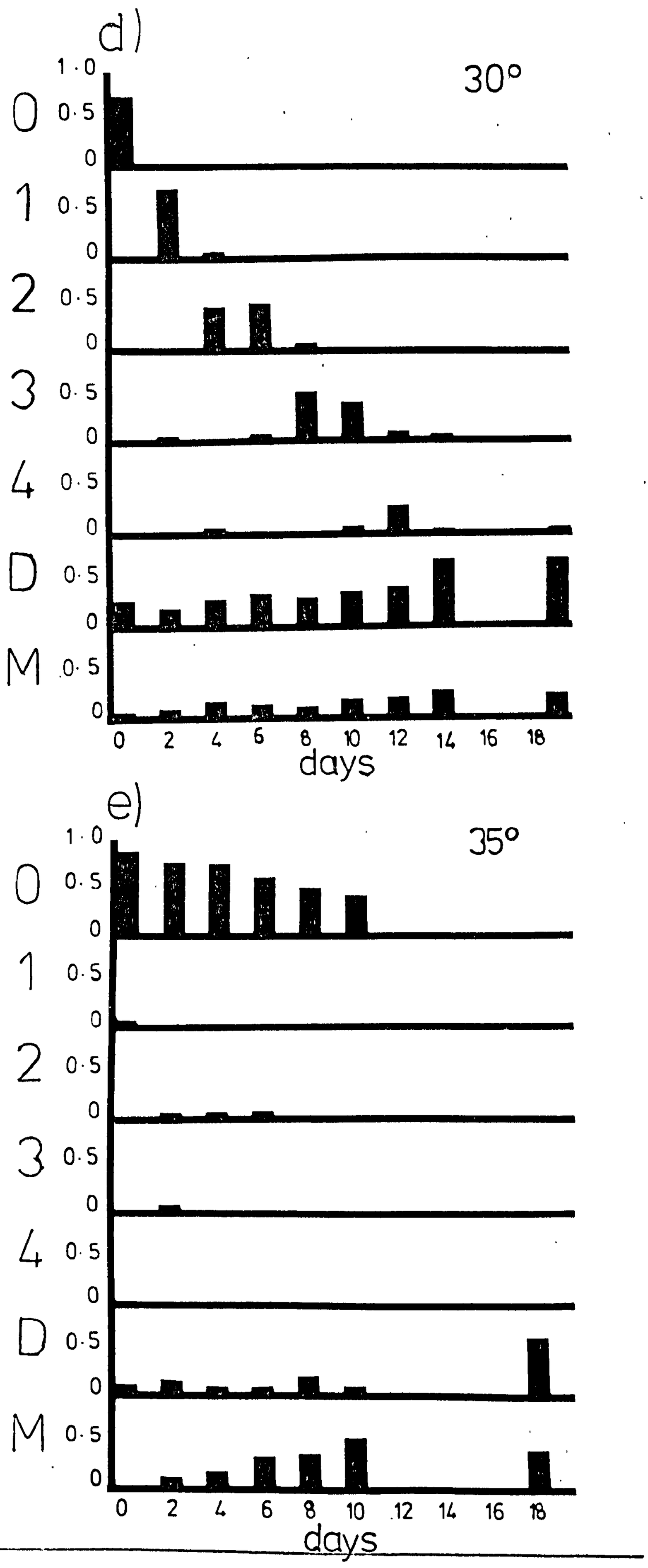
d)
30°
1·0
0·5
0
0
1
2
3
4
D
M
0·5
0
0 2 4 6 8 10 12 14 16 18
days
e)
35°
1·0
0·5
0
0
1
2
3
4
D
M
0·5
0
0 2 4 6 8 10 12 14 16 18
days

the Figures this is represented as a move along the time axis and down to the next developmental stage level. Occasional eggs were found at a much higher stage than the rest of the population (Figures 5.1c and 5.1d). These were assumed to have been at a more advanced stage at the time of collection. These represented a very small proportion of the samples and need not confuse the overall pattern. The grouped histograms give a striking impression of developmental flow from one stage to the next through time.

After the proportion of eggs at developmental stage 4 reached a peak there was an abrupt increase in the proportion of dis-operculate eggs. The timing of this event coincided with the hatching period (Section 6) and suggests that these dis-operculate eggs result from loss of the operculum during miracidial emergence.

At 35°C and 10°C no development was observed. At 15°C hatching was not recorded although this may have been a function of the small proportion of viable eggs available to hatch.

In the egg populations examined over the temperature range 15-30°C there was an increase in the proportion of moribund eggs throughout the developmental period. After the period of hatching had been completed there was very little or no increase in the proportion of moribund eggs present. This may be a natural consequence of the fact that moribund eggs can only arise from the population of developing eggs, presumably as a result of pathological changes in the developing embryo. After the hatching period a negligible number of developing embryos remained and there were, therefore, few eggs capable of contributing to the moribund population and hence the moribund population remained constant.

The relationship between the developing and non-developing populations is best illustrated by examining the relative proportions of the total developing and non-developing populations. The developing population at a given time is the sum of the proportions in all developing stages. The non-developing population is represented separately by the moribund and dis-operculate proportions. The results for the different temperatures are presented as follows: 10°C, Figure 5.2a; 15°C, Figure 5.2b; 20°C, Figure 5.2c; 25°C, Figure 5.2d; 30°C, Figure 5.2e and 35°C, Figure 5.2f.

In interpreting such graphs it should be noted that the numbers of moribund and dis-operculate eggs are cumulative since the proportions were determined by sequential aliquots from a population of eggs.

In considering the behaviour of these populations it is essential to understand how they are interrelated. The maximum developing population was fixed at the time of collection, there can be no subsequent birth process contributing to this egg population. Over any interval of time eggs may move from the developing population. Eggs leaving the developing population may directly join the dis-operculate population, by opercular loss due to damage or hatching, or alternatively may join the moribund population, due to extrinsic or intrinsic lethal effects. Eggs may subsequently leave the moribund population, through opercular loss due to damage, and contribute indirectly to the dis-operculate population. This complex of interactions, with its essentially uni-directional flow, is represented diagrammatically in Figure 5.3.

Figure 5.2: Proportion of eggs developing, moribund and disoperculate with increasing age (see Text). Results shown for temperatures:

a) 10°C, b) 15°C, c) 20°C, d) 25°C,

e) 30°C, f) 35°C.

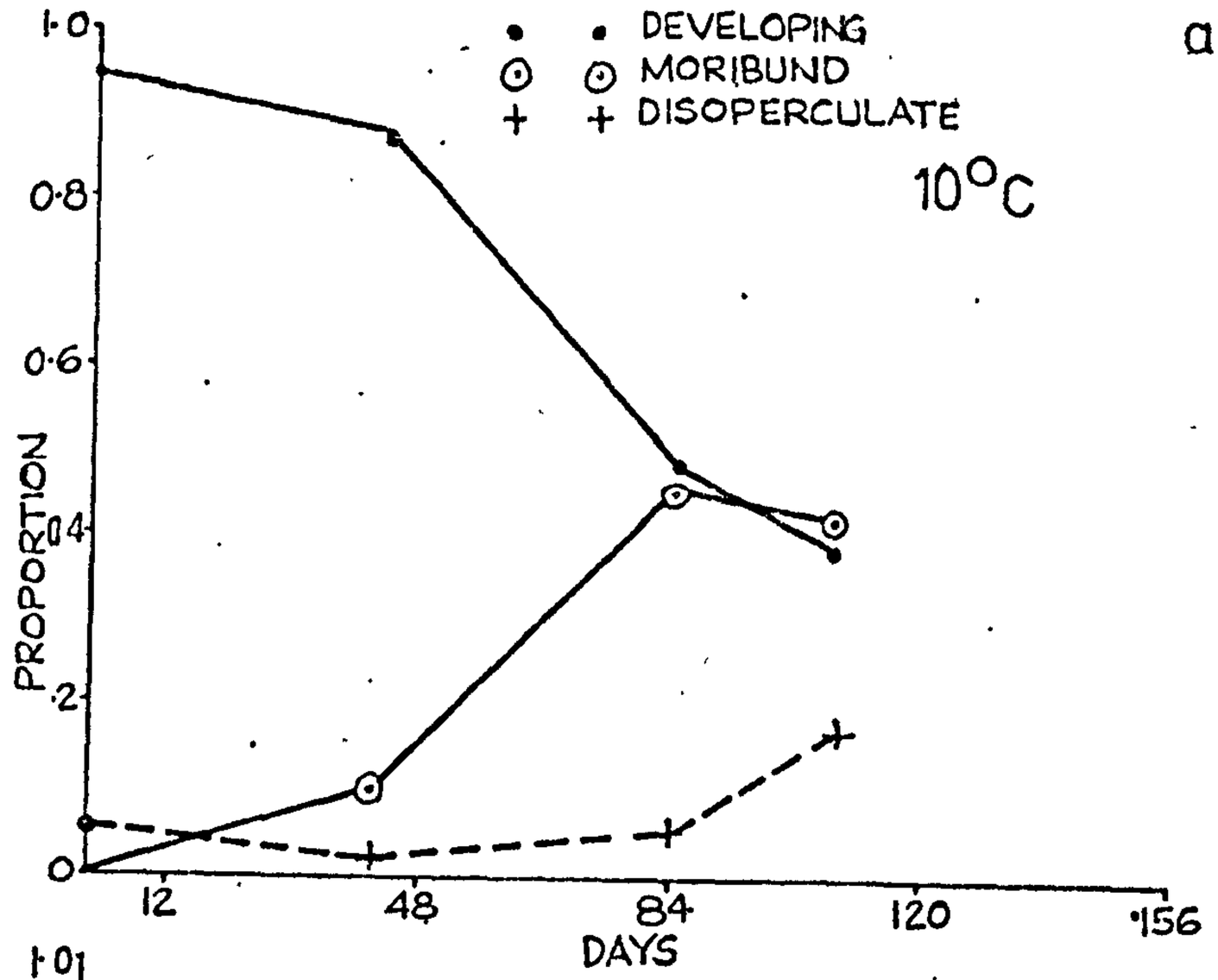
DEVELOPING
MORIBUND
DISOPERCULATE
a)
10°C
1·0
0·8
0·6
0·4
·2
0
PROPORTION
12
48
84
120
156
DAYS

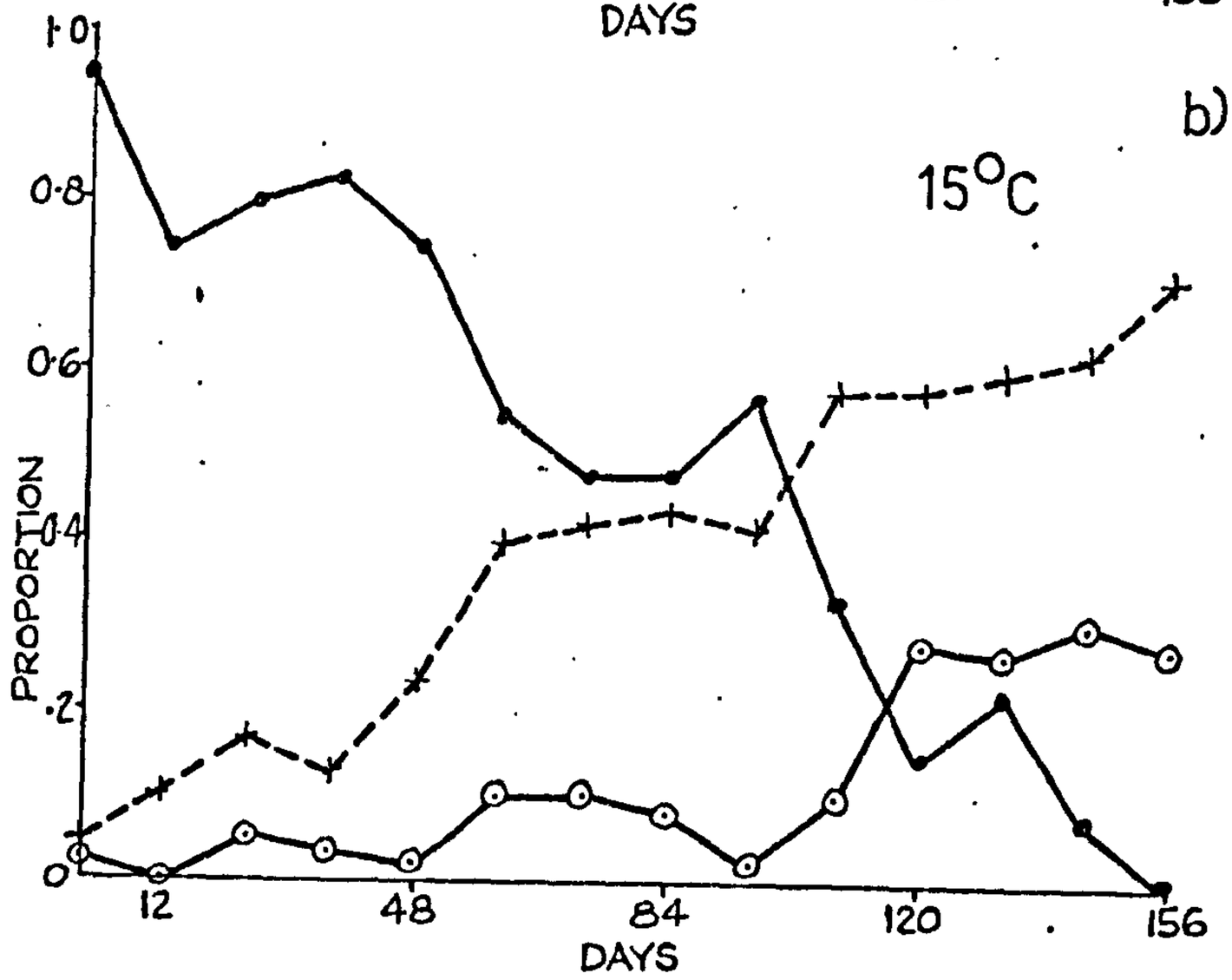
b)
15°C
1·0
0·8
0·6
0·4
·2
0
PROPORTION
12
48
84
120
156
DAYS

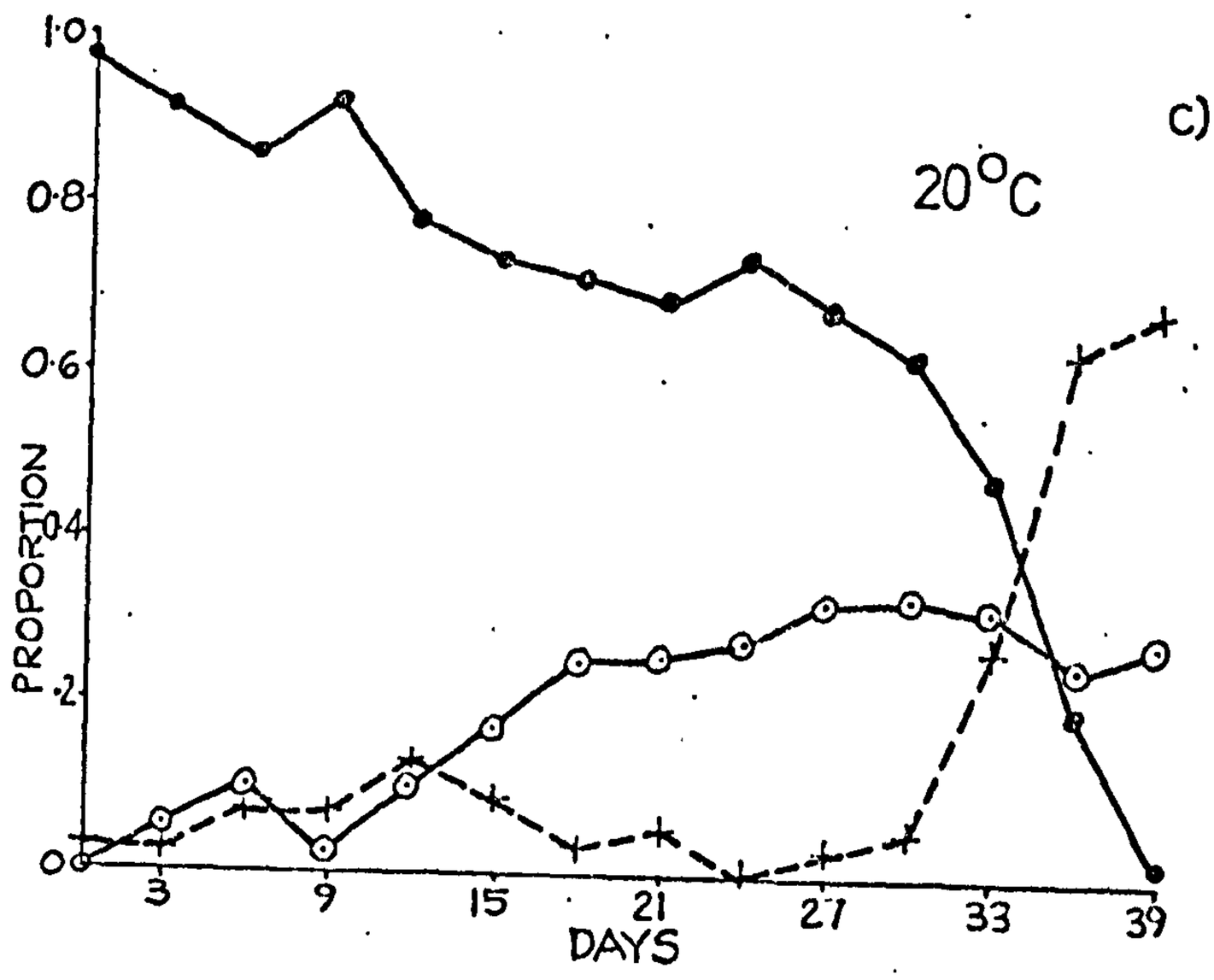
c)
20°C
1·0
0·8
0·6
0·4
·2
0
PROPORTION
3
9
15
21
27
33
39
DAYS

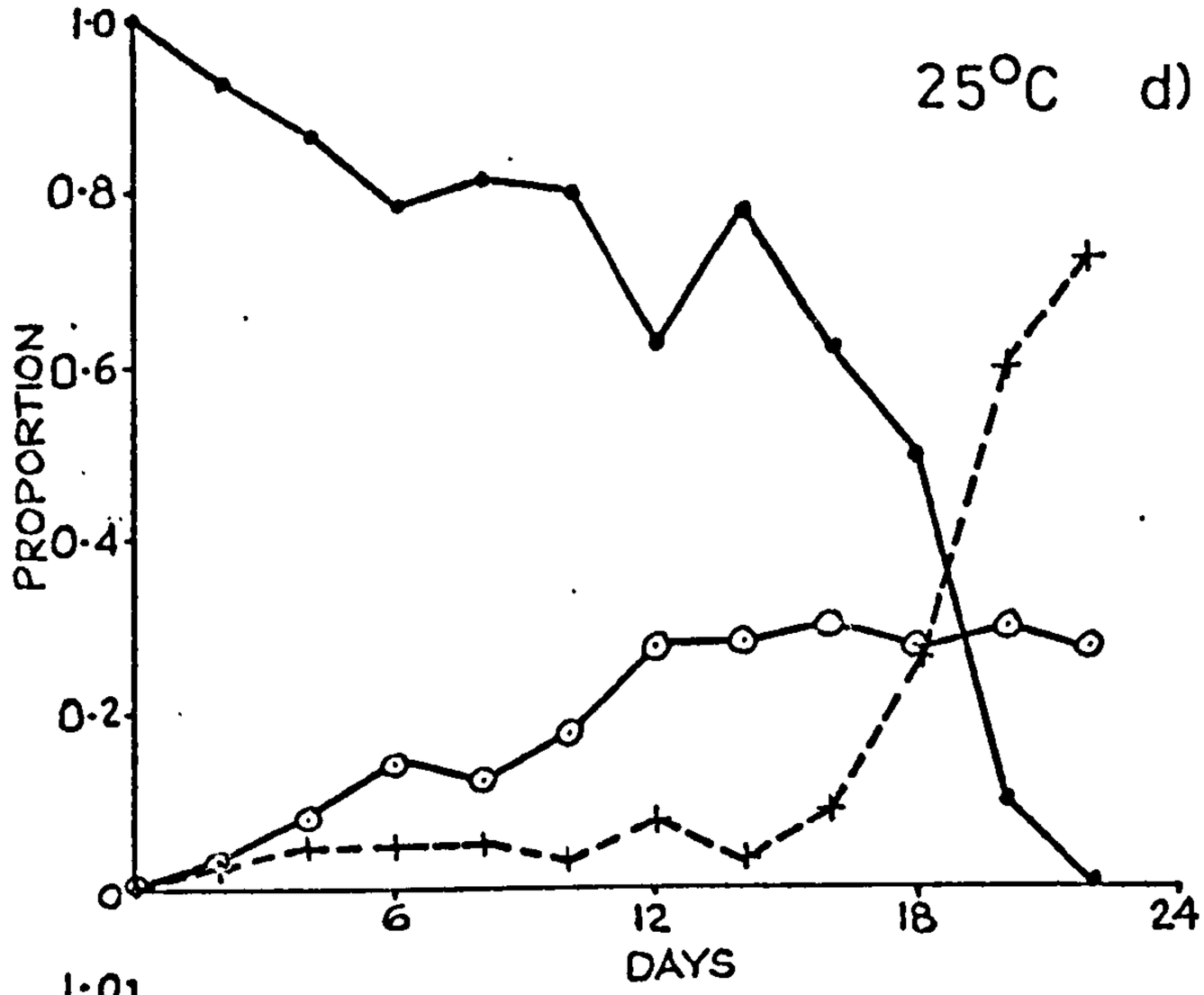
25°C d)
1·0
0·8
0·6
0·4
0·2
0
PROPORTION
6
12
18
24
DAYS

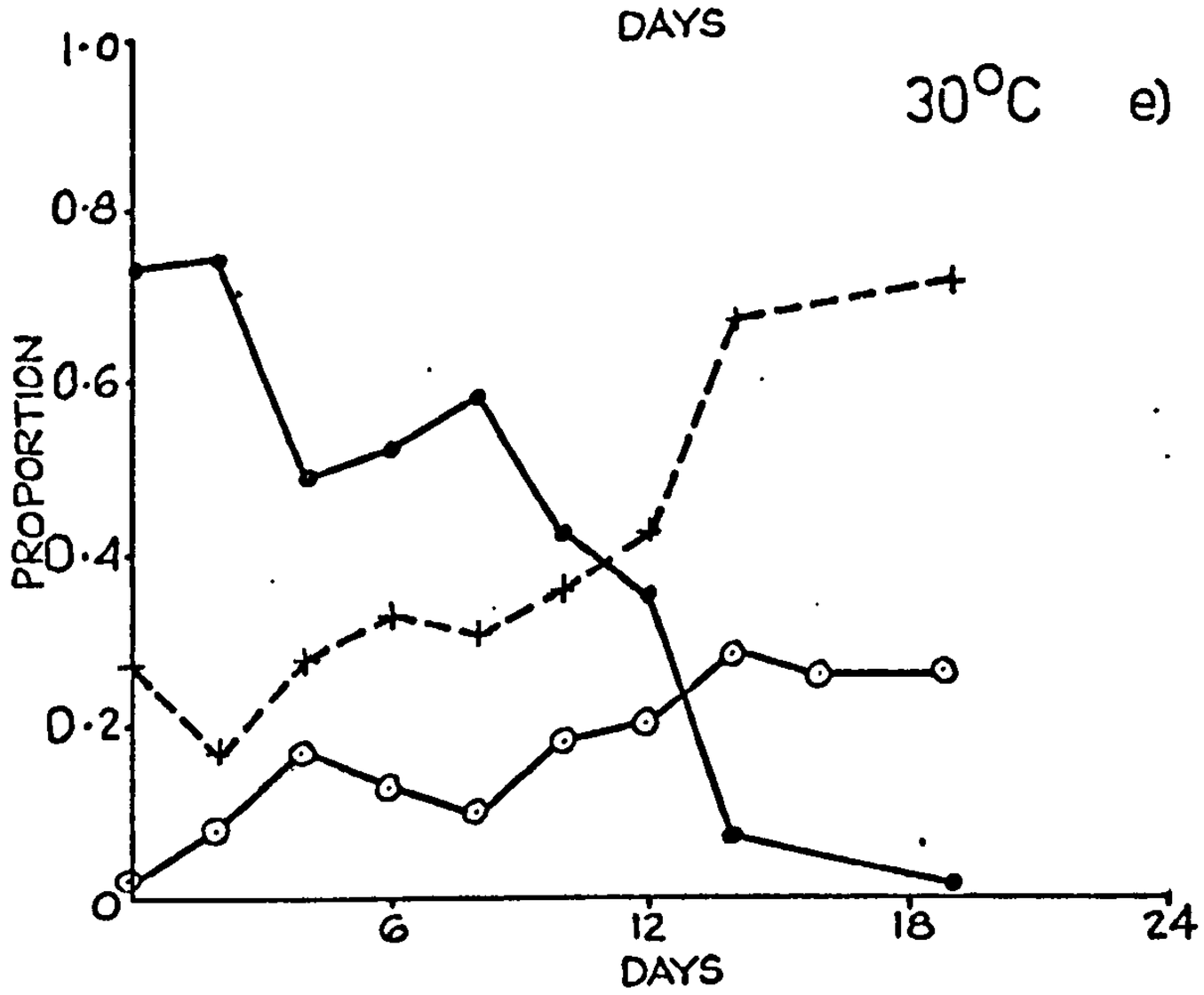
30°C e)
1·0
0·8
0·6
0·4
0·2
0
PROPORTION
6
12
18
24
DAYS

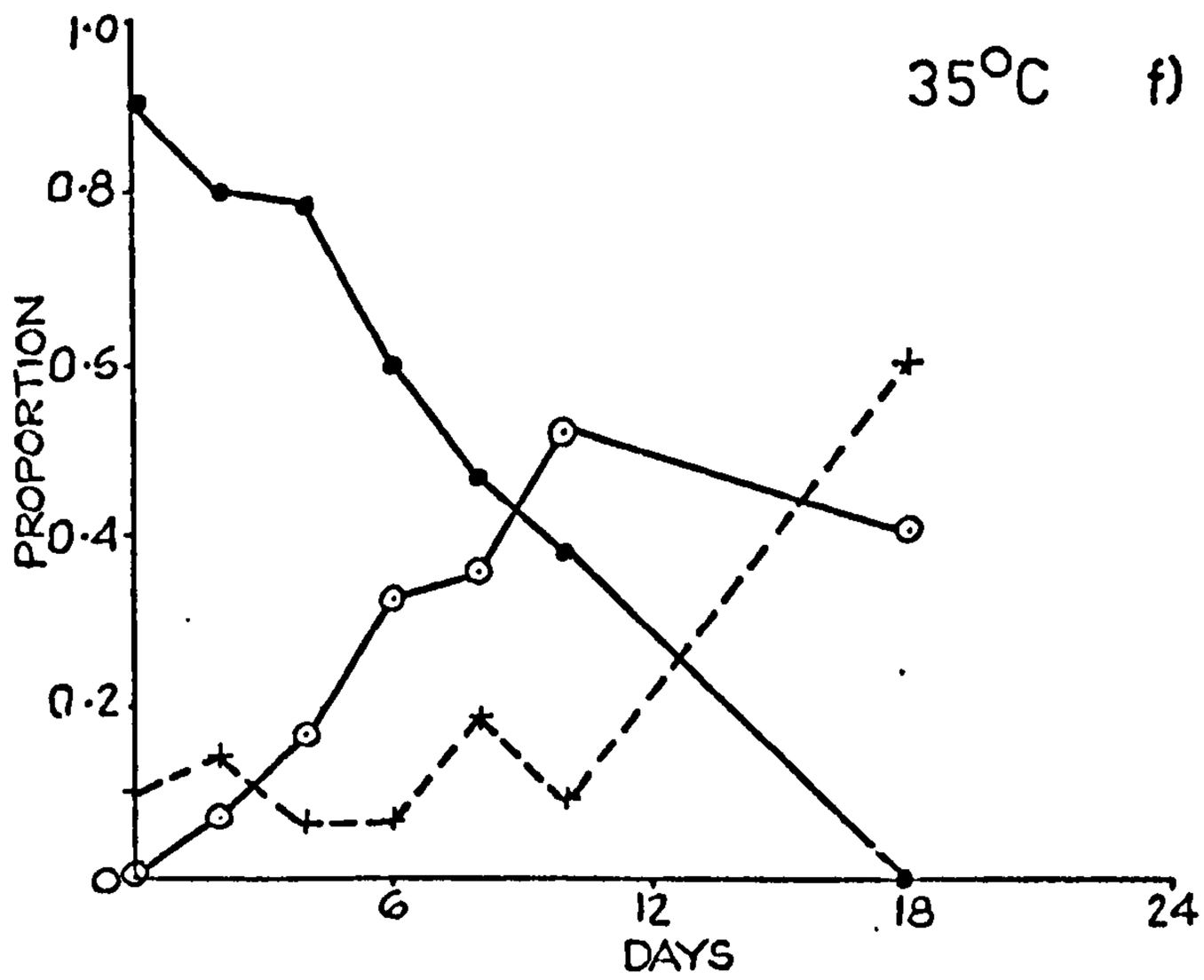
35°C f)
1·0
0·8
0·6
0·5
0·4
0·2
0
PROPORTION
6
12
18
24
DAYS

Figure 5.3: Schematic representation of the possible fates of developing eggs.

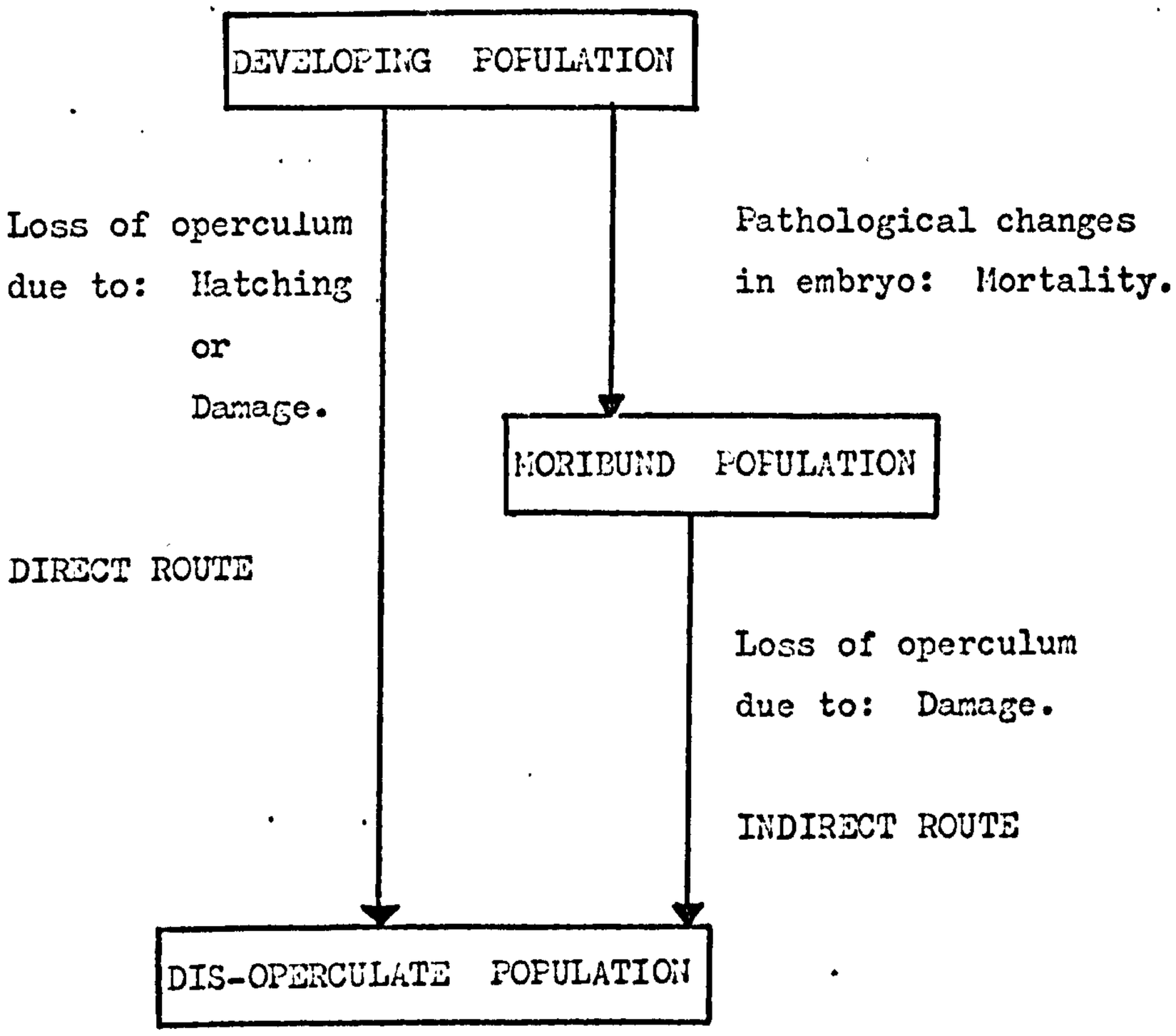
DEVELOPING POPULATION
Loss of operculum due to: Hatching or Damage.
DIRECT ROUTE
Pathological changes in embryo: Mortality.
MORIBUND POPULATION
Loss of operculum due to: Damage.
INDIRECT ROUTE
DIS-OPERCULATE POPULATION

Unfortunately, these interelationships were not quantifiable in the present experimental design. The relative importance of the different routes is unknown and the effect of temperature on the relative importance of these routes is undefined.

Some indication of the effect of temperature on these processes can be obtained by examining the instantaneous rate of loss from the developing populations. This rate was determined using the formula:

$$\mu_t = \ln At_1 - \ln At_2/t_2 - t_1$$

where μ_t = instantaneous rate of loss from the developing population per day per egg

At_1 = proportion of the developing population at time t_1.

At_2 = proportion of the developing population at time t_2.

$t_2 - t_1$ = time interval in days.

Data from the present investigation were treated in this manner and are shown for all temperatures in Appendix 1. Graphical presentation is as follows: 15°C, Figure 5.4a; 20°C, Figure 5.4b; 25°C, Figure 5.4c; 30°C, Figure 5.4d; and 35°C, Figure 5.4e.

The developmental patterns at 20°C and 25°C showed basic similarities (Figure 5.2c and d). In addition the rates of loss from the developing populations were similar at the two temperatures (Figure 5.4b and c). The developing population declined at a low, and approximately constant, rate until the time of hatching. When hatching commenced the rate of loss from the developing population increased considerably. Similarly, the proportion of the dis-operculate population was low and relatively constant until hatching

Figure 5.4: Instantaneous rate of loss per egg per day from the developing egg population (see text).
a) 15°C, b) 20°C, c) 25°C, d) 30°C, e) 35°C.

15°C

a)

20°C

b)

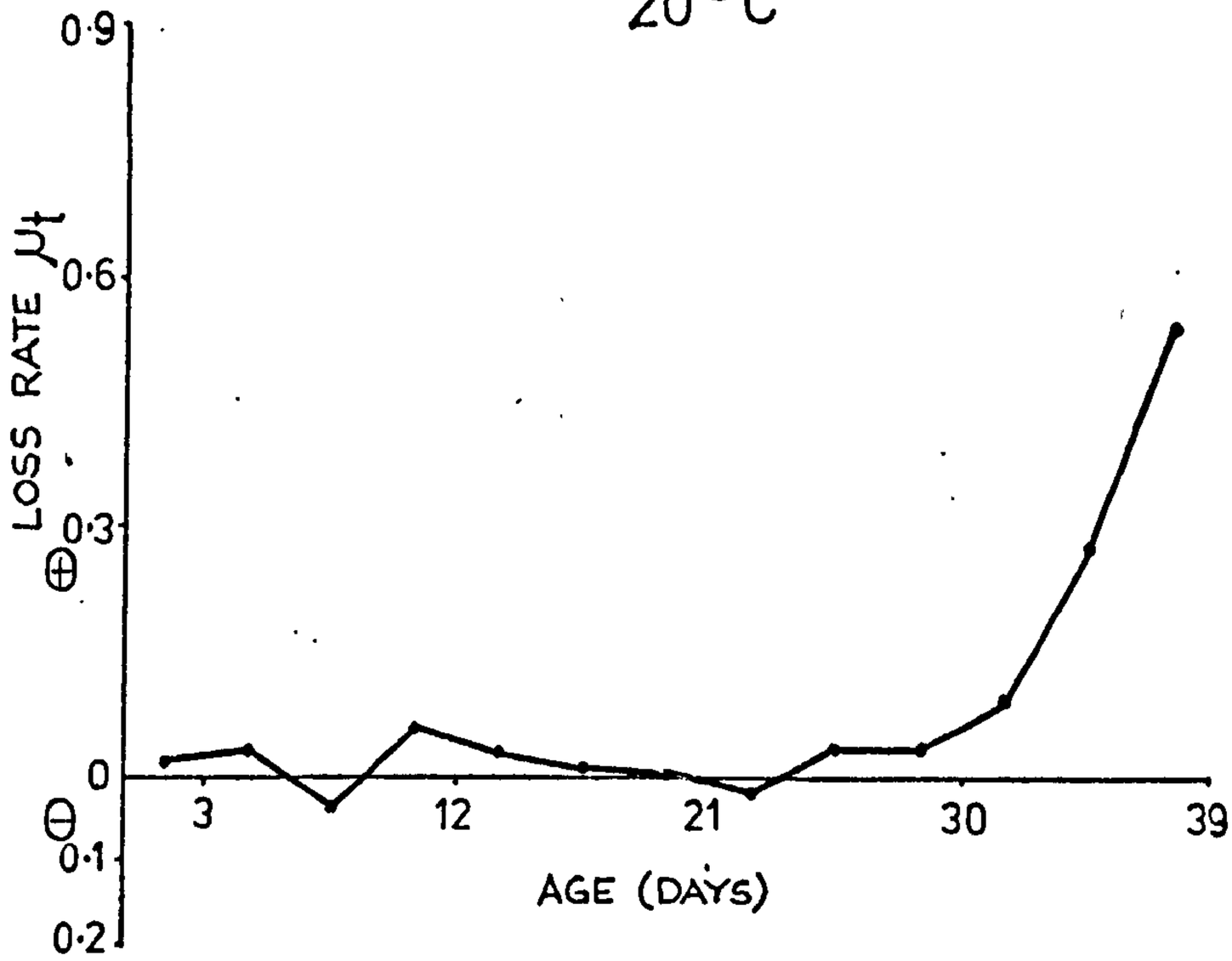

25°C

c)

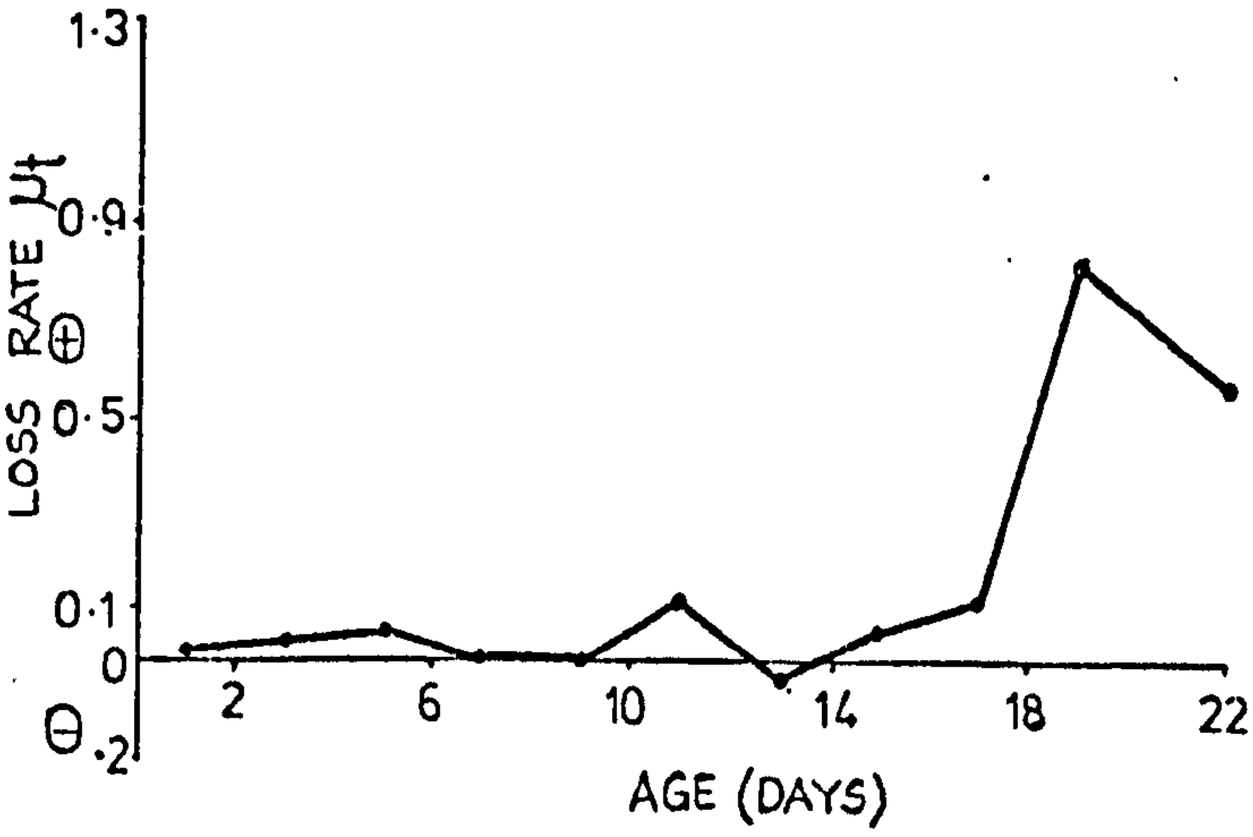

30°C

d)

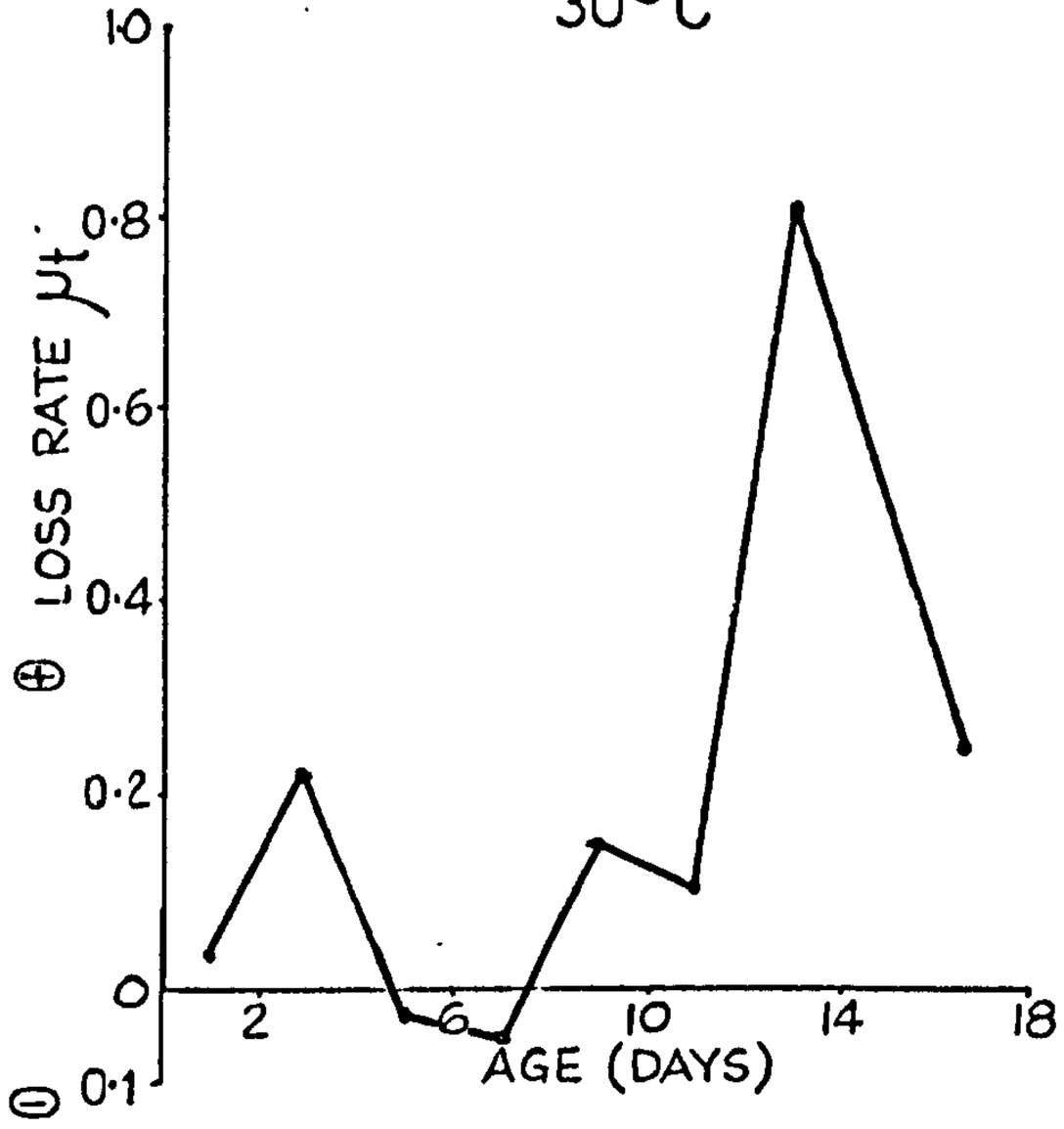
1·0
0·8
0·6
0·4
0·2
0
0·1
⊕ LOSS RATE μ_t
⊖
2
6
10
14
18
AGE (DAYS)

35°C

e)

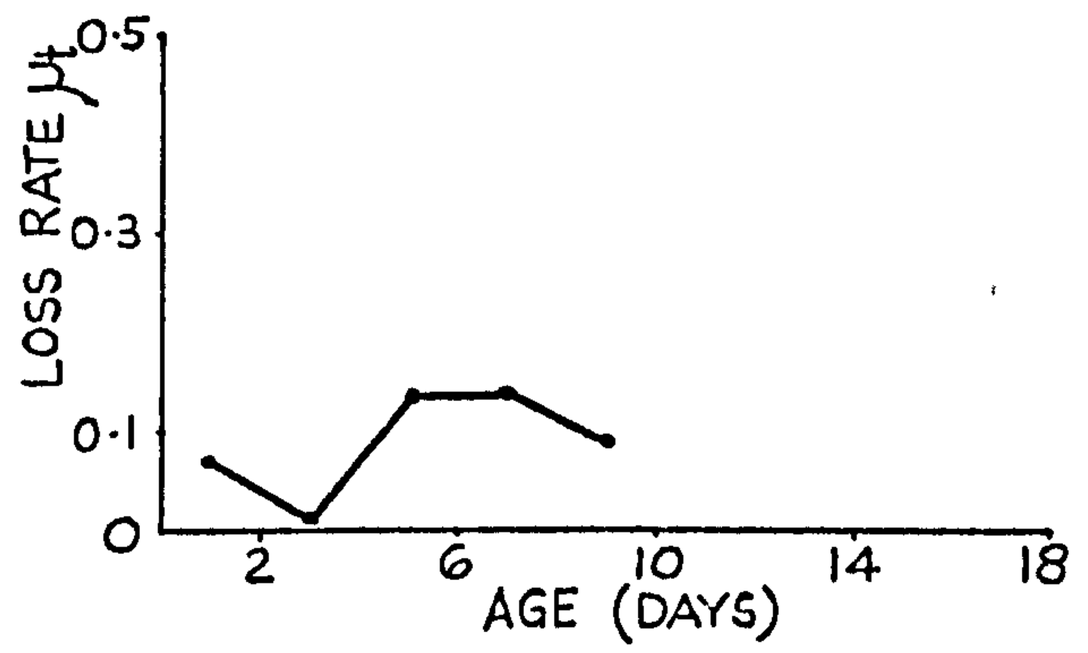
LOSS RATE μ_t
0·5
0·3
0·1
0
2
6
10
14
18
AGE (DAYS)

when an increase occurred. The proportion moribund rose during development but remained constant after the time of hatching.

Inspection of Figure 5.2 c and d indicates that the losses from the developing population resulted in approximately 60% of eggs being viable at the time of hatching. 30% of eggs in the period before hatching becoming moribund and 10% dis-operculate.

At 15°C and 30°C the interelationships between the developing and non-developing populations (Figure 5.2b and e) are superficially very similar at the two temperatures. However, the rates of loss from the developing populations (Figure 5.4a and d) were very different. This serves to illustrate the misleading influence of the differences in time scale. The rate of loss from the developing population was much lower at 15°C than at 30°C but because the former low rate was maintained over a longer period of time the ultimate result was approximately the same at the two temperatures. By the time of hatching only 15-30% of eggs were viable.

Inspection of the increase in proportion of moribund eggs at 15 and 30°C reveals qualitative similarities. As with the proportion of developing eggs, however, this apparent similarity masks what in fact are very different time scales at the two temperatures, the rate of increase in the moribund proportion being much slower at the lower temperature.

Comparison with the results at 20 and 25°C indicates that the proportion of dis-operculate eggs is larger at 15 and 30°C. This result suggests that at these latter two temperatures a greater proportion of eggs suffer opercular loss, although it is not apparent whether these eggs arise from the developing or moribund populations.

At 30°C the time of hatching coincided with a sudden increase in the rate of loss from the developing population (Figure 5.2e). This is assumed to be a consequence of hatching, and resultant opercular loss, of stage 4 eggs. At 15°C no such increase occurred (Figure 5.2b), nor was hatching observed. This may have been a consequence of the very small size of the viable developed population (about 15%) or some inhibition of the hatching process due to the low temperature.

At 35°C no development was observed (Figure 5.1e). The supposed "developing population" in fact consisted of eggs apparently at a normal Stage 0 which were assumed capable of development. The rate of loss from this "developing population" was higher than that recorded at 20 and 25°C (Figure 5.4e). The relationship between this "developing population" and the non-developing population was of a form unique to this temperature (Figure 5.2f). Mortality was apparently high, the moribund proportion increasing to levels not observed at other temperatures. The dis-operculate proportion was initially low but became larger than the moribund proportion when the developing proportion was negligible. This relationship can only be explained by indirect contribution to the dis-operculate population via the moribund population.

The results at 10°C were incomplete due to the greatly extended time scale at this temperature. Development did not occur (Table 5.1) and the rate of loss from the developing population was very low (Appendix 1).

The data obtained in these analyses were used to examine some aspects of the effects of temperature on the rate and period of

development.

The developmental period of each of the five developmental stages (0-4) at each of the experimental temperatures was determined by calculating the mid-stage point. This is the point in time post collection at which the proportion of eggs already recorded in a particular stage is equal to the subsequent proportion of eggs passing through that stage. It may also be expressed as the median, the point in the frequency distribution of eggs at a developmental stage where the area enclosed on either side of the point is the same.

The mid-stage point was determined in the same way as the median of a distribution. For any of the developmental stages at a given temperature there is a distribution of proportions of eggs at that stage, the proportions changing with age P.C. (Figure 5.1). For each stage considered these proportions were summed to give an index of the total number of eggs which passed through a particular developmental stage. By summing the proportions sequentially along the time axis the age P.C. at which half the total was achieved could be determined. This point in time P.C. was taken to be the mid-stage point of all eggs at that stage.

Table 5.2 shows the age P.C. at mid-stage for all five developmental stages at each experimental temperature.

Figure 5.5 illustrates the effect of temperature on the mid-stage points for stages 1 and 4. The intermediate stages 2 and 3 would complete this family of curves, lying between the two extremes. The experimental points were fitted with exponential curves by a linearizing least squares method using the model $y = ae^{bx}$. The parameters generated by the family of curves are given in Table 5.3.

Figure 5.5: Effect of temperature on the period required to attain the mid-stage points for Developmental Stages 1 and 4 (see text).

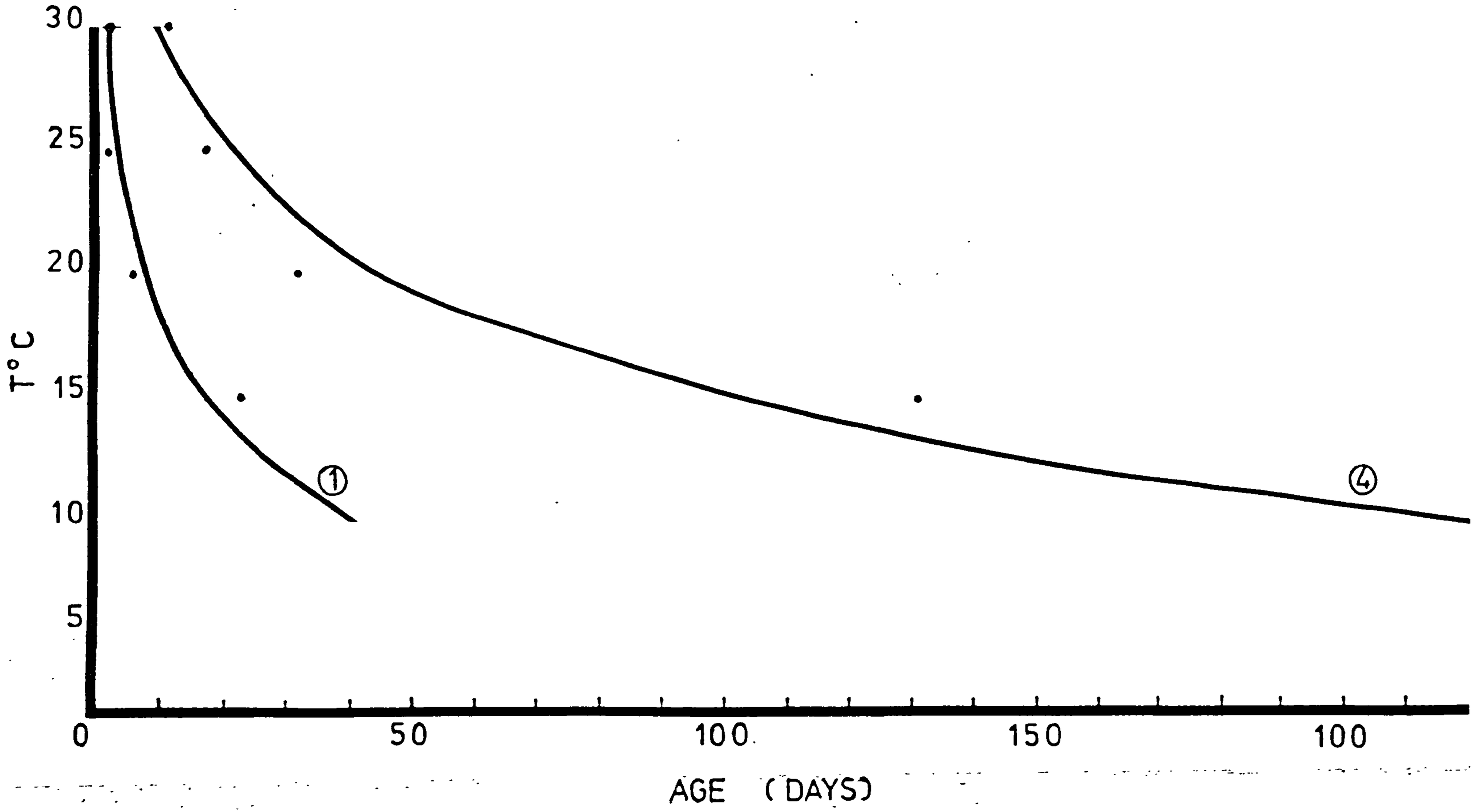
30
25
20
15
10
5
T°C
0
50
100
150
100
AGE (DAYS)
①
④

TABLE 5.2 Age in days of eggs at mid-stage of developmental stages 0-4 for the temperature range 10-35°C

TEMPERATURE °C	AGE (DAYS) AT MID-STAGE				
	0	1	2	3	4
35	0	-	-	-	-
30	0	2	6	8	12
25	0	2	6	12	18
20	0	6	15	24	33
15	0	24	60	108	132
10	0	-	-	-	-

TABLE 5.3 Parameters of the exponential model fitted to time to mid-stage against temperature experimental data for developmental stages 1, 2, 3 and 4 (see text)

STAGE	MODEL PARAMETERS		
	a	b	r^2
1	229.99	-0.171	0.877
2	428.27	-0.151	0.901
3	848.29	-0.160	0.930
4	1041.66	-0.160	0.922

These results indicate that the period of egg development is temperature dependent over the range 15-30°C.

The exponential model was employed because of its close correlation with the experimental data (Table 5.3) rather than any assumed biological validity. As discussed in Section 5.4 the effect of temperature on the development of organisms is highly complex since temperature influences the development of different components of the organism in different ways. No simple model can hope to adequately describe thermal relationships but empirically fitting a curve to the experimental data does provide a general, if arbitrary, conceptual framework within which different sets of data can be compared.

The close similarity of the b parameter (Table 5.3) describing the gradient of these curves suggests that the effect of temperature was the same for all stages. This effect can be examined by determining the relative temporal proportions of the developmental stages, that is by expressing the time to mid-stage point of developmental stages 1, 2 and 3 as a proportion of the time to mid-stage point of developmental stage 4 (Table 5.4). The proportions of the overall development period occupied by the developmental stages are similar over the range 15-30°C.

These results indicate that the proportion of time spent in attaining any given developmental stage expressed as a proportion of the total development period is independent of temperature over the range 15-30°C.

The process of development may also be described in terms of rates rather than periods. The rate is simply the reciprocal of the period and represents the proportion of the developmental period

TABLE 5.4

Proportion of developmental period, relative to age at mid-point of stage 4, spent in attaining the mid-point of stages 0, 1, 2 and 3. Examined over the temperature range 15-30°C.

TEMPERATURE °C	PROPORTION OF DEVELOPMENT PERIOD			
	0	1	2	3
30	0	0.16	0.50	0.67
25	0	0.11	0.33	0.67
20	0	0.18	0.45	0.73
15	0	0.18	0.45	0.82

which occurs per day. Figure 5.6a and Table 5.5 show the relationship between development rate and temperature for the eggs of T. patialense attaining stage 4. The linear regression curve fitted to the experimental points only approximates to the real form of the rate curve (Section 5.4). The intercept on the x-axis predicts the temperature at which no development occurs - the developmental zero or critical temperature. For T. patialense eggs under the present experimental conditions this was 13.75°C.

A quantity termed the "thermal constant" can be determined by taking the reciprocal of the slope of the rate curve. The thermal constant is a characteristic of the effect of temperature on development, relating the development period to the temperature above the developmental zero. In practice this allows estimation of the developmental period for any given temperature using the formula:

$$P_t = \mu / t - t_o$$

Figure 5.6:

a) The effect of temperature on the egg development rate (per egg per day) of four digenean species. Experimental data points fitted with linear regression curves.

b) Variation with temperature of the thermal constant (day degrees) of egg development for four digenean species.

Sources of experimental data:

Strigea tarda (Mathias, 1925;

Fasciola hepatica (Rowcliffe and Ollerenshaw, 1961);

Posthodiplostomum cuticola (Donges, 1964);

Transversotrema patialense (Present study).

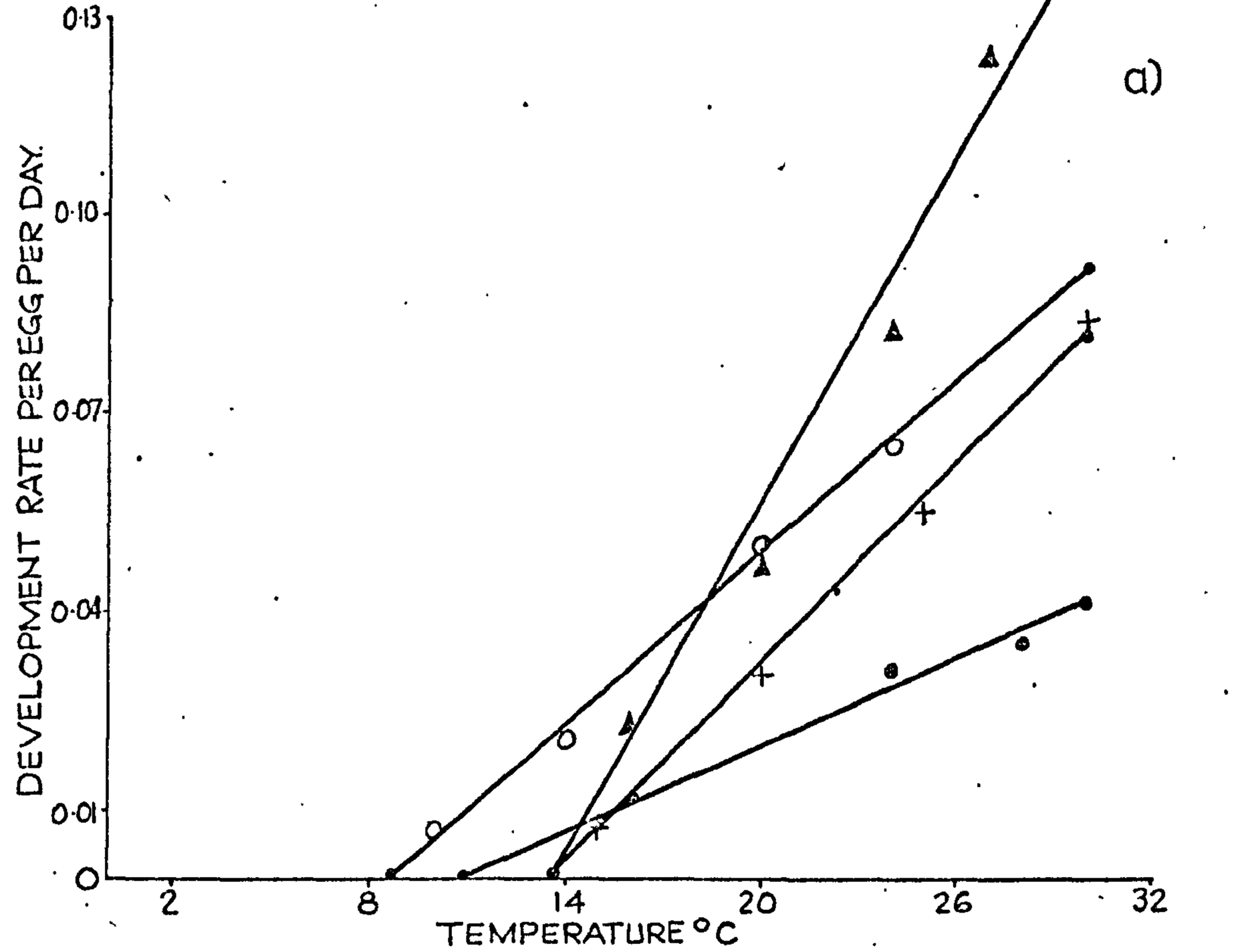
a)
0·13
0·10
0·07
0·04
0·01
0
DEVELOPMENT RATE PER EGG PER DAY.
2
8
14
20
26
32
TEMPERATURE °C
▲ STRIGEA TARDA
o POSTHODIPLOSTOMUM CUTICOLA
+ TRANSVERSOTREMA PATIALENSE
o FASCIOLA HEPATICA

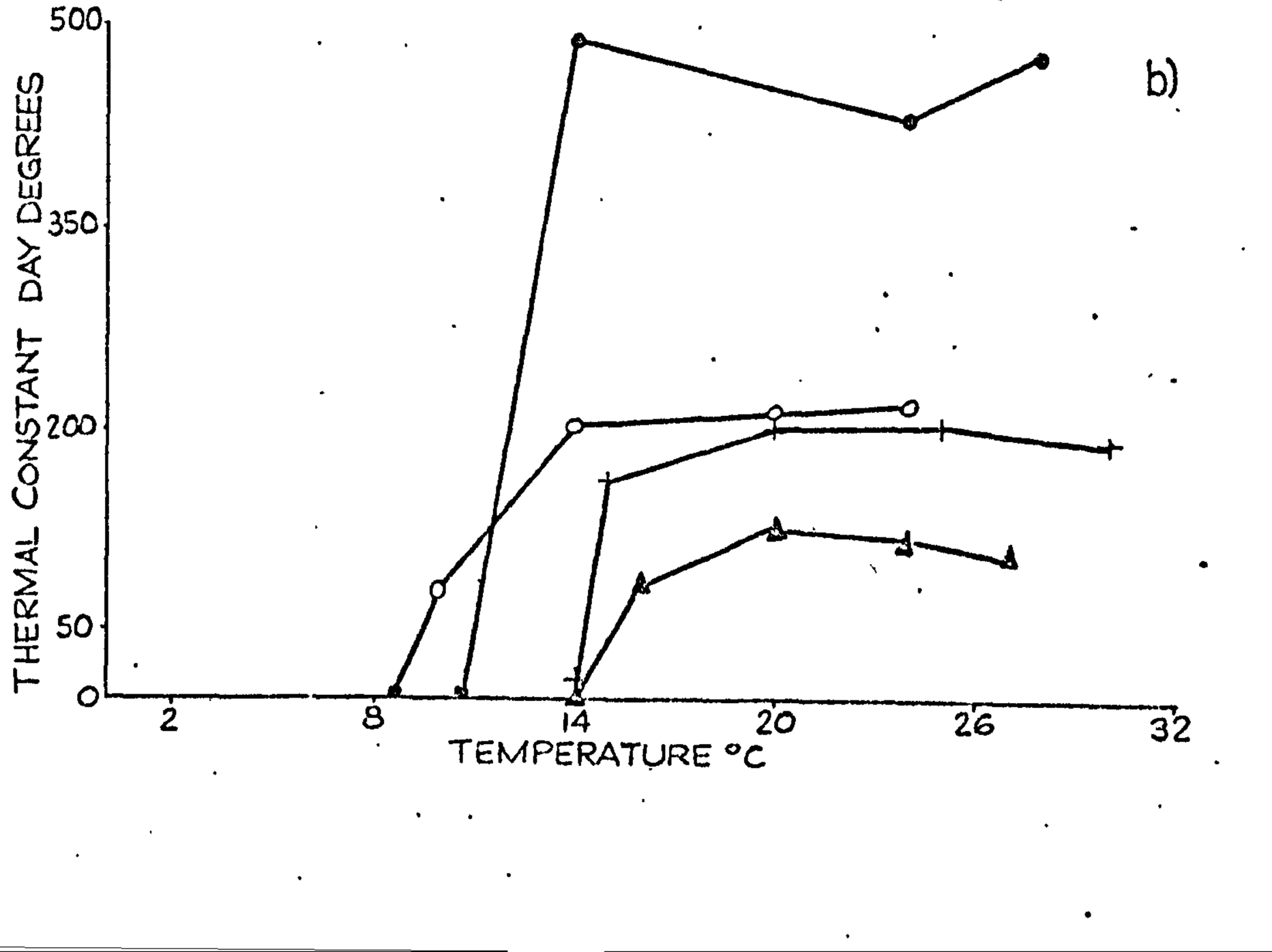
b)
500
350
200
50
0
DAY DEGREES
THERMAL CONSTANT
2
8
14
20
26
32
TEMPERATURE °C

Where P_t = period of development in days at temperature t; μ = thermal constant in day degrees; and t_o = developmental zero temperature in degrees. The formula only applies where $t_o \leqslant t <$ the upper lethal limit.

For eggs of T. patialense under the present conditions the thermal constant is 198 day degrees.

Alternatively, values of the thermal constant may be determined directly from the experimental data for each experimental temperature using the formula: $\mu_t = P_t(t-t_o)$. In which case the theraml constant μ_t has a specific value for each temperature t. Figure 5.6b and Table 5.5 indicate the changing values of the thermal constant in day degrees at the experimental temperatures for the developing eggs of T. patialense. The reasons for the variability with respect to temperature of this "constant" are discussed in Section 5.4.

Figure 5.7a shows the relationship between temperature and the Q_{10} of the development rate of the eggs of T. patialense. This parameter was obtained using the formula:

$$Q_{10} = (k_1/k_2)^{10/(t_1-t_2)}$$

where k_1 = development rate at temperature $t_1{}^oC$ and k_2 = development rate at temperature $t_2{}^oC$.

The significance of this parameter is discussed in Section 5.4.

5.3.2 Effect of storage at 10°C on subsequent egg viability at 25°C

Eggs transferred to 25°C after incubation at 10°C became invested with a bacterial film. This superficial layer impaired

Figure 5.7:

a) Variation with temperature of the Q_{10} of egg development for four digenean species.

b) Effect of temperature on the period of development (days) to a mature miracidium for four digenean species.

Sources of experimental data:

Strigea tarda (Mathias, 1925);

Fasciola hepatica (Rowcliffe and Ollerenshaw, 1961);

Posthodiplostomum cuticola (Donges, 1964);

Transversotrema patialense (Present study).

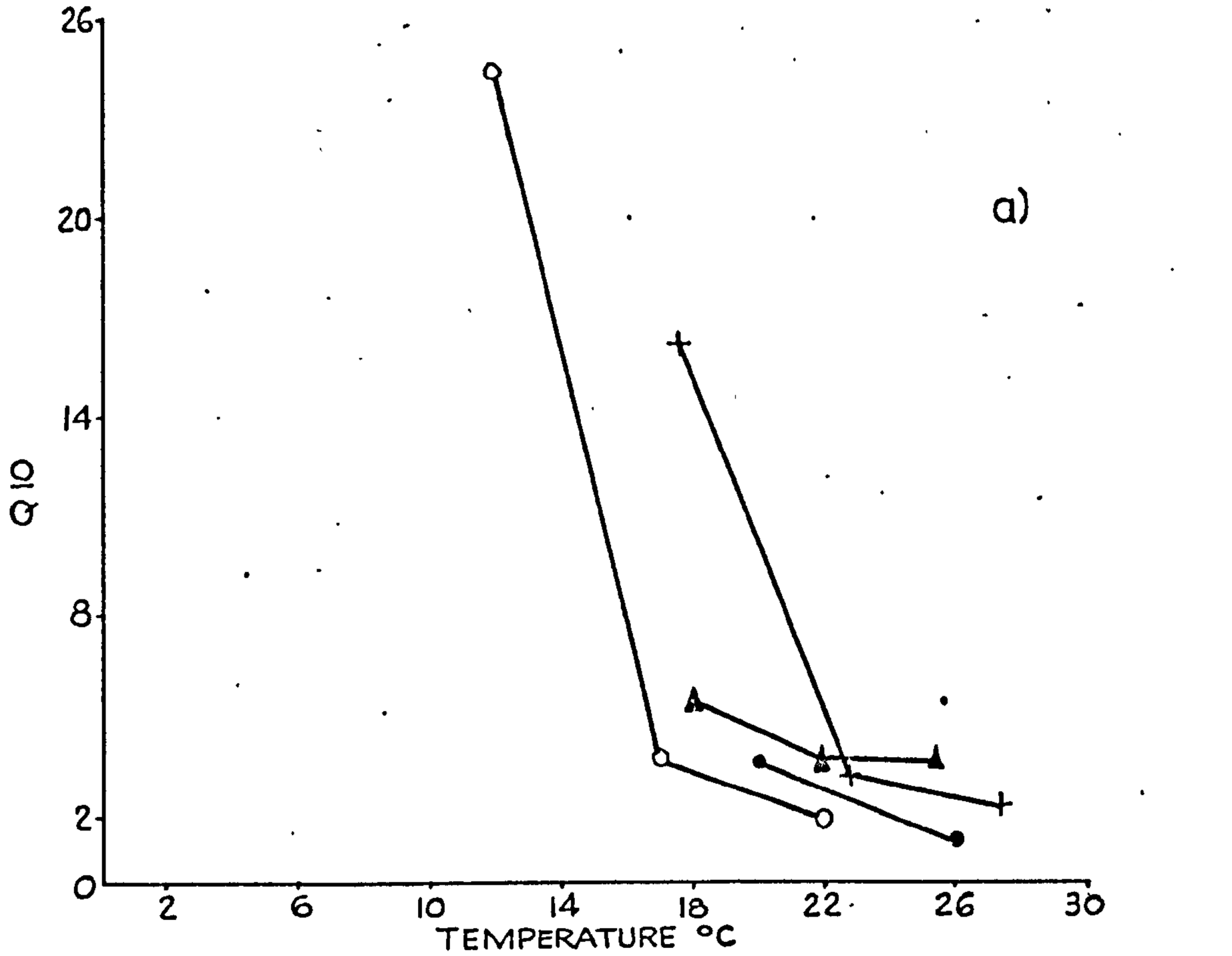
26
20
14
8
2
0
2
6
10
14
18
22
26
30
TEMPERATURE °C
a)
STRIGEA TARDA
POSTHODIPLOSTOMUM CUTICOLA
TRANSVERSOTREMA PATIALENSE
FASCIOLA HEPATICA

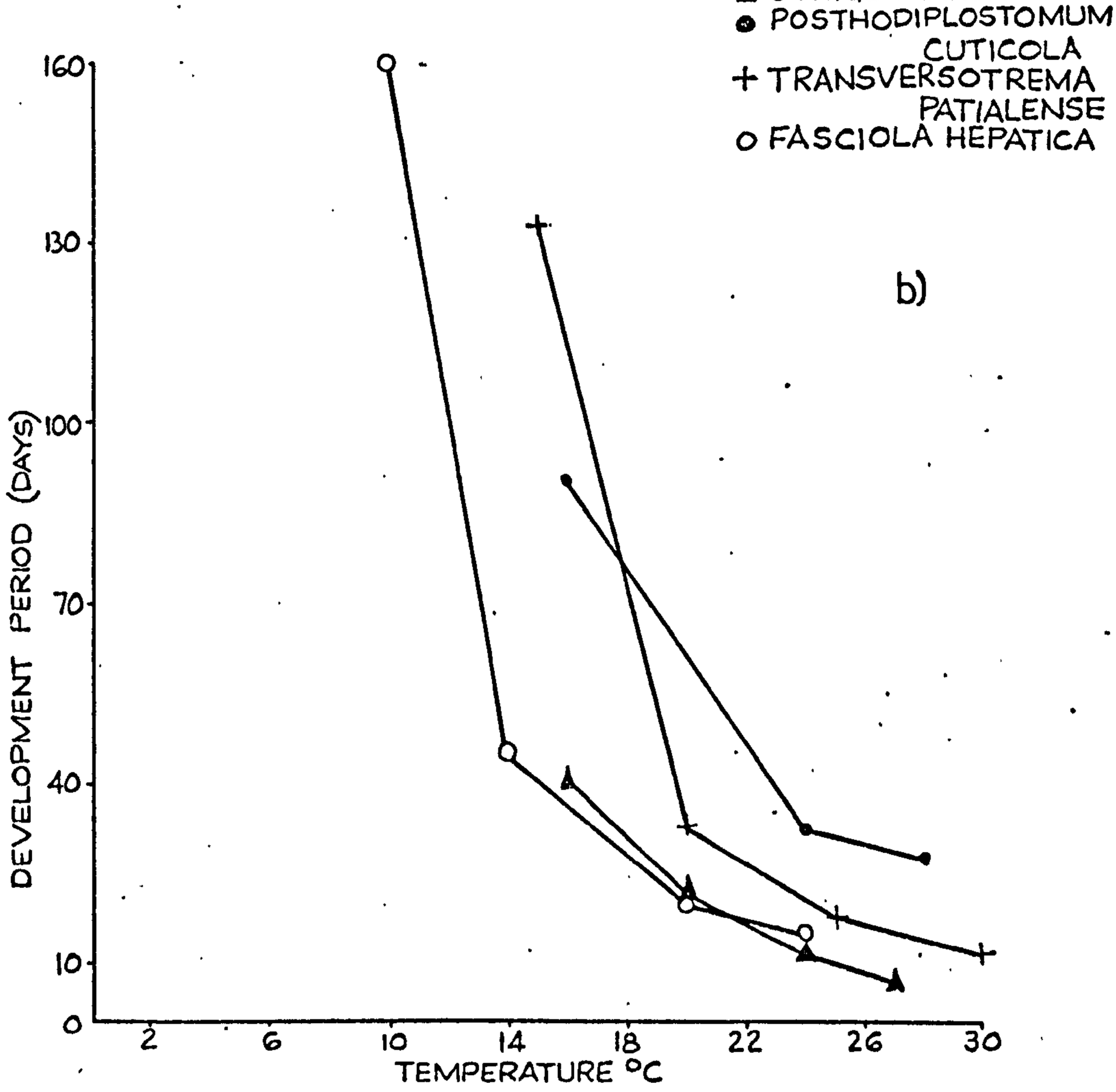
160
130
100
70
40
10
0
DEVELOPMENT PERIOD (DAYS)
2
6
10
14
18
22
26
30
TEMPERATURE °C
b)

TABLE 5.5

The effect of temperature on egg development

TEMPERATURE °C	PARAMETERS OF EGG DEVELOPMENT			
	PERIOD TO MID-STAGE 4 (DAYS)	RATE (PER EGG PER DAY)	THERMAL CONSTANT (DAY DEGREES)	Q10
30	12	0.0833	195.0	
				2.25
25	18	0.0555	202.5	
				3.35
20	33	0.0333	206.2	
				16.02
15	132	0.0076	165.0	

Parameters of linear regression model of development rate against temperature:

$a = -0.06945$

$b = 0.00505$

$r^2 = 0.99800$

developmental zero = 13.75

observation of egg contents and so prevented random sampling of developmental state. On this basis quantitative analyses of the type described above were inapplicable and hence the results were described qualitatively.

The eggs transferred to 25°C after 4 weeks at 10°C developed in an apparently normal manner. Miracidial embryos with pigmented ocelli were present in the culture. Transfer after 12 weeks at 10°C did not induce observable development. In no instance was an embryo or vitelline rind observed.

5.3.3 Effect of illumination period on egg development

Table 5.6 shows the mean proportions, from three replicates of 20 eggs each, of eggs developing at day 14 P.C. under three light regimes (12/12h D/L, L/L and D/D) at 25°C.

The period of illumination does not appear to significantly effect the rate of development or the viability of the eggs.

TABLE 5.6

Proportional development under different light regimes at 25°C. Eggs examined on day 14 P.C.

LIGHT REGIME	PROPORTION						
(12/12h)	0	1	2	3	4	D	M
D/D	0	0	0.05	0.65	0	0.05	0.25
D/L	0	0	0.05	0.58	0.05	0.03	0.29
L/L	0	0	0.02	0.53	0.07	0.05	0.33

5.4 Discussion

The results presented here indicate that the rate, and hence period, of development of the eggs of T. patialense is temperature dependent over the range 15-30°C. Temperature dependency is demonstrable for other digenean species. Published data on three other species, namely Strigea tarda (Mathias, 1925), Fasciola hepatica (Rowcliffe and Ollerenshaw, 1961), Posthodiplostomum cuticola (Donges, 1964), were analysed in the same way as for T. patialense (Figures 5.6a and 5.7b, and Table 5.7).

The effect of temperature on simple chemical reactions can be described using the Van t'Hoff and Arrhenius equations. The underlying principle is the same for both these approaches and describes the temperature dependent formation of activation complexes. For many reactions the Q_{10} (Van t'Hoff) and thermal increment (Arrhenius) have a constant linear relationship with the reaction rate with respect to temperature (Johnson, Eyring and Polissar, 1954). In many biological processes, however, the relationship exhibits asymmetric change with temperature (Crozier, 1924; Prosser, 1973). Figure 5.7a illustrates how Q_{10} alters with temperature for egg development in four digenean species.

The problem in applying physico-chemical reaction equations to biological processes arises from the complexity of the latter. Many different reactions are involved in a process such as egg development and each of these may exhibit different thermal responses. Furthermore the effect of temperature on physical factors such as viscosity and diffusion rates may be of more significance to the efficiency of the biological process than any temperature induced change in

TABLE 5.7

Effect of temperature on egg development for three digenean species

SPECIES (SOURCE)	TEMPERATURE (°C)	DEVELOPMENTAL ZERO (°C)	RATE (PER EGG PER DAY)	PERIOD (DAYS)	THERMAL CONSTANT (DAY DEGREES)	Q10
Fasciola hepatica (Rowcliffe and Ollernshaw, 1961)	24		0.0667	15	217.5	
	20		0.0500	20	210.0	2.05
	14		0.0222	45	202.5	3.87
	10		0.0062	160	80.0	24.26
		8.70				
Posthodiplostomum cuticola (Donges, 1964)	28		0.0364	27.5	479.7	
	24		0.0312	32	430.2	1.47
	16		0.0111	90	490.0	3.64
		10.56				
Strigea tarda (Mathias, 1925)	27		0.1250	8	105.1	
	24		0.0833	12	121.7	3.87
	20		0.0488	20.5	125.9	3.81
	16		0.0250	40	85.6	5.32
		13.86				

biochemical reaction rates. In general, therefore, values of Q_{10} and thermal increment are of limited use in aiding understanding of the thermal dependence of biological processes, and in the present context can only be usefully applied to developmental processes over a restricted temperature range.

Dubois (1929) suggested that the development of digenean eggs exhibits thermal relationship of the form predicted by the Van t'Hoff and Arrhenius equations. The present results suggest that this is only true over a limited temperature range.

Because of the difficulty of adequately describing the thermal relationships of biological processes the emphasis has moved away from the physico-chemical approach and towards the use of empirical descriptors with practical applications. The basis of this approach is the modelling of the thermal reaction rate curve. Techniques have been proposed for empirical models based on log-linearisation, the catenary curve and the logistic curve (Davidson, 1944). The equations of these curves, in conjunction with experimentally derived parameters, may be used to estimate the development rate at a given temperature.

These techniques have their relative advantages and disadvantages but all suffer from a necessary complexity which makes their use cumbersome. Further, they presuppose an accuracy of rate determination which is rarely achieved in the study of biological systems. For most biological purposes the simple thermal constant provides an adequate approximation (Varley, Gradwell and Hassel, 1973).

The thermal constant is the reciprocal of the slope of a thermal reaction rate curve. Figure 5.6a shows the effect of temperature on the rate of egg development, with linear regression models fitted to the data, for four species of digeneans. It is from such curves that the thermal constant is derived.

The approximate nature of the thermal constant may be readily demonstrated. Figure 5.6b shows the temperature dependency of individual values of the thermal constant derived for each temperature (see Section 5.3). The thermal constant remains constant for most of the temperature range but markedly decreases at low temperatures. This is a consequence of the linearising assumption of the equation, that is, that the development rates change in linear manner with temperature. In fact because this relationship is exponential rather than hyperbolic the reciprocal is sigmoid rather than linear and hence departs from the linear model at extremes of the range. Note that this departure from linearity may be exacerbated by adaptive physiological changes at temperature extremes as discussed below.

Despite these drawbacks the thermal constant has proved an extremely useful first approximation to the thermal relationships of development in poikilotherms. It has been successfully used in predicting climatic effects on the development of invertebrate populations (Shelford, 1927; Ollerenshaw, 1971; Nice and Wilson, 1974).

Any relationship between temperature and development will only hold over the range of physiological tolerance of the organism. With some notable exceptions poikilotherms only survive within the

temperature range 0-40°C (Vernberg and Vernberg, 1970). Within this range each organism has a specific range - the range of tolerance - bounded by upper and lower lethal limits (Fry, 1947). The lethal limits are labile and may be shifted by previous thermal conditioning so that there are "realms of resistance" at extremes of the range of tolerance (Brett, 1970).

The upper lethal limit of T. patialense eggs under the stated experimental conditions would appear to be between 30°C and 35°C. This is comparable with the upper lethal level of other digeneans with poikilothermic hosts. Endoparasites of homiotherms, such as schistosomes, generally have a higher level compatible with the elevated body temperature of their host.

The causes of thermal death at high temperatures are only partly understood but probably involve changes in cell membrane permeability, reduced enzyme activity and differential acceleration of enzymic reactions (Prosser, 1973). In many cases thermal death appears to inactivate organ systems differentially, the invertebrate nervous system often being the first to succumb (Vernberg & Vernberg, 1972).

The lethal level temperature does not have an independent existence but must be considered as a function of both time and temperature. The eggs of Fasciola hepatica fail to develop and eventually succumb if maintained at 37°C, but if transferred to 25°C before death occurs will develop normally (Rowcliffe and Ollerenshaw, 1961). The crucial factor is the period of exposure to the lethal temperature.

This complexity may be compounded by the state of development of the egg. The eggs of poikilotherms show an exponential increase in metabolic rate, as determined by oxygen consumption, throughout ontogeny (Brachet, 1968). Horstmann (1962) has demonstrated a similar functional relationship for the eggs of digéneans. The enhanced energetic demands of late embryos may result in increased susceptibility to thermal damage (Davidson, 1944; Kinne and Kinne, 1962). The eggs of Fascioloides magna initially develop normally at 34°C but after six days of development become aberrant and fail to form miracidia (Campbell, 1961).

Cold effects show a similar variability with developmental stage in Fascioloides magna eggs. At -5°C eggs containing miracidia are rapidly killed while unembryonated eggs survive for 6 weeks at the same temperature (Swales, 1935 and 1936).

The causes of cold death are even less well understood than those of heat death but are believed to function in a different manner. It has been suggested that the primary causes of physiological failure at low temperatures are inactivation of ionic pumps and mis-matching of component chains (Prosser, 1973).

Low temperatures reduce the activity of enzyme systems. In poikilotherms this often has the effect of slowing the rate of metabolism and inducing a state of quiescence. In digeneans the rate of egg development is similarily reduced by cold and development will eventually be inhibited. An ability to remain dormant during unfavourable conditions may have adaptive significance. In practical terms this may mean that eggs can overwinter and remain infective. Avoidance of cold damage by temporarily inhibiting metabolism would

seem to be a resistance adaptation of the type predicted by Precht (1958). Dormancy of this type is not a diapause, as defined by Andrewartha (1952), since it is non-essential to development and is readily reversed by temperature changes.

The value of dormancy is entirely dependent on the relationship between the period of development and the period of adverse conditions. In some platyelminths egg dormancy is highly developed suggesting an ability to withstand long periods of cold weather. The eggs of Fasciola hepatica and Spirometra mansonoides, for example, can survive over 2 years at 5°C (Boray, 1969; Krull, 1934; Mueller, 1961). In other species this ability is less developed and presumably less important to the life cycle: Neodiplostomum intermedium, survives for 90 days at 5°C (Pearson, 1961); Posthodiplostomum cuticola, 52 days at 3°C (Donges, 1964); Fascioloides magna, 6 months at 5°C (Campbell, 1961); and Isthmiophora melis, 90 days at 15°C (Donges, 1973). T. patialense must be a member of the latter category since its egg survive for one month at 10°C. This differential ability to withstand cold conditions cannot simply be a function of latitudinal differences, however, since the group with poorly developed dormancy abilities includes both a/tropical transversotrematid and temperate echinostomes and diplostomes.

In some platyhelminths resistance adaptation involves an ability to withstand sub-zero temperatures. This appears well developed in the Fascioloidiae: Fasciola gigantica eggs will survive for 23 days at -3°C and 17 days at -5°C while F. hepatica can withstand -12°C for 24h. (Kirakini, 1961; Shaw and Simms, 1930). It is among the cestodes, however, that the greatest levels of

resistance are found. The arctic species Echinococcus sibiricensis will remain infective after exposure to -26°C for 35 days or -31°C to -51°C for 120h (Schiller, 1955).

These resistance adaptations are a response to extremes of the tolerance range. In many organisms physiological adaptations occur within the normal range of temperatures in an attempt to maintain metabolic levels independent of ambient temperature. This process of "capacity adaptation" has three levels of expression (Precht, 1958).

Capacity adaptation of the first-type involves a sudden change in metabolic rate in response to changes in temperature. In the case of developing eggs this response would take the form of a rapid rise or fall in the development rate when eggs are first transferred to a different temperature but after some time the rate would stabilise to a level characteristic of the new temperature. In the present experiments all the eggs were initially at 25°C, the temperature of egg collection, and were then incubated at higher or lower temperatures except for those incubated at 25°C. With this exception, therefore, all eggs suffered a temperature change at the beginning of development and this should be reflected by some perturbation in rate during the initial stages of development if capacity adaptation occurs. In fact, the period of development of eggs to Stage 1 shows similar proportional responses to changes in temperature as were observed for the developmental period from Stage 0 to Stage 4. This suggests that if any capacity adaptation occurs it is of such short duration and minimal influence that it was undetected by the present experimental design.

The second form of capacity adaptation is acclimation, a physiological response to long term changes in ambient temperature. It has already been shown (Figures 5.6a and 5.7b) that the development rate of digenean eggs is temperature dependent and does not, therefore, exhibit thermal acclimation.

The final form of capacity adaptation is acclimatization, a long term genetic response to environmental factors (Prosser and Brown, 1961). Figures 5.6a and 5.7b reveal that the curves of thermal response of egg development in Fasciola hepatica and T. patialense are of similar form but occupy different positions on the temperature axis. F. hepatica achieves the same rate of egg development as T. patialense but at a lower temperature. This result implies that the development rate of T. patialense is adapted to higher temperatures and it is tempting to correlate this with the tropical and temperate environments of the two flukes. Evidence for acclimatization based on specific differences, however, must be regarded with circumspection, any firm conclusions awaiting comparisons between the thermal responses of the same species at different lattitudes (Kinne, 1964; Bullard, 1964).

The discussion so far has examined the temperature dependence of digenean egg development. Not all features of the developmental process show dependency, however, The proportion of time spent in attaining any given developmental stage expressed as a proportion of the total developmental period appears to be temperature independent over the range 15-30°C for T. patialense eggs. Barrett (1968) has similarly shown that for the larvae of Strongyloides ratti increasing temperature speeds up the rate of development of all the larval stages equally over the range 15-34°C. This

relationship does not seem to have been previously demonstrated for digenean eggs.

The development period of digenean eggs has been considered a specific characteristic; broader consideration of the group, however, shows surprising similarities. Table 5.8 shows the period of egg development, at temperatures between 20 and 33.5°C, of a wide range of digenean species from six Families. When these developmental periods are plotted in histogram form (Figure 5.8) it can be seen that there is a restricted distribution with a mean value of 15-20 days. This result contrasts markedly with the responses of the eggs of Schistosoma spp. which hatch instantaneously, under suitable conditions, on emergence from the host (Standen, 1951). Whether external development of eggs is constrained to such a defined period because of common ancestry, physical restraints on egg size, ecological factors relating to the importance of time delays in the stability of population dynamical processes, or yet other factors is at present unknown.

The period of illumination of the eggs of T. patialense did not appear to effect their rate of development. Eggs developed equally quickly in 12/12h D/L, D/D and L/L at 25°C. The rate of embryogenesis appears to be independent of photoperiod.

Brett (1970) concluded that, apart from desiccation, temperature is the most potent influence on the fate of reproductive cells of aquatic poikilotherms during development. The results of the present investigation similarly indicate that temperature is of central importance in determining the fate of the eggs of T. patialense.

TABLE 5.8

Egg development period for different species of Digenea

	T°C	PERIOD (DAYS)	SOURCE	
F. DIPLOSTOMIDAE				
Neodiplostomum intermedium	22.5	11	Pearson,	1961
Posthodiplsotomum cuticola	28	27.5	Donges,	1964
F. ECHINOSTOMATIDAE				
Isthmiophora melis	22	18	Donges,	1973
Paryphostomum sufrartyfex	32.5	10.5	Dissmarn et al.,	1966
F. FASCIOLIDAE				
Fasciola hepatica	24	15	Rowcliffe & Ollerenshaw,	1961
F. gigantica	26	17	Dinnik & Dinnik,	1963
Fascioloides magna	25	22	Campbell,	1961
F. PARAMPHISTOMATIDAE				
Paramphistomum kellicotti	27	21	Yokogawa,	1965
P. ichikawai	27	17	Durie,	1953
P. iloktsuensis	27	21	Yokogawa,	1965
P. microbothrium	27	15	Dinnik & Dinnik,	1954
P. daubneyi	27	9.5	Sey,	1972
Cotylophoron cotylophorum	26	18	Varma,	1961
C. indicum	33.5	12.5	Mukherjee,	1969
F. STRIGEIDAE				
Cotylurus c. cucullus	20	22	Odening et al.,	1970
Strigea tarda	24	12	Mathias,	1925
F. TRANSVERSOTREMATIDAE				
Transversotrema patialense	25	18	Present Study	

Figure 5.8: The period of development of the eggs of different digenean species (see text).

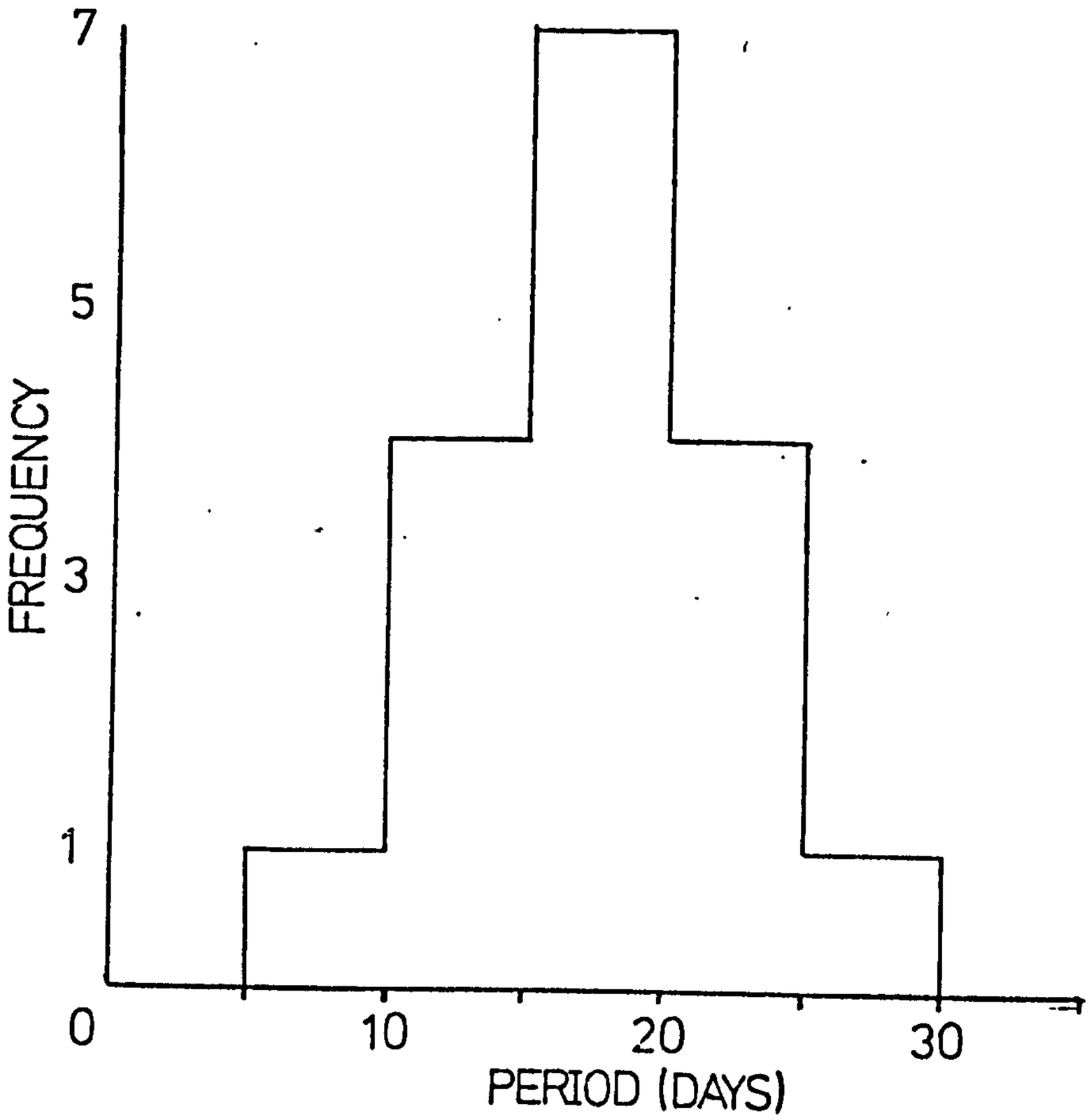
7
5
3
1
0
10
20
30
FREQUENCY
PERIOD (DAYS)

6. Egg Hatching

6.1 Introduction

In most digenean life cycles infection of a molluscan intermediate host is achieved by miracidial penetration. The hatching of the miracidium from the egg is, therefore, an important aspect of digenean biology. In the literature to date emphasis and interest has centered around the physical phenomenon of hatching and emergence from the capsule (Rowan, 1956 and 1957; Wilson, 1968; Kusel, 1970). An important aspect which has been neglected is the temporal patterning of the release of infective stages from the egg. This gap in our understanding of the hatching biology of digeneans is unfortunate as studies on, for instance, monogeneans (Kearn, 1973 and 1974; MacDonald, 1975) suggest that particular temporal patterns of egg hatching can have considerable significance in optimizing contacts between infective larvae and their hosts.

The investigation reported here is an attempt to determine the detailed timing of release of Transversotrema patialense miracidia from their egg capsules, and to correlate this with the temporal distribution of host mollusc activity.

6.2 Materials and Methods

6.2.1 Effect of alternating light and dark periods on the temporal distribution of hatching at 30°C

Eggs were collected overnight from infected fish and thoroughly washed (Section 2.6). The eggs were maintained in autoclaved conditioned water, without antibiotics, in an incubator at 30°C.

The eggs were illuminated cyclically with artifical light of 2,400 lux intensity. Illumination was automatically switched on at 06.00h and off at 18.00h so that the eggs were exposed to alternating twelve hour periods with and without illumination (12/12h D/L).

Four vials, each containing over 100 eggs, were prepared as above. On day 10 post collection (P.C.) the contents of the vials were poured into four separate 10 ml observation vessels and the number of eggs per vessel reduced to 100.

From 09.00h on day 12 P.C. the collections were checked at hourly intervals for the presence of free swimming miracidia using the following procedure. Approximately 8 ml of supernatant were pipetted from each of the observation vessels and placed in individual 10 ml vessels for microscopic examination. The observation vessel was then refilled with conditioned water at 30°C and returned to the incubator. During the dark period of incubation this procedure was carried out under the reduced intensity illumination of photographic "safe-lights".

The number of miracidia present in each sample of supernatant at each time of observation was recorded. The experiment was terminated at 18.00h on day 18 P.C.

The presence of a miracidium in an egg collection was considered indicative of the hatching of a single egg. The results were, therefore, expressed in terms of the mean proportion of all eggs present which hatched within any one hourly period.

6.2.2 Effect of mechanical stimulation on the temporal distribution of hatching

The transfer of eggs from incubation vials to observation vessels at day 10 P.C., as described above, may have been a source of stimulation of hatching rhythm. Two collections of 100 eggs each were, therefore, observed at approximately 4h intervals within incubation vials throughout the hatching period. The eggs were maintained in the same vials during development at 30°C, 12/12 D/L.

6.2.3 Effect of temperature on the temporal distribution of hatching

Eggs were collected and cleaned using the techniques described in Section 2.6 and then incubated as in Section 6.2.1 but at the lower temperature of 25°C.

Preliminary observations had shown that at this temperature the hatching period extended from 16 days P.C. until 24 days P.C. Due to the long period involved sustained 24h observation throughout this period was considered impractical. For 5 separate egg collections hourly observations were made over periods, which totalled 4 to 5 days for each egg collection, during 16 to 24 days P.C. By overlapping, the individual periods of observation were arranged to cover the whole hatching period so that when the results were summated at least two replicate egg collections were observed at any given time throughout the period 16 to 24 days P.C.

The results were expressed in terms of the mean proportion of all eggs present which hatched in any hourly observational period.

6.2.4 Effect of constant illumination on the temporal distribution of hatching

Eggs were collected and washed as described previously (Section 2.6). Four batches of 100 eggs each were incubated in autoclaved conditioned water at 30°C under constant light conditions (L/L) at 2400 lux intensity. Eggs were transferred to observational cells on day 10 P.C. and checked at two hourly intervals for the presence of miracidia (Section 6.2.1) from 12 days P.C. until 17 days P.C.

6.2.5 Effect of constant darkness on egg hatching and development

1) Eggs were collected and washed (Section 2.6). Two batches of over 200 eggs each were placed in vials of autoclaved conditioned water and the vials enclosed in light-tight covers of aluminium foil. The vials were then incubated at 30°C.

   At 16 days P.C. the vials were taken into a dark-room and two aliquots of eggs removed from each. The vials were then recovered with foil and returned to the incubator without being exposed to light.

   One aliquot from each collection was placed in an incubation vial of autoclaved conditioned water at 30°C and incubated at 12/12 D/L.

   The second aliquot from each collection was mounted on a vaseline supported slide and the proportion of eggs in different developmental states determined as described in Section 4.

On day 18 P.C. the aliquots incubated under 12/12h D/L and D/D were slide mounted and their developmental state assessed.

ii) Two washed egg collections were incubated at 30°C in light-tight vials of autoclaved conditioned water. On days 14, 15, 17 and 18 P.C. aliquots of eggs were removed from the vials in a dark-room and the vials recovered with foil and returned to the incubator.

The aliquots were exposed to light in observation vessels and observed for evidence of miracidial hatching.

6.3 Results

6.3.1 Effect of alternating light and dark periods on the temporal distribution of hatching

The percentage of eggs hatching within any hourly period under 12/12h D/L conditions at 30°C is shown in Table 6.1 and Figure 6.1.

It can be seen that no eggs hatched during the hours of darkness and that most eggs hatched between 13.00 and 16.00h.

Figure 6.2a shows the temporal distribution within a single 24h period when data from all the days of observation were superimposed.

Figure 6.3 shows the number of miracidia hatching per day P.C.

6.3.2 Effect of mechanical stimulation on the temporal distribution of hatching

In the above experiment eggs were transferred to observational vessels on day 10 P.C. in order to facilitate observation. Eggs which were not transferred but observed within the incubation vials

TABLE 6.1

Temporal distribution of egg hatching at 30°C, 12/12h L/D. Data expressed as mean percentage hatched of all eggs examined (four replicates, n = 400)

TIME OF DAY (h)	DAYS P.C.					TOTALS FOR
	13	14	15	16	17	TIME OF DAY
24-9	0	0	0	0	0	0
9-10	0.25	0	0	0	0	0.25
10-11	0	0	0.25	0.25	0	0.50
11-12	0	0.25	1.50	0.75	0.25	2.75
12-13	0	2.50	0.25	1.25	0	4.00
13-14	0.25	2.50	9.25	2.00	1.75	15.75
14-15	0	6.50	3.50	4.75	0.50	15.25
15-16	0	1.25	6.25	1.25	0	8.75
16-17	0	0.25	0.75	1.00	0	2.00
17-18	0	0.25	0.75	0	0	1.00
18-19	0	0	0	0	0	0
19-24	0	0	0	0	0	0
TOTALS FOR DAYS P.C.	0.50	13.50	22.50	11.25	2.50	50.25
						TOTAL

Figure 6.1: Percentage of eggs hatching during any hourly period. 12/12h D/L, 30°C. Black bar is dark period of 24hr cycle.

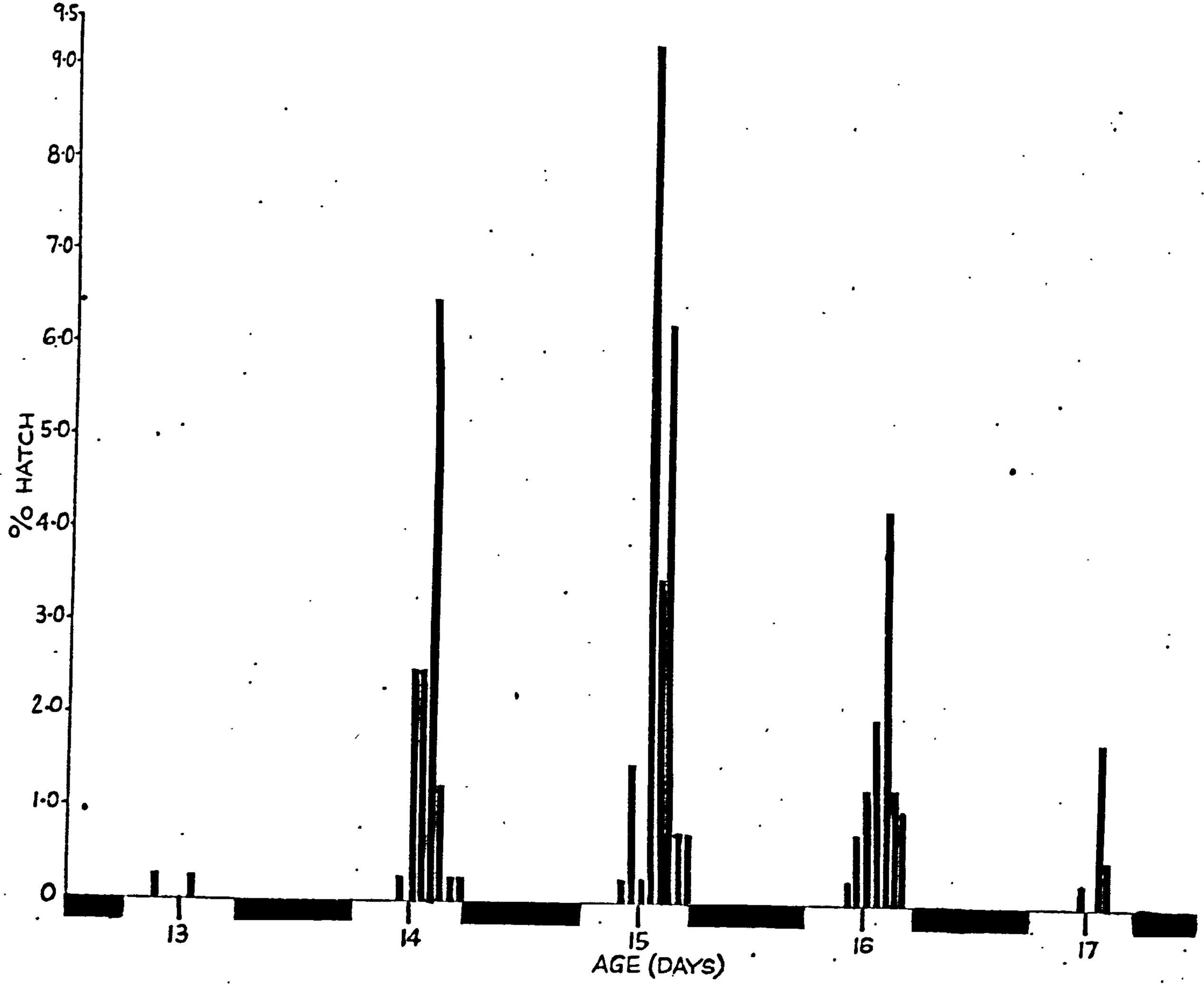
9·5
9·0
8·0
7·0
6·0
5·0
4·0
3·0
2·0
1·0
0
% HATCH
13
14
15
16
17
AGE (DAYS)

Figure 6.2: Percentage of eggs hatching during one hour periods at different times of day.

Illumination regime: 12/12h, D/L.

a) At 30°C

b) At 25°C.

a)

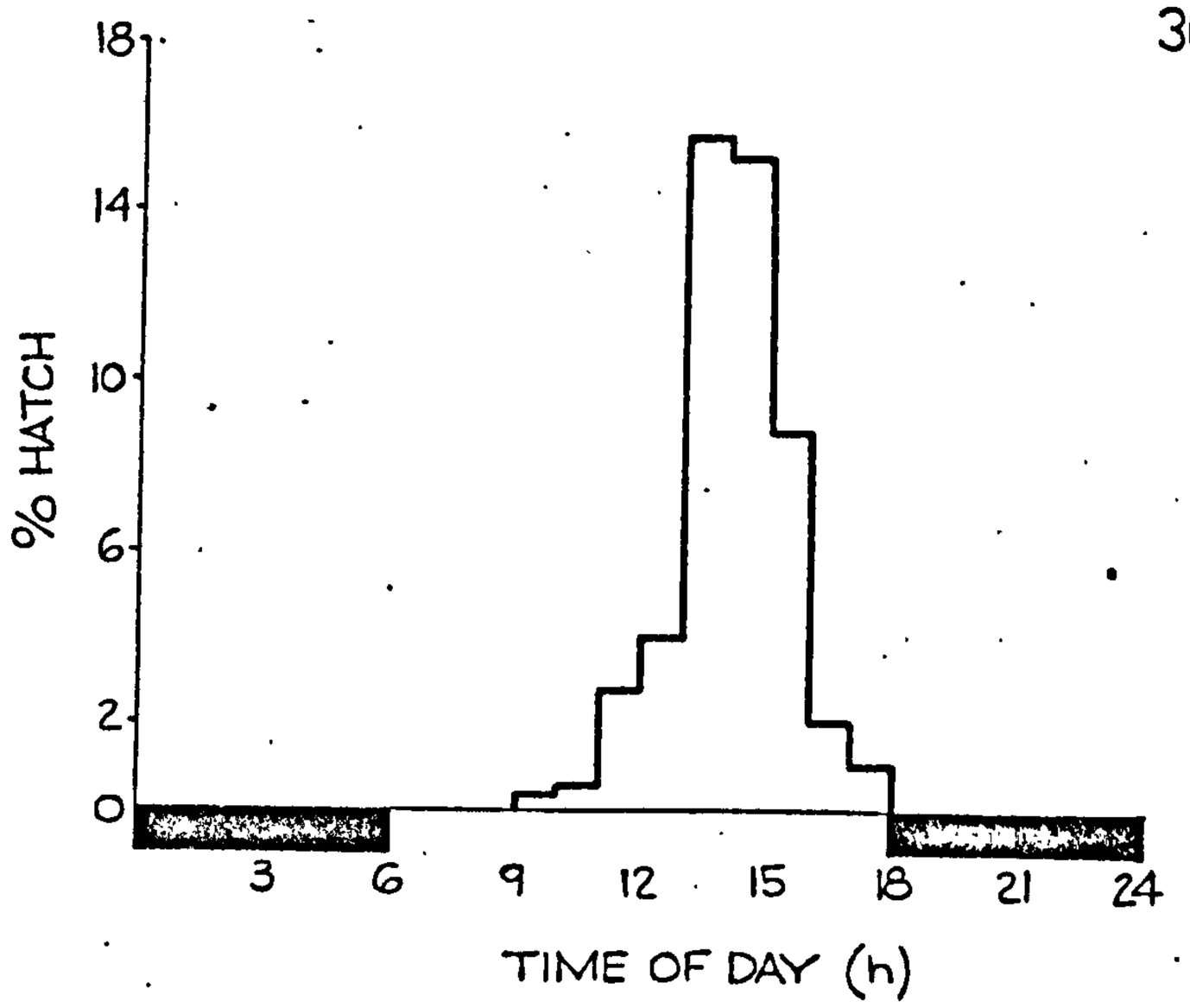
30°C
18
14
10
6
2
0
% HATCH
3
6
9
12
15
18
21
24
TIME OF DAY (h)

b)

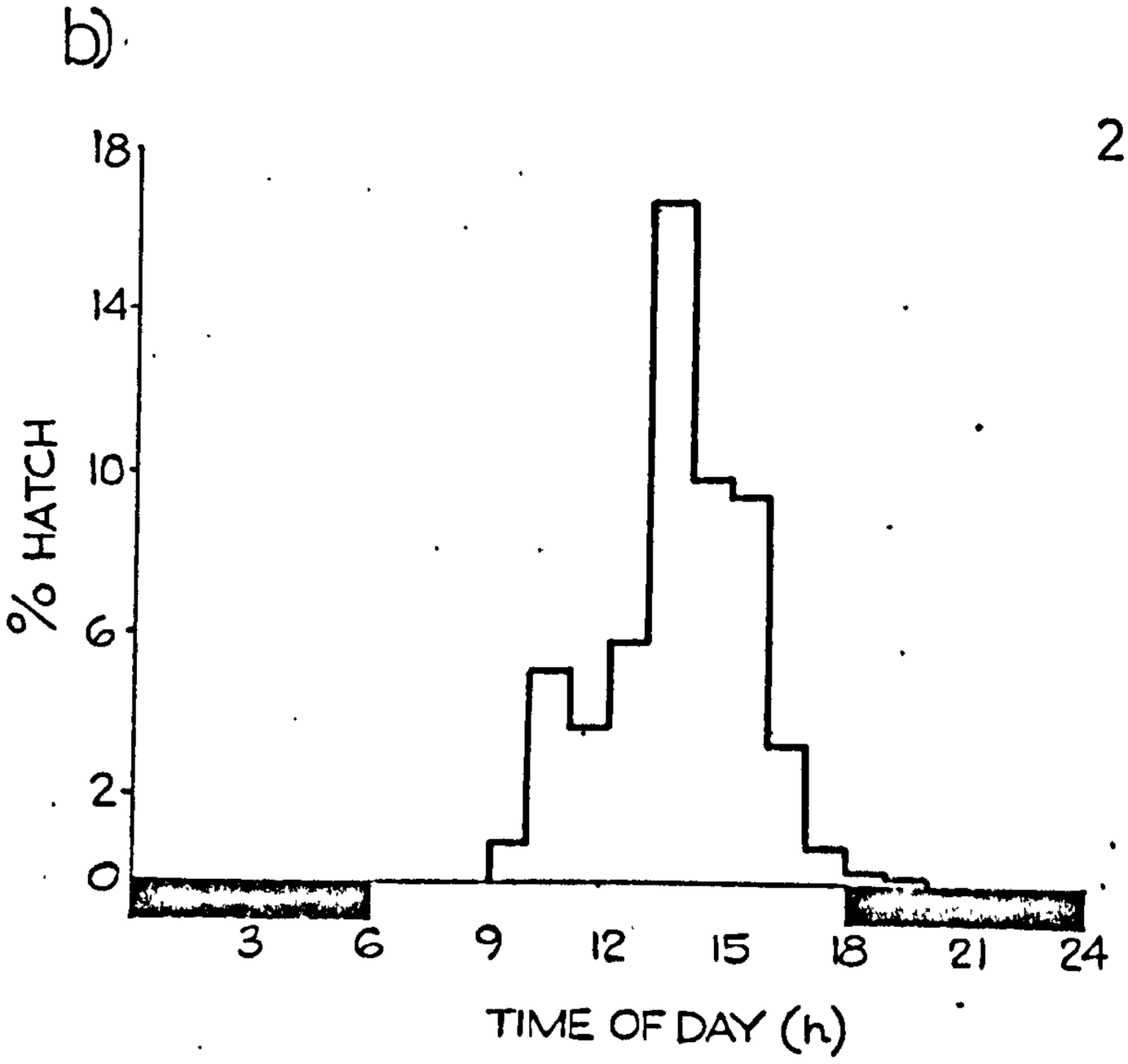
25°C
18
14
10
6
2
0
% HATCH
3
6
9
12
15
18
21
24
TIME OF DAY (h)

Figure 6.3: Percentage of eggs hatching per day post egg collection.

Eggs maintained under 12/12h D/L at 30°C and 25°C.

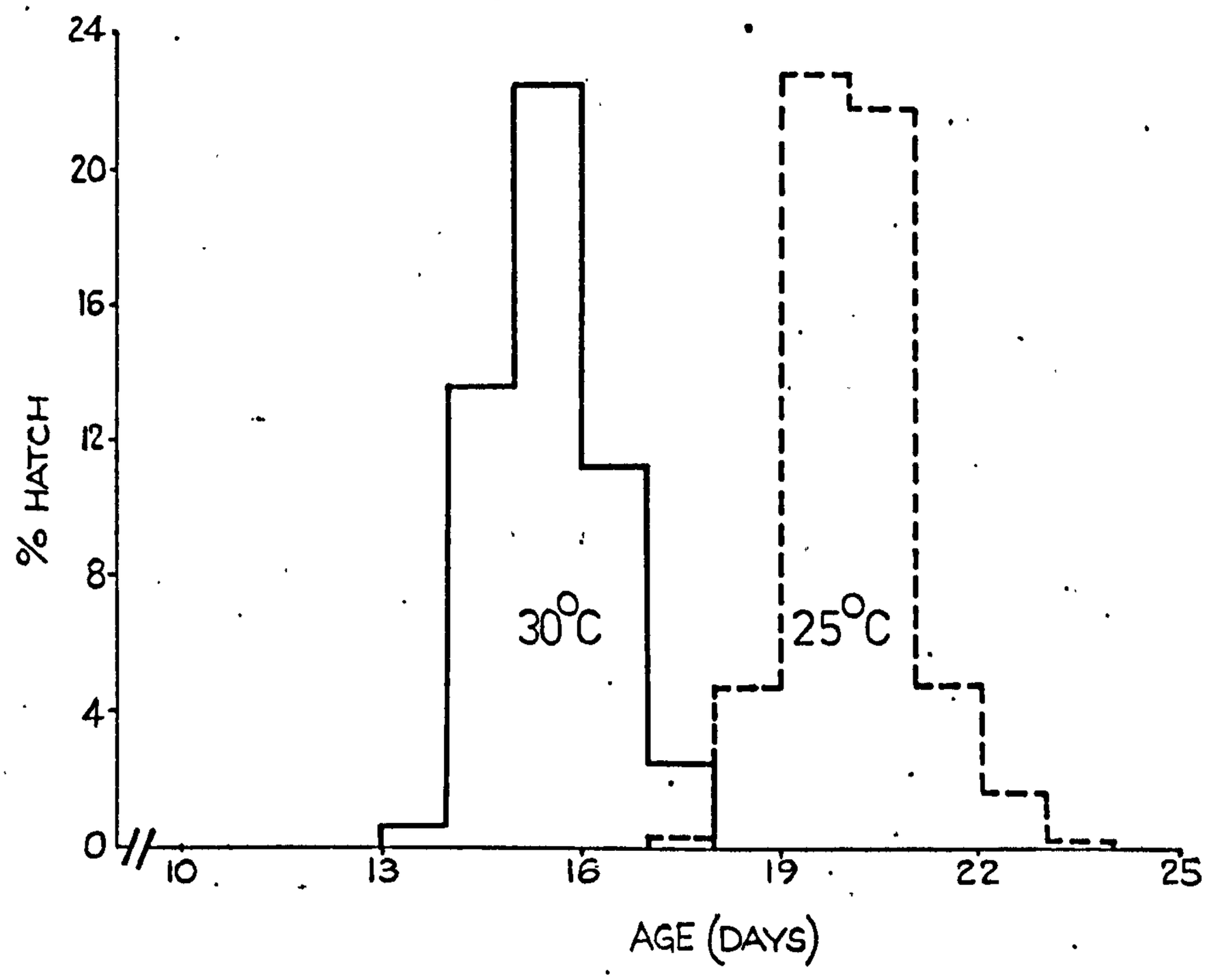
24
20
16
12
8
4
0
% HATCH
30°C
25°C
10
13
16
19
22
25
AGE (DAYS)

for the presence or absence of miracidia showed the same qualitative temporal response - no eggs hatched during the dark period and the majority of miracidia hatched in the early afternoon.

6.3.3 Effect of temperature on the temporal distribution of hatching

At 25°C eggs first hatched on day 17 P.C. and continued to hatch until day 23 P.C. Figure 6.3 shows the proportion of eggs hatching per day P.C.

Table 6.2 and Figure 6.4 show the temporal distribution of egg hatching.

Figure 6.2b shows the daily distributions of egg hatching superimposed on a single 24h period.

A decline in temperature appeared to increase the time taken to attain a developmental state capable of hatching (confirming the results in Section 5.) and also to increase the period of days over which hatching occurred. The temporal distribution of hatching within each 24h period, however, appeared to be independent of temperature over the range 25-30°C.

6.3.4 Effect of constant light on the temporal distribution of hatching

Under constant light conditions (L/L) at 30°C eggs first hatched on day 13 P.C. and continued until day 17 P.C. (Table 6.3).

The temporal distribution of hatching and the superimposed 24h pattern of hatching are shown in Table 6.3.

These patterns resembled those recorded for 12/12h D/L at 30°C (Table 6.1), except that the overall percentage hatching decreased

TABLE 6.2

Temporal distribution of egg hatching at 25°C, 12/12h L/D. Data expressed as percentage hatched of all eggs examined (for each observation 2 replicates, n = 400)

TIME OF DAY (h)	DAYS P.C. 17	18	19	20	21	22	23	TOTALS FOR TIME OF DAY
24- 9	0	0	0	0	0	0	0	0
9-10	0	0	0	0.58	0.32	0	0	0.90
10-11	0	0	0	4.61	0.29	0.22	0	5.12
11-12	0.12	0.34	1.02	0.58	1.28	0.39	0	3.73
12-13	0.12	0.34	2.30	1.31	1.37	0.39	0	5.83
13-14	0	1.24	7.43	6.24	1.28	0.49	0.12	16.80
14-15	0	1.35	3.07	5.37	0	0.20	0	9.99
15-16	0	0.45	6.53	2.19	0.42	0	0	9.59
16-17	0	0.81	1.79	0.66	0	0	0	3.26
17-18	0	0.20	0.38	0.26	0	0	0	0.84
18-19	0	0	0.22	0	0	0	0	0.22
19-20	0	0	0.11	0	0	0	0	0.11
20-24	0	0	0	0	0	0	0	0
TOTALS FOR DAYS P.C.	0.24	4.73	22.85	21.80	4.96	1.69	0.12	56.39
								TOTAL

Figure 6.4: Percentage eggs hatching during any hourly period.
12/12 D/L, 25°C. Black bar is dark period of 24hr cycle.

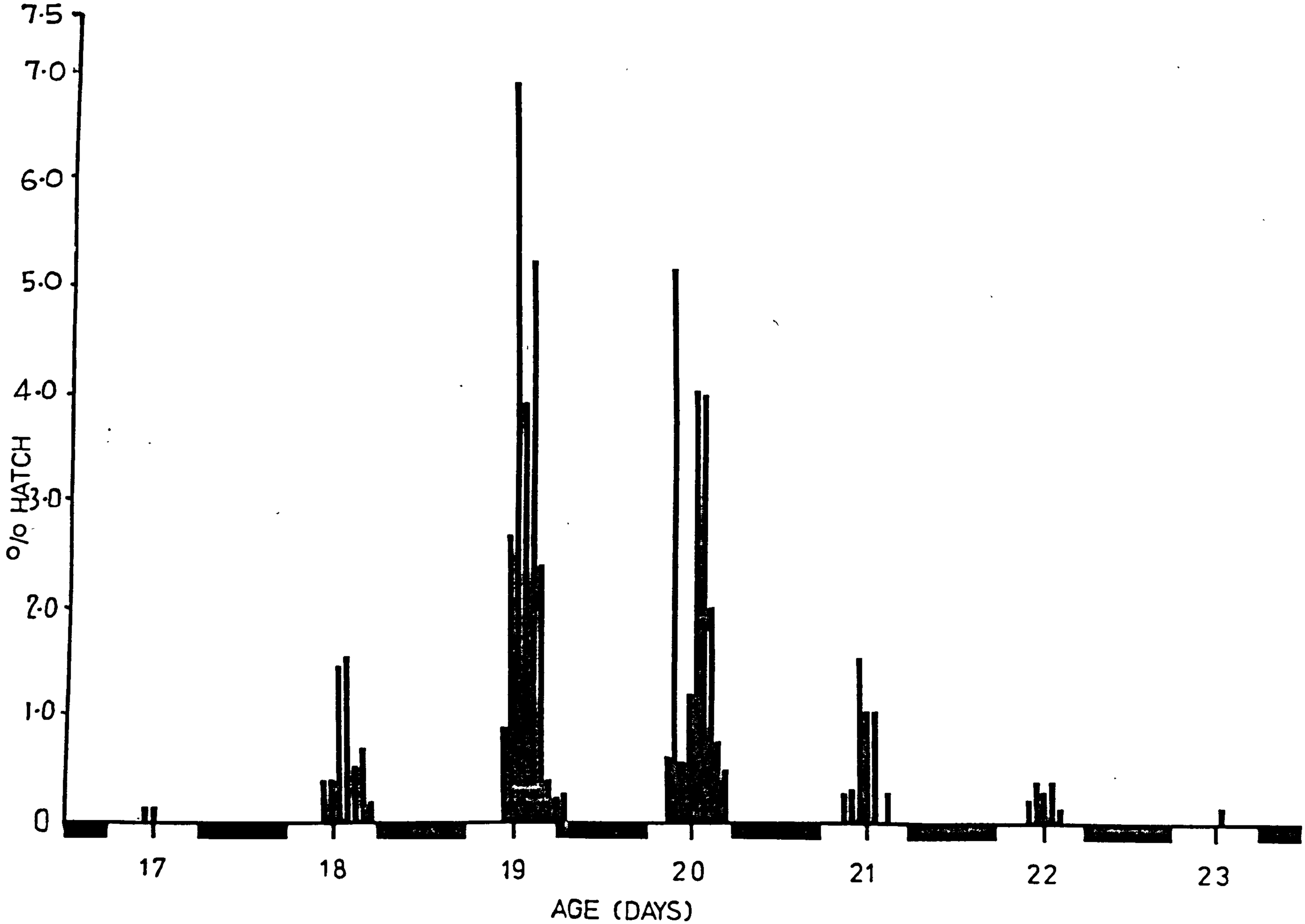
7·5
7·0
6·0
5·0
4·0
3·0
2·0
1·0
0
% HATCH
17
18
19
20
21
22
23
AGE (DAYS)

TABLE 6.3

Temporal distribution of egg hatching at 30°C, 12/12h L/L. Data expressed as percentage hatched of all eggs examined (four replicates, n = 400)

TIME OF DAY (h)	DAYS P.C.				TOTALS FOR TIME OF DAY
24- 9	0	0	0	0	0
9-11	0	0.50	0.25	0	0.75
11-13	0	1.75	6.50	0.25	8.50
13-15	0	6.00	7.50	2.50	16.00
15-17	0	3.75	1.75	0.75	6.25
17-19	0.75	1.25	0	1.25	3.25
19-21	0.50	0.50	0	0	1.00
21-24	0	0	0	0	0
TOTALS FOR DAYS P.C.	1.25	13.75	16.00	4.75	35.75 TOTAL

under constant light.

It appears that the hatching rhythm is maintained even under unstimulated conditions.

6.3.5 Effect of constant darkness on egg hatching and development

i) The results are shown in Table 6.4. It is apparent that a negligible number of eggs were dis-operculate (presumed hatched) by day 16 when maintained at 30°C in the dark. This contrasts with the result for eggs maintained under 12/12h D/L and L/L at 30°C (Table 6.1 and 6.3) when most eggs had hatched by 16 days P.C. The present result implies that constant dark conditions retard hatching or development.

TABLE 6.4

Effect of light on development and hatching of eggs at 30°C. Expressed as mean proportion in developmental stages (2 replicates, n = 150)

LIGHT REGIME (12/12h)	AGE (DAYS P.C.)	DEVELOPMENTAL STAGES						
		0	1	2	3	4	D	M
D/D	16	0	0	0.09	0.23	0.39	0.06	0.23
D/D	18	0	0	0.11	0.16	0.26	0.23	0.24
D/D (16 days) D/L (2 days)	18	0	0	0.02	0.06	0.12	0.34	0.46

By 18 days P.C. eggs maintained in 12/12h D/D at 30°C showed some evidence of hatching in that the number of disoperculate eggs had increased and the number of stage 4 eggs decreased (Table 6.4).

A significant proportion of eggs transferred from constant darkness to 12/12h D/L on day 16 P.C. showed evidence of hatching by 18 days P.C. (Table 6.4).

These results indicate that very few eggs hatched under constant dark conditions, and that a significantly greater proportion were induced to hatch by transfer to D/L conditions.

ii) Transfer from constant dark to light did not induce an immediate hatching response, nor had any eggs hatched by 4h after transfer.

Exposure to light clearly did not act as an immediate hatching "trigger" in eggs maintained in constant darkness.

The temporal distribution of hatching of eggs developing under these conditions is unknown.

6.4 Discussion

Before discussing the biological significance of the present results some consideration must be given to the reliability of the experimental methods. The fundamental experiments purport to expose digenean eggs to an environment in which the only variable was illumination. In practice this ideal is extremely difficult to achieve, not least because the experimenter must interupt the experiment during periods of observation.

In the present investigation the following factors should be considered. Firstly, eggs for all experiments were collected from infected fish maintained at 25°C in 12/12h D/L. This situation is amenable to manipulation, for instance it would theoretically be possible to maintain fish under the same conditions as in subsequent

egg incubation. It was, however, considered that eggs should be obtained from flukes maintained under the natural conditions of alternating dark and light periods so that their natural responses could be assessed. Secondly, observation of the eggs involved exposure to mechanical stimulation. As observations occurred at regular intervals throughout the day and night it was considered that the level of stimulation was constant and, therefore, unlikely to materially affect the temporal distribution of hatching. Finally, observation of the eggs involved exposure to light. This factor may have had a significant effect on the response of eggs during the dark phase of a 12/12h D/L illumination regime, although such an effect was hopefully minimised by the use of low intensity illumination of long wavelength. Light exposure during observation in constant light regimes is unlikely to have any effect and it is encouraging that the results for 12/12h D/L and L/L were very similar at the same temperature. This suggests that the mode of observation had a negligible effect in the present experimental design.

In Section 5 it was demonstrated that at the start of the hatching period in 12/12h D/L approximately 55% of eggs were in the developing population at 25°C and 35% of eggs at 30°C. The present results show that 56.39% of eggs hatched at 25°C and 50.25% at 30°C. Given the variation resulting from the different experimental procedures these results are sufficiently similar to suggest that eggs attaining stage 4 are capable of hatching and suffer minimal mortality.

Under constant light conditions 35.75% of eggs hatched at 30°C compared with 50.25% under 12/12h D/L. This reduced viability may

be a consequence of continuous algal growth under constant illumination reducing the suitability of the culture conditions.

The hatching of a digenean egg is an all-or-nothing event that results in the release of the infective miracidium from the egg capsule. Many exogenous stimuli have been implicated in the initiation or "triggering" of this response. It should be noted, however, that such stimuli may only act in the presence of suitable "permissive" factors, most notably moisture and physiological ranges of pH and temperature (Rowcliffe and Ollerenshaw, 1960; Gold & Goldberg, 1976; Sugiura, Sasaki, Hosaka and Ono, 1954).

One of the most widely known and experimentally useful hatching triggers is the effect of ionic dilution on schistosome eggs (Kusel, 1970; Becker, 1973). Eggs of several species of Schistosoma may be maintained unhatched in saline but will rapidly hatch if transferred to distilled water.

Changes in light intensity may also act as triggers to hatching. Sugiura et al. (1954) found that Schistosoma japonicum eggs exhibit a 60% increase in hatching if exposed to light as well as ionic stimuli, although this difference was not observed by Ingalls, Hunter, McMullen and Bauman (1949). Rowan (1956) and Gold and Goldberg (1976) found that Fasciola hepatica eggs were stimulated to hatch by a light stimulus, although this effect could also be achieved in the dark by a temperature shock. Wilson (1968) considered light to ach as a specific trigger for the hatching of F. hepatica eggs.

Temperature shocks may also act as a hatching trigger. For Isthmiophora melis eggs Donges (1973) considered a rise in temperature

far more important than increasing light intensity in triggering hatching.

The characteristic of all these forms of stimuli is that hatching follows rapidly on the reception of the environmental change. The rhythmic form of hatching of T. patialense eggs does not appear to be generated in this manner. The eggs were exposed to a step-function increase in light intensity, from zero to 2,400 lux, at 06.00h and yet the period over which hatching occurred did not begin until 3h later. Furthermore, hatching did not occur as a sudden response from all eggs present but instead, over a period of several hours, the proportion of eggs hatching rose gradually and then declined. This pattern was recorded from eggs incubated in 12/12h D/L and L/L and had a periodicity of approximately 24h.

There are two possible explanations for this result. It is possible that some subtle trigger was operating to initiate the hatching activity, but if so this exogenous stimulus remained undetected during all experiments and would have had to have operated in the three separate laboratories where these experiments were conducted. Nevertheless, the possibility of exogenous cues cannot be completely discounted and must always be a consideration in analyses of biological rhythms. Assuming that, as was intended, the only significant variable within the present system was the illumination regime it is possible that endogenous factors were involved in the control of hatching.

The concept of endogenous control mechanisms in biological systems is relatively modern and like many new areas of science has generated its own complex terminology, subsequent discussion

will utilise the nomenclature suggested by Saunders (1977). Temporal control of biological functions is achieved by a balance between exogenous and endogenous factors. In few, if any, systems does the latter operate alone. Most "biological clocks" consist of an endogenous oscillator - of unspecified location and morphology - whose rhythm is precisely entrained by some exogenous stimulus - the zeitgeber - to run in a precise temporal period. In the present context this period is a 24h cycle or circadian rhythm.

The period of the oscillator rhythm is made to equal the period of a solar day (approximately 24h) by the fine-tuning effect of the zeitgeber. In many instances the zeitgeber is a change in light intensity, although there are many other physical phenomena which may operate. The experimenter observes the period of the biological oscillator by the rhythmic appearance of some overt event, in the present case the hatching of eggs. The experimenter observes the period of the solar day by reference to a chronometer or similar instrument.

In order to increase confidence in the probability that an endogenous circadian rhythm is operating, the system observed must fulfil a number of conditions. The most basic condition is that the rhythm persists when all environmental periodicities are excluded. The biological oscillator is then said to be "freed" from its zeitgeber and to be in the free running condition. The overt event should then show a natural period which is, according to Saunders (1977): "close to but rarely equal to that of the period of the solar day; surprisingly accurate (for a biological phenomenon); and temperature compensated."

As previously stated the hatching rhythm of T. patialense eggs persisted under constant light and temperature conditions i.e. in the absence of environmental periodicities.

Under such conditions the "free running" period of hatching showed no obvious tendency to "drift". In most endogenously controlled phenomena the oscillator alters its phase with respect to solar time due to the lack of the fine-tuning zeitgeber. The presence of this drift away from the solar day rhythm is considered strong evidence for endogenous control. Unfortunately, with egg hatching one is observing a population phenomenon occurring over a relatively few days so that any individual drift would be obscured. Furthermore, because egg hatching is a unique event for each individual egg it is not possible to determine the rhythm of individuals but only of populations. Drift cannot be used as an indicator of endogenous control in the present context.

Temporal accuracy in biological terms implies that the rhythmic recurrence of overt events has a circadian cycle accurate to within ± one hour. The recurrence of hatching peaks recorded here are within these limits.

Peak egg hatching at 25°C and 30°C occurred at the same time during the experimental day and hence exhibited the same circadian rhythm. The developmental period at these two temperatures, however, was markedly different. This implies that the factors controlling egg development are temperature dependent while those controlling the time of hatching during any 24h period are not. The period of the oscillator is, therefore, temperature compensated.

There are grounds, therefore, for supposing the temporal control of egg hatching in T. patialense is due to endogenous mechanisms. The physiological nature of the oscillator in digenean eggs cannot be usefully discussed here although it is probably linked to the presumed illumination detecting function of the miracidial ocelli or ciliated photoreceptors. The mechanism controlling the timing of hatching may be considered to act on the principle of "allowed zones". A group of eggs collected over 24h may be assumed to be at slightly different stages of development. Over the period required to achieve the mature miracidial phase these differences may become enhanced. When the contents of an individual egg capsule achieve the required morphogenetic degree of development they are ready to hatch. Hatching, however, may only be permitted during certain "allowed zones" or "gates" at specific times of day. In the present context the gate would be the hatching period from approximately 09.00h to 19.00h. Eggs attaining full development when the gate was closed, that is during the "forbidden zone", would have to await the next gate on the following day. As mircidia attained maturity over several days the eggs would also hatch over several days within sequential time gates.

This latter concept of a gating mechanism is purely speculative and may have little relevance to the underlying biological mechanisms controlling hatching. It does, however, assist the formulation of hypotheses, the testing of which may hopefully lead to better understanding of the physiological mechanism involved.

There are few records of diurnal rhythms occurring in digeneans. The discharge of Schistosoma haematobium and S. mansoni eggs from man occurs with a circadian rhythm, althought it is as yet unclear

whether this is a function of cyclical behaviour on the part of the worm or the host (Dukes & Davidson, 1968; Pitchford and Visser, 1972).

The timing of emergence of cercariae from snails has also been shown to exhibit a diurnal rhythm. In reviewing this topic Erasmus (1972) lists 11 digenean species for which this phenomenon has been recorded. It appears, however, that this cyclical activity may be mediated by exogenous stimuli rather than an endogenous oscillator. In Schistosomatium douthitti reversal of the environmental light pattern produced a concomittant reversal of the emergence pattern (Olivier, 1951) and in Cercaria purpurae the rhythm was immediately abolished by free-running conditions of constant dark or illumination (Rees, 1947). The importance of exogenous cues was particularly clearly demonstrated for Cercaria X which emerged in response to specific levels of light intensity (Probert, 1963).

Circadian rhythms of egg hatching have not been adequately demonstrated for digeneans. In the present literature survey the only apparent rhythm discovered was that of Spirorchis artericola whose eggs hatch around the same period of the morning (Pieper, 1953).

In the Monogenea a number of species have been reported to exhibit circadian rhythms of egg hatching. The eggs of Entobdella hippoglossi and three species of Diclidophora hatch at specific times during a 12/12h D/L regime (Kearn, 1974; MacDonald, 1975). No attempt has been made to assess the free-running responses of these rhythms hence it cannot be stated to what extent they are exogenously or endogenously controlled. In E. soleae eggs the hatching rhythm persists in D/D and L/L provided they are exposed to

12/12 L/D until hatching begins (Kearn, 1973). This would suggest that the oscillator is only functional very late in ontogeny or that the requirement for entrainment is exceptionally great. This is, however, good evidence of some endogenous temporal control.

There are, therefore, some examples of endogenous control mechanisms within the Digenea or their close relatives. What then is the function of these mechanisms?

The hatching of the egg of T. patialense has the effect of releasing a miracidium. Within a relatively short period (Section 7) this larva must find, identify and infect the molluscan intermediate host if the life cycle is to continue. The probability of infection would be greatly enhanced if miracidial hatching occurred at a time when the probability of host-parasite contact was greatest. A rhythmic pattern of miracidial hatching might, therefore, be expected to reflect some cyclical feature of molluscan availability.

As may have been predicted from the above, Melanoides tuberculata does exhibit a circadian activity rhythm. Beeston (1977) demonstrated a crepuscular rhythm of locomotor activity which was persistent under unstimulated conditions. In the laboratory this activity took the form of vertical migration within experimental tanks at dawn and dusk. It is unclear whether this movement is a result of attempted lateral dispersion in a vertically constrained environment or a true reflection of behaviour in the wild (pers. com. D. Beeston, Zoology Department, University of Birmingham). In two species of the closely related genus Semisulcospira, field studies have revealed a rhythmic change in the molluscs' geotropic response (Mori, 1946). It is possible, therefore, that wild

populations of M. tuberculata also undergo vertical migrations within aquatic vegetation at dawn and dusk.

These studies show that the mollusc exhibits cyclical activity, but it is open to speculation as to which features of this activity might influence their availability to the parasite. M. tuberculata is a prosobranch mollusc and has an operculum which seals the mouth of the shell when the foot is retracted. In this configuration penetration by a miracidium would be very unlikely as the soft tissues of the mollusc are sealed within the shell. During both the active and quiescent periods of M. tuberculata, however, the foot remains extended, attaching the mollusc to the substrate, and so the epidermis is exposed to penetration during both periods. Availability of penetration sites would, therefore, appear to be equivalent whether the mollusc was actively migrating or quiescent on the substrate. Similarly, because the miracidium swims very rapidly, in comparison to the sluggish movements of the mollusc, the latter probably presents an equally available target whether it is moving or stationary. Neither availability of penetration sites nor host movement would appear, therefore, to differentially effect the probability of infection during the cyclical activity of the host. Of more probable significance for infection is the location of the host relative to the emergent miracidia, since a host situated close to the hatching eggs is more likely to be encountered by a miracidium. The miracidia hatch from eggs located on the substrate so it would appear that the presence of a host mollusc on the substrate at the time of hatching would provide more appropriate conditions for miracidial infection than if the snail were situated vertically distant in aquatic vegetation. In fact, the results presented here

show that miracidia hatch in their greatest numbers around midday, coinciding with the period when the host mollusc is located on the substrate between its dawn and dusk periods of vertical migration.

This begs the question why there is no apparently equally suitable midnight hatching of miracidia. This is possibly a consequence of miracidial biology alone. The miracidium is apparently equipped with two ocelli each of which is directional due to the presence of a pigment cup, these sense organs may be used for monitoring the direction of incident light rather than simply its intensity (Isseroff, 1964). Perhaps co-ordinated miracidial activity, therefore, requires light and hence nocturnal emergence would be a positive disadvantage.

Finally, a note of caution. The apparent correlation, discussed above, between the timing of parasite emergence and host activity may be entirely fortuitous. Firm conclusions on this relationship can only be drawn once the process of host location and infection is understood. In particular, since this host-parasite system evolved in the wild it is essential that laboratory activity studies are corroborated by investigations in the natural habitat.

Section 7:

Miracidial Survival

7. Miracidial Survival

7.1 Introduction

Since 1883 when Thomas first described the life span of the miracidium of Fasciola hepatica as having an "average maximum duration" of 8h it has been repeatedly shown that digenean miracidia have a very short life span in which to locate, identify and infect the intermediate host. For example, the miracidium of Fascioloides magna lives for 8-12h at 25°C (Campbell, 1961), Isthmiophora melis for 11h at 22°C (Donges, 1973) and Neodiplostomum intermedium for 3h at 25°C (Donges, 1964).

The present investigation seeks to determine the longevity of Transversotrema patialense miracidia and to examine the temporal relationships of the mortality rate.

7.2 Materials and Methods

Eggs were collected, cleaned and then incubated at 25°C as described in Section 4.2.

On days 19 and 20 P.C. the cultured eggs were placed in conditioned water in 10 ml crystallizing dishes and, between 12.00h and 17.00h, examined every 30 min. for the presence of swimming miracidia. All the miracidia that had hatched in the previous 30 min. were removed. Miracidia were transferred individually in a wide-bore pipette and maintained separately in individual 10 ml dishes containing conditioned water at 25°C. The age of the miracidium at transfer was taken to be zero time post emergence (P.C.) ± 15 min.

By this means 4 replicate batches of approximately 10 miracidia each were prepared. Each batch originated from a separate egg collection.

The dishes containing the miracidia were glass covered to reduce evaporation and placed in an incubator at 25°C under constant light conditions at 2,400 lux intensity. At one hour intervals P.E. the dishes were examined and the number of miracidia showing movement discernable at 40x magnification was determined. The experiment was terminated when two consecutive observational periods failed to reveal any miracidial activity.

7.3 Results

The miracidia of T. patialense swam in the spiral fashion characteristic of most digenean miracidia (MacInnis, 1965). Having traversed the vessel the larva would turn right or left and follow the vessel wall or turn round and recross the chamber. While a miracidium would occasionally perform local revolving movements against an egg capsule or vessel wall on no occasion did they stop moving completely and then resume activity.

A miracidium which had ceased activity for a 10 sec. period of observation was assumed dead for the purposes of this investigation. This does not imply a cessation of metabolic activity nor an inability to respond to novel stimuli. The period during which a miracidium exhibited active movements was, therefore, considered in the present context to represent its period of survival.

For each of the four batches of miracidia examined, the number of miracidia surviving was determined for each hour P.E. that the

miracidia survived. From these data the mean proportion surviving at each hour post emergence could be calculated (Table 7.1 and Figure 7.1b).

Subsequent manipulations of the survival data followed the procedures suggested by Anderson and Whitfield (1975).

The mean instantaneous mortality rate (μ) during each hour was determined (Table 7.1) using the formula:

$$\mu = \ln P_t - \ln P_{t+1}/t+1 - t$$

where: μ = instantaneous mortality rate per miracidium; P_t = mean proportion surviving at time t; and P_{t+1} = mean proportion surviving at time t plus unit time interval.

The instantaneous mortality rates determined from the experimental data are represented by the data points in Figure 7.1a.

The experimental mortality data was fitted (Figure 7.1a), using a linear least-squares technique, with the exponential model: $\mu(t) = a.\exp(bt)$. The parameters of which were: a = 0.00534; b = 0.90181; and r = 0.98547.

The solution of the time-dependent process described by the exponential model is:

$$P_{(t)} = 1.0 \exp\left[a/b \left[1-\exp(bt)\right]\right]$$

Hence using the parameters of the mortality model the proportional time-dependent survival of the miracidium of T. patialense could be predicted.

Figure 7.1b shows the close correspondence between the predicted curve and experimental data points.

TABLE 7.1

Survival and mortality parameters of the miracidium of T. patialense at 25°C

AGE (h)	PROPORTIONAL SURVIVAL REPLICATES (n) 1(9)	2(12)	3(11)	4(8)	MEAN	INSTANTANEOUS MORTALITY RATE
0.0	1.00	1.00	1.00	1.00	1.00	
0.5						0.000
1.0	1.00	1.00	1.00	1.00	1.00	
1.5						0.0305
2.0	1.00	1.00	1.00	0.87	0.97	
2.5						0.0314
3.0	0.89	1.00	1.00	0.87	0.94	
3.5						0.1125
4.0	0.89	0.83	0.91	0.75	0.84	
4.5						0.3365
5.0	0.55	0.66	0.45	0.75	0.60	
5.5						0.8755
6.0	0.22	0.25	0.27	0.25	0.25	
6.5						1.8326
7.0	0.00	0.08	0.09	0.00	0.04	
7.5						
8.0	0.00	0.00	0.00	0.00	0.00	

Figure 7.1:

a) Points represent the mean instantaneous mortality rate per miracidium (μ_t). Fitted with exponential model (see text).

b) Proportional survival of miracidia. Fitted with predicted survial curve (see text).

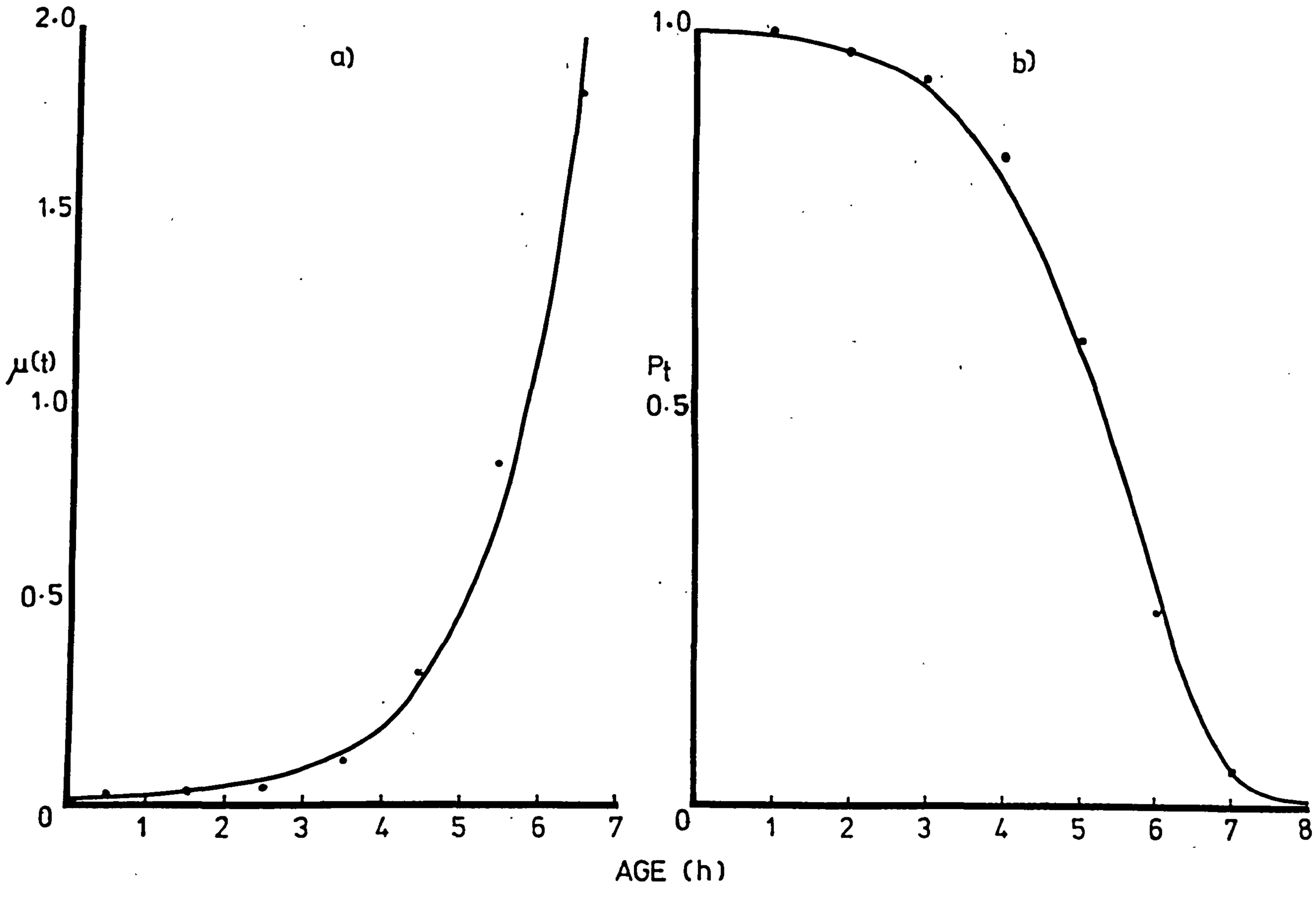
a)
b)
2·0
1·5
μ(t)
1·0
0·5
0
1
2
3
4
5
6
7
1·0
Pt
0·5
0
1
2
3
4
5
6
7
8
AGE (h)

It appears, therefore, that the maximum life-span of the miracidium of T. patialense under the stated experimental conditions was approximately 8h, with 50% of larvae failing to survive beyond 5.5h P.E.

7.4 Discussion

The miracidium of Transversotrema patialense is shown here to have a maximum life-span of about 8h at 25°C. The rate of mortality, however, does not remain constant throughout this period but increases exponentially with age. Age dependent mortality of this form has been previously demonstrated for the miracidia of Schistosomatium douthitti, Schistosoma mansoni and S. haematobium (Schreiber and Schubert, 1949; Oliver and Short, 1956; Anderson, 1976 and 1978; Prah and James, 1977). A similar phenomenon occurs in other infective stages of helminths such as the hexacanths of Hymenolepis diminuta (Anderson and Lethbridge, 1975), the L3 larvae of Bunostomum trignocephalum (Anderson, 1976), and the cercariae of T. patialense (Anderson and Whitfield, 1975; Anderson, Whitfield and Mills, 1977).

In the present investigation the age dependent mortality of T. patialense miracidia may be generated by a progressive adverse change in the experimental environment. This could take the form of a reduction in the suitability of the medium, the metabolic activities of the larvae conspiring to deplete oxygen levels and enhance the concentration of toxic metabolites. This possibility may be discounted, however, because the large volume of medium relative to the volume of the miracidium should be of sufficient capacity to buffer any such changes during the short active life

of the larva.

A more likely hypothesis, and one applicable to the other helminth systems, is that the changing mortality pattern is generated by age dependent depletion of nutrient reserves. Miracidia contain relatively large quantities of glycogen, in the case of Fasciola hepatica this represents 15% of the dry weight of the newly emerged larva and falls to an undetectable level by the end of the active period (Wagner, 1965; Axmann, 1947; Horstmann, 1962). During active swimming the polysaccharide may be mobilised to provide the energy for ciliary activity, and since the miracidium is apparently non-feeding the amount of available glycogen will progressively decrease. Similar relationships between finite nutrient reserves and activity levels have been proposed to exist between the hexacanth of Hymenolepis diminuta and its hook musculature (Anderson and Lethbridge, 1975) and between the cercaria of T. patialense and its tail musculature (Anderson and Whitfield, 1975). The implication, therefore, is that these larvae utilise their energy depots without replacement and hence are ultimately unable to sustain their activity.

Age dependent mortality of miracidia has consequences for their infectivity. Infection by these larval digeneans involves active penetration of intermediate host epidermis and is, therefore, energetically demanding. It may be assumed that some finite limit exists on the levels of available nutrients which allow for infection, that is there is a minimum requirement of glycogen which will permit completion of the penetration process. It would be expected, therefore, that infectivity is age dependent and that the infectivity-age curve would be of similar form to the survival-age

curve but not extend so far along the time axis. Functional relationships of this form have been described for the cercaria of T. patialense infecting Brachydanio rerio (Anderson and Whitfield, 1975), the miracidium of Fasciola hepatica infecting Lymnea truncatula (Christensen, Nansen and Frandsen, 1976), and the miracidium of Schistosoma mansoni infecting Biomphalaria globosus and B. pfeifferi (Prah and James, 1977; Anderson, 1978) all of which have active infection processes.

These age dependent survival and infectivity relationships of helminth larval stages may be modified by external factors. The period of miracidial and cercarial survival and infectivity is inversely related to temperature (Schreiber and Schubert, 1949; DeWitt, 1955; Benex and Deschiens, 1963; Purnell, 1966a; Christensen et al., 1976; Whitfield, Anderson and Bundy, 1977). Miracidial activity and infection rates show a similar inverse relationship to temperature (DeWitt, 1955; Purnell, 1966b; Mason and Fripp, 1976). Naturally, these factors can only obtain within the range of physiological tolerance of the larvae; extremes of salinity, pH, temperature and water movement all prevent or inhibit infection (Benex and Deschiens, 1963; Webbe, 1966; Upatham, 1972).

Finally, it should not be supposed that abiotic parameters are the sole determinants of infection sucess. Recent theoretical studies indicate that a wide range of endogenous biological factors, such as host activity, host susceptibility, density of hosts and infective stages, may affect the rate of infection (May and Anderson, 1978; Anderson, 1978).

SECTION 8:

MIRACIDIAL ULTRASTRUCTURE

8. Miracidial Ultrastructure

8.1 Introduction

The previous two sections considered miracidial biology in respect of the temporal relationship of hatching and the longevity of the resulting larvae. No attempt was made to relate these factors to miracidial physiology. Indeed there is an apparent lack of attention to miracidial physiology in the literature, presumably due to the difficulties of experimentation on such small and short lived organisms. Surprisingly, however, functionally significant aspects of miracidial ultrastructure have been similarly neglected.

The ultrastructure of the miracidial body wall has been investigated in detail in only two species: Fasciola hepatica (Wilson, 1969a and 1969b; Wilson, Pullin and Denison, 1971; Southgate, 1970) and Schistosoma mansoni (Basch and DiConza, 1974; Meuleman, Lyaruu, Khan, Holzmann and Sminia, 1978). The structure of the body wall, however, is of particular functional significance. It is the physical and physiological interface with the external environment, it provides the locomotive mechanism for activity and is probably the main site for sensory interrogation of the environment.

The ultrastructure of the miracidial protonephridial system has been investigated only in F. hepatica (Wilson, 1967c and 1969c; Kummel, 1958). Yet this system probably mediates miracidial osmoregulation and excretion.

In an attempt to improve understanding of some of the functionally significant aspects of the structure of miracidia the present

investigation centres on an examination of the ultrastructure of the body wall and protonephridial system of Transversotrema patialense.

8.2 Materials and Methods

Eggs of T. patialense were collected and cultured at 25°C as described in Section 4.2. At 19 to 22 days after collection the eggs were observed around 12 noon and any newly emerged miracidia pipetted into 2.5% glutaraldehyde in cacodylate buffer at 4°C. Individual miracidia were then pipetted through the preparative solutions for T.E.M. (Section 2.8).

Miracidia were blocked out individually and the blocks trimmed to present the larvae in the correct orientation for transverse sectioning. Sections were cut and stained using the techniques described in Section 2.8.

8.3 Results

8.3.1 The miracidial body wall and associated structures

Descriptions of miracidial morphology utilise the nomenclature of Wilson (1969a) with the exception that "vesiculated cells" are considered together as a subepithelial layer of cell bodies (see discussion Section 8.4).

General

In terms of the structure of the body wall a miracidium may be considered to have two distinct regions: an aciliate apical papilla and a ciliated body region posterior to the papilla (Figure 8.1). The present investigation concerns the latter region only.

Figure 8.1: Schematic diagram of the miracidium of T. patialense. ap: apical papilla; ct: convoluted region of tubule; ec: ciliated epithelial cells; ep: excretory pore; fc: flame cell; ic: intercellular ridge; po: pigmented ocelli.

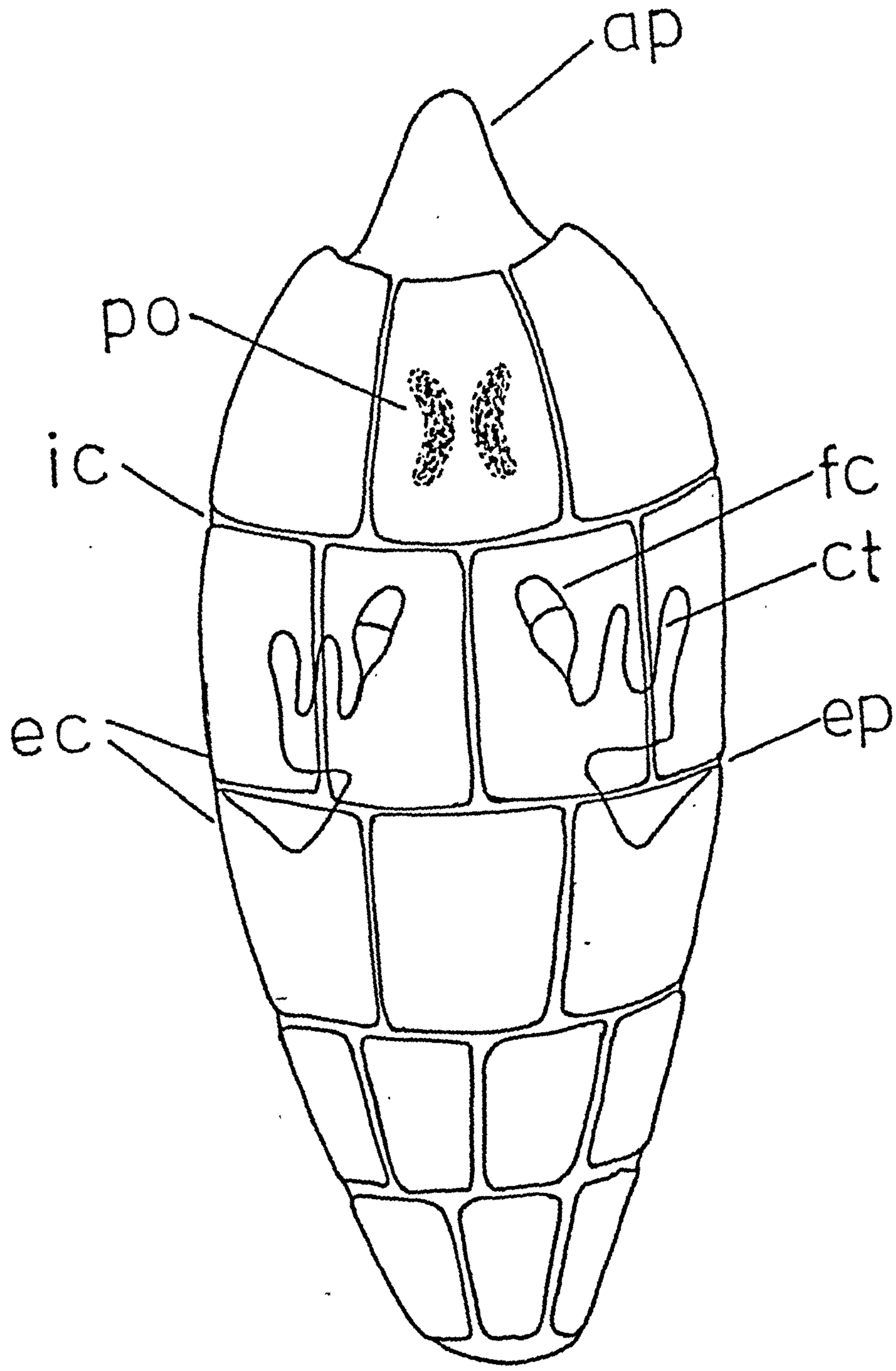
ap
po
ic
fc
ct
ec
ep

The miracidium, with the exception of the apical papilla, is invested with plate-like ciliated epithelial cells (Plate 2 and Figure 8.2). These flattened cells are not continuous over the whole surface but are separated along their lateral margins by prominent intercellular ridges (Southgate, 1970). Beneath the epithelial cells is a thin cytoplasmic layer which is connected both to the intercellular ridges and to a sub-epithelial layer of cell bodies. Subjacent to the thin cytoplasmic layer are the muscles of the body wall, outer circular and inner longitudinal. Beneath the muscle layers is the discontinuous sub-epithelial layer of cell bodies.

Epithelial Cells

The epithelial cells took the form of curved external plates approximately 1.2μm thick around the circumference of the miracidium. The number which encircled the larva varied with the region sectioned although the overall disposition of the plates was not accurately determined. Attachment of the epithelial cells to the remainder of the miracidium is achieved by two methods. Where the lateral surfaces of the cells contact the intercellular ridges the membranes of cell and ridge are joined by septate desmosomes (Plate 3a). The inner surface of the epithelial cells appears to attach irregularly to the thin cytoplasmic layer. The inner membrane of the epithelial cell is projected downwards at these points of attachment (Plate 3a and b).

The epithelial cell nuclei are situated against the inner membrane of the cells (Plates 4a and 5a). The nucleus is very electron dense and contains dense granules presumed to be condensed

Figure 8.2: The body wall of the miracidium of T. patialense.

a, Type A inclusion; cm, circular muscle; ec, epithelial cell; el, epithelial layer; ic, intercellular ridge; lc, locomotory cilium; lm, longitudinal muscle; mi, mitochondrion; mv, microvillus; n, nucleus; sc, sub-epithelial layer cell body; sd, septate desmosome; sl, sub-epithelial layer of cell bodies; tc, thin cytoplasmic layer; v, vesicular inclusions.

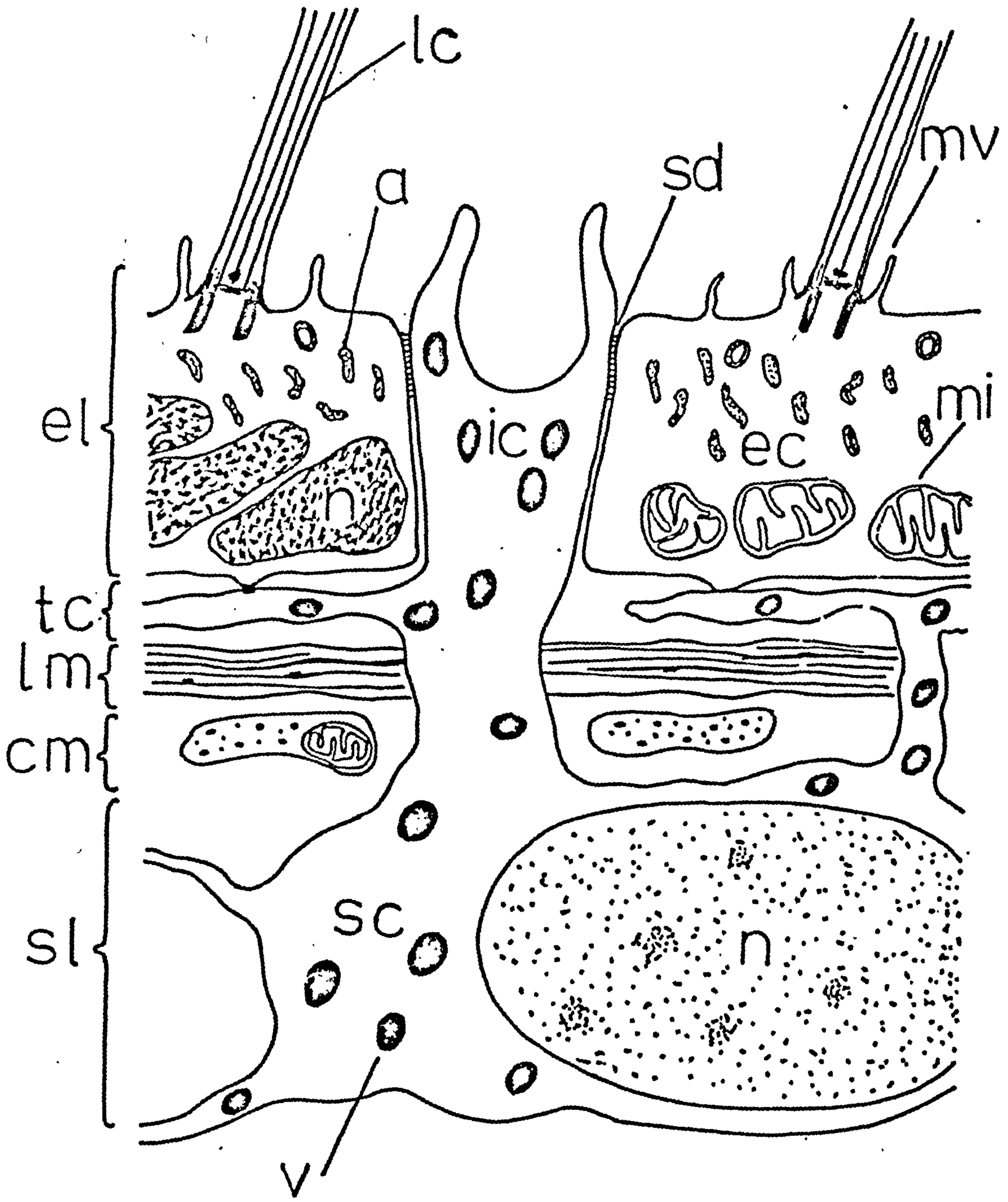
lc
a
sd
mv
el
ic
ec
mi
n
tc
lm
cm
sl
sc
n

chromatin. Since most sections showed several profiles of the nucleus within a single epithelial cell it is assmed that the nucleus is dendritic and extensive.

Locomotory cilia are present on the external surface of epithelial cells, as are 0.3μm microvilli (Plate 3a). Microvilli are present over the whole surface but are most numerous around the bases of cilia.

Mitochondria are present in the epithelial cells, generally forming a layer against the inner membrane (Plate 3a and 4b). Above this mitochondrial layer is a region containing electron dense inclusions. These inclusions, designated Type A, are irregular in shape and have an average size of 0.05 x 0.15μm (Plate 3a). They are often surrounded by electron lucent areas which may have been of artifactual origin. Associated characteristically with the outer membrane of the epithelial cells are electron dense rings of approximately 0.12μm diameter enclosing an electron lucent core (Plate 3a). On the basis of their position and conformation these were interpreted as transverse profiles of ciliary rootlets.

<u>Locomotory Cilia</u>

The cilia of the epithelial cells form a 6μm thick layer around the periphery of the miracidium (Plates 5a and 6a). The shaft or axoneme of each cilium has a typical 9 + 2 conformation of nine peripheral doublet microtubules and two central microtubules, and has an overall diameter of 0.17μm (Plate 3c).

The surface membrane of the cilium was not preserved intact by the T.E.M. procedures. Membranes of deeper structures, however, were well preserved suggesting that the fixative had penetrated efficiently. This result suggest either that ciliary membranes have a different sensitivity to fixation or that the surface structures degenerate more rapidly during the preparative procedures.

Figure 8.3 illustrates the structure of the basal body, or kinetosome, and the zone of transition to the axoneme. The kinetosome is covered by a dense matrix which extends up to the level of the epithelial cell outer surface. At this point the matrix extends laterally, to form a skirt around the base of the cilium, and vertically to form a membrane collar. Approximately half way up the kinetosome lumen a moderately electron dense band extends across the diameter for approximately 0.03μm. This is interpreted as a series of "proximal cartwheels". A ciliary rootlet projects laterally from the distal region of the kinetosome (Plate 4a).

The transition zone between kinetosome and axoneme is characterised by the presence of a band of electron dense material - the distal transverse plate - and a dense granule or axosome. The axosome is the origin of the central microtubules and is on average 0.18μm above the general level of the epithelial cell surface. This suggests that the locomotory cilia basal bodies are of Type II form (see discussion Section 8.4).

The ciliary root structure is at an acute angle to the insertion of the cilium (Plate 4a). The root is banded with repeating striations at 30 nm intervals.

Figure 8.3: Median longitudinal section of epithelial cell locomotory cilium.

A, axoneme; a, axosome; cm, ciliary membrane; ct, central microtubules; cr, ciliary rootlet; dt, distal transverse plate; ec, epithelial cell membrane; K, Kinetosome; km, kinetosomal matrix; mc, membrane collar; pc, proximal cartwheels; pt, peripheral microtubules; s, skirt; T, transition zone.

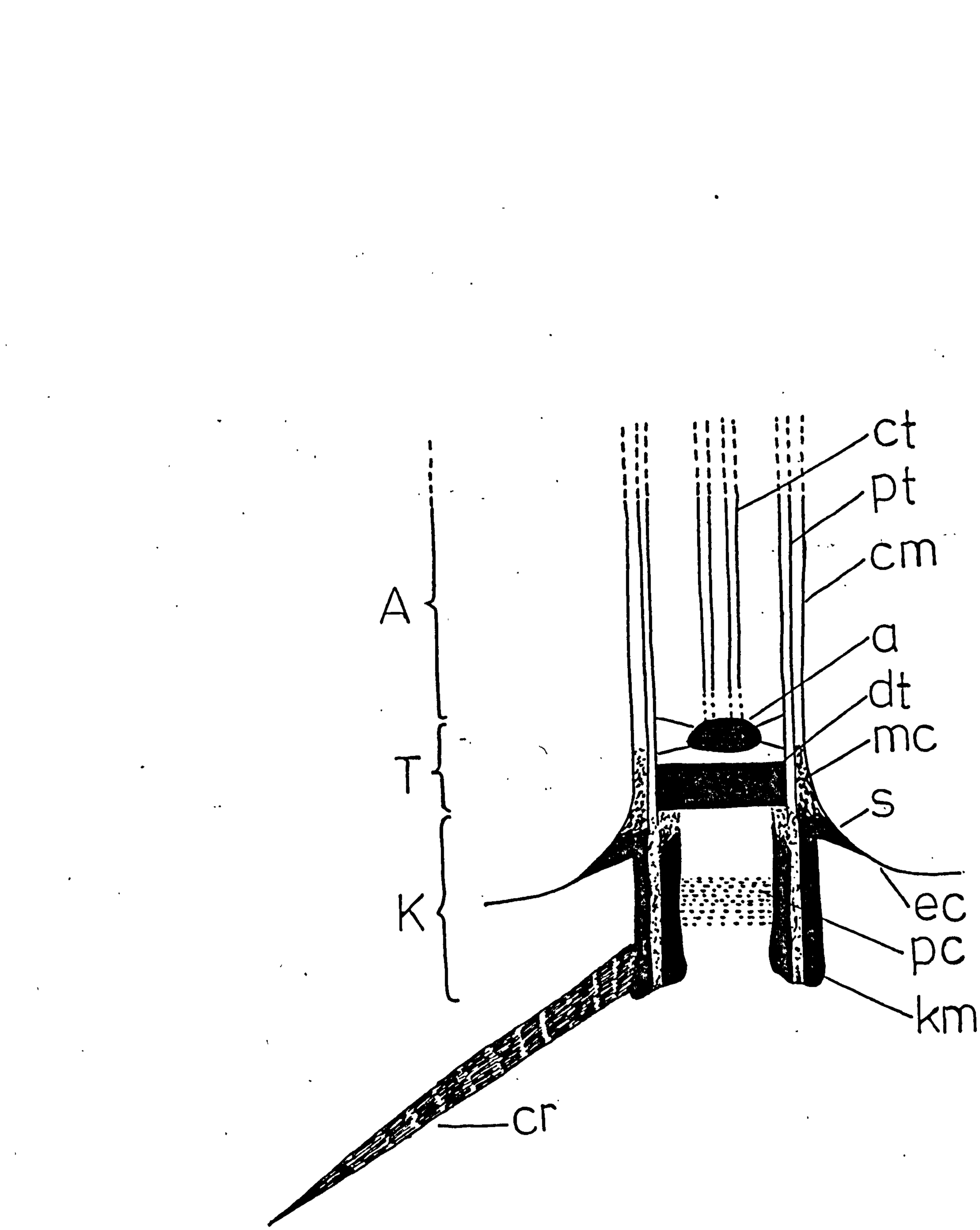
A
T
K
ct
pt
cm
a
dt
mc
s
ec
pc
km
cr

Intercellular ridges

A 0.7μm wide ridge of cytoplasm separates the epithelial cells (Figure 8.2 and Plates 2 and 3a). The epithelial cells are attached to these intercellular ridges by peripheral septate desmosomes along the external margins. The external surface of the ridges is not at the same level as the general surface of the epithelial cells but is invaginated approximately 0.6μm to form a "gutter" between adjoining epithelial cells.

The cytoplasm of the ridges is finely granular and characterised by the presence of electron dense membrane bound inclusions of approximately 0.17μm diameter. These are identical to those found in the sub-epithelial layer of cell bodies, to which the ridges are attached, and presumably derive from this region.

The intercellular ridges are the site of presumed sensory structures. Sensory endings are never observed within the epithelial cells.

Sensory structures

Three types of sensory structures were observed using TE microscopy: papillae, ciliary endings and ciliary eyes.

Papillae and ciliary endings are associated with the intercellular ridges while the ciliary eyes are located at a deeper level beneath the epithelial cell layer. All these sensory structures are found between the first and second tier of epithelial cells.

Papillae are illustrated in Plates 4a and 7a and Figure 8.4a. The terminal bulb is approximately 1μm in diameter and located within the intercellular ridge cytoplasm and entirely enclosed by

Figure 8.4: Superficial sensory endings of the miracidium of T. patialense.

a) Papilla.

b) Uniciliate ending.

c) Ciliate papilla.

cr, ciliary rootlet; ea, electron lucent area;

ec, epithelial cell, di, electron dense inclusion;

ir, intercellular ridge; nt, neurotubule;

rc, ridge collar; sd, septate desmosome;

se, sensory cilium; sr, septate desmosomal ring.

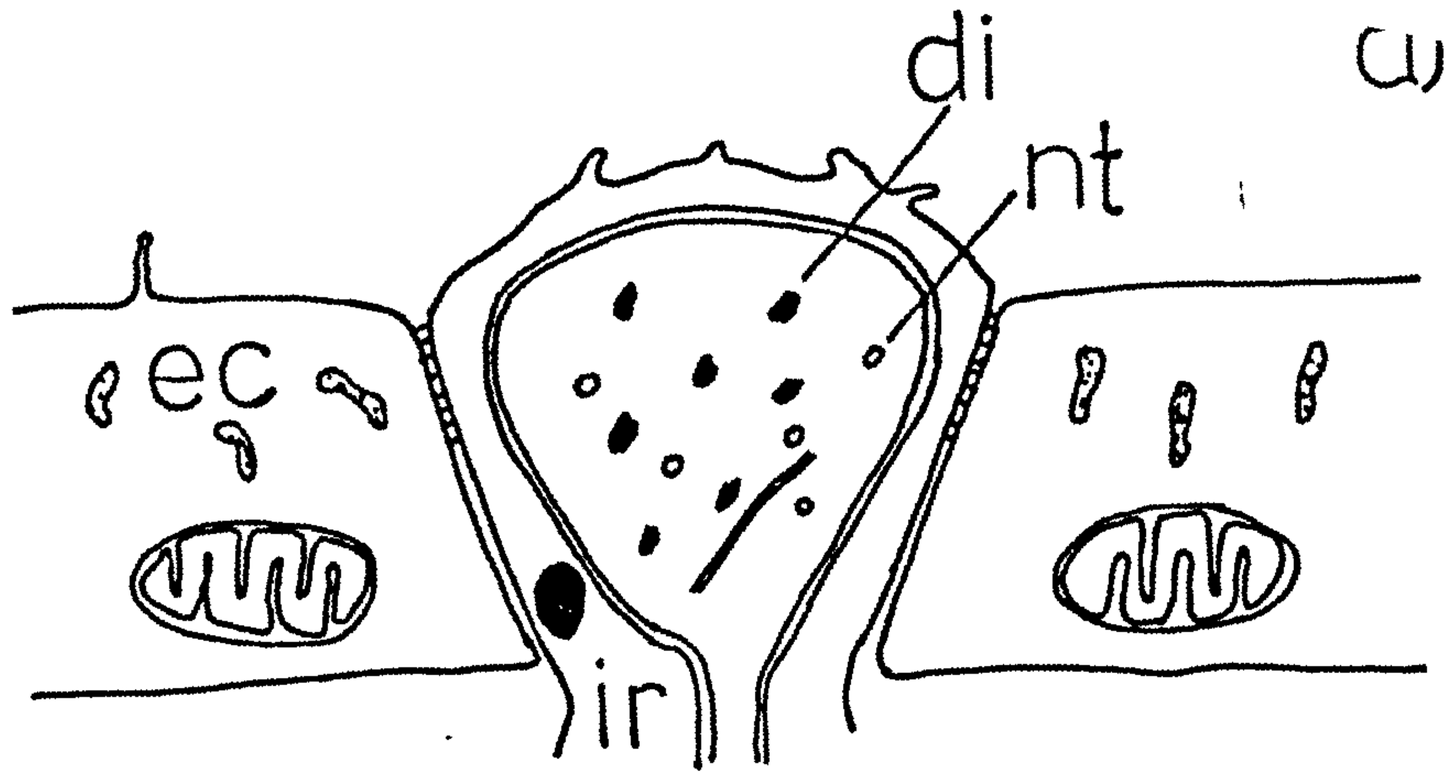

a)

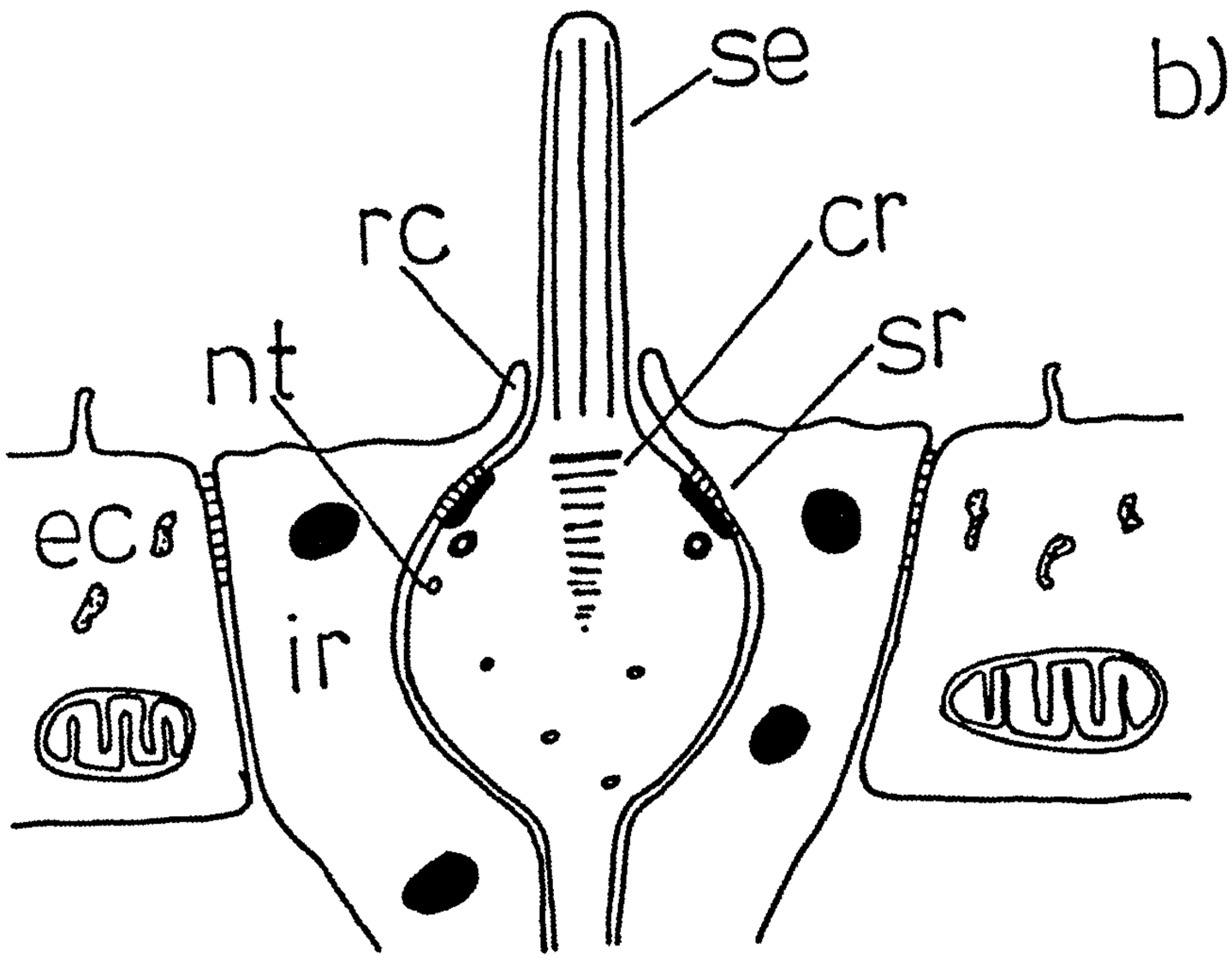

b)

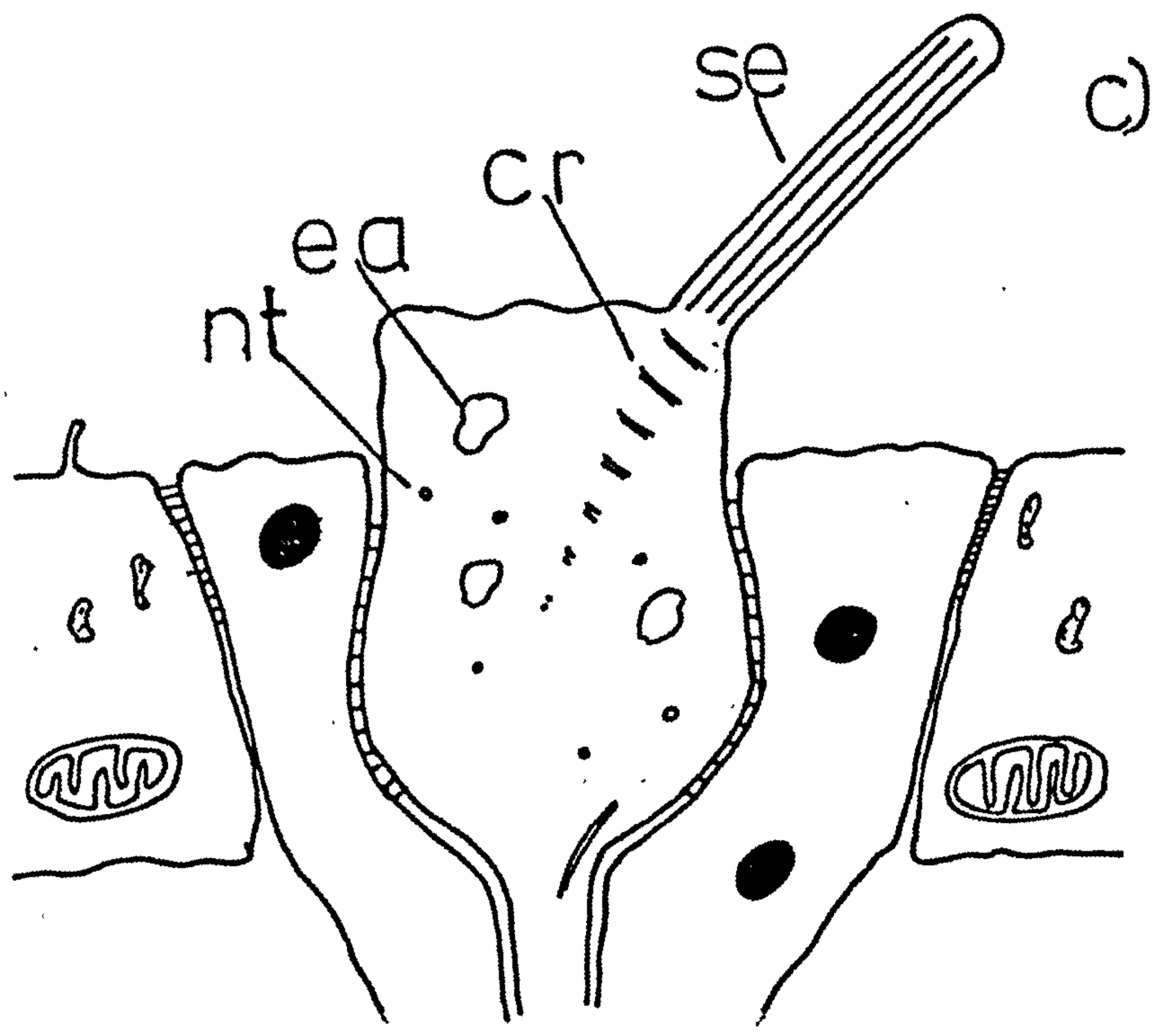

c)

it, except perhaps at the point of attachment of the sensory neurite. This has the effect of distorting the external surface of the intercellular ridge so that the surface projects above the general level of the epithelial cells. There is, however no direct contact between the bulb and the external medium, in the sections observed, due to the enclosing layer of ridge cytoplasm. There is a consistent gap of 25 nm between the membrane of the bulb and enveloping ridge with no evidence of a junctional complex between the two membranes.

The cytoplasm of the bulb is generally diffuse, with numerous electron lucent areas in a finely granular cytoplasm. Small (0.05μm) electron dens inclusions and neurotubules are also present.

The ciliated endings are of two types. In one form there is a single cilium attached to a bulb (0.75 x 1.25μm) situated within the intercellular ridge and surrounded distally by a collar of ridge cytoplasm (Plate 8 and Figure 8.4b). The bulb and ridge membranes are attached by a distal septate desmosomal ring. The 0.26μm diameter cilium has an apparently normal 9 + 2 axonemal complex. In the second form of ciliated ending the bulb (o.60 x 0.56μm) projects above the level of the adjacent epithelial cells (Plate 7 and Figure 8.4c). Ciliary endings of this type have been described as ciliate papilla (Brooker, 1972). The bulb membrane is attached to the ridge membrane by an extensive lateral septate desmosomal ring. The number of cilia present was not determined but the oblique orientation of the cilia suggests that several could be dispersed around the projecting portion of the bulb. All examples of ciliary endings of this type that have been observed have been located closely adjacent to papilla. The granular cytoplasm of the bulb contains irregular electron lucent

areas, neurotubules and at least one ciliary rootlet.

Located adjacent to papillae and ciliated endings, but below the epithelial cell layer, are structures (2.5 x 2μm) containing basal bodies and axonemes (Plates 4a, 6 and 7a). The basal bodies are inwardly directed from a thin peripheral rind of cytoplasm (Plate 6b). The axonemes had a 9 + 0 microtubular structure with a doublet ring diameter of 0.15μm. The central region of these lamellate structures contains a complex folded area of cytoplasmic projections, each projection appearing circular in cross-section. These sensory structures were interpreted as ciliary eyes.

The cytoplasmic projections were not discernable in Plates 4a and 7a either because the section passes through a densely cytoplasmic portion of the sensory structure or possibly because these are sections of a different form of sensory structure.

Thin cytoplasmic layer

Immediately beneath the epithelial cells is a layer of finely granular cytoplasm designated the thin cytoplasmic layer (Figure 8.2). This layer is diffuse and difficult to trace but appeared to form a zone of separation between the epithelial cells and the underlying circular muscles.

Occasionally the thin cytoplasmic layer became thickened and contained electron dense membrane bound vesicles identical in size to those found in the intercellular ridges (Plate 3a). Tenuous connections could also be traced to the underlying sub-epithelial layer of cell bodies which gave rise to the intercellular ridges. It appears, therefore, that the thin cytoplasmic layer, the

intercellular ridges and the sub-epithelial layer are in cytoplasmic communication.

Muscle layer

Beneath the thin cytoplasmic layer are the muscles of the body wall (Figure 8.2). These consist of an outer layer of circular and an inner layer of longitudinal muscle fibres each of approximately 0.4 μm diameter (Plate 3b).

The cytoplasm of the muscle fibres is granular and contains aggregates of electron dense material presumed to be glycogen. Large mitochondria are located peripherally but no nuclei are observed.

The fibres have a characteristic content of thick and thin myofilaments (Plate 3b). No banding or striations are discernable. The thick filaments have a diameter of 20 nm and the thin filaments 5 nm.

The outer circular muscle fibres have irregular connections to the thin cytoplasmic layer, apparently consisting of tight junctions of closely applied unit membranes (Plate 3b). No other connections between muscle fibres or between fibres and other cells were observed.

The sub-epithelial layer of cell bodies

The sub-epithelial layer cell bodies are in cytoplasmic continuity with the thin cytoplasmic layer and intercellular ridges (Figure 8.2). Transverse sections through the miracidium at successively more posterior positions showed that the sub-epithelial layer is present throughout the length of the miracidium (Plates 2, 6a and 5a). In some regions the nucleate cell bodies form a

discontinuous ring around the periphery (Plate 6a). Nucleate flame cell bodies occasionally interupt this peripheral ring (Plate 5a).

8.3.2 The protonephridial system

The description presented here utilises the nomenclature of Wilson (1969c).

Under light microscopical observation the protonephridial system is seen to be paired (Figure 8.1). A flame cell is situated on either side of the body one third distant from the anterior end of the miracidium. The head of the flame cell is directed anteriorly and a tubule runs posteriorly from the tapered tip. Proximal to the flame cells the tubules are greatly convoluted but became straightened posteriorly. At about two thirds distance from the anterior of the miracidium the tubules bend abruptly towards the lateral margin of the larva and open to the surface at two lateral excretory pores.

Miracidial sections examined using TE microscopy revealed the structure of the flame cells and tubules. Unfortunately, no sections were cut whose plane ran through the excretory pores and hence their structure was not observed.

The head of the flame cell consists of a nucleated cell region from the cytoplasm of which arises the ciliary flame (Plate 5b). The nucleus is large and the cytoplasm contained generally distributed mitochondria.

The cytoplasm of the nucleated cell appears to be drawn into thin projections, or "inner ribs", which extend posteriorly around

the ciliary flame (Plate 5b). From the inner ribs arise cytoplasmic extensions or leptotriches. Surrounding the inner ribs, and joined to them by desmosomes, are outer ribs. There are apparently no leptotriches associated with the outer ribs. The orientation of the sections through the present material did not allow unambiguous interpretation of the origin of the outer and inner ribs.

The tubules of the protonephridial system contain large nuclei proximal to the flame cells. The tubule cytoplasm is granular and contained mitochondria (Plate 9a). The tubules are formed by two flaps of cytoplasm projecting peripherally from the tubule cell and joined together with a desmosome to enclose a lumen (Plate 9b).

More posteriorly the nucleate tubule cell bodies are absent. The tubules are simple tubes with a cytoplasmic wall and desmosomal "seam" running across from the lumen to the external surface (Figure 8.5). The luminal surface is drawn into thin projections enclosed in the trilaminate plasma membrane of the tubule wall (Plate 10).

In some sections two desmosomal seams were present in the tubule wall (Plate 10a). There are two probable explanations for this phenomenon. Firstly, this may represent a zone of transition from one tubule cell to the next since it is at present unknown whether the tubule system is composed of one or several cells. In the latter case the cells may be connected by desmosomes. Secondly, the double seam may arise due to the plane of the section. If the plane of the section were to cross the apex of a tubule convolution the resulting section would contain two parts of the same desmosomal seam (Figure 8.5). It was not possible to determine whether or not the present result was the result of a sectioning

Figure 8.5: Schematic representation of protonephridial tubule convolution of T. patialense miracidium Section along AA produces double seam appearance. Section along BB produces single seam appearance (see text).

ds, desomosomal seam; lu, protonephridial tubule lumen.

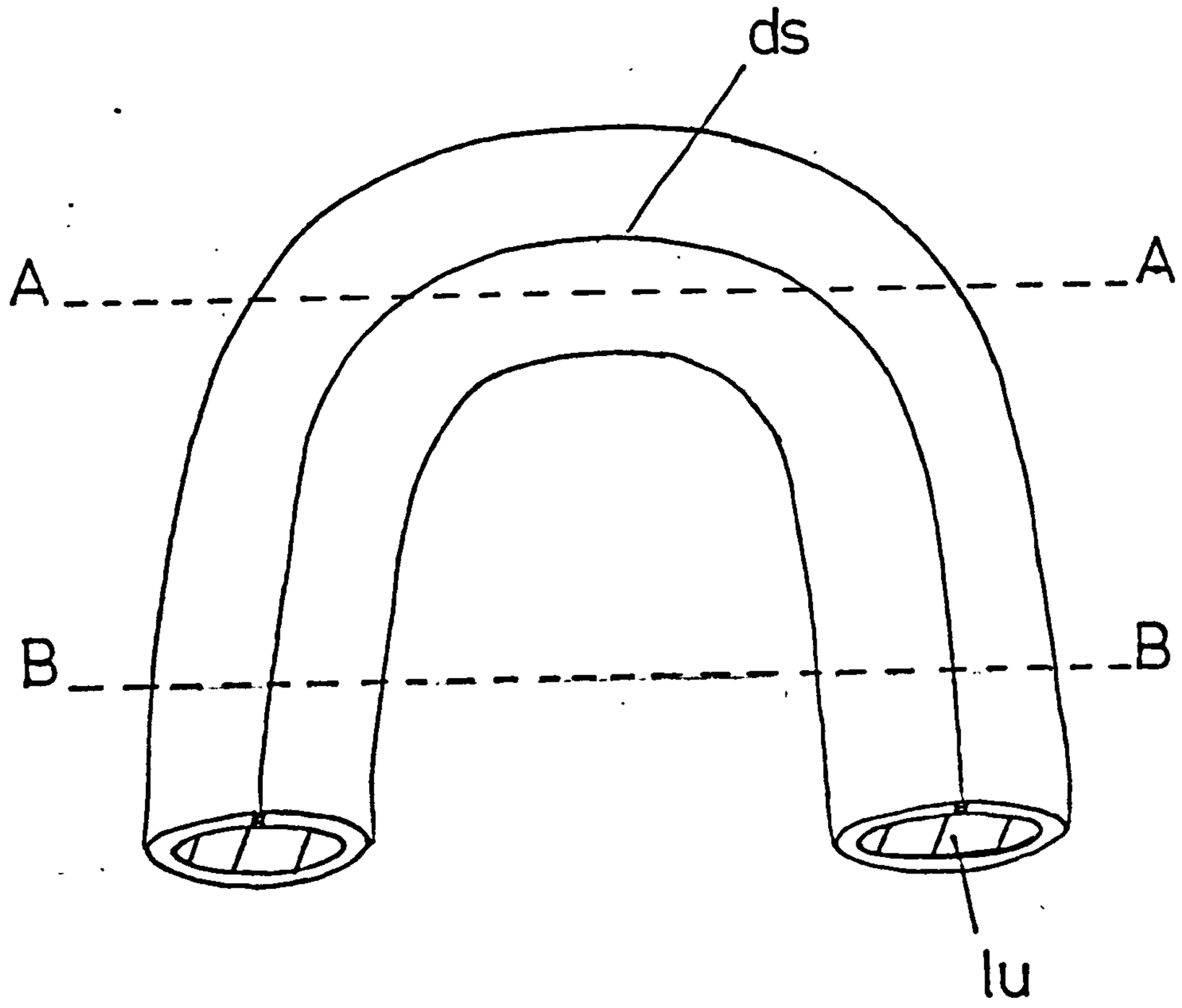
ds
A
A
B
B
lu

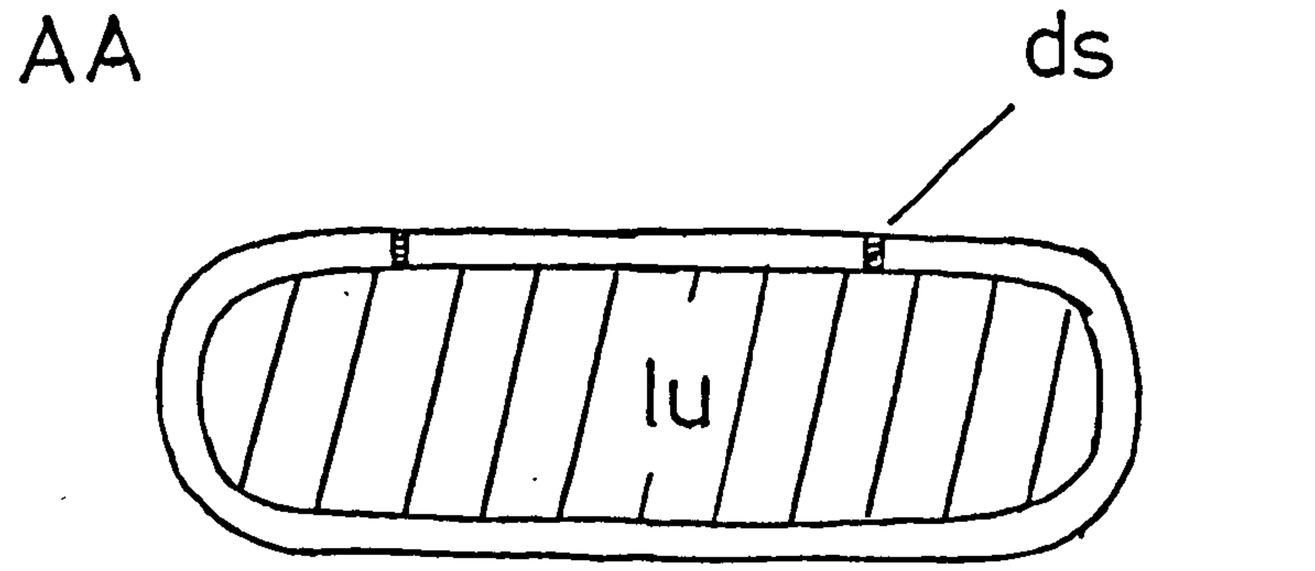
AA
ds
lu


BB
ds
lu

artefact.

The inclusion of two transverse profiles in the tubule section shown in Plate 10a is likely to be due to the section passing through the tubules in an area of convolution.

8.4 Discussion

The work of Southgate (1970) and Wilson et al. (1971) on Fasciola hepatica and that of Basch and DiConza (1974) and Meulemann et al. (1978) on Schistosoma mansoni has elucidated the developmental changes that occur in the body wall during the transition from miracidium to sporocyst. The important feature of this phase is that the cellular epithelium is lost and replaced by a syncytical tegument. The tegument of the sporocyst apparently arises from the confluence of previously discontinuous regions, the thin cytoplasmic layer and the intercellular ridges, material being provided by the sub-epithelial layer of cell bodies. Because of the apparent continuity of the intercellular ridges it is likely that, even at the miracidial stage, the sub-epithelial layer cell bodies are in cytoplasmic connection and therefore form a syncytium. It is because of this syncytial nature, and the fact that many other unrelated cell systems contain vesicular inclusions, that the term "sub-epithelial layer cell bodies" (Southgate, 1970) is preferred to "vesiculated cells" (Wilson, 1969a) in the present discussion.

The fate of the epithelial cells during the miracidium - sporocyst transformation apparently show species - specific variation. In Fasciola hepatica miracidia the epithelial cells

are nucleate and superficial and are shed during molluscan penetration (Wilson, 1970; Southgate, 1970; Wilson et al., 1971). Wright (1971), referring to unpublished work of Brooker, and Hockley (1973) claimed that the epithelial cells of Schistosoma mansoni miracidia are not designed to be shed. The in vitro studies of Basch and DiConza (1974) showed that shedding can and does occur, and Meuleman et al. (1978) demonstrated that this happened after the miracidium had penetrated its snail host.

The early doubts about the feasibility of epithelial cell loss in S. mansoni miracidia were stimulated by Brooker, in personal communications to Wright (1971) and in a later publication (Brooker, 1972), when he described the epithelial cells as "superficial extensions of a deeper cell". Meuleman et al. (1978) also described the epithelial cells of S. mansoni miracidia as being "joined by cytoplasmic projections to nucleated parts below the muscle layers" but did not explain how these connections were severed during their observed cell shedding.

This arrangement is entirely different from that of Fasciola hepatica and Transversotrema patialense miracidia. In these species the epithelial cells are themselves nucleate and are an entirely superficial component of the body wall. Unfortunately, neither Brooker (1972) nor Meuleman et al. (1978) published photographic evidence of cytoplasmic connectives or supposed epithelial cell bodies. In the light of the profound evolutionary and functional significance of such a major difference in miracidial structure more detailed studies of the apparently anomalous condition in schistosome miracidia are required.

The epithelial cells of T. patialense miracidia contain inclusions (Type A) that resemble the lysosome-like structures (Basch and DiConza, 1974) and membrane bound bodies (Wikel and Bogitsh, 1974) of S. mansoni miracidia. Fasciola hepatica miracidial epithelial cells differ from both these species in possessing only a very few moderately dense inclusions (Wilson, 1969a; Southgate, 1970).

Basch and DiConza (1974) suggested that the lysosome-like structures could autolyse the epithelial cells after shedding. Meuleman et al. (1978), however, failed to detect acid phosphatase within the inclusions and observed that the shed epithelial cells were not autolysed but were phagocytosed by molluscan amoebocytes. On little apparent evidence they suggested that the inclusions were degenerate mitochondria.

The surface topography of the intercellular ridge also appears to show species - specific variation. In F. hepatica the ridges have flat external surfaces at the same level as the epithelial cell outer surface (Wilson, 1969a; Southgate, 1970). In S. mansoni the ridge is extended into long granule-laden filaments (Basch and DiConza, 1974). T. patialense miracidia have a third form of intercellular ridge, in this case the ridge is deeply invaginated to form a gutter running between the epithelial cells.

Basch and DiConza (1974) suggested that the ridge filaments of S. mansoni serve to aid contact-recognition between trematode surface and molluscan cells, necessary in S. mansoni to carry "surface-active granules" beyond the periphery of the unshed epithelial cells at penetration. These authors did not explain the necessity for host recognition after penetration was initiated nor did they demonstrate that the ridge filaments extended beyond

the dense mat of locomotory cilia to contact the molluscan cells.

In T. patialense miracidial penetration of the molluscan host results in the production of a sporocyst stage (Section 9). Changes in the body wall during this transformation were not observed but because the morphology of the miracidial body wall closely resembles that of other species it is assumed to transform in a similar manner to those previously described (Southgate, 1970; Wilson et al., 1971).

The fine structure of the locomotory cilia of miracidia has been described in detail only for Fasciola hepatica (Wilson, 1969a). The locomotory cilia of T. patialense miracidia differ in only two minor respects. In F. hepatica the distal transverse plate is perforated by a central apperture which appears to be absent in the present species. The second difference concerns the kineto-somal lumen. In T. patialense miracidia it is suggested that a series of "proximal cartwheels" serve to form a filamentous connection between the triplet microtubules of the basal body. No equivalent structure was described in F. hepatica miracidia. All the ciliary components described have been reported from cilia of other organisms although not necessarily in the same combination.

The basal bodies of cilia may be of Type I or Type II (Pitelka, 1974). In Type I basal bodies the origin of the central microtubules projects less than 0.1 μm above the general level of the cell surface from which the cilium arises. In Type II basal bodies this difference is around 0.2 μm. Evidence from known ciliary types suggests that Type I basal bodies are characteristic of birds and mammals while Type II basal bodies are found in a wide

range of taxa. The locomotory cilia of T. patialense miracidia are apparently of Type II. The fine structure of cilia has been described for relatively few platyhelminths but in every case, namely Fasciola hepatica miracidia (Wilson, 1969c), adults of five species of acoelous turbellaria (Dorey, 1965) and the endoparasitic neorhabdocoel Kronborgia amphipodicola (Bresciani and Koie, 1970) were of Type II.

The uniciliate sensory endings of T. patialense miracidia are similar to those described for miracidia of other species. In Fasciola hepatica the ciliated endings have a tubular sheath of cytoplasm, with extensive superficial corrugations, around the proximal region of the sensory cilium (Wilson, 1970). A sheath was also present around the sensory cilium of Schistosoma mansoni (Brooker, 1972) and T. patialense, but lacked the superficial corrugations.

The ciliate papillae closely resemble the dorsal papillae of Diplostomum spathaceum (Brooker, 1972).

The aciliate papillae of T. patialense are different from the lateral papillae described from other species. Schistosoma mansoni and Diplostomum spathaceum miracidia have bulbous endings characterised by the presence of numerous electron lucent vesicles with an electron dense periphery (Brooker, 1972). Fasciola hepatica miracidia have an apparently unique double papillary structure with two closely adjacent bulbous endings (Wilson, 1970). The smaller of these paired endings resembles that of T. patialense miracidia.

These sensory endings of T. patialense miracidia were all located in the intercellular ridges of the epithelial cell covered

posterior region. The apical papilla was not examined but it is almost certain that this region possesses sensory structure of different form and function. Regional specialization of this type has been recorded from T.E.M. and S.E.M. observations of other species (Wilson, 1970; Brooker, 1972; Kinoti, 1971; Koie and Frandsen, 1976; Koie, Christensen and Nansen, 1976; Blankespoor and Van der Schalie, 1976).

Due to the small size of these superficial sensory structures it is extremely difficult to demonstrate their function by direct means, however, comparison of their morphology with that of proven sensory structures in other organisms may provide some indication of their function.

Uniciliate receptors have been recorded in larval and adult digeneans where they are generally considered to function as mechanoreceptors (Dixon and Mercer, 1965; Erasmus, 1967; Brooker, 1972; Matricon-Gondran, 1971). This function is ascribed on the basis of morphological similarity to sensory endings in other invertebrates (Wilson, 1970; Gray, 1960).

There is, however, some dispute as to the function of papillae. Wilson (1970) argues that the lack of direct contact between bulb and external environment precludes a sensory function and suggests instead that the papillae are either secretory, after rupture of the cytoplasmic sheath, or some early stage in the development of a sensory ending. The former of these suggested functions would appear unsatisfactory because the presence of an apparent sensory neurite and neurotubules associated with papillae (Wilson, 1970; Brooker, 1972) argues strongly for a sensory function. In

Diplostomum spathaceum, Fasciola hepatica and Schistosoma mansoni each lateral papilla is situated adjacent to a sensory cilium (Brooker, 1972) and a similar arrangement is present in T. patialense miracidia. Rees (1940) noted that the lateral papilla of Parorchis acanthus miracidia are capable of considerable extension, and it has been suggested that the extended lateral papilla could impinge upon the sensory cilium providing information on miracidial orientation and acceleration (Brooker, 1972). The presence of some form of gravity receptor is indicated by behavioural studies which suggest that miracidia are responsive to gravity (Wilson and Denison, 1970).

In T. patialense it is the protruberant ciliate papilla which is associated with the papilla. Ciliate papilla of this form are believed to be chemoreceptors on the basis of their structural similarity to the olfactory receptors of vertebrates (Brooker, 1972). It seems improbable that the ciliate papilla of T. patialense would function both as a chemoreceptor and, in conjunction with the papilla, as a mechanoreceptor but its true role cannot be decided on present evidence.

Bodies with an organisation similar to the lamellate structure adjacent to the sub-epithelial layer of cell bodies in T. patialense miracidia have been previously recorded in the miracidia of Schistosoma mansoni and Diplostomum spathaceum (Brooker, 1972), the oncomiracidia of Entobdella soleae (Lyons, 1972), and the cercariae of Schistosoma mansoni (Short and Gagne, 1975). In all these larvae the structure was interpreted as a light sensitive ciliary eye. Wilson (1970) describes a similar structure in the miracidium of Fasciola hepatica, but he considers it to be a "club-shaped ending" possibly functioning as a gravity receptor. However,

the morphological similarity between these structures and the proven photoreceptors of molluscs and annelids makes light detection the most likely interpretation of function (Lyons, 1972).

Light microscopical examination of the miracidium of T. patialense shows that paired ocelli with pigment cups are present. These appear to be of similar form to those described for other miracidia (Isseroff and Cable, 1968; Brooker, 1972). Unfortunately they were not observed in sections prepared for T.E.M.

The presence of two types of photoreceptors in a miracidium suggests that they have different functions. Pigmented rhabdomeric eyes are believed to provide information on the direction of incident light (Isseroff and Cable, 1968). In a natural aquatic habitat surface water will always be better illuminated than deeper layers and hence a miracidium could orientate itself using the pigmented ocelli. Ciliary eyes in molluses respond to decreasing illumination, the "off" response, which is a component of protective shadow responses on the part of the organism (Land, 1968). Lyons (1972 and 1973), however, points out that it is unlikely that all ciliate photoreceptors signal shadowing, and suggests instead that the ciliary eyes of Entobdella soleae oncomiracidia may act as a long term photoreceptor involved in temporal control of the egg hatching rhythm (Kearn, 1973). This hypothesis is particularly attractive in relation to the function of ciliary eyes in T. patialense miracidia since, as previously described (Section 6), the temporal distribution of egg hatching in this species also exhibits circadian rhythmicity with light acting as the postulated zeitgeber.

Schistosome miracidia also posess ciliary eyes, yet changes in

light intensity do not induce any discernable hatching rhythm in schistosome eggs but instead increasing illumination acts as an almost instantaneous hatching trigger (Standen, 1951; Wilson, 1968). Furthermore, schistosome miracidia exhibit phototaxis (Chernin and Dunavan, 1962) despite the absence of rhabdomeric eyes. These results suggest that the ciliary eye is more versatile than was supposed, and indicate the need for further studies on photoreceptor function.

The protonephridia of T. patialense and Fasciola hepatica miracidia differ only superficially in structure. In F. hepatica the perinuclear cytoplasm is characterised by a peripheral ring of mitochondria and generally distributed granular vesicles (Wilson, 1969c). In T. patialense the mitochondria were not confined to a particular region and granular vesicles were not apparent.

Kummel (1958) described fine cytoplasmic processes covering the nucleated region of the flame cell of Fasciola hepatica miracidia. These were not observed by Wilson (1969c) in the same species nor were they apparent in T. patialense miracidia.

The flame cell cytoplasm of Fasciola hepatica miracidia extended into inner ribs surrounding the ciliary flame and these were connected by desmosomes to outer ribs extending from the tubule cell cytoplasm (Wilson, 1969c). The origins of the inner and outer ribs were not determined for the present species.

Both inner and outer ribs of the protonephridia of Fasciola hepatica miracidia and the cyrtocytes of priapulid worms are covered with thin cytoplasmic extensions or leptotriches (Kummel, 1964; Wilson, 1969c). Leptotriches were only present on the inner

ribs of T. patialense miracidial protonephridia.

It is unfortunate that this morphological familiarity with protonephridia has not been complemented by a better understanding of their physiology. Attempts to elucidate the function of the protonephridial system have as yet proved relatively unsuccessful. Wilson (1967b) was unable to demonstrate any relationship between the flame cell activity of Fasciola hepatica miracidia and the osmotic pressure of the external medium, although flame cell activity of mature miracidia within the egg capsule increased markedly as a prelude to hatching (Wilson, 1969c).

An interdigitating mass of supposed parenchyma cells are present in the core of the miracidium of T. patialense and Fasciola hepatica (Wilson, 1969a). In the cells of both species glycogen granules are present, the cells presumably acting as a glycogen storage site. As previously described (Section 7) the miracidial mortality rate has an exponential age-dependent form compatible with progressive exhaustion of available nutrients. In F. hepatica miracidia there is a decrease in glycogen content from 15% of dry weight to zero over the active life of the organism (Horstmann, 1962). It is assumed that this decrease corresponds to depletion of glycogen levels within the parenchyma cells.

In conclusion, it appears that miracidial ultrastructure exhibits a fundamental homogeneity among the species described to date. The only major difference concerns the relationship of the epithelial cells to underlying structures. The presence of connectives to epithelial cell bodies in Schistosoma mansoni miracidia requires confirmation and the fate of these connectives during epithelial

cell loss must be clarified. It is to be hoped that a more thorough understanding of these and other miracidial structures will ultimately lead to comprehension of the functions to which they relate.

SECTION 9:

INTRAMOLLUSCAN DEVELOPMENT

9. Intramolluscan Development

9.1 Introduction

In nearly all digenean life cycles a mollusc serves as the first intermediate host, a miracidium establishing an infection which eventually results in the production of numerous cercariae infective to subsequent hosts.

Digenean intramolluscan larval development was first described nearly a century ago by Leuckart and Thomas. While opinions have varied there is still no coherent concept of the factors controlling the development patterns of the multiplicative intramolluscan larval stages.

The present investigation attempts to describe quantitatively the intramolluscan development of Transversotrema patialense in the cerithiacean mollusc Melanoides tuberculata. The technique adopted was to infect molluscs and determine the changes in intramolluscan larval population parameters during the development of the infection.

9.2 Materials and Methods

9.2.1 Early development

Eggs were collected and incubated at 25°C as described in Section 5. 19 to 22 days after collection the eggs were observed and miracidia removed as they emerged.

Individual uninfected Melanoides tuberculata in 100 ml of conditioned water were exposed to 20 miracidia overnight. The snails were transferred to a maintenance tank (Section 2.2) and

kept for 7 days at 25°C before being prepared for histochemical examination.

The shell was dissected from the snail and the body tissues fixed in formal acetic alcohol for 24h. The fixed material was embedded in wax and transverse serial sections cut of the entire mollusc. Slide mounted sections were stained using Cason's stain, dehydrated and mounted in Canada Balsam.

The serial sections were examined for evidence of early intramolluscan larval stages.

9.2.2 Time course of the development of intramolluscan stages

100 uninfected snails of similar size (initial shell whorl diameter 3-5 mm) were acclimated to a maintenance tank at 25°C (Section 2.2). Eggs of T. patialense were indirectly introduced into the tank over a 14 day period by the addition of fifteen infected Brachydanio rerio for this period of time.

Previous results (Sections 6 and 7) indicated that at 25°C miracidial hatching occurs over a period of six days, from 17 to 23 days after emergence of eggs from the fluke, and that miracidial survival and presumably infectivity is of short duration. It was assumed, therefore, for the purposes of the present investigation that the molluscs would be exposed to infective miracidia for a period of twenty days. That is from 17 days (eggs deposited on the first day developing in 17 days) to 37 days (eggs deposited on the fourteenth day developing in 23 days) after the introduction of the infected fish. The median time of possible molluscan infection was therefore 27 ± 10 days after the fish were introduced.

60 and 95 days after the introduction of the fish (33 ± 10 and 68 ± 10 days post possible infection (PPI)) five snails were dissected and the level of infection assessed as described below.

From day 100 after the introduction of the infected fish (73 ± 10 days PPI) all the snails present were examined for cercarial release. Twice weekly the molluscs were placed separately in individual specimen vessels of tank water at 25°C and kept in the dark for one hour. Any emergent cercariae were readily observable using oblique illumination.

When a previously refractory snail was found to produce cercariae the mollusc was dissected and the level of infection assertained as shown below. Four snails were examined on their first day of observed cercarial production.

Within one period of eleven days three snails began to emit cercariae. These three molluscs were isolated in a separate maintenance tank for a further 60 days before dissection. The snails were, therefore, examined at 185 ± 13 days PPI.

In all the above examinations the level of molluscan infection was assessed in the same manner after the snails had been dissected according to the procedure described in Section 2.7.

All intramolluscan cercariae were pipetted onto vaseline ringed slides, small numbers being mounted on each slide to facilitate subsequent examination. All intramolluscan rediae were similarly mounted but in this case individual larvae were mounted in separate vaseline rings.

Slides of larvae were scanned at 100 X magnification and each larva encountered was measured using an eye-piece micrometer. The characteristics measured were different for the two larval forms.

With cercariae measurement was made along the long axis from the anterior tip of the body to the furcal cleft at the distal region of the tail. Specimens were measured at 100 X or 250 X magnification, the dimensions of the specimen dictating the most convenient scale.

Two factors complicated this procedure. Firstly, the movements of the larvae prevented accurate measurement in the fully extended position. Measurements were therefore estimated with an accuracy of $\pm$ 2.5 eye-piece micrometer units, equivalent to $\pm$ 25μm at 100 X and $\pm$ 10μm at 250 X magnification. Secondly, some cercariae shed their tails during the preparative phase. From measurements of body length and tails plus body length on twenty intact cercariae a correlation between body and overall length was obtained, allowing an estimate of cercarial length from body length measurements alone (Table 9.1).

Redial measurements were made of length and width of rediae. Because of the sluggish movements of the rediae it was not possible to obtain a measurement at maximum contraction or extension without protracting the period of observation. Hence the product of length and width was used as a compromise measure of redial dimensions.

This compound figure allowed for relative variation in width and length due to extension and contraction, and permitted comparison of the size of rediae in different configurations. The values are expressed in arbitrary units where one arbitrary unit = $10^3 \mu m^2$.

TABLE 9.1

Use of regression to determine overall cercarial length from body length measurements

SAMPLE DATA

OVERALL LENGTH (x) (μm)	BODY LENGTH (y) (μm)
190	114
209	114
247	133
266	114
285	114
304	138
323	133
342	152
361	171
380	176
485	144
533	144
582	226
630	194
679	242
727	291
776	242
873	242
921	291
970	291

Linear regression model:

$$y = a + xb$$

where:

a = intersect of regression line
= 68.3615
= slope of regression line
= 0.2379

hence:

$$x = (y - 68.3615)/0.2379$$

After measurement rediae were examined at 400 X magnification for the presence of intra-redial larvae. If larvae were present the cover slip was lifted and the redia pipetted into fresh Sorensen's phosphate buffer (Section 2.7) on another vaseline ringed slide. Using fine needles the redial wall was incised and internal larvae drawn out. A cover slip was replaced and the slide scanned at 250 X magnification.

Intra-redial larvae were only included in this analysis where they could be absolutely identified as cercariae or rediae. An intra-redial redia was characterized by dimensions of approximately 150 x 40μm (equivalent to 6 arbitrary units), motility and the possession of a pharynx. An intra-redial cercaria in contrast was characterized by a longitudinal measurement of approximately 120μm, the possession of a protruberant pimordial ventral sucker and a bifurcating tail region. Very immature intra-redial larvae which were insufficiently differentiated to accord with either of the above descriptions were not included in the results.

9.2.3 Period of development of infection

Fifteen of the snails infected during the experiment described in Section 9.2.2 were isolated from the maintenance tank on day 80 $\pm$ 10 PPI. These molluscs were maintained separately under the conditions described.in Section 2.2.

At approximately weekly intervals individual molluscs were placed in specimen vessels of aquarium water at 25^{o}C and kept in the dark for one hour. Emergent cercariae were observable by oblique illumination.

The age of the infection in days PPI was noted for each snail when cercariae first emerged under the above conditions. The experiment was terminated at 160 ± 10 days PPI.

9.3 Results

9.3.1 Early development

Serial sections of snails seven days after exposure to miracidia revealed the presence of sporocysts within the muscular tissues of the foot (Plate 11). The sporocysts were approximately 60 μm long and 30 μm wide and retained the paired pigmented ocelli (5 μm diameter) of the miracidium. Large cells with distinctive nucleoli were present in the posterior portion of the larva. These were presumed to be germinative cells.

The epithelial cells of the miracidial stage were absent from the surface of the sporocyst and there was no evidence of the cells in the adjacent molluscan tissue. No snail tissue reaction to the sporocyst was apparent.

9.3.2 Time course of the development of intramolluscan stages

9.3.2a Observations at known intervals during the development of the intramolluscan larval stages

In addition to the above mentioned sporocyst two larval forms were found within the snail host.

Rediae (Plate 12) had a pharynx and sac-like intestine, the remainder of the internal volume of the larva being occupied by free cells, cellular masses or developing intra-redial larvae. The rediae were characteristically active, displaying locomotion by the

production of body wall peristaltic waves, and were very variable in size.

Cercariae showed a considerable range of morphological variation associated with their size (Section 10). It was assumed that the cercariae underwent growth and differentiation within the molluscan host and that the smaller and morphologically less differentiated forms were at an early stage in development.

The larvae within the molluscan host were considered to conform to the following categories. Firstly, rediae of variable size but otherwise morphologically similar. Secondly, intra-redial larval forms contained within the rediae. These forms consisted of unidientifiable early stages in larval development, intra-redial cercariae and intra-redial rediae. Thirdly, cercariae free in the snail tissues displaying considerable variation in size and a corresponding degree of differentiation from immature to fully developed for emergence from the host.

Intra-redial larvae were observed to emerge from rediae via a birth pore situated about one third of the body length from the anterior end. These emergent larvae corresponded in size and morphology to the most differentiated intra-redial cercariae and intra-redial rediae and also to the least developed rediae and cercariae.

9.3.2b Location of intramolluscan larval stages

Table 9.2 lists the age of the infection in days PPI on which snails were examined. The nature of the developing larvae was, therefore, determined before, during and after the period of infection at which cercariae first emerged from their hosts.

TABLE 9.2

Experimental parameters of snail dissections

EXPERIMENT	MEAN AGE OF INFECTION (± 10 DAYS PPI)	COMMENTS
A	33	3 snails infected of 5 examined
B	68	3 snails infected of 5 examined
C	102.5	4 snails, first emitting cercariae at 91, 100, 107 and 112 days PPI
D	183	3 snails, first emitting cercariae 60 days before examination

The distribution of the larvae within the host could not be determined precisely. Due to the thinness of the snail epidermis it was readily torn during dissection and as a result larvae would occassionally be moved from their original location. The location of larvae was, therefore, not recorded unless it was considered improbable that they had reached their observed location by displacement. The following general features of larval distribution were noted.

At 33 ± 10 days PPI large rediae were found within the haemocoel spaces around the heart of the mollusc. Small rediae were found within the digestive gland. No sporocysts or cercariae were present.

At 68 ± 10 days PPI a variety of sizes of rediae were found in the digestive gland only. Immature cercariae were present in the digestive gland.

At 102.5 ± 10 days and 183 ± 13 days PPI a variety of sizes of rediae and cercariae were present in the digestive gland. They formed a white undulating mass visible through the thin shells of young snails. Incising the wall of the digestive gland caused the larvae to stream out as if under pressure. Only rarely were larvae observed deep within the tissues of the digestive gland. Fully developed cercariae were also present in the haemocoel spaces around the heart of the mollusc.

9.3.2c Time course of development of intramolluscan rediae and cercariae

The sizes of rediae were recorded from each snail examined at the four stages of infection (Table 9.3 and Appendix 2). Note that the dimension parameter was the product of width and length and is

TABLE 9.3

Numbers and proportions of rediae per snail at different stages of infection. Expressed as mean number and proportion of the total redial population in each redial size class

REDIAL SIZE CLASS	STAGES OF INFECTION (± 10 days PPI)							
(ARBITRARY UNITS)	33		68		102.5		183	
	N	P	N	P	N	P	N	P
0– 50	11.0	0.53	11.0	0.42	16.7	0.49	25.3	0.50
50–100	5.0	0.35	11.7	0.41	3.8	0.09	13.7	0.30
100–150	1.0	0.09	3.7	0.14	7.7	0.22	9.0	0.18
150–200	0.3	0.01	0.3	0.01	4	0.15	1.0	0.02
200–250	0	0	0	0	1.2	0.03	0	0
250–300	0	0.02	0.7	0.02	0.5	0.01	0	0
300–350	0	0	0	0	0	0	0	0
350–400	0	0	0	0	0	0	0	0
400–450	0	0	0	0	0	0	0	0
450–500	0	0	0	0	0.2	0.005	0	0
MEAN TOTAL NUMBER (n)	17.7 (3)		27.3 (3)		34.2 (4)		49.0 (3)	

where: N, mean number of rediae per size class;

P, mean proportion of rediae per size class;

n, number of replicates

expressed in arbitrary units (see Section 9.2).

From these data it is apparent that the mean number of rediae per snail increased during infection, tending towards a constant number of approximately 50 rediae per snail (Figure 9.1).

The mean proportion of rediae in each size class changed little over the period 33 to 183 ± 10 days PPI. The proportion of small rediae was always much greater than that of larger rediae (Figure 9.2).

The sizes of cercariae were recorded from each snail examined at the four stages of infection (Table 9.4 and Appendix 2). Note that in some cases the cercarial total length was estimated from body length alone, the proportion requiring estimation was always less than 10% of those present per snail.

From these data it is apparent that cercariae were absent during the early stages of infection but increased rapidly from approximately 70 days PPI (Figure 9.1). This figure indicates that the number of cercariae may be approaching a constant level although this has clearly not bee n attained by 183 ± 13 days PPI.

The mean proportion of free cercariae in each size class showed considerable variation over the period of observation (Figure 9.3). At 33 days PPI no cercariae were present. At 68 days PPI the few cercariae present were immature, corresponding in size with recently emerged intra-redial cercariae. At 102.5 days PPI cercariae over the full size range from immature to fully developed were present. The greater proportion, however, were in the least developed size class. At 183 days PPI there was less size-dependent variability, cercariae were present in similar proportions in all

Figure 9.1: Mean number of cercariae and rediae per snail at different times during the development of intra-molluscan infection.

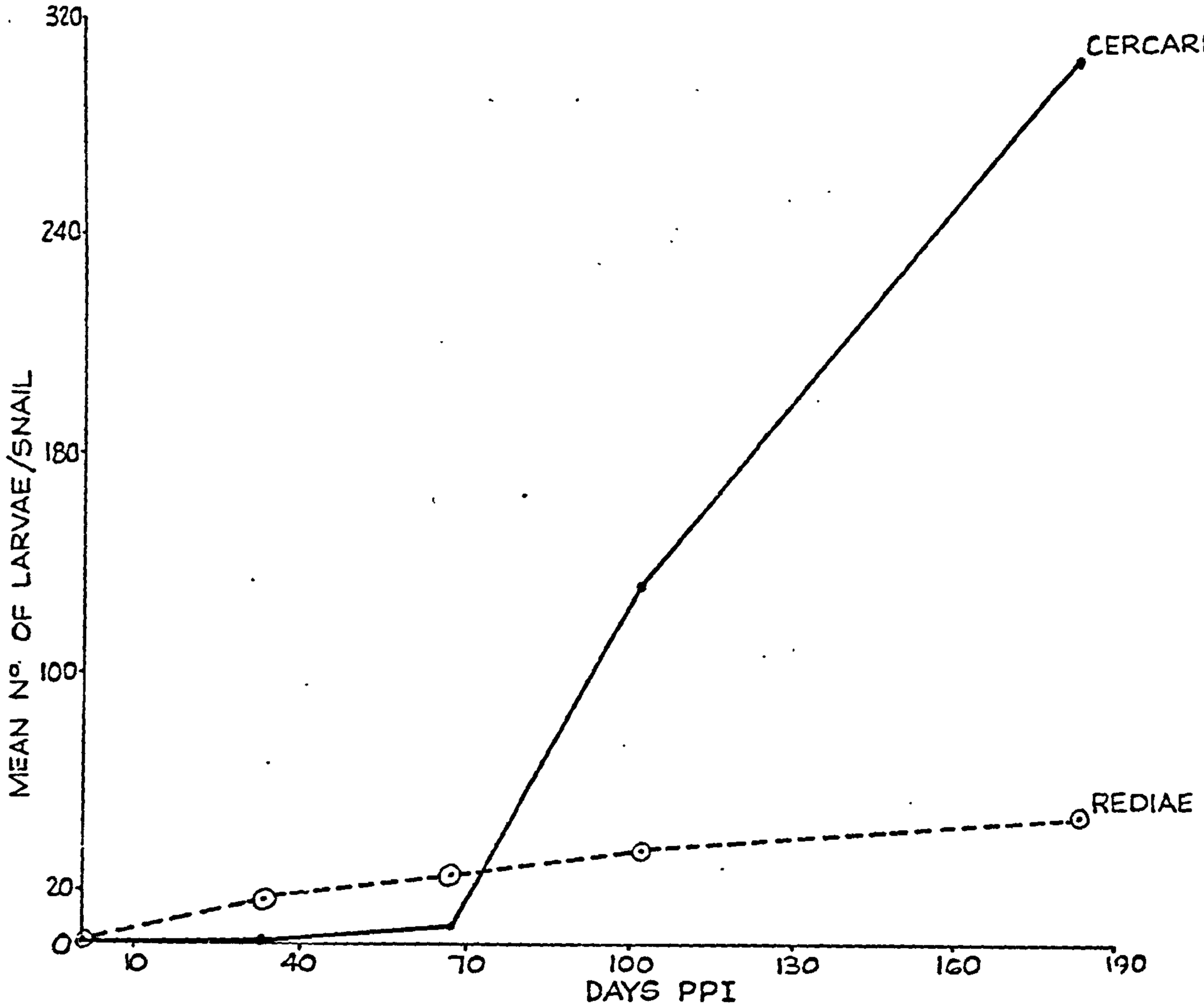
320
240
180
100
20
0
MEAN No. OF LARVAE/SNAIL
CERCARIAE
REDIAE
10
40
70
100
130
160
190
DAYS PPI

Figure 9.2: Mean proportion of rediae per snail in different size classes of rediae. Results shown at different stages of infection (± 10 days PPI): a) 33 days, b) 68 days, c) 102.5 days, and d) 183 days.

a)

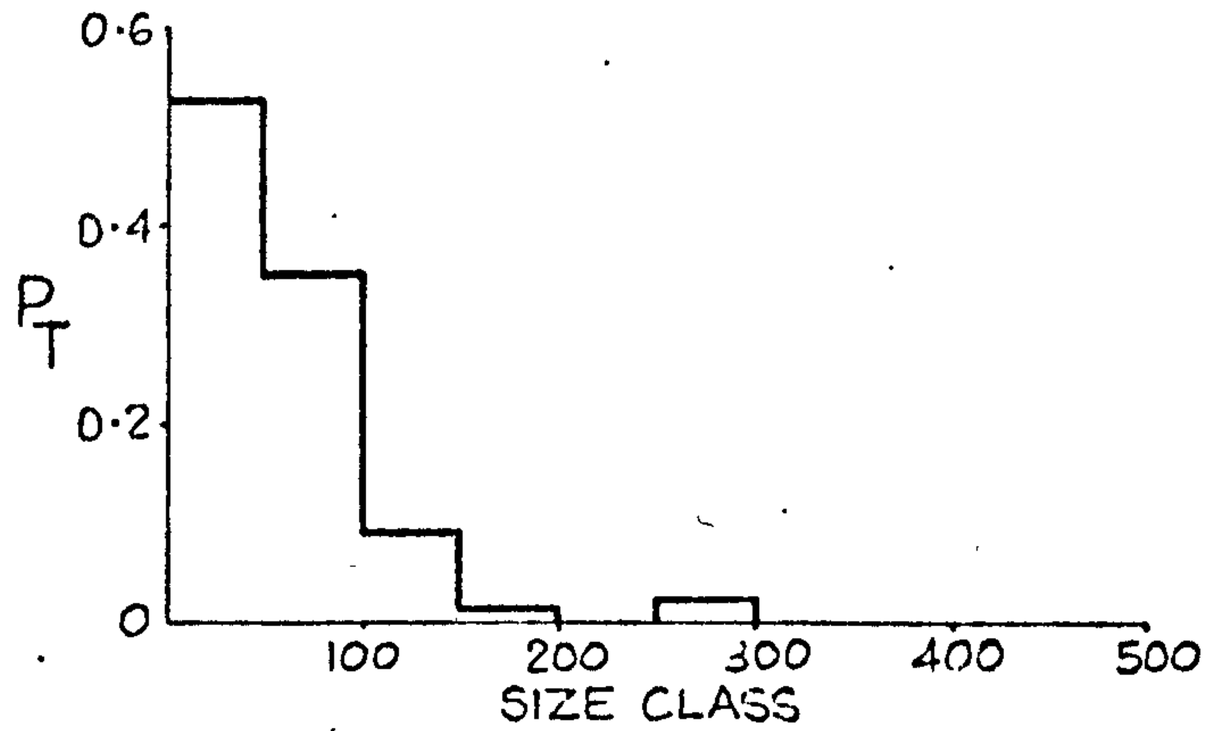
0·6
0·4
0·2
0
P_T
100
200
300
400
500
SIZE CLASS

b)

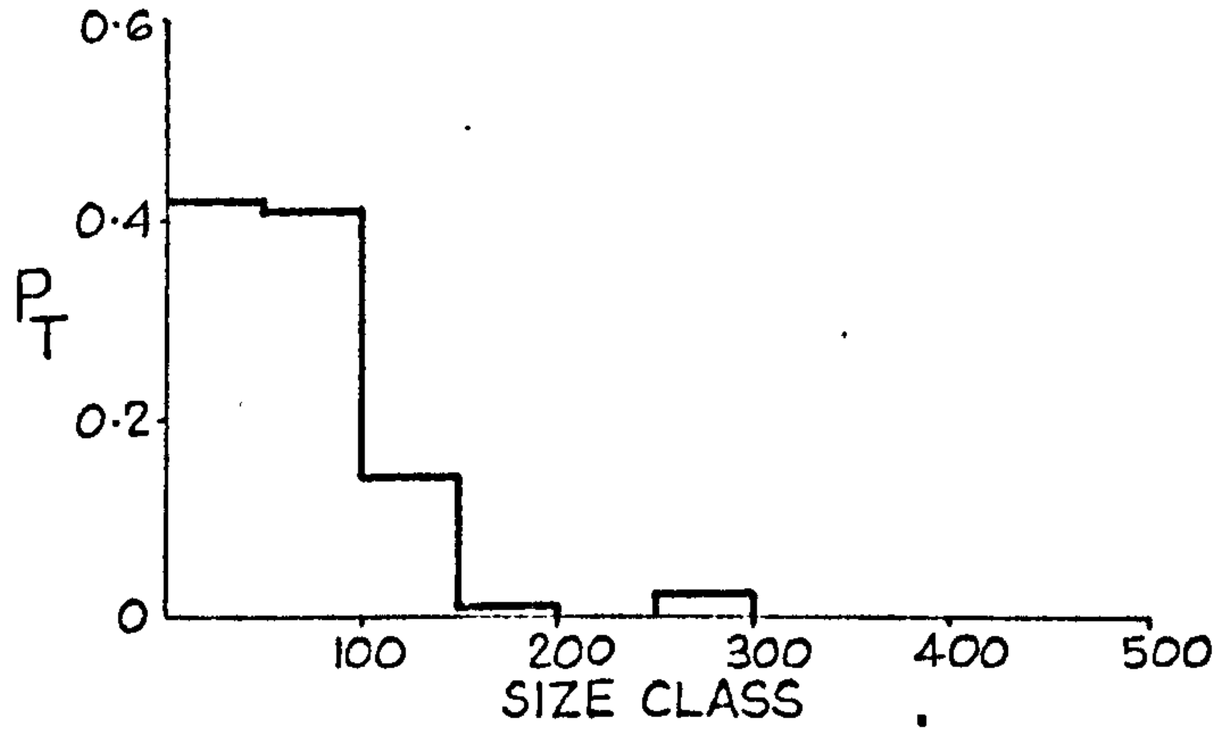
0·6
0·4
0·2
0
P_T
100
200
300
400
500
SIZE CLASS

c)

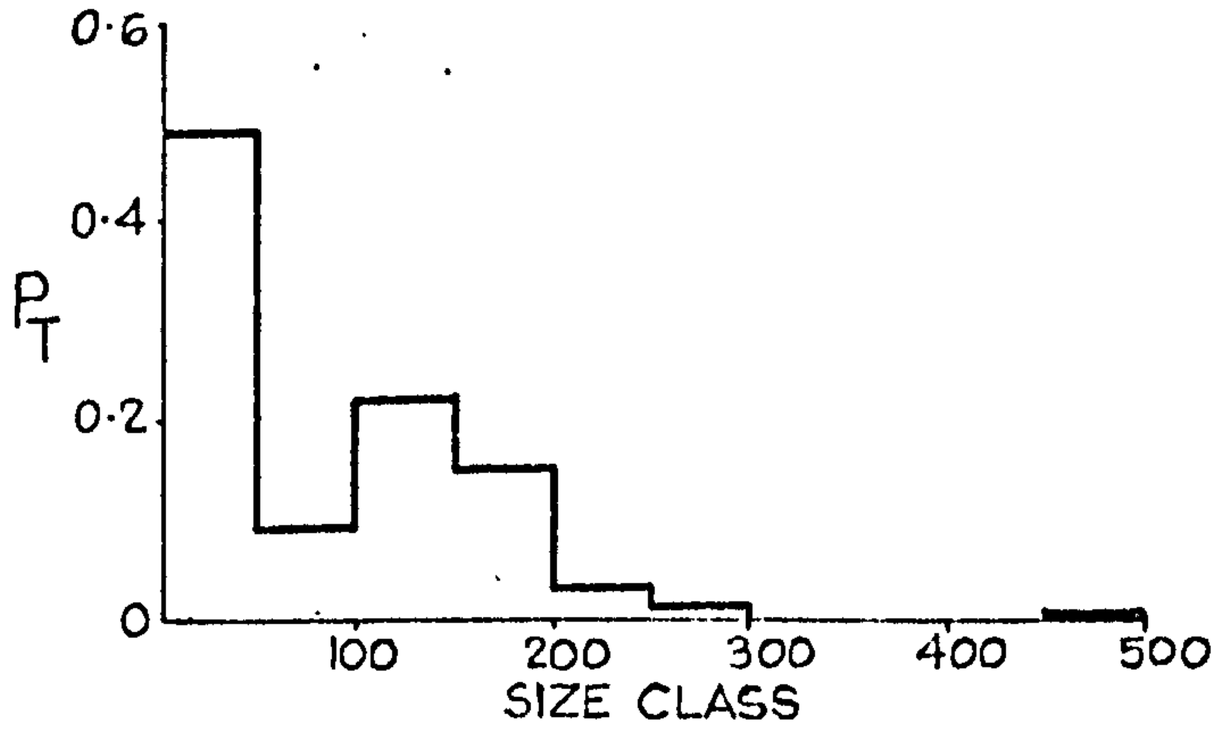
0·6
0·4
0·2
0
P_T
100
200
300
400
500
SIZE CLASS

d)

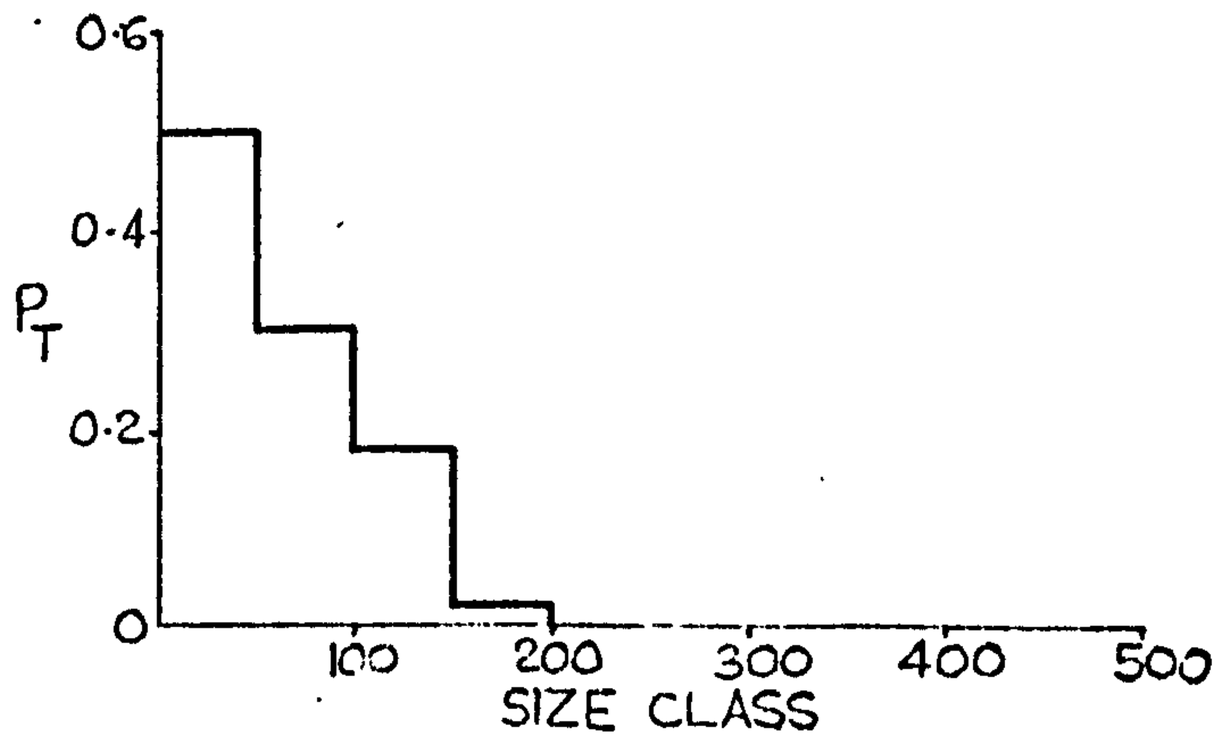
0·6
0·4
0·2
0
P_T
100
200
300
400
500
SIZE CLASS

TABLE 9.4

Numbers and proportions of cercariae/snail at different stages of infection. Expressed as mean number and proportion in each cercarial size class

CERCARIAL SIZE CLASS	STAGES OF INFECTION (± 10 days PPI)							
(μm)	33		68		102.5		183	
	N	P	N	P	N	P	N	P
0– 100	0	0	0.67	0.09	0	0	0	0
100– 200	0	0	5.67	0.91	24.25	0.23	45.33	0.14
200– 300	0	0	0	0	33.75	0.28	67.00	0.22
300– 400	0	0	0	0	34.00	0.25	45.33	0.15
400– 500	0	0	0	0	7.25	0.04	25.00	0.08
500– 600	0	0	0	0	8.00	0.04	20.67	0.07
600– 700	0	0	0	0	5.25	0.03	15.00	0.06
700– 800	0	0	0	0	5.50	0.03	20.33	0.06
800– 900	0	0	0	0	5.50	0.04	12.67	0.05
900–1000	0	0	0	0	4.25	0.03	31.00	0.10
1000–1100	0	0	0	0	5.00	0.03	21.67	0.07
MEAN TOTAL NUMBERS (n)	0(3)		6.3 (3)		130.7 (4)		304 (3)	

where: N, mean number of cercariae per size class;

P, mean proportion of cercariae per size class;

n, number of replicates

Figure 9.3: Mean proportion of cercariae per snail in different size classes of cercariae. Results shown at different stages of infection (± 10 days PPI): a) 68 days, b) 102.5 days and c) 183 days. No cercariae were observed at 33 ± 10 days PPI.

a)

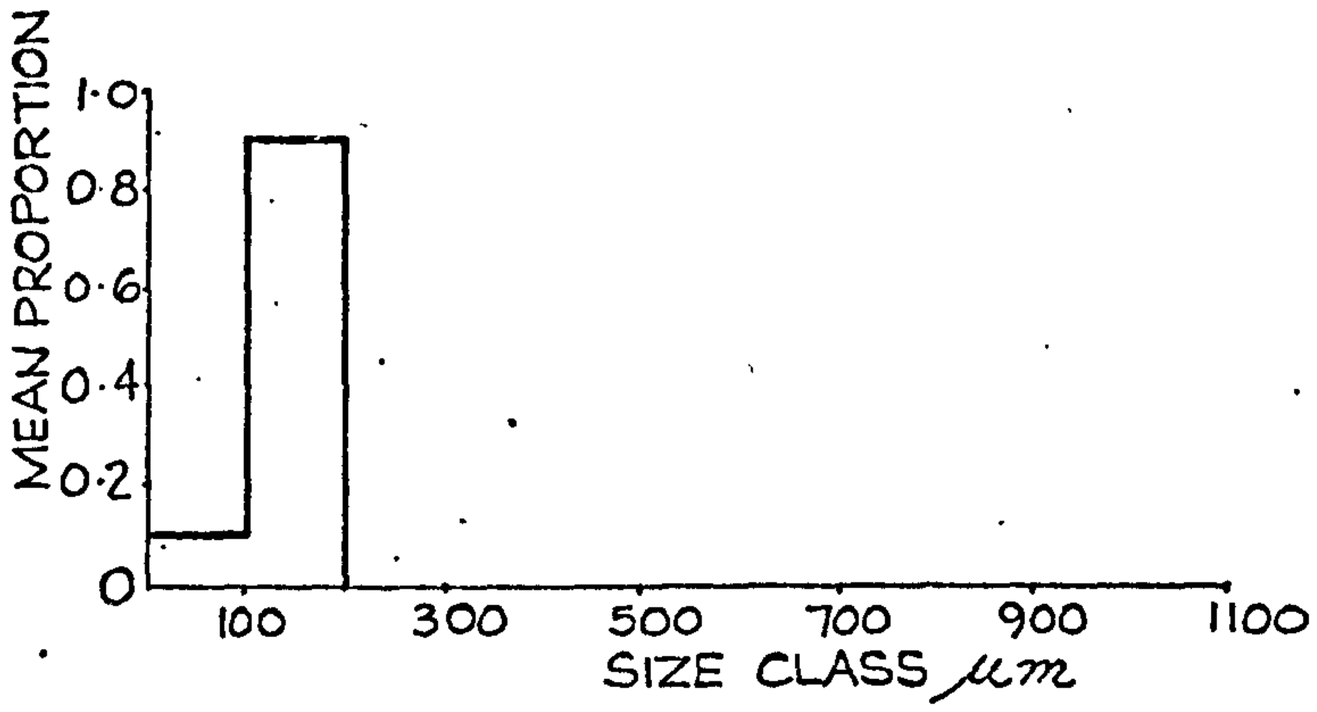
MEAN PROPORTION
1·0
0·8
0·6
0·4
0·2
0
100
300
500
700
900
1100
SIZE CLASS μm

b)

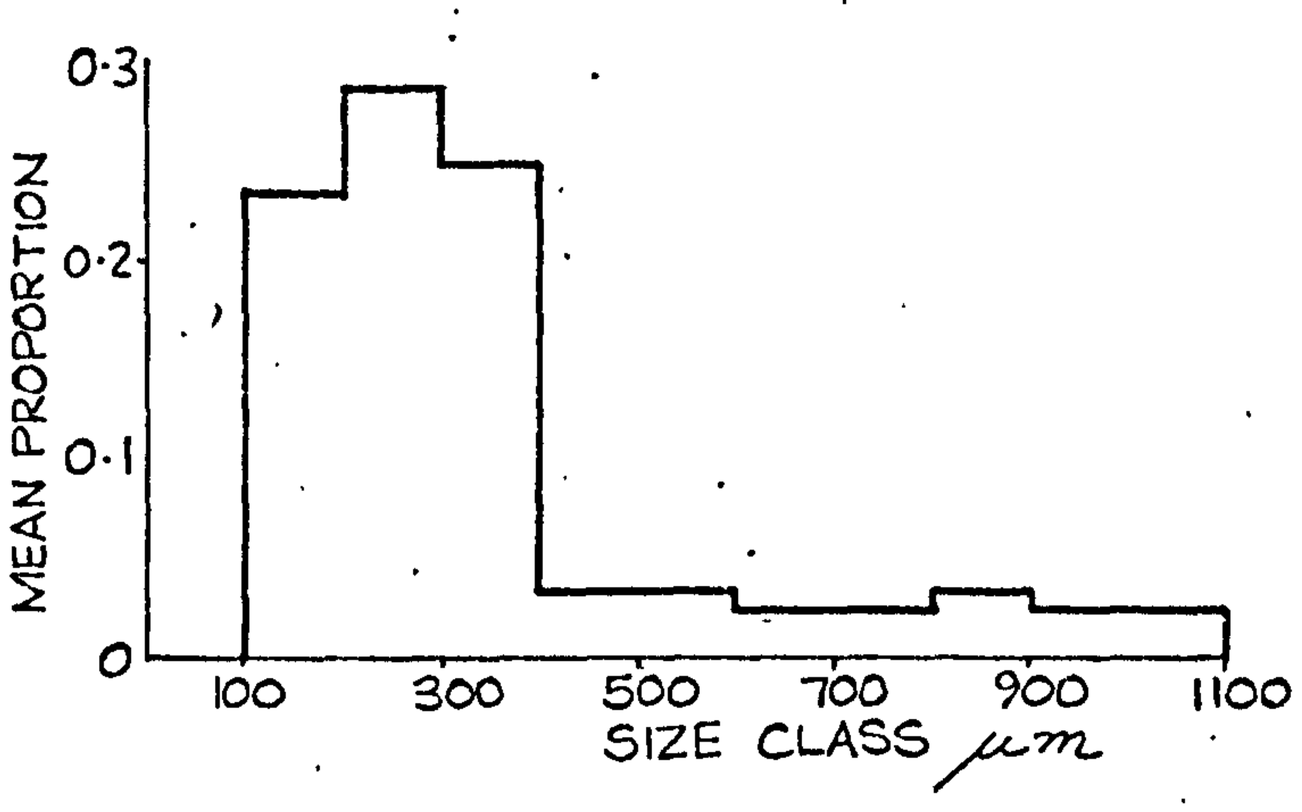
MEAN PROPORTION
0·3
0·2
0·1
0
100
300
500
700
900
1100
SIZE CLASS μm

c)

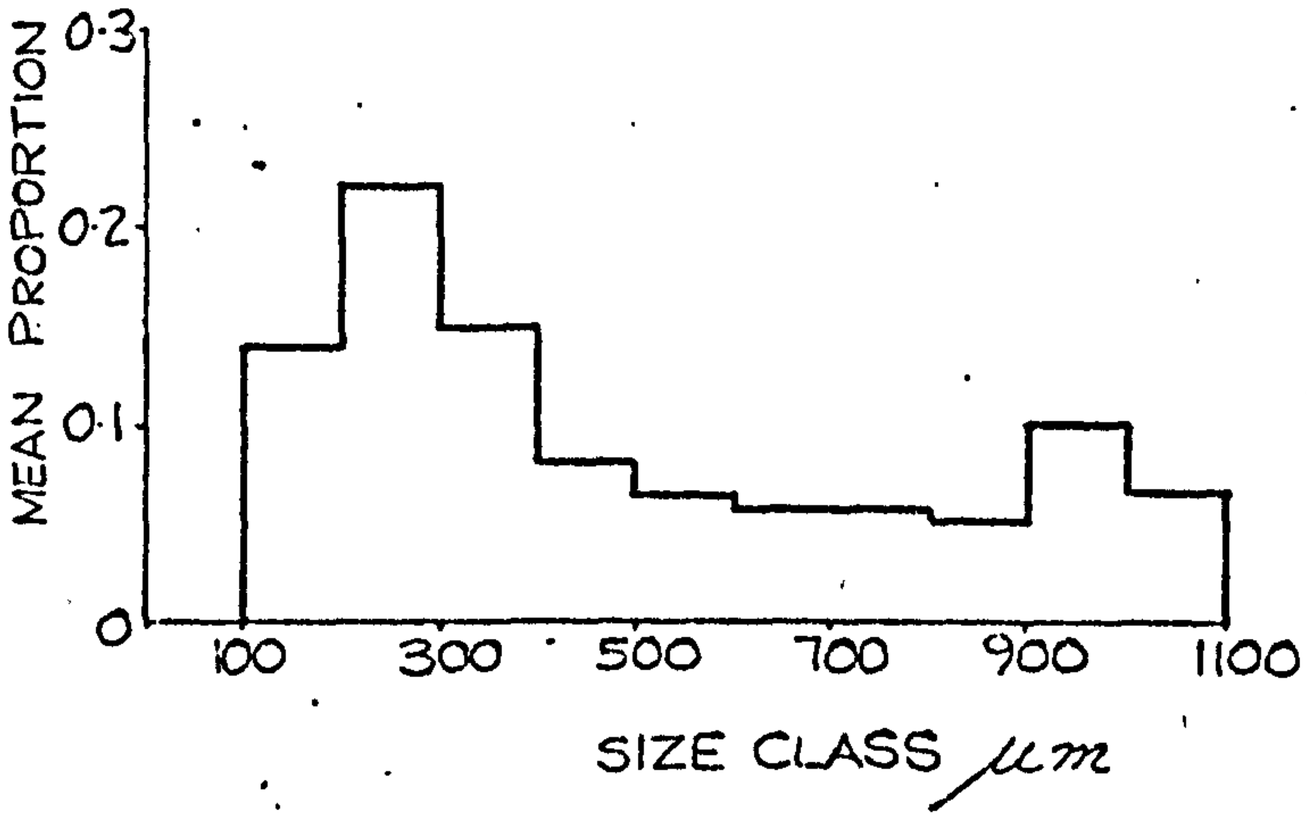
MEAN PROPORTION
0·3
0·2
0·1
0
100
300
500
700
900
1100
SIZE CLASS μm

size classes.

Figure 9.4 also shows how the size frequency distribution changed with age of infection, but the data in this case are presented as absolute numbers rather than proportions.

9.3.2d Intra-redial larvae

Appendix 2 contains the raw data of intra-redial larval numbers in all rediae examined. These data are summarised below.

Intra-redial rediae were present in rediae of snails examined from 33 to 183 days PPI, that is intra-redial were found at all observed stages of infection from 33 days PPI onwards.

Intra-redial cercariae were present in rediae from 68 days PPI onwards, they were not observed in snails at 33 days PPI.

At any stage in infection a redia within a snail may be classified into one of four categories. A redia may contain no intra-redial larvae, intra-redial rediae only, intra-redial cercariae only or both intra-redial larval forms together. Hence for each group of snails examined at a particular time PPI it was possible to determined the mean proportion of rediae per snail which fell into each category. These data are shown in Table 9.5.

From Table 9.5 it can be deduced that usually less than 50% of rediae per snail contained intra-redial larvae. At 33 days PPI intraredial rediae only were produced. From 68 days PPI onwards the greatest proportion of rediae, with intra-redial larvae, contained intra-redial cercariae. The smallest proportion contained intra-redial rediae only, and the remainder produced both intra-redial larval forms at the same time.

Figure 9.4: Mean number of cercariae per snail in different size classes of cercariae. Results shown at different stages of infection (± 10 days PPI): B) 68 days, C) 102.5 days and D) 183 days.

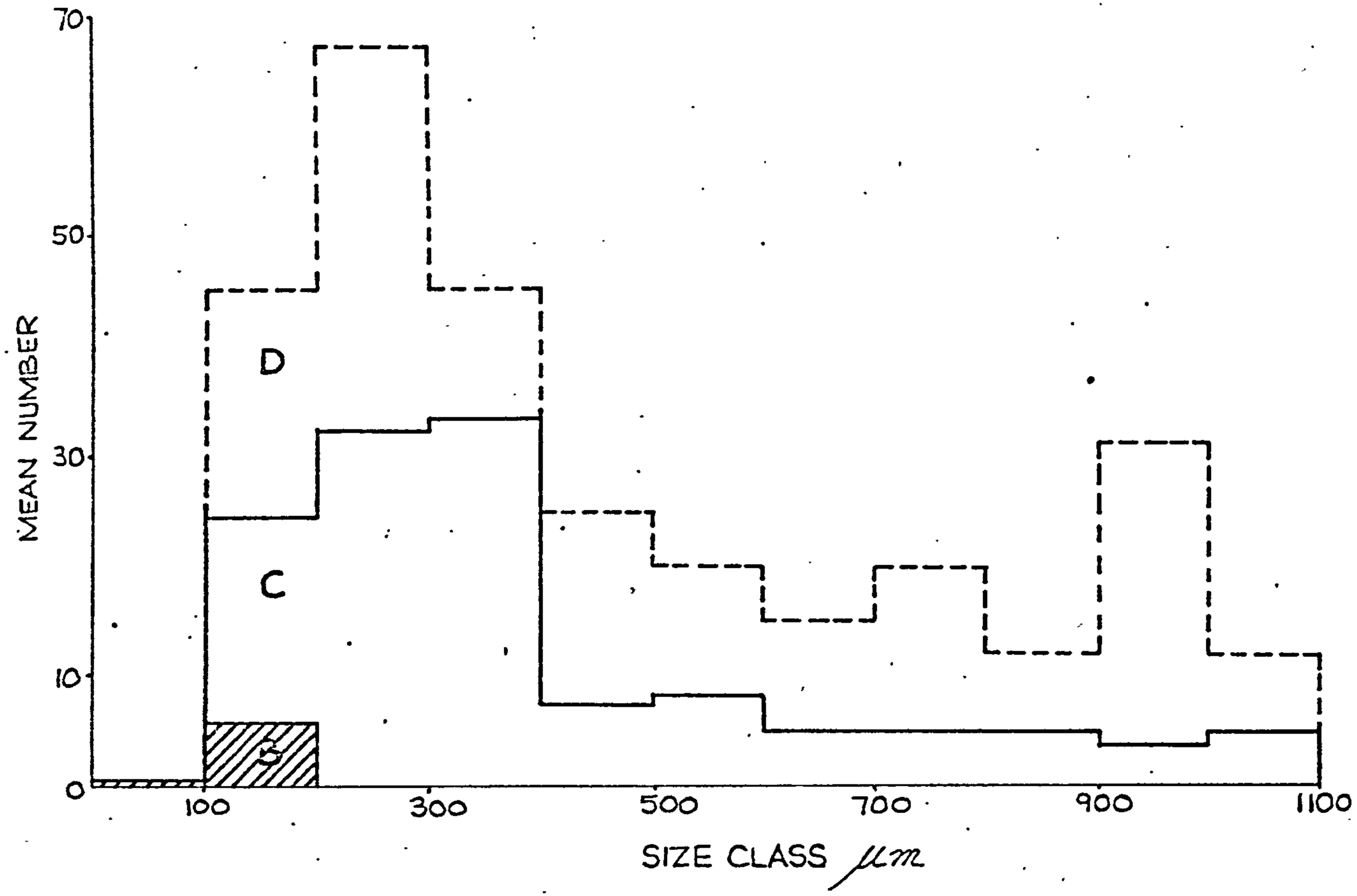
70
50
30
10
0
MEAN NUMBER
D
C
S
100
300
500
700
900
1100
SIZE CLASS μm

TABLE 9.5

Intra-redial contents at different stages of infection. Expressed as mean proportion of rediae per snail (P)

INTRA-REDIAL CONTENTS	STAGE OF INFECTION (± 10 days PPI)			
	33	68	102.5	183
	P	P	P	P
NO INTRA-REDIAL LARVAE	0.72	0.46	0.52	0.65
INTRA-REDIAL REDIAE ONLY	0.28	0.01	0.02	0.00
INTRA-REDIAL CERCARIAE ONLY	0.00	0.30	0.35	0.24
BOTH INTRA-REDIAL LARVAL TYPES	0.00	0.23	0.11	0.11

Table 9.6 shows the mean number, rather than the mean proportion, of intra-redial larvae within each redia. From 68 days PPI onwards it is apparent that the number of intra-redial rediae per redia containing intra-redial rediae was approximately 1-2 individuals, regardless of whether they were present alone or in conjunction with intra-redial cercariae. Similarly, the mean number of intra-redial cercariae remained constant at 4-6 individuals per redia containing intra-redial cercariae whether alone or in conjunction with intra-redial rediae.

It appears, considering Tables 9.5 and 9.6 together, that from 68 days PPI onwards more intra-redial rediae per snail were present in conjunction with intra-redial cercariae than were present alone. Conversely, more intra-redial cercariae per snail were present alone in rediae than were present in conjunction with intra-redial rediae.

At 33 days PPI there were a mean number of 13.21 intra-redial rediae per redia containing intra-redial rediae.

These mean values give little impression of the frequency distributions of intra-redial larval numbers which generate the means. Table 9.7 and Figure 9.5 show the frequency distributions of numbers of intra-redial rediae per redia. From 68 days PPI onwards the distributions had a very short tail, most intra-redial rediae occurred singly. At 33 days PPI the tail was much longer indicating that intra-redial rediae occurred in large numbers in a few individual rediae.

The frequency distributions of intra-redial cercariae had an unusual cyclical form due to the fact that even numbers of

TABLE 9.6

Mean number of intra-redial larvae per redia at different stages of infection. Mean determined only from rediae containing intra-redial larvae

INTRA-REDIAL CONTENTS	STAGE OF INFECTION (± 10 days PPI)							
	33		68		102.5		183	
	R	C	R	C	R	C	R	C
INTRA-REDIAL REDIAE ONLY	13.21	-	1	-	2.12	-	0	-
INTRA-REDIAL CERCARIAE ONLY	-	0	-	5.21	-	4.06	-	4.68
BOTH INTRA-REDIAL LARVAL TYPES	0	0	1.28	4.72	0.98	6.19	1.32	4.40

where: R, mean number of intra-redial rediae per redia;

C, mean number of intra-redial cercariae per redia.

TABLE 9.7

Frequency distribution of intra-redial rediae, numbers per redia at different stages of infection. Expressed as mean proportions (P) per snail for rediae which contained intra-redial rediae alone or in conjunction with intra-redial cercariae

NUMBER OF INTRA-REDIAL REDIAE	STAGE OF INFECTION (± 10 days PPI)			
	33	68	102.5	183
	P	P	P	P
0	0.76	0.73	0.86	0.88
1	0	0.19	0.08	0.08
2	0.06	0.05	0.04	0.04
3	0.02	0.01	0.01	0
4	0.04	0.01	0.02	0
5	0.06	0	0.01	0
10	0.02	0	0	0
19	0.02	0	0	0
26	0.02	0	0	0
40	0.02	0	0	0

Figure 9.5: Frequency distribution of intra-redial rediae, numbers per redia at different stages of infection. Expressed as the mean proportion of rediae per snail which contain a particular number of intra-redial rediae.

Results shown at different stages of infection ($\pm$ 10 days PPI): a) 33 days, b) 68 days, c) 102.5 days and d) 183 days.

a)

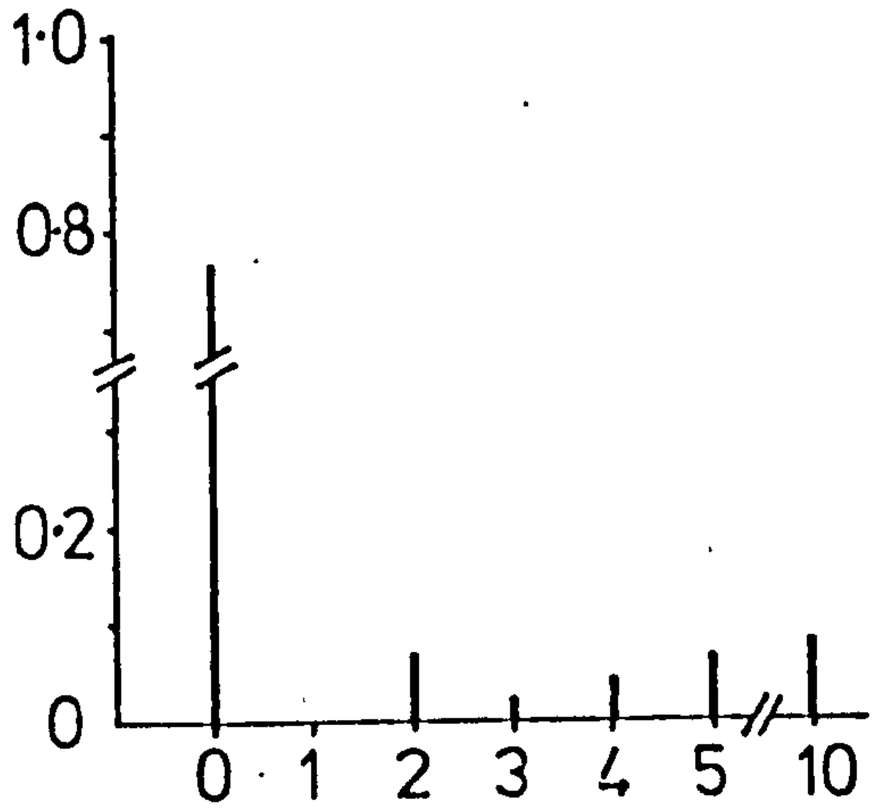
1·0
0·8
0·2
0
0 1 2 3 4 5 10

b)

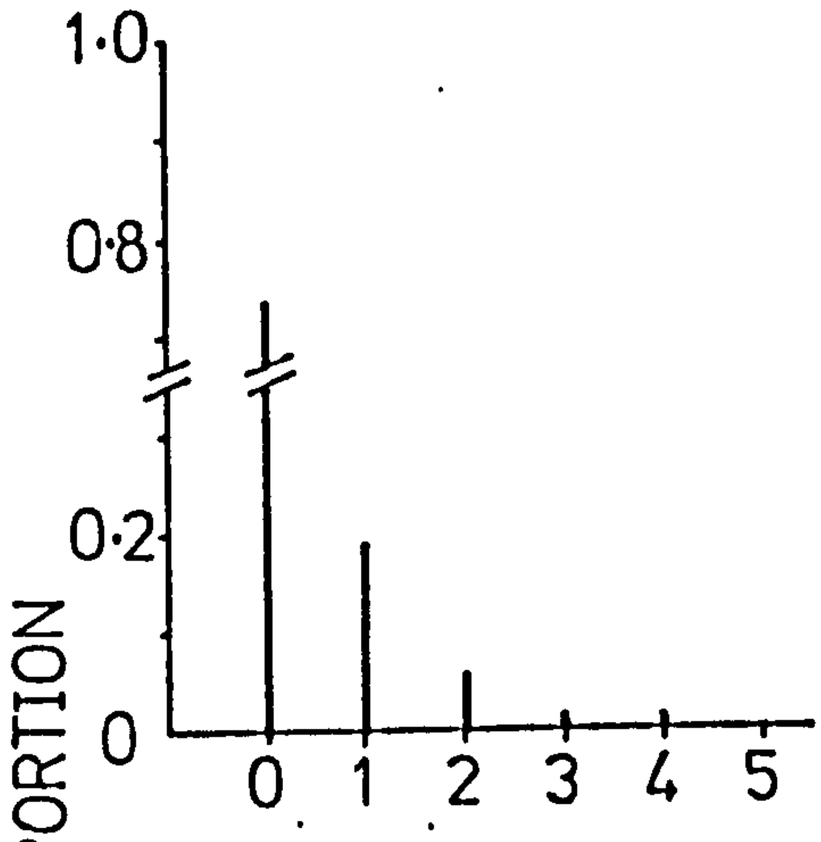
1·0
0·8
0·2
0
PROPORTION
0 1 2 3 4 5

c)

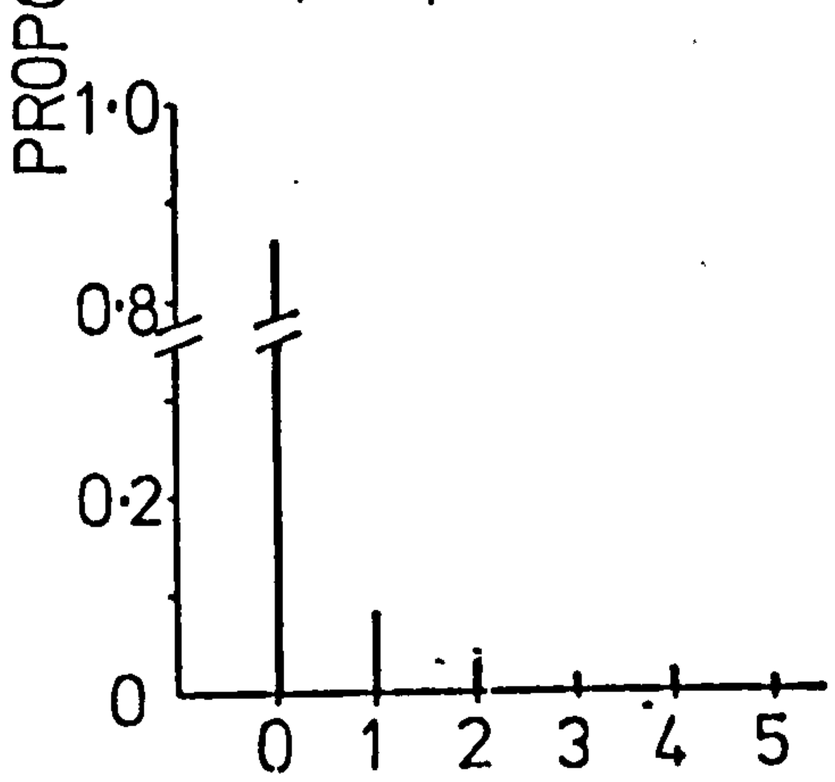
PROP
1·0
0·8
0·2
0
0 1 2 3 4 5

d)

1·0
0·8
0·2
0
0 1 2 3 4 5
NUMBER OF INTRAREDIAL REDIAE

larvae per redia were more common than odd numbers (Table 9.8 and Figure 9.6). The most common number of intra-redial cercariae per redia appeared to be 4 or 6.

The effect of redial size on intra-redial number is described in Table 9.9 and Figure 9.7. It can be seen that for intra-redial rediae at 33 days PPI there was an apparent correlation between redial size and the number of intra-redial rediae per redia. From 68 days PPI onwards, however, this relationship was lost and the number of intra-redial rediae per redia appeared independent of the size of the parent redia. Intra-redial cercariae were not present at 33 days PPI. From 68 days PPI onwards the number of intra-redial cercariae per redia appeared to be positively correlated to the size of the parent redia.

Table 9.10 examines the effect of redial size on the type of intra-redial larvae present. These data are illustrated in Figure 9.8. In the early stages of infection only intra-redial rediae were present so no conclusion can be drawn. From 68 days PPI onwards, however, intra-redial rediae occurred both alone and in conjunction with intra-redial cercariae. There was no apparent difference between the sizes of rediae which contained either type of intra-redial larvae alone or together. It appears, therefore, that the size of the parent redia does not influence the type of intra-redial larvae produced.

9.3.3 The period of development of infection

Table 9.11 shows the age of infection in days PPI at which members of a population of 15 snails first began emitting cercariae. Cercariae emerged from the first individual 91 $\pm$ 10 days PPI. By

TABLE 9.8

Frequency distribution of intra-redial cercariae, numbers per redia at different stages of infection. Expressed as mean proportions (P) per snail

NUMBER OF INTRA-REDIAL CERCARIAE	STAGE OF INFECTION (± 10 days PPI)			
	33	68	102.5	183
	P	P	P	P
0	1.0	0.41	0.54	0.64
1	0	0	0	0
2	0	0.08	0.05	0.05
3	0	0.06	0.02	0.04
4	0	0.16	0.09	0.12
5	0	0.11	0.03	0.06
6	0	0.09	0.12	0.05
7	0	0.04	0.02	0.02
8	0	0.06	0.11	0
9	0	0.03	0.01	0.01
10	0	0	0.01	0.02
11	0	0	0.01	0

Figure 9.6: Frequency distribution of intra-redial cercariae, numbers per redia at different stages of infection. Expressed as the mean proportion of rediae per snail which contain a particular number of intra-redial cercariae.

Results shown at different stages of infection (± 10 days PPI): a) 33 days, b) 68 days, c) 102.5 days and d) 183 days.

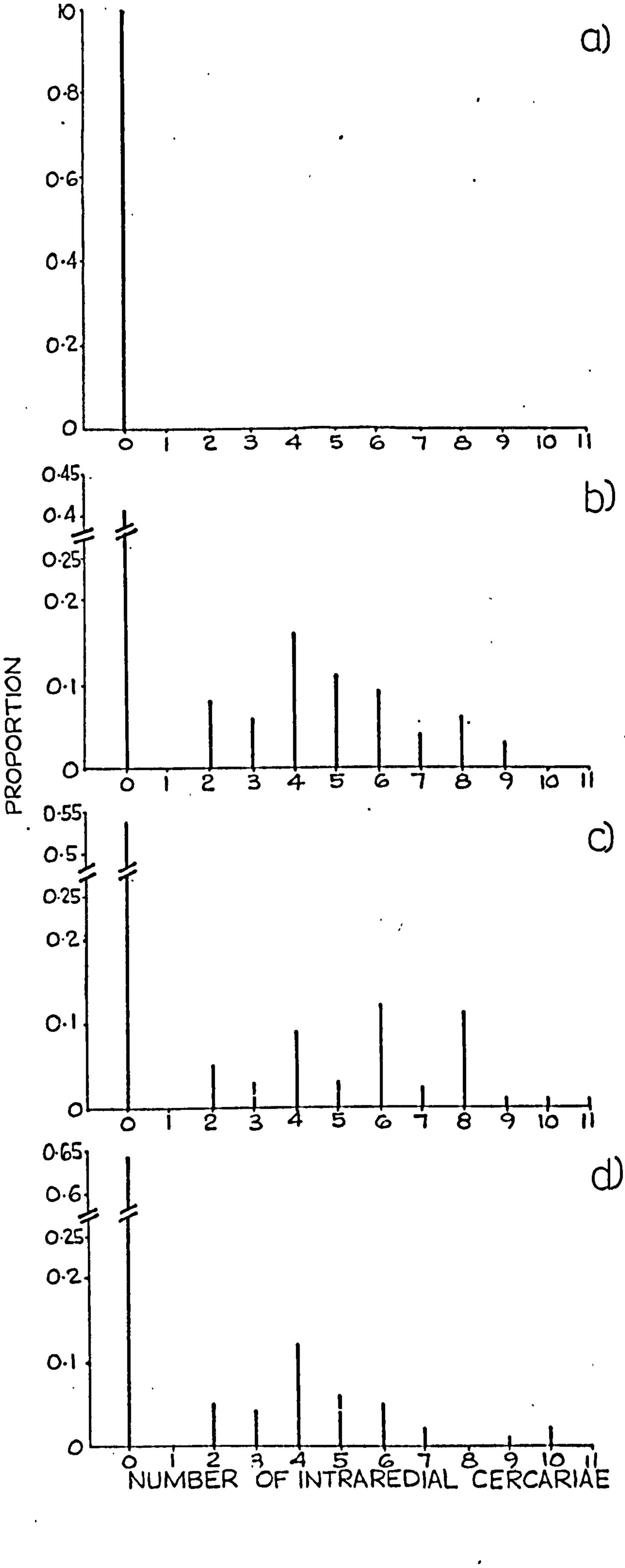
a)
10
0·8
0·6
0·4
0·2
0
0 1 2 3 4 5 6 7 8 9 10 11
b)
0·45
0·4
0·25
0·2
0·1
0
0 1 2 3 4 5 6 7 8 9 10 11
PROPORTION
c)
0·55
0·5
0·25
0·2
0·1
0
0 1 2 3 4 5 6 7 8 9 10 11
d)
0·65
0·6
0·25
0·2
0·1
0
0 1 2 3 4 5 6 7 8 9 10 11
NUMBER OF INTRAREDIAL CERCARIAE

TABLE 9.9

Effect of redial size on the number of intra-redial larvae. Expressed as the mean number of intra-redial rediae (R) or intra-redial cercariae (C) per redia for different redial size classes

REDIAL SIZE CLASS (ARBITRARY UNITS)	33		68		102.5		183	
	R	C	R	C	R	C	R	C
0- 50	0	0	1.5	3.4	1.0	3.0	0	0
50-100	3.5	0	1.1	4.5	1.5	3.7	1.0	2.2
100-150	18.0	0	1.3	6.5	2.3	5.4	1.4	4.9
150-200	26.0	0	4.0	9.0	1.3	6.7	1.3	5.0
200-250	0	0	0	0	1.0	8.0	0	0
250-300	19.0	0	2.0	6.0	0	8.0	0	0
300-350	0	0	0	0	0	0	0	0
350-400	0	0	0	0	0	0	0	0
400-450	0	0	0	0	0	0	0	0
450-500	0	0	0	0	3.0	6.0	0	0

Figure 9.7: Effect of redial size on the number of intra-redial larvae. Expressed as the mean number of intra-redial rediae or intra-redial cercariae per redia for different redial size classes.

Results shown at different stages of infection ($\pm$ 10 days PPI): A) 33 days, B) 68 days C) 102.5 days and D) 183 days.

INTRAREDIAL REDIAE PER REDIA

INTRAREDIAL CERCARIAE PER REDIA

TABLE 9.10

Effect of redial size on the type of intra-redial contents. Expressed as the mean number of rediae per snail which contain intra-redial cercariae only (C), intra-redial rediae only (R), or both intra-redial larval stages together (RC), for different redial size classes

REDIAL SIZE CLASS	STAGES OF INFECTION (± 10 days PPI)											
(ARBITRARY UNITS)	33			68			102.5			183		
	C	R	RC	C	R	RC	C	R	RC	C	R	RC
0 - 50	0	0	0	1.0	0	0.7	0.2	0	0.2	0	0	0
50 - 100	0	2.7	0	7.0	0	3.3	1.7	0	1.0	7.0	0	1.0
100 - 150	0	1.0	0	0.7	0	2.0	5.2	0.7	1.5	4.3	0	3.7
150 - 200	0	0.3	0	0	0	0.3	3.2	0	0.7	0	0	1.0
200 - 250	0	0	0	0	0	0	1.0	0	0.2	0	0	0
250 - 300	0	0.3	0	0	0.3	0.3	0.5	0	0	0	0	0
300 - 350	0	0	0	0	0	0	0	0	0	0	0	0
350 - 400	0	0	0	0	0	0	0	0	0	0	0	0
400 - 450	0	0	0	0	0	0	0	0	0	0	0	0
450 - 500	0	0	0	0	0	0	0	0	0.2	0	0	0

Figure 9.8: Effect of redial size on the type of intra-redial contents. Expressed as the mean number of rediae per snail which contain intra-redial cercariae only, intra-redial rediae only or both intra-redial larval stages together, for different redial size classes.

Results shown for different stages of infection (± 10 days PPI): a) 33 days, b) 68 days, c) 102.5 days and d) 183 days.

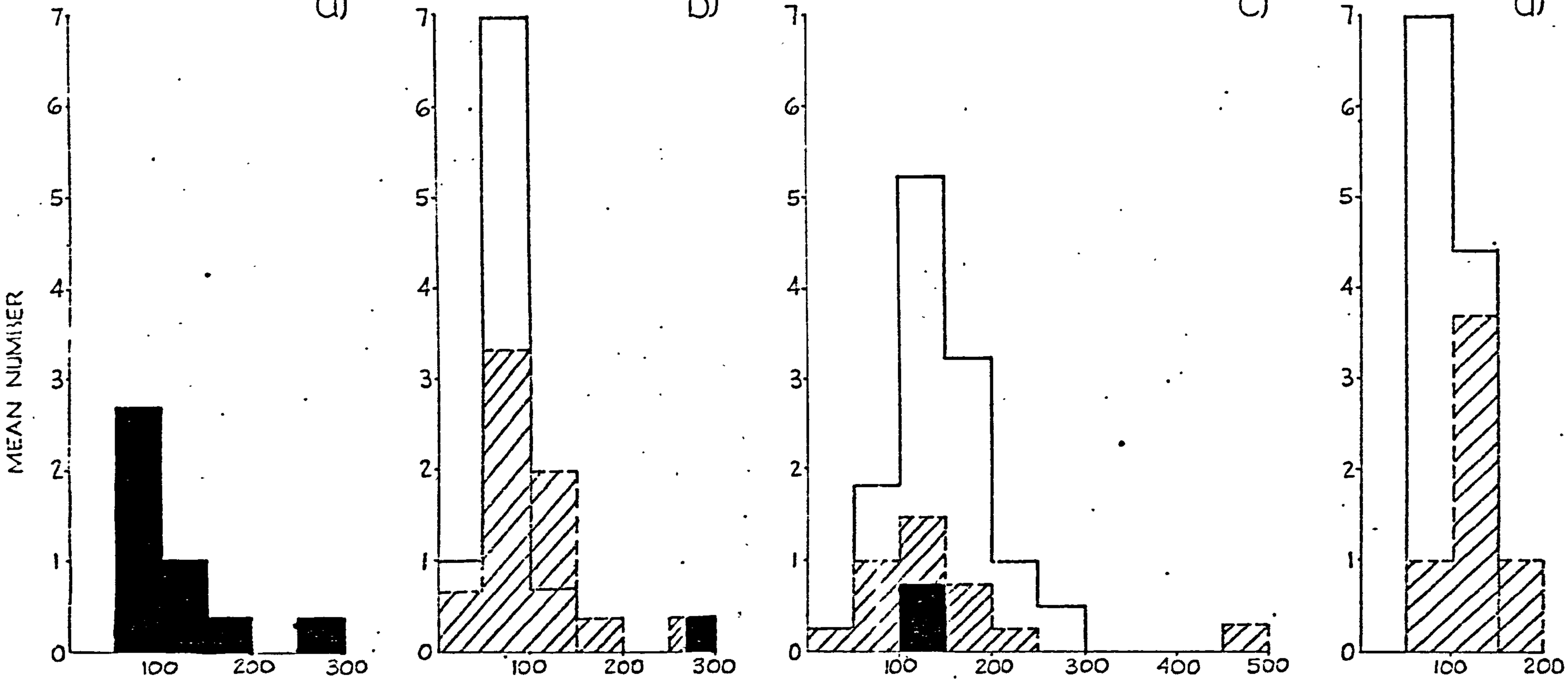
a)
b)
c)
d)
MEAN NUMBER
0
1
2
3
4
5
6
7
100
200
300
400
500
SIZE CLASS
INTRAREDIAL CERCARIAE ONLY
INTRAREDIAL REDIAE ONLY
BOTH INTRAREDIAL LARVAL STAGES

TABLE 9.11

Age of infection in days PPI at which members of a population of 15 snails first emitted cercariae

AGE OF INFECTION (± 10 days PPI)	PROPORTION OF SNAILS EMITTING CERCARIAE
80	0
84	0
91	0.07
100	0.13
107	0.20
112	0.27
119	0.40
130	0.47
136	0.60
147	0.60
160	0.60

136 ± 10 days PPI 60% of the snails were producing cercariae and this proportion remained constant until 160 ± 10 days PPI when the experiment was terminated.

It appears, therefore, that only 9 out of 15 snails had become infected. 50% of this infected population were emitting ceracriae by 115 ± 10 days PPI and this was taken to be the mean period of time required for the development of the intramolluscan infection to the cercarial emission stage at 25°C.

9.3.4 Effects of infection on the molluscan host

Macroscopic observation of host tissues during the dissection of infected Melanoides tuberculata did not reveal overt damage at any stage during the time course of intramolluscan development. As described in Section 9.3.2, however, the digestive glands of infected snails examined from 102.5 days PPI onwards were swollen by the numerous parasites present, the larvae streaming out of the gland when the epidermis was punctured during dissection. This may indicate increased internal pressure within the digestive gland which could result in local tissue damage.

M. tuberculata populations are comprised almost entirely of females which reproduce by ameiotic parthenogenesis (Jacob, 1957; Berry and Kadri, 1974). Oocytes discharged from the ovary adjacent to the digestive gland move down the oviduct into a cephalic brood pouch where, after two maturation divisions, development continues to a small, shelled juvenile. During dissection the cephalic brood pouch of the mollusc was routinely examined. Infected snails at 33 and 68 days PPI had an apparently normal complement of developing embryos and young. Snails examined later in infection, 102.5 and

183 days PPI, had no young snails and only a few embryos in the brood pouch.

9.4 Discussion

Quantitative interpretation of the results presented here must be tempered with caution since the scale of the initial infection was unknown. The procedure involved exposing a known population of snails to an unknown population of infective miracidia and hence the experimental design did not reveal the number of miracidia penetrating each host. There are cogent reasons, however, why information on this point is not essential to useful interpretation of results.

Firstly, the experiment relates to the natural situation. Variability in the results is an expression of real variability within the populations of host and parasite.

Secondly, the small amount of variability between replicates at each developmental stage suggests that the degree of exposure and susceptibility of each host snail was similar.

Finally, there is a growing body of evidence to suggest that the ultimate parasite burden of a mollusc is independent of the size of the initial miracidial infection.

Due to the enormous asexual reproductive potential of larval digeneans they have the ability to saturate the carrying capacity of the parasite micro-environment within the molluscan host independently of the number of parasites initially penetrating (Wilson and Draskau, 1976; Anderson, Whitfield and Mills, 1977).

Given these three mitigating factors it is apparent that some useful conclusions may be drawn from the present results.

The information presented here represents the state of development of infection at particular points in time. The course of infection during the intervening periods was unknown. Clearly, however, development is a continuous process and hence projections can be made to describe the overall process. Figure 9.9 is a flow diagram of intramolluscan development, based on present evidence, in which possible alternatives at each stage are indicated.

When the miracidium had penetrated the mollusc it transformed to a mother sporocyst in the muscular foot region adjacent to the site of penetration. An initial larval form of this type was described by Sim (1972) for the present species.

At 33 days PPI large and very small rediae were observed in the cardiac haemocoel spaces and digestive gland. In every case the largest rediae were observed in the cardiac haemocoel. In this site they were surrounded by immature rediae which were also present in the digestive gland. The implication of this spatial distribution is that larger, and presumably older, rediae in the mid-region of the mollusc give birth to daughter rediae which themselves migrate to the digestive gland or produce a second generation of rediae which do so.

The large mid-region rediae were almost certainly progeny of the mother sporocyst, arriving in the mid-region after migrating from the foot. It is unknown whether these large rediae were first or second generation daughters of the mother sporocyst.

Figure 9.9: Schematic representation of intra-molluscan cycle.

AQUATIC HABITAT

MIRACIDIUM

Penetration

MOLLUSCAN HOST

FOOT

Only sporocysts present at 7 days PI.

MOTHER SPOROCYST

REDIA(E)

Several generations(?)

Migration

MID-REGION

Only rediae present from 33 to 68 days PI.

REDIA(E)

CERCARIAE ——— Emergence →

Several generations(?)

Migration

Migration

DIGESTIVE GLAND

Cercariae first present at 68 days PI.

REDIA(E)

Several generations(?)

CERCARIAE

CERCARIAE

By 68 days PPI the mid-region rediae were absent. Their daughters in the digestive gland had produced several generations so that rediae were present at different developmental stages within the digestive gland.

Very immature cercariae were also present in the digestive gland at 68 days PPI, first emerging from the snail as fully developed forms 34·5 days later on average. From the time when cercariae first emerge from the mollusc the digestive gland contained cercariae in different developmental states from immature to fully developed. Only fully developed cercariae, however, were found outside the digestive gland implying that migration to the exterior only occurs once the larvae are mature.

This then is the basic intramolluscan cycle and it is with this framework in mind that one can begin to consider the dynamics of the intramolluscan populations of parasitic larval stages. Rediae entered the intramolluscan population due to the birth of intra-redial rediae. Embryonic rediae have been observed within the rediae of Transversotrema laruei (Velasquez, 1961), T. koliensis (Olivier, 1947); T. soparkari (Pandey, 1971), and T. chackai (Nadakal, Mohandas and Sunderaraman, 1969). The size frequency distributions of the redial population had the same form throughout the observed developmental period, with the numbers present in each size class in inverse proportion to redial size. If it is assumed that redial size is an index of age, that is that older rediae are larger, then it is apparent that there were always more young than old rediae even when the overall redial population size was relatively constant.

It appears, therefore, that the age structure of the redial population, within the digestive gland, was relatively constant in mature infections. Quantification of the factors maintaining this constancy of population structure is extremely difficult due to the multiplicity, and interrelated nature, of the factors involved. For example, the addition of new members to the redial population is the result of birth processes within the population itself, hence the birth rate is dependent on the population structure while, conversely, the population structure is dependent on the birth rate. This complexity may be further compounded by death processes since mortality rates may also be a function of the age structure of the population. The present experimental design did not indicate the relative importance of these different components nor did it permit the determination of birth or mortality rates. In fact, due to the inaccessibility of the intramolluscan larval stages and the complex of factors determining their population structure, it is difficult to envisage any simple experimental system which would allow rigorous quantitative analysis of the population parameters involved. Aspects of the dynamics of the redial population are, therefore, considered here only in qualitative terms.

It appears that in mature infections the redial population age structure and size is stable. This stability could only result from a balance of birth and death processes, that is the birth rate of rediae reaches an equilibrium with the mortality rate of rediae.

A number of factors could cause redial mortality. Competition for digestive gland nutrients could be one source of this mortality. Competition may not, however, only occur between rediae but also

between cercariae and rediae. It has already been shown that the reproductive efficiency of infected molluses is greatly impaired once intramolluscan cercarial development is initiated, and this may indicate that the cercariae utilise nutrients to the detriment of the host. This cercarial utilisation would also reduce the availability of nutrients to rediae. A more direct effect causing redial mortality is redial cannabilism. In the present investigation the ingestion of one redia by another was observed on three occasions. A similar phenomenon was observed by Olivier (1947) who recorded the presence of dead rediae within the gut of rediae of T. koliensis. Further causes of redial mortality may include ageing and host reactions. Clearly this is a complex issue and yet it only concerns one aspect of the redial population - mortality. This mortality must be balanced by births and an examination of the birth processes again indicates the complexity of the population dynamics.

The redial population arises from the intra-redial redial population. The number of intra-redial rediae per redia appeared to change during the course of infection. During the early phase, parent rediae contained a mean number of 13.21 intra-redial rediae but from 68 days PPI onwards only 1-2 intra-redial rediae per redia were present. Without information on the actual birth rate of rediae it is not possible to decide whether early parent rediae were more fecund than rediae later in the infection. It appears, however, that the early rediae differed significantly from later forms perhaps due to the lack of competition in the early stages of the infection or some relative advantage of their location in the cardiac haemocoel rather than the digestive gland.

The production of rediae in mature infections also differed from that earlier in development in that intra-redial rediae could develop with intra-redial cercariae within the same parent redia. Anantaraman (1948) and Brien (1954) described intra-redial cercariae within the redia of T. patialense. In no other species of Transversotrema were such forms discerned although their presence must be assumed from the records of very immature cercariae in the molluscan digestive gland. Nadakal et al. (1969) described a fully formed cercaria within a redia of T. chackai on a single occasion. This may have been the result of imprecise observation or could conceivably represent anomalous development.

Simultaneous development of rediae and cercariae within a single redia has been observed for other digenean species although the mechanisms causing it to occur in some rediae but not others have not been explained. The original life cycle studies on Fasciola hepatica by Leuckart and Thomas in 1883 both concluded that rediae were capable of producing cercariae or rediae but not both. Subsequent work on this species, however, has shown that simultaneous production does occur (Kendal, 1965; Wilson and Draskau, 1976). In F. gigantica this phenomenon has also been observed and has been considered to be a consequence of "sucession of generations" (Dinnik and Dinnik, 1956 and 1964). According to this hypothesis parent rediae initially produce daughter rediae uniquely and as the parent redia ages it initiates cercarial production, simultaneous production only occurring during the period of overlap from production of one form to the other. In T. patialense production of intra-redial rediae alone was observed in a very small proportion of rediae, implying that if sucession of generations does occur the uniquely redial phase must

be of extremely short duration. Furthermore, rediae producing the two intra-redial larvae alone or simultaneously have the same size frequency distribution, the size and presumably age of the rediae is not an indicator of the type of intra-redial larvae produced.

A surprising feature of simultaneous production of intra-redial larval forms in T. patialense is that it does not affect the number of larvae produced. Rediae contained approximately 1-2 intra-redial rediae or 4-6 intra-redial cercariae whether each intra-redial larval form was present alone or with the other. In fact, because there were more rediae producing both intra-redial rediae and intra-redial cercariae together than intra-redial rediae alone, rediae producing both larval forms made the major contribution to the redial population. This result is surprising since it might be expected that if only intra-redial rediae were produced they might receive the share of nutrients otherwise utilised by co-developing cercariae. A similar result was obtained by Wilson and Draskau (1976) who, using temperature manipulation, could not materially alter the production of rediae at the expense of cercariae in Fasciola hepatica. In direct contradiction, however, such a change has been achieved with F. gigantica (Dinnik and Dinnik, 1964). In the face of such conflicting evidence it is apparent that the processes controlling intramolluscan development require further investigation.

The dynamics of the intramolluscan cercarial population are very different from those of rediae. This difference primarily arises due to the losses from the intramolluscan population when cercariae emerge from the host mollusc. During the development of T. patialense infections the size frequency distribution of the

cercarial population changed markedly. Early in infections immature cercariae predominated but as the infection matured there was a more even distribution of cercariae in the size, and presumably age, classes. This may imply that cercarial output occurs on a "production line" basis, the rate of input of immature cercariae eventually being balanced by the rate of output of mature infective cercariae. That is, the number of immature cercariae emerging from parent rediae is equivalent to the rate of emergence of infective cercariae from the host.

An interesting feature of intra-redial cercarial production was the preponderance of even numbers of larvae per parent redia. This may have implications for the method of cercarial embryogenesis since it implies that intra-redial cercariae are produced in pairs. Simultaneous production of this type could occur if a cercarial germinative cells divides initially to give two cells each of which develops to a cercaria or, alternatively, if two germinative cells initiate development at the same time. The presence of infrequent odd numbers of larvae within parent rediae may simply be a consequence of emergence from parent rediae occurring for one member of a developing pair at a time. The structure of the intra-redial cercarial population within each parent redia would then be a consequence of the initiation rate of germinative cells, the development rate of intra-redial cercariae and the rate of emergence from the parent redia. In this context it is significant that no rediae were observed to contain a single intra-redial cercaria, the minimum number was two. This suggests that by the time either of the first two intra-redial cercariae were ready to emerge a second pair of germinative cells had initiated development and were

recognisable as intra-redial cercariae.

It should be noted that single intra-redial rediae were frequently observed within parent rediae and there was no tendency for even numbers to occur more frequently. This supports the hypothesis that the germinative cells producing rediae are fundamentally different from those producing cercariae.

From the above discussion it should be apparent that the processes involved in controlling intramolluscan development are incompletely understood. The concept of a germinal lineage preserving the genotype throughout larval development is now well documented and generally accepted (see Cort et al., 1954 for review and discussion), but the mechanisms involved in this process and the role of the genetic material remain obscure despite the interest shown in this topic (James and Bowers, 1967; Khalil and Cable, 1967; Cable, 1971; Pearson, 1972; Clark, 1974). It is perhaps a measure of the complexity of the problems that so little progress has been made since Seenstrup first proposed the concept of alternation of generations 137 years ago.

The present discussion has centered around the intramolluscan parasite population but consideration must also be given to the effects of the parasite on its environment - the host molluso.

Infection of Melanoides tuberculata with T. patialense resulted in an inhibition or reduction in the reproductive ability of the snail. In parasitised snails no young were observed in the brood pouch from 102-5 days PPI.

The reproductive ability of infected snails may be reduced directly, by disruptive changes to reproductive structures, or indirectly, by reduction of nutrient supplies to developing stages.

Four forms of direct disruptive effects have been described. The most common form is parasitic castration, generally resulting from the invasion of the gonads by intramolluscan larvae (Rees, 1936; Cheng and Snyder, 1962; James, 1965; Robson and Williams, 1971; Huizinga, 1973). Less common forms are: sex reversal; mechanical occlusion of oviducts by cercariae; and inhibition of gametogenesis by disruption of gonadal vascularization (Krull, 1935; McArthur and Featherstone, 1976; Uzmann, 1953).

The intramolluscan larvae of T. patialense were not observed within the reproductive system of M. tuberculata.

Indirect inhibition of mollusc reproductive ability by interruption of nutrient supply to gonads and developing young has been ascribed to two main causes.

Firstly, pathological changes in the morphology of the digestive gland. This has been observed in many trematode-mollusc relationships (James, 1965; Reader, 1971 and 1976; Robson and Williams, 1971; Meuleman, 1972; Huizinga, 1973; Yoshino, 1976) including those involving M. tuberculata (Lal and Premvati, 1955; Mohandas, 1974). The digestive gland may degenerate due to: physical occlusion of digestive tubules; accumulation of toxic wastes and lytic enzymes; or ingestion and disruption of gland cells by browsing rediae (Rees, 1934; Rees, 1936; Cheng, 1963; James, 1965; Robson and Williams, 1971). Whatever the mechanism, or combination of mechanisms, involved the result is to reduce the

assimilation efficiency of the digestive gland.

Secondly, competition between parasite and host for ingested nutrients. Host glycogen is utilised for parasitic larval development hence the host has less available nutrients to support its own reproduction.

It is suggested that the depressed reproductive ability of M. tuberculata infected with T. patialense is a consequence of reduced availability of host nutrients. The snail is involved in competition with its parasitic population for ingested nutrients while at the same time the presence of the larvae within the host digestive gland almost certainly reduces assimilation efficiency.

Significantly, the loss of reproductive ability coincided with the development of the large intramolluscan cercarial population. While approximately 40 rediae were the only inhabitants of the digestive gland (up to 68 days PPI) the snail was able to reproduce. When the large population of developing cercariae also began to make demands on the available nutrients there was a decline in the reproductive ability of the snail.

SECTION 10:

CERCARIAL DEVELOPMENT

10. Cercarial Development

10.1 Introduction

Development of the intramolluscan stages of Transversotrema patialense was described in the previous section (Section 9). An unusual aspect of this process was the extra-redial development of the cercariae. Cercarial development external to rediae or sporocysts is known in only four families other than the Transversotrematidae: the Paramphistomatidae, Notocotylidae, Azygiidae and Opisthorchiidae (Pearson, 1972). Development of this type greatly facilitates the experimental isolation of individual immature larvae, permitting observation of single organisms at different stages of development.

The transformation to the adult, in T. patialense, involves loss of the cercarial tail during attachment to the piscine definitive host, the cercarial body region developing to the ovigerous adult with few overt signs of morphological differentiation (Whitfield et al., 1975; Mills, 1977).

The present investigation takes advantage of the accessability of the cercarial and adult stages to describe cercarial morphogenesis and cercarial-adult transformation of T. patialense using scanning and transmission electron microscopical techniques.

10.2 Materials and Methods

Intramolluscan larval stages were obtained by dissection of infected snails (Section 2.7).

Mature free-living cercariae were collected as they emerged from infected snails (Section 2.3).

Adult flukes were removed from infected Brachydanio rerio (Section 2.5).

The different stages in the life cycle were fixed immediately after collection in 2.5% glutaraldehyde at 4°C. Individual organisms were then prepared for SEM and TEM (Section 2.8).

The internal structure of adult flukes was studied using living material.

10.3 Results

10.3.1 General

Primordial cercariae were produced by rediae within the digestive gland of Melanoides tuberculata. The rediae had a characteristic shape, possessing a large anterior opening, a bulbous mid-region and a short caudal extension (Plate 12a and b). A muscular pharynx was present within the anterior opening (Plate 12b). The body wall possessed bands of circular muscles which were obscured posteriorly by wrinkled surface projections (Plate 12a). The general body surface and the projections were covered with 100 nm wide minute folds or microplica (Plate 12c and d).

Intra-redial cercariae produced by the rediae escaped via a birth pore. The newly emerged cercariae, body region length approximately 100 μm, exhibited little regional differentiation although a primordial tail 50 μm long could be discerned (Plate 13a). The pharynx was represented by a series of longitudinal striations

(Plate 13b) while the primordial ventral sucker (25 x 35μm) was apparent as a protruberant area (Plate 13c). The general body surface was covered with microplica approximately 80 nm wide (Plate 13d).

By the time the body region length attained 140μm the tail region was 125μm long and consisted of a tail stem with a distal bifurcation into primordial furcae (Plate 14a). A proximal thickening of the tail stem indicated the future location of the arm processes. The primordial pharyngeal region became insunk but was apparently imperforate (Plate 14b). The ventral sucker (32μm diameter) was distinctly pedunculate, its surface retaining the wrinkled appearance of the rest of the body surface (Plate 14c). The general body surface was still covered with 80 nm wide microplica (Plate 14d).

When the cercariae had attained a body length of approximately 150μm and a tail length of 210μm the arm processes had appeared (Plate 15a). The pharyngeal aperture remained imperforate but with a deep circumferential invagination (Plate 15b). The surface of the ventral sucker (64μm diameter) was more clearly separated from the surrounding body surface (Plate 15c). Microplica of the same size and form as earlier stages were present on the body surface (Plate 15d).

Fully developed cercariae had a mean body length of approximately 350μm and a tail length of 560μm. As they approached this size tegumental spines first became apparent, while the body surface still retained microplica (Plate 16c). When fully developed the surface was corrugated and spinous but the microplica were absent

(Plate 16d). The ventral sucker (100μm diameter) developed to the pedunculate form characteristic of mature cercariae before spines first became discernable (Plate 16a).

The growth and distribution of tegumental spines is discussed elsewhere (Section 11) and will not be described here.

The pharynx was perforate and apparently functional (Plate 17d). A genital pore was present (Plate 18a).

The SEM ultrastructure of the mature cercarial tail region has been described elsewhere (Whitfield et al., 1975). The tail region showed an exceptional degree of differentiation: the distal region of the tail stem bifurcated into spatulate furcae: the proximal region of the tail stem was laterally extended into two arm processes which terminated in adhesive pads and sensory structures supposedly involved in identification of, and attachment to, the definitive host. These structures are discussed further in Section 12.

The adult fluke was, apart from its larger size, indistinguishable externally from the body region of the mature cercaria without the tail and associated structures (Plate 19a). Tail loss resulted in a dorsally situated decaudation lesion surrounded by a sub-tegumental sphincter 23μm in diameter (Plate 19b).

The ovigerous adult deposited eggs via the genital atrium (Plate 18b and c). This was also the apparent site of exit or reception of sperm (Plate 18d). Laurer's canal opened on the dorsal surface via an aperture approximately 6 x 15μm (Plate 20c).

The distribution of the adult fluke organ systems is illustrated in Figure 10.1.

In subsequent discussions cercarial development is considered in three arbitrary divisions (Figure 10.2). Type One intramolluscan cercariae are those that have recently emerged from a redia (Plate 13a). Type Two intramolluscan cercariae have reached a stage of development where the arm processes and furcae are apparent and the ventral sucker pedunculate. The genital pore and pharyngeal aperture, however, remain imperforate (Plate 15). The morphologically indistinguisable fully developed intramolluscan and free-living cercariae are considered together as Type Three. These arbitrary divisions clearly permit large areas of overlap and are intended only as convenient stages within the continuum of development from newly emerged intra-redial cercaria to free-living cercaria.

10.3.2 Structure of the body surface during development from intra-molluscan cercaria to adult

The structure of the spines found in the body walls of mature cercariae and adults is discussed in Section 11 and will not be considered here.

The sequence of development of the body surface from Type One cercaria to adult is illustrated diagrammatically in Figure 10.3.

Although all material was prepared for TEM in a similar manner sections of Type One cercariae were consistently of lower contrast than those of more mature stages. This differential resolution may be a reflection of differences in cytoplasmic organisation at this early differentiating stage. Because of the poor image quality

Figure 10.1: Structure of the adult of Transversotrema patialense.

Key: cc, cellular region of caecum; ev, excretory vesicle; ga, genital atrium; lc, laurer's canal; oc, pigmented cup of ocellus; ov, ovary; ph, pharynx; sv, seminal vesicle; tc, tegumental region of caecum; te, testis; ut, uterus; vd, vas deferens; vf, vitelline follicle; vr, vitelline reservoir.

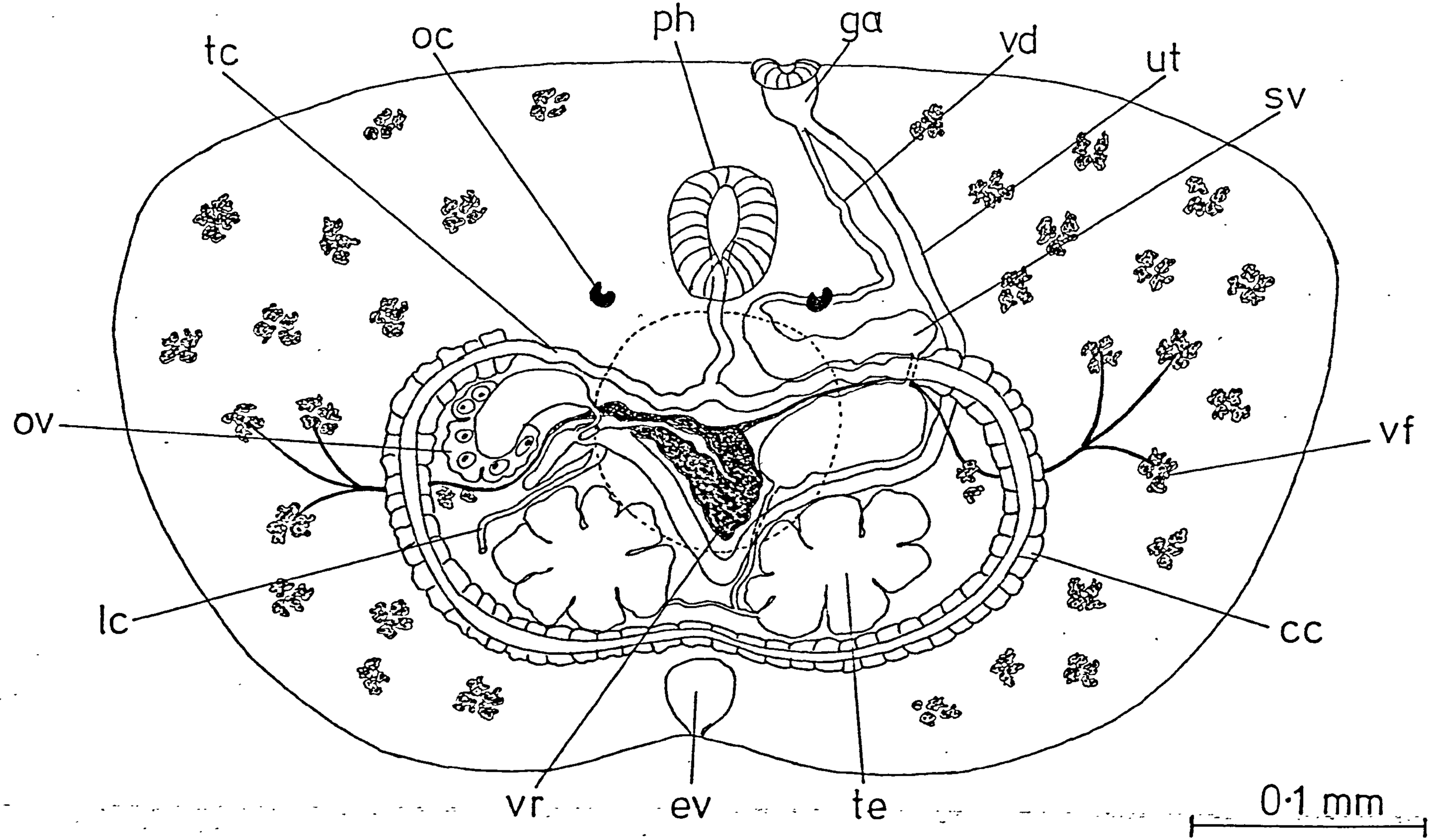
tc
oc
ph
ga
vd
ut
sv
ov
vf
lc
cc
vr
ev
te
0·1 mm

Figure 10.2: Size relationships during growth from newly emerged intra-redial cercaria to adult fluke.

a) Type One cercaria.

b) Type Two cercaria.

c) Type Three cercaria.

d) Adult fluke.

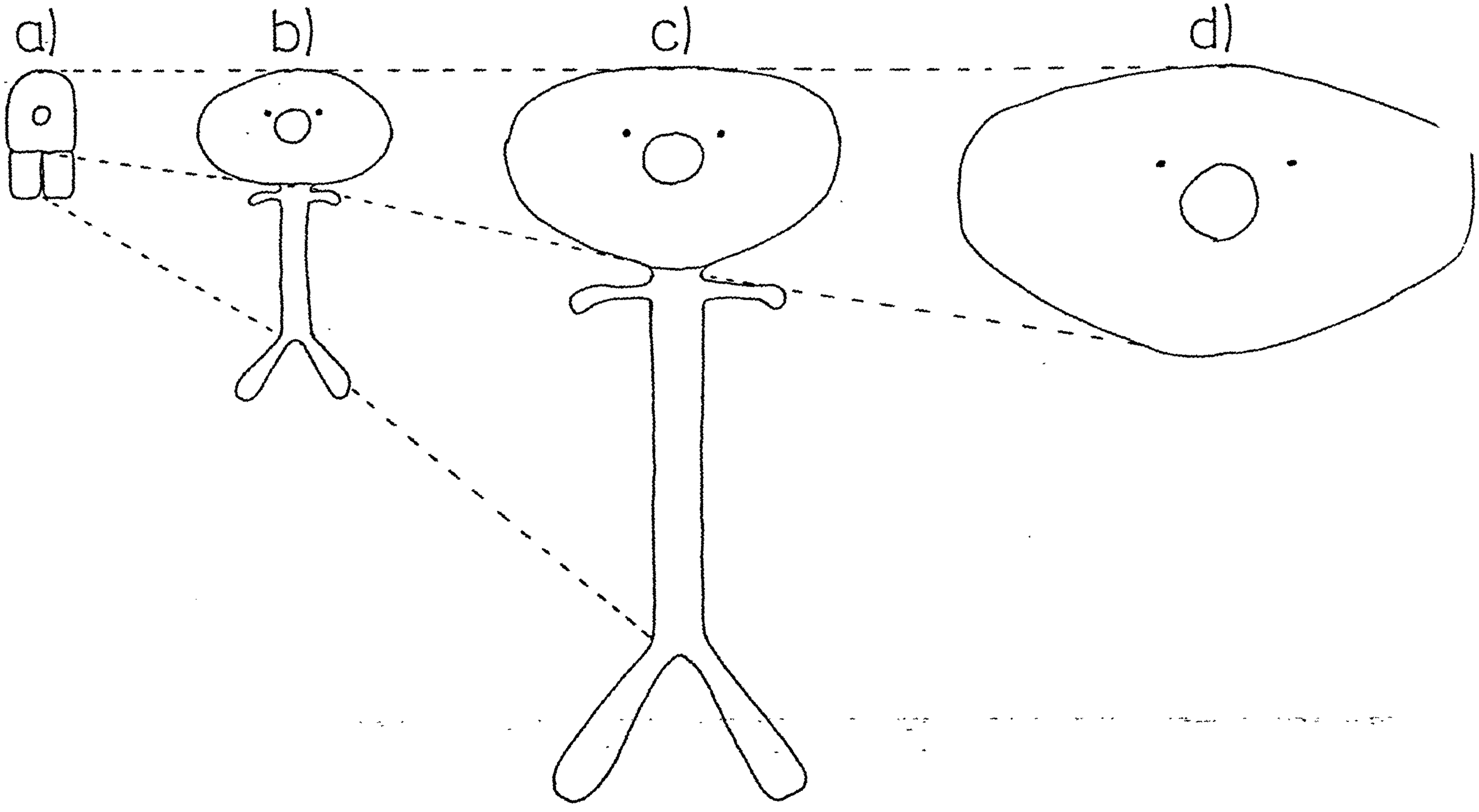
a)
b)
c)
d)

Figure 10.3: The structure of the body surface during development from newly emerged intra-redial cercaria to the adult fluke.

a) Type One cercaria.

b) Type Two cercaria.

c) Type Three cercaria.

d) Adult fluke.

Key: am, apical plasma membrane; bi, basal invagination; bl, basal lamina; bm, basal plasma membrane; c, cytoplasmic connective; cb, tegumental cell body; dl, dense layer; ei, electron lucent inclusion; h, hemi-desmosome; mt, mitochondrion; mp, microplica; mw, membranous whorl; n, nucleus; pn, pycnotic nucleus (?).

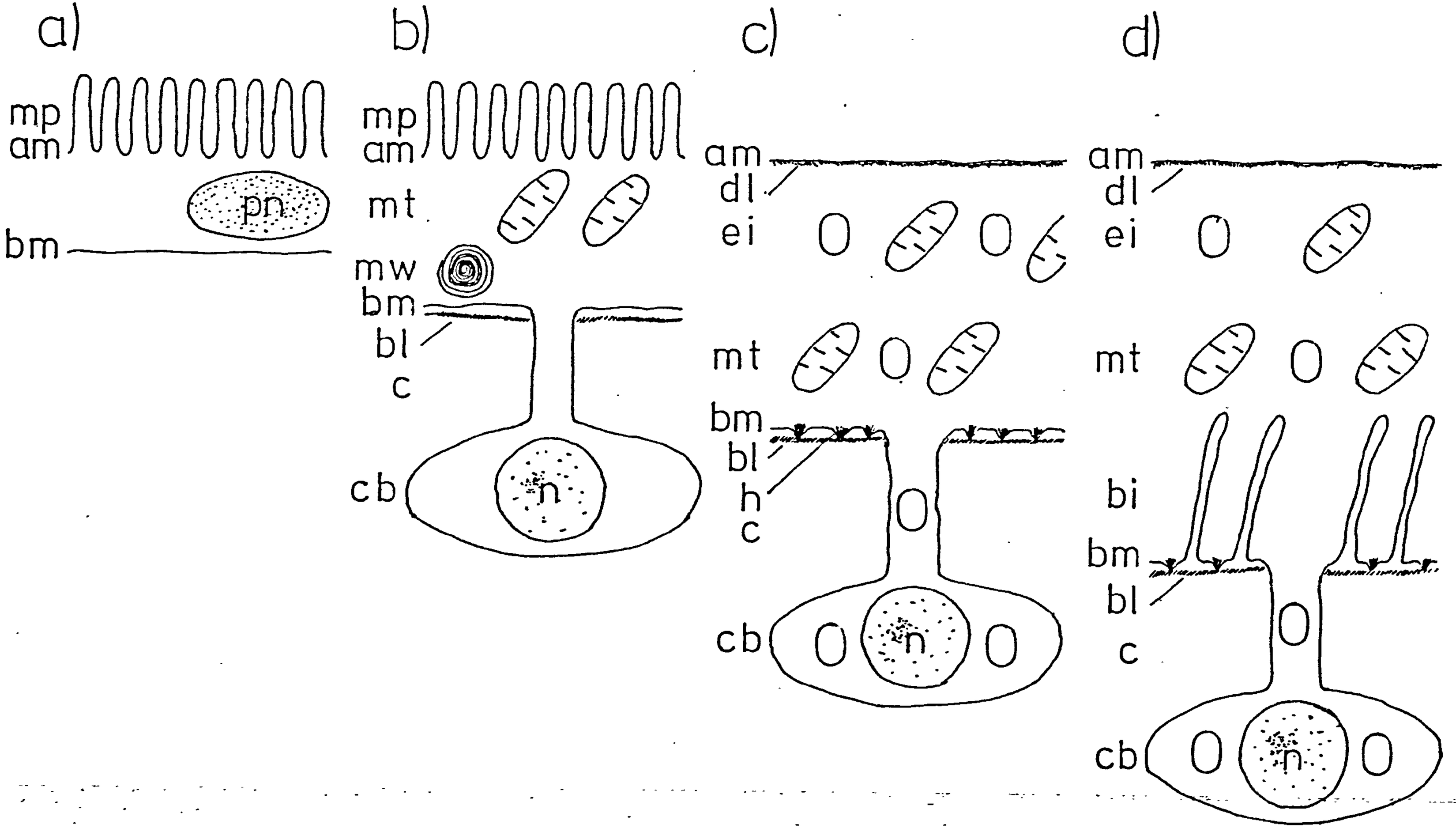
a)
mp
am
pn
bm
b)
mp
am
mt
mw
bm
bl
c
cb
n
c)
am
dl
ei
mt
bm
bl
h
c
cb
n
d)
am
dl
ei
mt
bi
bm
bl
c
cb
n

few details of the structure of the body wall could be discerned.

In Type One cercariae the surface layer was approximately 0.25 μm thick. The apical surface was folded into microplica 50-100 μm wide and 200 nm deep and was covered with a trilaminate apical plasma membrane (Plate 21). The base of the surface layer appeared to be delineated by a trilaminate basal plasma membrane (Plate 21). There were no discernable junctional complexes between the basal plasma membrane and the subjacent regions nor was it possible to distinguish cytoplasmic connections between the surface layer and the regions beneath.

The surface layer contained dense bodies interpreted as ribosomes on the basis of their size and form (Plate 21). In occasional sections the surface layer contained electron-dense structures 0.2-0.3 μm in diameter which appeared to be partially enclosed by, or closely associated with, unit membranes (Plate 21). These structures may have been pycnotic nuclei.

In Type Two intramolluscan cercariae the surface tegument was approximately 0.30 μm thick. Microplica surmounted by the trilaminate apical plasma membrane were present (Plate 22). The trilaminate basal plasma membrane had a subjacent dense layer - the basal lamina (Plate 22a and c). Dense bodies, resembling ribosomes, and mitochondria were distributed throughout the surface tegumental cytoplasm (Plate 22a and c). Membranous whorls were also present (Plate 22b). The surface tegument was connected to presumbed subtegumentary cell bodies by connectives (Plate 22a).

In Type Three cercariae spines were first apparent (Section 11). The surface tegument was approximately 0.8 μm thick (Plate 23).

As for less mature cercariae, the surface tegument was enclosed by an apical plasma membrane and a basal plasma membrane (Plate 24a). Subjacent to the apical plasma membrane was a 12 nm thick electron-dense layer. The cytoplasm was granular and contained spines, mitochondria and 0.2 μm diameter membrane bound electron-lucent inclusions (Plate 23a + 24a). The electron lucent inclusions reached the surface tegument from the sub-tegumentary cell bodies, in which they appeared to be manufactured, via cytoplasmic connectives (Plate 24a and Section 11). The sub-tegumentary cell bodies were nucleate and contained golgi apparatus, electron lucent inclusions, dense bodies, crystalline bodies, mitochondria, and dense arrays of ribosomes (Plate 23a + b, 24b, 25 and Section 11).

The electron lucent inclusions were very variable in size and shape. This was attributed to the orientation of the section and the inherent plasticity of the inclusions. The plasticity of the inclusion is clearly demonstrated by the distortion undergone during passage through the cytoplasmic connectives (Plate 24a).

In some sections the electron lucent inclusions appear to have an electron dense core (Plate 24a and 25a). This appearance may also be due to the highly variable shape of the inclusions. In Plate 25 inclusions can be seen to partially surround dense regions of cytoplasm. Certain sections through inclusions in this conformation would give the appearance of a dense core despite the fact that the dense material remains external to the unit membrane of the inclusion.

The basal plasma membrane was attached to an underlying 30 nm thick basal lamina by irregularly occuring hemidesmosomes (Plate 24a),

the basal plasma membrane being evaginated at the points of attachment (Plate 24a). Subjacent to the basal lamina was a layer of interstitial matrix containing fibres approximately 5 nm thick (Plate 24a). Beneath this region were layers of outer circular and inner longitudinal muscle fibres (Plate 23a). The fibres were approximately 0.4 μm in diameter and contained thick and thin filaments 20 nm and 5 nm in diameter.

The surface tegument of the adult was approximately 1.2 μm thick (Plate 26). It resembled the surface tegument of Type Three cercariae except for the following features. The electron lucent inclusions were infrequent (Plate 26). The basal plasma membrane was extended deeply into the cytoplasm of the surface tegument, forming invaginations approximately 0.4 μm long and giving the basal region of the surface tegument a lamellate appearance (Plate 26b).

10.3.3 The digestive tract

It was apparent from light microscopical observations that the digestive tract of the adult fluke was lined with two different components (Figure 10.1). The pharynx, oesophagus and anterior transverse regions had a syncytial lining while the posterior transverse and lateral regions had a cellular lining.

Plate 27a shows a section through the anterior transverse region of a Type Three cercaria at approximately the level of the ocelli. The intestine was lined with a 1.1 μm thick layer which closely resembled, apart from the absence of spines, the surface tegument of the general body surface. In some sections inclusions were present which may represent a different form to those in the surface tegument or may be another morphological variant of the

electron lucent inclusions (Plate 28a).

Plate 27b shows a section through the posterior transverse region of the digestive tract of a Type Three cercaria. In this region the intestine was lined with a gastrodermis of nulceated cells. Junctions between the cells can be seen where the cell junction abuts the lumenal surface. The apical surface of the cells was drawn into 30 nm wide extensions projecting 1.6 μm into the lumen (Plate 27a + 28a). Membrane bound densely granular 0.5 μm inclusions were associated with the apical cytoplasm (Plate 27a + 28a). Granular endoplasmic reticulum and mitochondria were present.

The disparate nature of the surface tegument and gastrodermal cells was most obvious at the junction between the two regions (Plate 27a). The two regions were joined by a septate desmosome (Plate 27b).

The regional differentiation of digestive tract lining was present in the adult as well as Type Three cercariae. The gastrodermis of the adult, however, differed markedly from that of the cercaria. The lamellar extensions of the apical surfaces of the gastrodermal cells formed a more extensive layer than previously (Plate 29a). The lamellae often described tortuous routes, occasionally anastomosing with other lamellae and returning to the cell surface. The lamellae appeared to subdivide at the tip into microvillar extensions. Each lamella was covered by the trilaminate plasma membrane of the gastrodermal cell (Plate 29b).

The membrane bound granular inclusions of cercarial gastrodermal cells were infrequent in the adult (Plate 29a). Membrane bound electron lucent regions adjacent to the apical plasma membrane

were interpreted as exhausted inclusions on the basis of their size and location (Plate 29a + b). Large numbers of mitochondria were present in the apical cytoplasm (Plate 29a). The gastrodermal cells were joined by desmosomal connections, associated with cisternae of the smooth endoplasmic reticulum (Plate 29b).

10.3.4 Protonephridia

Flame cells were distributed throughout the body of the Type Three cercaria including the ventral sucker and tail (Plate 30). They were first discernable in Type One cercariae (Plate 31a) and were apparently fully developed in early Type Three cercariae. At the time of emergence a complex tubule system joined approximately 60 flame cells.

The flame cells were apparently of typical digenean form (Plate 31b). A central ciliary "flame" was surrounded by inner ribs presumably derived from the flame cell body (Plate 32b). Cytoplasmic processes, or leptotriches, arose from the inner ribs and filled the area adjacent to the flame. Outer ribs, presumably arising from the adjacent excretory tubule, were attached to the inner ribs by desmosomes. The orientation of each cilium within the flame was identical (Plate 32a).

10.3.5 Vitelline cells

In Type Two intramolluscan cercariae the vitelline cells had a large nucleus with a peripheral rind of cytoplasm containing a very few vitelline granules (Plate 33a). In Type Three cercariae the cytoplasm/nucleus ratio was greatly increased and numerous vitelline granules were present (Plate 33b).

10.3.6 Sensory structures

The adult fluke was biocellate. The rhabdomeric ocelli first appeared in Type Two cercariae in which the pigment granules were sparse (Plate 34a). In Type Three cercariae the ocelli were fully developed (Plate 34b + 33c).

The surface of Type Three cercariae and adult flukes had unciliate sensory endings. These were distributed throughout the body surface where they occurred between spines ventrally and dorsally (Plate 35). Sensory endings were also associated with the ventral sucker (Plate 16b).

The sensory endings consisted a bulb with a single projecting cilium. The bulb was approximately 1.25 μm in diameter and enclosed within the surface tegument (Plate 36). A septate desmosomal ring attached the bulb to the tegument (Plate 36c). Associated with the desmosome was an electron dense ring with a second proximal ring independently attached to the sensory bulb plasma membrane (Plate 36b). Apart from these osmiophilic rings the bulb cytoplasm also contained characteristic inclusions (Plate 36c). The inclusions were 80 nm in diameter and consisted of a dense core surrounded by a moderately dense region, the whole enclosed by a membrane.

The projecting cilium had a diameter of 0.22 μm and extended 2.5 μm from the bulb. The proximal region of the cilium was surrounded by a collar of surface tegumentary material (Plate 36c).

10.3.7 Sperm development

Mature sperm were present in the seminal receptacle and uterus of Type Three cercariae (Figure 10.1). These were apparently of typical digenean structure (Plate 37). Mechanical pressure on

cercariae or adults caused the extrusion of sperm from the genital pore (Plate 18d).

In Type Two cercariae the germinal cells of the testis were present (Plate 38). These cells had a large nucleus surrounded by a peripheral rind of cytoplasm. The nuclei contained synaptonemal complexes indicative of meiotic activity.

10.4 Discussion

10.4.1 General

The surface topography of rediae has been examined in two other species: Opechona bacillaris and Fasciola hepatica (Koie, 1975; Koie et al., 1976). In both species supposed sensory structures were associated with the anterior opening into the pharynx. These were not discerned in the redia of T. patialense, possibly as a result of preparative techniques since it would appear unlikely that an actively foraging organism could function efficiently without anterior sensory input.

All these rediae described had a body surface folded into microplica. This would tend to increase the surface area and hence the absorptive capabilities of the body wall. Koie et al. (1976) suggested that this was an adaptation to trans-tegumental metabolic activity, implying that the pharynx and gut alone are unable to satisfy the nutrient requirements of the redia and its developing larvae.

Cercarial development external to rediae or sporocysts is known from only four families other than the transversotrematids (Pearson, 1972). SEM techniques, however, have apparently only

been used to describe the extra-redial cercarial development of Opechona bacillaris (Koie, 1975). In T. patialense and O. bacillaris the immature cercarial body was typically much larger than the tail region, subsequent growth causing a disproportionate increase in tail length relative to body length.

The surfaces of early cercariae were folded into microplica. The relevance of this increase in surface area to nutrient acquisition is discussed in Section 10.4.3.

The fully developed intramolluscan and free-living cercariae of T. patialense were morphologically indistinguishable. Furthermore, apart from its larger size, the adult fluke was indistinguishable externally from the cercarial body. Tail loss by the cercaria resulted in a lesion of presumed traumatised tissue on the posterior dorsal surface of the adult. This was similar to that described from the schistosomulum of Schistosoma mansoni (Howells, Gerken, Ramacho-Pinto, Kawazoe, Gazzinelli and Pellegrino, 1975). It was suggested by these workers that the lesion formed at the cercaria-schistosomulum transformation caused the temporally associated changes in osmotic tolerance. A similar tolerance change is associated with tail loss in T. patialense (Mills, 1977). In both species, however, subsequent long term changes in adult tolerances, are almost certainly a consequence of changes in the body surface tegument (Howells, Ramacho-Pinto, Gazzinelli, De Oliveria, Figueiredo and Pellegrino, 1974; Howells et al., 1975).

10.4.2 The body surface

In 1963 Threadgold, using TEM techniques, demonstrated for the first time that the covering layer of Fasciola hepatica adults

was a living syncytium, consisting of an anucleate superficial layer in cytoplasmic continuity with nucleated cell bodies within the tissues of the fluke. This basic structure has since been described from every adult digenean examined using TEM techniques and is probably a universal feature of the group.

Unfortunately, this unanamity of structure has not extended to the descriptive nomenclature. The early term "cuticle" was abandoned on the suggestion of Threadgold (1963), presumably to avoid confusion with the inert coverings of other taxa. Instead the terms tegument (Threadgold, 1963) or epidermis (Lee, 1966 and 1972) have been suggested. Despite the simplicity of the latter term, tegument has become generally accepted possibly because of its primogenetive position. The derivative "integument" is more commonly used in the U.S.A. (Burton, 1964). In the present investigation the term tegument is adopted because of its wide acceptance.

The problems of nomenclature, however, do not stop at the naming of the overall structure, the component parts have themselves been variously described. The difficulties arise because the tegument is not simply a covering layer but exists at two levels. An anucleate syncytium covers the surface of the flukes, and to a limited extent lines the gut and excretory passages. Beneath this outer layer, and its subjacent musculature, is a second layer composed of nucleate cell bodies connected to the outer layer by cytoplasmic processes but without lateral connections. As predicted by Lee (1966) many authors have referred to the surface layer alone as though it were an independent structure, variously terming it the tegument (Bogitsh, 1968 and 1972), syncytial

tegument (Hockley, 1973), general tegument (Erasmus, 1967) and integument (Bils and Martin, 1966; Burton, 1966). A similarly misleading practice is the description of the nucleate regions of the tegumental syncytium as cells, despite the fact that these regions are not discrete units but are in cytoplasmic continuity: for example, tegumentary cells (Threadgold, 1967 and 1976; Erasmus, 1967) and subtegumentary cells (Bogitsh, 1968; Hockley, 1972). The common practice in the U.S.A. of referring to these regions as perinuclear cytoplasm (Burton, 1964; Bogitsh, 1972) is also misleading since it might be thought to exclude the nucleus and outer plasma membrane. In the present investigation the tegument will be considered to consist of a surface tegument in communication via cytoplasmic connectives with a layer of nucleate tegumentary cell bodies. This terminology is sufficiently similar to that commonly used to be readily interpreted while avoiding most of the ambiguities.

Tegumental morphogenesis during the cercarial/adult generation has been examined in very few species, yet different findings have been reported for each. The only unifying characteristic is that the developing cercarial embryo is surrounded by a cellular rind beneath which the tegument develops. Even this simplification is disputed by Rifkin (1970).

The intrasporocyst cercarial embryo of Schistosoma mansoni is invested with a "primitive epithelium" of cells, derived from the embryo (Hockley, 1972) or the sporocyst (Meuleman and Holzmann, 1975). A thin nucleate covering syncytium develops beneath the primitive epithelium the latter is then sloughed off. The nuclei of the syncytium become pycnotic and subjacent cells extend

processes which fuse with the surface syncytium so forming a true tegument which persists through to the adult (Hockley, 1973).

Rifkin's (1970) description of S. mansoni tegumental morphogenesis uniquely omitted the primitive epithelium and ascribed the origin of the surface tegument to the sporocyst. Elongate sporocyst cells are said to surround the cercarial embryo, fuse to form a syncytium and then become connected to nucleate subjacent cells to form the tegument.

Tegumental development in Acanthoparyphium spinulosum and Cloacitrema narrabeenensis cercariae is apparently similar to that described for S. mansoni by workers other than Rifkin (1970) (Bils and Martin, 1966; Dixon, 1970). A rind of cells invests the cercarial embryo, originating from the embryo in A. spinulosum and the sporocyst in C. narrabeenensis. Peripheral embryonic cells form a syncytium beneath the primitive epithelium which is then shed. Nuclear regions of the surface syncytium migrate down into the cercarial body to complete the structural development of the cercarial tegument. In C. narrabeenensis this cercarial tegument is lost during the process of metacercarial encystment and replaced by a tegument which persists through to the adult (Dixon, 1970). The new tegument is formed by the coalescence of superficial processes from cystogenous cells.

In Fasciola hepatica an embryo derived primitive epithelium covers the cercaria until metacercarial encystment (Dixon and Mercer, 1967). The metacercaria then becomes covered by a true tegument originating from cystogenous cells.

Immature cercariae of T. patialense possessed a syncytial covering layer. This was clearly not a cellular primitive epithelium. although the existence of a cellular investing layer at some earlier stage, possibly within the redia, cannot be discounted.

The origins of this surface syncytium are obscure. The membrane bound dense regions present within the surface syncytium may represent degenerate nuclei in which case the syncytium could arise from coalesced embryonic or redial cells. The apparent absence of cytoplasmic connections to any deeper cell bodies implies that the surface layer was formed entirely from peripheral material and not from processes of subjacent cells.

Type Two cercariae had a true tegument. The surface tegument was of similar thickness to the surface syncytium and carried microplica of identical form and dimensions. It is probable that the surface tegument is equivalent to the early surface syncytium. Connection with tegumental cell bodies probably arises by fusion with peripherally directed processes of subjacent cells, rather than the sinking of nuclei, in the absence of discernable intact nuclei within the surface syncytium.

The mature cercaria of T. patialense had a thicker surface tegument than the immature forms, i.e. 0.8μm rather than 0.25μm. It should be noted that the tegument considered here is that of the general body surface. It has been demonstrated in other species and T. patialense cercariae (Anderson et al., 1975) that the structure of the surface tegument is regionally specialized so that at different sites on the same individual it may vary in topography and composition (see Lee, 1972 and Erasmus, 1972 for reviews of this literature).

The thicker surface tegument of the mature cercaria contained spines and electron lucent inclusions. The nature of the spines is discussed in Section 11. The electron lucent inclusions resemble those described from the cercariae of Zoogonoides viviparus as "light bodies" (Koie, 1971) and from Podocotyle staffordi as "osmiophobic vesicles" (Gibson, 1974). The cercarial surface tegument of Acantharium oregonense and Schistosoma mansoni contains membrane bound electron lucent inclusions, but these differ from those of the present species in possessing a dense fibrillar core (Belton and Harris, 1967; Hockley, 1973).

The electron lucent inclusions were present in the surface tegument of adult T. patialense although they were less numerous than in the cercaria. This reduction in frequency was too great to be explained by the slight increase in surface tegument thickness between the adult and cercarial stages.

The presence of a single type of inclusion is uncharacteristic of the tegument of adult digeneans. Of nine species examined, representing seven families, in no case were less than two types of inclusion present (Threadgold, 1963, 1967 and 1968; Burton, 1964 and 1966; Erasmus, 1967; Bogitsh, 1968 and 1972; Morris and Threadgold, 1968; Smith, Reynolds and Von Lichtenberg, 1969; Bibby and Rees, 1971; Harris, Cheng and Cali, 1974; Bennett and Threadgold, 1975). Furthermore, none of the inclusions described closely resembles that of the present species. The surface tegument of Megalodiscus temporatus does contain an electron lucent inclusion, but this is much larger and characteristically associated with the apical plasma membrane (Bogitsh, 1968).

As described in Section 10.3 the tegumental inclusions exhibit considerable morphological variation which was attributed to sectioning artifacts and inclusion plasticity. This assumption is supported by the apparent gradation from one morphological form to another. Nevertheless, it is not possible to define the nature of the inclusions without supporting histochemical evidence. It is tentatively suggested, therefore, that there is a single type of inclusion in the tegument of T. patialense but confirmation must await more rigorous experimental analysis.

The function of the inclusions in T. patialense is unknown. In Section 11 a possible involvement in glycocalyx formation is discussed but in the absence of histochemical evidence any suggestions must be purely speculative.

Rambourg (1971) has shown that the external plasma membranes of all cells are coated with a polyanionic carbohydrate rich layer or glycocalyx. In typical endoparasitic digeneans a complex of secretory granules deposits this presumed protective layer on the external surface of the tegument (Threadgold, 1976; Hanna and Threadgold, 1976). Typically ectoparasitic monogeneans apparently solve their problem of exposure to the external environment in a similar manner (Morris and Halton, 1971).

In other respects the surface tegument of this species resembles that of other digeneans. Mitochondria were present in 8 of the 9 species mentioned above and deeply invaginated basal plasma membranes were described in five of them.

10.4.3 The digestive tract

Lamellar projections of gastrodermal cells have been described from the adults of Schistosoma mansoni (Morris, 1968), Schistosomatium douthitti (Dike, 1969), Haematoloechus medioplexus (Davis, Bogitsh and Nunnally, 1968; Shannon and Bogitsh, 1969), 6 species of Paragonimus (Fujino and Ishii, 1978), and Fasciola hepatica (Robinson and Threadgold, 1975); and from the cercariae of Zoogonoides viviparus (Koie, 1971) and Neophasis lageniformis (Koie, 1973).

The secretory and absorptive function ascribed to lamellate gastrodermal cells (Shannon and Bogitsh, 1969; Robinson and Threadgold, 1975) almost certainly does not include the tegument lined region of the digestive tract and hence consideration of gut activity is confined here to the gastrodermal cells.

The relative importance of the body surface and the intestine as routes for nutrient absorption appears to alter during the transformation from cercaria to adult in T. patialense. It is probable that in Type One and Two cercariae trans-tegumental absorption is the exclusive route for nutrient uptake since the pharyngeal aperture is imperforate, and the intestine therefore inaccessible, while the surface tegument has a greatly enhanced surface area due to the microplicae. In adults and presumably non-feeding cercariae, however, the pharynx is perforate and microplica absent implying that the intestinal route predominates.

The location of mature cercariae within the digestive gland suggests that the contents of the gland are used as a nutrient source.

Similar circumstantial evidence suggests that the adult feeds on fish mucus (Section 11). The enormous proliferation of gastrodermal lamellae in the adult may be a reflection of the relative nutrient value of these two diets or of increased metabolic demands in the adult stage.

The apical dense granules observed within the cercarial gastrodermis probably have a secretory function. In the adult these were less frequent although their evacuated membranes were present. This may suggest that the adult gut is more active, secreting material into the lumen more rapidly than it can be formed, an hypothesis supported by the proliferation of the mitochondria.

Perhaps the cercarial gastrodermal cells have a limited secretory and absorptive role but act as a depot for secretory material which is immediately available to the established adult.

The ultrastructure of the gastrodermal cells of Fasciola hepatica has been described from the cercarial to the adult stage (Bennett and Threadgold, 1973; Bennett, 1975a). The cercaria and migrating juvenile have characteristic gastrodermal cells ("A cells") which contain large (1.3μm) dense inclusions involved in disrupting host cells to facilitate penetration (Bennett, 1975a). On entering the hepatic site of the adult the gastrodermal cells change their nature to "B cells", with small (0.5μm) inclusions and extensive lamellae, and adopt an absorptive and secretory role.

In T. patialense the gastrodermal cells of cercaria and adult resemble "B cells". It is possible, however, that the dense inclusions of the cercarial gastrodermis are involved in producing lytic secretions to facilitate migrations within the mollusc. In

the adult the dense inclusions could have a digestive function.

10.4.4 Protonephridia

Development of protonephridia in the cercaria of T. patialense had apparently started before the primordial cercaria emerged from its redia. By the time the fully developed cercaria emerged from the snail host a large number of flame cells (approximately 60) were present and an extensive tubule system had developed. This indicates a high degree of sophistication in larval differentiation and development reducing subsequent development on the definitive host.

An interesting feature of the structure of the protonephridial flames is the highly ordered orientation of the cilia. It is apparent that the planes determined by the pairs of central microtubules were all approximately parallel to one another. This phenomenon is apparent in TE micrographs of the cercarial flame cells of Himasthla quissetensis and the miracidial flame of Fasciola hepatica (Cardell, 1962; Wilson, 1969c). This pattern arises because the flame cilia are required to beat unidirectionally. A cilium bends in a plane precisely normal to a plane running through both central axonemal microtubules (Tamm and Horridge, 1970; Satir, 1974), since all the flame cilia bend in the same direction their structural orientation must also be identical.

10.4.5 Vitelline cells

Mills (1977) showed by histochemical means that the amount of vitelline material produced by T. patialense increased with age from the free-swimming cercarial to the adult stage. This would be intuitively expected since the vitelline material is primarily

involved in oogenesis and would be in most demand in the ovigerous adult. The present results indicate that vitelline granules are present in Type Two cercariae, a much earlier occurence than had been assumed. Previous work on the development of vitelline cells has concentrated on vitellogenesis in adult platyhelminths (see Swiderski and Mackiewicz, 1976 for extensive review) but there seem to be no previous records which accurately determine the earliest developmental stage at which vitelline production can be demonstrated.

10.4.6 Sensory structures

The ocelli of the cercaria of T. patialense appeared to each consist of a single rhadbdomere surrounded by a cup-shaped pigment cell. This structure resembles that of the eyespots of Crepidostomum sp. cercariae (Pond and Cable, 1966). The cercariae of Macrovestibulum eversum, Skrjabinopsolus manteri and Spirorchis sp. all have double rhabdomeres (Pond and Cable 1966; Isseroff and Cable, 1968).

The presence of ocelli in early intramolluscan cercariae is a novel finding. It is highly improbable that a light receptor is functional or useful within molluscan tissues and yet the eyespot only requires additional condensation of pigment to attain the differentiation apparent in the free-living cercaria.

An unusual feature of transversotrematids is the persistence of eyespots into and throughout the adult stage. All species of the genus Transversotrema are now known to possess this character. The original description of the marine species T. haasi by Witenberg (1944) failed to record the presence of ocelli in the adult, however a recent redescription by Velasquez (1975) confirmed that

this species also is biocellate.

Supposed sensory receptors, consisting of a bulb and single cilium-like projection, have been recorded from cestodes, monogeneans and digeneans. Attempts to compare these structures in the different taxa on the basis of ciliary rootlet structure and relative numbers of membrane bound vesicles have met with limited success (Matricon-Gondran, 1971). Neither of these characters is satisfactory since sectioning artifacts make precise interpretation difficult (Weibel, 1969).

A more satisfactory character would appear to be the structure of the osmiophilic rings within the bulb. The sensory bulb plasma membrane is attached to the tegumental membrane by a desmosome which entirely encircles the distal margin of the bulb. Associated with the desmosome within the bulb cytoplasm is a dense body which also forms a continuous ring. A second intra-cytoplasmic dense ring, apparently attached to the inner surface of the bulb plasma membrane but not associated with any desmosomal connection, is situated below the first ring. This double structure was first identified, in the adult of Schistosoma mansoni, by Morris and Threadgold (1967) who also noted that the proximal ring may possess one or more lumena. Chapman and Wilson (1970), in the cercaria of Himasthla secunda, interpreted the proximal ring as a second desmosome. No inter-membranous septae are discernable at this locus in their published TE micrographs nor are they apparent in TE micrographs of T. patialense cercariae and adults, Cyathocotyle bushiensis adults (Erasmus, 1967), S. mansoni cercariae (Nuttman, 1971), Echinostomum paraensei cercariae (Matricon-Gondran, 1971),

Diplostomum phoxini cercariae (Bibby and Rees, 1971), and Zoogonoides viviparus cercariae (Koie, 1971). On the available evidence it appears that the characteristic structure of digenean uniciliate sensory endings includes a pair of osmiophilic rings, only the most distal of which is closely associated with a desmosomal connection.

In adult monogeneans an entirely different structure is present. An osmiophilic cylinder is associated with the desmosome of uniciliate receptors in Gyrodactylus sp. and Entobdella soleae, while in Diclidophora several osmiophilic rings are present (Lyons, 1969; Halton and Morris, 1969). These structures were ascribed a cytoskeletal function by Lyons (1972) and the osmiophilic rings of digeneans may similarly serve to support the sensory bulb.

TE micrographs of sensory bulbs in the tegument of the cestode Echinococcus granulosus only show a single osmiophilic ring (Morseth, 1967).

From present evidence it would appear that the uniciliate sensory bulbs of cestodes, digeneans and monogeneans may be distinguished on the conformation of cytoskeletal structures.

Section 11:

Spine Morphology

11. Spine Morphology

11.1 Introduction

Hard structures have been observed in the surface tegument of a sufficiently wide range of unrelated species for them to be considered a digenean characteristic. These structures have been variously described as spines, scales and hooks; descriptions which all rely on the shape of the structures. The term spine is sufficiently commonly used to be accepted and is the terminology adopted here. It has the further advantage of avoiding confusion with the hooks of the other major groups of the Platyhelminths, the Cestoda.

The taxonomy of the Digenea is notoriously difficult due to the lack of hard tissues unaffected by preparative techniques. The apparent relative constancy of form of eggs and spines has, therefore, encouraged their use in taxonomic descriptions. The distribution and form of spines is frequently described in specific diagnoses, in increasing detail following such improvements in observational techniques as the introduction of the scanning electron microscope (Kuntz, Tulloch, Huang and Davidson, 1977; Sakamoto and Ishii, 1977).

Regardless of the observational technique, however, the usefulness of these characters is dependent on an understanding of their variability within a species. Age and environmental factors might be expected to influence the development of spines so that flukes of the same speceis but with different histories exhibit differing patterns and sizes of spines. Unless the range of this

variation is known no conclusions can be drawn as to the relationship of individuals on spine characteristics alone.

The present investigation attempts to provide information on spine structure and formation in transversotrematids while examining the age dependency of spine morphometrics.

11.2 Materials and Methods

11.2.1 Preparation for microscopy

Intramolluscan cercariae, free-living cercariae and adults of Transversotrema patialense were obtained using the techniques described in Sections 2.3, 2.5 and 2.7.

Newly emerged cercariae and removed adults were fixed in 70% ethanol. After dehydrating through the alcohol series the material was cleared in xylene. Undistorted specimens were selected for the preparation of whole mounts in Canada Balsam. Permanent mounts of this type were used in the analyses of spine and fluke morphometrics described below.

Intramolluscan cercariae, free-living cercariae and adults were prepared for SEM and TEM as described in Section 2.8. This material was utilised for examination of spine distribution and morphogenesis.

Material for the examination of the fluke-host interface was treated differently. Anaesthetised infected fish (Section 2.5) were immersed in boiling formaldehyde solution causing instantaneous fixation of host and parasites. Fish scales were removed and the exposed flukes floated off in a stream of pipetted water. The

sides of the fish were then dissected off, dehydrated through an alcohol series and immersed in acetone before preparation for SEM (Section 2.8).

11.2.2 Spine growth

Fish were infected at mid-day so that flukes removed at noon on subsequent days could be ascribed an exact age in days post infection (P.I.).

Adult flukes were removed (Section 2.5) at six ages: 0, 1, 3, 7, 14 and 21 days P.I. Permanent mounts of two flukes at each age were prepared. For each specimen the information recorded and method of examination were the same.

Each adult was observed at 1000 X magnification using an eye-piece graticule. Ten spines were measured at each of the spine row positions 10, 20, 30, 40 and 50 on the ventral and dorsal surfaces (Figure 11.1). The length (L) of each spine was measured from the base to the apex and the width (W) across the spine base.

From the 100 measurements of L and W on each surface a mean value was determined. This was then the mean spine size on a given surface at a particular fluke age.

11.2.3 Spine density

An eye-piece graticule was etched with a square of dimensions such that at 1000 X magnification it enclosed an area of $400\mu m^2$. Slide mounted flukes of ages 0, 3, 7, 14 and 21 days P.I. were examined at row positions 10, 20, 30, 40 and 50 on the dorsal and ventral surfaces (Figure 11.1). The graticule was orientated in the same way for each row position: one spine from the row lay

Figure 11.1: Schematic representation of the position of spine rows on the dorsal and ventral surface of adult flukes.

The left portion of the diagram represents the ventral surface, and the right portion the dorsal surface. The most anterior row on either surface was designated "row one" and subsequent rows were numbered in sequence posteriorly.

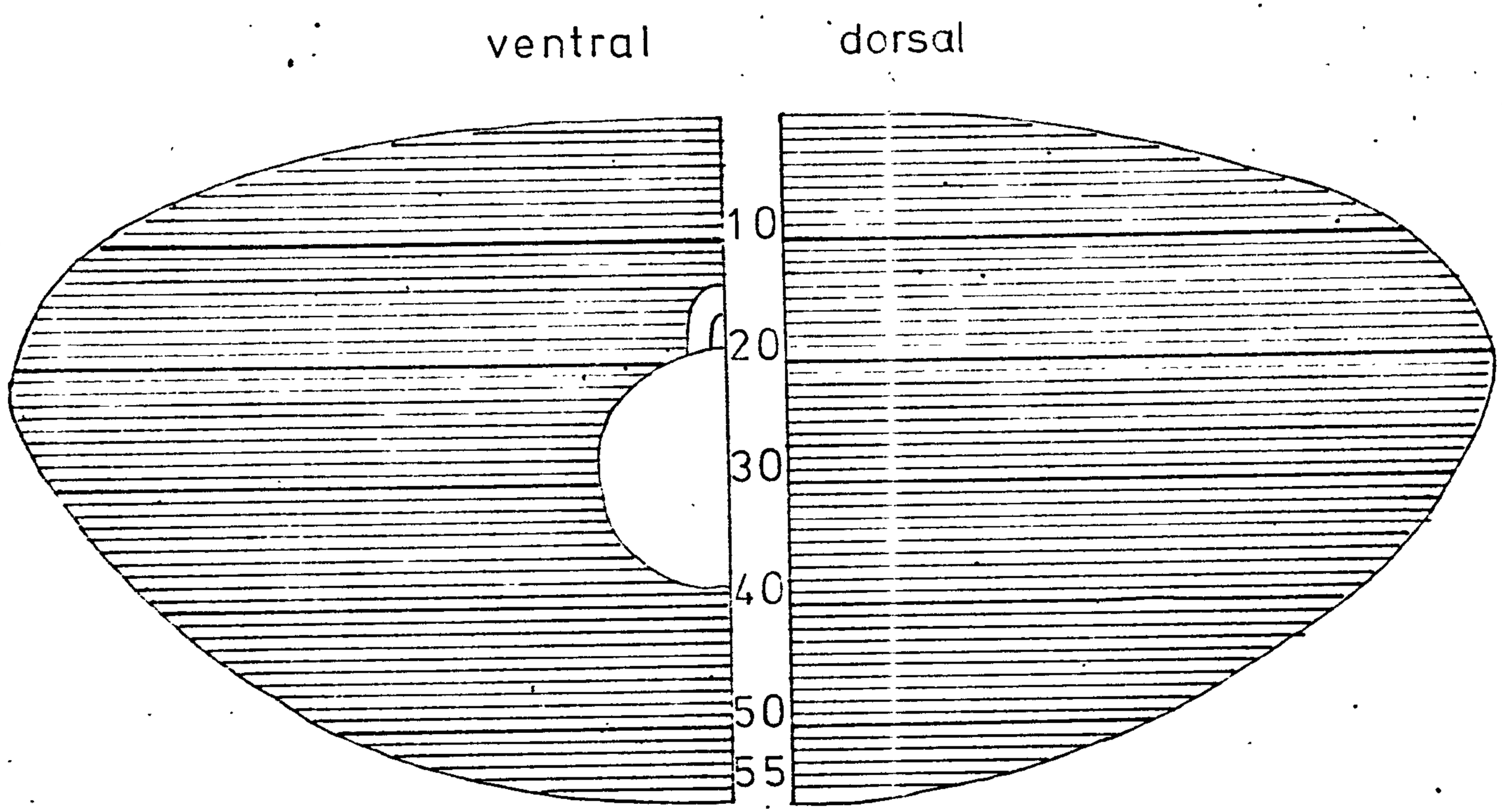
ventral
dorsal
10
20
30
40
50
55

at the mid-point of the left hand margin of the square. The number of spine bases within the area of the square was then determined.

From the 5 measurements of density on both surfaces of two flukes examined at each age a mean density was determined for each stage in development.

11.2.4 Number of spine rows

S.E. micrographs were prepared of the ventral surface of six flukes for each of the ages 0, 7 and 21 days P.I. The number of rows of spines was then determined by direct counting.

11.2.5 Spine number

Permanent mounts of 2 flukes at 0 and 21 days P.I. were prepared. Every fifth row of spines between rows 5 and 55 on the ventral surface was examined (Figure 11.1). For each of these rows the number of spines between the mid anterior-posterior axis and the margin of the fluke was determined; that is half the total number of spines in each row. Taking a mean of these values for each fluke gave the mean number of spines per half row on the ventral surface. Doubling this figure provided an estimate of the mean number of spines per row which multiplied by the number of rows indicated the total number of spines present.

S.E. micrographs of the ventral surface of two 21 day old flukes were prepared. The number of spines on the ventral surface and ventral sucker was counted directly.

11.2.6 Fluke growth

Fluke growth was estimated in terms of area. Permanent mounts were prepared of flukes 0, 3, 7, 14 and 21 days P.I. Micrographs

of five flukes from each age were printed at the same magnification and the image of the worms cut out and weighed. By a weight/area conversion the area of one surface of the fluke was determined.

The surface area measurement was the plane projected area of the fluke, that is the area apparent in a precisely normal observation of the dorsal or ventral surface. It was assumed that the area in either dorsal or ventral view was identical. All subsequent references to fluke surface area refer to the area apparent for a single surface, whether ventral or dorsal.

11.3 Results

11.3.1 General distribution of spines

Under SEM examination Type One and Two intramolluscan cercariae were aspinose (Plates 13 and 15).

Spines were first apparent in Type Three intramolluscan cercariae although partially concealed by corrugations of the surface tegument (Plate 35a).

In late Type Three cercariae the spination was essentially that of the adult and these are, therefore, considered together.

In Type Three cercariae and newly attached adult spines were absent from the posterior third of the dorsal surface although as the adults matured the ventral and dorsal surface were covered with spines (Plates 17c, 20a and d, 42d).

The spines were scale-like, due to dorso-ventral compression, and directed with apex posteriad. The pattern of the surface spines was similar on the dorsal and ventral surfaces. The rows

ran transverse with each alternate row displaced laterally so that each spine lay between the spines of the rows immediately before and after (Plate 17c) (see Section 11.4).

Spines were absent from the body margins and the regions immediately adjacent to the genital pore, pharynx and the opening of laurer's canal (Plates 17d, 18a and 20c).

Spines were also absent from the ventral surface beneath the ventral sucker (Plate 16b). The ventral sucker, while aspinose until the late Type Three cercarial stage (Plate 16a), had a characteristic spination in all later stages. There appeared to be two regional divisions: a peripheral palisade of spines forming a complete ring within the periphery of the ventral sucker, and a central spinous region in which no regular pattern could be distinguished (Plate 16b).

11.3.2 Spine and related tegumental ultrastructure

Neither spines nor spine primordia were identifiable in T.E. micrographs of Type One and Two intramolluscan cercariae (Plates 21 and 22).

Spines first became apparent in early Type Three intramolluscan cercariae where they were partly concealed by the surrounding microplicae and tegumental corrugations (Plate 39a). Dense granules of 10 nm diameter, interpreted as ribosomes, were observed closely associated with spines (Plate 39b).

The region of spine attachment to the basal plasma membrane and basal lamina was less dense than in later forms (Plate 39b).

Mature spines were scale-like, dorso-ventrally compressed and directed with the apex posteriad (Plate 23). The exterior surface of the spine was almost flat with a slight convex curvature. The underside of the spine, the surface most closely apposed to the tegumental surface, possessed a proximal central keel. Distally the keel was lost, the apex of the spine becoming thin and blade-like. Figure 11.2 shows diagrammatically the relationship of the spine to the tegument. The spine structure may be discerned with reference to the sequential transverse sections of Plate 40 and the longitudinal section of Plate 23b.

The spines were entirely enclosed within the surface tegument of the fluke. The external surface and apex of the spine was covered by the trilaminate apical plasma membrane of the surface tegument and its subjacent dense layer (Plate 41a).

The base of the spine abutted against the trilaminate basal plasma membrane of the surface tegument. In this region the basal lamina was more dense than elsewhere and this enhanced density was also apparent in the adjacent region of the spine base (Plate 23b and 41b). The increased density of the basal lamina was not apparently due to condensation of fibres from the interstitial matrix but due to the presence of dense globular units approximately 10 nm in diameter.

Due to the posteriad orientation of the spine apex there was considerable asymmetric distortion of the associated membranes (Figure 11.2 and Plate 23b). Reflexion of the spine resulted in the formation of a surface invagination between the apical plasma membrane where it enclosed the underside of the spine and its

Figure 11.2: The structure of the spine and related body wall of cercariae and adults.

a) Longtitudinal section of spine.

b) Transverse section of spine at XX in (a).

Key: am, apical plasma membrane; bl, basal lamina; db, dense region of basal lamina; dl, dense layer; ei, electron lucent inclusion; h, hemi-desmosome; i, isthums of interstitial matrix; im, interstitial matrix; m, mitochondrion; mf, muscle fibre; s, spine; st, surface tegument.

a)

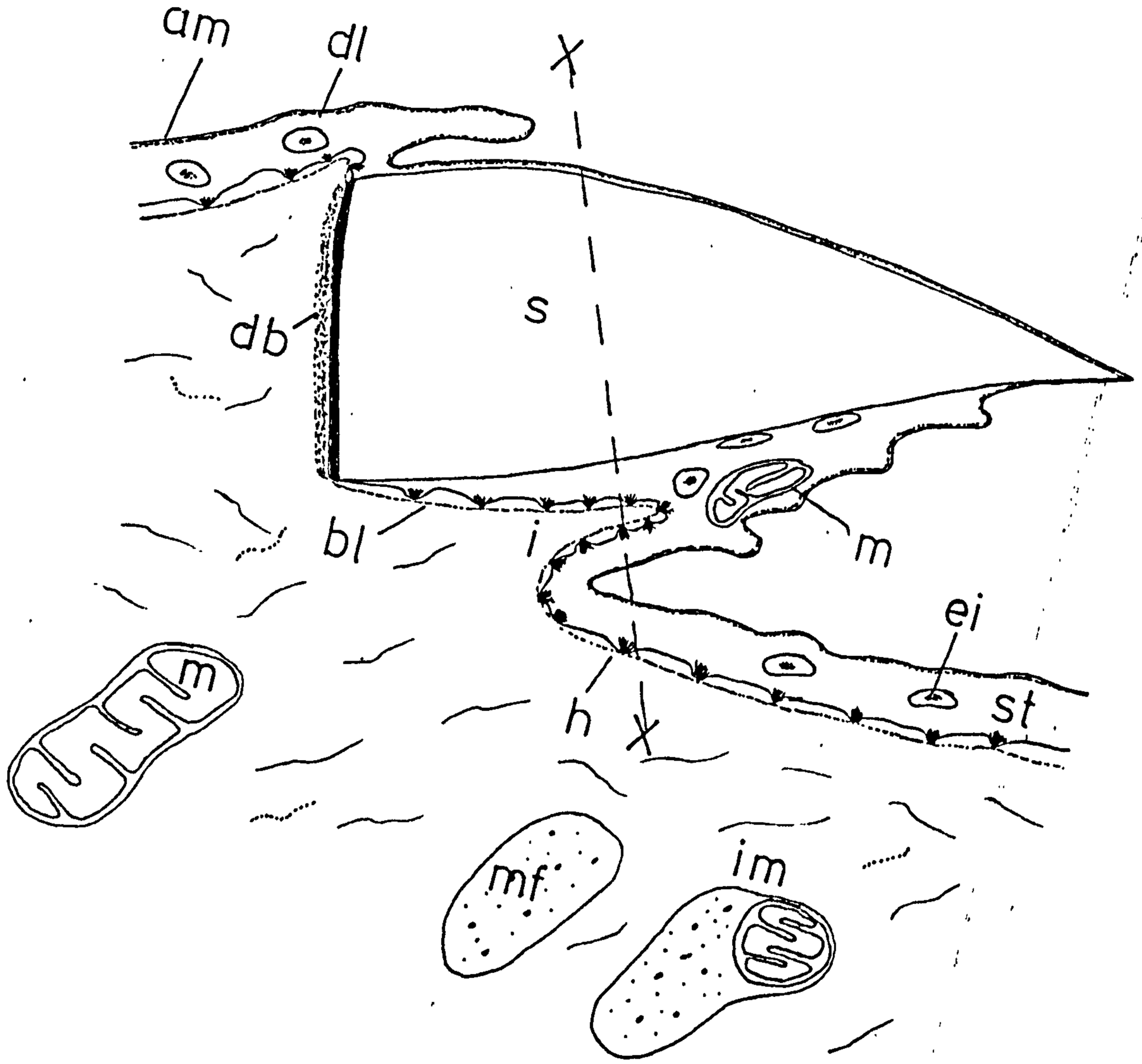

b)

general tegumental level. Similarly, the basal plasma membrane was drawn into a "step" around the spine base.

The nature of the surface invagination could be clearly discerned from transverse sections of the spine (Figure 11.2 and Plate 23a and 40). From such sections it was apparent that the underside of the spine incorporated a layer of surface tegumental cytoplasm between the apical plasma membrane and the spine, and that this cytoplasmic layer was penetrated by a narrow isthmus of interstitial matrix (Plate 41c).

Apart from the region of the spine base the basal plasma membrane was attached to the underlying basal lamina by hemidesmosomes (Plate 24a). These were also present around the narrow isthmus of interstitial matrix underlying the spines (Plate 41c).

The posterior third of the dorsal surface of cercariae bore spines in a completely different relationship to the tegument. Under LM and SEM observation this region was apparently aspinose. T.E. micrographs, however, revealed the presence of minute spines which did not extend to the apical plasma membrane and hence were not observable as external features (Plate 39c). These spines were attached to the trilaminate basal plasma membrane in the normal manner but did not cause local distortion. The subsequent presence of normal spines in this region of mature adults suggests that these diminutive spines represent an early stage in spine morphogenesis.

The infrastructure of spines appeared as an amorphous matrix, alternating electron dense and electron lucent striations or electron lucent globular units in a dense matrix (Plates 23b and 41).

This variability in appearence was ascribed to sectioning artifacts and the structure was believed to consist of parallel electron lucent "rods" 5 nm in diameter lying at 5 nm intervals in an electron dense matrix (see Section 11.4).

The infrastructure of spines of Type Three cercariae lacked the precise ordering of later spines although the "rods" were of the same diameter (Plate 39b). Regions in which the striations occurred at different relative angles were present and in some cases the rods appeared to be curved.

The structure of the tegument is discussed elsewhere (see Section 10) and hence only spine-related components will be examined here. Of possible significance to spine formation are the electron lucent membrane-bound inclusions present in the surface tegument of all stages more mature than early Type Three cercariae (Plates 23a and 24a). These inclusions appeared to reach the surface tegument from the tegumentary cell bodies via the connectives (Plate 24a).

Within the surface tegument the inclusions were generally spherical and 0.2 m diameter although they exhibited considerable plasticity (Plate 25), suffering distortion during passage through the connectives (Plate 24a). Where the inclusions were found in close approximation to spines they were generally flattened (Plate 41c).

The electron lucent inclusions appeared to be manufactured in the tegumentary cell bodies most probably by the golgi-apparatus (Plate 25a).

The tegumentary cell bodies of Type Three cercariae also contained amorphous electron dense bodies and crystalline bodies. While these often appeared together (Plate 25b) they also appeared independently (Plate 24b and 25a). The crystalline bodies had an infrastructure resembling that of the spines in that it involved alternate electron lucent and electron dense 5 nm subunits. The units were rarely parallel, however, and were present in a variety of different forms (Plate 24b and 25b).

In adult fluke tegumentary cell bodies the dense bodies were absent and the crystalline bodies were generally smaller (less than 1μm diameter) than in cercariae (more than 2μm diameter). The membrane bound electron lucent inclusions were often closely associated with the dense bodies and crystalline inclusions of cercarial tegumentary cell bodies. In several instances they were observed to have a large invagination containing dense material apparently of cytoplasmic origin (Plate 25). This behaviour may explain the occasional appearance of dense material in the centre of otherwise typical electron lucent inclusions (Plate 25a).

11.3.3 Fluke-host interface

Examination of the host fish surface beneath a scale, after removal of an adult fluke, (Plate 42c) revealed indentations which appeared to be of fluke origin (Plates 17a and b, 42a). A circular trough indicated the limits of the ventral sucker (Plate 17b). The area within the ventral sucker region and the adjacent area were marked with indentations of the same shape and pattern as fluke ventral spines (Plate 42a and b).

Mid-anterior to the ventral sucker indentation there was a crest of material, surrounded by an indentation, running anteriorly normal to the rim of the ventral sucker rim imprint. These features are compatible with pharynx feeding activity (Plate 17b and d).

11.3.4 Spine growth

For the dorsal and ventral surfaces of flukes at different ages 100 measurements of a particular spine dimension (L or W) were obtained. These measurements were the sum of 10 values at 5 different row positions on two flukes. A mean of these 100 values would, therefore, include in a single value the variation due to spine size distribution on a given surface and be characteristic of flukes at a specific age.

The mean results are shown in Table 11.1 and Figure 11.3. Note that no values were obtained for the dorsal surface of flukes at 0 days P.I. since at this age spines were not present over the whole surface.

Spine size appears to increase with fluke age and ventral spines were longer than dorsal spines.

TABLE 11.1

Change in mean spine dimensions with fluke age

FLUKE AGE (DAYS P.I.)	SPINE DIMENSIONS (μm) (n = 100)			
	VENTRAL		DORSAL	
	LENGTH	WIDTH	LENGTH	WIDTH
0	3.96	2.93	-	-
1	4.27	3.04	3.38	2.02
3	5.26	3.49	4.04	2.81
7	5.93	4.02	5.28	2.81
14	6.74	4.63	4.98	2.74
21	6.90	4.30	5.93	3.16

Figure 11.3: Spine growth from 0 to 21 days after attachment.
Data points fitted with 95% confidence limits.

VL: length of ventral surface spines.

DL: length of dorsal surface spines.

VW: width of ventral surface spines.

DW: width of dorsal surface spines.

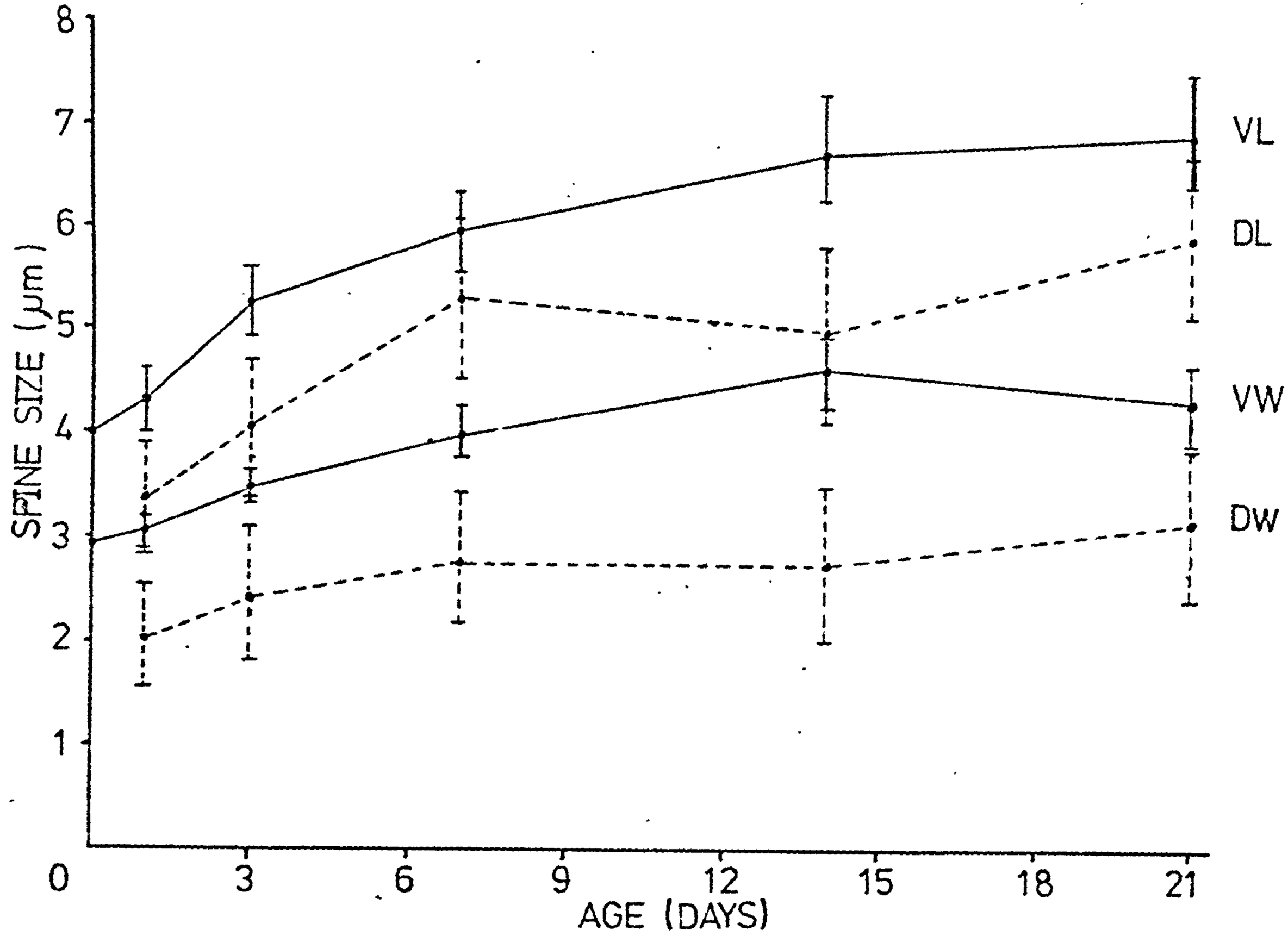
8
7
6
5
4
3
2
1
0
SPINE SIZE (μm)
3
6
9
12
15
18
21
AGE (DAYS)
VL
DL
VW
DW

11.3.5 Spine density

The results are shown in Table 11.2 and illustrated in Figure 11.4.

TABLE 11.2

Change in mean spine density with fluke age

FLUKE AGE (DAYS P.I.)	Mean number of spines/400μm^2 (n = 10) VENTRAL	DORSAL
0	8.7	9.5
3	6.0	6.5
7	5.4	5.6
14	4.6	5.0
21	4.5	4.4

It is apparent that spine density was similar on the dorsal and ventral surfaces of flukes of the same age, and that the spine density declined with fluke age.

11.3.6 Number of spine rows

Six flukes at three different ages were examined. The number of spine rows was determined from S.E. micrographs and mean values calculated (Table 11.3). It is apparent that the number of spine rows was independent of fluke age.

TABLE 11.3

Effect of fluke age on the mean number of spine rows

FLUKE AGE (DAYS P.I.)	NUMBER OF SPINE ROWS REPLICATES						MEAN
0	60	54	54	52	62	58	56.66
7	53	54	58	56	59	53	55.55
21	56	52	59	57	53	57	55.66

Figure 11.4: Relationship between spine density (per 400μm^2) and fluke surface area (mm^2).

a) Ventral surface.

b) Dorsal surface.

Data points for mean surface area (continuous line) fitted with 95% confidence limits.

a)

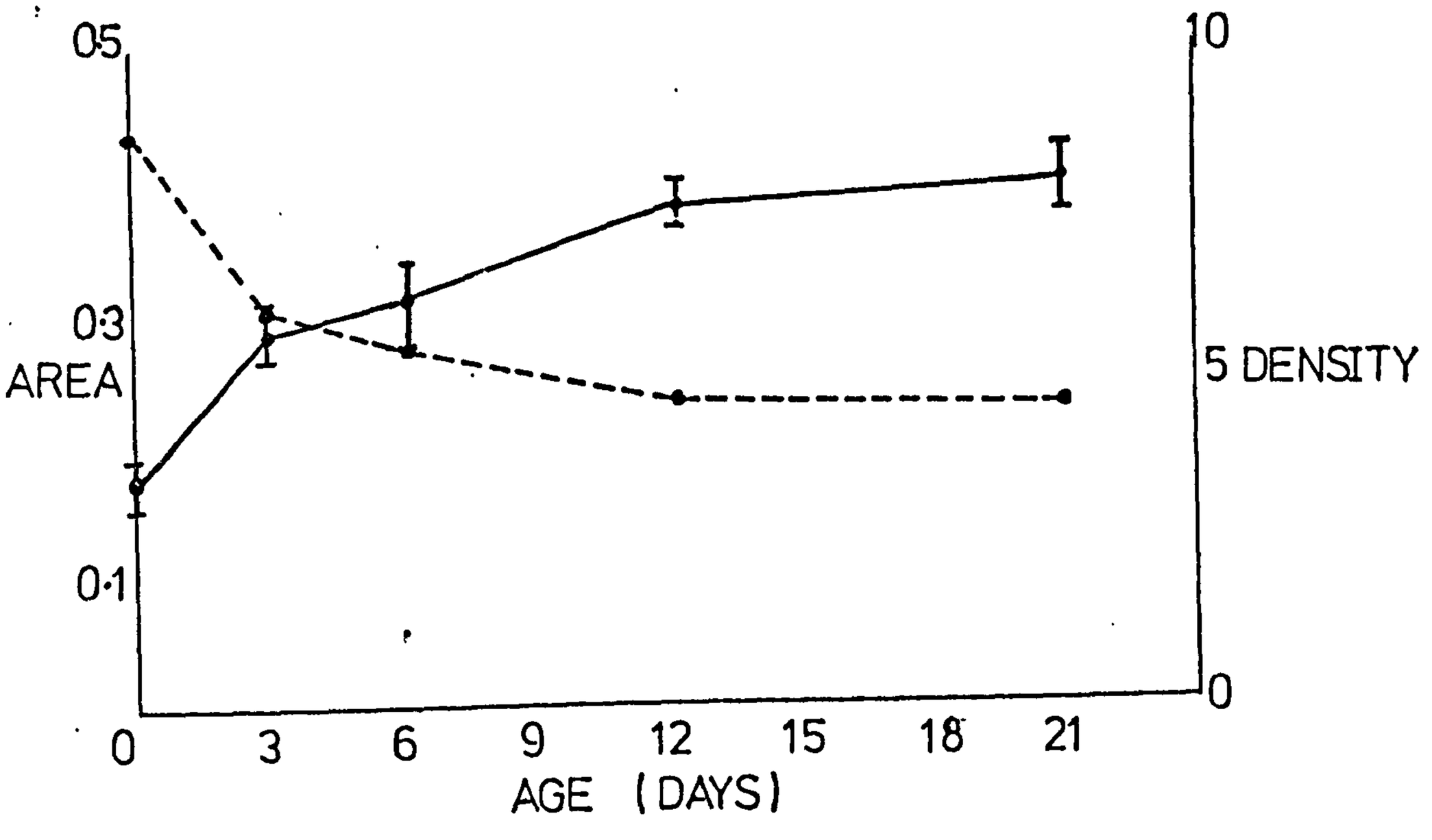
0·5
0·3
AREA
0·1
0
3
6
9
12
15
18
21
AGE (DAYS)
10
5 DENSITY
0

b)

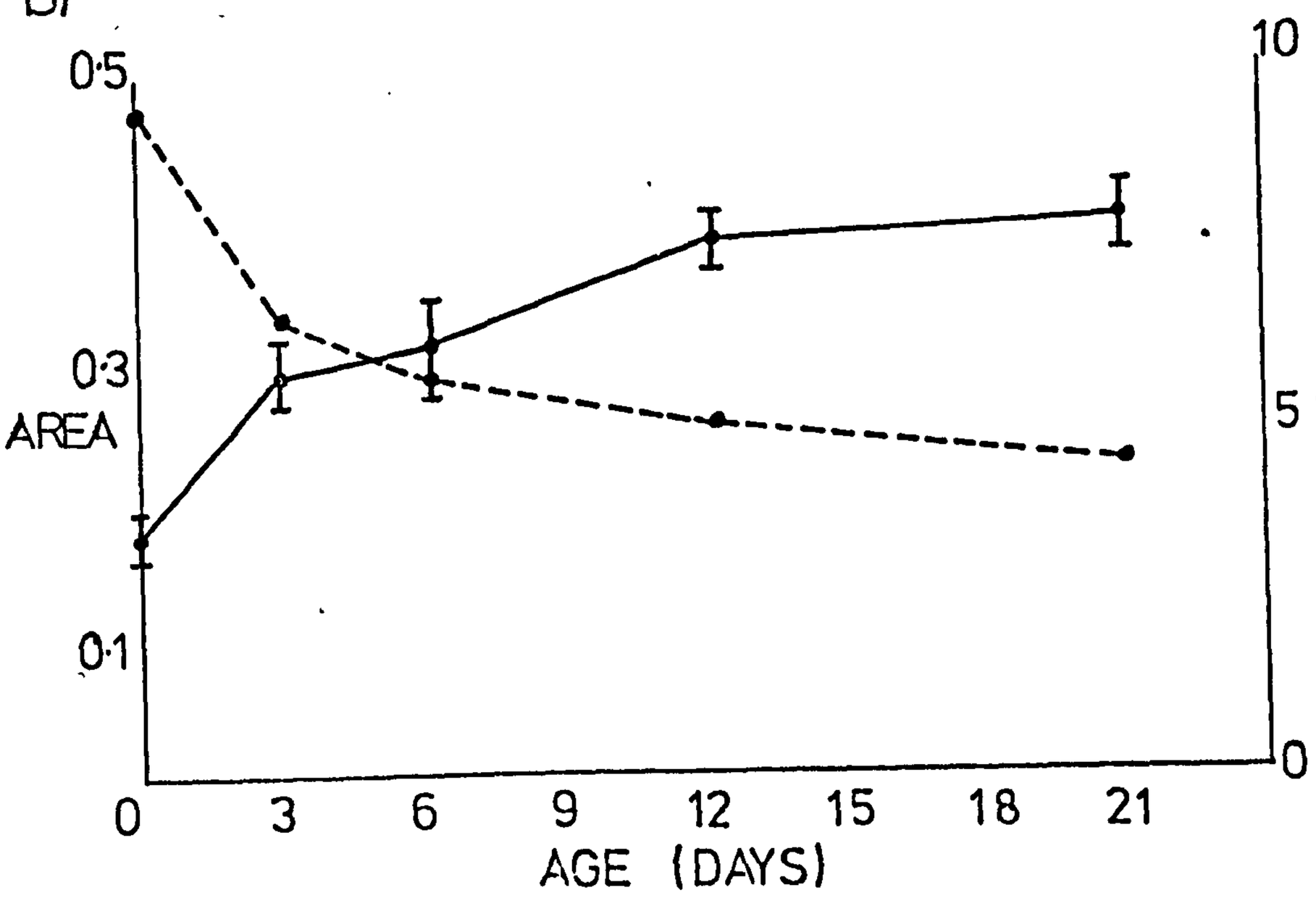
0·5
0·3
AREA
0·1
0
3
6
9
12
15
18
21
AGE (DAYS)
10
5 DENSITY
0

An early Type Two cercaria was fortuitously fixed so that the circular muscle bundles were apparent under SEM (Plate 14). This individual had 58 rows of circular muscles, equivalent to the number of spine rows on older cercariae and adults.

Spines at all fluke ages were associated with the circular muscle bundles, spine rows alternating with circular muscles bundles.

11.3.7 Spine number

Table 11.4 shows the results of the LM estimates of spine number. Because of the indirect approach used to determine these values a comparison was made with direct counts from S.E. micrographs. Two 21 day adults had 3366 and 3692 spines on the ventral surface, numbers that compare favourably with the indirect results.

It is apparent that if any change in spine number does occur with age it represents a very small proportion of the total number of spines present.

The ventral sucker of adult flukes carried spines in the peripheral and central region. 21 day old flukes had 247 ($s^2 = 7.4$, $n = 5$) central spines and 75 ($s^2 = 8.5$, $n = 5$) peripheral spines. An early Type Three intramolluscan cercaria, on which spines were first becoming apparent, had 252 central and 72 peripheral spines.

It is apparent that ventral sucker spination does not change markedly with age.

11.3.8

The mean area of the ventral or dorsal surface of fixed

TABLE 11.4

Estimated spine number from LM observation of fluke ventral surface. A and B, and C and D are replicate flukes at 0 and 21 days P.I. respectively

	NUMBER OF SPINES IN HALF ROW			
	0 DAYS P.I.		21 DAYS P.I.	
ROW NUMBER	A	B	C	D
5	27	28	28	27
10	35	32	35	34
15	31	34	33	34
20	31	35	36	33
25	34	34	36	29
30	35	31	35	34
35	30	31	35	31
40	31	33	38	31
45	33	30	36	30
50	29	30	29	30
55	24	25	29	26
MEAN SPINE NUMBER PER ROW :	61.82	62.36	67.28	61.64
TOTAL NUMBER SPINES IF 55.96 ROWS :	3460	3490	3764	3450

flukes at different ages are shown in Table 11.5 and Figure 11.4. It is apparent that the surface area approximately doubled over the period 0-21 days P.I.

TABLE 11.5

Change in fluke surface area with fluke age

FLUKE AGE (DAYS P.I.)	MEAN SURFACE AREA (n = 5) (mm^2)
0	0.171
3	0.285
7	0.303
14	0.377
21	0.394

The relationship between fluke surface area and spine density allows an indirect estimate of spine numbers to be made. Table 11.6 shows the number of spines on the ventral surface of flukes at ages 0-21 days P.I. estimated from spine density x fluke surface area using data from Tables 11.2 and 11.5. These are overestimates since they assume the entire surface of the fluke to be evenly covered with spines while in practice there are disruptions in the pattern due to the presence of the ventral sucker, pharynx, genital pore and aspinose periphery. The spine order is, however, of the same number as estimates derived by other means, and significantly does not change markedly with age.

TABLE 11.6

Indirect estimate of total spine number on the surface of flukes of known age. Spine number estimated from fluke surface area x spine density

FLUKE AGE (DAYS P.I.)	TOTAL SPINE NUMBER	
	VENTRAL	DORSAL
0	3719	4061
3	4275	4631
7	4090	4242
14	4335	4712
21	4432	4334

11.4 Discussion

Spines in the Digenea are cytoplasmic organelles entirely enclosed within the tegument, the spine apex being closely apposed to the apical plasma membrane and the spine base abutting the basal plasma membrane.

The mode of attachment of the spines to the basal lamina and basal plasma membrane apparently shows taxonomic variation. The spine base of Transversotrema patialense was associated with a dense zone of basal lamina. A similar attachment is apparent in T.E. micrographs of Cyathocotyle bushiensis, Fasciola hepatica and Cercaria buchanani (Erasmus, 1967; Bennett and Threadgold, 1973; Bils and Martin, 1966). In Schistosoma mansoni, however, the spine is attached to the basal lamina by small dense bodies (Morris and Threadgold, 1968; Hockley, 1970; Wilson and Barnes, 1974). These dense bodies have the same structure as those attaching the basal

plasma membrane to the basal lamina in all regions of T. patialense except the spine bases, and are interpreted as hemi-desmosomes.

11.4.1 The structure and composition of tegumental spines

The structure and composition of spines is incompletely understood and such evidence that exists is conflicting. The evidence presented here is morphological but in order to interpret these results it is necessary to have some understanding of the chemical properties of spines.

The spines of Schistosoma mansoni and Haematoloechus medioplexus gave positive results to histochemical tests for proteins containing unusually high concentrations of sulphur groups (Smith, Reynolds and Von Lichtenberg, 1969; Burton, 1964). Of the structural proteins keratin is characterised by a high sulphur content (Filshie and Rogers, 1962).

More extensive analyses have been undertaken on cestodes. The composition of Hydatigera taeniaformis strobilocercus hooks has been shown to resemble a protein of keratin-type on the basis of solubility, elemental, amino acid and infrared spectrophotometric analyses (Crusz, 1947; Dvorak, 1969a, b and c). Similarly the hooks of Echinococcus granulosus hydatid scolices are primarily composed of a protein with amino acid components, sulphur content, pH responses and resistance to proteolytic enzymes compatible with it being of keratin-type (Gallagher, 1964).

The series of results suggests that platyhelminth hooks and spines are primarily composed of a keratin-like protein. Keratins are not simple homogeneous proteins but are composed of one or more proteins or polypeptides, and may be "predominantly filamentous,

predominantly amorphous or mixtures of filamentous and amorphous elements" (Mercer, Rogers, Munger and Roth, 1964). Keratins are, therefore, usually biphasic consisting of two primary components: the filaments, consisting of a highly organised assembly of fibrous molecules, and the matrix, of amorphous ground substance (Rogers, 1959a and b; Filshie and Rogers, 1961; Seifter and Gallop, 1966). Electron microscopic examination reveals this formation as osmiophobic rods (filaments) in an osmiophilic globular ground substance (matrix). In most animal hairs and porcupine quills the filaments have a diameter of 8-9 nm (Crewther, Fraser, Lennox and Lindley, 1965) while in feather keratins this diameter may be as small as 3 nm (Filshie and Rogers, 1962).

Incubation of animal hair keratins in 0.5 M thioglycollic acid (TGA) reduces the cystine content of the matrix and enhances its affinity for osmium (Filshie and Rogers, 1961). This technique reveals the presence of a filament sub-structure under TEM observation, each filament consisting of nine 2 nm protofilaments surrounding a core of intrafilamentous matrix (Fraser, MacRae and Rogers, 1962; Dobb, 1965; Crewther and Harrap, 1965). In feather keratin, however, no protofilaments are observable after TGA-osmium treatment, perhaps because of a lack of differential staining of the matrix and filaments due to their similar sulphur content (Filshie and Rogers, 1962).

If digenean spines are composed of keratin then some of these features should be apparent under T.E. microscopic examination.

The spines of cercarial and adult Schistosoma mansoni and cercarial Zoogonoides viviparus have a "crystalline" substructure

consisting of 4-5 nm wide repeating electron lucent and electron dense bands (Morris and Threadgold, 1968; Morris, 1971; Koie, 1975). Smith et al. (1969), however, recorded that the repeating units of S. mansoni were 7-7.5 nm wide. This agrees with the dimensions of the "lamellar crossbridges" of Haematoloechus medioplexus spine infrastructure (Burton, 1964).

These results may all be interpreted in terms of a biphasic keratin-like structure. Each description mentions, or figures, repeating 5-7 nm electron lucent and electron opaque subunits. While in one case (Morris, 1971) the electron lucent unit is referred to as a "gap" in most cases the structural implications of these differential staining phenomena are ignored. It is suggested here that the electron lucent unit is the keratin filament and the electron opaque unit the matrix. The results may then be interpreted to describe 5-7 nm electron lucent filaments, of protein or polypeptides, lying in an electron opaque matrix. In cross sections the filaments can be seen to be in repeating units of four, arranged in equilateral parallelograms with internal angles of 60° and 120° so that they appear to form two rows at 60° to each other.

The description of T. patialense spine infrastructure recorded here is compatible with the above arrangement.

Smith et al. (1969) demonstrated that TGA-osmium treatment did not enhance the staining properties of Schistosoma mansoni spines, and suggested that this militated against a keratin composition. However, as previously mentioned feather keratin also does not respond to this treatment. According to Filshie and Rogers (1962) this should not be considered as a test for keratin but rather an

indication of the differential sulphur content of filaments and matrix.

It is apparent both from the present results for T. patialense and published T.E. micrographs that sections of digenean spines do not always show a clear pattern of filaments, the perfect transverse or parallel view is exceptional. This can be explained in terms of the plane of section, a factor which was mentioned by Rogers (1959b) with reference to animal hairs and examined in detail by Whitfield (1973) in a study on the keratin envelope of acanthocephalan eggs. This latter work demonstrated that even with thin (50 nm) TEM sections deviations as small as 2^{o} from a section orientation exactly normal to the longitudinal axes of the filaments will cause overlap of the electron lucent filament profiles so that the electron opaque matrix is obscured. In this situation the filament profiles form an electron lucent band or "pseudoplane" so that an only slightly displaced transverse section appears to show longitudinal elements. A similar phenomenon can cause total overlap of filament profiles so that the intervening matrix is obliterated producing a homogeneous appearance.

A significant feature of all sections of T. patialense spines is that the appearance of the infrastructure was uniform over the whole spine section. This suggests that all filaments within the spine have the same parallel orientation, the filaments alligned parallel with the longitudinal axis of the spine from base to apex.

11.4.2 Tegumental spine formation

From the above it appears probable that digenean spines are composed of keratin. How this material is supplied for spine

elaboration is unknown but three hypotheses have been suggested. Firstly, it has been suggested that tegumental inclusions, contribute directly to spine formation since inclusions of the surface tegument and apical plasma membrane are often closely associated with spines and may provide structural components (Smith et al., 1969; Morris, 1971; McLaren and Hockley, 1976). Secondly, it has been suggested that tegumental inclusions, contribute indirectly to spine formation by dissassembling and so contributing to the general cytoplasm of the surface tegument from which the spines derive structural materials (Burton, 1966; Spence and Silk, 1970; Hockley, 1973; Bennett and Threadgold, 1975). Thirdly, the dense areas of basal lamina associated with spine base may act as a route for transport of spine material (Bils and Martin, 1966).

These hypotheses all rely on circumstantial evidence derived from observations of extant spines. In the Cestoda, however, consideration has been given to sequential changes in hook development and these investigations may give some insight into spine development in the Digenea.

The rostellar hooks of cyclophylidean cestodes arise from the electron dense caps of strobilar microtrichs (Mount, 1970; Slais and Machnicka, 1976). They do not arise <u>de novo</u> or by the fusion of microtrichs as previously suggested (Crusz, 1947; Bilques and Freeman, 1969). Material for subsequent development arises from the subjacent tegumental cytoplasm and tegumental dense vesicles (Mount, 1970).

While the parallels that can be drawn between cestode hooks and digenean spines are limited it is instructive that hook material is entirely derived from the tegument. This resembles the deposition of keratin in vertebrate cells, Mercer et al. (1964) defining keratins as "proteins produced by epithelial cells, and usually retained within the cell". This entirely cytoplasmic origin argues strongly against the basal assembly hypothesis of Bils and Martin (1966) since the route they suggest would require transport of extra-tegumental material across the basal plasma membrane of the tegument.

In mature cercariae and adults the most likely regions of keratin production are the tegumentary cell bodies since polyribosomes are largely confined to these regions and these are the organelles usually concerned with keratin synthesis (Rhodin and Reith, 1962). Other inclusions of these regions also suggest a productive role, the aggregates of spine-like material described in T. patialense and previously in Haplometra cylindracea (Threadgold, 1968) and Fasciola hepatica (Bennett and Threadgold, 1973) appear to be alligments of keratin filaments. Such aggregates closely resemble the fibrils found in keratinizing vertebrate germinative cells (Rhodin and Reith, 1962). The precursor of keratin is either such fibrils alone or in collaboration with electron dense granules (Matoltsy, 1962). In T. patialense dense graunles similar to those in vertebrate germinative cells were also present in the tegumentary cell bodies.

In Fasciola hepatica layer IV of the metacercarial cyst is composed of keratin produced by "Keratin Cells" (Mercer and Dixon, 1967). These cells produce the juvenile and adult tegument and

then become the tegumentary cell bodies (Dixon and Mercer, 1967). It is these tegumentary cell bodies, with a demonstrated ability to produce keratin, in which the crystalline aggregates of spine-like material became apparent (Bennett and Threadgold, 1973).

Aggregates of spine-like material were absent from the tegumentary cell bodies of early Type Three cercariae of T. patialense. Polyribosomes were observed in the tegument adjacent to the spines and they may serve to produce keratin precursors in the surface tegument at this early stage. The irregular arrangement of filaments within spines at this stage is compatible with the filaments having aggregated into the initial fibrillar form (Rhodin and Reith, 1962).

If keratin originates in the tegumentary cell bodies it presumably reaches the surface tegument via the connectives. Crystalline bodies and dense bodies were not observed within the connectives and it is therefore assumed that keratins travel to the surface in a disassembled form, perhaps as monomer, and are then added to the growing spines.

The electron lucent inclusions were present in the tegumentary cell bodies, connectives and surface tegument. These inclusions were probably produced in the tegumentary cell bodies by the GER-golgi complex (Hanna and Threadgold, 1976). Despite the close apposition of the electron lucent inclusions to the crystalline bodies and dense bodies within the tegumentary cell bodies, and to the spines in the surface tegument, it is improbable that these membrane bound inclusions are involved in keratin transport. More probably these inclusions are involved in the carriage of material to the superficial glycocalyx of the surface tegument.

11.4.3 Growth of tegumental spines

Spine growth should not be considered in isolation but relative to somatic growth if spines are to have any relevance as taxonomic criteria. The present results indicate that for T. patialense maximal fluke and spine size are attained at approximately the same age, spines continuing growth from the intramolluscan cercaria to the ovigerous adult. For other species there is a paucity of quantitative data spanning a similar developmental range. The spines of Schistosoma mansoni are said to be larger on the adult than the cercaria, the males showing a greater increase (Hockley, 1973; Smith et al., 1969). Spine growth in Fasciola hepatica has been recorded from the newly excysted juvenile to the adult stage (Bennett, 1975c). In this species spine size increases in the preacetabular region between 0 and 8 days post excystment (P.E.) and thereafter remains constant. In the postacetabular region spine growth is still apparent at 26 days P.E. Somatic growth shows a similar trend in these two regions, ceasing in the preacetabular and continuing in the postacetabular.

It should be noted in considering the results of Bennett (1975c) that measurements were made from S.E. micrographs hence only the portion of the spine projecting from the tegument was measurable, the remainder of the spine being enclosed within the surface tegument. In this case, therefore, the thickness of the tegument must be assumed constant during growth if spine measurements from different age classes are to be comparable.. Constancy of tegumental thickness is not a digenean characteristic, in fact in extreme cases such as Hypoderaeum sp. the spines are gradually engulfed by the surface tegument during adult growth until they

are no longer visible as surface features (pers. com. E. A. Williams, Royal Holloway College, University of London).

Age dependent morphometric features of cestode hooks have also been investigated. The rostellar hooks of Taenia pisiformis and the bothridial hooks of Acanthobothrium quadripartitum attain their adult size early in ontogeny and do not grow further despite the increase in strobilar length (Beveridge and Rickard, 1976; McVicar, 1977). These cestodes do not, therefore, show the same relationship between hook and somatic growth as was found for spine and somatic growth in the Digenea.

In many species of Digenea spine morphology changes with fluke somatic growth. In its extreme form this may represent a change from a simple conical spine to a plate-like form in which the tip is pectinate or "toothed": for example Diplostomum phoxini (Erasmus, 1970), Neophasis lageniformis (Koie, 1973a), Opechona bacillaris (Koie, 1975), Fasciola hepatica (Bennett, 1975b), Cryptocotyle lingua (Koie, 1977), Meiogymnocephalus minutus and Microphallus similis (Davies, 1976).

In T. patialense there was no change in spine morphology associated with somatic growth.

Hockley (1973) observed that spines on the schistosomulum of Schistosoma mansoni appeared more dispersed than on the cercaria, attributable to an increase in surface area as recorded by Clegg (1965). Significantly, Hockley (1973) could find no evidence for the addition of new spines, the cercarial spination being fundamentally that of the adult. Conversely, Bennett (1975c) recorded a large increase in spine number on the postacetabular region of

Fasciola hepatica although spine number was constant on the preacetabular region.

In T. patialense there was an increase in spine dispersion with growth. On the ventral surface the increase in dispersion was compatible with the increased fluke surface area with no evidence for the addition of spines. On the dorsal surface, however, spines could not be detected posteriorly on the cercaria but becams apparent in the adult.

The findings for T. patialense, Schistosoma mansoni and the preacetabular region of Fasciola hepatica are compatible: as somatic growth occurs the surface area increases, the spines grow and become more widely dispersed. There is no evidence that spines are added to cover the increased surface area, the existing spines increasing their separation to fill the area available to them.

The results for the dorsal surface of T. patialense and the postacetabular region of Fasciola hepatica may not in fact conflict with this scheme. It was shown that the posterior third of the dorsal surface of T. patialense cercariae possessed spines visible under TEM but which were not discernable as surface features because they did not appose the apical plasma membrane. Similarly, SEM observation of the postacetabular region of F. hepatica would not reveal such intra-tegumental spines. The apparent de novo appearance of spines could, therefore, simply be a function of observational techniques - spines only being recorded as present when they distort the surface and become visible for SEM observation.

This hypothesis implies that the pattern of spination is fixed early in ontogeny. The location of spines in T. patialense has been shown to be related to the distribution of the somatic musculature, the number of circular muscles and spine rows being a constant feature. The number of muscle rows is apparently determined at a very early stage and spine distribution may be said to be prescribed from this point if spine primodia are located within this framework.

11.4.4 The fluke-host interface

The extent of parasite-host contact in adult T. patialense on the zebra danio (Brachydanio rerio) is illustrated by the S.E. micrographs of the fluke imprint. Care must be taken in interpreting this result. Observations on anaesthetised fish showed flukes moving beneath the scales and even from scale to scale, such migrations would be expected since copulation appears to be a prerequisite of fertile egg production (Section 5). At the least flukes showed an undulant movement similar to the "breathing movements" of Entobdella soleae (Kearn, 1962). The surface imprint, however, did not show the scarring that might be expected from repeated spine contact but coversely exhibited a single discrete pattern of spines. A possible interpretation of this result is that the rapid fixation technique maintained the superficial fish mucus layer in a distended pattern and showed the position of the fluke at the moment of fixation, the viscous properties of the mucus normally removing any trace of spine contact once the fluke has changed position and the distorting effects are removed. There are, therefore, no indications of spine initiated damage to the epidermis of the fish host.

The other features of the fluke imprint are readily related to the morphology of the fluke ventral surface. The circular imprint was of a size, shape and position compatible with it being of ventral sucker origin. Kearn (1963) demonstrated a similar "footprint" on the skin of the sole caused by the haptor of Entobdella soleae. The crest of mucus anterior to the ventral sucker imprint was surrounded by a depression possibly originating from protrusion of the pharynx. This suggests that the fluke feeds on mucus by the pumping action of the pharynx. This mode of feeding has more affinities with that of the Monopisthocotylea monogeneans than either Polyopisthocotylea monogeneans or digeneans (Kearn, 1963; Halton and Jennings, 1965; Halton, 1963).

11.4.5 Spines as a taxonomic feature

Finally, attention is drawn to the use of spines as taxonomic criteria. The following descriptions of spination have been recorded for members of the Family Transversotrematidae:

T. patialense: thick, short triangular spines in alternating rows on both surfaces, smaller dorsally (Rao and Ganapati, 1967; Crusz et al., 1964; Soparkar, 1924; Anantaraman, 1948).

T. chackai: triangular, scale-like spines in alternating rows throughout the body (Mohandas, 1973; Nadakal et al., 1969).

T. soparkari: prominent, triangular scales in alternating rows over dorsal and ventral surfaces, except anterior margin (Pande and Shukla, 1972; Pandy, 1971).

T. koliensis: large, conspicuous, plate-like spines, five sided and thickened posteriorly, in quincunx pattern over dorsal and ventral surfaces, smaller dorsally and present only in anterior third of cercaria (Olivier, 1947).

T. laruei: large, conspicuous, scale-like spines, diagonally arranged on both surfaces, minute dorsally (Velasquez, 1958 and 1961).

T. licinum: scales prominent near anterior border on both surfaces. Less developed posteriorly and gradually replaced by fine spines along posterior border (Manter, 1970).

T. haasi: short (15μm) stout spines, disposed quincuntially, covering both surfaces, larger ventrally (Witenberg, 1944).

Prototransversotrema steeri: scale-like spines (4μm), closely set on ventral surface, absent dorsally (Angel, 1969).

With the single exception of the large spined T. haasi all the descriptions of Transversotrema species agree with that of the species described here. The apparently differing descriptions of spine pattern are all attempts to describe the same pattern. This confusion may be directly attributed to a lack of accepted nomenclature. By definition, a symmetrical pattern contains repeating units and it is the various descriptors of these repeating units that cause confusion (Figure 11.5). What compounds this situation is that without an accepted notation all modes of description are valid.

It is suggested that some of the underlying concepts of the descriptive notation of morphological crystallography be adopted for taxonomic diagnoses of spine pattern. The system used in crystallography provides, within its definitions, information on the translation, reflection and rotation periodicity of three-dimensional symmetrical structures (see for example Bishop, 1967; Buerger, 1963). A pattern of digenean spines is essentially a symmetrical two-dimensional array of points - a plane-lattice.

Figure 11.5: The same symmetrical pattern described for different repeating units.

a) Hexagonal

b) Square (1)

c) Square (2), Rhombic (1) or Diamond (1)

d) Diamond (2) or Rhombic (2) .

e) Triangular

f) Quincuntial.

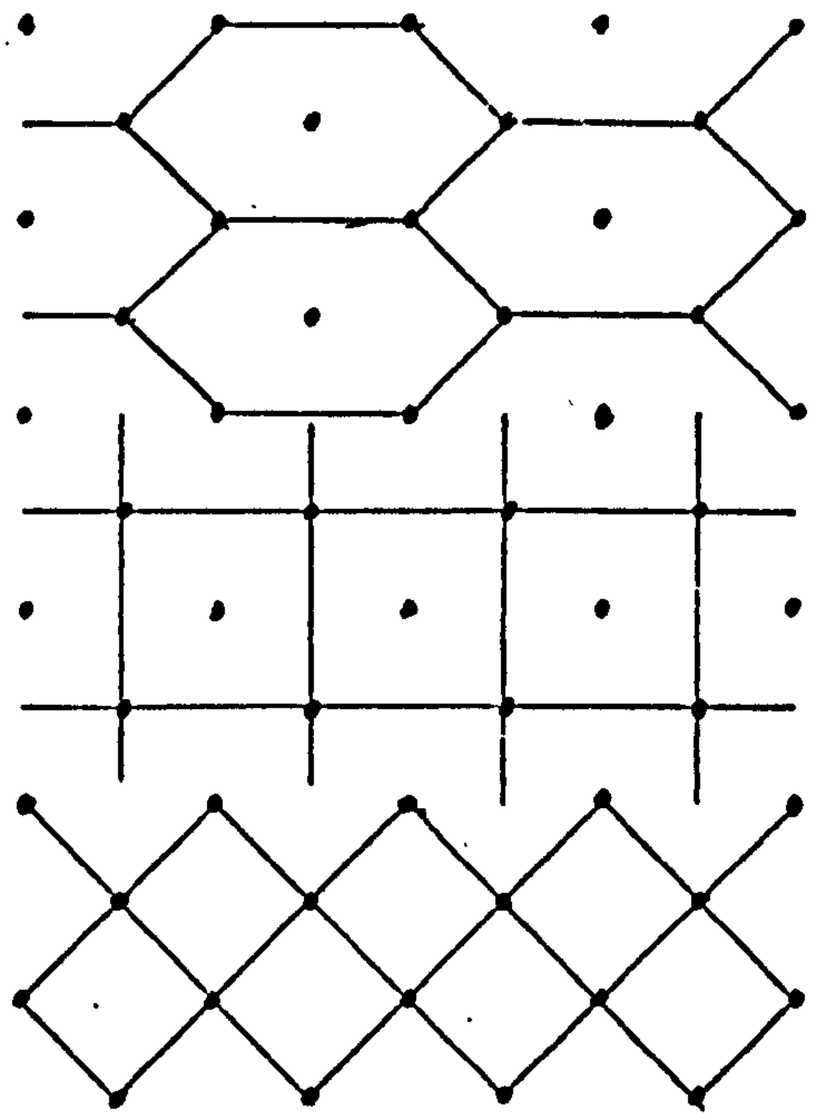

a)

b)

c)

d)

e)

f)

Any such plane-lattice is composed of basic repeating units or primitive cells. Since there may be a variety of possible primitive cells it is usual to adopt and define a particular cell form and term this the unit cell upon which comparison can be based.

In describing the plane-lattice of digenean spine pattern it is suggested that the following procedure be adopted:

1) The spine rows most nearly parallel to the transverse axis of the fluke are taken to be the horizontal rows of a plane-lattice. Since, as previously mentioned, spine rows are usually related to transverse musculature this orientation is intuitively adopted in any case (Figure 11.6a).

2) The centre of each spine base is taken as a point in a plane-lattice (Figure 11.6a).

3) A unit cell is defined so that the translation t_1 along the horizontal row, the translation t_2 between rows and their equal and opposite translations t_1^1 and t_2^1 incorporate as few points as possible in a repeating unit (Figure 11.6a).

4) The unit cell is figured for comparative purposes. If it aids comprehension the approximate internal angles and relative proportions are indicated (Figure 11.6b).

The unit cell of T. patialense has the following parameters and characteristics:

$$A \triangleq B, \quad \alpha \triangleq 60^\circ \text{ and } \quad \beta \triangleq 120^\circ.$$

If this procedure is followed than an unambiguous and directly comparable description of spine pattern is achieved.

Figure 11.6: Description of the plane lattice of digenean spine distribution.

a) The plane lattice. Each point represents the centre of a spine base. t_1 is the horizontal translation and t_2 the vertical translation. t_1^1 and t_2^1 are equal and opposite translations which enclose the unit cell.

b) The unit cell of spine distribution.

a)

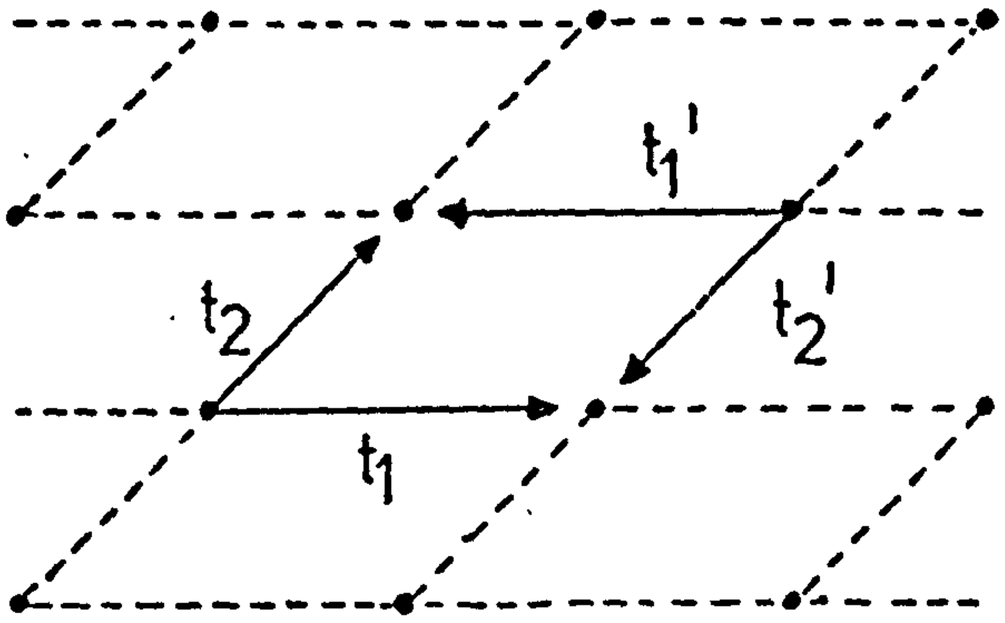

b)

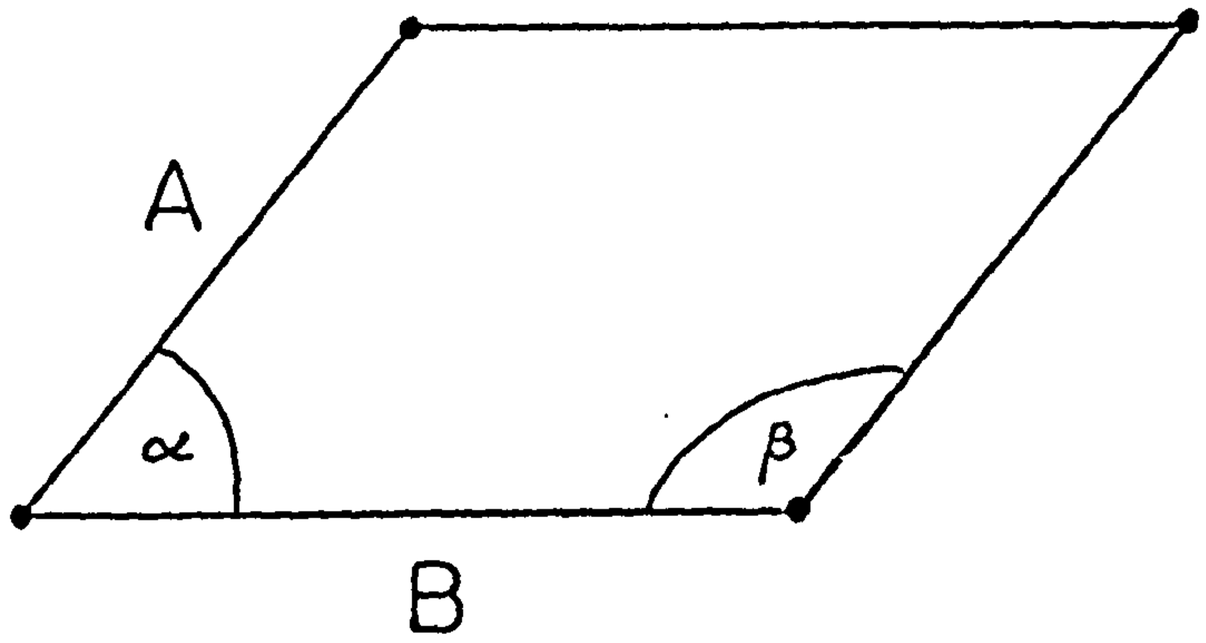

The unit cell of T. patialense appears to be of the same form as for many other species of digeneans as revealed by inspection of published S.E. micrographs. It may be that this basic form is the norm and only deviations from it have relevance as diagnostic characters. The fact that even this basic information is lacking emphasises the need for standardised notation.

Section 12:

Cercarial Locomotion

12. Cercarial Locomotion

12.1 Introduction

In the majority of digenean life cycles cercariae have a dispersive and infective function in which cercarial behaviour plays a crucial role. In many life cycles there are three phases of this behaviour: emergence from the molluscan host, dispersive or host finding activity in the water column and infection. The dispersive phase usually involves active swimming and, in furcocercous cercariae at least, passive dropping. The complex relationship of these two activity modes has been examined elsewhere (Chapman, 1975; Whitfield, Anderson and Bundy, 1977). The nature of cercarial locomotion, however, have received scant attention.

Early interest in cercarial locomotion generally took the form of brief qualitative descriptions (Wunder, 1924; Mathias, 1925; Cort and Brooks, 1928; Dubois, 1929; Wesenberg-Lund, 1934). The superficiality of this approach in early studies is almost certainly a reflection of the experimental techniques available. Any study of cercarial locomotion is complicated by the small size (i.e. less than 1 mm) of the organisms and the extreme rapidity of their motion.

In 1967 Graefe, Hohorst and Drager utilised high speed micro-cinematography to record the swimming motion of Schistosoma mansoni cercariae and so produced the first quantitative description of cercarial swimming. After the publication of this pioneering study three further investigations were conducted using modifications of the same technique (Rees, 1971; Chapman and Wilson, 1973;

Nuttman, 1975). These four investigations provided quantitative descriptions of cercarial locomotion but did not attempt to discuss the hydrodynamic features of small animal aquatic locomotion.

The present investigation utilises still and microcinematographic techniques to illustrate, and quantitatively describe, cercarial behaviour in Transversotrema patialense. The hydrodynamic consequences of this locomotion are discussed.

12.2 Materials and Methods

12.2.1 Cine and microflash photography

Cercariae were obtained using the technique described in Section 2.3. All experiments were conducted with cercariae approximately one hour after emergence from the snail.

The swimming behaviour of cercariae was photographed using a high-speed cinematographic technique, the arrangement of the apparatus is illustrated in Figure 12.1. A Hadland Hyspeed camera mounted with an f4.4 Zeiss Luminar macrolens on 180 mm extension tube was used to film the cercaria on double perforated Kodak 4X 16 mm negative film. The subject was illuminated with a quartz-halogen projector, two glass neutral density filters separated by an air gap serving to reduce the heating effects of the light beam.

Freshly shed cercariae were placed in a thin, vertical transparent cell filled with conditioned water at 24°C. The dimensions of the cell were 6 x 6 x 1.5 mm thus each cercaria was constrained to swim in a two dimensional vertical plane at right angles to the optical axis of the apparatus and at the focal length of the photographic lens system.

Figure 12.1: Arrangement of photographic apparatus.

Key: ca, camera; ls, light source; ml, macrolens system; ned, neutral density filters; and oc, observation cell.

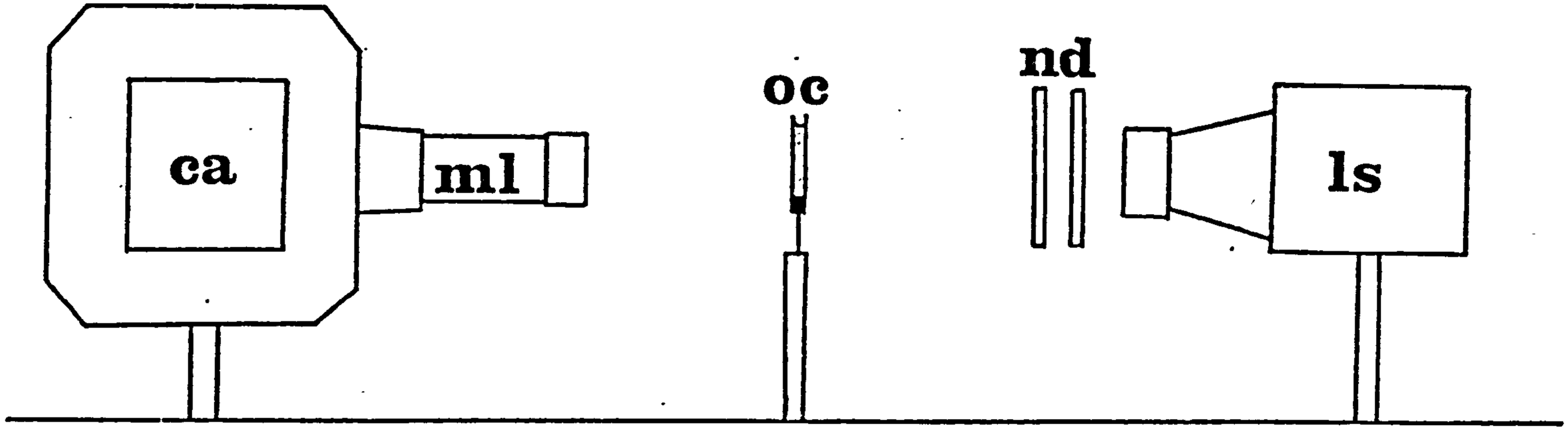
ca
ml
oc
nd
ls

The filming procedure was as follows. With the illumination switched on, an Ashai Pentax spotmeter was introduced into the optical axis and exposure readings computed. A framing rate of 1000 pictures per second (pps) and shutter speed of 1/2500 sec. at f8 were utilised throughout. A cercaria was introduced into the cell and the camera activated when swimming commenced. During each filming period an one hundred foot casette of film was automatically exposed. An in-frame timing light applied a time scale to the moving film during exposure. The time scale was applied at 1/10 of the framing rate, in this case one mark per 100 frames.

The first 10 feet of each developed casette were discarded since during this initial period the camera was still accelerating to the desired framing rate. The remaining exposed film was examined for suitable swimming sequences. Selected sequences were printed as individual frames enlarged to 5 x 4" and were used for analyses.

Microflash photography utilises illumination of high intensity and short duration to produce a single image of a moving subject.

Two alignments of the photographic system were used to provide lateral and dorsal views of cercarial movement. Lateral views were obtained using a similar arrangement to that used for cinematography (Figure 12.1). A 6 x 6 x 1.5 mm flat cell was placed at right angles to the horizontal optical axis and at the focal length of the photographic lens system. Vertical views from above were obtained using a similar photographic system rotated through 90° so that the optical axis was vertical. A cylindrical cell 3 mm

high and 2 mm in diameter was placed with its major axis parallel to the optical axis.

A Lindhof Technical camera with f4.5 Zeiss Luminar macrolens was used with illumination provided by a Courtenay and Co. Microflash supplying 8 kV output to a microhead with diffuser. The flash duration was 2 μ sec.

Newly emerged cercariae were introduced into the photographic cells filled with conditioned water at 24°C. Exposures were made to record different aspects of cercarial behaviour and 5 x 4" enlargements of the negatives were utilised for analyses.

12.2.2 Estimation of cercarial density

Cercarial density was estimated by examining the bouyancy of cold-immobilised cercariae in sucrose solutions of known density.

Analar sucrose solutions in distilled water were prepared over a range of concentrations. The solution density at a given concentration was determined from the tables of Lange and Forker (1956).

Newly emerged cercariae were immobilised by cooling to 0°C. For each test solution the same procedure was followed. The immobilised cercariae were placed in 5 ml of cold solution. The cercariae plus test solution were pipetted into a 30 ml graduated cylinder of more test solution at 0°C and the drift of cercariae up or down in the column recorded. Neutral bouyancy would be achieved if the density of cercaria and solution were the same.

12.3 Results

12.3.1 General structure of the cercaria

The cercaria of T. patialense is furcocercous. The cercaria in a relaxed configuration is illustrated in Figure 12.2. As with most cercariae the larva consisted of two regions - the body and the tail. This cercaria was unusual in the degree of transverse extension and dorso-ventral compression of the body. The body had a mean length of 350μm and mean width of 510μm. In contrast the dorso-ventral dimension was only 40μm.

The cercarial tail was attached to the posterior dorsal surface of the body. The 560μm x 80μm cylindrical tail stem contained four blocks of longitudinal striated muscle (Plate 30). Distally the tail bifurcated to form two 370μm long furcae. Each furca increased in width, from 60 to 120μm, and decreased in depth, from 50 to 10μm, towards the tip.

A unique feature of transversotrematid cercariae is the presence of 100μm long arm processes projecting laterally from the proximal region of the tail stem. The ultrastructure of these processes has been described elsewhere (Whitfield, Anderson and Moloney, 1975).

12.3.2 Phases of cercarial behaviour

There were three phases of cercarial activity each of which involved specific behavioural responses. Firstly, the cercaria emerged from the molluscan host. Secondly, the cercaria had a period of free living activity. Finally, the cercaria attached to the piscine definitive host.

Cercarial emergence was not observed in detail but, in the absence of penetration glands, was assumed to occur via some

existing aperture in the molluscan body wall.

During the free living phase the cercaria exhibited three distinct behavioural modes as described previously (Whitfield et al., 1977): swimming in the water column, dropping in the water column or resting on the substrate. Regardless of which mode was adopted, however, the cercaria maintained a reflexed configuration characteristic of the free living activity phase. This configuration was achieved by a change in the conformation of the body as illustrated in Figure 12.2. The essential feature was the ventral reflexion of the body region about the tail stem so that the ventral surface of the body came into contact with the ventral surface of the tail stem. The lateral extremities of the body were wrapped about the tail stem. Maintenance of this configuration was assumed to be achieved by adhesion of the ventral sucker to the tail stem and contraction of the body somatic musculature (Figure 12.2).

This change in conformation had consequences for the steric relationships of the cercarial components. Firstly, a cercaria in the reflexed configuration had the arm processes projecting from the anterior extremity. Secondly, the predominantly ventral body region enclosed a large proportion of the tail stem so that only 275 μm of tail stem remained exposed.

Unless stated otherwise, all subsequent discussions of free living cercarial activity assume the cercaria is in the reflexed configuration. To facilitate discussion the reflexed body and the portion of tail stem it enclosed were considered together as the "reflexed body region", while the remaining portion of the tail stem was considered as the "exposed tail stem" (Figure 12.2d and f). A convenient marker of reflexed cercarial orientation was

Figure 12.2: Cercaria in extended and reflexed configuration.

a) to c): extended

d) to f): reflexed.

Key: ap, arm process; b, extended body;

et, exposed tail stem, f, furcae;

rb, reflexed body region; ts, tail stem.

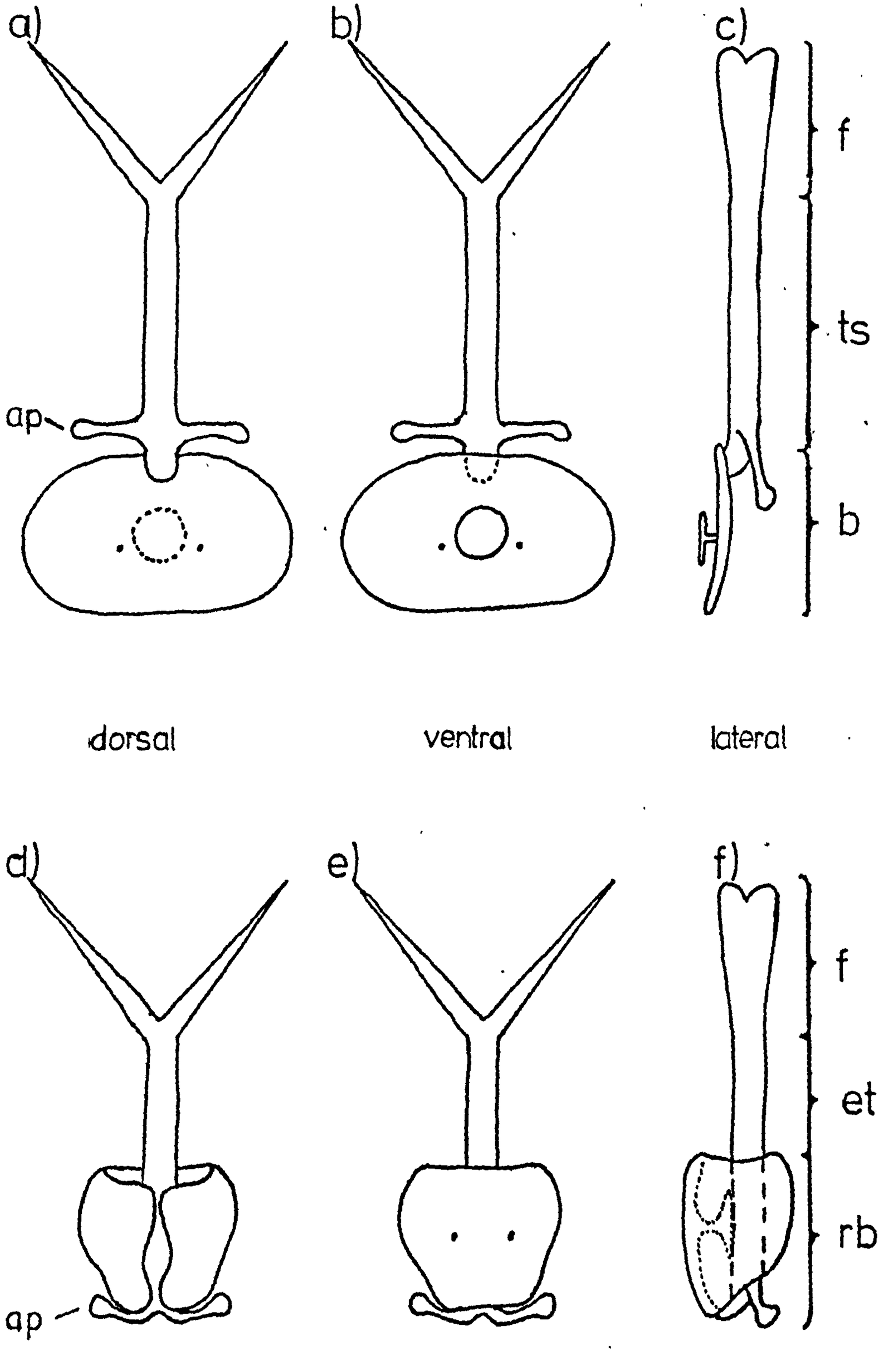
a)
b)
c)
f
ts
b
ap
dorsal
ventral
lateral
d)
e)
f)
f
et
rb
ap

the pigmented ocelli which were only visible in ventral view (Figure 12.2e).

Swimming in the water column always occurred in a tail first direction, the tail stem describing an arc in the lateral plane. Although the route followed by a swimming cercaria was usually tortuous it generally had a predominantly vertical component which caused the larva to rise in the water column.

A cercaria descended in the water column during the dropping behavioural mode. During dropping the reflexed configuration was maintained, with the reflexed body region downward and the rigid exposed tail stem and symmetrically spread furcae trailing. The furcae had a characteristic mean internal angle of $120^{\circ} \pm 4$ (Whitfield et al., 1977).

Plate 43 shows photographs of a dropping cercaria in dorsal and lateral view.

When the dropping cercaria contacted the substrate it initiated either swimming or resting behaviour. In the latter case the cercaria lay horizontally on the substrate in the reflexed configuration with the ventral surface of the exposed tail stem in contact with the substrate (Plate 44d).

The free living phase of activity ended when either the cercaria died or attached to its piscine definitive host. In the latter case a characteristic four stage attachment behaviour was initiated as described previously (Whitfield et al., 1975).

Attachment behaviour was described previously from microscopical examination of cercariae on anaesthetised fish. The

photographic evidence presented here was obtained using an unnatural system of aged cercariae in conditioned water attaching to components of an observation cell. The behavioural responses appeared consistent with those from the published observations.

Initial attachment - a dropping cercaria contacts the host with the arm processes and attaches by means of its adhesive pads (Plate 45a).

Body extension - the body unfolds from the reflexed configuration (Plates 45b and 46).

Inversion - the arm processes detach and the whole cercaria rotates about its long axis to bring the ventral sucker into contact with the host (Plate 45c).

Decaudation - the tail performs rapid lateral movements and separates from the body which then develop to the adult (see Section 11).

During extension and inversion of the body the furcae were often closely adpressed (Plate 45c). This was reversible, some cercariae subsequently spreading the furcae and detaching to swim and drop in the normal configuration.

12.3.3 Quantitative description of cercarial swimming

To simplify comprehension of swimming behaviour it was assumed that in any short interval of time the cercaria persued a straight-line path.

Swimming behaviour was analysed from three high speed cinematographic sequences of individual cercariae. These were

designated sequence A, B and C and represented real time durations of 49, 44 and 37 msec respectively. Since the framing rate was 1000 pps each sequence had one recorded frame for each msec of elapsed time.

Sequence A is illustrated in Plate 47. It can be seen in this typical sequence that the cercaria lashed its tail from side to side when swimming. As will be shown below the time taken for the tail to complete each swimming stroke - from extreme extension on one side to extreme extension on the other and back to the original side - was on average 33.5 msec. Hence each of the three cine sequences examined included one complete swimming stroke.

It is apparent from Plate 47 that the reflexed body region did not maintain a fixed position relative to the direction of movement of the cercaria but yawed from side to side. The reflexed body region may be considered to be a disc slicing edge-on through the water and simultaneously oscillating in the same plane about its centre point. Figure 12.3 is a tracing of the changing position of the reflexed head region during motion in sequence A.

Quantitative descriptions of the angular oscillations of the reflexed body region, or any other cercarial component, relative to the straight line trajectory of the whole organism require that this trajectory be accurately known. The practical difficulties of filming permitted only relatively short swimming sequences to be recorded and fitting the mean straight-line path by eye to such short sequences proved inaccurate. A statistical technique was therefore developed. The use of this technique and its application to determine the trajectories of the cercariae in sequences A, B and C are described in Appendix 3.

Figure 12.3: Tracings of sequential orientation of reflexed body region during swimming sequence A.
The position of the reflexed body region is shown at one msec. intervals during the progress of the whole organism along the trajectory indicated by the arrow.

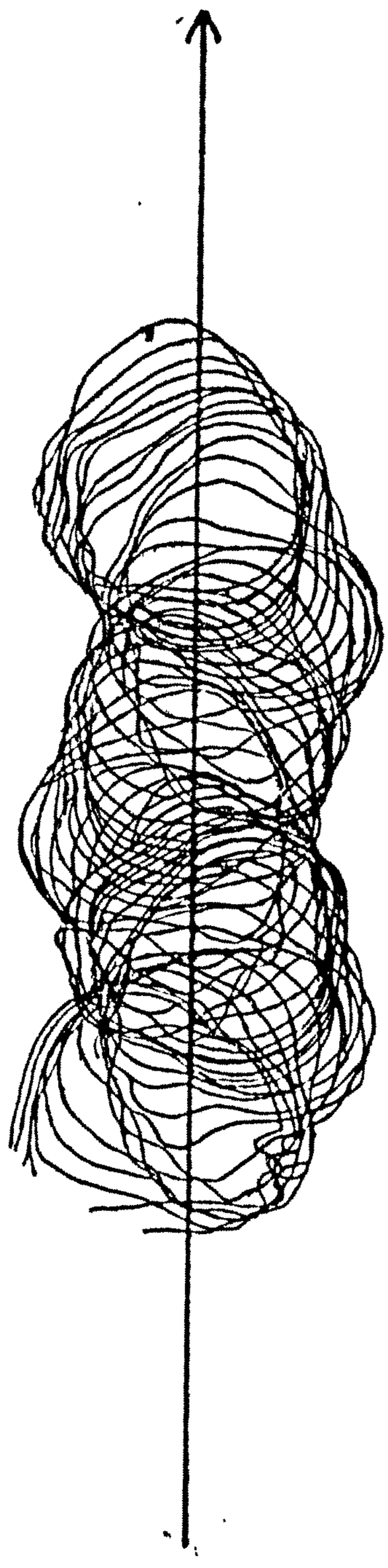

The angle (i) between the mid-anterio-posterior axis of the reflexed body region and the direction of movement of the whole organism was determined. Figure 12.4 shows the relationships of these components and the conventions used in describing the angles.

Figure 12.5 illustrates the changing values of i in the swimming sequences A, B and C. It can be seen that the angle changes cyclically with a mean period of 33.5 msec and amplitude (defined as the extreme angular displacement from the mean position) of approximately 90^{o}. That is, the reflexed body region moved from being at right angles on one side of the direction of movement of the cercaria to the same position on the other side every 16.75 msec.

There was relative movement between the reflexed body region and the exposed tail stem. This movement was clearly demonstrated if one or other of these components was conceptually maintained in a constant position and the other component allowed to move relative to it. This is effectively what is achieved in Figure 12.6 where the motion of the exposed tail stem and furcae are shown relative to the reflexed body region. To obtain these figures an approximate outline of the reflexed body region was traced and the position of the other components relative to this profile traced from frames of sequence A. In Figure 12.6a and b only the left margin of the exposed tail stem and the left furca were outlined, in Figure 12.6c only the right margin and furcae.

Figure 12.6 a and b show the changing relative positions throughout sequence A while Figure 12.6c shows the positions during the same part of the sequence as in Figure 12.6b.

Figure 12.4: Conventional description of relative angles during swimming.

Arrow indicates trajectory of swimming cercaria.

Y = angle of exposed tail stem to anterio-posterior axis of reflexed body region.

ψ = angle of exposed tail stem to trajectory

i = angle of anteio-posterior axis of reflexed body region to trajectory.

Hence from convention Right = + ve, Left = -ve:

a) Y = - ve

ψ = + ve

i = - ve

b) Y = 0

ψ = 0

i = 0

c) Y = + ve

ψ = - ve

i = + ve

a)

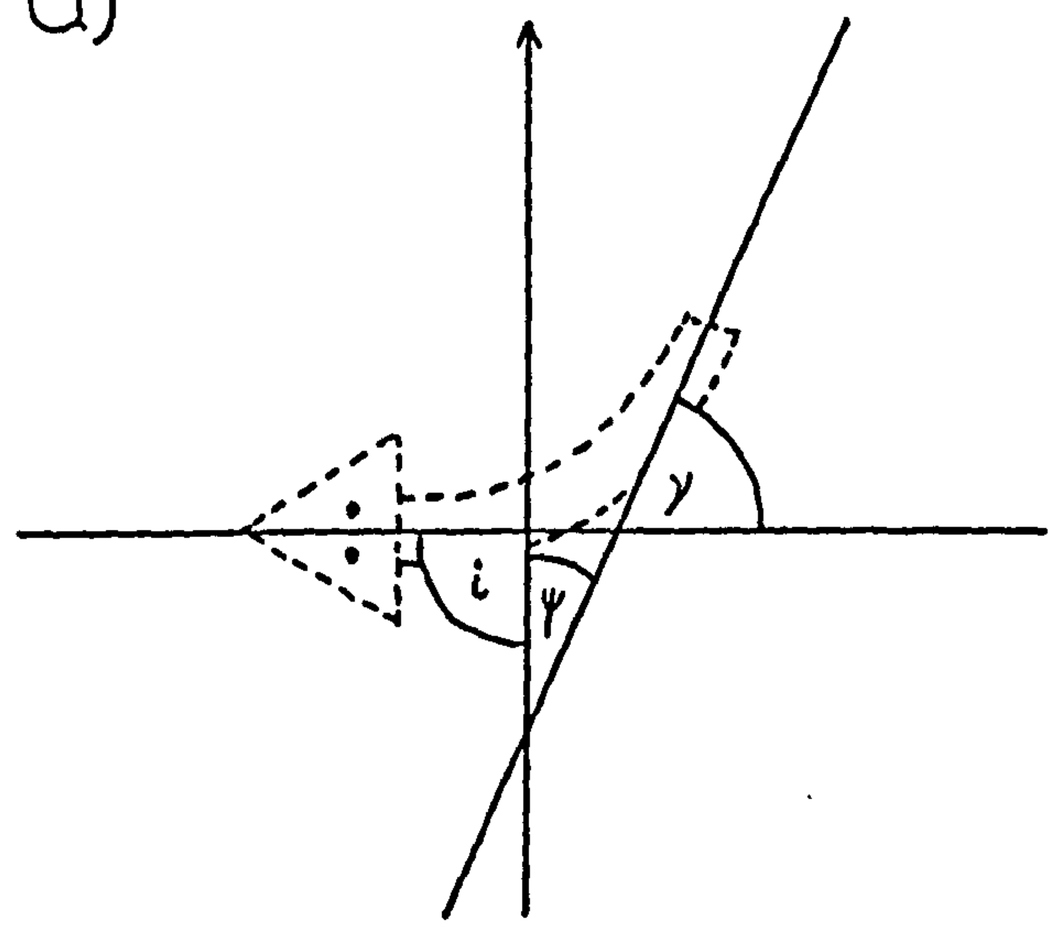

b)

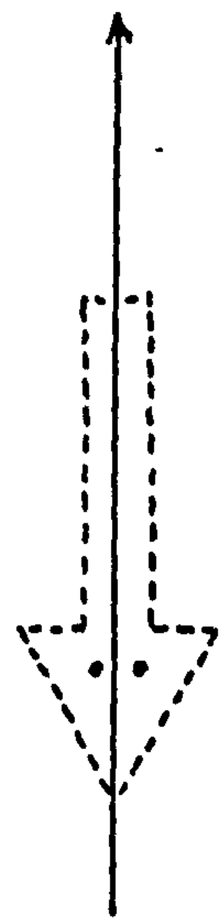

c)

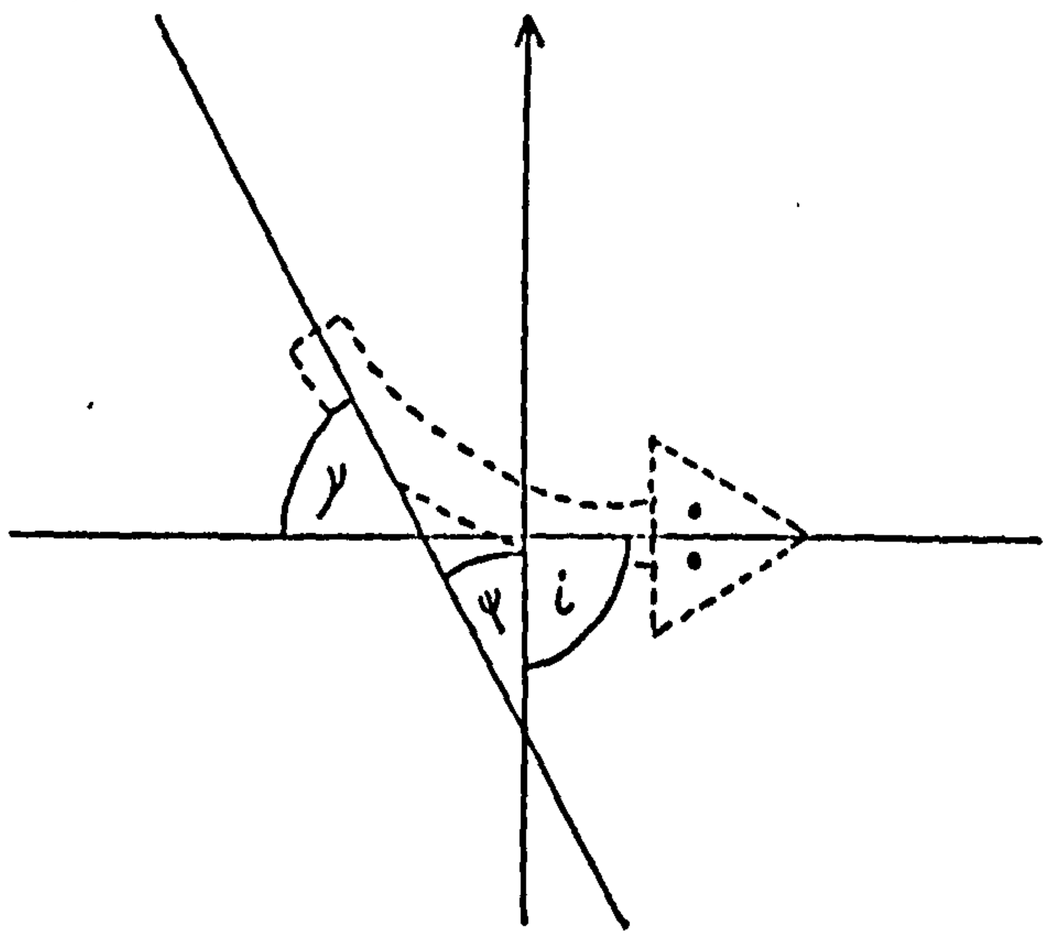

Figure 12.5: Angles subtended by cercarial components to trajectory of whole organism.

a) Swimming sequence A.

b) Swimming sequence B.

c) Swimming sequence C.

Angles above zero line (+ ve) to right of trajectory, angles below zero line (- ve) to left of trajectory.

Key (reading from top of Figure):

Bold dashed line, anterio-posterior axis of reflexed body region;

Feint continuous line, right furca;

Bold continuous line, exposed tail stem;

Feint dashed line, left furca;

Bold dashed line, anterio-posterior axis of reflexed body region (continued).

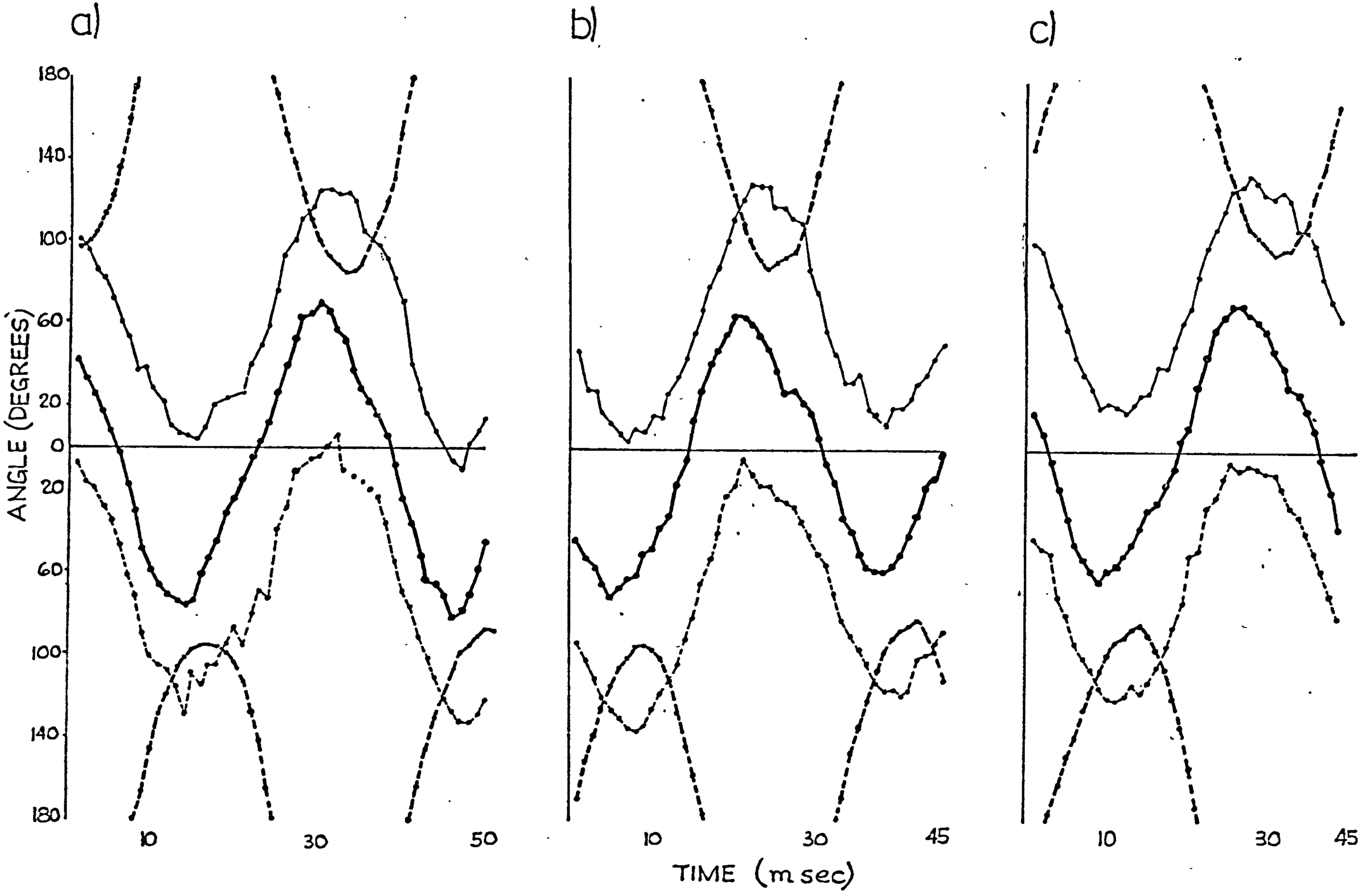
a)
b)
c)
180
140
100
60
20
0
20
60
100
140
180
ANGLE (DEGREES)
10
30
50
10
30
45
10
30
45
TIME (m sec)

Figure 12.6: Motion of exposed tail stem and furcae relative to conceptually constrained body region. Selected from sequence A.

a) Left margin of exposed tail stem and left furca. Effective stroke.

b) Left margin of exposed tail stem and left furca. Recovery stroke preceeding (a) above.

c) Right margin of exposed tail stem and right furca. Effective stroke simultaneous to (b) above.

a)

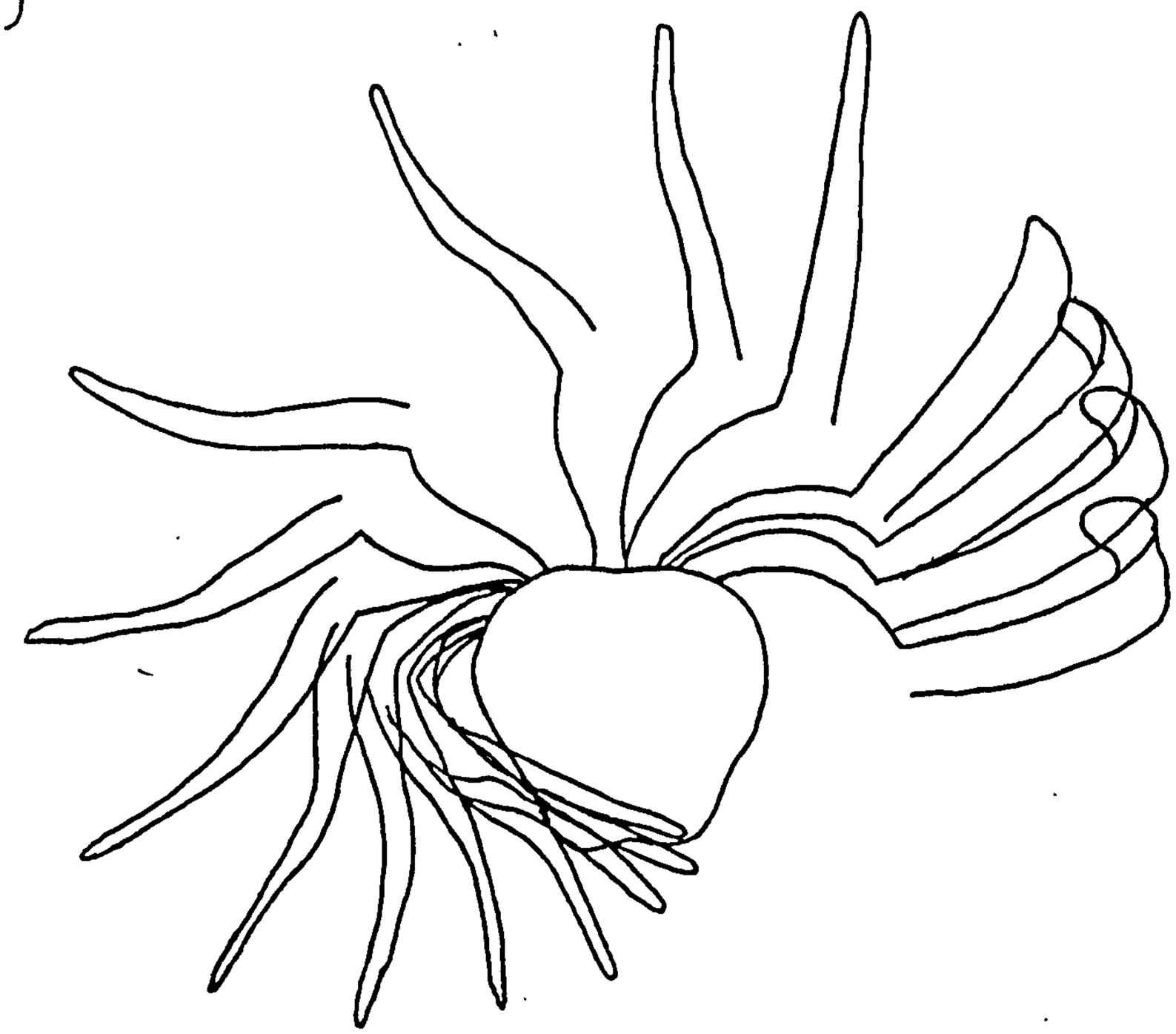

b)

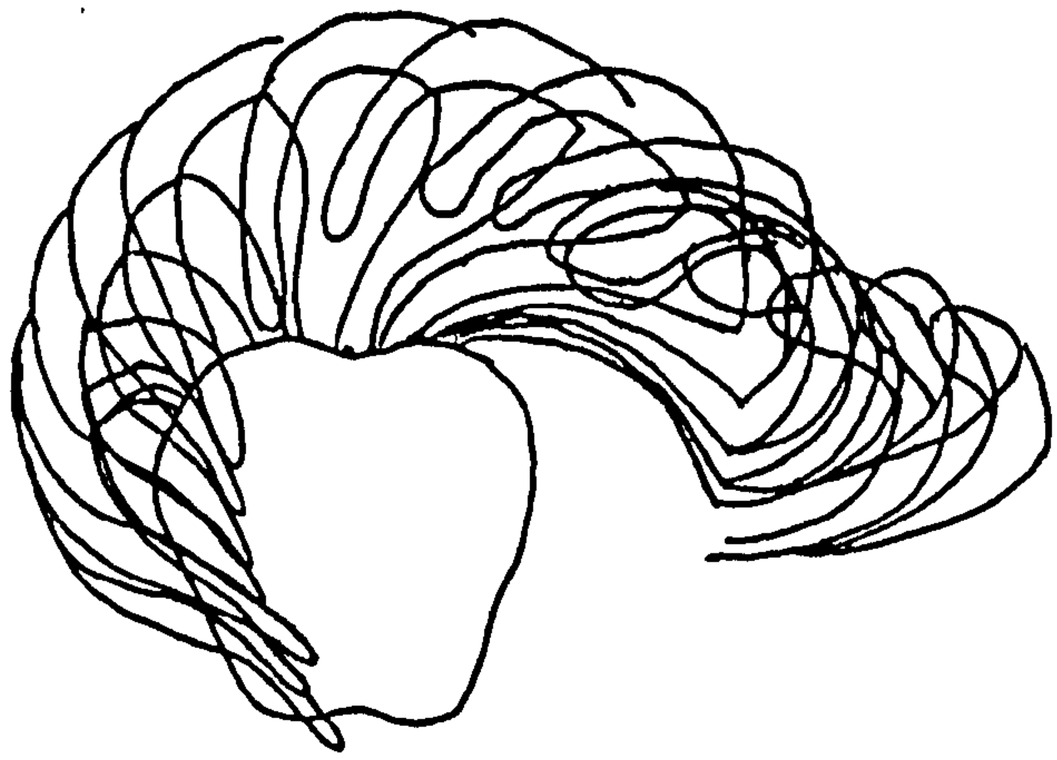

c)

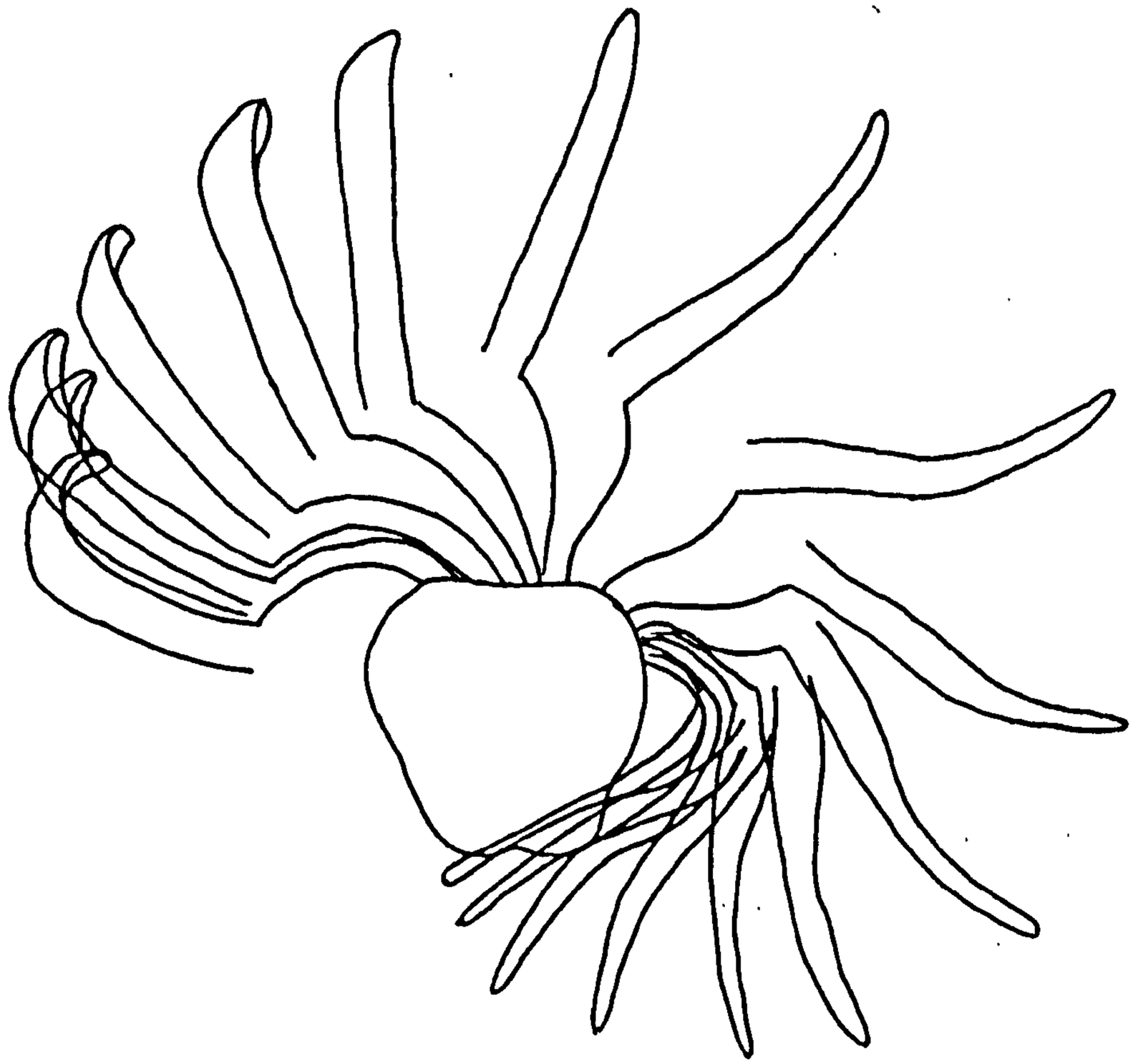

Considering only the exposed tail stem for the moment it is apparent that this structure moved from left to right and back to left again. This movement was achieved by lateral curvature of the tail stem relative to the mid-anterio-posterior axis of the reflexed body region.

To quantify the relative angular change of these cercarial components the procedures and conventions shown in Figure 12.7 were adopted. Using this approach the angle r between the tangent to the long axis of the exposed tail stem and the mid-anterio-posterior axis of the reflexed body region could be determined for each one msec interval in sequences A, B and C. These results are shown in Figure 12.8.

It is apparent that the exposed tail stem swept through an arc of 280-320^{o} in its movement from one extreme lateral position to the other. The mean length of time required to achieve this movement was approximately 16.75 msec. Note that the period of this activity corresponded to the period of the lateral movements of the reflexed body region relative to the direction of movement of the whole organism. Significantly, however, the oscillations were almost exactly out of phase so that while the exposed tail stem rotated through 280-320^{o} relative to the reflexed body region in one direction, the reflexed body region rotated through 180^{o} in the opposite direction. In consequence the arc swept by the exposed tail stem relative to the direction of movement of the cercaria must be approximately equivalent to 280-300^{o} minus 180^{o}, or 100-120^{o}. The simple geometrical reasons for this are perhaps more readily understood with reference to Figure 12.4.

Figure 12.7: Conventional angles relative to exposed tail stem and furcae.

a) Angle of left (α) and right (β) margin of exposed tail stem to antero-posterior axis of reflexed body region. Hence mean angle (r) = $\alpha + \beta/2$.

b) Angle of left (δ) and right (ε) furca to exposed tail stem. Angle between furcae (γ).

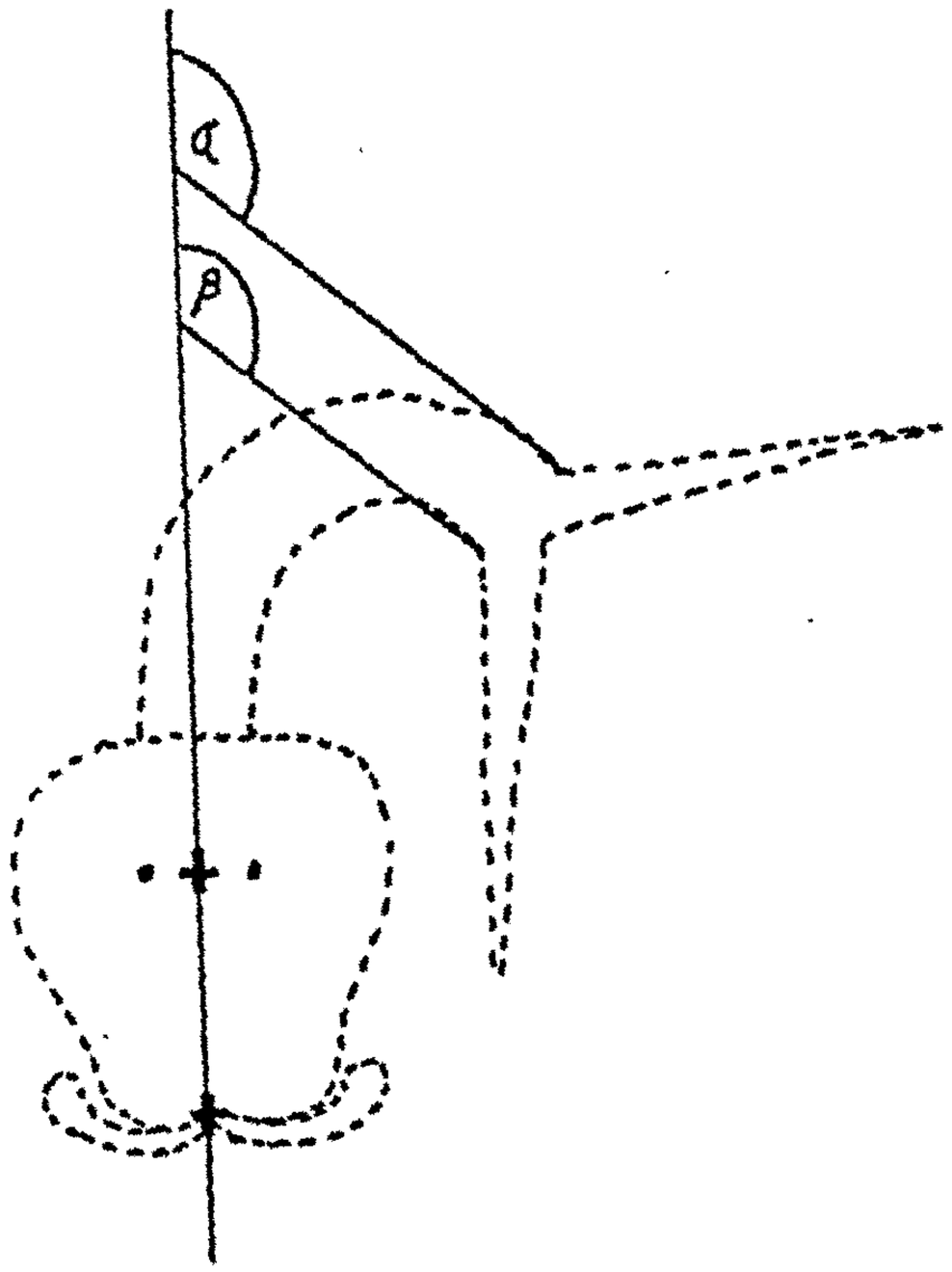

b)

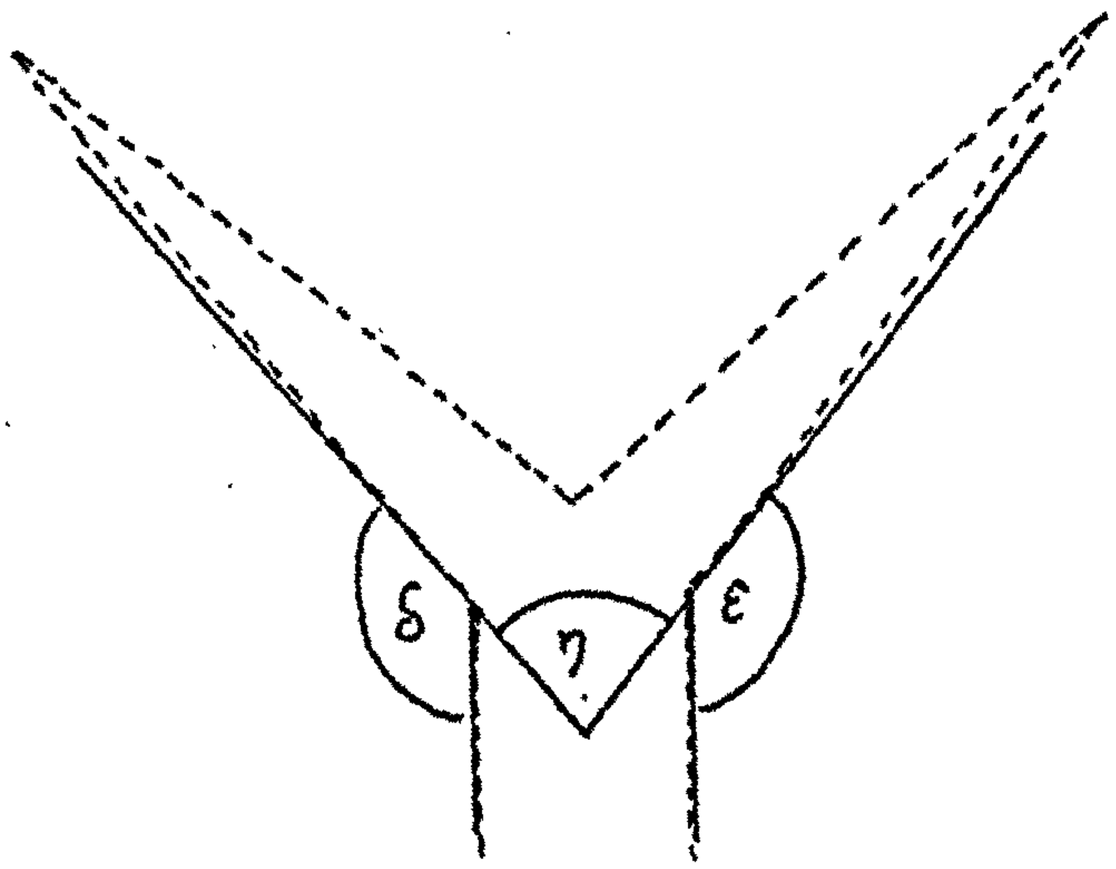

Figure 12.8: Angle subtended by exposed tail stem to anterio-posterior axis of reflexed body region. This is the angle r described in Figure 12.7a.

a) Swimming sequence A.

b) Swimming sequence B.

c) Swimming sequence C.

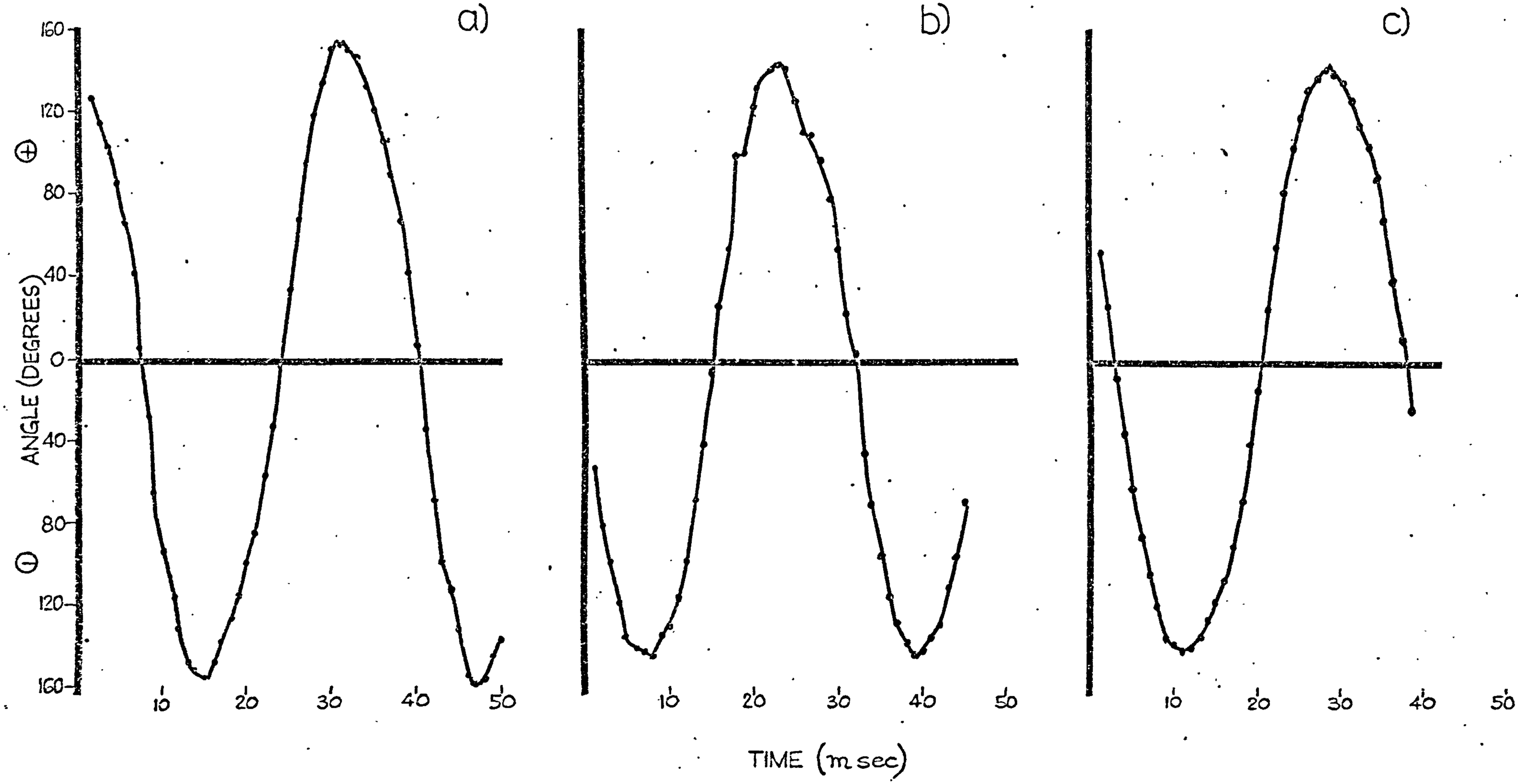
a)
b)
c)
160
120
80
40
0
40
80
120
160
⊕
⊖
ANGLE (DEGREES)
1'0
2'0
3'0
4'0
5'0
TIME (m sec)

This prediction was tested by measuring the angle between exposed tail stem and direction of movement in the sequences A, B and C according to the procedures and conventions of Figure 12.4. The results are shown in Figure 12.5. The angle oscillated approximately 60-70° either side of the direction of movement, in agreement with the predicted value. The oscillations had a mean period of 32.7 msec.

The results so far have described the swimming cercaria as moving along a straight-line path, with the reflexed body region and exposed tail stem oscillating about this path at the same frequency but in opposite directions. The role of the furcae in this movement was examined.

The furcae bifurcated symmetrically from the distal tip of the exposed tail stem. Figure 12.6 a and b shows the fate of the left furca in sequence A during one complete swimming stroke. It should be remebered that this figure represents movement with the reflexed body region artifically constrained. It can be seen that during the left-to-right motion of the exposed tail stem (Figure 12.6b) the furca gradually straightened. This process continued at the start of the right-to-left movement (Figure 12.6a) and then the furcal tip became slightly recurved before the furca again curled. For reasons discussed below the lateral motion during which the furca uncurled was considered to be the recovery stroke while the lateral motion in which the furca finally straightened was the effective stroke, together comprising the propulsive cycle or swimming stroke of the cercaria.

Figure 12.6c shows the fate of the right furca during the same sequence as Figure 12.6b. It is apparent that the right furca was on an effective stroke while the left furca was on its recovery stroke. In fact, during a single lateral sweep of the exposed tail stem one furca performed an effective stroke and the other a recovery stroke. Consequently, each propulsive cycle involved two symmetrical effective strokes and two symmetrical recovery strokes.

The angle of curvature of the furcal tip relative to the exposed tail stem was difficult to measure. The difficulty arose due to twisting of the furcal tip during the recovery stroke, this phenomenon was not obvious in lateral view but was apparent when the swimming cercaria was viewed from other angles (Plate 44a, b and c). A compromise was adopted and the angles measured relative to the furcal bases (Figure 12.7b).

The changing angles between furcae and tail stem are shown for swimming sequences A, B and C in Figure 12.9. The angle oscillated between 140° and 90° with a period of approximately 30 msec. The angle was maximal during the effective stroke and minimal during the recovery stroke.

This result would suggest that the angle between the furcae remained relatively constant since as one furca-tail angle increased the other decreased by a concomittant amount. To test this prediction the angle between the furcae was measured for sequences A, B and C according to Figure 12.7. The results are shown in Figure 12.10. The interfurcal angle did not vary cyclically but in an apparently random manner. The angle appeared to vary about a value of 120-130°.

Figure 12.9: Angles subtended by right and left furcae to exposed tail stem. These are the angles δ (dashed line), and ε (continuous line) described in Figure 12.7b.

a) Swimming sequence A.

b) Swimming sequence C.

c) Swimming sequence D.

a)

b)

c)

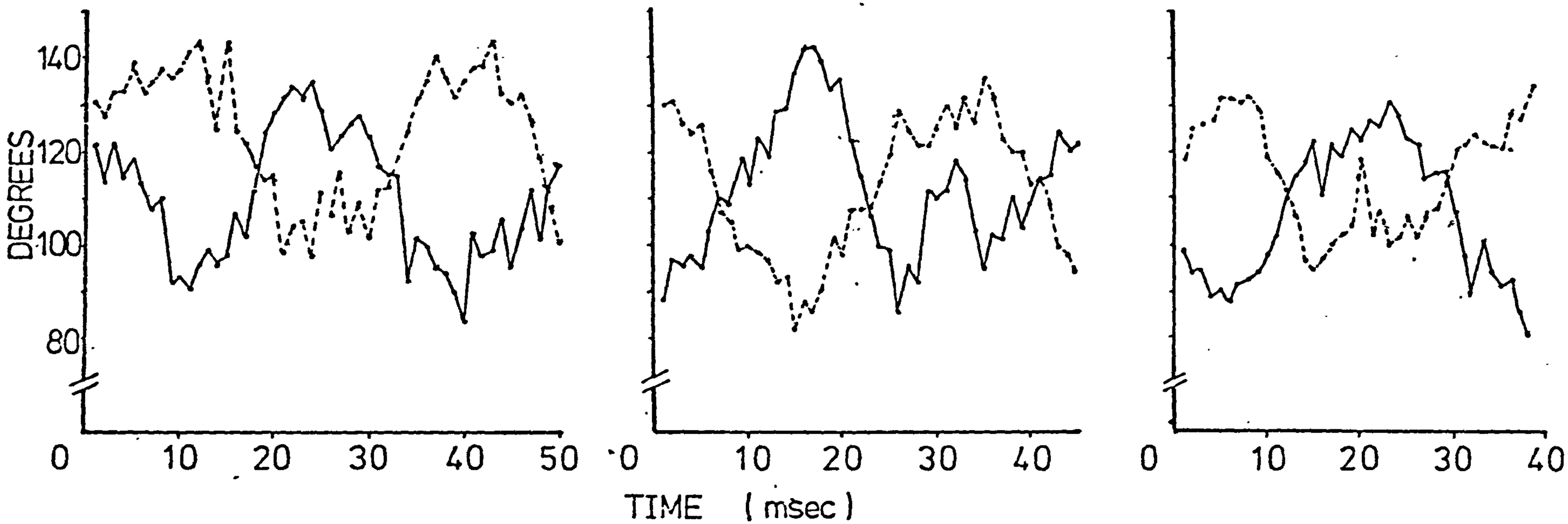
140
120
100
80
DEGREES
0
10
20
30
40
50
0
10
20
30
40
0
10
20
30
40
TIME (msec)

Figure 12.10: Angle between furcae.

This is the angle η described in Figure 12.7b.

a) Swimming sequence A.

b) Swimming sequence B.

c) Swimming sequence C.

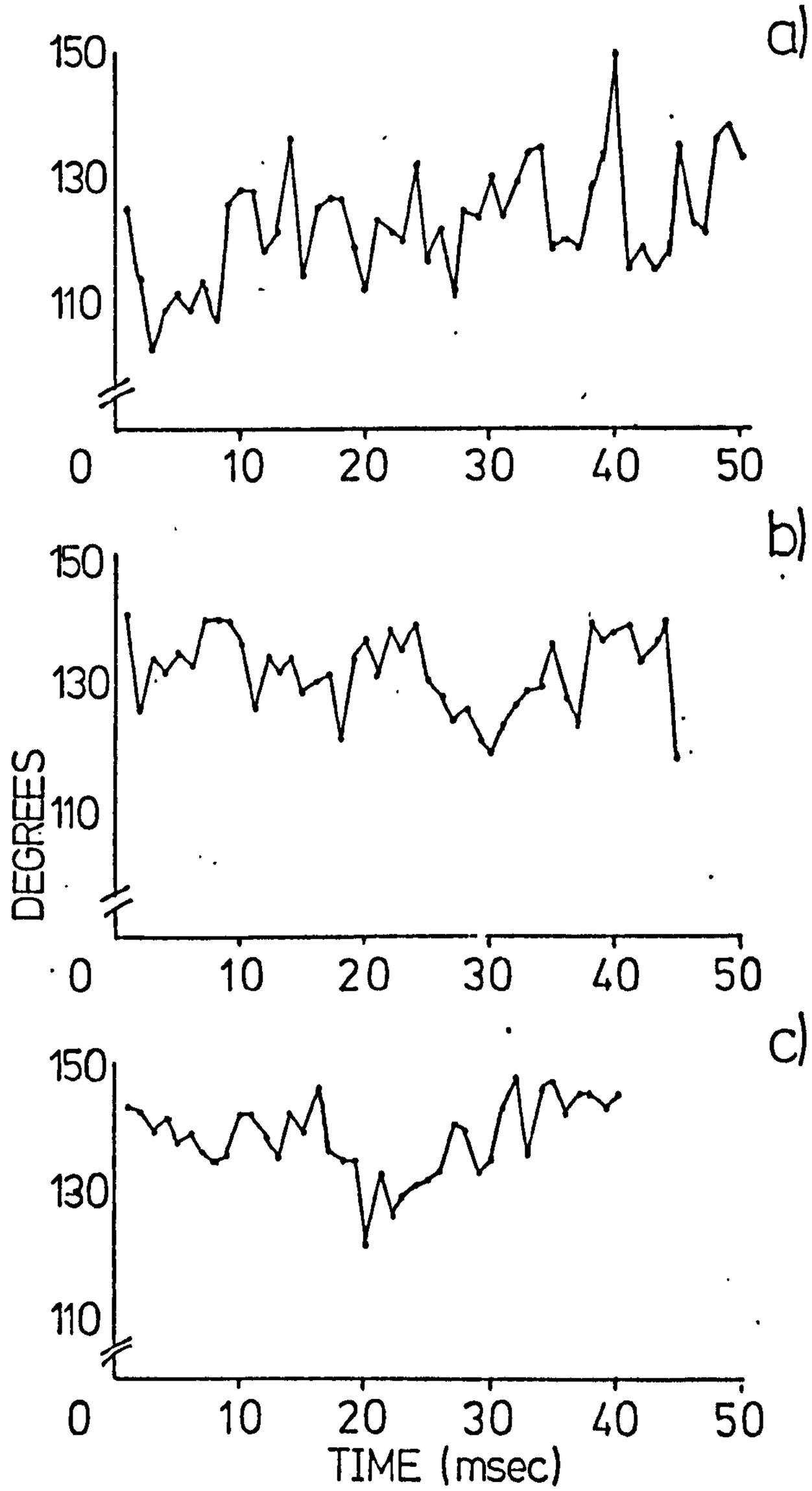
a)
150
130
110
0
10
20
30
40
50
b)
150
130
110
DEGREES
0
10
20
30
40
50
c)
150
130
110
0
10
20
30
40
50
TIME (msec)

The angles of the furcal bases relative to the direction of movement of the cercaria are shown in Figure 12.5. It is apparent that the furcal base angle oscillated from 0^{o} to 120^{o} with a period of approximately 30 msec.

As explained previously the furcal tip curled and twisted independently of the base. Figure 12.11 shows arbitrarily selected tracings during a recovery stroke in sequence A. In Figure 12.11a the reflexed body region is represented in a constant position while in Figure 12.11b the orientation of the left furca was traced as it moved relative to the cercaria.

At position 1 the exposed tail stem was at one lateral extreme. The furcal tip was curled away from the direction of movement of the cercaria and was effectively trailing. At position 6 the base of the furca was pointing in the direction of movement of the cercaria but due to curling and twisting the furcal tip was pointing in the opposite direction. This whole recovery stroke sequence had the effect of projecting the furca laterally, a movement clearly demonstrated by the tracing of the whole sequence in Figure 12.12a.

The effective stroke of the left furca is shown in Figure 12.12b. During the effective stroke the furca became straightened so that it was in line with the furcal base. This occurred as the furca reached a position at 90^{o} to the direction of movement of the cercaria, so that the furca was moving at right angles in the opposite direction to that of the cercaria. The furcal tip became reflexed during this phase.

Figure 12.11: Orientation of the left furca during a recovery stroke. 1-6 are arbitrarily selected sequential positions of the left furca during swimming sequence A.

a) Movement of left margin of exposed tail stem and left furca relative to conceptually constrained reflexed body region.

b) Movement of left furca during unconstrained swimming. Arrow represents trajectory of cercaria.

a)

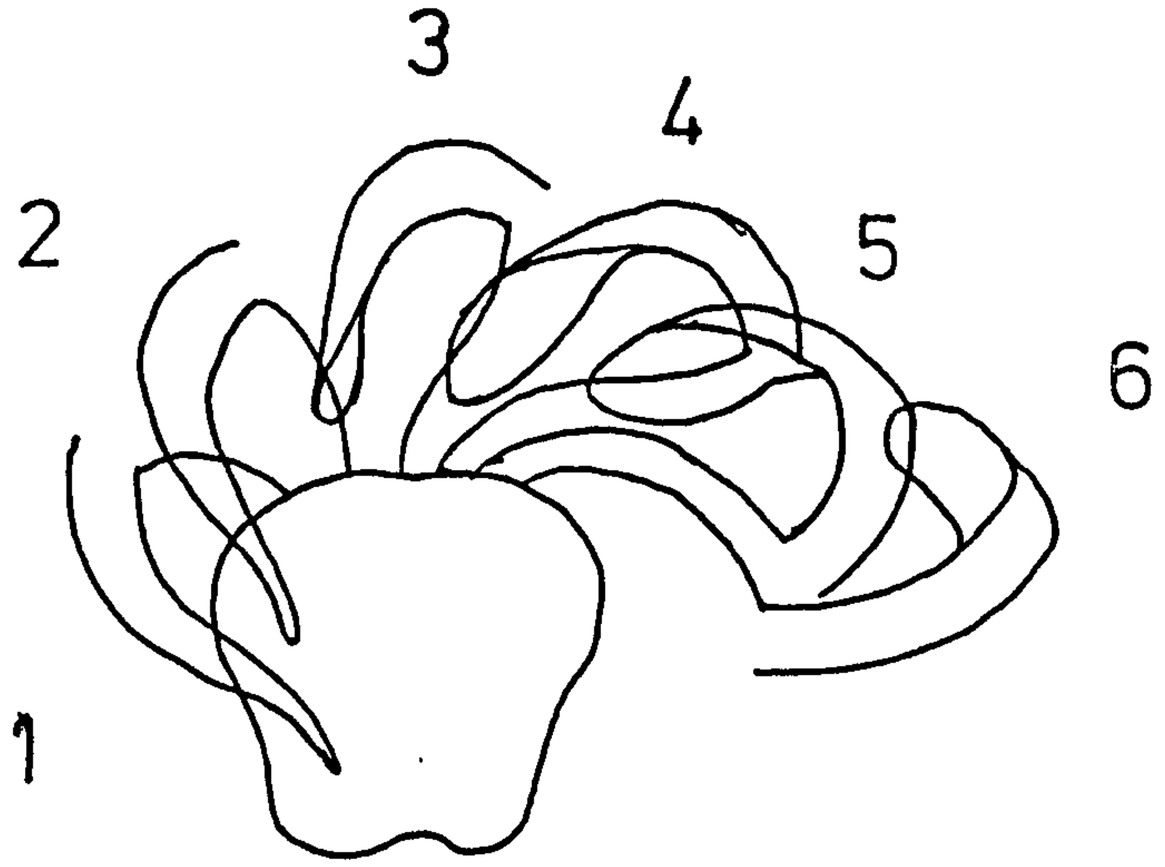

b)

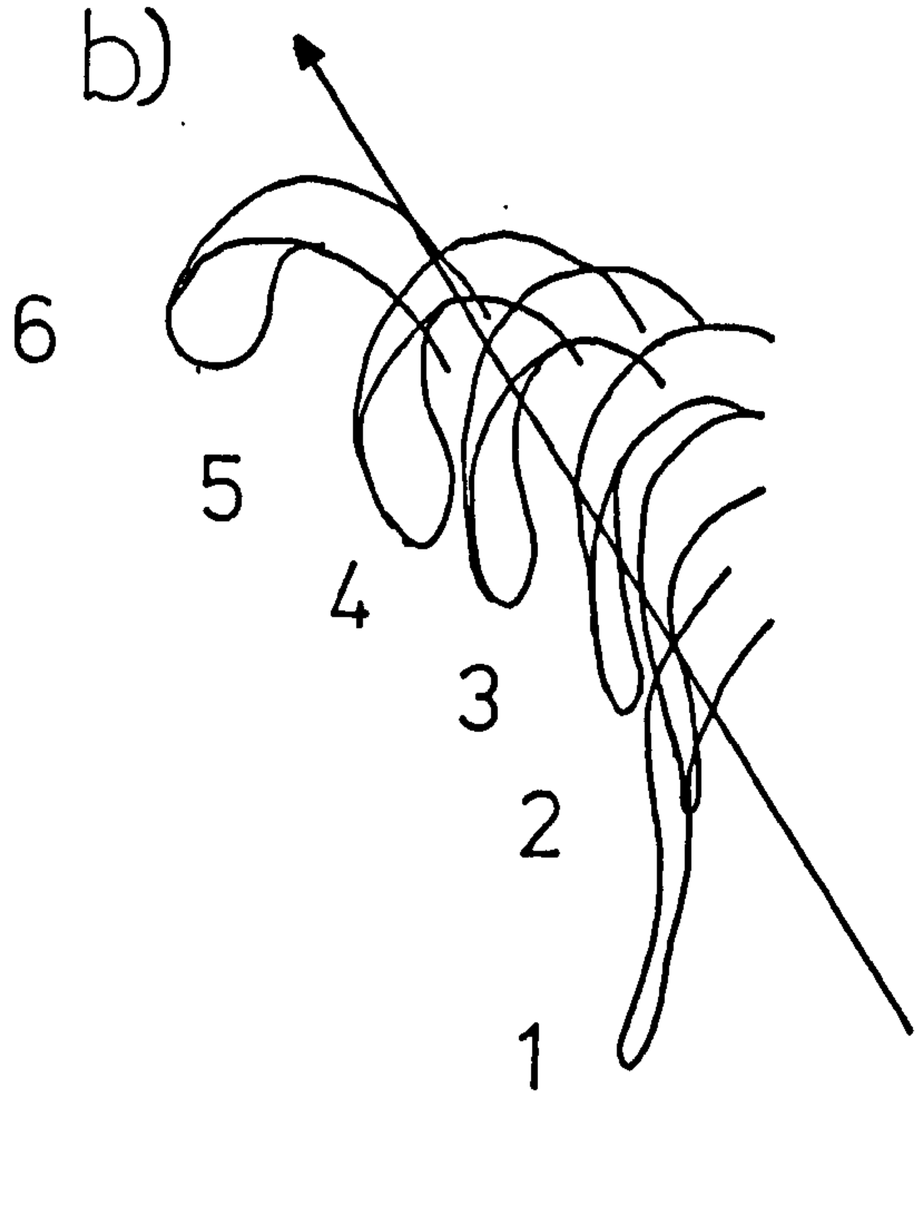

Figure 12.12: Orientation of furca during recovery and effective stroke.

The sequential position of the left furca at one msec. intervals during swimming sequence A. The arrow represents the trajectory of the cercaria.

a) recovery stroke.

b) effective stroke.

a)

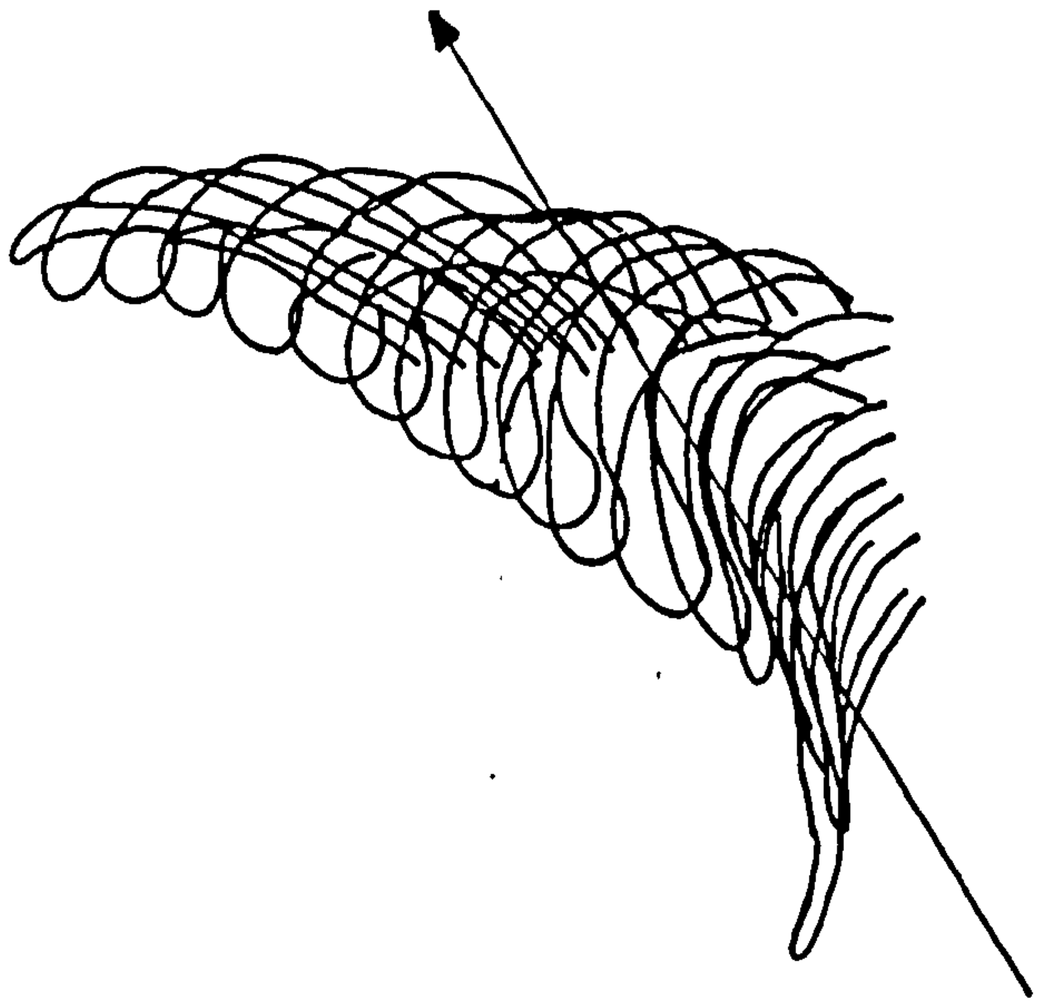

b)

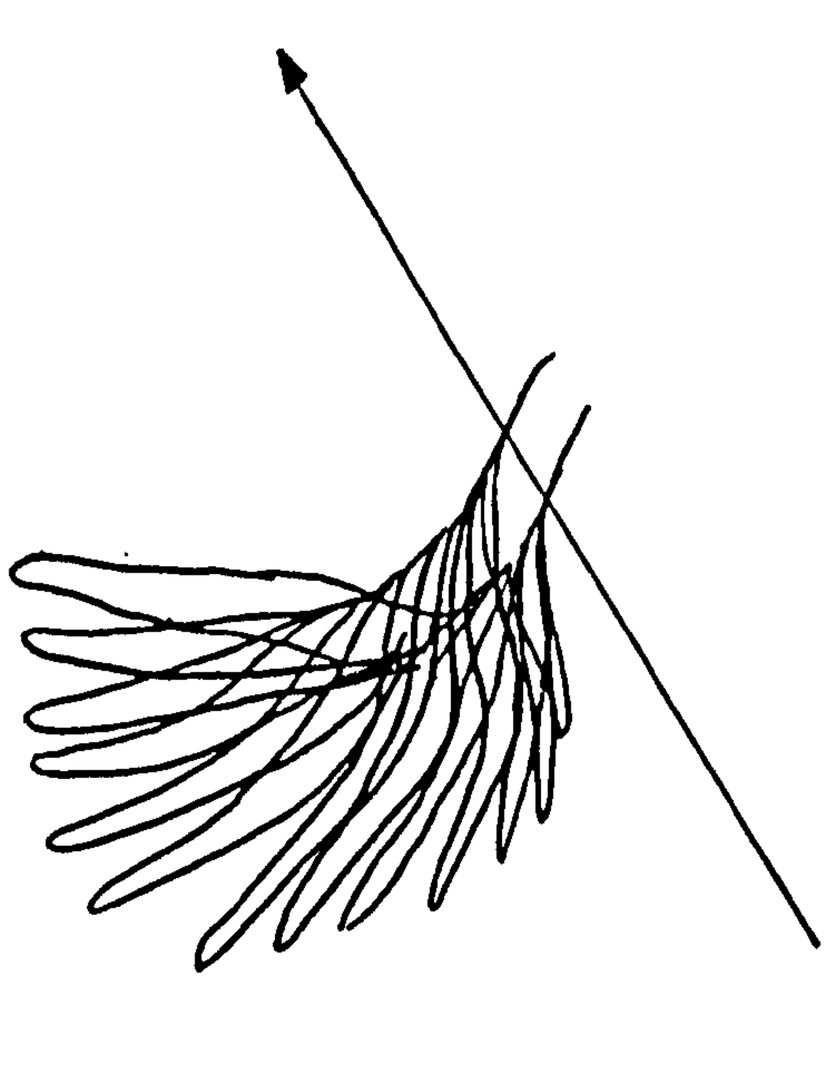

The whole sequence of recovery and effective strokes of the left furca is illustrated in Figure 12.13. Figure 12.13 illustrates the simultaneous orientation of the right furca. It is apparent that the two furcae were always involved in exactly opposite stages of the propulsive cycle.

The whole complex of interacting events described in these results are difficult to appreciate or comprehend simultaneously. Plate 48 shows six arbitrarily selected frames from swimming sequence A. Each on its own may be interpreted in terms of the angular relationships of its component parts. When the six frames are superimposed to illustrate the sequential cycle of events the true complexity of the relationships is revealed (Frontispiece).

In considering the totality of events during cercarial swimming it was apparent that the arm processes were also involved. Normally the arm processes were folded against the reflexed body region but at certain stages during the propulsive cycle one or other, but never both, was extended. When the propulsive cycle was at the lateral extreme, with exposed tail stem maximally flexed and reflexed body region at 90° to the direction of movement, both arm processes were folded.

With the initiation of the next lateral sweep the reflexed body region turned towards the path of the organism and at the same time the arm process distal to the path was extended. This sequence is apparent in Plates 47 and 48. As the reflexed body region arrived at its new lateral extremity the arm process was again folded and the cycle restarted in the opposite direction.

Figure 12.13: Simultaneous orientation of right and left furcae during a propulsive cycle.

Sequential positions of furcae arbitrarily selected from swimming sequence A. Arrow represents the trajectory of the cercaria.

a) left furca.

b) right furca.

a)

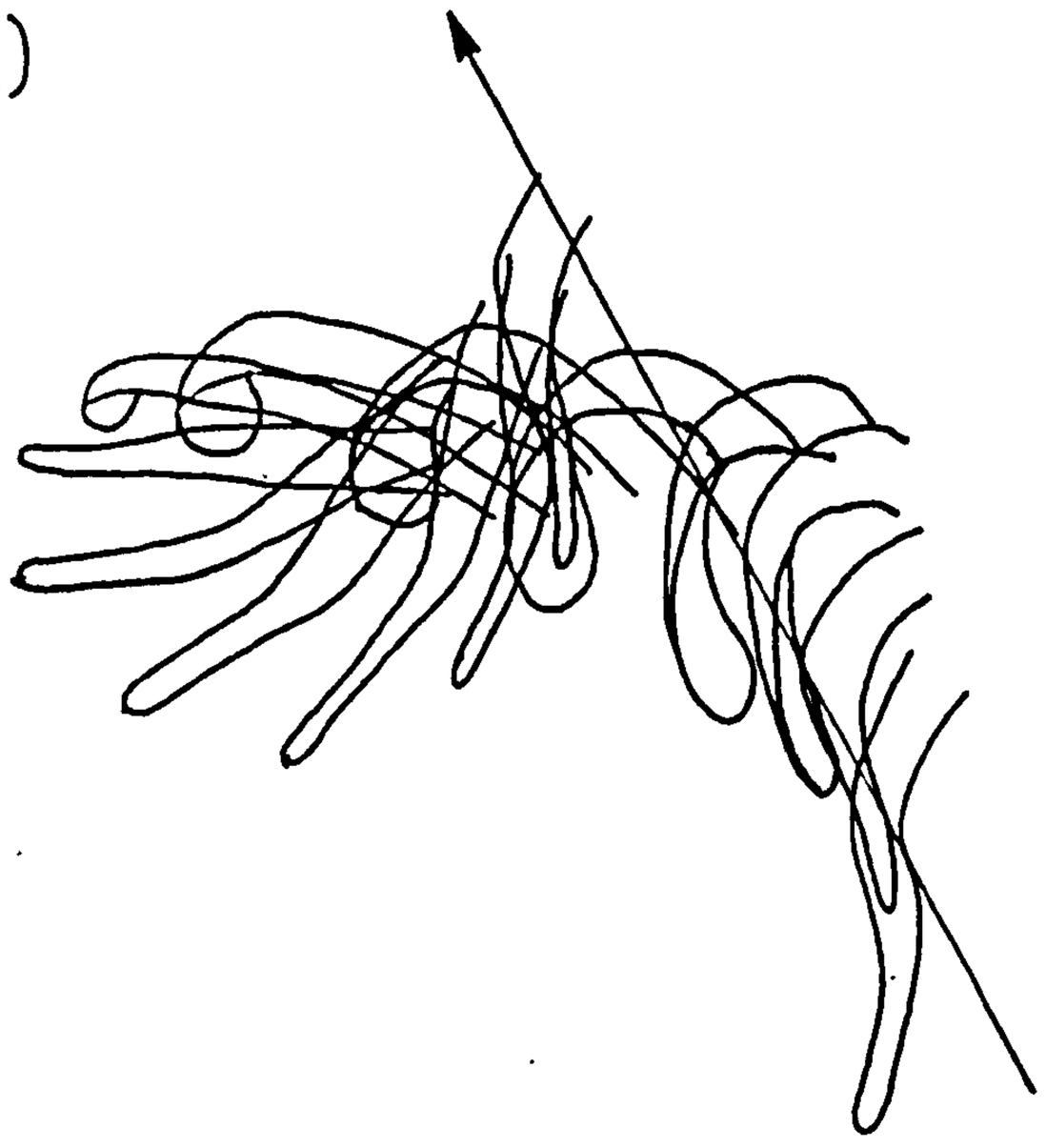

b)

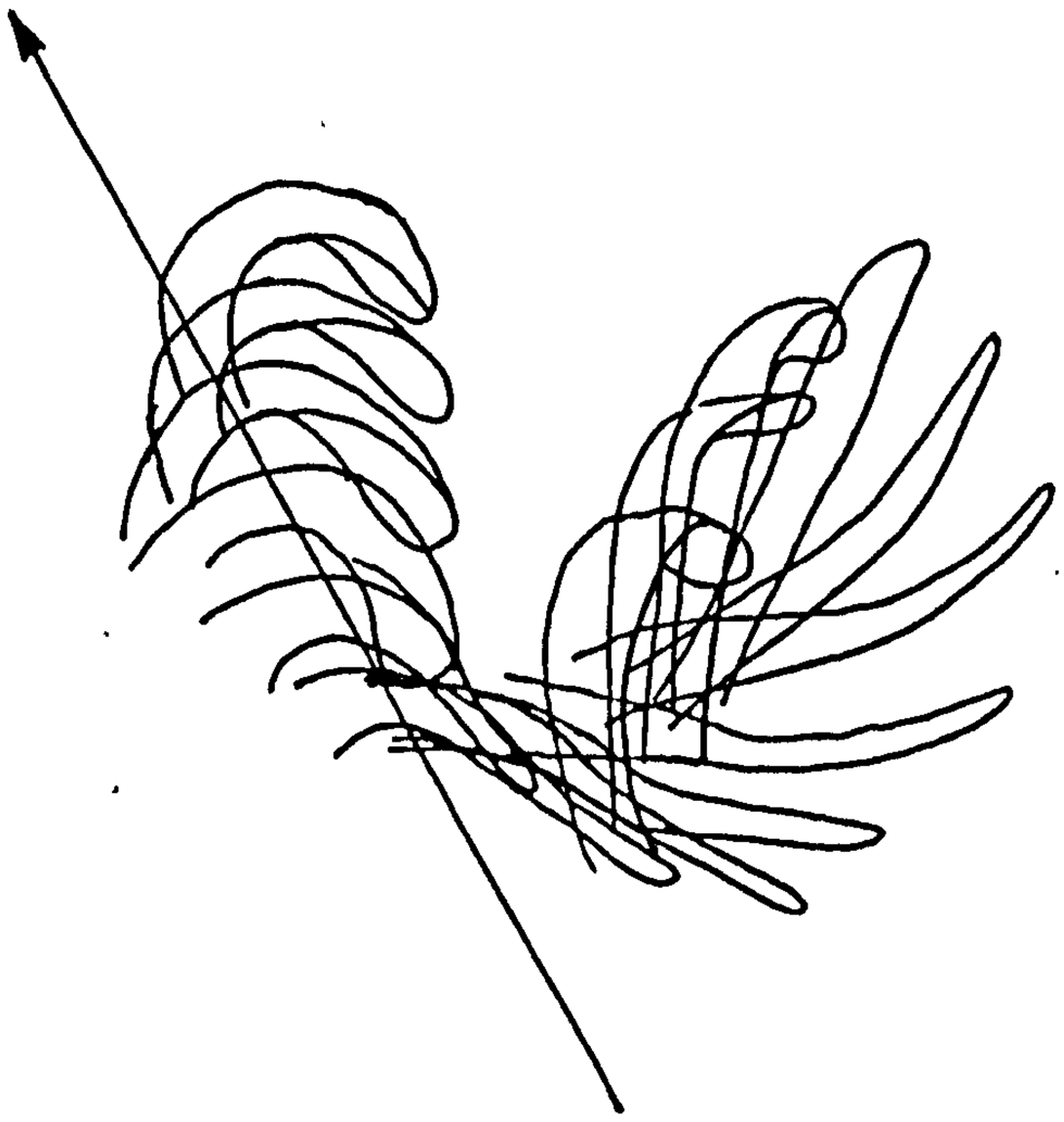

12.3.4 Cercarial density

Cercarial density was determined in order to estimate the gravitational force on a dropping cercaria (see Section 12.3.6).

Due to the low temperature utilised the cercariae were unable to swim and hence their drift up or down in the sucrose solution was dependent on the density difference between solution and cercaria. The ideal condition of neutral bouyancy was never satisfied due to the disrupting effects of local convection currents in the solution. Cercarial density was, therefore, taken to be an intermediate value between the solution density which just caused an appreciable upward drift and that which caused an appreciable downward drift.

The density was found to be between 1.158 and 1.183 g cm^{-3}, equivalent to 33 and 40% sucrose solutions. The density was, therefore, estimated at 1.17 g cm^{-3}.

12.3.5 Reynolds Number for cercarial swimming

The Reynolds Number gives an indication of the relative importance of inertial and viscous forces during aquatic locomotion. For the cercaria of T. patialense the supposed propulsive organs were the furcae, and therefore activity parameters of these during the effective stroke were determined in order to calculate the Reynolds Number.

The velocity of furcal tip movement was calculated by determining the absolute distance in μm moved by the furcal tip between sequential frames at 1 msec intervals during the effective stroke. From these data the velocity of 10 sequential movements

was determined for 5 separate effective strokes, and a mean value calculated (Table 12.1).

The Reynolds Number is given by:

$$R_e = \rho l v / \eta$$

where ρ = density of water (10^3 Kg m^{-3})

l = depth of furca (40×10^{-6} m)

v = velocity of furcal tip (52×10^{-3} $msec^{-1}$)

η = coefficient of viscosity of water

(1.2×10^{-3} Kg m^{-1} sec^{-1})

Hence Reynolds Number (R_e) for a swimming cercaria has an approximate value of 2. This result suggests that both inertial and viscous forces were involved in the swimming activity of T. patialense cercariae.

12.3.6 Viscous effects on the dropping cercaria

It has been shown elsewhere (Whitfield et al., 1977) that cercariae in water at 25°C drop with a terminal velocity of 1.09 mm/sec if intact, 1.35 mm/sec with one furca amputated, and 1.58 mm/sec with both furcae amputated.

In the present investigation these experimentally derived results were compared with theoretical estimates of terminal dropping velocity. The following parameters had to be estimated: cercarial density, cercarial volume and the viscous resistance to cercarial dropping.

Methods of calculating volume and viscous resistance are described in Appendix 4.

TABLE 12.1

Velocity of the furcal tip during the effective stroke

Replicate Furcal Positions	Replicate effective strokes (Velocity in mm sec^{-1})				
	1	2	3	4	5
1	27	40	27	38	28
2	40	49	58	57	43
3	31	45	58	66	43
4	45	67	63	38	33
5	63	54	81	95	47
6	45	72	49	57	57
7	76	54	76	47	66
8	63	49	54	52	52
9	58	40	40	47	47
10	54	45	45	62	47

Mean furcal tip velocity = 51.8 mm sec^{-1}

The cercarial density was 1.17 g cm^{-3} (see Section 12.3.4), representing a density difference (ρ_D) between cercaria and water of 0.17 Kg m^{-3}.

The equation of motion of a small body dropping at its terminal velocity (u) in an aquatic medium is given by:

gravitational force = viscous resistance

Therefore, for a dropping cercaria:

cercarial volume x ρ_D x g = sum of viscous resistance due to reflexed body region, exposed tail stem and furcae.

Hence given the constants: acceleration due to gravity (g) = 9.8 x 10^{-6} $msec^{-2}$; and coefficient of viscosity for water (η) = 1.2 x 10^{-3} Kg $m^{-1}sec^{-1}$; it is possible to determine the terminal velocity of cercariae with two, one or no furcae.

The calculations are shown in full in Appendix 5.

The terminal dropping velocity of cercariae determined by experimental techniques and theoretical calculations are shown in Table 12.2. It is apparent that the theoretical estimates predict a greater dropping velocity than was determined experimentally, and that the proportionate increases in dropping velocity due to furcal amputation were broadly similar in the experimental and theoretical results.

TABLE 12.2

Terminal velocity of dropping T. patialense cercariae, determined by experimental and theoretical means. Experimental data from Whitfield et al., 1977

	EXPERIMENTAL		THEORETICAL	
CONDITION OF CERCARIA	V	P_v	V	P_v
INTACT	1.09		3.01	
WITH SINGLE FURCA	1.35	0.24	3.72	0.24
WITH NO FURCAE	1.58	0.45	5.11	0.69

where: P_v = proportional increase in dropping velocity due to furcal amputation.

V = terminal dropping velocity (mm sec^{-1})

12.4 Discussion

12.4.1 Hydrodynamic aspects of dropping behaviour

The theoretical estimates of terminal dropping velocity of cercariae were of the same order of magnitude as the experimentally derived values but differed from them by a factor of 3. Despite this discrepancy the effect of removing the relevant furcal parameters from the predictive equations caused a similar proportional increase in dropping velocity as was achieved by physical amputation of furcae in the experimental system. That is, the model system responded to change in a similar manner to the real situation. This response increases faith in the applicability of the fundamental assumptions of the model to the physical parameters controlling the rate of dropping of the cercaria.

The lack of precise correspondence between the theoretical and experimental results was probably due to the method of estimation of the physical parameters. For estimating viscous drag and volume the cercarial components were assumed to be of precise and uniform shape to facilitate calculations. Projections and irregularities in form were ignored, due to their considerable complexity, and these almost certainly contribute to the hydrodynamical properties of the cercaria and could generate the discrepancy between predicted and experimental values.

If one accepts that the theoretical model is a reasonable approximation to the real situation then some of the assumptions of the model may be used to explain hydrodynamic aspects of cercarial dropping. The most significant feature is that dropping could be described with respect to viscous forces alone; since inertial

forces due to the fluid were not required in the predictive equations they may be considered negligible. The dominance of viscous forces implies that the dimensions and surface area of structures have more significance for the dropping velocity than their configuration or aspect. The furcal amputation experiment provides a good example of this effect. If one furca is removed the resultant increase in terminal dropping velocity can be reproduced by removing the resistive force due to the loss of the effective surface of the furca from the relevant equations. There was no necessity to include analyses of the change in configuration. This situation is very different from that found in inertia dominated systems. For example removal of a flight from a dart or arrow would cause considerable changes in the dynamical properties of these missiles, their dynamic stability being primarily dependent on their conformation.

The limited effect of conformational changes in viscous dominated situations is also illustrated by examining the effect of changing the angle between the furcae and the direction of movement of the cercaria. In Appendix 4 equations were presented which allowed the resistance due to the furcae to be determined. By substituting in these equations it is possible to estimate the resistance with different furcal angles. With furcae normal to the direction of dropping the viscous resistance is 2714 $\eta u N$, while with furcae parallel to the direction of dropping the force is 1898 $\eta u N$. Clearly the smaller the angle the less resistance is created, but even with the furcae parallel to the direction of movement the viscous drag created is of considerable magnitude.

This result is markedly different to that expected if inertial forces played a significant role. For example, consider a flat plate moving through a fluid. If inertial forces dominated then the resistance to movement of the plate with its broad surface normal to the direction of movement would be very much greater than if the plate were moved edge-on. If viscous forces dominated the resistance would be appreciable and similar in both situations.

The angle between the furcae in dropping cercariae of T. patialense is approximately 120°, or 60° with respect to the direction of dropping. The inter-furcal angle is rigidly maintained in this and many other species, indeed the constancy of dropping configuration within a species is such that it has been suggested as a useful diagnostic feature (Blair, 1977). In most species studied the angle between the furcae is obtuse and approximately 120° (Cort and Brooks, 1928; Cort and Talbot, 1936; Wesenberg-Lund, 1934; Donges, 1964; Blair, 1977). There are some notable exceptions, in Apharyngostrigea pipientis the angle is 60° while the aptly named Cercaria anchoroides resembles an inverted anchor due to its furcae being spread in excess of 180° (Olivier, 1940; Wesenberg-Lund, 1934). It is suggested that the 120° angle is a compromise imposed on the cercariae by a combination of the demands of the swimming mode and tail structure, the actual angle being of little significance to the rate of dropping of the cercaria. This relationship is discussed below.

12.4.2 Hydrodynamic aspects of swimming behaviour

It appears that although the dropping mode of T. patialense cercariae is explicable in terms of viscous forces alone swimming involves a much more complex situation with both inertial and

viscous forces playing significant roles. This relationship can be deduced from the fact that the Reynolds Number approaches unity.

The Reynold Number in respect of aquatic motion indicates the ratio of viscous forces to inertial forces determining the characteristics of the motion. A Reynolds Number of one indicates that inertial and viscous forces are equally important, a value less than one indicates that viscous forces are dominant and more than one indicates that inertial forces predominate. In practice the Reynolds Number has to be very small or very large for either inertial or viscous forces respectively to be entirely ignored. A flagellate protozoan or a spermatazoan may have a Reynolds Number as low as 10^{-3}, while large fish and cetaceans swimming normally have values as high as 10^{4}-10^{8} (Wu, 1978). Values around unity are rare but have been recorded for the undulant swimming motion of some free-living nematodes (Lighthill, 1951).

Reynolds Numbers do not appear to have been previously determined for swimming cercariae. From the data of Nuttman (1975) on the swimming motion of Schistosoma mansoni cercariae it is possible to estimate the furcal tip velocity (17 mm sec^{-1}) and furcal width (20μm) and hence obtain a Reynolds Number of 0.28. This compares with a Reynolds Number of 2 for swimming T. patialense cercariae. It would appear, therefore, that although these two cercariae differ markedly in size and swimming velocity, the Reynolds Number approaches unity in both cases and hence inertial and viscous forces must be considered together in any discussion of their swimming behaviour. Simultaneous calculation of inertial and viscous effects is extremely difficult, for which reason hydrodynamicists have largely avoided consideration of problems in

this boundary zone of unitary Reynolds Numbers. This discussion will, therefore, confine itself to considering the forces involved in cercarial swimming without quantification.

The resistance to aquatic movement due to inertial forces is determined by such characteristics as angle of attack and aspect ratio of the moving body. This particularly applies to propulsive components, in the present considerations the furcae. During the recovery stroke the flattened furcae are curled and twisted to present a minimal surface area to the direction of movement, in effect presenting a narrow edge rather than a flat surface. During the effective stroke the flat surface is presented to increase the surface area and so increase the inertial forces during the supposed propulsive stroke. Both the reflexion of the furcal tip during the effective stroke and the increased angle between tail stem and furca suggest that the furca is subject to greater forces during the effective stroke than the recovery stroke.

Twisting and curling of furcae during swimming have been recorded from the cercariae of Posthodiplostomum cuticola and Diplostomum spathaceum (Donges, 1964; Haas, 1974). In Schistosoma mansoni cercariae, however, the furcae remain straight throughout (Graefe et al., 1967; Nuttman, 1975). These dissimilar results may be a reflection of the differential importance of inertial forces to these different species. Certainly S. mansoni has a lower Reynolds Number than T. patialense suggesting viscous forces are marginally more significant. Viscous forces depend on the effective surface area of the propulsive structure and not on the area presented to the direction of movement and hence conformational changes would be irrelevant.

In this investigation it was shown that the furcae of T. patialense move through a restricted arc of 0–120° relative to the path of the organism. That is, each furca reaches a maximum angular displacement in a lateral position of 120°, while when the furca is most closely approximated to the path of the organism it is parallel to the path and points straight forward. In simple terms the furca does not cross the line of motion of the cercaria. This constrained arc might be expected to avoid retarding forces since if the furca did cross the line of motion this would produce a force tending to act in the opposite direction to the propulsive forces.

From the data of Nuttman (1975) on the swimming motion of Schistosoma mansoni it is possible to determine the swept arc of the furcae in a similar manner. The furcae of S. mansoni describe a greater arc and do cross the path of movement. However, the angle formed is only 7.5° and would produce minimal retardation.

The spread configuration of the furcae of T. patialense remained remarkably constant during swimming despite the considerable forces acting against them. This postural rigidity is also described for Apharyngostrigea pipientis (Olivier, 1940), Neodiplostomum intermedium (Pearson, 1961), Posthodiplostomum cuticola (Donges, 1964), Schistosoma mansoni (Graefe et al., 1967), and Diplostomum spathaceum (Haas, 1974). The mechanism maintaining the configuration is obscure.

The "extensor" muscles in the furcae of N. intermedium and the similarly situated "cruciform" muscles of T. patialense seem inadequate to this role (Pearson, 1961; Whitfield et al., 1975). Pearson (1961) suggests that contraction of the longitudinal and

circular tail stem muscles causes an increase in turgor pressure maintaining the rigidity of the furcae. Presumably the furcal extensor muscles could then act for fine control of furcal orientation.

The implications of this hypothesis have significance for other aspects of cercarial activity. The furcae are closed together during attachment to the piscine host. This configuration is reversible, detached cercariae being capable of spreading the furcae and swimming and dropping normally. Possibly this phenomenon occurs due to loss of turgor when the tail stem muscles relax. It is suggested that there are essentially two possible configurations for the furcae: when tail stem muscles contract the furcae are spread, when the muscles relax the furcae are adpressed, any intermediate position being less stable than the two extremes. If this is the case then the spreading of furcae during swimming and dropping is readily explained. Adpressed furcae present a reduced surface area, the closely apposed surfaces creating negligible viscous drag, hence the furcae are spread during dropping to maximise drag. As explained previously the spread angle is relatively unimportant to this function. The interfurcal angle, however, is crucial to efficient and stable swimming since it determines the arc of movement of the furcae. Hence the angle between the furcae is a function of its value in the swimming mode and is only incidentally adopted in the dropping mode. Determination of the general applicability of this relationship would require comparison of inter-furcal angles during swimming and dropping for other species to determine whether they are the same for both modes as they are in T. patialense and Schistosoma mansoni.

The reflexion of the body region of T. patialense cercariae is presumably a consequence of the hydrodynamic forces involved in locomotion. Without knowledge of the streamlines of fluid around the reflexed body region no firm conclusions may be drawn as to its properties. It is probable, however, that the extended body could not be maintained in a constant configuration and would effectively act like a flat plate of continually altering angle relative to the movement of the cercaria. Such a structure would be fundamentally destabilising in both viscous and inertial terms, and would therefore be undesirable.

The reflexed body region tended to oscillate or "yaw" about the path of movement of the cercaria in sympathy with tail stem oscillations. As described in Section 12.3 these movements coincide with extension of one or other arm process depending on the direction of oscillation. Whitfield et al. (1977) tentatively suggested that the arm processes were passively extended as a consequence of fluid flow. This conclusion was based on a misinterpretation of the phase relationships of extension: due to the analysis of individual photographs rather than a cinematographic sequence the arm processes were assumed to extend in exactly reverse sequence to that described here. The present results make passive extension improbable and suggests that the arm processes are actively extended and retracted. They could then function to create viscous and inertial resistance, retarding the rate of reflexed body region angular rotation and so reduce the arc of oscillation. Such a constrained arc would be desirable since with the tail stem and furcae producing the main propulsive drive the reflexed body region should remain as stable as possible.

Stable propulsion is a problem with which all cercariae must contend. Furcocercous cercariae produce a propulsive stroke on either side of the path of movement of the cercaria so that the forces resolve themselves into a single component. Symmetrical propulsive thrusts are therefore achieved by having the right and left furcae separately producing propulsive force. With monocercous cercariae the problems are much greater since a single propulsive organ must produce a symmetrical force. This problem is apparently solved in different ways by different species. The swimming cycle of Himasthla secunda cercariae contrives to produce two effective strokes, one either side of the direction of movement of the cercaria, during a single cycle (Chapman and Wilson, 1973). In Cryptocotyle lingua the cercaria moves body foremost while continually reversing wave forms move down the tail stem in the opposite direction to the movement of the organism (Chapman and Wilson, 1973). The cercaria of Parochis acanthus apparently involves the body region in producing propulsive thrust, the tail and body region performing separate effective strokes which become resolved unidirectionally (Rees, 1971). These three swimming techniques are extremely complex when compared with the simple lateral lashing of the tail of furcocercariae.

All the components of swimming T. patialense cercariae oscillated at approximately 30 Hz. This suggests a single motor system is in operation for which the most likely candidate is the tail stem with its longitudinal striated muscles. Muscles of this type have been recorded within the tail stems of several species of cercariae (Vickers, 1940; Olivier, 1940; Pearson, 1956 and 1961; Chapman, 1973; Rees, 1975 and 1977). These muscles seem the most

probable drive system for two reasons. Firstly, their position is compatible with the production of bending moments within the tail stem, all recorded swimming activities involving flexure of the tail stem.. Secondly, they are the only striated muscles present in cercariae and striated muscle is much more likely to achieve the rapid phasic contractions required. .In vertebrates the z-discs of striated muscle are said to coordinate the movement of myofilaments within the myofibres during rapid contraction (Franzini-Armstrong and Porter, 1964). A similar structural coordination of muscle elements would be an expected requirement of rapidly contracting cercarial tail muscles and these, therefore, would also be expected to be striated (Lumsden and Foor, 1968).

The requirement for rapid contraction appears to vary somewhat between furcocercous and monocercous cercariae. The tail of T. patialense beats at 30 Hz at 24°C, and therefore requires sixty alternate contractions per second. The tail of Schistosoma mansoni beats at 22.1 Hz (25-30°C), approximately 44 alternate contractions per second (Graefe et al., 1967). Monocercous cercariae, however, appear to utilise much slower rates of tail beat: Parorchis acanthus 2.91 Hz (22°C), Himasthla secunda 4 Hz (5°C) and Crypotcotyle lingua 5.33 Hz (5°C) (Rees, 1971; Chapman and Wilson, 1973). Whether this is a biologically significant difference, or a consequence of the species selected and temperatures employed, can only be confirmed by results from a wider range of species.

The swimming behaviour of cercariae is clearly a complex activity in which many factors play a significant role. The velocity of swimming, however, is a parameter that resolves these interacting components into a single comparative value. Before

comparing the swimming velocities of different species, however, a note of caution must be introduced. The mechanisms achieving propulsion are fundamentally dependent on physico-chemical processes and hence exhibit temperature dependency. The swimming velocity of Schistosoma mansoni cercariae exhibits a linear relationship to temperature over the range 15-40°C, so that at 20°C the velocity is 0.7 mm sec^{-1} while at 30°C it is 1.4 mm sec^{-1} (Valle, Pellegrino and Gazzinelli, 1974). Unfortunately, in the majority of cases where swimming velocity is quoted the temperature is not recorded and, therefore, there must be some reservations as to their comparability.

Table 12.3 shows the swimming velocities of furcocercous and monocercous cercariae. The species in each group are shown in descending order of magnitude. From these few results it would appear that swimming velocity of furcocercariae in absolute terms and relative to body length is directly proportional to cercarial size. Until the hydrodynamic factors involved in furcocercarial swimming are better understood the reasons for this relationsip must remain obscure. No such relationship is apparent in the monocercous group whose swimming velocity, however expressed, shows considerable variation between species. This variability may be a consequence of the hydrodynamic efficiency achieved by the widely differing swimming techniques. In overall terms, however, it would appear that furcocercous cercariae are faster swimmers than monocercous cercariae.

This investigation has, hopefully, indicated that quantitative analyses of cercarial locomotion can lead to greater understanding of the fundamental processes involved in this stage of the digenean

TABLE 12.3

Relationship between cercarial swimming velocity and cercarial size

CERCARIAL SPECIES - IN DESCENDING ORDER OF SIZE FOR EACH GROUP	SWIMMING VELOCITY ABSOLUTE ($mm\ sec^{-1}$)	RELATIVE (body lengths/sec)	SOURCE
FURCOCERCOUS:			
Transversotrema patialense	25.9	32	(1)
Posthodiplostomum cuticola	10.0	20	(2)
Diplostomum spathaceum	3.7	10	(3)
Schistosoma mansoni	1.4	3	(4)
MONOCERCOUS:			
Parorchis acanthus	0.017	.009	(5)
Echinostoma sp.	4.0	3.81	(6,7)
Cercaria helvetica XXII	2.22	2.47	(6,7)
Cercaria helvetica XXXIII	1.54	2.57	(6,7)
Cercaria hypoderai conoidei	1.11	2.22	(6,7)
Echinoparyphium sp.	2.5	10	(8)

Calculated from the results of:

(1) Whitfield, Anderson and Bundy, 1977;

(2) Donges, 1964;

(3) Haas, 1974;

(4) Graefe et al., 1967;

(5) Rees, 1971;

(6) Dubois, 1929;

(7) Dawes, 1946;

(8) Graefe and Burkert, 1972

life cycle. It has certainly shown that the hydrodynamic principles involved are not trivial and perhaps require more complementary elucidation of the biological processes involved. As Professor T.Y. Wu stated in his introduction to the 1977 Symposium on "Scale Effects in Animal Locomotion":

"we can actually make a better estimate of the drag of a fish from biological measurements than from direct flow measurements, because the latter is formidably hard".

Section 13:

General Discussion

13. General Discussion

The investigations described in this thesis have examined aspects of the life cycle of Transversotrema patialense from the development of the egg, through the multiplicative intramolluscan stages, to the attachment of cercariae to the definitive host. The various topics considered were treated separately within their relevant sections, the significance of each aspect being discussed both specifically and in relation to its broader implications for digenean biology. These investigations, however, were intended not only to consider isolated aspects of transversotrematid biology but also to improve comprehension of interrelated factors of the life cycle.

The cercarial/adult generation of T. patialense has attracted experimental attention due to the simplicity of maintaining the host-parasite system in the laboratory and the practical accessibility of these stages. In consequence cercarial survival, behaviour and infection dynamics have been described in quantitative detail (Anderson and Whitfield, 1975; Whitfield et al., 1975 and 1977) and adult survival and fecundity has received similar attention (Whitfield et al., 1975; Anderson, 1976; Anderson et al., 1977; Mills, 1977). The accessibility of these stages was utilized in the present investigations to provide extensive quantitative information on the locomotion of cercariae and tegumental spine development during the cercarial/adult generation. An understanding of cercarial and adult biology is a necessary component of understanding the whole life cycle, but however thorough the investigations they cannot alone provide an adequate understanding of the whole system. The cercarial/adult generation does not exist in isolation but is

an integral part of the total life cycle.

The main aim of this thesis, therefore, was to provide information on the less accessible, and consequently less understood, remaining stages of the life cycle, that is the egg, miracidium and intramolluscan larvae. Their ultrastructure, developmental biology, reproductive biology and behaviour were, therefore, examined.

The results of these investigations were intended either to contribute directly to comprehension of the population processes of these stages or equally importantly to define experimental techniques which would allow the design of specific experiments to elucidate the population parameters.

Previous studies have shown that at 25°C the cercariae live for approximately two days (Anderson and Whitfield, 1975) and the adults for 10 weeks (Anderson et al., 1977). The present investigations show that at the same temperature eggs develop in three weeks, miracidia survive for 8h. and intramolluscan development to first release of cercariae takes approximately 16 weeks. These results, therefore, provide the additional information necessary to describe the developmental period of all segments of the life cycle. Comprehensive information of this type has been obtained for few digeneans and yet the developmental period may be of considerable importance in understanding their population dynamics. In particular Anderson (1978) has demonstrated theoretically that parasite developmental time delays may significantly affect the extent to which parasites regulate their host populations.

In describing egg development perhaps the most novel finding was the existence of a circadian rhythm of egg hatching. This appears to be the first quantitative record of cyclical egg hatching in digeneans. This result may have considerable significance for the understanding of the transmission of infection since it could materially increase the proportion of successful miracidial/ snail contacts by constraining miracidial release to the period when such contacts were most probable. This postulated enhanced infectivity rate per miracidium could have the effect of offsetting the demonstrated low egg (Anderson et al., 1978) and cercarial (Mills, 1977) output of T. patialense. Design of quantitative experiments to analyse the consequent temporal relationships of miracidial population infectivity would now be relatively straightforward since techniques for egg culture, miracidial hatching and identification of intramolluscan sporocysts have all been described and quantitative data made available on egg development and miracidial mortality rates.

As well as temporal effects,analyses of miracidial infectivity would also incorporate such exogenous influences as temperature and illumination. The present investigations could contribute materially to the design of such experiments, particularly in relation to the demonstrated significance of temperature and light for the rate of miracidial morphogenesis.

The investigations presented here have also demonstrated the complexity of intramolluscan development and indicated the difficulty of isolating components of the population processes during this segment of the life cycle. Despite the establishment of a comprehensive data base the present investigations did not

reveal the rate parameters essential for describing the population dynamics of the intramolluscan larval stages. This analysis will hopefully, however, provide a useful basis for further work. In particular the description of morphological differentiation during cercarial development and the records of redial and cercarial morphometrics during the development of infection should facilitate the accurate identification of intramolluscan larval developmental states. This would be particularly useful in determining the rate of development of transplanted larvae. Transplantation of individual immature rediae and cercariae to uninfected snails and subsequent examination at known time intervals could be utilized to assess the size and degree of differentiation of larvae and hence to determine their rates of development. In a similar manner parent rediae could be transplanted and their progeny assessed over a known period to determine birth rates.

Experimental analyses of this type would establish a unique level of understanding of a digenean life cycle. The demonstrated manipulability of the system and the established quantitative descriptions of the intramolluscan stages of T. patialense make such an approach feasible.

It may be concluded that the investigations presented here have made a significant contribution to understanding of the biology of T. patialense. With the exception of the sporocyst, all stages in the life cycle have been described at the ultrastructural level. Experimental techniques have been established for obtaining and maintaining all stages of the life cycle and these techniques now have proven reliability in obtaining repeatable quantitative data on all these stages. T. patialense has been described as

an ideal model system for the study of digenean biology (Whitfield et al., 1975) because of its inexpensive, hardy and diminutive hosts and ectoparasitic habit. With the present contribution it is hoped that understanding of the disparate parts of the life cycle will soon be complemented by comprehension of the dynamics of the life cycle as a whole.

REFERENCES

ANANTARAMAN, M. 1948. Observations on Cercaria patialensis Soparkar, 1924, and its relationships

Ind. J. Helm., 1: 11-12.

ANDERSEN, K. and HALUORSEN, O. 1978. Egg size and form as taxonomic criteria in Diphyllobothrium (Cestoda, Pseudophyllidea).

Parasitology, 76: 229-240.

ANDERSON, R.M. 1976. Dynamic aspects of parasite population ecology. In: "Ecological aspects of Parasitology". Chapt. 21. Ed.: C.R. Kennedy.

North Holland Pub. Co., Amsterdam.

ANDERSON, R.M. 1978. Population dynamics of snail infection by miracidia.

Parasitology, 77: 201-224.

ANDERSON, R.M. and LETHBRIDGE, R.C. 1975. An experimental study of the survival characteristics, activity and energy reserves of the hexacanths of Hymenolepis diminuta.

Parasitology, 71: 137-151.

ANDERSON, R.M. and WHITFIELD, P.J. 1975. Survival characteristics of the free-living cercarial population of the ectoparasitic digenean Transversotrema patialense (Soparkar, 1924).

Parasitology, 70: 295-310.

ANDERSON, R.M., WHITFIELD, P.J. and MILLS, C.A. 1977. An experimental study of the population dynamics of an ectoparasitic digenean Transversotrema patialense: the cercarial and adult stages.

J. Anim. Ecol., 46: 555-580.

ANDREWARTHA, H.G. 1952. Diapause in relation to the ecology of insects.

Biol. Rev., 27: 50-107.

ANGEL, L.M. 1969. Prototransversotrema steeri gen. nov., sp. nov. (Digenea: Transversotrematidae) from a South Australian fish. Parasitology, 59: 719-724.

AXMANN, M.C. 1947. Morphological studies on glycogen deposition in schistosomes and other flukes. J. Morph., 80: 321-334.

BACHA, W.J. 1966. Viable egg production in Zygocotyle lunata following mono-metacercarial infections. J. Parasit., 52: 1216-1217.

BARRETT, J. 1968. The effect of temperature on the development and survival of the infective larvae of Strongyloides ratti Sandground, 1925. Parasitology, 58: 641-651.

BASCH, P.F. and DiCONZA, J.J. 1974. The miracidium-sporocyst transition in Schistosoma mansoni: surface changes in vitro with ultrastructural correlation. J. Parasit., 60: 935-941.

BEAVER, P.C. 1937. Experimental studies on Echinostoma revoltum (Froelich), a fluke from birds and mammals. ILL. Biol. Monog., 15: 1-96.

BECKER, W. 1973. Aktivierung und Inaktivierung der Miracidien von Schistosoma mansoni innerhalb der Eischale. Z. ParasitKde, 42: 235-242.

BEESTON, D.C. 1977. The locomotor activity rhythm of a tropical freshwater prosobranch mollusc Melanoides tuberculata (Muller). 184th Conference of the Society for Experimental Biology. Abstract.

BELTON, C.M. and HARRIS, P.J. 1967. Fine structure of the cuticle of the cercaria of Acanthatrium oregonense (Macy). J. Parasit., 53: 715-724.

BENEX, J. and DESCHIENS, R. 1963. Incidence des facteurs extremes sur la longevite et la vitalite des miracidiums de Schistosoma mansoni Bull. Soc. Path. exot., 56: 987.

BENNETT, C.E. 197a. Fasciola hepatica - development of caecal epithelium during migration in the mouse. Expl Parasit., 37: 426-441.

BENNETT, C.E. 1975b. Surface features, sensory structures, and movement of the newly excysted juvenile Fasciola hepatica L. J. Parasit., 61: 886-891.

BENNETT, C.E. 1975c. Scanning electron microscopy of Fasciola hepatica L. during growth and maturation in the mouse. J. Parasit., 61: 892-898.

BENNETT, C.E. and THREADGOLD, L.T. 1973. Electron microscope studies of Fasciola hepatica. XIII. Fine structure of newly excysted juvenile. Exptl Parasit., 34: 85-99.

BENNETT, C.E. and THREADGOLD, L.T. 1975. Fasciola hepatica: Development of tegument during migration in the mouse. Exptl Parasit., 38: 38-55.

BERRY, A.J. and KADRI, A. 1974. Reproduction in the Malayan freshwater cerithiacean gastropod Melanoides tuberculata. J. Zool., Lond., 172, 369-381.

BEVERIDGE, I. and RICKARD, M.D. 1976. The development of the rostellar hooks of Taenia pisiformis. Int. J. Parasit., 6, 55-59.

BIBBY, M.C. and REES, F.G. 1971. The ultrastructure of the epidermis and associated structures in the metacercaria, cercaria and sporocysts of Diplostomum phoxini (Faust, 1918).

Z. ParasitKde., 37: 169-186.

BILQEES, F.M. and FREEMAN, R.S. 1969. Histogenesis of the rostellum of Taenia crassiceps (Zeder, 1880) (Cestoda) with special reference to hook development.

Can. J. Zool., 47: 251-261.

BILS, R.F. and MARTIN, W.E. 1966. Fine structure and development of the trematode integument.

Trans. Am. microsc. Soc., 85: 78-88.

BISHOP, A.C. 1967. An outline of crystal morphology.

Hutchinson, Lond.

BLAIR, D. 1977. A key to cercariae of British strigeoids (Digenea) for which the life-cycles are known, and notes on the characters used.

J. Helminth., 51: 155-166.

BLANKESPOOR, H.D. and VAN DER SCHALIE, H. 1976. Attachment and penetration of miracidia observed by scanning electron microscopy.

Science, 191: 291-293.

BOGITSH, B.J. 1968. Cytochemical and ultrastructural observations on the tegument of the trematode Megalodisus temporatus.

Trans. Am. microsc. Soc., 87: 477-486.

BOGITSH, B.J. 1972. Additional cytochemical and morphological observations on the tegument of Haematoloechus medioplexus.

Trans. Am. microsc. Soc., 91: 47-55.

BORAY, J.C. 1969. Experimental fascioliasis in Australia.

Adv. Parasit., 7: 96-211.

BRACHET, J. 1968. Chemical embryology.

Hafner, N.Y.

BRESCIANI, J. and KOIE, M. 1970. On the ultrastructure of the epidermis of the adult female of Kronborgia amphipodicola Christensen and Kanneworff, 1964 (Turbellaria, Neorhabdocoela).

Ophelia, 8: 209-230.

BRETT, J.R. 1970. Temperature and fish. IN: "Marine Biology". Vol. 1. Ed. O. KINNE.

Wiley Interscience, Lond.

BRIEN, P. 1954. Deux formes larvaires de Trematodés congolais: La parthenogonie - le cycle des cellules germinales.

Ann. Mus. Congo Tervuren, 4, ZOOL, 1, 153-162.

BROOKER, B.E. 1972. The sense organs of trematode miracidia. In: "Behavioural aspects of parasite transmission". Eds. E.U. Canning and C.A. Wright.

Suppl. 1. Zool. J. Linn. Soc., 51: 171-181.

BUERGER, M.J. 1963. Elementary crystallography.

J. Wiley and Sons. Inc., N.Y.

BULLARD, R.T. 1964. Animals in aquatic environments: Annelids and Molluscs. In: "Handbook of Physiology". Chapt 42. Sect. 4. Ed. Dill, D.B.

Am Physiol. Soc., Washington D.C.

BURTON, P.R. 1964. The ultrastructure of the Integument of the frog lung-fluke, Haematoloechus medioplexus (Trematoda: Plagiorchiidae).

J. Morph., 115: 305-318.

BURTON, P.R. 1966. The ultrastructure of the integument of the frog bladder fluke, Gorgoderina sp.

J. Parasit., 52: 926-934.

CABLE, R.M. 1971. Parthenogenesis in parasitic helminths.
Am. Zool., 11: 267-272.

CALENTINE, R.L. AND ULMER, M.J. 1961. Khawia iowensis n. sp. (Cestoda: Caryophylleidae) from Cyprinus carpio L. in Iowa.
J. Parasit., 47: 795-805.

CAMPBELL, W.C. 1961. Notes on the egg and miracidium of Fascioloides magna (Trematoda).
Trans. Am. microsc. Soc., 80: 308-319.

CARDELL, R.R. 1962. Observations on the ultrastructure of the body of the cercaria of Himasthla quissetensis (Miller and Northup, 1926).
Trans. Am. microsc. Soc., 81: 124-131.

CHAPMAN, H.D. 1973. The functional organisation and fine structure of the tail musculature of the cercariae of Cryptocotyle lingua and Himasthla secunda.
Parasitology, 66: 487-497.

CHAPMAN, H.D. 1975. The behaviour of the cercaria of Cryptocotyle lingua.
Z. ParasitKde, 44: 211-226.

CHAPMAN, H.D. and WILSON, R.A. 1970. The distribution and fine structure of the integumentary papillae of the cercaria of Himasthla secunda (Nicoll).
Parasitology, 61: 219-227.

CHAPMAN, H.D. and WILSON, R.A. 1973. The propulsion of the cercariae of Himasthla secunda (Nicoll) and Cryptocotyle lingua.
Parasitology, 67: 1-15.

CHENG, T.C. 1963. The effects of Echinoparyphium larvae on the structure of and glycogen deposition in the hepatopancreas of Helisoma trivolis and glycogenesis in the parasite larvae.
Malacologia, 1: 291-303.

CHENG, T.C. and SNYDER, R.W. 1962. Studies on host-parasite relationships between larval trematodes and their host. I. A review. II. The utilization of the host's glycogen by the intramolluscan larvae of Glypthelmins pennsylvaniensis Cheng, and associated phenomena.

Trans. Am. microsc. Soc., 81: 209-228.

CHERNIN, E. and DUNAVAN, C.A. 1962. The influence of host-parasite dispersion upon the capacity of Schistosoma mansoni miracidia to infect Australorbis glabratus.

Am. J. trop. Med. Hyg., 11: 455-471.

CHRISTENSEN, N.O., NANSEN, P. and FRANDSEN, F. 1976. The influence of temperature on the infectivity of Fasciola hepatica miracidia to Lymnea truncatula.

J. Parasit., 62: 698-701.

CLARK, W.C. 1974. Interpretation of the life history pattern in the digenea.

Int. J. Parasit., 4: 115-123.

CLEGG, J.A. 1965. In vitro cultivation of Schistosoma mansoni.

Exptl. Parasit., 16: 133-147.

COCHRAN, W.G. 1954. Some methods for strengthening the common Chi-squared Tests.

Biometrics, 10: 417-451.

CORT, W.W., AMEEL, D.J. and VAN DER WOUDE, A. 1954. Germinal development in the sporocysts and rediae of the digenetic trematodes.

Exptl. Parasit., 3: 185-216.

CORT, W.W. and BROOKS, S.P. 1928. Studies on the holostome cercariae from Douglas Lake, Michigan.

Trans. Am. microsc. Soc., 47: 179-221.

CORT, W.W. and TALBOT, S.B. 1936. Studies on schistosome dermititis. Observations on the behaviour of the dermatitis producing schistosome cercariae.

Am. J. Hyg., 23: 385-396.

CREWTHER, W.G., FRASER, R.D.B., LENNOX, F.G. and LINDLEY, H. 1965. The chemistry of keratins.

Adv. Protein Chem., 20: 191-346.

CREWTHER, W.G. and HARRAP, B.S. 1965. Helix-rich fractions from the low sulphur proteins of wool.

Nature, 207: 295.

CRISP, D.J. and WILLIAMS, R. 1971. Direct measurement of pore-size distribution on artifical and natural deposits, and prediction of pore space accessible to interstitial organisms.

Int. J. Life in Oceans and Coastal Waters, 10: 214-226.

CROZIER, W.J. 1924. On biological oxidations as a function of temperature.

J. gen. Physiol. 7: 189-216.

CRUSZ, H. 1947. The early development of the rostellum of Cysticercus fasciolaris Rud., and the chemical nature of its hooks.

J. Parasit., 33: 87-98.

CRUSZ, H. 1956. The progenetic trematode Cercaria patialensis Soparkar, in Ceylon.

J. Parasit., 42: 245.

CRUSZ, H., RATNAYAKE, W.E. and SATHANANTHAN, A.H. 1964. Observations on the structure and life-cycle of the digenetic fish trematode Transversotrema patialense (Soparkar).

Ceylon J. Sci. (Bio. Sci.), 5: 8-17.

CRUSZ, H. and SATHANANTHAN, A.H. 1960. Metacercaria of Transversotrema patialensis in the freshwater fish Macropodus cupanus.

J. Parasit., 46: 613.

DAVIDSON, J. 1944. On the relationship between temperature and rate of development of insects at constant temperatures.

J. Anim. Ecol., 13: 26-38.

DAVIES, C. 1976. Development and in vitro culture of some digenea.

Ph.D. Thesis, 2 vols. University of Lond.

DAVIES, R.G. 1971. Computer programming in quantitative biology.

Academic Press.

DAVIS, D.A., BOGITSH, B.J. and NUNNALLY, D.A. 1968. Cytochemical and biochemical observations on the digestive tracts of digenetic trematodes. I. Ultrastructure of Haematoloechus medioplexus gut.

Exptl. Parasit. 22: 98-106.

DAWES, B. 1946. The Trematoda.

Cambridge Univ. Press.

DeWITT, W.B. 1955. Influence of temperature on the penetration of the snail host by Schistosoma mansoni miracidia.

Exptl. Parasit., 4: 271-276.

DIKE, S.C. 1969. Acid phosphatase activity and ferritin incorporation in the ceca of digenetic trematodes.

J. Parasit., 55: 111-23.

DINNIK, J.A. and DINNIK, N.N. 1954. The life cycle of Paramphistomum microbothrium Fischoeder, 1901 (Trematoda, Paramphistomatidae).

Parasitology, 44: 285-299.

DINNIK, J.A. and DINNIK, N.N. 1956. Observations on the succession of redial generations of Fasciola gigantica Cobbold in a snail host.

Z. Tropenmed. Parasit., 7: 397-419.

DINNIK, J.A. and DINNIK, N.N. 1963. Effect of the seasonal variations of temperature on the development of Fasciola gigantica in the snail host in the Kenya Highlands.

Bull. epizoot. Dis. Afr., 11: 197-207.

DINNIK, J.A. and DINNIK, N.N. 1964. The influence of temperature on the succession of redial and cercarial generations of Fasciola gigantica in a snail host.

Parasitology, 54: 65-69.

DISSAMARN, R., ARANYAKANANDA, P., SRIVORANATH, P., CHAI-ANAN, P., THIRAPAT, K. and CHITRAKORN, P. 1966. The life history of Paryphostomum sufrartyfex (Lane, 1915) Bhalerao, 1931.

J. Thai. Vet. Med. Ass., 17: 11-16.

DIXON, K.E. 1970. Absorption by developing cercariae of Cloacitrema narrabeenensis (Philophthalmidae).

J. Parasit., 56, supplement, 416-417.

DIXON, K.E. and MERCER, E.H. 1967. The formation of the cyst wall of the metacercaria of Fasciola hepatica L.

Z. Zellforsch. mikrosk. Anat., 77: 345-360.

DOBB, M.G. 1965. α-helix in fibrous proteins.

Nature, 207: 293.

DONGES, J. 1964. Der Lebenszyklus von Posthodiplostomum cuticola (V. Nordmann, 1832) Dubois, 1936 (Trematoda, Diplostomatidae).

Z. ParasitKde., 24: 169-248.

DONGES, J. 1973. Das miracidium von Isthmiophora melis (Schrank, 1788) (Echinostomatidae).

Z. ParasitKde., 41: 215-230.

DOREY, A.E. 1965. The organisation and replacement of the epidermis in acoelous turbellarians.

Q. Jl. microsc. Sci., 106: 147-172.

DUBOIS, G. 1929. Les cercaires de la region de Neuchatel.

Bull. Soc. neuchatel. Sci. nat., 53, N.S. 2, year 1928, 3-177.

DUKES, D.C. and DAVIDSON, L. 1968. Some factors affecting the output of schistosome ova in the urine.

Cent. Afr. J. Med., 14: 115-122.

DURIE, P.H. 1953. The paramphistomes (Trematoda) of Australian ruminants. II. The life history of Ceylonocotyle streptocoelium (Fischoeder) Nasmark and Paramphistomum ichikawai Fukui.

Aust. J. Zool., 1: 193-222.

DVORAK, J.A. 1969a. Hydatigera taeniaeformis: Strobilocerci hooks. 1. Collection and preparation; elemental, amino acid, and infrared spectrophotometric analyses.

Exptl. Parasit., 26: 111-121.

DVORAK, J.A. 1969b. Hydatigera taeniaeformis: Strobilocerci hooks. II. Solubility and structural homogeneity.

Exptl. Parasit., 26: 122-127.

DVORAK, J.A. 1969c. Hydatigera taeniaeformis: Strobilocerci hooks. III. Molecular weight and N-terminal amino acid determinations.

Exptl. Parasit., 26: 128-133.

ERASMUS, D.A. 1967. The host-parasite interface of Cyathocotyle bushiensis Khan, 1962 (Trematoda: Strigeoidea). II. Electron microscope studies of the tegument.

J. Parasit., 53: 703-714.

ERASMUS, D.A. 1970. The host-parasite interface of strigeoid trematodes. IX. A probe and transmission electron microscope study of the tegument of Diplostomum phoxini (Faust, 1918).

Parasitology, 61: 35-41.

ERASMUS, D.A. 1972. The biology of trematodes.

Edward Arnold, Univ. Press Belfast.

FILSHIE, B.K. and ROGERS, G.E. 1961. The fine structure of α-keratin.

J. molec. Biol., 3: 784-6.

FILSHIE, B.K. and ROGERS, G.E. 1962. Electron microscope studies of feather keratin.

J. Cell. Biol., 13: 1-12.

FRANZINI-ARMSTRONG, C. and PORTER, K. 1964. The Z-disc of skeletal muscle fibures.

Z. Zellforsch. mikrosk. Anat., 61: 661-672.

FRASER, H.J. 1935. Experimental study of the porosity and permeability of Clastic sediments.

J. Geol., 43: 910-1010.

FRASER, R.D.B., MACRAE, T.P. and ROGERS, G.E. 1962. Molecular organisation of α-keratin.

Nature, 193: 1052-1055.

FREEMAN, R.F.H. 1949. Notes on the morphology and life cycle of the genus Monoecocestus Beddard, 1914 (Cestoda: Anoplocephalidae) from the porcupine.

J. Parasit., 35: 605-612.

FRIED, B. 1962. Growth of Philophthalamus sp. (Trematoda) in the eyes of chicks.

J. Parasit., 48: 395-399.

FRY, F.E.J. 1947 Effects of the environment on animal activity.
Univ. Toronto Stud. Biol., 55, (Pub.
Ontario Fish. Res. Lab.), 68: 1-62.

FUJINO, T. and ISHII, Y. 1978. Comparative ultrastructural topography of the gut epithelium of the lung fluke Paragonimus (Trematoda: Troglotrematidae).
Int. J. Parasit. 8: 139-148.

GALLAGHER, I.H.C. 1964. Chemical composition of hooks isolated from Hydatid scolices.
Exptl. Parasit., 15: 110-117.

GIBSON, D.I. 1974. Aspects of the ultrastructure of the daughter-sporocyst and cercaria of Podocotyle staffordi Miller, 1941 (Digenea: Opecoelidae).
Norw. J. Zool., 22: 237-252.

GOLD, D. and GOLDBERG, M. 1976. Effect of light and temperature on hatching in Fasciola hepatica (Trematoda: Fasciolidae).
Israel J. Zool., 25: 178-185.

GONNERT, R. 1948. Die Struktur der Korperoberflache von Bilharzia mansoni (Sambon, 1907).
Z. Tropemed. Parasit., 1: 105-112.

GRAEFE, G. and BURKERT, D.G. 1972. Zur Lokomotionsmeckanik von Diplostomatiden - und Echinostomatiden - Cercarien (Trematoda).
Zool. Anz., 188: 366-369.

GRAEFE, G., HOHORST, W. and DRAGER, H. 1967. Forked tail of the cercaria of Schistosoma mansoni - a rowing device.
Nature, 215: 207-208.

GRAFTON, L.C. and FRASER, H.J. 1935. Systematic packing of spheres - with particular reference to porosity and permeability.
J. Geol., 43: 785-909.

GRAY, E.G. 1960. The fine structure of the insect ear.
Phil. Trans. R. Soc. B., 243: 75-94.

GUILFORD, H.G. 1961. Gametogenesis, egg-capsule formation, and early miracidial development in the digenetic trematode Halipegus eccentricus Thomas.
J. Parasit., 47: 757-764.

HAAS, W. 1974. Analyse der Invasionmechanismen der Cercarie von Diplostomum spathaceum. 1. Fixation und penetration.
Int. J. Parasit., 4: 311-319.

HAAS, W. 1976. Die Anheftung (Fixation) der Cercariae von Schistosoma mansoni.
Z. ParasitKde., 49: 63-72.

HALTON, D.W. 1967. Observations on the nutrition of digenetic trematodes.
Parasitology, 57: 639-660.

HALTON, D.W. and JENNINGS, J.B. 1965. Observations on the nutrition of monogenetic trematodes.
Biol. Bull., 129: 257-272.

HALTON, D.W. and MORRIS, G.P. 1969. Occurrence of cholinesterase and ciliated sensory structures in a fish gill-fluke Diclidophora merlangi (Trematoda: Monogenea).
Z. ParasitKde., 33: 21-30.

HANNA, R.E.B. and THREADGOLD, L.T. 1976. Fasciola hepatica: Stereological analysis of effects of certain metabolic inhibitors on synthesis of secretory bodies by the tegument of tissue slices.
Exptl. Parasit., 39: 106-114.

HARRIS, K.R., CHENG, T.C. and CALI, A. 1974. An electron microscope study of the tegument of the metacercaria and adult of Leucochloridiomorpha constantiae (Trematoda: Brachylaemidae). Parasitology, 68: 57-67.

HASTINGS, C. 1955. Approximations for digital computers. University Press, Princeton.

HILLIARD, D.K. 1960. Studies on the helminth fauna of Alaska. XXXVIII. The taxonomic significance of eggs and coracidia of some Diphyllobothriid cestodes. J. Parasit., 46: 703-716.

HOCKLEY, D.J. 1968. Small spines on the eggshell of Schistosoma. Parasitology, 58: 367-370.

HOCKLEY, D.J. 1970. An ultrastructural study of the cuticle of Schistosoma mansoni Sambon, 1907. Ph.D. Thesis, University of London.

HOCKLEY, D.J. 1972. Schistosoma mansoni: the development of the cercarial tegument. Parasitology, 64: 245-252.

HOCKLEY, D.J. 1973. Ultrastructure of the tegument of Schistosoma. Adv. Parasit., 11: 233-305.

HORSTMANN, H.J. 1962. Sauerstoffverbrauch und glykogengehalt der eier von Fasciola hepatica wahrend der entwicklung der miracidien. Z. ParasitKde., 21: 437-445.

HOWELLS, R.E., GERKEN, S.E., RAMACHO-PINTO, F.J., KAWAZOE, U., GAZZINELLI, G. and PELLEGRINO, J. 1975. Schistosoma mansoni: tail loss in relation to permeability changes during cercaria-schistosomulum transformation. Parasitology, 71: 9-18.

HOWELLS, R.E., RAMACHO-PINTO, F.J., GAZZINELLI, G., De OLIVERIA, C.C., FIGUEIREDO, E.A. and PELLEGRINO, J. 1974. Schistosoma mansoni: mechanism of cercarial tail loss and its significance to host penetration.

Exptl. Parasit., 36: 373-385.

HSU, H.F. and HSU, S.Y. 1958. On the size and shape of the eggs of the geographic strains of Schistosoma japonicum.

Am. J. trop. Med. Hyg., 7: 125-134.

HUIZINGA, H.W. 1973. Ribeiroia marini: pathogenesis and larval trematode antagonism in the snail, Biomphalaria glabrata.

Exptl. Parasit., 33: 350-364.

INGALLS, J.W., HUNTER, G.W., McMULLEN, D.B. and BAUMAN, P.M. 1949. The molluscan intermediate host and schistosomiasis japonica. 1. Observations on the conditions governing the hatching of the eggs of Schistosoma japonicum.

J. Parasit., 35: 147-151.

ISSEROFF, H. 1964. Fine structure of the eysepot in the miracidium of Philophthalmus megalurus (Cort, 1914).

J. Parasit., 50: 549-554.

ISSEROFF, H. and CABLE, R.M. 1968. Fine structure of photoreceptors in larval trematodes.

Z. Zellforsch. mikrosk. Anat., 86: 511-534.

JACOB, J. 1957. Cytological studies of Melaniidae (Mollusca) with special reference to parthenogenesis and polyploidy I. Oogenesis of the parthenogenetic species of Melanoides (Prosobranchia-Gastropoda).

Trans. R. Soc. Edinb., 63: 341-352.

JAMES, B.L. 1965. The effects of parasitism by larval digenea on the digestive gland of the intertidal prosobranch Littorina saxatilis (Oliv.) tenebrosa (Montagu).

Parasitology, 55: 93-115.

JAMES, B.L. and BOWERS, E.A. 1967. Reporoduction in the daughter sporocysts of Cercaria bucephalopsis haimeana (Lacaze-Duthiers, 1854) (Bucephalidae) and Cercaria dichotoma Lebour, 1911 (von Muller) (Gymnophallidae).

Parasitology, 57: 607-625.

JOHNSON, F.H., EYRING, H. and POLISSAR, M.J. 1954. The kinetic basis of molecular biology.

Wiley, N.Y.

KEARN, G.C. 1962. Breathing movements in Entobdella soleae (Trematoda: Monogenea) from the skin of the common sole.

J. mar. biol. Ass. U.K., 42: 93-104.

KEARN, G.C. 1963. Feeding in some monogenean skin parasites. Entobdella soleae on Solea solea and Acanthocotyle sp. on Raia clavata.

J. mar. biol. Ass. U.K., 43: 749-766.

KEARN, G.C. 1973. An endogenous circadian hatching rhythm in the monogenean skin parasite Entobdella soleae, and its relationship to the activity rhythm of the host (Solea solea).

Parasitology, 66: 101-122.

KEARN, G.C. 1974. Nocturnal hatching in the monogenean skin parasite Entobdella hippoglossi from the halibut, Hippoglossus hippoglossus.

Parasitology, 68: 161-172.

KENDALL, S.B. 1965. Relationships between the species of Fasciola and their molluscan hosts.

Adv. Parasit., 3: 59-98.

KHALIL, G.M. and CABLE, R.M. 1967. Germinal development in Philophthalmus megalurus (Cort, 1914) (Trematoda: Digenea).
Z. ParasitKde., 31: 211-231.

KINNE, O. 1964. Animals in aquatic environments: Crustaceans.
In: "Handbook of Physiology". Chapt. 41. Ed. D.B. Dill.
Am. Physiol. Soc., Washington, D.C.

KINNE, O. 1970. Temperature. In: "Marine Biology", Vol. 1.
Ed. O. Kinne.
Wiley Interscience, London.

KINNE, O. and KINNE, E.M. 1962. Rates of development in embryos of cyprinodont fish exposed to different temperature - salinity - oxygen combinations.
Can. J. Zool., 40: 231-253.

KINOTI, G.K. 1971. The attachment and penetration apparatus of the miracidium of Schistosoma.
J. Helm., 45: 229-235.

KIRAKINI, V.V. 1961. The epizootiology of fascioliasis in sheep in the Turman SSSR.
Conf. Nat. Focal. Occur. Dis. and Prob. In: Parasites of Kazakhstan and Central Asian Republics". 4th Alma-Ata, 1959, 3: 389-393. (In Russian).

KOIE, M. 1971. On the histochemistry and ultrastructure of the tegument and associated structures of the cercaria of Zoogonoides viviparus in the first intermediate host.
Ophelia, 9: 165-206.

KOIE, M. 1973a. The host-parasite interface and associated structures of the cercaria and adult Neophasis lageniformis (Lebour, 1910).
Ophelia, 12: 205-219.

KOIE, M. 1973b. The ultrastructure of the caecal epithelium of the intraredial cercaria of Neophasis lageniformis (Lebour, 1910) (Trematoda, Acanthocolpidae).

Z. Zellforsch. mikrosk. Anat., 139: 405-416.

KOIE, M. 1975. On the morphology and life history of Opechona bacillaris (Molin, 1859) Looss, 1907 (Trematoda, Lepocreadiidae).

Ophelia, 13: 63-86.

KOIE, M. 1976. On the morphology and life-history of Zoogonoides vivparus (Olsson, 1868) Odhner, 1902 (Trematoda, Zoogonidae).

Ophelia, 15: 1-14.

KOIE, M. 1977. Steroscan studies of cercariae, metacercariae and adults of Cryptocotyle lingua (Creplin, 1825) Fischoeder 1903 (Trematoda: Heterophyidae).

J. Parasit., 63: 835-839.

KOIE, M., CHRISTENSEN, N.O. and NANSEN, P. 1976. Sterescan studies of eggs, free-swimming and penetrating miracidia and early sporocysts of Fasciola hepatica.

Z. ParasitKde., 51: 79-90.

KOIE, M. and FRANDSEN, F. 1976. Stereoscan observations of the miracidium and early sporocysts of Schistosoma mansoni.

Z. ParasitKde., 50: 335-344.

KOMIYA, Y. 1966. Clonorchis and clonorchiasis.

Adv. Parasit., 4: 53-106.

KRULL, W.H. 1934. Notes on the hatchability and infectivity of refrigerated eggs of Fasciola hepatica L.

Proc. Iowa Acad. Sci., 41: 309.

KRULL, W.H. 1935. Studies on the life history of Helipegus occidentalis Stafford, 1905.

Am. Midl. Nat., 16: 129-143.

KRUPA, P.L. 1974. Ultrastructural topography of a trematode eggshell.
Exptl. Parasit., 35: 244-247.

KUMMEL, G. 1958. Terminalorgan der Protonephridien. Feinstruktur und Dentung der Funktion.
Z. Naturf., 13 B, 677-679.

KUMMEL, G. 1964. Die Feinstruktur der Terminalzellen (Cyrtocyten) an den Protonephridien der Priapuliden.
Z. Zellforsch. mikrosk. Anat., 62: 468-484.

KUNTZ, R.E., TULLOCH, G.S., DAVIDSON, D.L. and HUANG, T.C. 1976. Scanning electron microscopy of the integumental surfaces of Schistosoma haematobium.
J. Parasit., 62: 63-69.

KUNTZ, R.E., TULLOCH, G.S., HUANG, T.C. and DAVIDSON, D.L. 1977. Scanning electron microscopy of integumental surfaces of Schistosoma intercalatum.
J. Parasit., 63: 401-406.

KUSEL, J.R. 1970. Studies on the structure and hatching of the eggs of Schistosoma mansoni.
Parasitology, 60: 79-88.

LAL, M.B. and PREMVATI, L. 1955. Studies in histopathology - changes induced by a larval monostome in the digestive gland of the snail, Melanoides tuberculata (Muller).
Proc. Ind. Acad. Sci., 42: 293-299.

LAND, M.F. 1968. Functional aspects of the optical and retinal organisation of the mollusc eye.
Symp. Zool. Soc. Lond., 23: 75-96.

LANGE, F. and FORKER, L. 1956. Handbook of Chemistry. ED. 9.
Sandusky.

LEE, D.L. 1966. The structure and composition of the helminth cuticle.
Adv. Parasit., 4: 187-254.

LEE, D.L. 1972. The structure of the helminth cuticle.
Adv. Parasit., 10: 347-379.

LETHBRIDGE, R.C. 1976. The architecture of the eggshell of
Hymenolepis diminuta.
Int. J. Parasit., 6: 87-90.

LEUCKART, K.G.F.R. 1886. Die Parasiten des Menschen und die
von ihnen herruhrenden Krankheiten.
2nd. Ed., Leipzig.

LIE, K.J. 1965. Studies on Echinostomatidae (Trematoda) in
Malaya. IX. The mehlis gland complex in echinostomes.
J. Parasit., 51: 789-792.

LIGHTHILL, M.J. 1969. Hydromechanics of aquatic animal propulsion.
Ann. Rev. Fluid. Mech., 1: 413-447.

LUMSDEN, R.D. and FOOR, W.E. 1968. Electron microscopy of
schistosome cercarial muscle.
J. Parasit., 54: 780-794.

LYONS, K.M. 1969. Sense organs of monogenean skin parasites
ending in a typical cilium.
Parasitology, 59: 611-623.

LYONS, K.M. 1972. Sense organs of monogeneans. In: "Behavioural
aspects of parasite transmission". Ed. E.U. Canning and
C.A. Wright.
Suppl. 1. Zool. J. Linn. Soc., 51: 181-199.

LYONS, K.M. 1973. The epidermis and sense organs of the monogenea
and some related groups.
Adv. Parasit., 11: 193-232.

MacDONALD, S. 1975. Hatching rhythms in three species of Diclidophora (Monogenea) with observations on host behaviour. Parasitology, 71: 211-228.

MacINNIS, A.J. 1965. Responses of Schistosoma mansoni miracidia to chemical attractants. J. Parasit., 51: 731-746.

MADHAVI, R. 1966. Egg-shell in Paramphistomatidae. (Trematoda: Digenea). Experentia, 22: 93-94.

MADHAVI, R. 1968. Diplodiscus mehrai: chemical nature of eggshell. Exptl. Parasit., 23: 392-397.

MANTER, H.W. 1965. A mature ectoparasitic digenean (Transversotrema sp. nov.) beneath scales of fishes. J. Parasit. 51, Suppl. 59 (abst.)

MANTER, H.W. 1970. A new species of Transversotrema (Trematoda: Digenea) from marine fishes of Australia. J. Parasit., 56: 486-489.

MASON, P.R. and FRIPP, P.J. 1976. Analysis of the movements of Schistosoma mansoni miracidia using dark-ground photography. J. Parasit., 62: 721-727.

MATHIAS, P. 1925. Recherches experimentales sur le cycle evolutif de quelques trematodes. Bull. Biol., 49: 1-123.

MATOLTSY, A.G. 1962. Mechanism of keratinization. In: "Fundamentals of keratinization". Ed. E.O. Butcher and R.F. Sognnaes. Pub. 70. AAAS, Washington D.C.

MATRICON-GONDRAN, M. 1971. Etude ultrastructurale des recepteurs sensoriels tegumentaires de quelques Trematodes Digenetiques larvaires.

Z. ParasitKde., 35: 318-333.

MAY, R.M. and ANDERSON, R.M. 1978. Regulation and stability of host-parasite interactions. II Destabilising processes.

J. Anim. Ecol., 47: 249-268.

McARTHUR, C.P. and FEATHERSTONE, D.W. 1976. Suppression of egg production in Potamopyrgus antipodarum (Gastropoda: Hydrobiidae) by larval trematodes.

N.Z. J. Zool., 3: 35-38.

McLAREN, D.J. and HOCKLEY, D.J. 1976. Schistosoma mansoni: The occurrence of microvilli on the surface of the tegument during transformation from cercaria to schistosomulum.

Parasitology, 73: 169-187.

McVICAR, A.H. 1977. The bothridial hooks of Acanthobothrium quadripartitum Williams, 1968 (Cestoda: Tetraphyllidea): their growth and use in taxonomy.

Int. J. Parasit., 7: 439-442.

MERCER, E.H. and DIXON, K.E. 1967. The fine structure of the cystogenic cells of the cercaria of Fasciola hepatica L.

Z. Zellforsch. mikrosk. Anat., 77: 331-344.

MERCER, E.H., ROGERS, G.E., MUNGER, B.L. and ROTH, S.I. 1964. A suggested nomenclature for fine structural components of keratin and keratin-like products of cells.

Nature, 201: 367-368.

MEULEMAN, E.A. 1972. Host-parasite interrelationships between the freshwater pulmonate Biomphalaria pfeifferi and the trematode Schistosoma mansoni.

Neth. J. Zool., 22: 355-427.

MEULEMAN, E.A. and HOLZMANN, P.J. 1975. The development of the primitive epithelium and true tegument in the cercaria of Schistosoma mansoni.

Z. ParasitKde., 45: 307-318.

MEULEMAN, E.A., LYARUU, D.M., KHAN, M.A., HOLZMANN, P.J. and SMINIA, T. 1978. Ultrastructural changes in the body wall of Schistosoma mansoni during the transformation of the miracidium into the mother sporocyst in the snail host Biomphalaria pfeifferi.

Z. ParasitKde., 56: 227-242.

MILLS, C.A. 1977. An experimental study of the population biology of an ectoparasitic digenean.

Ph.D. Thesis. University of London.

MOHANDAS, A. 1973. Transversotrema chackai sp. nov., adult of Cercaria chackai, from fishes (Digenea: Transversotrematidae).

Hydrobiologia, 43: 183-188.

MOHANDAS, A. 1974. The pathological effects of larval trematodes on the digestive glands of four species of gastropods.

Folia. Parasit., 21: 219-224.

MORI, S. 1946. Daily rhythmic activities of two Japanese fresh-water snails.

Physiol. Ecol. Contr. Otsu. Hydrobiol. Station, (Kyoto Univ.), 60: 1-17.

MORRIS, G.P. 1968. Fine structure of the gut epithelium of Schistosoma mansoni.

Experientia, 24: 480-482.

MORRIS, G.P. 1971. The fine structure of the tegument and associated structures of the cercaria of Schistosoma mansoni.

Z. ParasitKde., 36: 15-31.

MORRIS, G.P. and HALTON, D.W. 1971. Electron microscope studies of Diclidophora merlangi (Monogenea: Polyophisthocotylea). II. Ultrastructure of the tegument.

J. Parasit., 57: 49-61.

MORRIS, G.P. and THREADGOLD, L.T. 1967. A presumed sensory structure associated with the tegument of Schistosoma mansoni

J. Parasit., 53: 537-539.

MORRIS, G.P. and THREADGOLD, L.T. 1968. Ultrastructure of the tegument of adult Schistosoma mansoni.

J. Parasit., 54: 15-27.

MORSETH, D.J. 1967. Observations on the fine structure of the nervous system of Echinococcus granulosus.

J. Parasit., 53: 492-500.

MOUNT, P.M. 1970. Histogenesis of the rostellar hooks of Taenia crassiceps (Zeder, 1800) (Cestoda).

J. Parasit., 56: 947-961.

MUELLER, F.J. 1961. The laboratory propagation of Spirometra mansonoides as an experimental tool. IV. Experimental inversion of the primary axis in the developing egg.

Exptl. Parasit., 11: 311-318.

MUKHERJEE, R.P. 1969. Studies on the life history of Cotylophoron indicum, an amphistomatous parasite of ruminants in India.

J. Zool. Soc. Ind., 20: 105-122.

MURTY, A.S. and RAO, K.H. 1968. On a new host record for the fish trematode Transversotrema patialensis (Soparkar).

Curr. Sci., 37: 652-653.

NADAKAL, A.M., MOHANDAS, A. and SUNDERARAMAN, V. 1969. Cercaria chackai sp. nov. (Transversotrematidae) from Kerala, India.

J. Parasit., 55: 1187-1190.

NELSON, G.S., TEESDALE, C. and HIGHTON, R.B. 1962. CIBA Foundation Symposium on Biharziasis.

Churchill, London.

NICE, G.G. and WILSON, R.A. 1974. A study of the effect of temperature on the growth of Fasciola hepatica in Lymnea truncatula.

Parasitology, 68: 47-56.

NOLLEN, P.M. 1968. Autoradiographic studies on reproduction in Philophthalmus megalurus (Cort, 1914) (Trematoda).

J. Parasitol., 54: 43-48.

NOLLEN, P.M. 1971. Digenetic trematodes: Quinone tanning system in eggshells.

Exptl. Parasit. 30: 64-72.

NUTTMAN, C.J. 1971. The fine structure of ciliated nerve endings in the cercaria of Schistosoma mansoni.

J. Parasit., 57: 855-859.

NUTTMAN, C.J. 1975: The structure and behaviour of the cercaria of Schistosoma mansoni.

Ph.D. Thesis. University of York.

ODENING, K., MATTHEIS, T., and BOCKHARD, T. 1970. (The life history of Cotylurus cucullus cucullus (Thoss) (Trematoda: Strigeida) in the Berlin region).

Zool. Jb. Syst., 97: 125-198. (In German).

OLIVER, J.H. and SHORT, R.B. 1956. Longevity of miracidia of Schistosomatium douthitti.

Extl. Parasit., 5: 238-249.

OLIVIER, L. 1940. Life history studies on two strigeid trematodes of the Douglas Lake region of Michigan.

J. Parasit., 26: 447-477.

OLIVIER, L. 1947. Cercaria koliensis, a new fork-tailed cercaria from Guadalcanal.

J. Parasit., 33: 234-240.

OLIVIER, L. 1951. The influence of light on the emergence of Schistosomatium douthitti cercariae from their snail host.

J. Parasit., 37: 201-204.

OLLERENSHAW, C.B. 1971. Forecasting liver fluke disease in England and Wales 1958-1968 with a comment on the influence of climate on the incidence of disease in some other countries.

Vet. Med. Rev. Nº 2/3: 289-312.

PANDE, B.P. and SHUKLA, R.P. 1972. On the juvenile and adult of an ectoparasitic fluke of some of our freshwater fishes.

Curr. Sci., 41: 682-684.

PANDEY, K.C. 1971. On a rare cercaria, Cercaria soparkari n.sp., (Transversotrematidae) from Lucknow, India.

J. Helm., 45: 321-326.

PEARSON, J.C. 1956. Studies on the life cycles and morphology of the larval stages of Alaria arisaemoides Augustine and Uribe, 1927 and Alaria canis LaRue and Fallis, 1936 (Trematoda: Diplostomidae).

Can. J. Zool., 34: 295-387.

PEARSON, J.C. 1961. Observations on the morphology and life cycle of Neodiplostomum intermedium. (Trematoda: Diplostomidae).

Parasitology, 51: 133-172.

PEARSON, J.C. 1972. A phylogeny of life cycle patterns of the digenea.

Adv. Parasit., 10: 153-189.

PECKAM, G. 1970. A new method for minimising a sum of squares without calculating gradients.

Comput. J., 13: 418-420.

PENCE, D.B. 1970. Electron microscope and histochemical studies on the eggs of Hymenolepis diminuta.

J. Parasit., 56: 84-97.

PIEPER, M.B. 1953. The life history and germ cell cycle of Spirorchis artericola (Ward, 1921).

J. Parasit., 39: 310-325.

PITCHFORD, R.J. and VISSER, P.S. 1972. Some observations on the hatching pattern of Schistosoma mansoni eggs.

Ann. trop. Med. Parasit., 66: 399-407.

PITELKA, D.R. 1974. Basal bodies and root structures. In: "Cilia and Flagella". Chapt. 16. Ed. M.A. Sleigh.

Academic Press., London.

POND, G.G. and CABLE, R.M. 1966. Fine structure of photoreceptors in three types of ocellate cercariae.

J. Parasit., 52: 483-493.

PRAH, S.K. and JAMES, C. 1977. The influence of physical factors on the survival and infectivity of miracidia of Schistosoma mansoni and S. haematobium. 1. Effect of temperature and U.V. light.

J. Helm., 51: 73-85.

PRECHT, H. 1958. Concepts of the temperature adaptation of unchanging reaction systems of cold-blooded animals. In: Physiological Adaptation". Ed. C.L. Prosser.

Am. Physiol. Soc., Washington D.C.

PRESTON, F.W. 1974. The volume of an egg.

Auk, 91: 132-138.

PROBERT, A.J. 1963. Biological studies on some helminths parasitic in the freshwater fauna of South Wales.

Ph.D. Thesis, Univ. of Wales.

PROSSER, C.L. 1973. Temperature. In: "Comparative Animal Physiology". Ed. C.L. Prosser, Saunders, U.S.A.

PROSSER, C.L. and BROWN, F.A. 1961. Comparative animal physiology. 2nd Ed. Saunders, U.S.A.

PURNELL, R.E. 1966a. Host-parasite relationships in schistosomiasis. 1. The effect of temperature on the infection of Biomphalaria sudanica tanganyicensis with Schistosoma mansoni miracidia and of laboratory mice with Schistosoma mansoni cercariae. Am. trop. Med. Parasit., 60: 90-93.

PURNELL, R.E. 1966b. Host-parasite relationships in schistosomiasis. III. The Effect of temperature on survival of Schistosoma mansoni miracidia and on the survival and infectivity of Schistosoma mansoni cercariae. Am. trop. Med. Parasit., 60: 182-186.

RAMALINGAM, K. 1973. The chemical nature of the eggshells of helminths. 1. Abscence of quinone tanning in the eggshell of the liver-fluke, Fasciola hepatica. Int. J. Parasit., 3: 67-75.

RAMBOURG, A. 1971. Morphological and histochemical aspects of glycoproteins at the surface of animal cells. Int. Rev. Cytol. 31: 57-114.

RAO, K.H. and GANAPATI, P.N. 1967. Observations on Transversotrema patialensis (Soparkar, 1924). (Trematoda) from Waltair, Andhra Pradesh (India). Parasitology, 57: 661-664.

READER, T.A.J. 1971. The pathological effects of sporocysts, rediae and metacercariae on the digestive gland of Bithynia tentaculata (Mollusca: Gastropoda).

Parasitology, 63: 483-489.

READER, T.A.J. 1976. Studies on the ultrastructure, histochemistry and cytochemistry of the uninfected digestive gland of Bithynia tentaculata (Mollusca: Gastropoda) and on the ultrastructure of this host organ in snails infected with larval digeneans.

Z. ParasitKde., 50: 11-30.

REES, F.G. 1934. Cercaria patellae Lebour, 1911, and its effect on the digestive gland of Patella vulgata.

Proc. zool. Soc. Lond., 1: 45-53.

REES, F.G. 1940. Studies on the germ cell cycle of the digenetic trematode Parorchis acanthus Nicoll. II. Structure of the miracidium and germinal development in the larval stages.

Parasitology, 32: 372-391.

REES, F.G. 1940. A study of the effect of light, temperature and salinity on the emergence of Cercaria purpurae Lebour from Nucella lapillus (L).

Parasitology, 38: 228-242.

REES, F.G. 1971. Locomotion of the cercaria of Parorchis acanthus Nicoll, and the ultrastructure of the tail.

Parasitology, 62: 489-503.

REES, F.G. 1975. The arrangement and ultrastructure of the musculature, nerves and epidermis in the tail of the cercaria of Cryptocotyle lingua (Creplin)from Littorina littorea (L).

Proc. R. Soc. B, 190: 165-186.

REES, F.G. 1977. The development of the tail and the excretory system in the cercaria of Cryptocotyle lingua (Creplin) (Digenea: Heterophyidae) from Littorina littorea (L).

Proc. R. Soc. B, 195: 425-452.

REES, W.J. 1936. The effect of parasitism by larval trematodes on the tissues of Littorina littorea.

Proc. zool. Soc. Lond., 2: 357-368.

REYNOLDS, E.S. 1963. The use of lead citrate at high pH as an electron-opaque stain in electron microscopy.

J. Cell. Biol., 17: 208.

RHODIN, A.G. and REITH, E.J. 1962. Ultrastructure of keratin in oral mucosa, skin, esophagus, claw and hair. In: "Fundamentals of keratinization". Ed. E.O. Butcher and R.F. Sognnaes. Pub. Nº 70, AAAS, Washington D.C.

RIFKIN, E. 1970. An ultrastructural study of the interaction between the sporocysts and the developing cercariae of Schistosoma mansoni.

J. Parasit., 56, suppl. 284.

ROBINSON, G. and THREADGOLD, L.T. 1975. Electron microscope studies of Fasciola hepatica. XII. The fine structure of the gastrodermis.

Exptl. Parasit., 37: 20-36.

ROBSON, E.M. and WILLIAMS, I.C. 1971. Relationship of some species of digenea with the marine prosobranch Littorina littorea (L). II. The effect of larval digenea on the reproductive biology of L. littorea.

J. Helm., 45: 145-159.

ROGERS, G.E. 1959a. Electron microscope studies of wool.

J. Ultrastruct. Res., 2: 309-330.

ROGERS, G.E. 1959b. Electron microscope studies of hair and wool.
Ann. N.Y. Acad. Sci., 83: 378.

ROWAN, W.B. 1956. The mode of hatching of the egg of Fasciola hepatica.
Exptl. Parasit., 5: 118-137.

ROWAN, W.B. 1957. The mode of hatching of the egg of Fasciola hepatica. II. Colloidal nature of the viscous cushion.
Exptl. Parasit., 6: 131-142.

ROWAN, W.B. 1958. Daily periodicity of Schistosoma mansoni cercariae in Puerto Rican Waters.
Am. J. trop. Med. Hyg., 7: 374-381.

ROWCLIFFE, S.A. and OLLERENSHAW, C.B. 1961. Observations on the bionomics of the egg of Fasciola.
Am. trop. Med. Parasit., 54: 172-181.

RYBICKA, K. 1966. Embryogenesis in cestodes.
Adv. Parasit., 4: 107-186.

RYBICKA, K. 1972. Ultrastructure of embryonic envelopes and their differentiation in Hymenolepis diminuta (Cestoda).
J. Parasit., 58: 849-863.

SAKAMOTO, K. and ISHII, Y. 1977. Scanning electron microscope observations on adult Schistosoma japonicum.
J. Parasit., 63: 407-412.

SATIR, P. 1974. The present status of the sliding microtubule model of ciliary motion. In: "Cilia and flagella". Chapt. 7. Ed. M.A. Sleigh.
Academic Press, London.

SAUNDERS, D.S. 1977. An introduction to biological rhythms.
Blackie, London.

SCHILLER, E.L. 1955. Studies on the helminth fauna of Alaska. XXVI. Some observations on the cold resistance of eggs of Echinococcus sibiricensis Rausch and Schiller, 1954.

J. Parasit., 41: 578-582.

SCHNITZER, B., SODEMAN, T., SODEMAN, W. and DURKEE, T. 1971. Microspines on Schistosoma japonicum and S. haematobium egg shells.

Parasitology, 62: 385-387.

SCHREIBER, F.G. and SCHUBERT, M. 1949. Experimental infection of the snail Australorbis glabratus with the trematode S. mansoni and the production of cercariae.

J. Parasit., 35: 91-100.

SEIFTER, S. and GALLOP, P.M. 1966. The structure proteins. IN: "The proteins: composition, structure and function". 2nd Edition, Vol. 4. Ed. H. Neurath.

Academic Press Inc. N.Y.

SEY, O. 1972. Investigations on the eggs, the process of embryo formation and the structure of the miracidium of Paramphistomum daubneyi Dinnik, 1962.

Parasit. Hung., 5: 17-38.

SHANNON, W.A. and BOGITSH, B.J. 1969. Cytochemical and biochemical observations of the digestive tracts of digenetic trematodes. V. Ultrastructure of Schistosomatium douthitti gut.

Exptl. Parasit., 26: 344-353.

SHAW, J.M. and SIMMS, B.T. 1930. Studies on fascioliasis in Oregon sheep and goats.

Oregon. Agr. Exptl. Sta. Bull., 266.

SHELFORD, V.E. 1927. An experimental investigation of the relations of the codling moth to weather and climate.

Bull. Ill. St. nat. Hist. Surv., 16: 311-440.

SHORT, R.B. and GAGNE, H.I. 1975. Fine structure of a possible photoreceptor in cercariae of Schistosoma mansoni.

J. Parasit., 61: 69-74.

SIM, E.K.P., 1972. The life cycle of a Malayan species of Transversotrema: a trematode parasite of fish.

M.Sc. Thesis, Univ. of Malaya, Kuala Lumpur.

SLAIS, J. and MACHNICKA, B. 1976. Appearance of a temporary hook anlages in the early development of Taenia saginata Goeze, 1782.

Zool. Anz., Jena, 196: 85-92.

SMITH, J.H., REYNOLDS, E.S. and VON LICHTENBERG, F. 1969. The integument of Schistosoma mansoni.

Am. J. trop. Med. Hyg., 18: 28-49.

SMYTH, J.D. and CLEGG, J.A. 1959. Egg shell formation in trematodes and cestodes.

Exptl. Parasit., 8: 286-323.

SOGANDARES-BERNAL, F. 1966. Studies on American paragonimiasis. IV. Observations on the pairing of adult worms in laboratory infections of domestic cats.

J. Parasit., 52: 701-703.

SOPARKAR, M.B. 1924. A new cercaria from Northern India. Cercaria patialensis nov. sp.

Indian J. med. Res., 11: 933-942.

SOUTHGATE, V.R. 1970. Observations on the epidermis of the miracidium and on the formation of the tegument of the sporocyst of Fasciola hepatica.

Parasitology, 61: 177-190.

SPENCE, I.M. and SILK, M.H. 1970. Ultrastructural studies of the blood fluke - Schistosoma mansoni. IV. Digestive system.

S. Afr. J. med. Sci., 35: 93-112.

STANDEN, O.D. 1951. The effects of temperature, light and salinity upon the hatching of the ova of Schistosoma mansoni.

Trans. R. Soc. trop. Med. Hyg., 45: 225-241.

STEELE, D.H. 1977. Correlation between egg size and developmental period.

Am. Nat., 111: 371-372.

STEPHENSON, W. 1947. Physiological and histochemical observations on the adult liver fluke Fasciola hepatica L. III. Egg shell formation.

Parasitology, 38: 128-139.

STRATHMAN, R.R. 1977. Egg size, larval development, and juvenile size in benthic marine invertebrates.

Am. Nat., 111: 372-376.

STUNKARD, H.W. 1950. Further observations on Cercaria parvicaudata Stunkard and Shaw, 1931.

Biol. Bull., 99: 136-142.

SUGIURA, S., SASAKI, T., HOSAKA, Y. and ONO, R. 1954. A study of several factors influencing hatching of Schistosoma japonicum eggs.

J. Parasit., 40: 381-386.

SWALES, C.W. 1935. The life cycle of Fascioloides magna (Bassi, 1875) the large liver fluke of ruminants in Canada.

Can. J. Res., 12: 177-215.

SWALES, C.W. 1936. Further studies on Fascioloides magna (Bassi, 1875) Ward, 1917, as a parasite of ruminants.

Can. J. Res., 14: 83-95.

SWIDERSKI, Z. and MACKIEWICZ, J.S. 1976. Electron microscope study of vitellogenesis in Glaridacris catostomi (Cestoidea: Caryophyllidea).

Int. J. Parasit., 6: 61-73.

TAMM, S.C. and HORRIDGE, C.A. 1970. The relation between the oreintation of the control fibrils and the direction of beat in cilia of Opalina.

Proc. R. Soc. B., 175: 219-233.

TATUM, J.B. 1975. Egg volume.

Auk., 92: 576-580.

THOMAS, A.P. 1883. The life history of the Liver-Fluke (Fasciola hepatica).

Q. J. microsc. Soc., 89: 99-133.

THREADGOLD, L.T. 1963. The tegument and associated structures of Fasciola hepatica.

Q. J. microsc. Sci., 104: 505-512.

THREADGOLD, L.T. 1967. Electron microscope studies of Fasciola hepatica. III. Further observations on the tegument and associated structures.

Parasitology, 57: 633-637.

THREADGOLD, L.T. 1968. The tegument and associated structures of Haplometra cylindracea.

Parasitology, 58: 1-7.

THREADGOLD, L.T. 1976. Fasciola hepatica: ultrastructure and histochemistry of the glycocalyx of the tegument.

Exptl. Parasit., 39: 119-134.

UJIIE, N. 1936. On the process of egg-shell formation of Clonorchis sinensis, a liver fluke.

J. Med. Ass., Formosa, 35: 1894-1896.

UNDERWOOD, A.J. 1974. On models for reproductive strategy in marine benthic invertebrates.

Am. Nat., 108: 874-878.

UPTHAM, E.S. 1972. Effects of some physico-chemical factors on the infection of Biomphalaria glabrata (Say) by miracidia of Schistosoma mansoni Sambon in St. Lucia, West Indies.

J. Helm., 46: 307-315.

UZMANN, J.R. 1953. Cercaria milfordensis nov. sp., a microcercous trematode larva from the marine bivalve, Mytilus edulis L. with special reference to its effect on the host.

J. Parasit., 39: 445-451.

VALLE, C., PELLEGRINO, J. and GAZZINELLI, G. 1974. Influence of temperature on the backward propulsion speed of Schistosoma mansoni cercariae.

J. Parasit., 60: 372-373.

VANCE, R.R. 1973a. On reproductive strategies in marine benthic invertebrates.

Am. Nat., 107: 339-352.

VANCE, R.R. 1973b. More on reproductive strategies in marine benthic invertebrates.

Am. Nat., 107: 353-361.

VANCE, R.R. 1974. Reply to Underwood.

Am. Nat., 108: 879-880.

VARLEY, G.C., GRADWELL, G.R. and HASSEL, M.P. 1973. Insect population ecology, an analytical approach.

Blackwells, Oxon.

VARMA, A.K. 1961. Observations on the biology and pathogenicity of Cotylophoron cotylophoron (Fischoeder, 1901).

J. Helm., 35: 161-168.

VELASQUEZ, C.C. 1958. Transversotrema laruei, a new trematode of Philippine fish (Digenea: Transversotrematidae).

J. Parasit., 44: 449-451.

VELASQUEZ, C.C. 1961. Further studies on Transversotrema laruei Velasquez with observations on the life cycle (Digenea: Transversotrematidae).

J. Parasit., 47: 65-70.

VELASQUEZ, C.C. 1975. Digenetic trematodes of Philippine fishes.

Univ. Philippines Press, Quezon City.

VERNBERG, F.J. and VERNBERG, W.B. 1970. The animal and the environment.

Holt, Rinehart and Wilson, U.S.A.

VERNBERG, W.B. and VERNBERG, F.J. 1972. Environmental physiology of marine animals.

Springer Verlag, N.Y.

VICKERS, G.G. 1940. On the anatomy of Cercaria macrocerca from Sphaerium corneum.

Q. J. microsc. Sci., 82: 311-326.

WAGNER, B. 1965. Untersuchungen uber ektogene Helminthenstadien. I. Experimentalle Untersuhungen zum Glykogen - und Fett-stoffwechsel der Mirazidien von Fasciola hepatica unter Berucksichtigung ihres Sauerstoffverbrauchs.

Angew. Parasit., 6: 142-150.

WEBBE, G. 1966. The effect of water velocities on the infection of Biomphalaria sudanica tanganyicensis to different numbers of Schistosoma mansoni miracidia.

Ann. trop. Med. Parasit., 60: 85-89.

WEIBEL, E.R. 1969. Stereological principles of morphometry in electron microscope cytology.

Int. Rev. Cytol., 26: 235-302.

WESENBERG-LUND, C. 1934. Contributions to the development of the Trematoda Digenea. II. The biology of the freshwater cercariae in Danish freshwaters.

Mem. Acad. Roy. Sci. Lett. Danemark. Sect. Sci., 2, tV: 1-223.

WHITFIELD, P.J. 1973. The egg envelopes of Polymorphus minutus (Acanthocephala).

Parasitology, 66: 387-403.

WHITFIELD, P.J., ANDERSON, R.M. and BUNDY, D.A.P. 1977. Experimental investigations on the behaviour of the cercariae of an ecto-parasitic digenean Transversotrema patialense: general activity patterns.

Parasitology, 75: 9-30.

WHITFIELD, P.J., ANDERSON, R.M. and MOLONEY, N.A. 1975. The attachment of cercariae of an ectoparasitic digenean, Transversotrema patialensis, to the fish host: behavioural and ultrastructural aspects.

Parasitology, 70: 311-329.

WHITFIELD, P.J. and WELIS, J. 1973. Observations on the ecto-parasitic digenean Transversotrema patialensis.

Parasitology, 67; Proc. B.S.P.: 27.

WIKEL, S.K. and BOGITSH, B.J. 1974. Schistosoma mansoni penetration apparatus and epidermis of the miracidium.

Exptl. Parasit., 36: 342-354.

WILSON, R.A. 1967a. The structure and permeability of the shell and vitelline membrane of the egg of Fasciola hepatica.

Parasitology, 57: 47-58.

WILSON, R.A. 1967b. The protonephridial system in the miracidium of the liver fluke, Fasciola hepatica L.

Comp. Biochem. Physiol., 20: 237-242.

WILSON, R.A. 1968. The hatching mechanism of the egg of Fasciola hepatica.

Parasitology, 58: 79-89.

WILSON, R.A. 1969a. Fine structure of the tegument of the miracidium of Fasciola hepatica L.

J. Parasit., 55: 124-133.

WILSON, R.A. 1969b. Fine structure and organization of the musculature in the miracidium of Fasciola hepatica.

J. Parasit., 55: 1153-1161.

WILSON, R.A. 1969c. The fine structure of the protonephridial system in the miracidium of Fasciola hepatica.

Parasitology, 59: 461-467.

WILSON, R.A. 1970. Fine structure of the nervous system and specialized nerve endings in the miracidium of Fasciola hepatica.

Parasitology, 60: 399-410.

WILSON, R.A. and BARNES, P.E. 1974. The tegument of Schistosoma mansoni: observations on the formation, structure and composition of cytoplasmic inclusions in relation to tegument function.

Parasitology, 68: 239-258.

WILSON, R.A. and DENISON, J. 1970. Studies on the activity of the miracidium of the common liver fluke: Fasciola hepatica.

Comp. Biochem. Physiol., 32: 301-313.

WILSON, R.A. and DRASKAU, T. 1976. The stimulation of daughter redia production during the larval development of Fasciola hepatica.

Parasitology, 72: 245-257.

WILSON, R.A. PULLIN, R. and DENISON, J. 1971. An investigation of the mechanism of infection by digenetic trematodes: the penetration of the miracidium of Fasciola hepatica into its snail host Lymnea truncatula.

Parasitology, 63: 491-506.

WITENBERG, G. 1944. Transversotrema haasi, a new fish trematode.

J. Parasit., 30: 179-180.

WRIGHT, C.A. 1971. Flukes and snails.

Allen and Unwin, Lond.

WU, T.Y. 1978. Introduction to the scaling of aquatic animal locomotion. In: "Scale effects in animal locomotion". Ed. T.J. Pedley.

Academic Press, Lond.

WUNDER, W. 1924. Bau, Entwicklung und Funktion des Cercarienschwanzes.

Jool. Jahrb. Abt. Anat., 46: 303-339.

YATES, F. 1934. Contingency tables involving small numbers and the X^2 Test.

J. R. statist. Soc. 1: 217-235.

YOKOGAWA, M. 1965. Paragonimus and Paragonimiasis.

Adv. Parasit., 3: 99-158.

YOSHINO, T.P. 1976. Histophathological effects of larval digenea on the digestive epithelium of the marine prosobranch Cerithidea californica: Fine structural changes in the digestive gland.

J. Invert. Path., 28: 209-216.

YULE, G.U. and KENDALL, M.G. 1965. An introduction to the theory of statistics.

Griffin, Lond.

List of Plates

1. S.E. micrographs of the egg capsule.

2. T.E. micrograph of transverse section of miracidium.

3. T.E. micrographs of miracidial body wall.

4. T.E. micrographs of miracidial sensory endings.

5. T.E. micrographs of miracidial T.S. and flame cell.

6. T.E. micrographs of miracidial T.S. and ciliary eye.

7. T.E. micrographs of miracidial sensory endings.

8. T.E. micrographs of miracidial sensory endings.

9. T.E. micrographs of miracidial protonephridial tubule.

10. T.E. micrographs of miracidial protonephridial tubule.

11. Micrographs of the egg surface and sporocyst.

12. S.E. micrographs of redia.

13. S.E. micrographs of Type One cercaria.

14. S.E. micrographs of early Type Two cercaria.

15. S.E. micrographs of late Type Two cercaria.

16. S.E. micrographs of ventral surface of Type Three cercaria.

17. S.E. micrographs of adult fluke/host interface.

18. S.E. micrographs of genital pore of adult.

19. S.E. micrographs of decaudate cercaria (= young adult).

20. S.E. micrographs of dorsal surface of adult.

21. T.E. micrograph of body wall of Type One cercaria.

22. T.E. micrographs of the body wall of Type Two cercariae.

23. T.E. micrographs of spines in the tegument of Type Three cercariae.

24. T.E. micrographs of tegument of Type Three cercariae.

25. T.E. micrographs of tegument cell bodies of Type Three cercariae.

26. T.E. micrographs of body wall of adult.

27. T.E. micrographs of digestive tract of Type Three cercariae.

28. T.E. micrographs of the junction between tegument and gastrodermis of Type Three cercariae.
29. T.E. micrographs of adult gastrodermis.
30. T.E. micrographs of T.S. through the tail stem of a Type Three cercaria
31. T.E. micrographs of cercarial flame cells.
32. T.E. micrographs of a flame cell of a Type Three cercaria.
33. T.E. micrographs of cercarial ocellus and vitelline cells.
34. T.E. micrographs of cercarial ocelli.
35. S.E. micrographs of the ventral surface of Type Three cercaria.
36. T.E. micrographs of uniciliate sensory endings of Type Three cercariae.
37. T.E. micrographs of sperm in Type Three cercariae.
38. T.E. micrographs of testis cell in Type Two cercaria.
39. T.E. micrographs of tegumental spines of early Type Three cercariae.
40. T.E. micrographs of T.S. tegumental spines of Type Three cercariae.
41. T.E. micrographs of tegumental spine infrastructure of Type Three cercariae.
42. S.E. micrographs of adult flukes at the host interface.
43. Microflash photographs of dropping cercariae.
44. Microflash photographs of swimming and resting cercariae.
45. Microflash photographs of attaching cercariae.
46. Microflash photographs of attached cercaria extending body region.
47. Highspeed microcinematographic record of swimming sequence A.
48. Selected frames of swimming sequence A.

Plate 1: S.E. micrographs of the egg capsule

a) Lateral view.

b) Apical view.

c) Felted appearance of egg capsule surface due to capsular extensions. Note adherent bacteria (ba).

d) Capsular extensions (ex) from capsular bosses (bo).

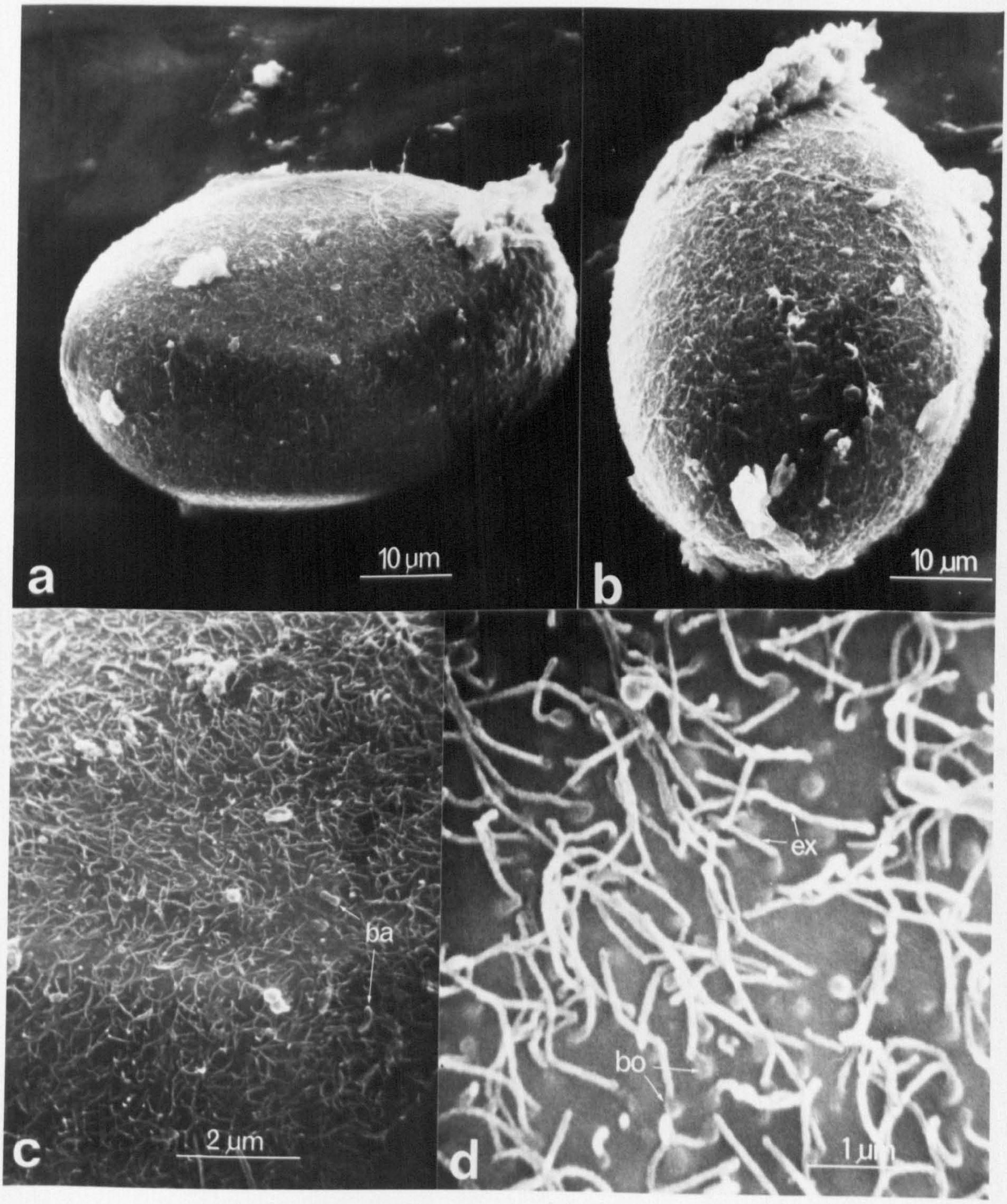
a
10 µm
b
10 µm
ba
c
2 µm
ex
bo
d
1 µm

Plate 2: T.E. micrograph of a transverse section of a miracidium. The periphery of the miracidium at the level of this section is covered with 6 epithelial cells (ec) separated by intercellular ridges (ir). The epithelial cells have an outer region containing inclusions and an inner region containing mitochondria. A subjacent muscle layer separates the epithelial cells from the cytoplasmic extensions of the sub-epithelial layer of cell bodies (sl). The centre of this section contains vesiculated regions (gc) presumed to be extensions of the apical gland cells.

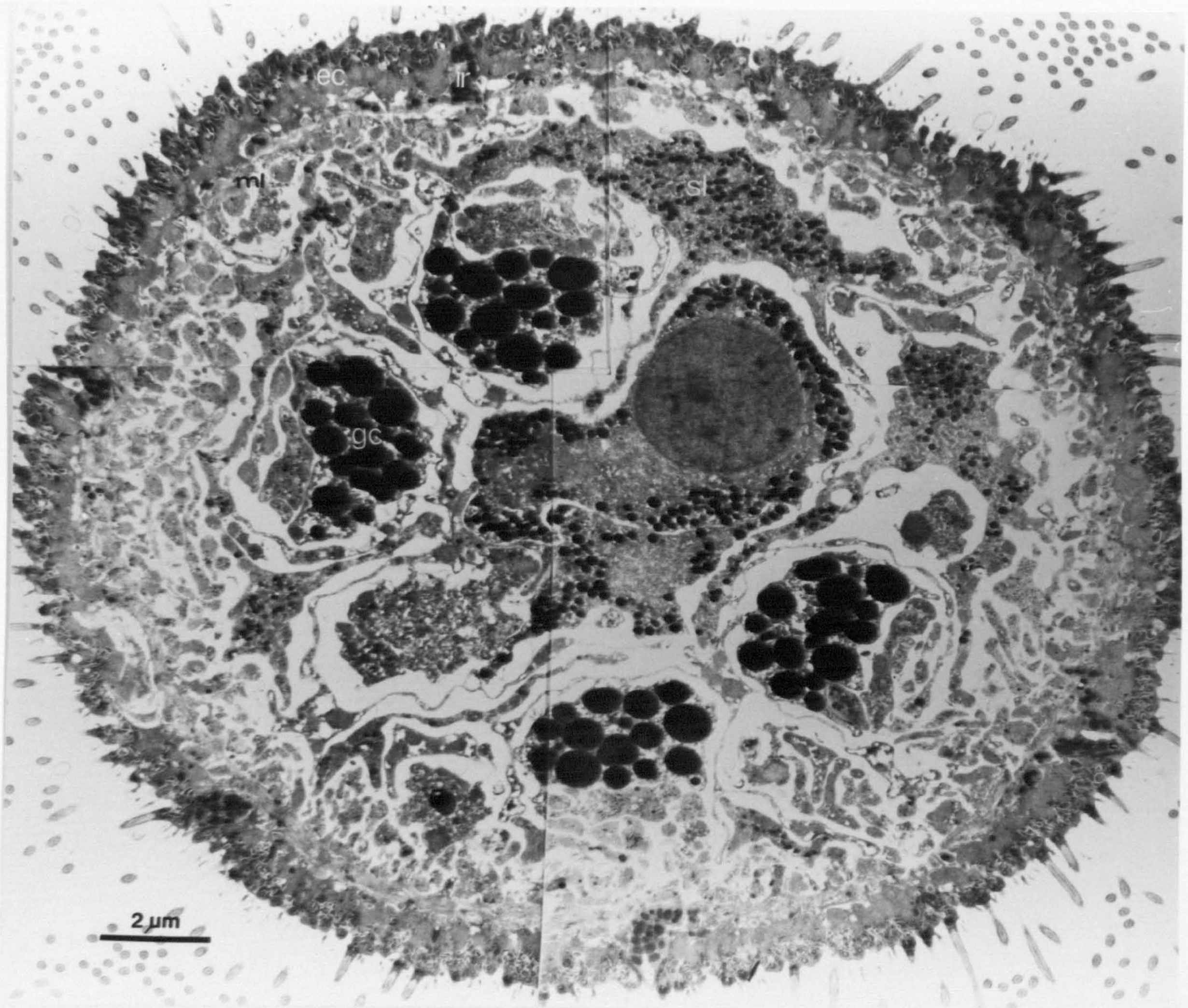
ec
ir
ml
sl
gc
2 µm

Plate 3: T.E. micrographs of the miracidial body wall.

a) Intercellular ridge (ir) attached laterally by septate desmosomes (sd) to epithelial cells (ec). The epithelial cells contain Type A inclusions (ta) and ciliary rootlets (cr) distally while the proximal region contains mitochondria (mi). The intercellular ridge contains vesicular inclusions (vi). The inner membranes of the epithelial cells are attached to subjacent regions by dense junctions (dj).

b) Epithelial cell (ec) overlying thin cytoplasmic layer (tc) and subjacent longitudinal (lm) and circular (cm) muscles. Supposed parenchyma cells contain glycogen granules. (SCALE AS ABOVE).

c) T.S. locomotory cilium. (× 150,000)

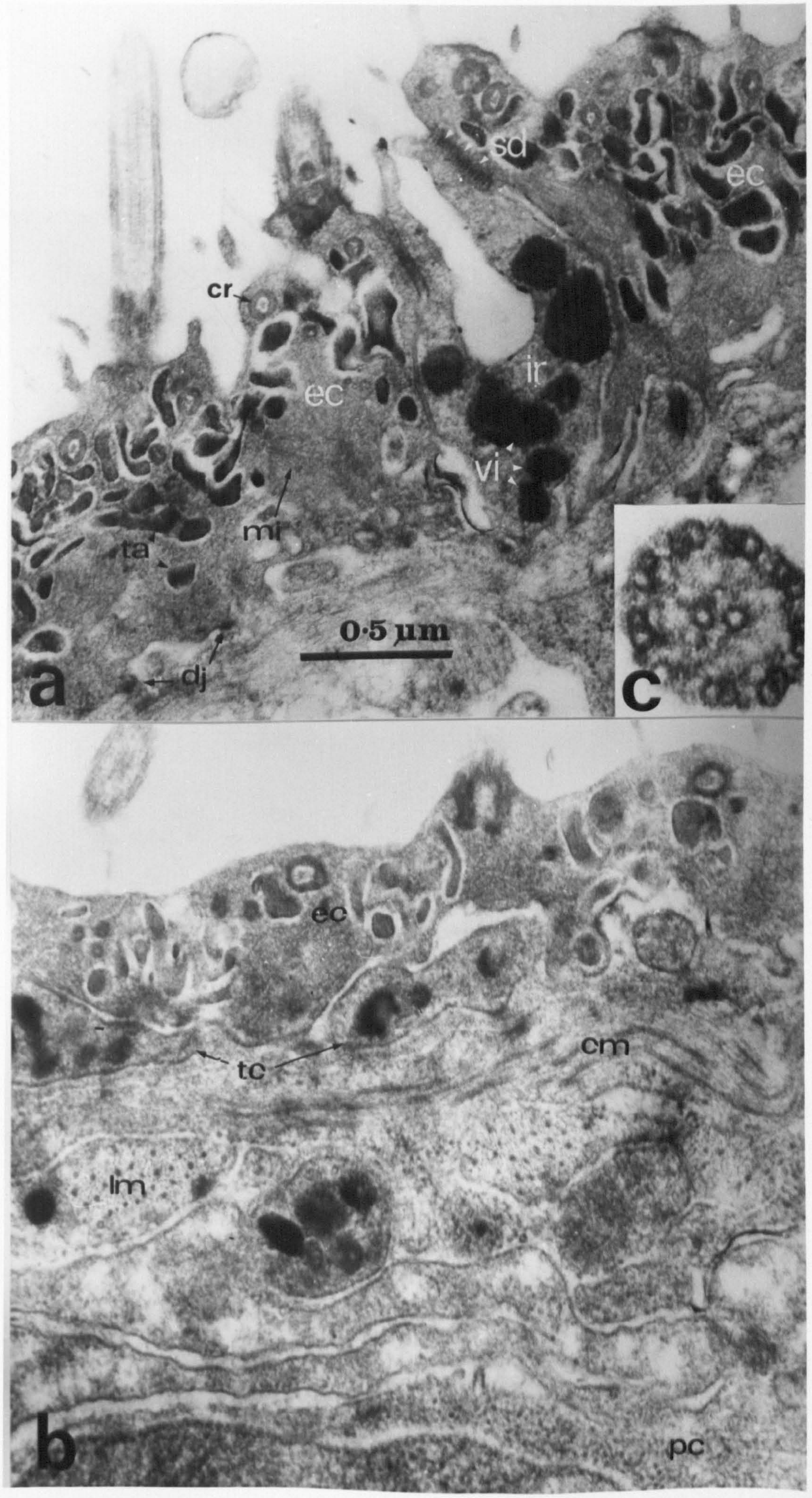
sd
ec
cr
ec
ir
vi
mi
ta
0·5 µm
dj
a
c
ec
tc
cm
im
b
pc

Plate 4: T.E. micrographs of miracidial sensory structures.

a) Body wall of miracidium containing papilla (pa in intercellular ridge (ir). A locomotory cilium (lc) in an adjacent epithelial cell (ec) has a discernable ciliary rootlet (cr). Epithelial cell nuclei (en) are present in both adjacent epithelial cells. Subjacent to the epithelial cells is a cytoplasmic portion of a ciliary eye (ce), containing 9 + 0 axonemes (ax) and basal bodies (bb).

b) Papilla (pa) separated by narrow gap (n) from intercellular ridge (ir). Papilla contains dense vesicles (dv) and neurotubules (nt). Intercellular ridge attacted to epithelial cells by sepate desmosome (sd).

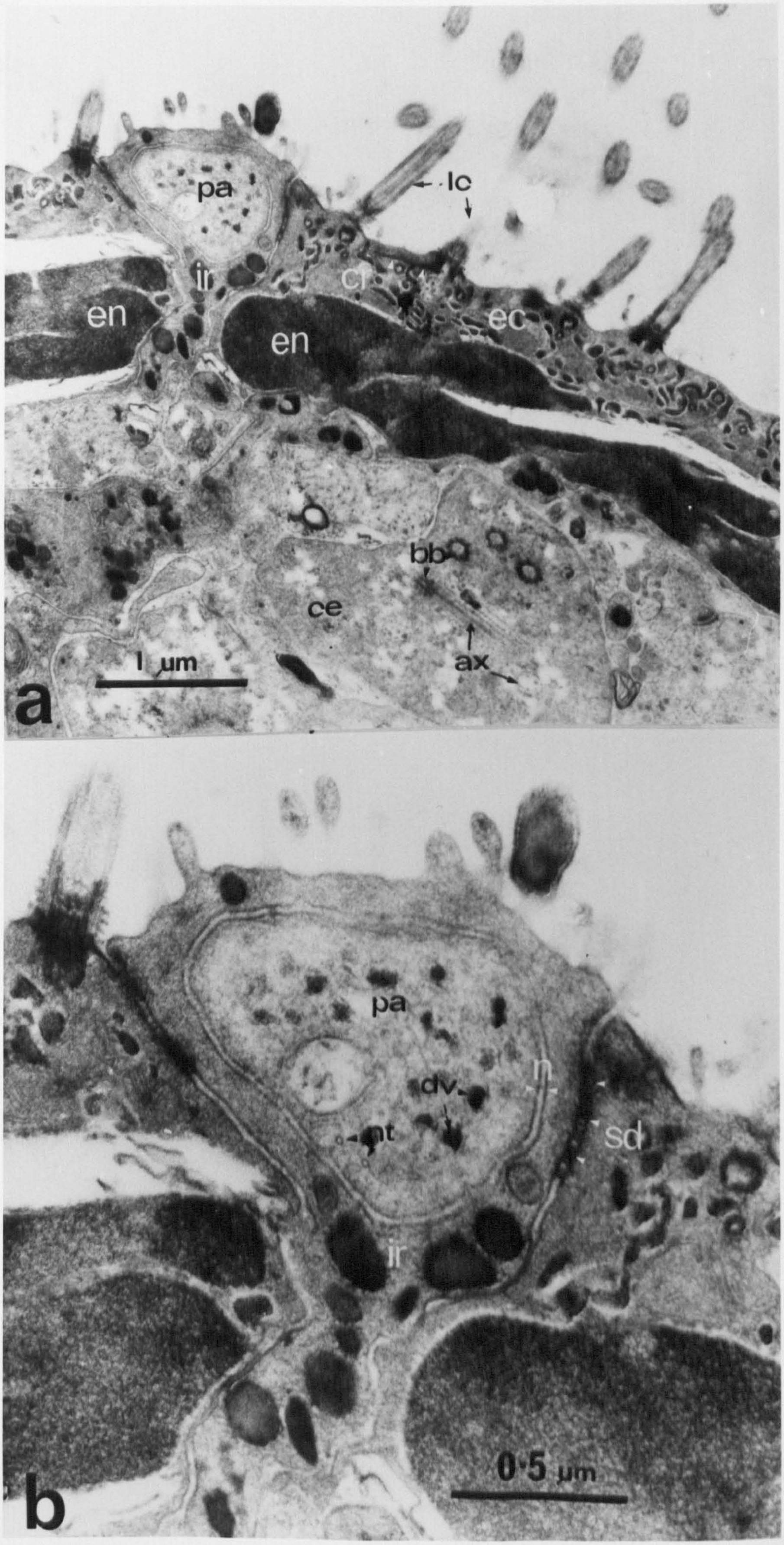
pa
lc
ir
cl
en
en
ec
ce
bb
ax
1 µm
a
pa
dv
m
nt
sd
ir
0·5 µm
b

Plate 5: T.E. micrographs of the miracidium.

a) T.S. miracidium. The sub-epithelial layer of cell bodies (sl) is interrupted by a flame cell (fc).

b) Miracidial flame cell. The section passes obliquely through the ciliary flame so that both basal bodies (bb) and axonmes (ax) are revealed in T.S. The inner ribs (in) give rise to leptotriches (le) adjacent to the cilia. The outer ribs (ou) are attached to the inner ribs by desmosomes (de). Mitochondria (mi) and a large nucleus (nu) are present in the cell body of the flame cell.

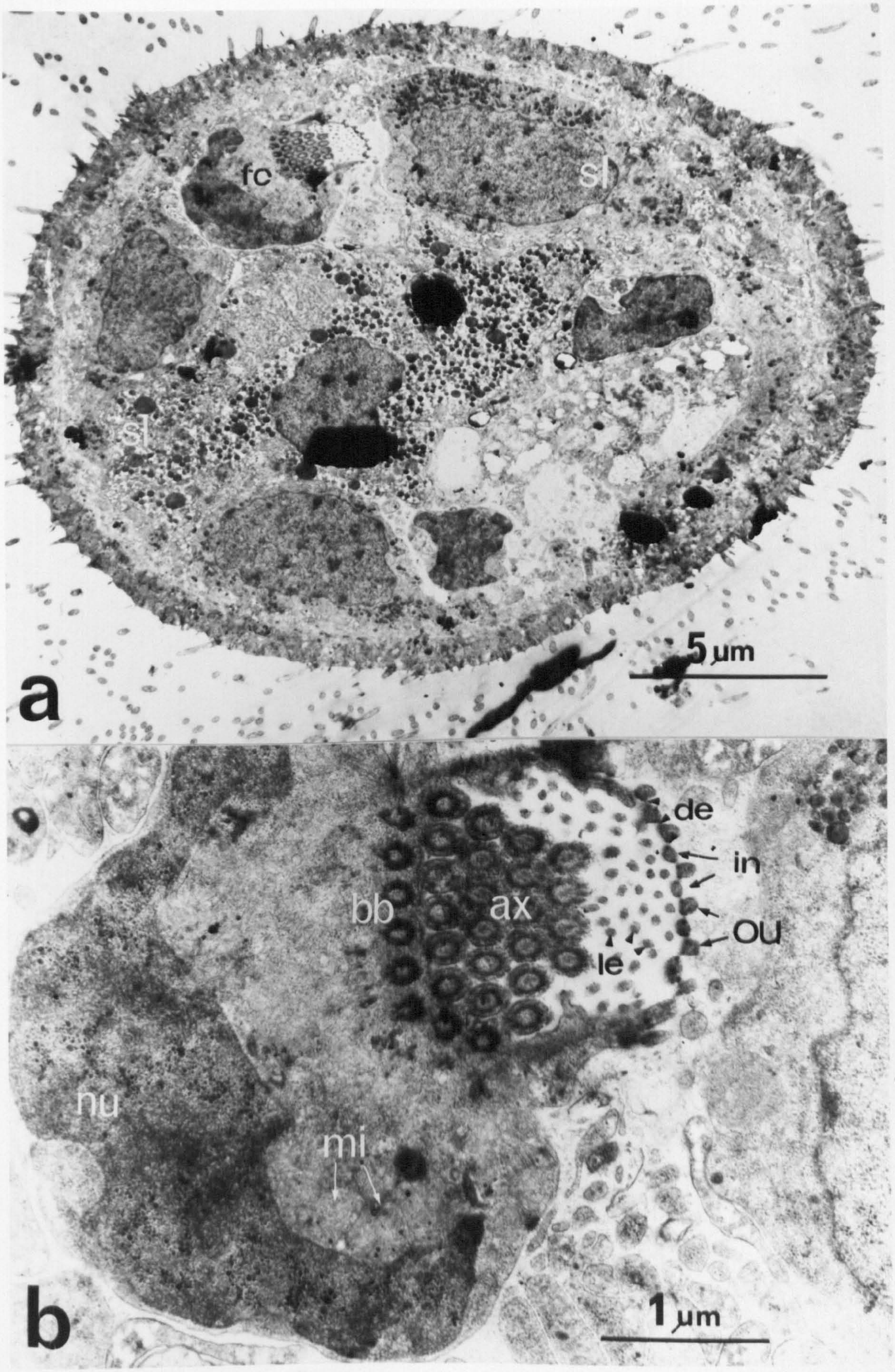
fc
sl
sl
5 µm
a
de
in
ou
bb
ax
le
nu
mi
1 µm
b

Plate 6: T.E. micrographs of the miracidium.

a) T.S. miracidium. Dendritic epithelial cell nuclei (en) are present within the epithelial cell layer (ec). The sub-epithelial layer of cell bodies (sl) is interrupted laterally by a ciliary eye (ce).

b) Ciliary eye. Basal bodies (bb) project inwards from the peripheral rind of cytoplasm towards the central lamellate region (lr).

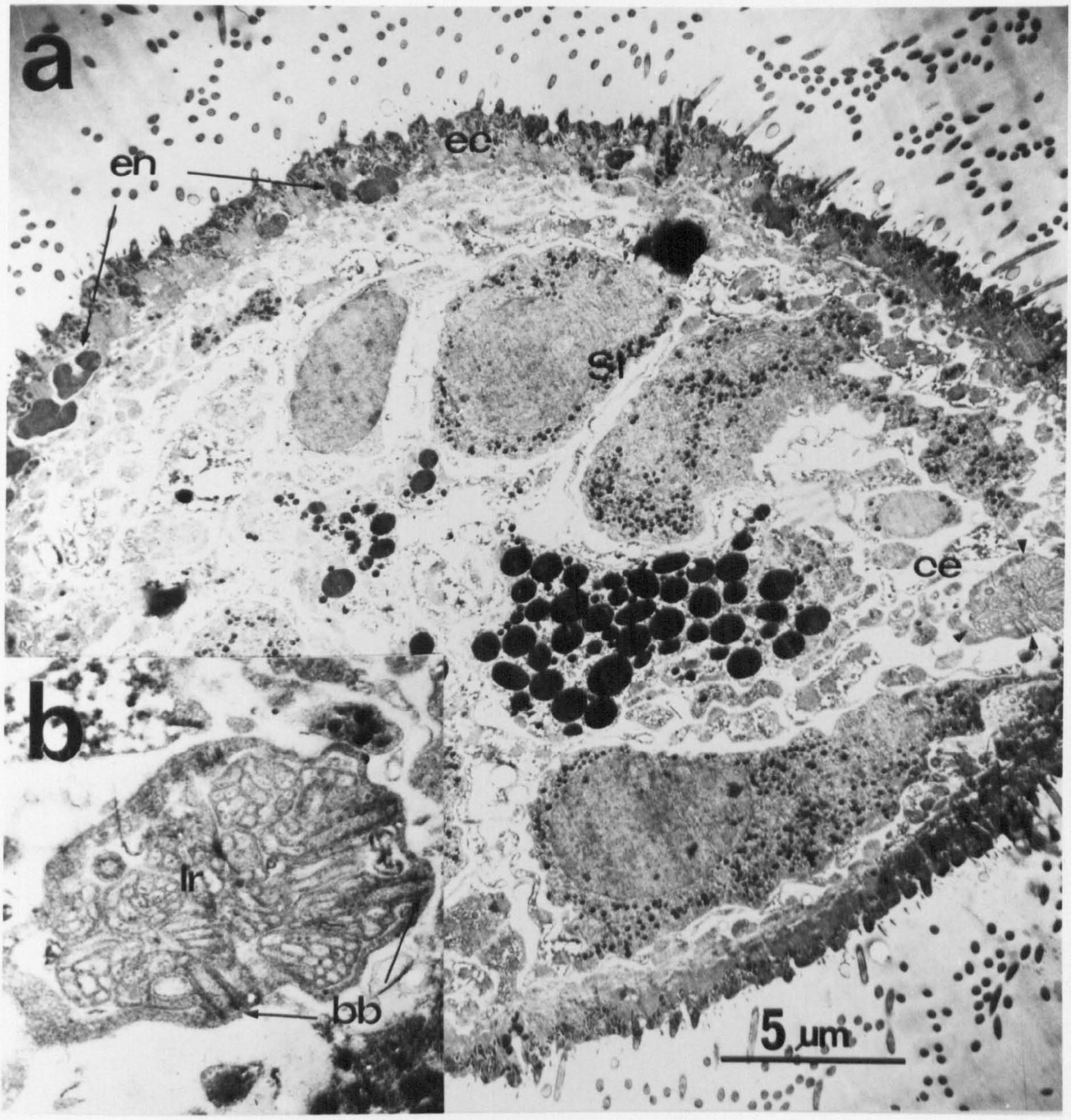
a
en
ec
sl
ce
b
lr
bb
5 µm

Plate 7: T.E. micrographs of miracidial sensory structures.

a) Miracidial body wall with ciliate papilla (cp) and papilla (pa) in intercellular ridge (ir). 9 + 0 axonemes (ax) can be distinguished in the cytoplasmic region of a ciliary eye (ce).

b) Ciliate papilla. The bulb (bu) is attached to the intercellular ridge by a dense lateral septate desmosome (sd). The bulb contains electron lucent regions (el) and a ciliary rootlet (cr). There appear to be two sensory cilia (sc) projecting from the bulb in this section.

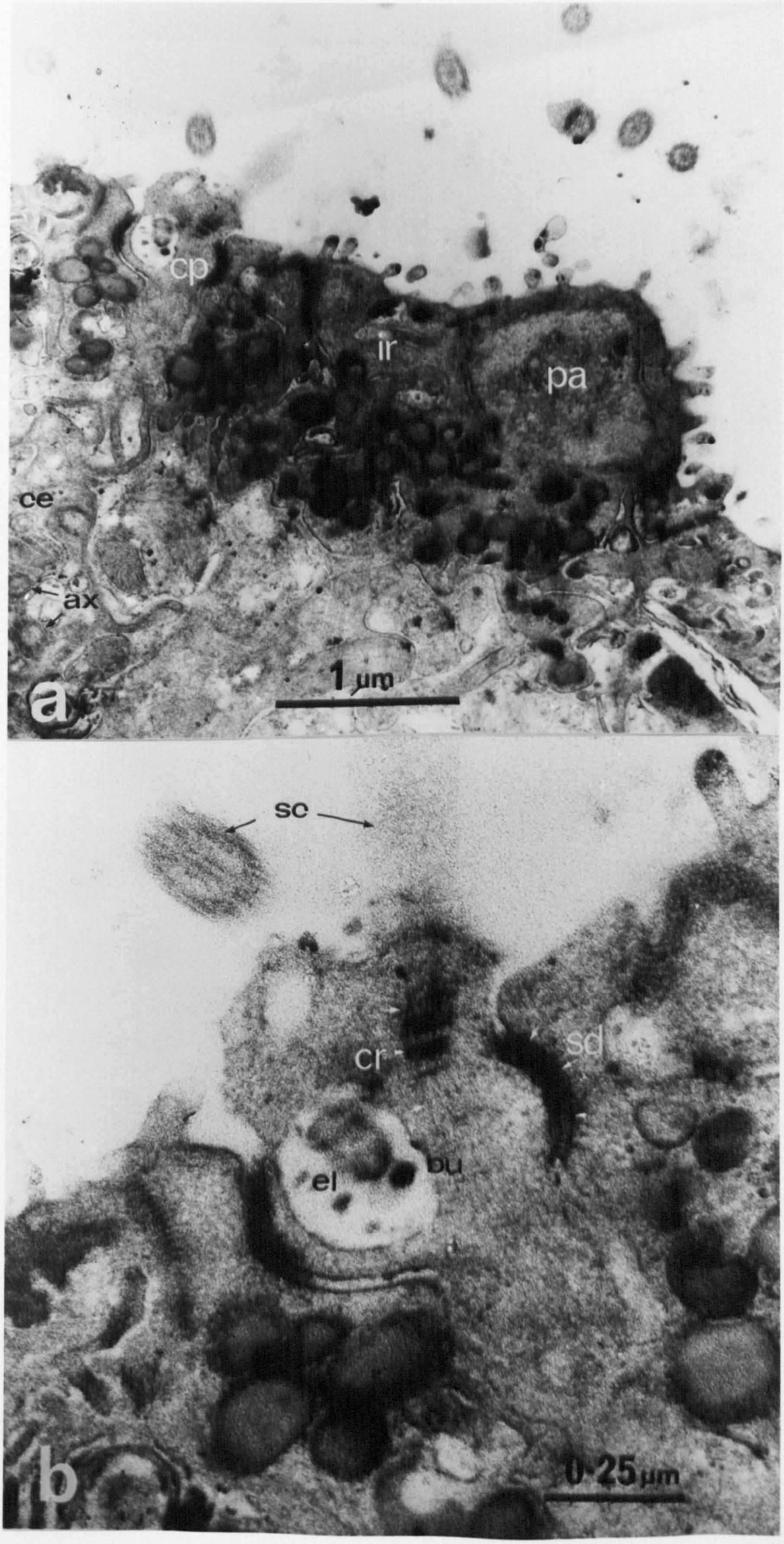
cp
ir
pa
ce
ax
1 µm
a
sc
cr
sd
el
bu
0·25µm
b

Plate 8: T.E. micrographs of miracidial sensory endings.

a) Body wall of miracidium showing uniciliate sensory ending (uc) in intercellular ridge (ir) with subjacent sub-epithelial cell body (sb) containing a nucleus (nu).

b) Uniciliate sensory ending. The sensory cilium (sc) projects through an intercellular ridge collar (ic). The bulb (bu) is attached to the intercellular ridge membrane by a septate desmosomal ring (sd).

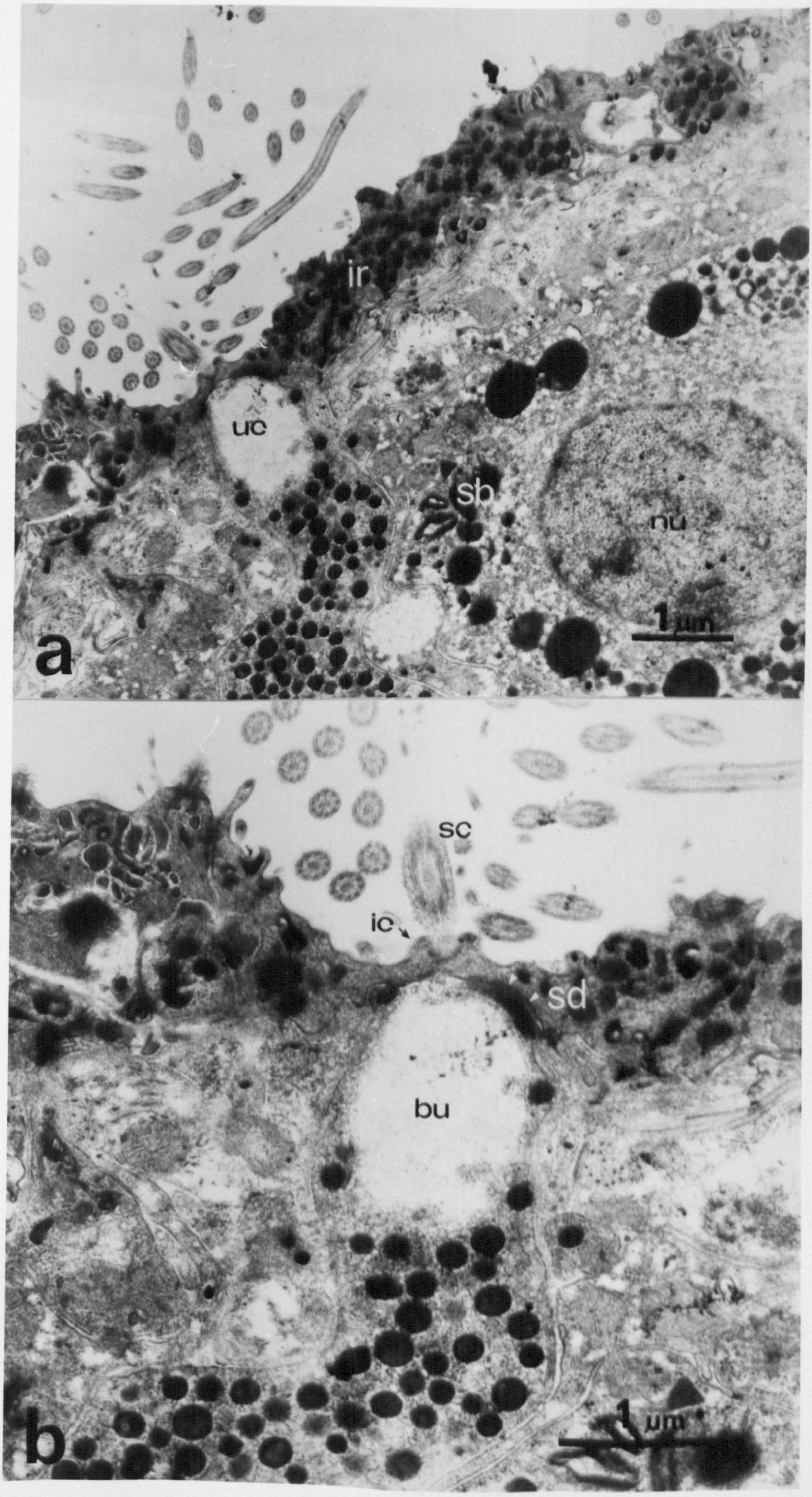
ir
uc
sb
nu
1 µm
a
sc
ic
sd
bu
1 µm
b

Plate 9: T.E. micrographs of miracidial protonephridial tubules.

a) Tubule cell. The nucleated tubule cell (tc) has two lateral transverse sections of tubules (tu) in this section.

b) Tubule structure. The lumen of the tubule is apparently enclosed by two cytoplasmic flaps (cf) joined with a septate desmosome (sd).

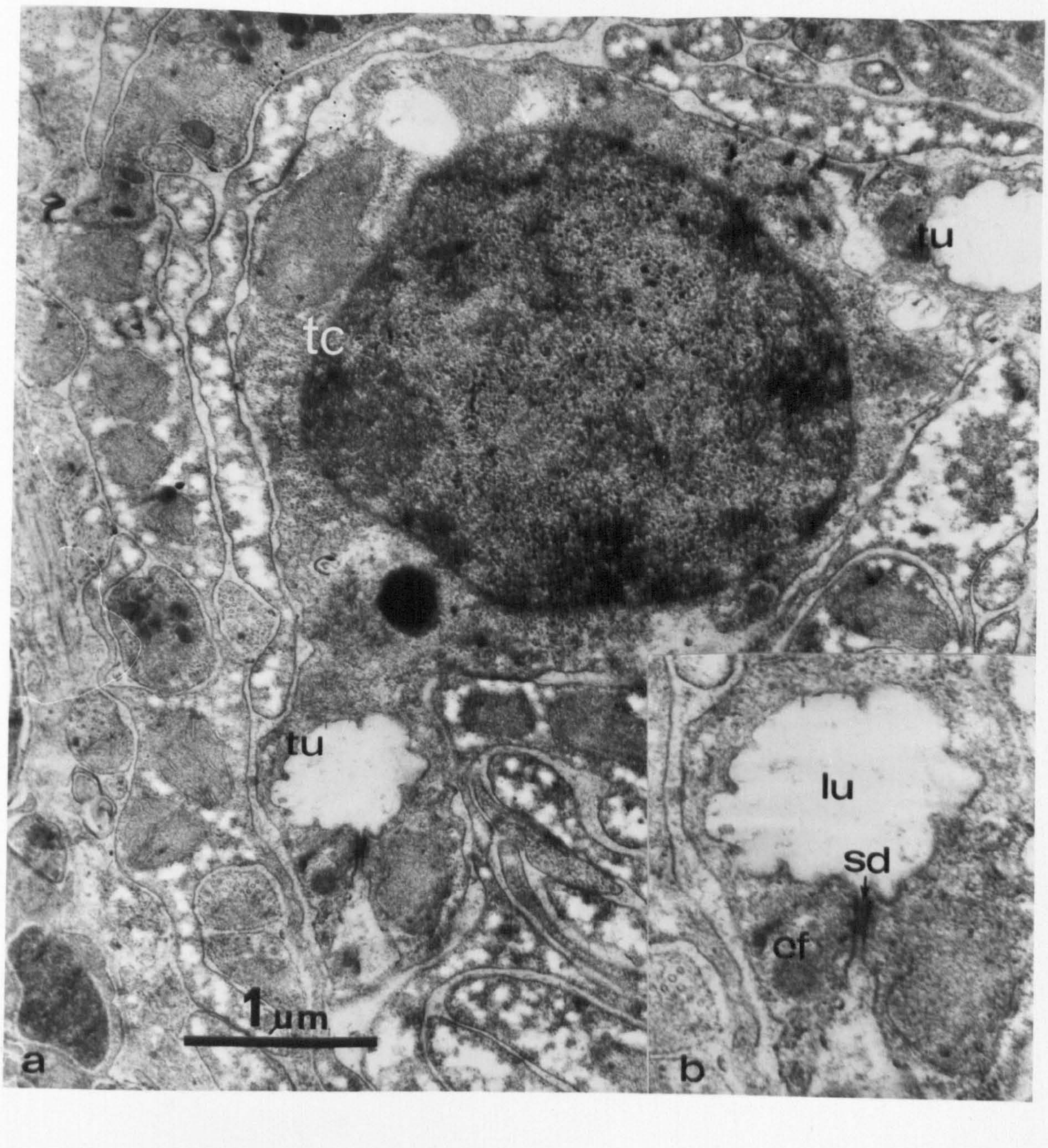
tc
tu
tu
lu
sd
cf
1 µm
a
b

Plate 10: T.E. micrographs of miracidial protonephridial tubule.

a) Protonephridial tubule. In this section two septate desmosomal junctions (sd) are discernable in the tubule wall.

b) Projections (pr) of the tubule wall cytoplasm are enclosed by the trilaminate plasma membrane (tp) of the tubule wall. A septate desmosome (sd) connects two flaps of cytoplasm to enclose the tubule lumen (lu).

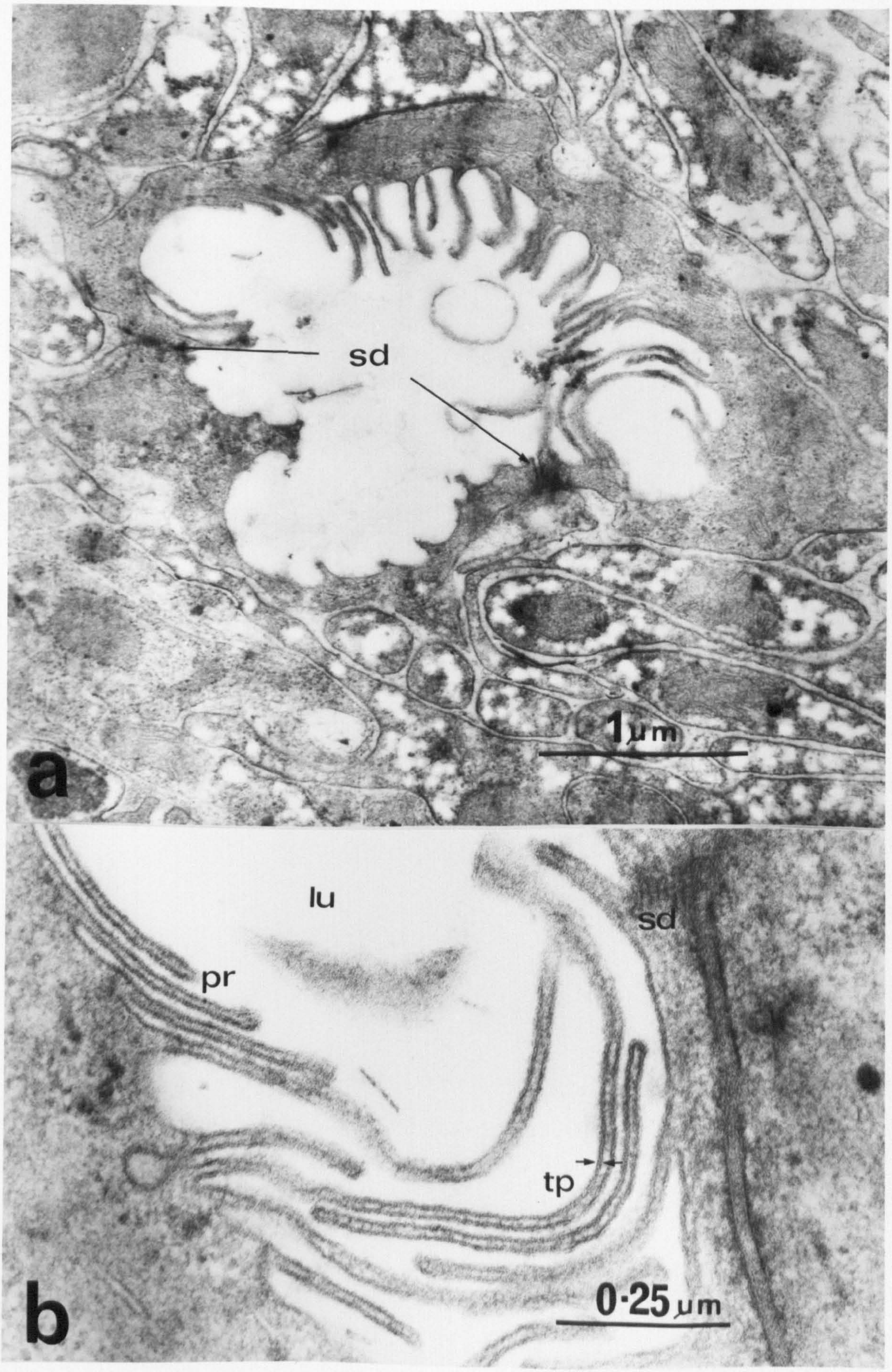
sd
1µm
a
lu
pr
sd
tp
0·25 µm
b

Plate 11: Micrographs of the egg surface and sporocyst.

a)-d) T.E. micrographs of egg capsule surface showing extensions (ex) each projecting from an individual boss (bo).

e) Light micrograph of 7 day old sporocyst in muscular tissues of the snail foot. Germinative cells (ge) and ocelli (o) can be distinguished.

Scale bars: a) 0.5 μm;

b) 0.1 μm;

c) and d) 0.5 μm;

e) 10 μm.

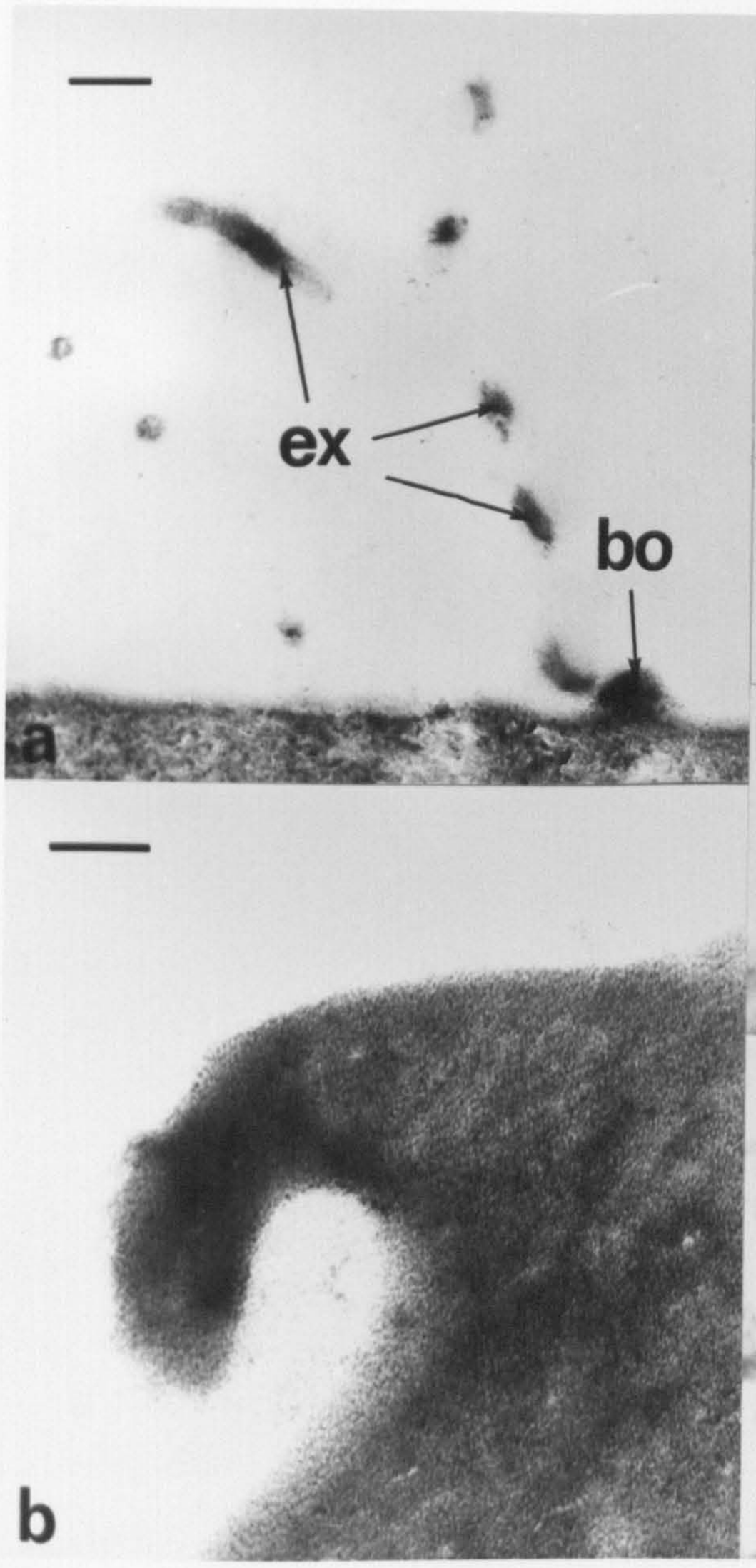
ex
bo
a
b

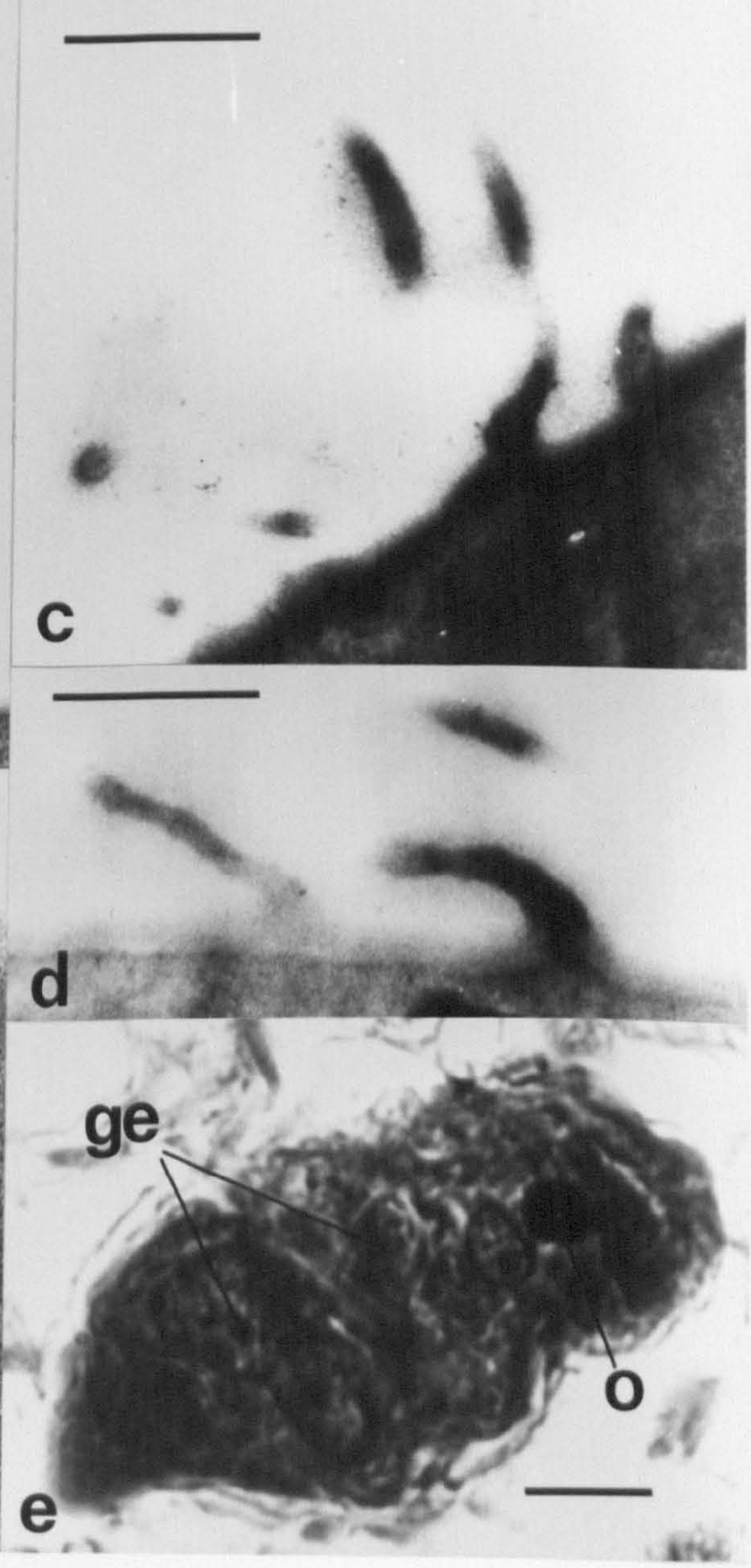
c
d
ge
o
e

Plate 12: S.E. micrographs of redia.

a) Lateral view showing numerous surface projections (pr) and caudal extension (ex)

Scale bar = 100 μm.

b) Anterior view showing muscular pharynx (ph)

Scale bar = 50 μm.

c) Surface projection.

Scale bar = 10 μm.

d) Microplicae (mp) on body surface.

Scale bar = 2 μm.

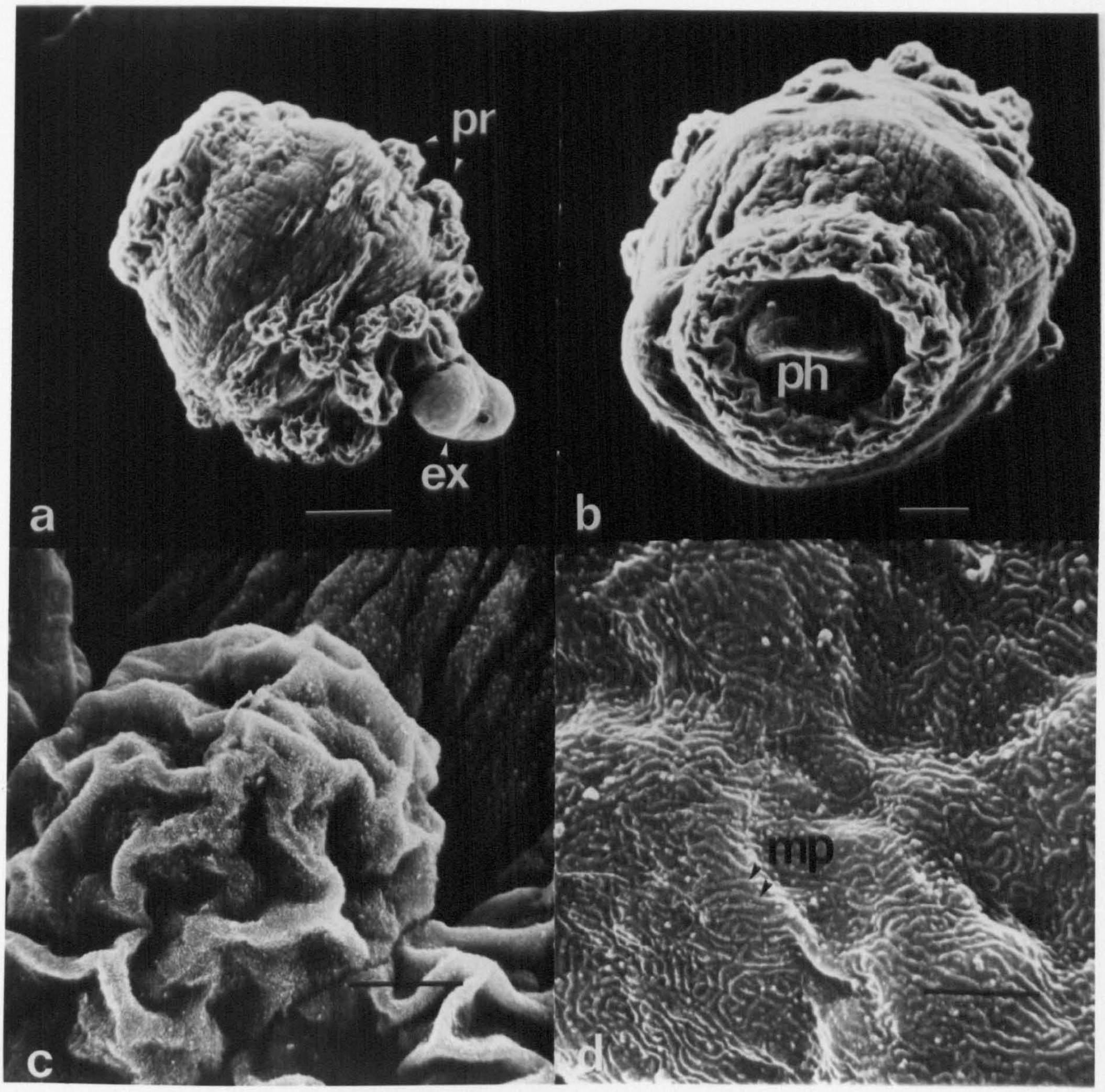
pr
ex
a
ph
b
mp
c
d

Plate 13: S.E. micrographs of Type One cercaria.

a) Regional differentiation into tail stem (ts), ventral sucker (vs) and pharynx (ph).

Scale bar = 30μm.

b) Pharynx primordium.

Scale bar = 5μm.

c) Ventral sucker primordium.

Scale bar = 10μm.

d) Microplicae (mp) on body surface.

Scale bar = 1μm.

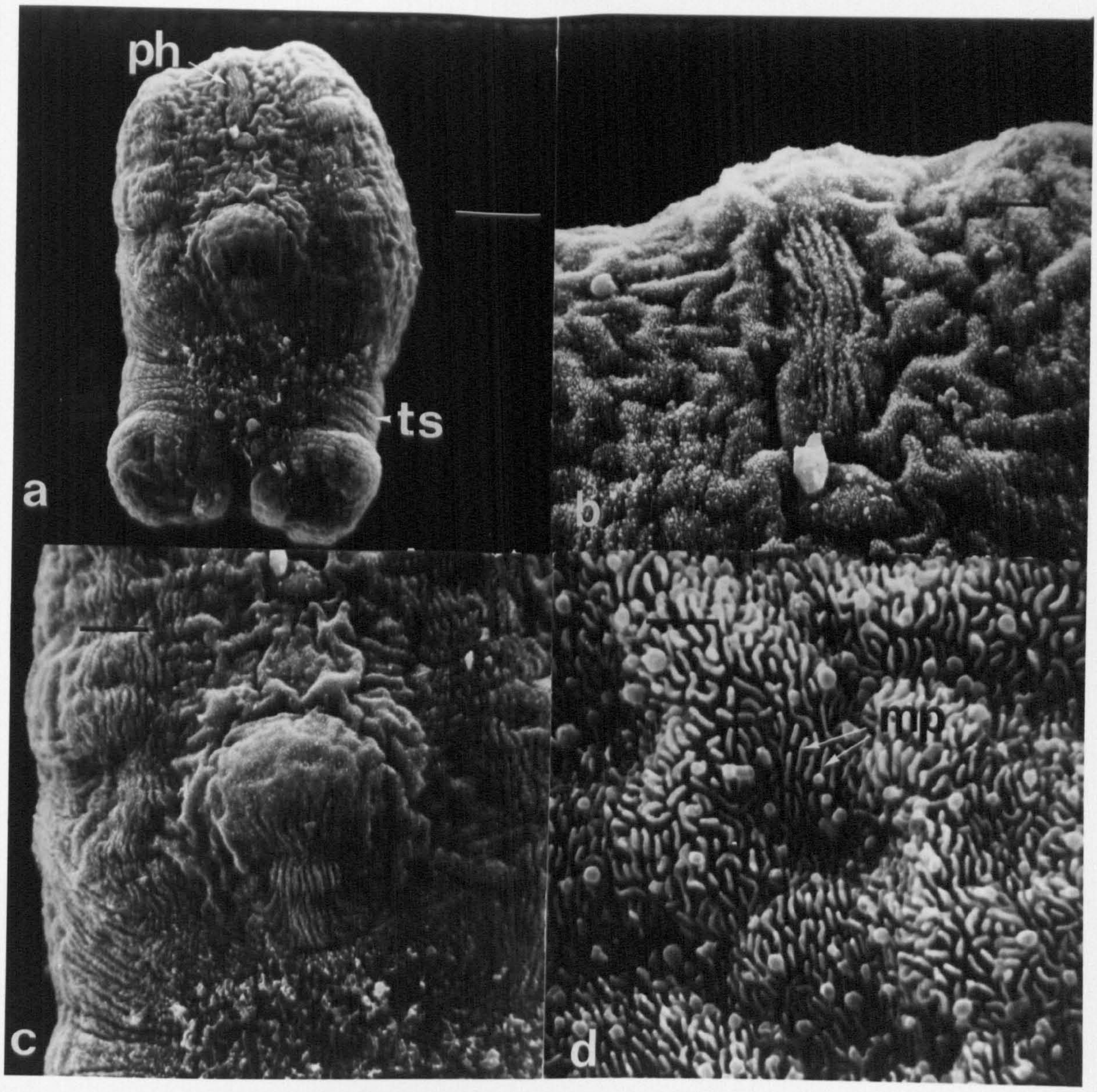
ph
ts
a
b
c
mp
d

Plate 14: S.E. micrographs of early Type Two cercaria.

a) Regional differentiation into tail stem (ts), furcae (fu) and ventral sucker (vs).

Scale bar = 50μm.

b) Pharynx.

Scale bar = 3μm.

c) Ventral sucker.

Scale bar = 5μm.

d) Microplicae (mp) on body surface.

Scale bar = 1μm.

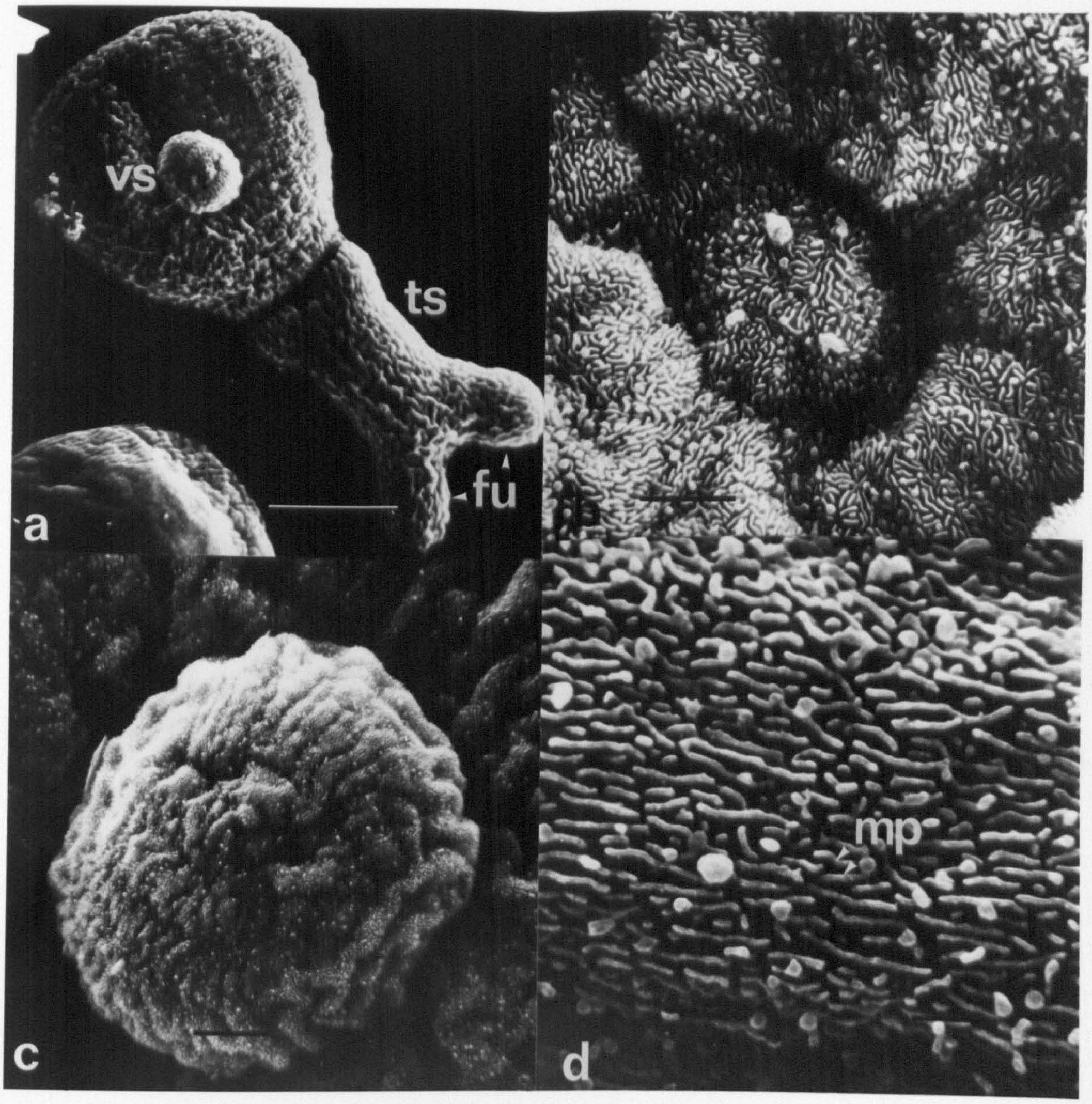
vs
ts
fu
a
c
d
mp

Plate 15: S.E. micrographs of late Type Two cercaria.

a) Regional differentiation into furcae (fu), ventral sucker (vs), tail stem (ts) and primordial arm processes (pr).

Scale bar = 250μm.

b) Pharynx.

Scale bar = 2.5μm.

c) Ventral sucker.

Scale bar = 5μm.

d) Microplicae (mp) on body surface.

Scale bar = 1μm.

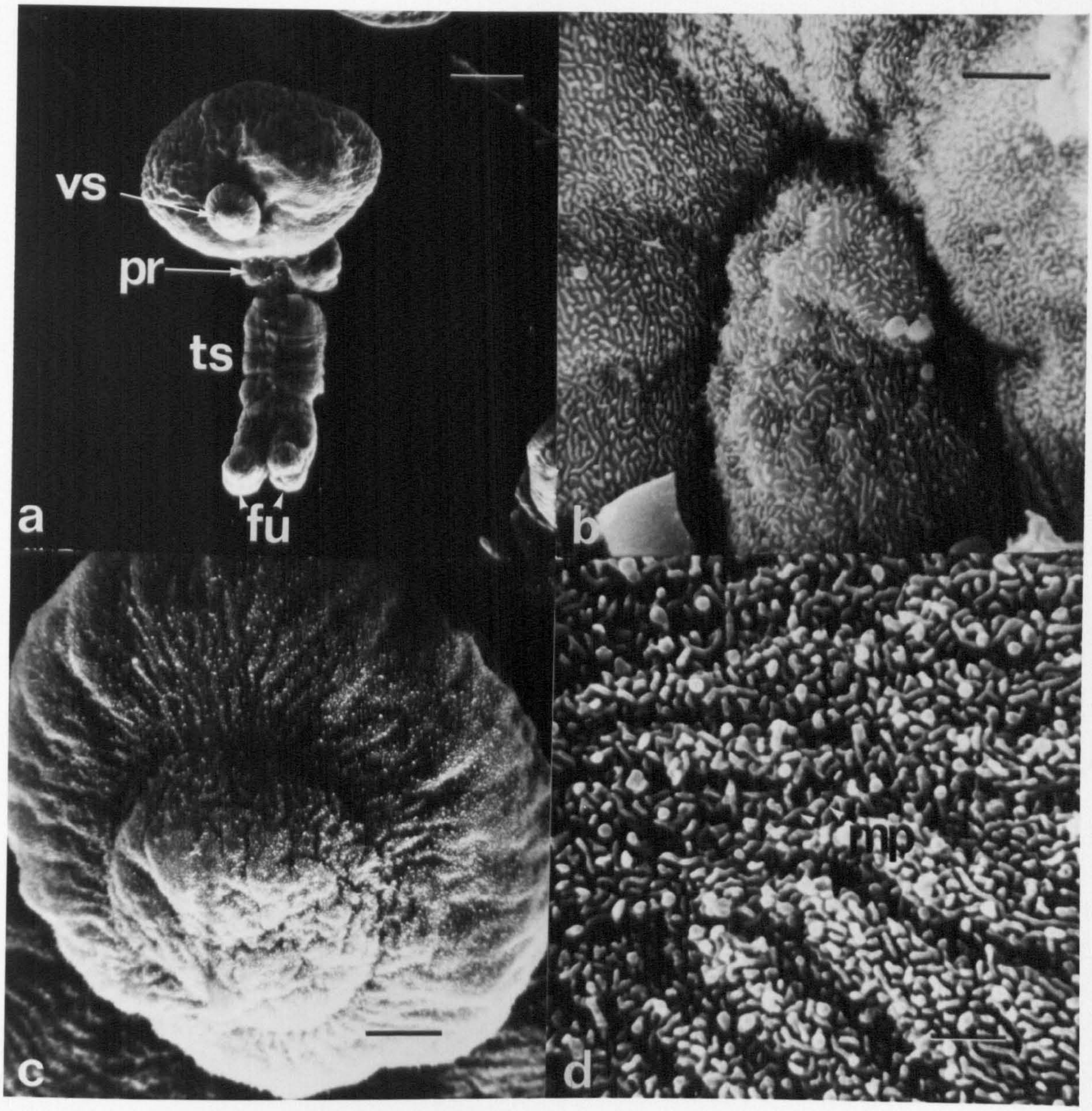
vs
pr
ts
fu
a
b
c
d
mp

Plate 16: S.E. micrographs of ventral surface of Type Three cercaria.

a) Aspinose ventral sucker of early Type Three cercaria. Scale bar = 10μm.

b) Ventral sucker of late Type Three cercaria with peripheral palisade (pp) of spines, marginal valve (mv) and sensory endings (black arrows). Scale bar = 10μm.

c) Body surface of early Type Three cercaria in which spines (si) are present together with microplicae (mp). Scale bar = 2.5μm.

d) Body surface of late Type Three cercaria with spines (si) and surface corrugations (su). Scale bar = 1μm.

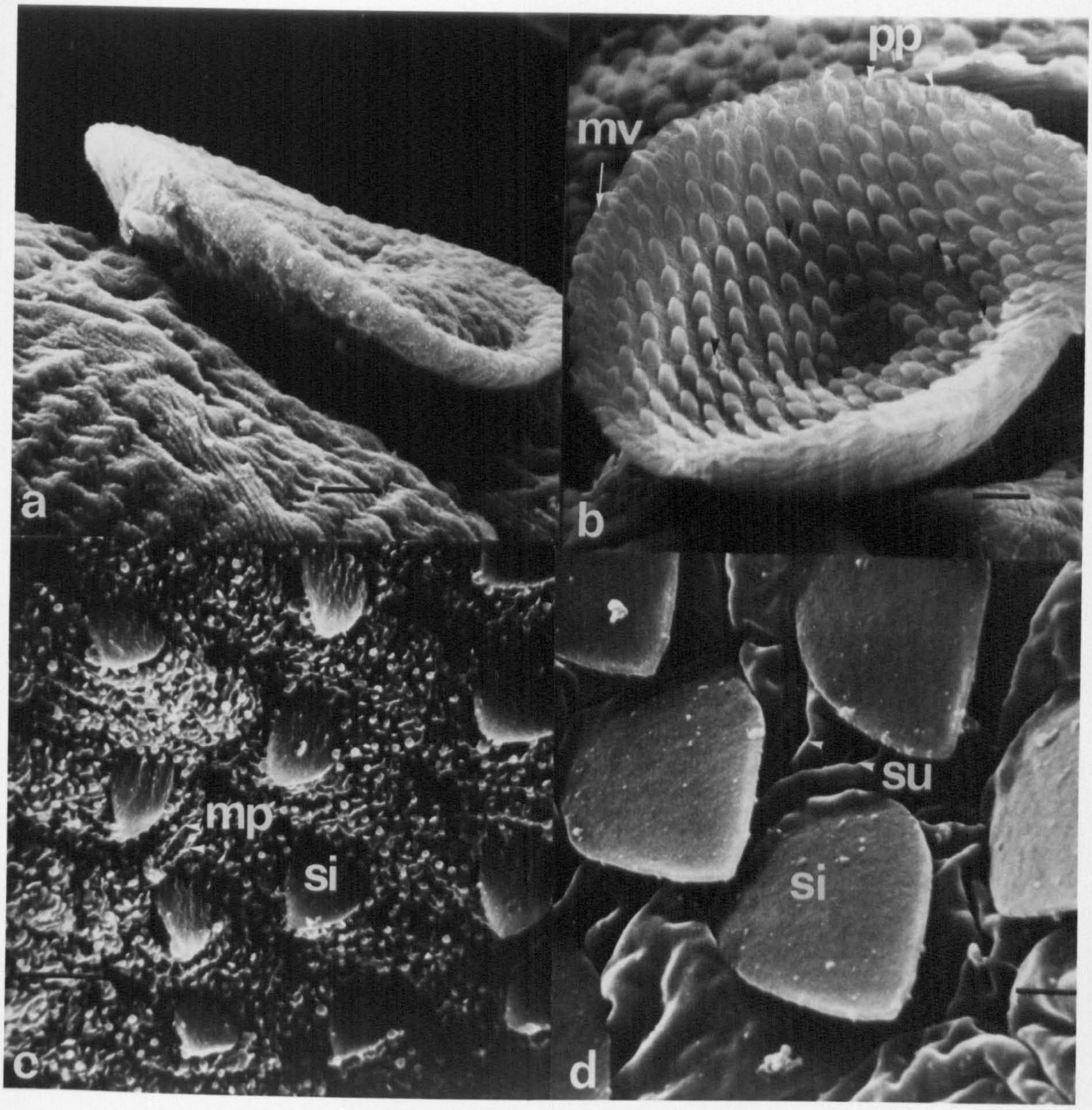
a
pp
mv
b
mp
si
c
su
si
d

Plate 17: S.E. micrographs of adult fluke/host interface.

a) Surface of fish host beneath scale. The superficial mucus surface shows the imprint of the ventral sucker (vs) and spines (si).
Scale bar = 50μm.

b) Imprint of ventral sucker. A ridge of mucus (rm), presumably due to pharynx activity, is located anterior to the circumferential margin (vm) of the ventral sucker imprint.
Scale bar = 30μm.

c) Ventral surface of adult fluke showing the surface features, such as the pharynx (ph) and ventral sucker (vs), which produced the imprint in (a) above.
Scale bar = 20μm.

d) Ventral surface of adult fluke showing the relationship of the pharynx (ph) to the ventral sucker which produced the imprint in (b) above.
Scale bar = 10μm.

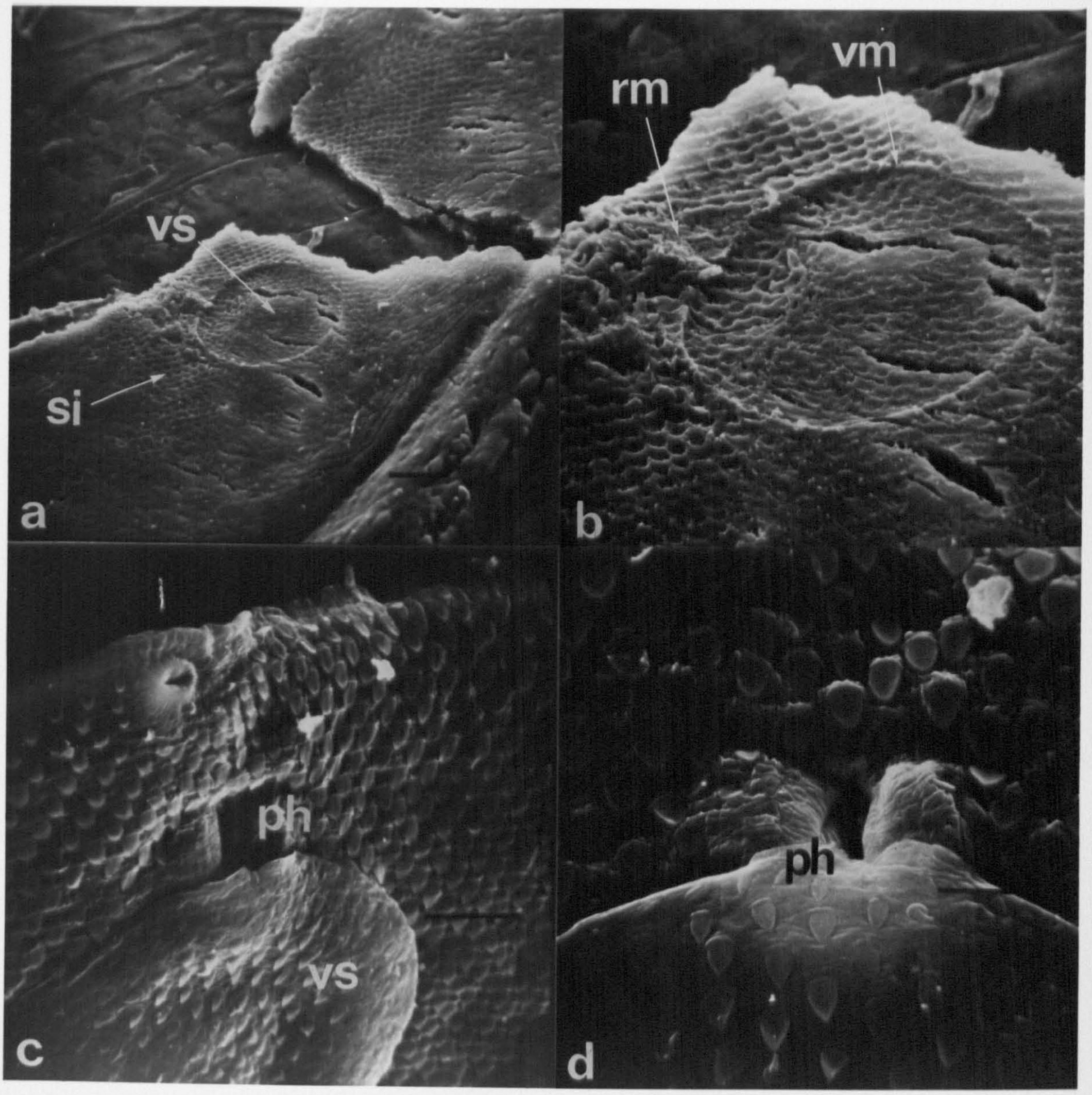
vs
si
a
rm
vm
b
ph
vs
c
ph
d

Plate 18: S.E. micrographs of genital pore of adult.

a) Genital pore (gp).

Scale bar = 5 μm.

b) and c) Genital pore distended during emergence of egg (eg).

Scale bar = 10 μm.

d) Sperm (sm) issuing from genital pore.

Scale bar = 20 μm.

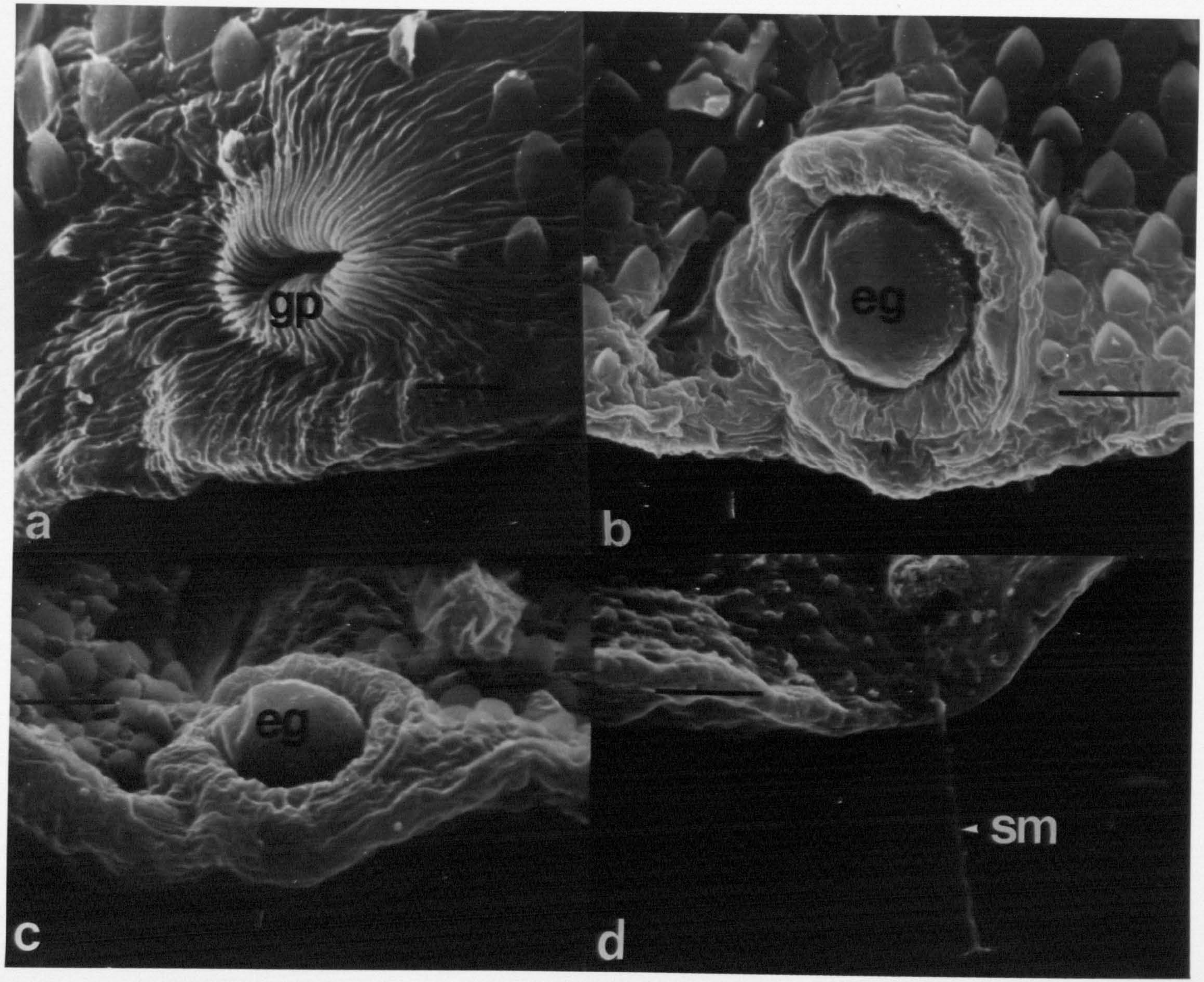
gp
a
eg
b
eg
c
sm
d

Plate 19: S.E. micrographs of decaudate cercaria (= young adult).

a) Posterior view showing decaudation lesion (dl).

Scale bar = 100 μm.

b) Decaudation lesion with characteristic circumferential sub-tegumental sphincter (cs).

Scale bar = 20 μm.

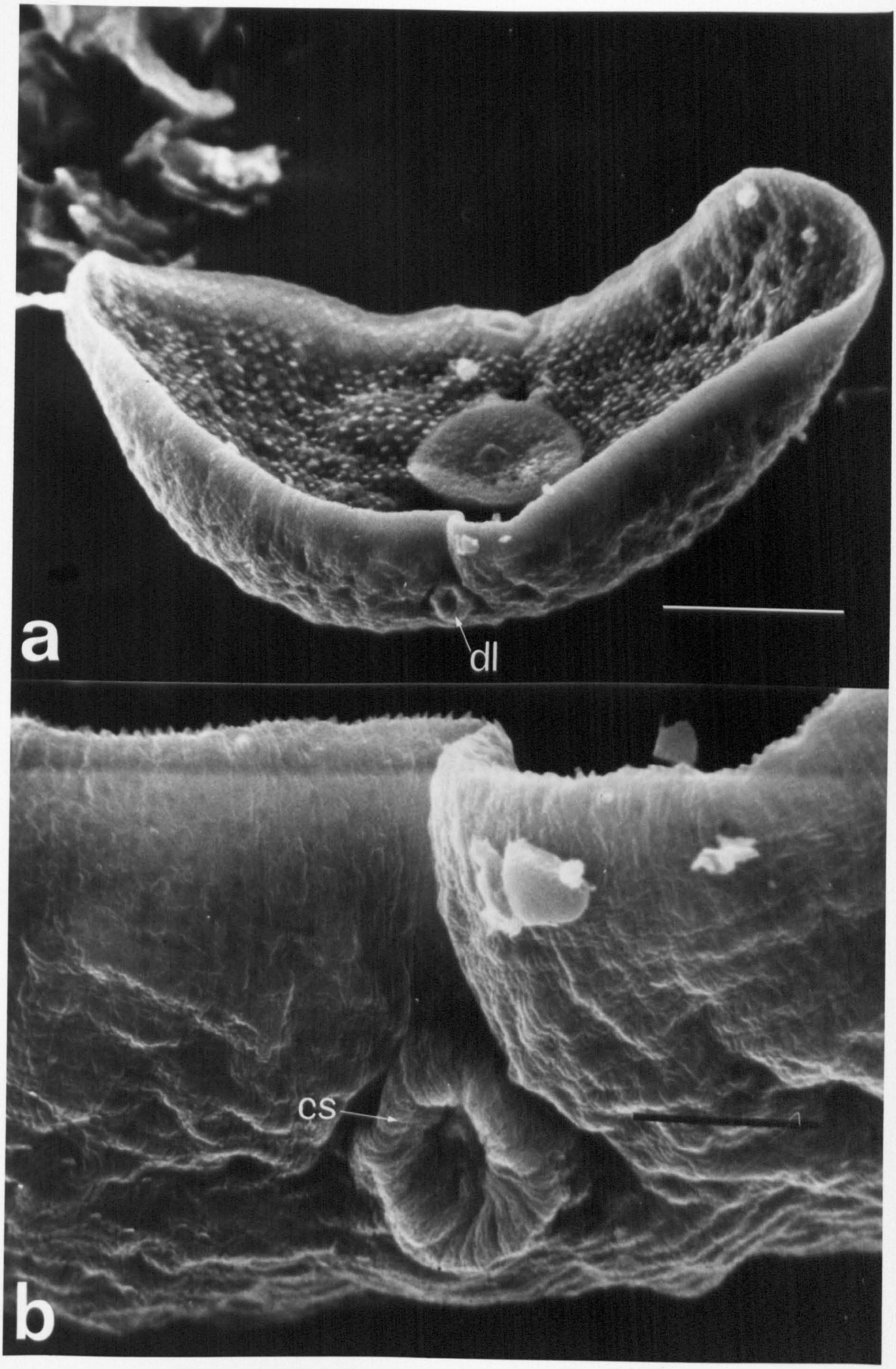
a
dl
cs
b

Plate 20: S.E. micrographs of dorsal surface of adult.

a) Adult displaced from location beneath fish scale.

The relatively smaller size of posterior spines may be discerned.

Scale bar = 100 μm.

b) Spine rows on dorsal surface.

Scale bar = 10 μm.

c) Laurer's canal aperture (lr) on dorsal surface.

Scale bar = 40 μm.

d) Dorsal surface showing gradation from large spines anteriorly (top) to small spines posteriorly.

Scale bar = 100 μm.

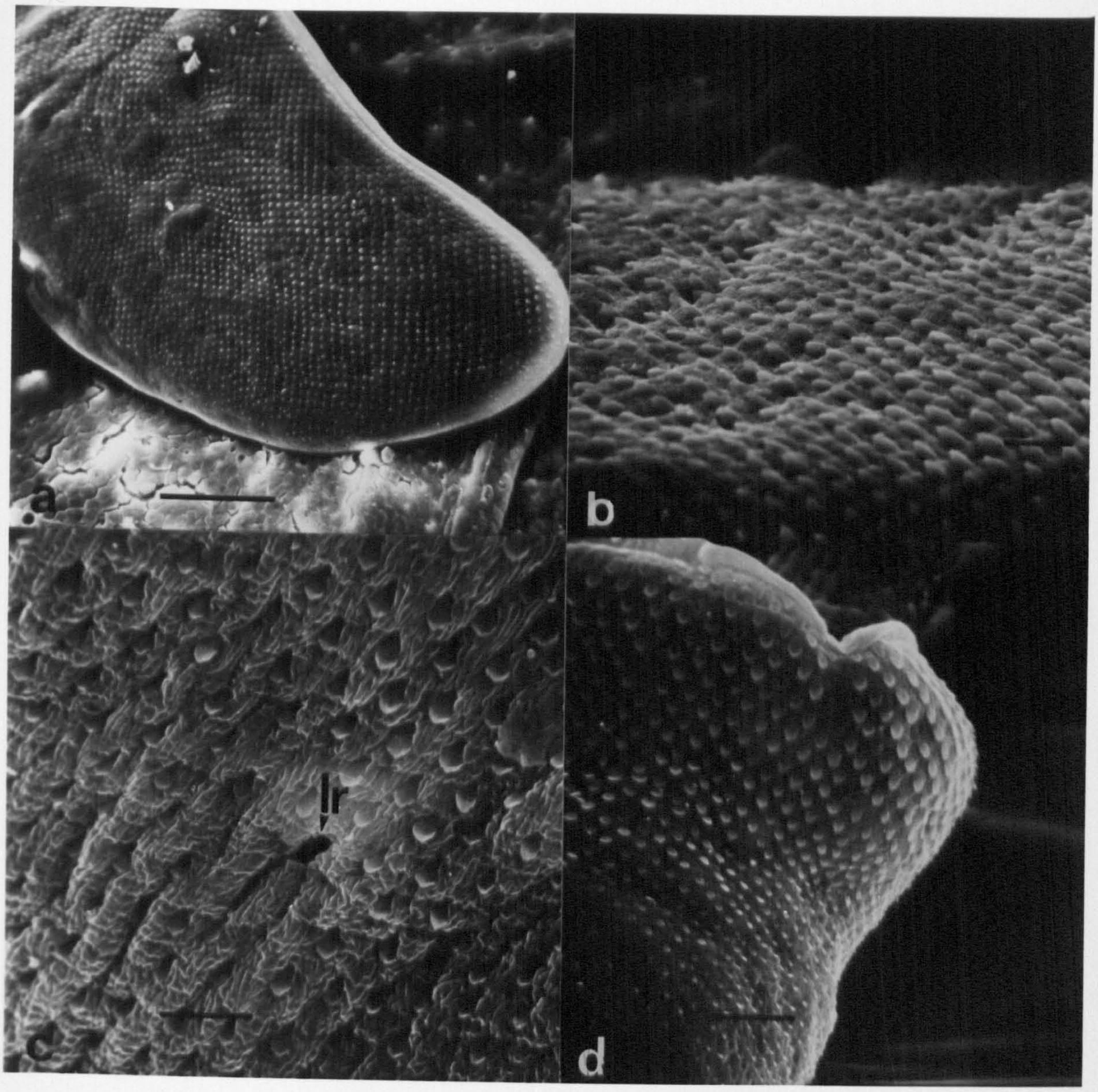
a
b
c
lr
d

Plate 21: T.E. micrograph of body wall of Type One cercaria. Surface syncytium bounded by trilaminate apical plasma membrane (am) and basal plasma membrane (bm). The surface is extended into microplicae (mp). A dense area may represent a pycnotic nucleus (pn) with associated unit membranes (white arrows). Ribosomes (ri) are scattered throughout the cytoplasm.

Scale bar = 0.2μm.

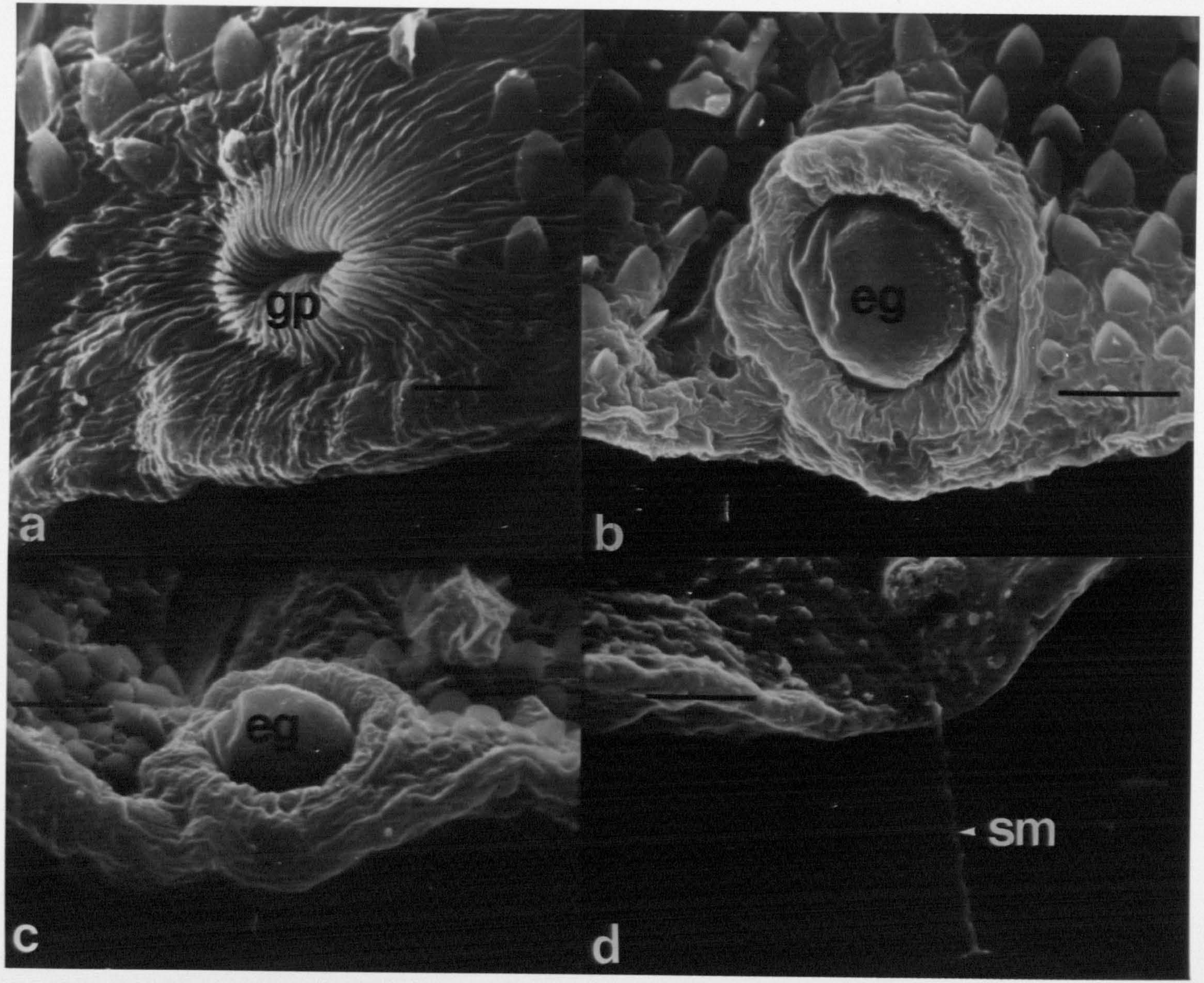
gp
a
eg
b
eg
c
sm
d

Plate 19: S.E. micrographs of decaudate cercaria (= young adult).

a) Posterior view showing decaudation lesion (dl).

Scale bar = 100 μm.

b) Decaudation lesion with characteristic circumferential sub-tegumental sphincter (cs).

Scale bar = 20 μm.

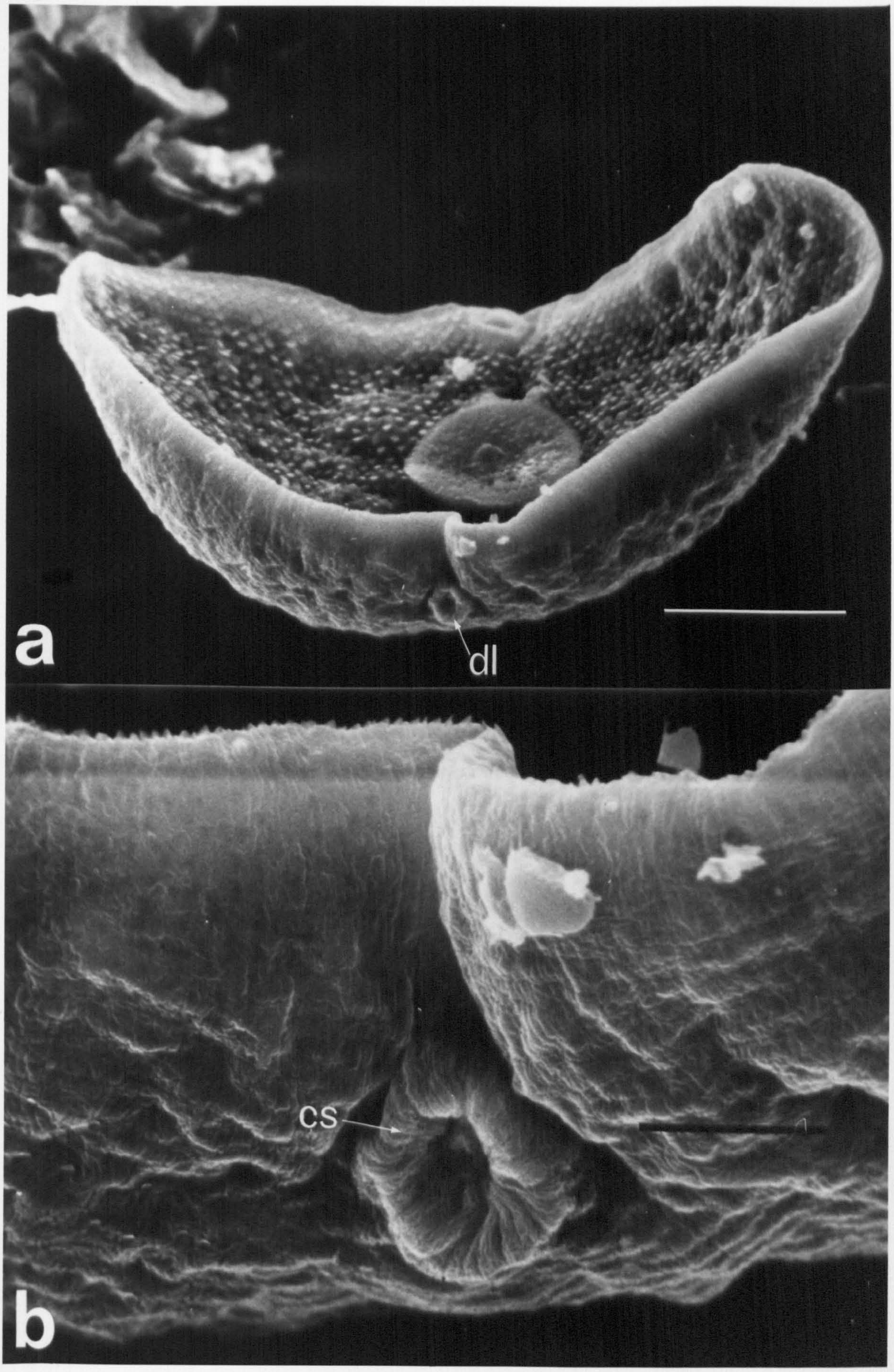
a
dl
cs
b

Plate 20: S.E. micrographs of dorsal surface of adult.

a) Adult displaced from location beneath fish scale.

The relatively smaller size of posterior spines may be discerned.

Scale bar = 100 μm.

b) Spine rows on dorsal surface.

Scale bar = 10 μm.

c) Laurer's canal aperture (lr) on dorsal surface.

Scale bar = 40 μm.

d) Dorsal surface showing gradation from large spines anteriorly (top) to small spines posteriorly.

Scale bar = 100 μm.

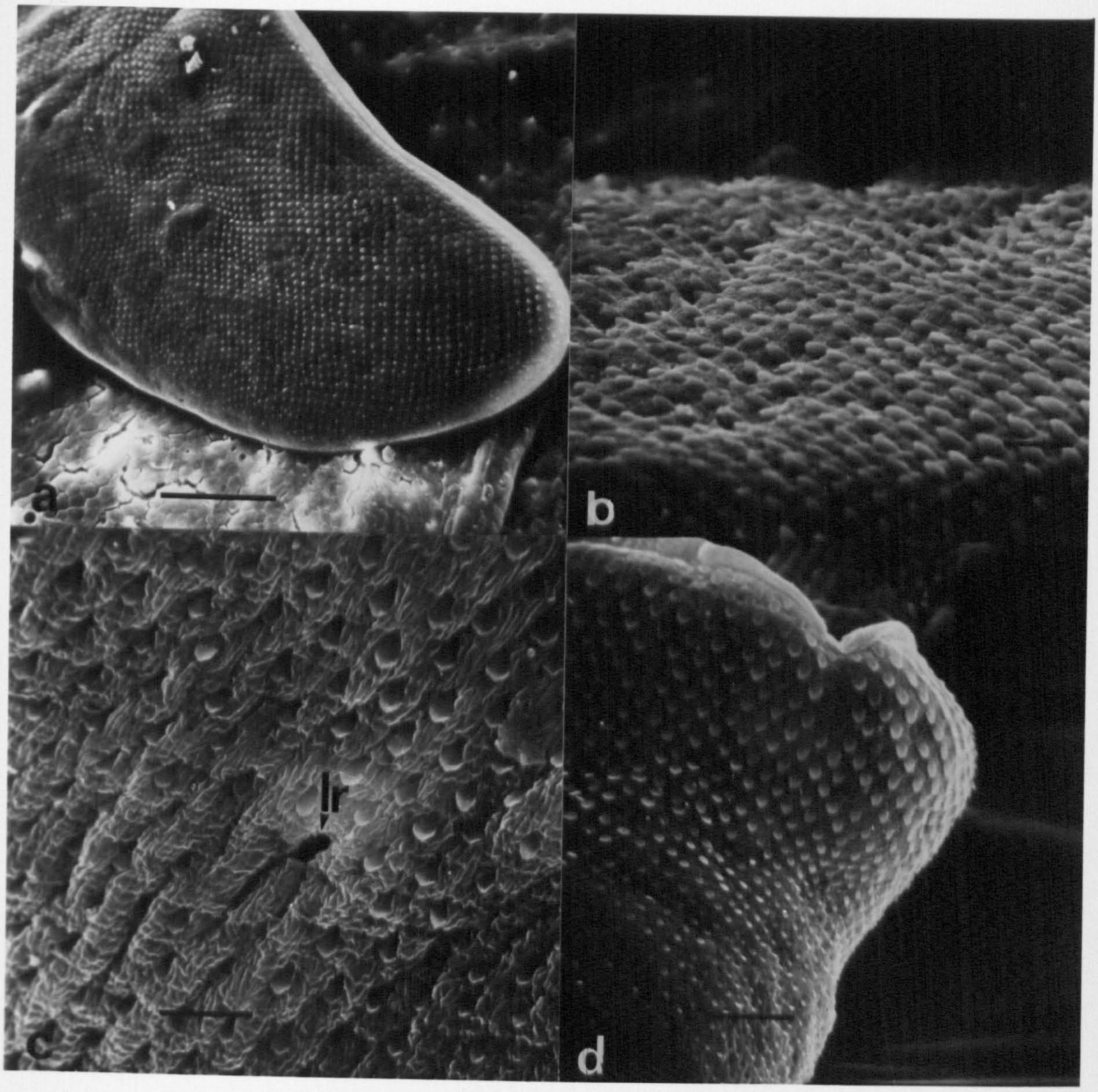
a
lr
b
c
d

Plate 21: T.E. micrograph of body wall of Type One cercaria. Surface syncytium bounded by trilaminate apical plasma membrane (am) and basal plasma membrane (bm). The surface is extended into microplicae (mp). A dense area may represent a pycnotic nucleus (pn) with associated unit membranes (white arrows). Ribosomes (ri) are scattered throughout the cytoplasm.

Scale bar = 0.2μm.

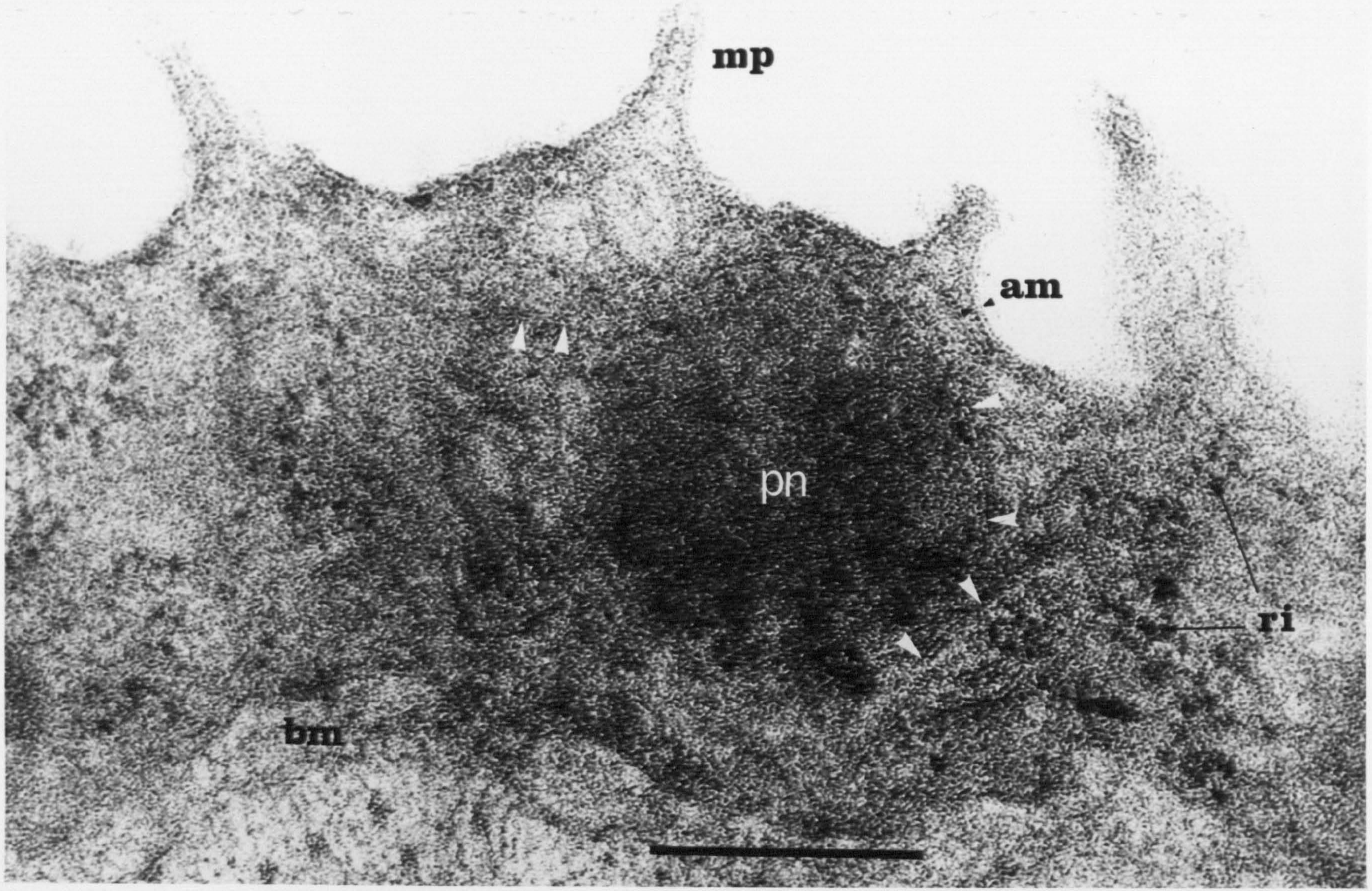
mp
am
pn
ri
bm

Plate 22: T.E. micrographs of the body wall of Type Two cercariae.

a) General section showing surface tegument (st) and cytoplasmic connective (cc). The surface tegument is covered by microplicae (mp) and enclosed by an apical plasma membrane (am) and basal plasma membrane (bm).

Scale bar = 0.5 μm.

b) Membranous whorl in surface tegument.

Scale bar = 0.2 μm.

c) Mitochondria (mi) in surface tegument.

Scale bar = 0.25 μm.

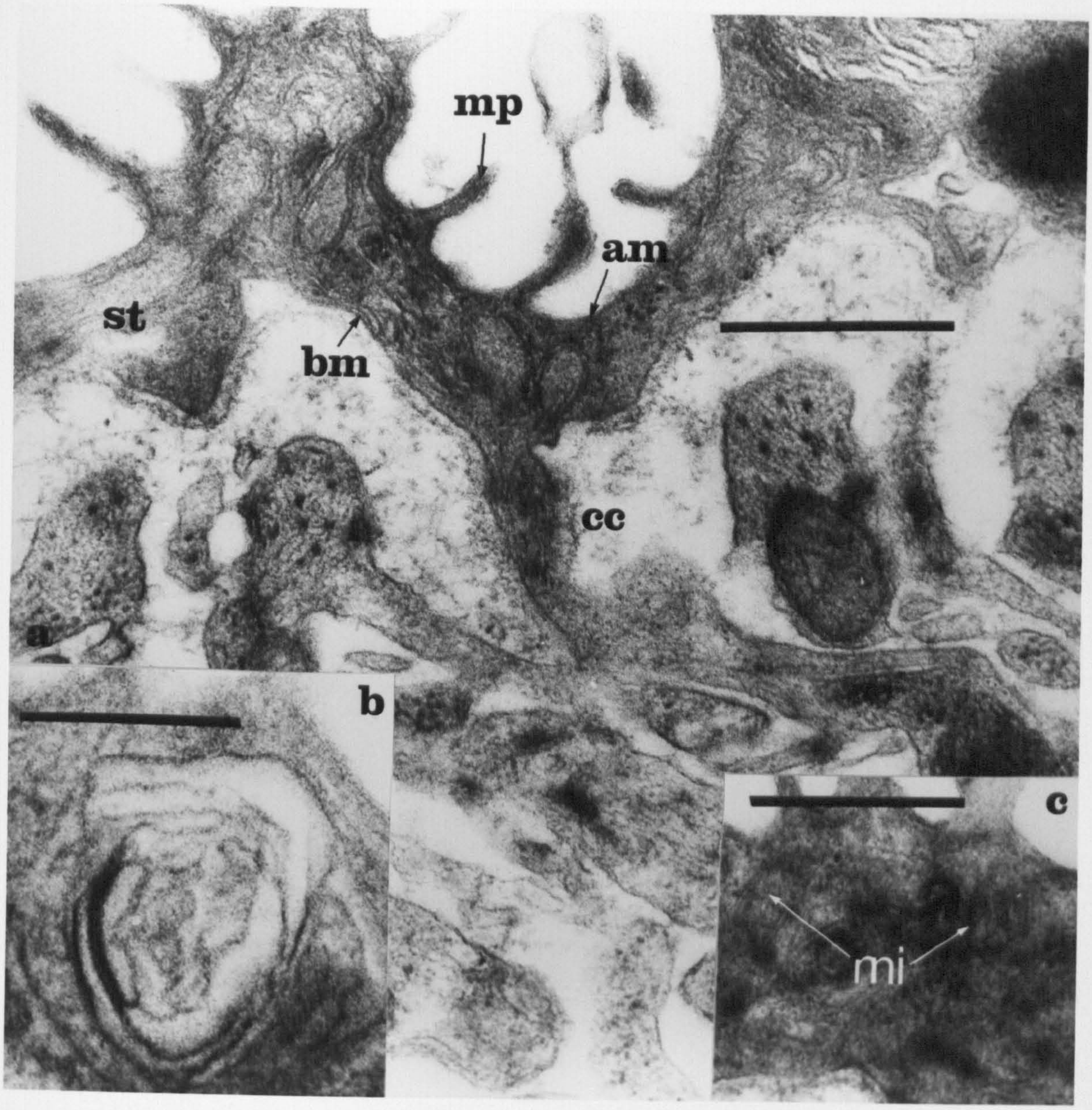
mp
am
st
bm
cc
a
b
c
mi

Plate 23: T.E. micrographs of spines in the tegument of Type Three cercariae.

a) Transverse section of spine (si) within the surface tegument (st). Surface tegument also contains a dense layer (dl) subjacent to the apical plasma membrane, electron lucent inclusions (ei) and mitochondria (mi). Beneath the surface tegument are circular muscle fibres (cf) and longitudinal muscle fibres (lf). A tegumental cell body (tb) contains electron lucent inclusions (ei) and a crystalline body (ry).

Scale bar = 2 μm.

b) Longtitudinal section of spine (si). The basal lamina (bl) of the surface tegument is denser in the region of the spine base (sb). A nucleate (nu) tegumental cell body contains mitochondria (mi).

Scale bar = 4 μm.

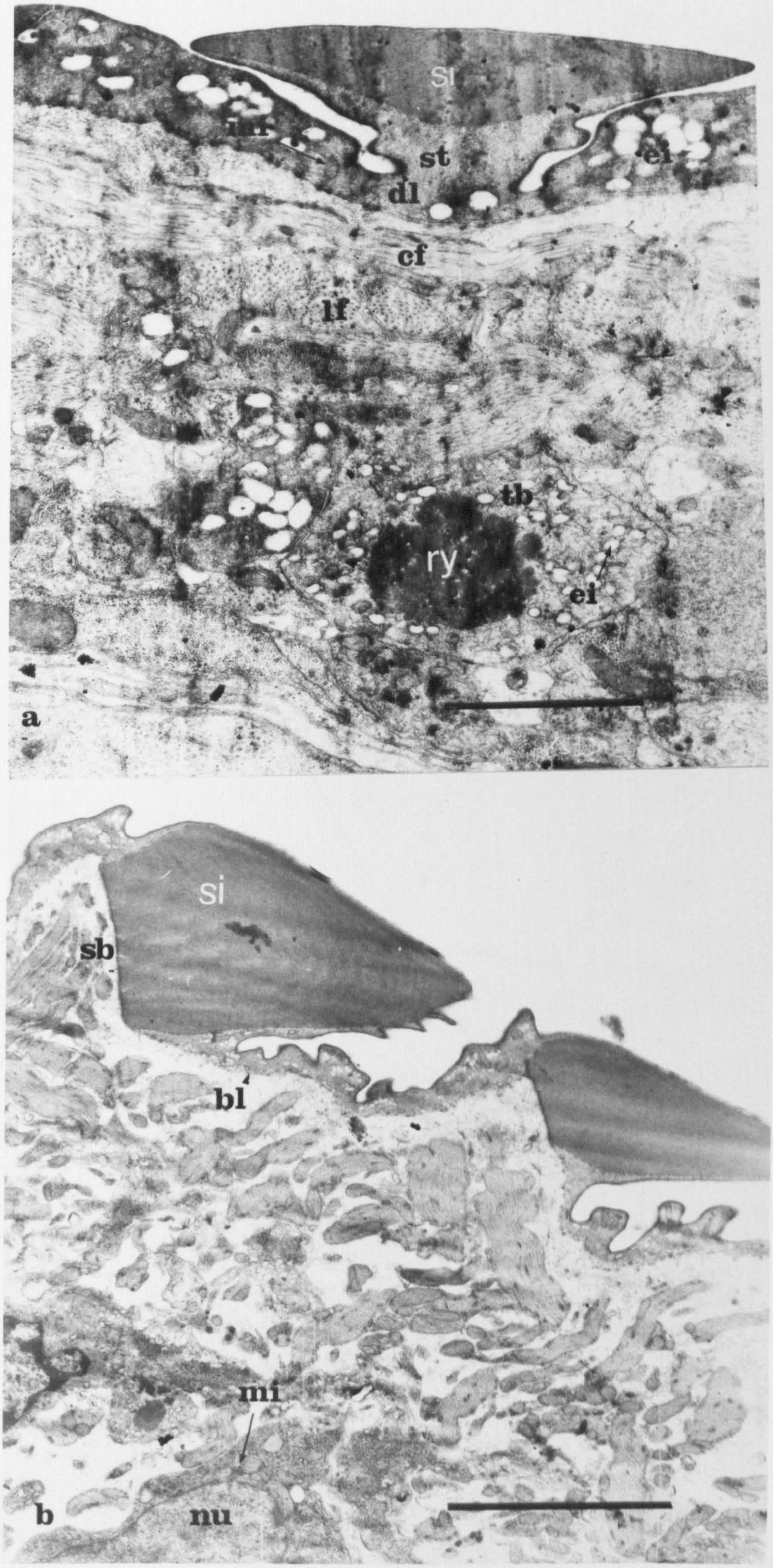
si
st
el
dl
cf
lf
tb
ry
ei
a
si
sb
bl
mi
b
nu

Plate 24: T.E. micrographs of tegument of Type Three cercariae.

a) Surface tegument (st) with cytoplasmic connective (cc). The membrane bound electron lucent inclusions (ei) are present in the surface tegument in a range of different forms. They undergo distortion (double arrows) during passage through the connective. A dense layer (dl) is present beneath the apical plasma membrane. The basal plasma membrane (bm) is attached to the basal lamina (bl) by hemidesmosomes (he). Subjacent to the basal lamina is a layer of interstitial matrix (im).
Scale bar = 1 μm.

b) Tegumental cell body containing a crystalline body (ry) with an irregular orientation of infrastructural components. Membrane bound electron lucent inclusions (ei) are present.
Scale bar = 0.5 μm.

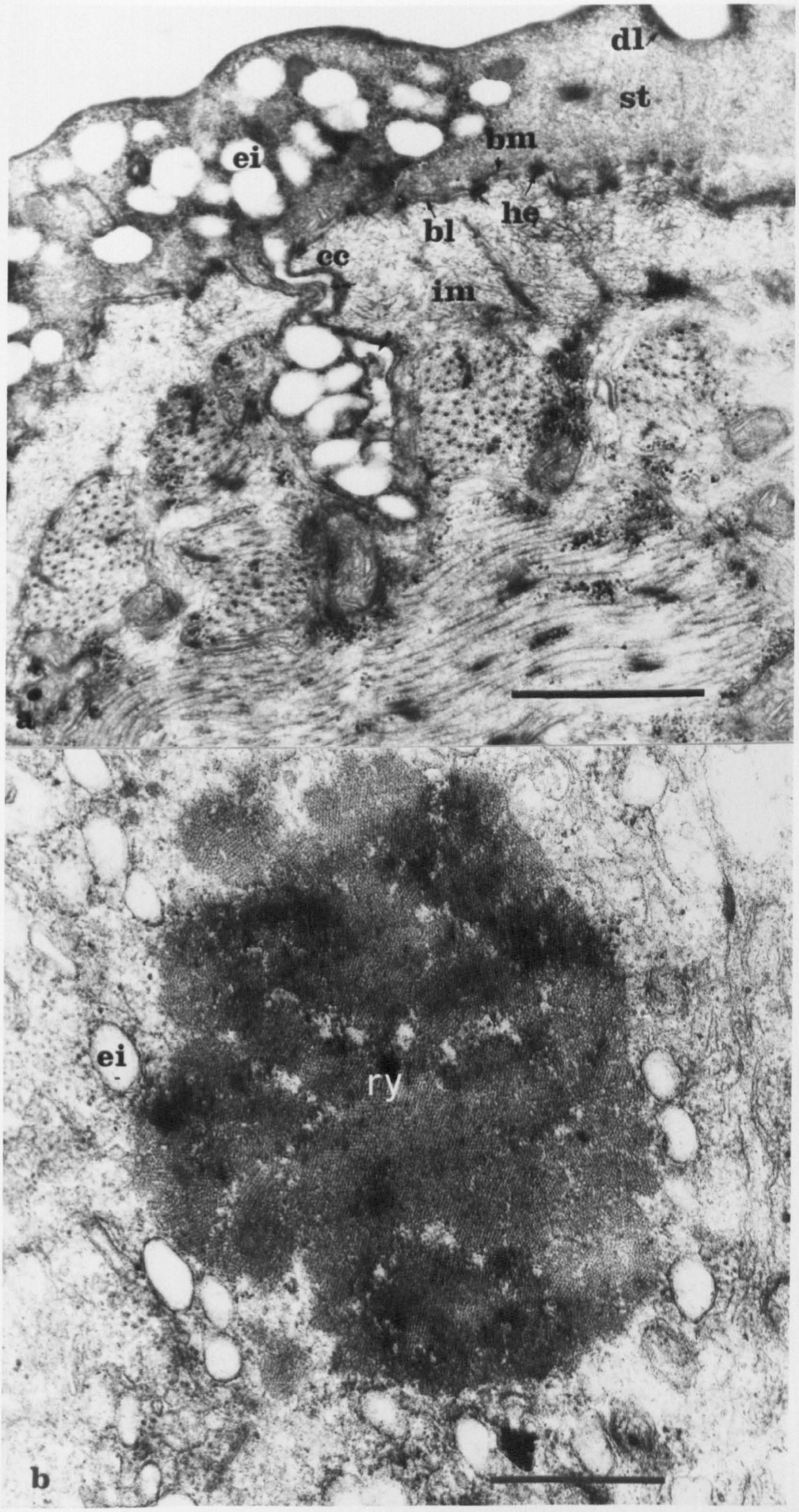
dl
st
bm
ei
he
bl
cc
im
ei
ry
b

Plate 25: T.E. micrographs of tegumental cell bodies of Type Three cercariae.

a) Dense bodies (db) surrounded by electron lucent inclusions (ei). Some inclusions appear to engulf dense material (1.) which may result in the apparent presence of a dense central core (2.). Arrays of ribosomes (ri) and a golgi complex (go) are present. Scale bar = 0.5 μm.

b) Dense bodies (db) are present together with a crystalline body (ry) which as an infrastructure differing from that shown in Plate 24b. Electron lucent inclusions again appear to engulf dense material (1.) apparently producing the anomalous appearance of other inclusions (2.).
Scale bar = 0.25 μm.

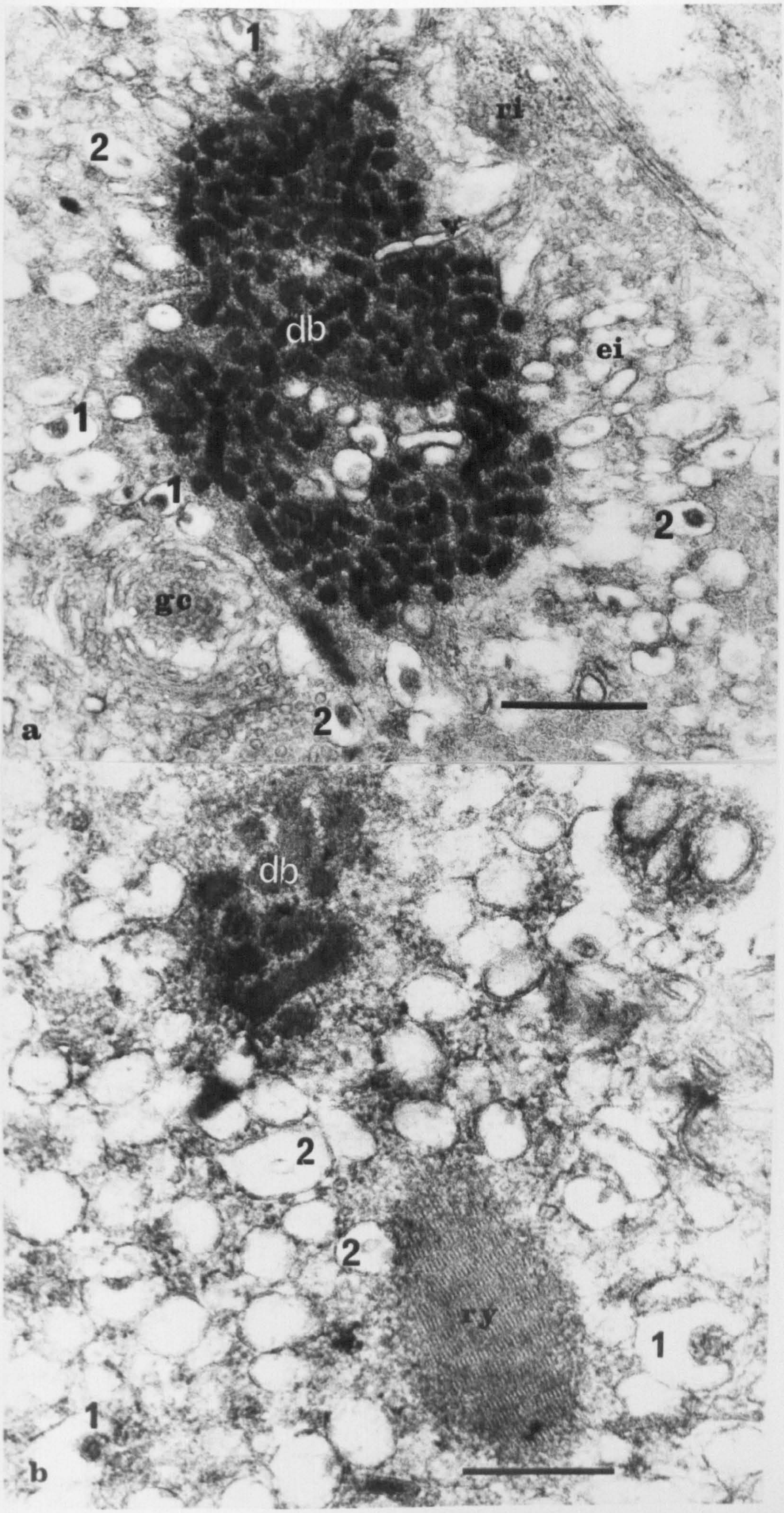
1
2
rl
db
ei
1
1
2
gc
2
a
db
2
2
ry
1
1
b

Plate 26: T.E. micrographs of body wall of adult.

a) Surface tegument (st) with cytoplasmic connective (cc). Few electron lucent inclusions (ei) are present in the surface tegument.
Scale bar = 2 μm.

b) Surface tegument with deep basal invaginations of basal plasma membrane.
Scale bar = 2 μm.

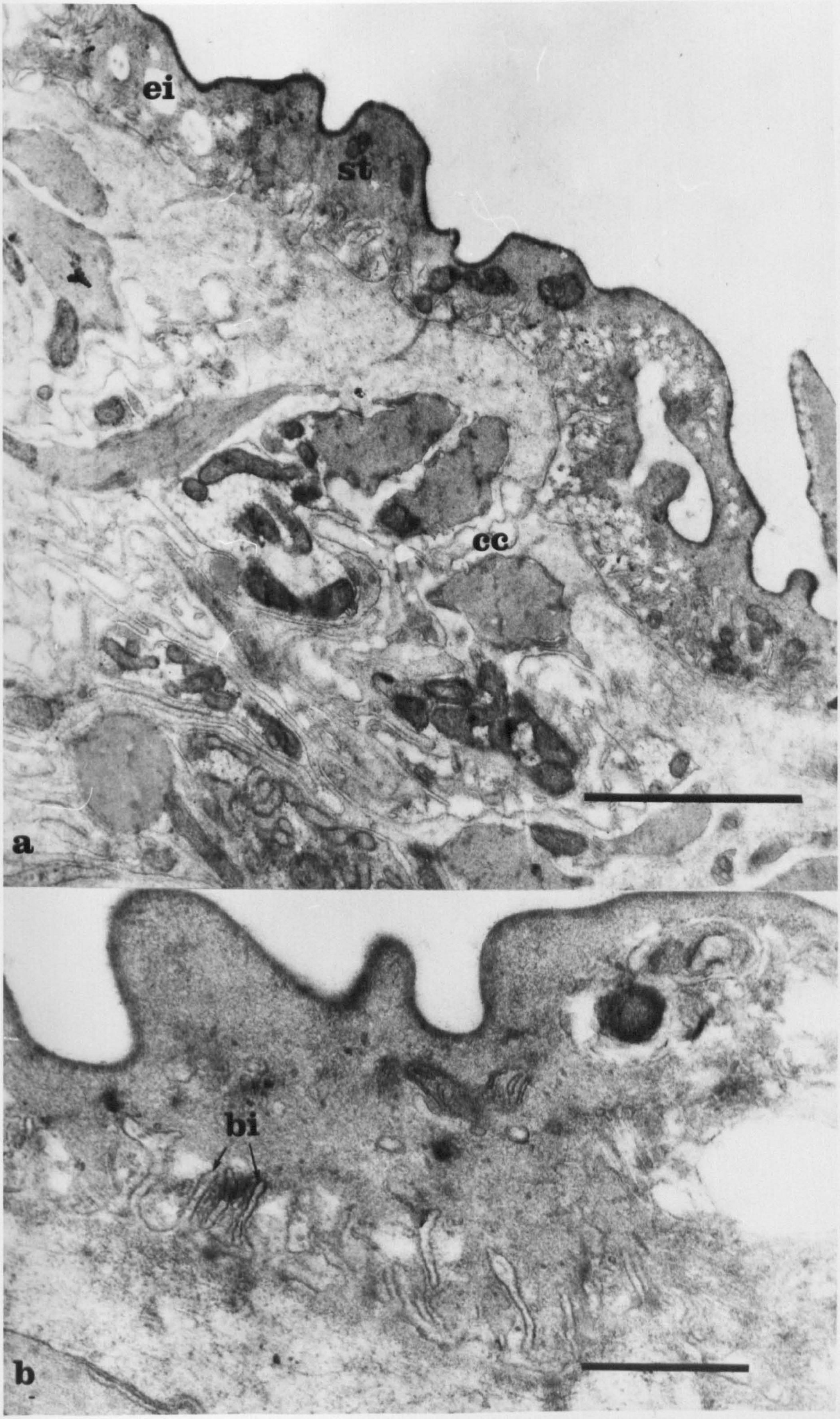
ei
st
cc
a
bi
b

Plate 27: T.E. micrographs of digestive tract of Type Three cercariae.

a) Region with tegumental lining.

Scale bar = 5μm.

b) Gastrodermal lining of gut. The gastrodermal cells have lateral junctions (gj) and contain both mitochondria (mi) and membrane bound granular inclusions (mg).

Scale bar = 5μm.

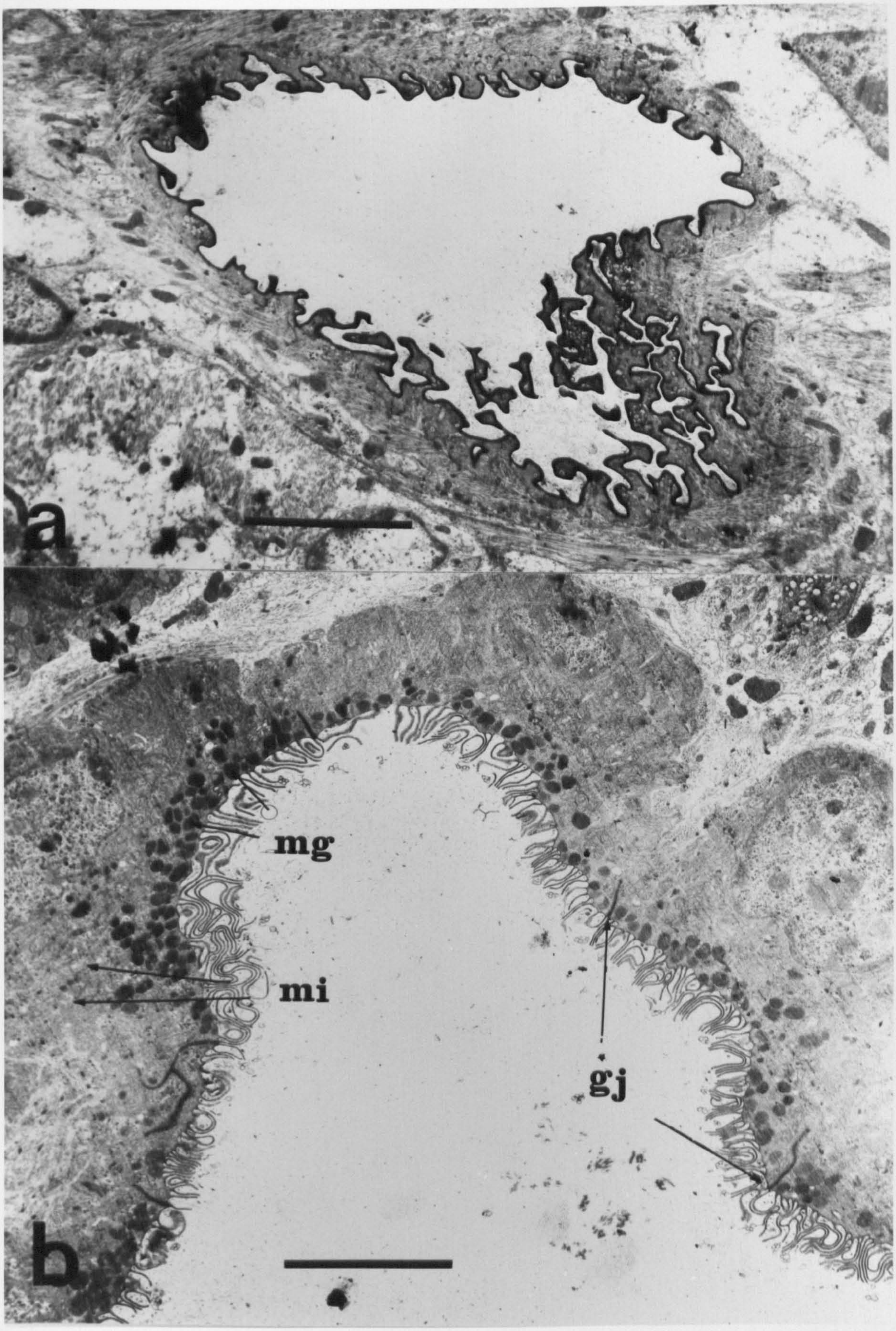
a
mg
mi
gj
b

Plate 28: T.E. micrographs of junction between tegument and gastrodermis of digestive tract of Type Three cercariae.

a) The gastrodermal cells are clearly differentiated by the presence of lamellar extensions (la), membrane bound granular inclusions (mg) and granular endoplasmic reticulum (gr). The cells are jointed to the gut tegumental lining by a desmosomal junction (dj). The surface tegument contains inclusions (qi) which may be a morphological variant of the electron lucent inclusions or possibly a specific inclusion of the gut tegument.

Scale bar = 1 μm.

b) Desmosomal connection between gastrodermis and tegument.

Scale bar = 0.25 μm.

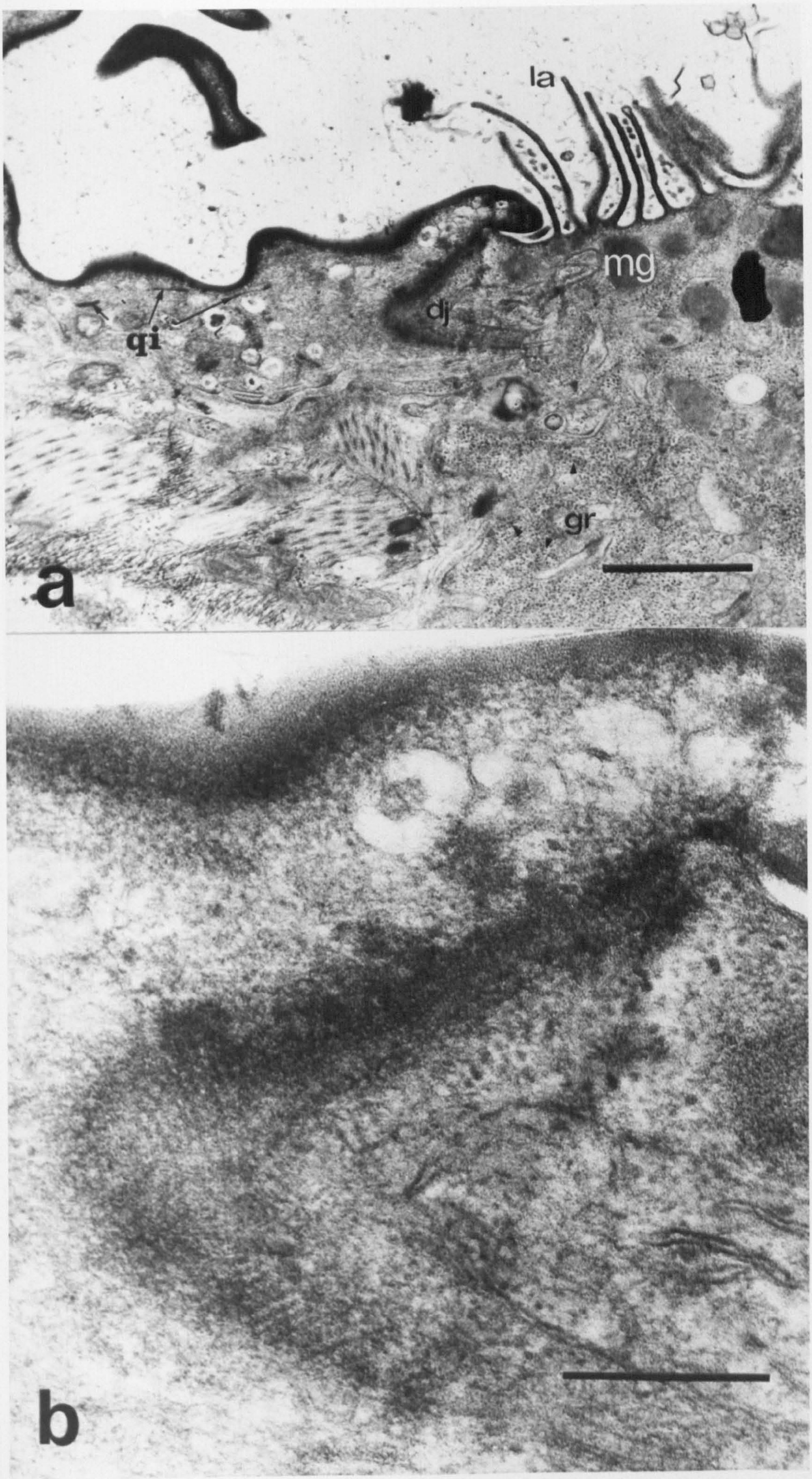
la
mg
dj
qi
gr
a
b

Plate 29: T.E. micrographs of adult gastrodermis.

a) The gastrodermal cells have lamellar extensions (la) from which may arise terminal microvilli (mv). The cells contain mitochondria (mi) and exhausted inclusions (double arrows).
Scale bar = 2 μm.

b) The gastrodermal cells are joined by septate desmosomes (sd). Cisternae of smooth endoplasmic reticulum (ci) are characteristically associated with this junction. The gastrodermal cells contain mitochondria (mi) and exhausted inclusions (ei).
Scale bar = 0.25 μm.

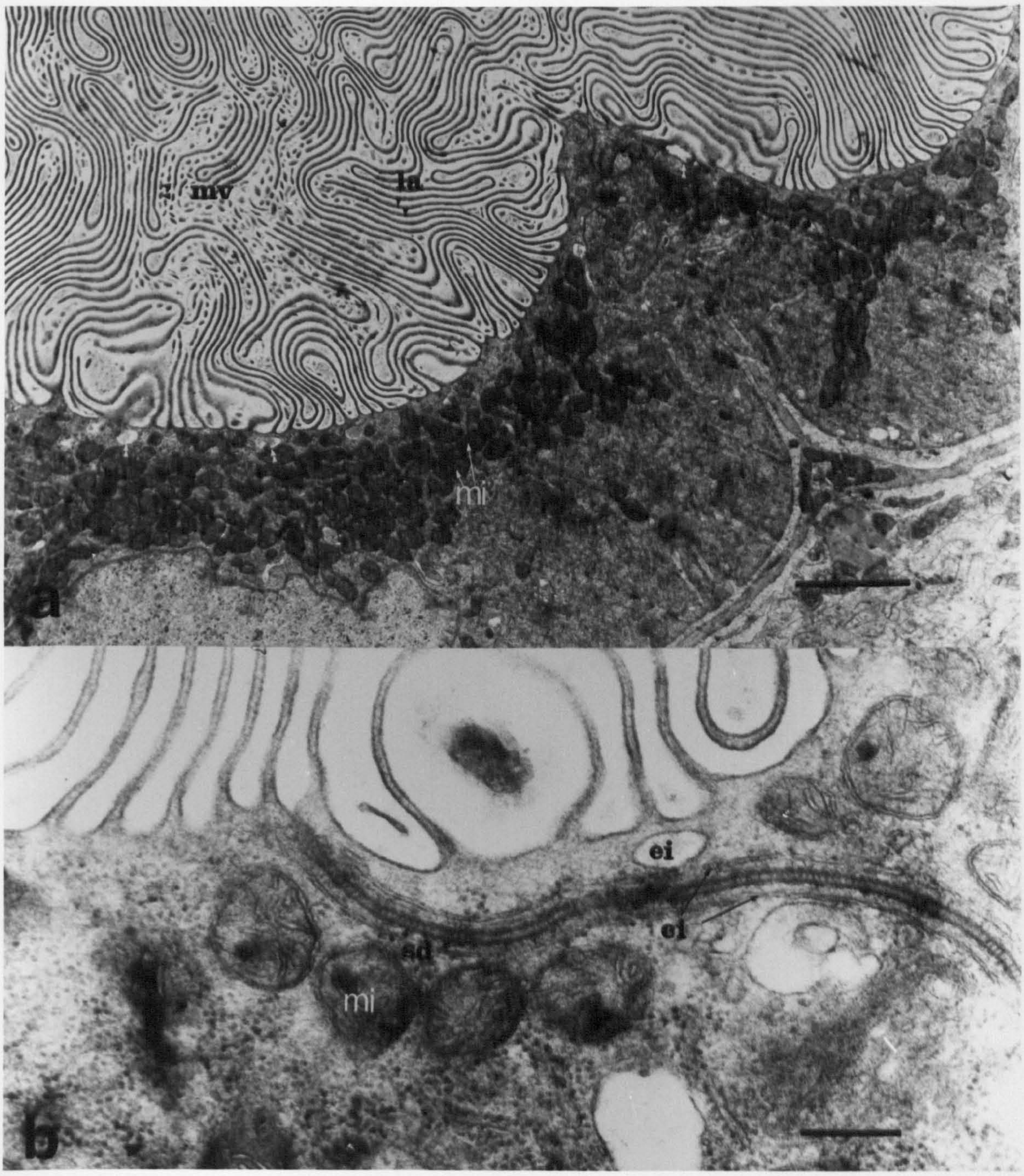
mv
la
mi
a
ei
ei
ed
mi
b

Plate 30: T.E. micrographs of a transverse section through the tail stem of a Type Three cercaria.

There are four blocks of longitudinal striated muscle (sl). An excretory tubule (et) and flame cell (fc) are present in this section.

Scale bar = 10 μm.

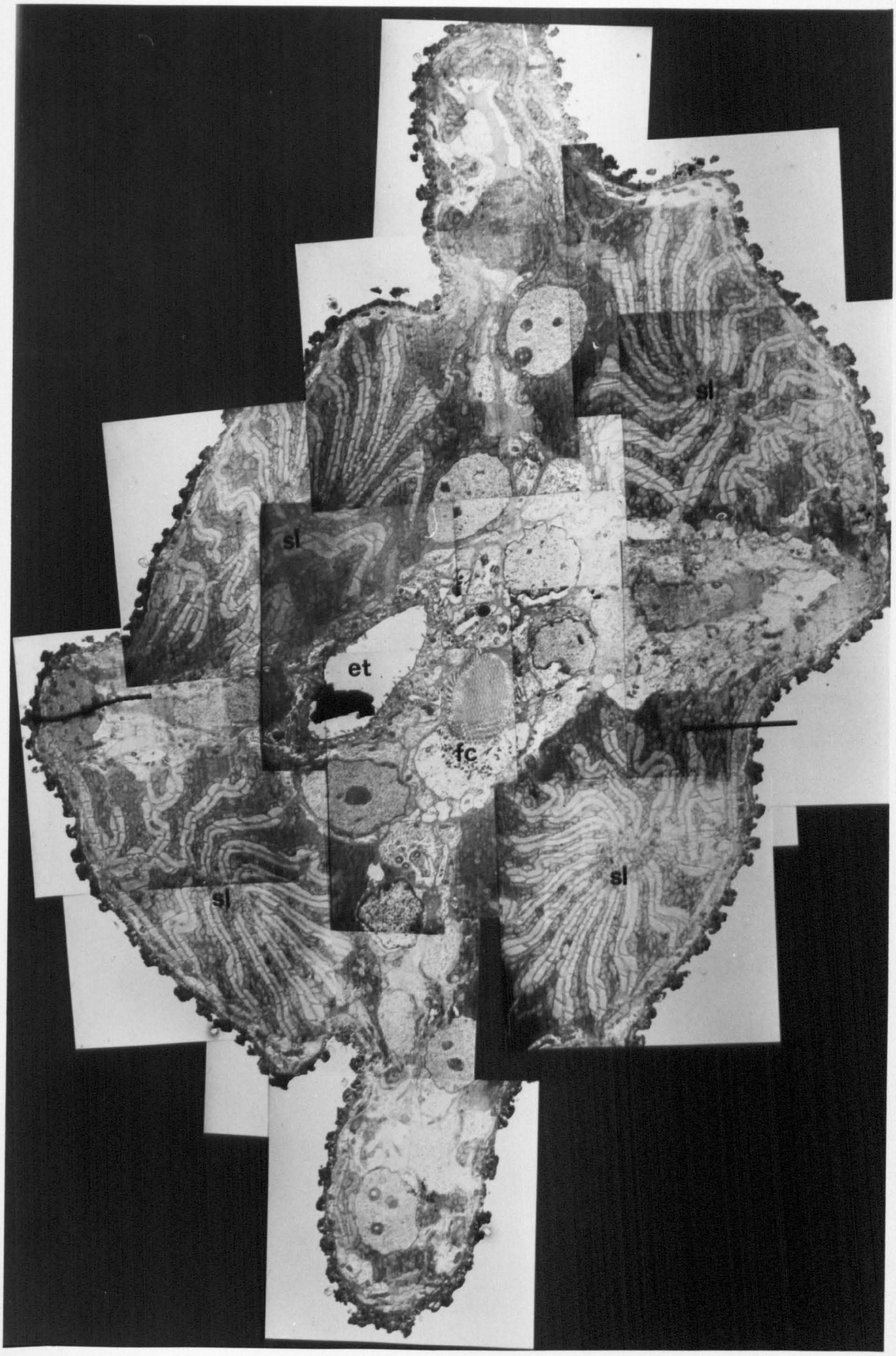
sl
sl
et
fc
sl
sl

Plate 31: T.E. micrographs of cercarial flame cells.

a) Type One cercaria.

Scale bar = 0.5μm.

b) Type Three cercaria.

Scale bar = 1 μm.

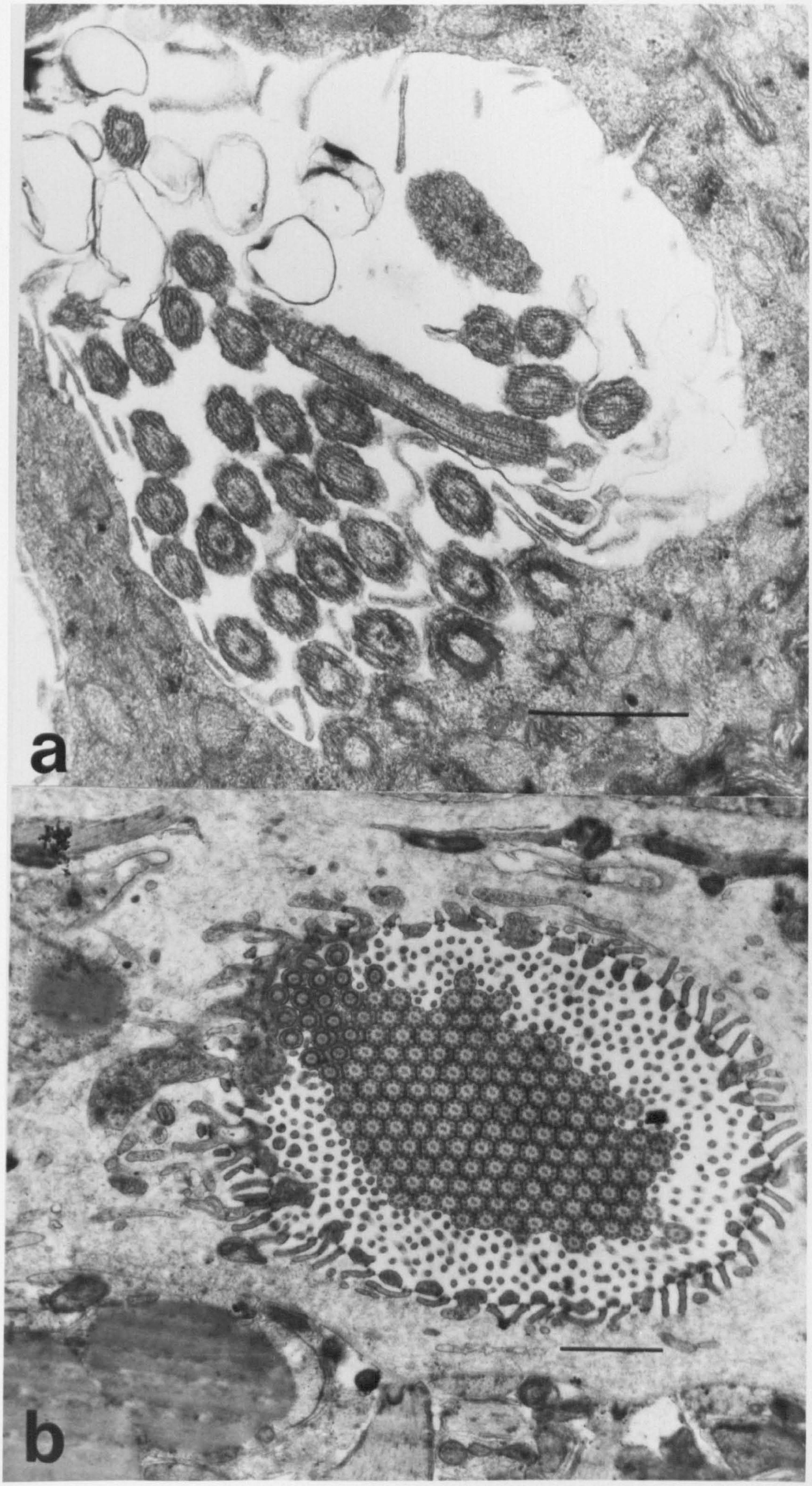
a
b

Plate 32: T.E. micrographs of a flame cell of a Type Three cercaria.

a) The central microtubules (arrowed) of the cilia in the "flame" have an identical orientation.
Scale bar = 0.25μm.

b) Around the "flame" the outer ribs (or) are joined by desmosomes (sd) to inner ribs (ir) from which leptotriches (lt) arise.
Scale bar = 0.5μm.

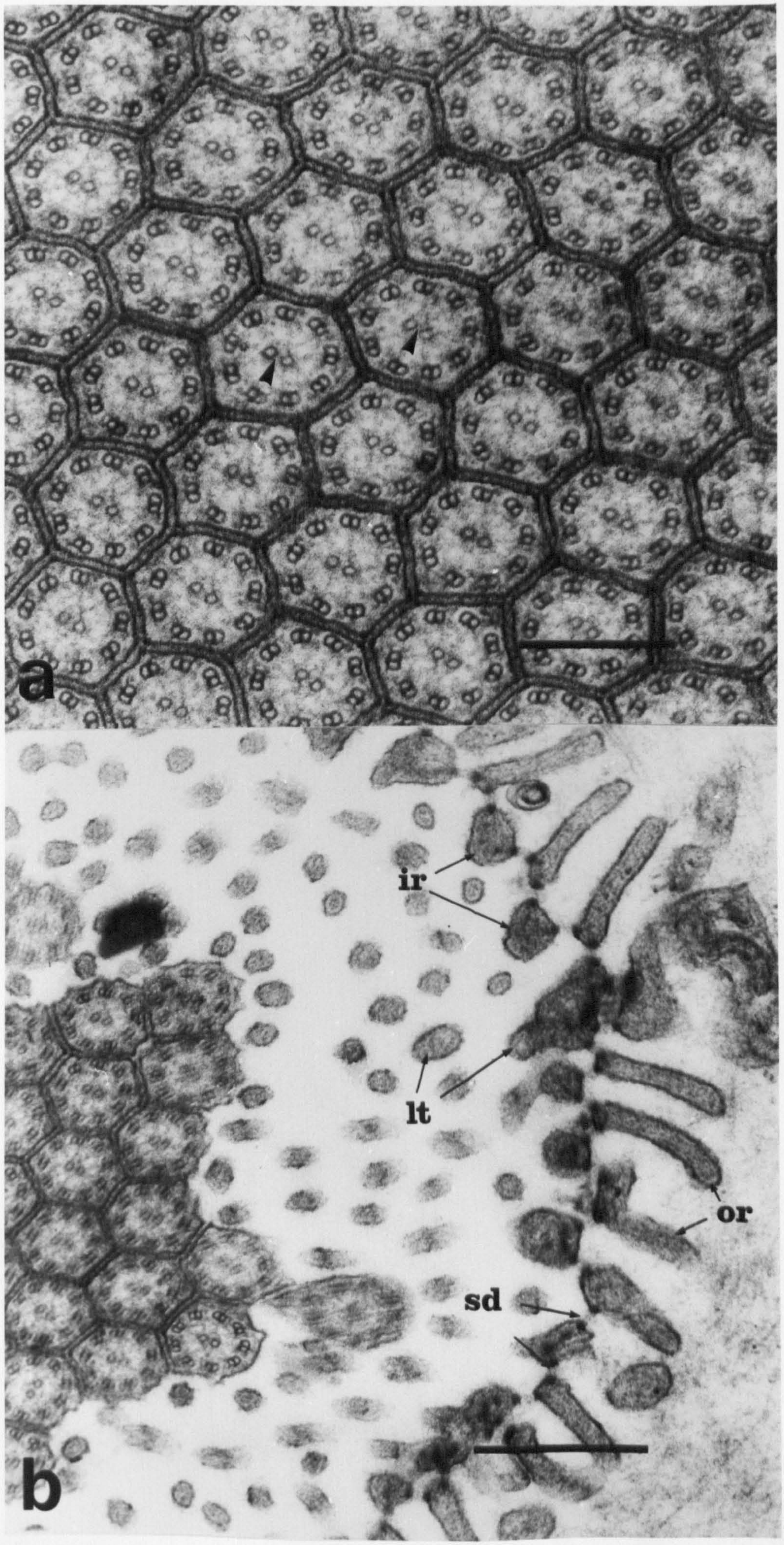
a
ir
lt
or
sd
b

Plate 33: T.E. micrographs of cercarial ocellus and vitelline cells.

a) Vitelline cells in Type Two cercaria, the nucleus (nu) is relatively large and vitelline granules (vg) sparse.

Scale bar = 2μm.

b) Vitelline cells in Type Three cercaria, the nucleus (nu) is relatively small and vitelline granules (vg) are numerous.

Scale bar = 10μm.

c) Ocellus of Type Three cercariae showing the lamellae of the rhabdomere (lr) surrounded by pigment granules (pg).

Scale bar = 2μm.

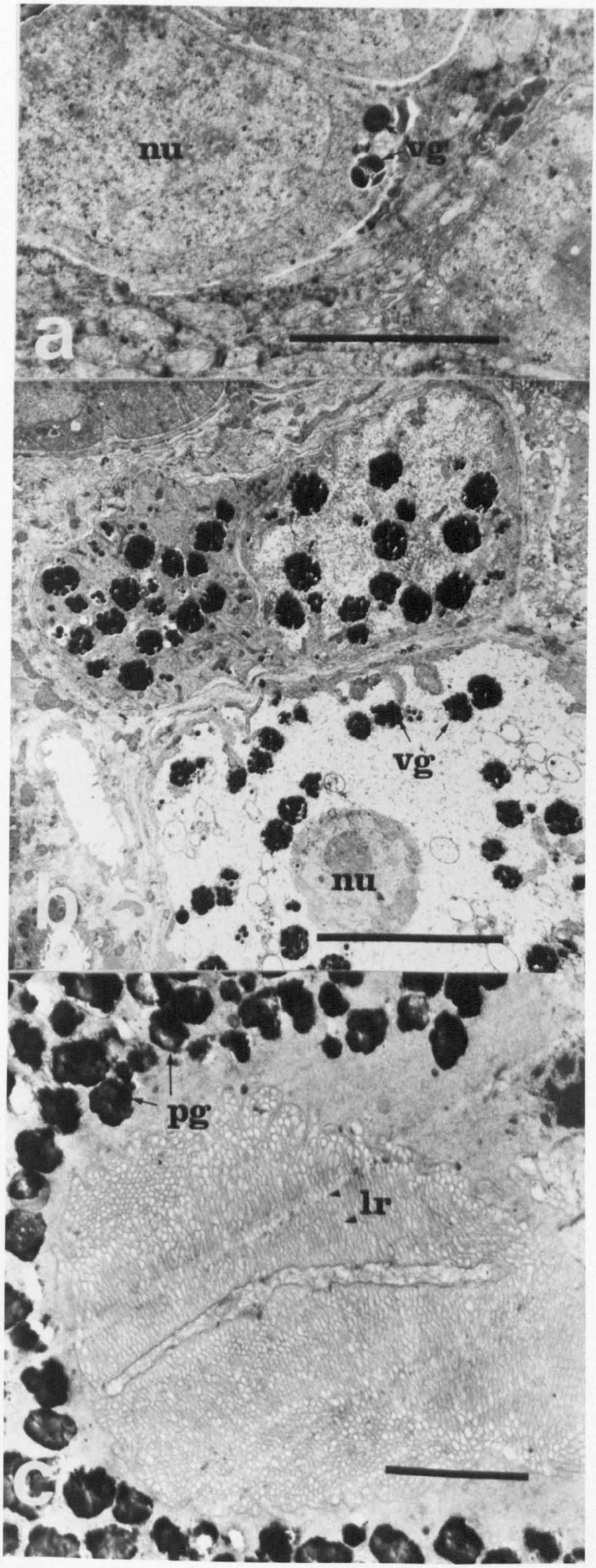
nu
vg
a
vg
nu
b
pg
lr
c

Plate 34: T.E. micrographs of cercarial ocelli.

a) Type Two cercaria. The rhabdomere (rh) is surrounded by relatively few pigment granules (pg).
Scale bar = 2μm.

b) Type Three cercaria. The rhabdomere (rh) extends from a rhabdomere cell body (ry) and is surrounded by a pigment cup cell (pc).
Scale bar = 5μm.

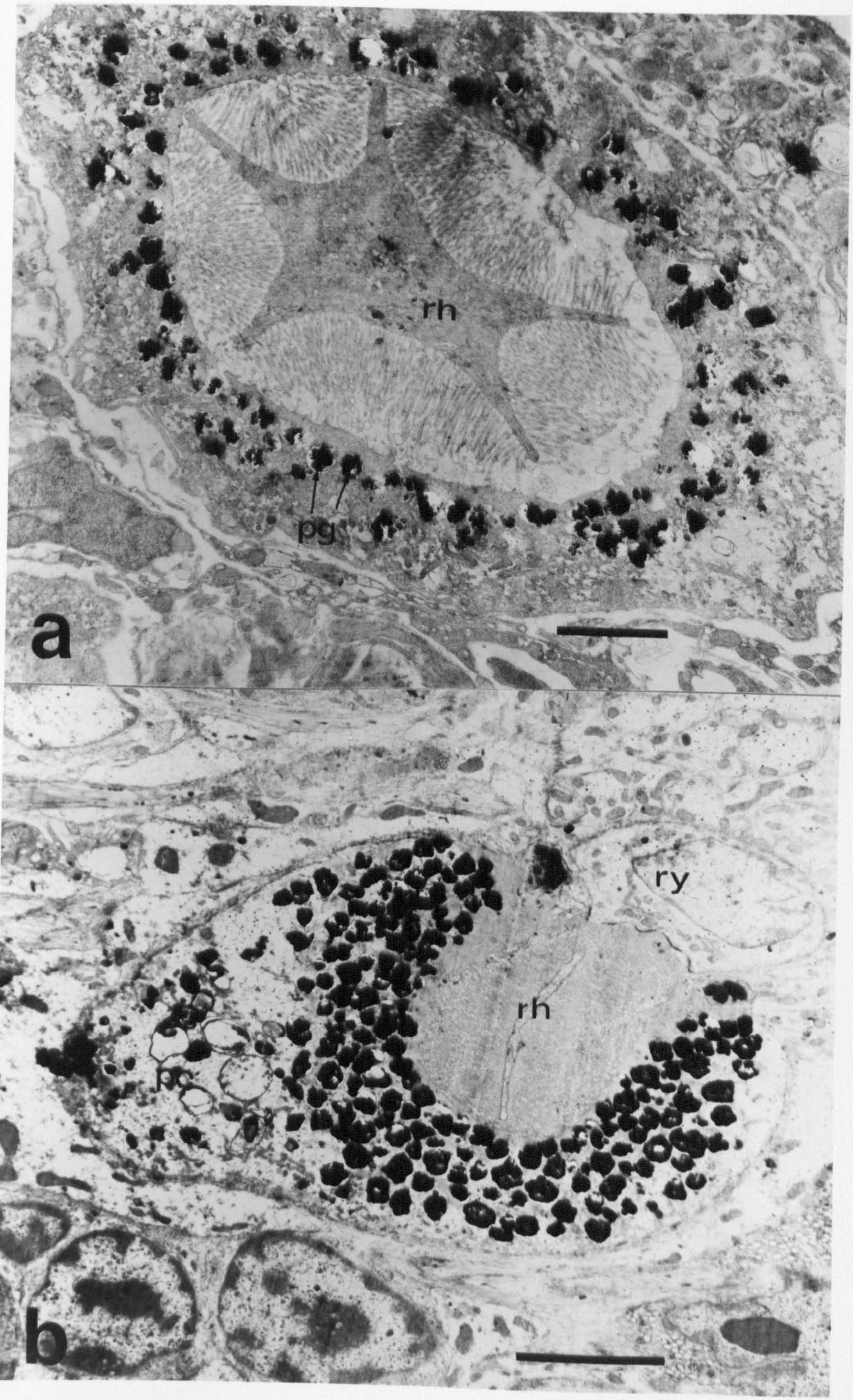
rh
pg
a
ry
rh
pg
b

Plate 35: S.E. micrographs of ventral surface of Type Three cercariae.

a) Early Type Three intramolluscan cercaria. Spines (sp) are partially concealed by surface corrugations (mp). A uniciliate sensory ending (us) is present. Scale bar = 5 μm.

b) Late Type Three free swimming cercaria. Spines (sp) protrude from surface corrugations. A uniciliate sensory ending (us) is present. Scale bar = 2.5 μm.

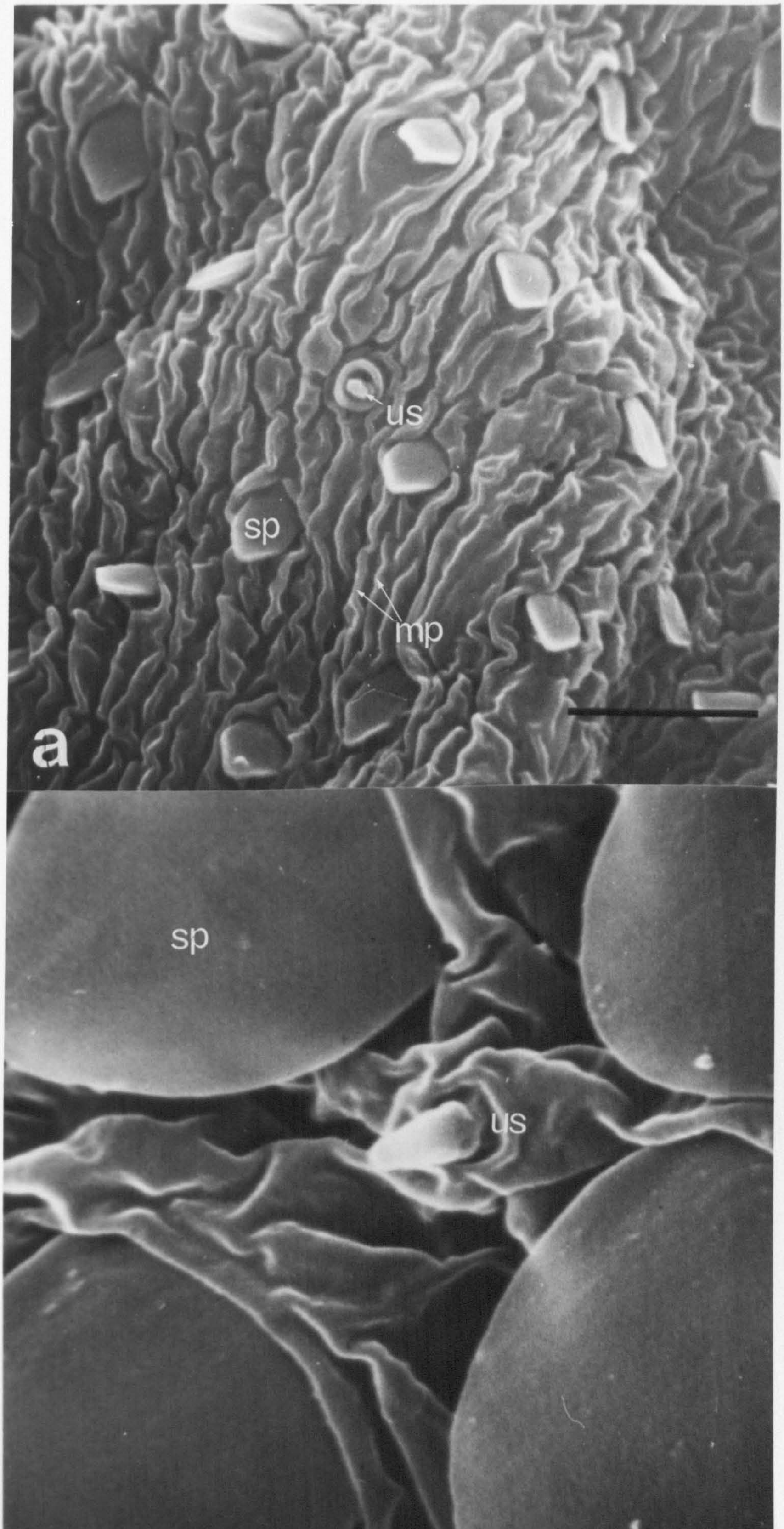
us
sp
mp
a
sp
us
b

Plate 36: T.E. micrographs of uniciliate sensory endings of Type Three cercaria.

Scale bar = 0.5μm.

a) The sensory cilium (sc) arises from a bulb (bu) and protrudes through a collar of surface tegument.

b) Two osmiophilic rings are associated with the bulb, a distal ring (dr) and a proximal ring (pr).

c) The distal ring is associated with a septate desmosome (sd). The bulb contains dense inclusions (di).

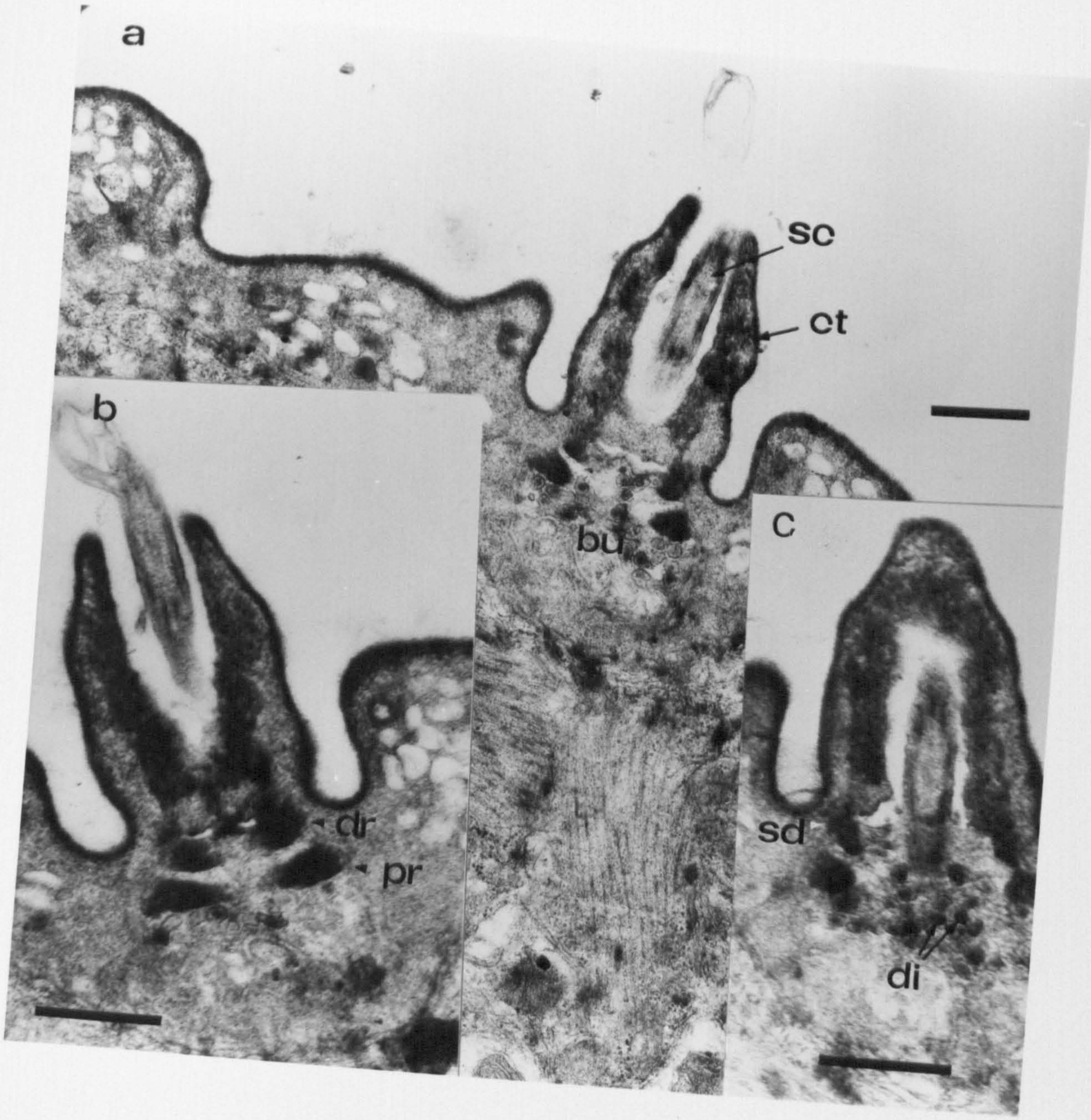
a
sc
ct
bu
b
dr
pr
c
sd
di

Plate 37: T.E. micrographs of sperm in Type Three cercariae.

Flagella (fa), a mitochondrion(mi), a nucleus (nu) and microtubules (mt) are present.

Scale bar = 0.5μm.

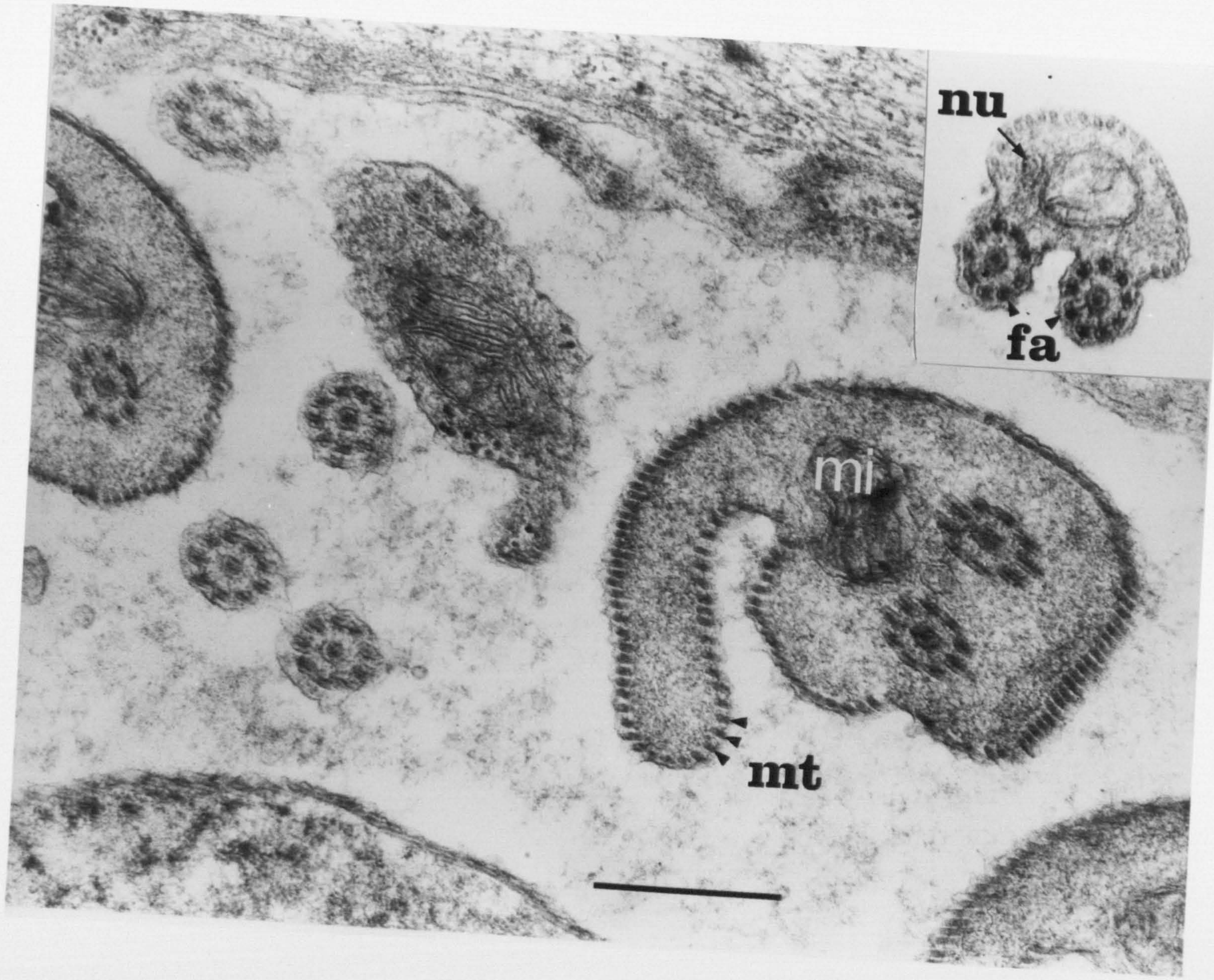
nu
fa
mi
mt

Plate 38: T.E. micrographs of testis cell in Type Two cercaria. Within the nucleus are condensed regions of chromatin (cc) and synaptonemal complexes (arrowed). Scale bar = 2 μm.

Insert: synaptonemal complex.

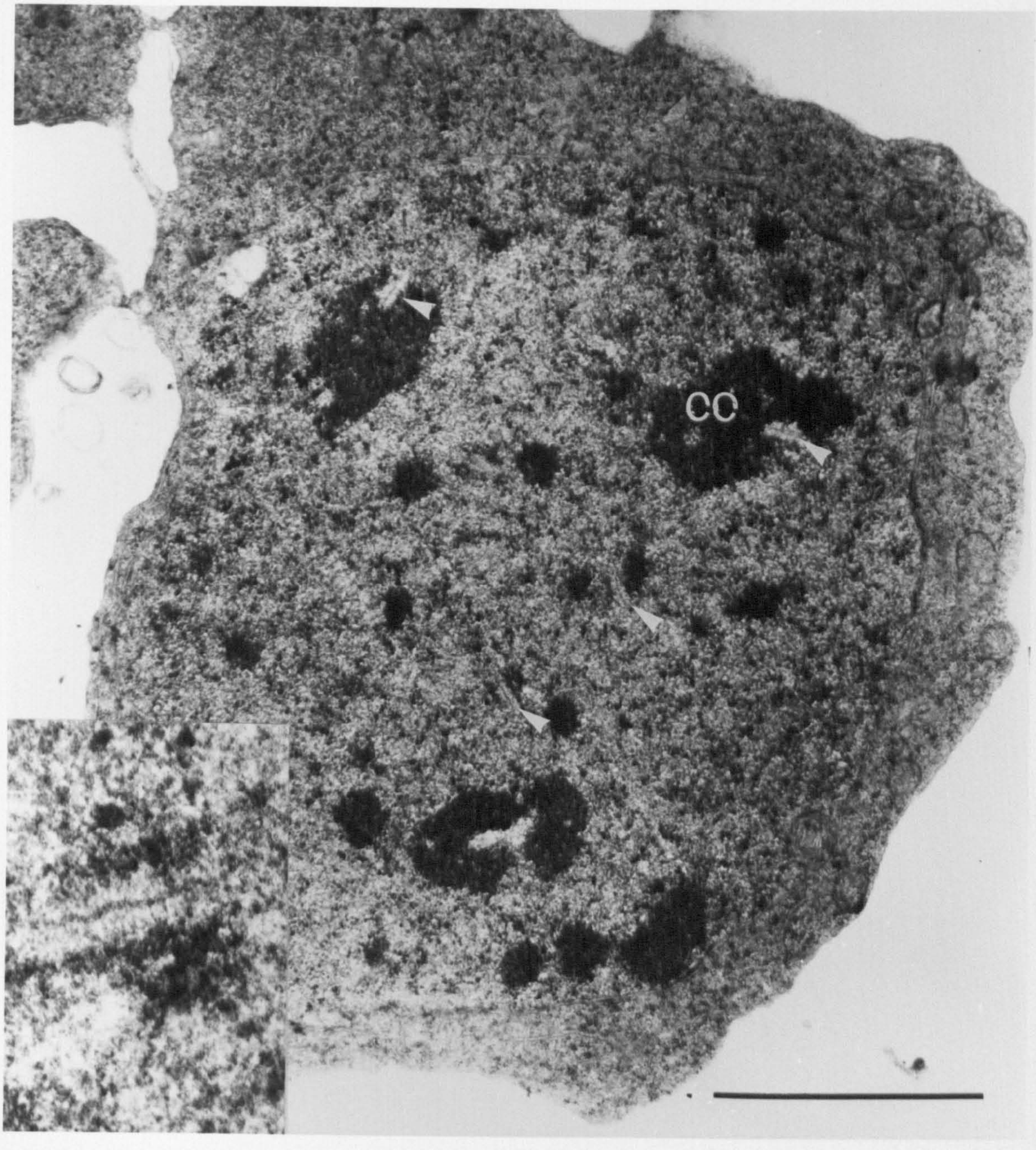
cc

Plate 39: T.E. micrographs of tegumental spines of early Type Three cercariae.

a) Spines (si) concealed within surface corrugations (sc) with microplicae (mp).
Scale bar = 2 μm.

b) Spine in which the infrastructure shows discontinuity (arrowed). The basal lamina (bl) is less dense than for later spines, and ribosomes (ri) appear to be associated with the spine.
Scale bar = 0.2 μm.

c) Dorsal spine (si) within the surface tegument (st) but not in contact with the apical plasma membrane (am).
Scale bar = 0.5 μm.

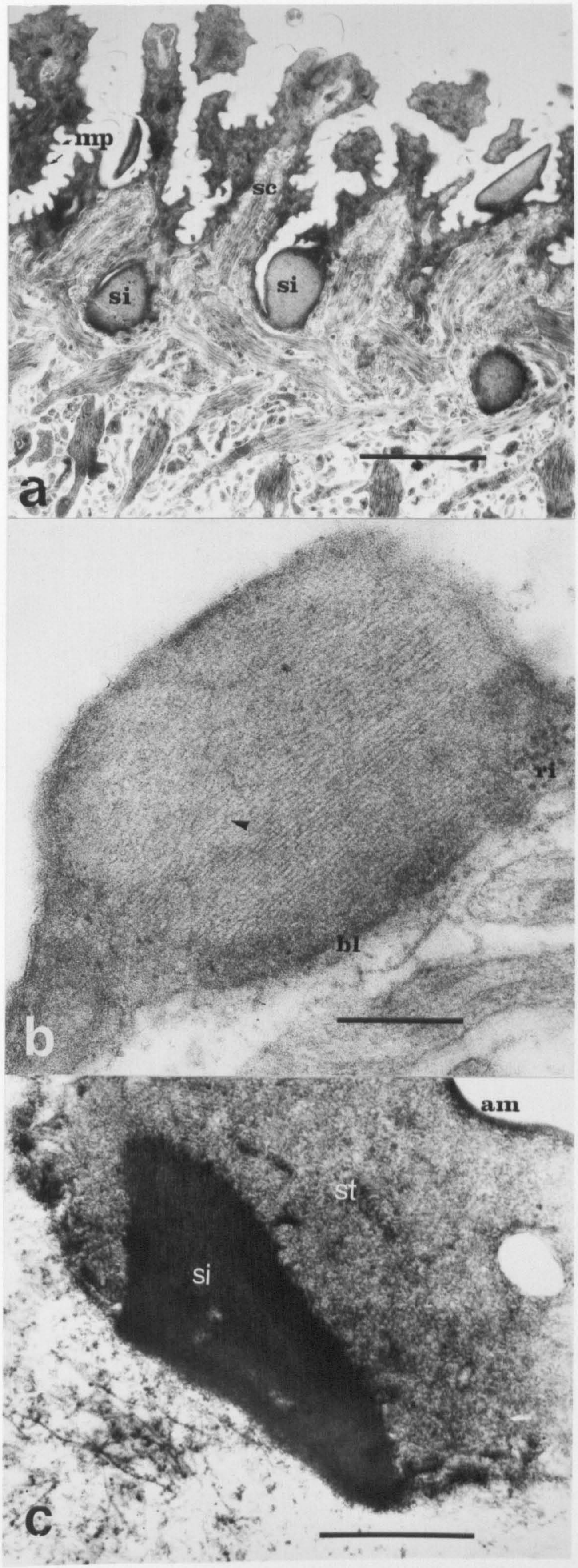
mp
sc
si
si
a
ri
bl
b
am
st
si
c

Plate 40: T.E. micrographs of transverse sections through tegumental spines of Type Three cercariae.

a) - e) shows sections of the spine taken from the apex at (a) to the region of attachment to these basal lamina at (e).

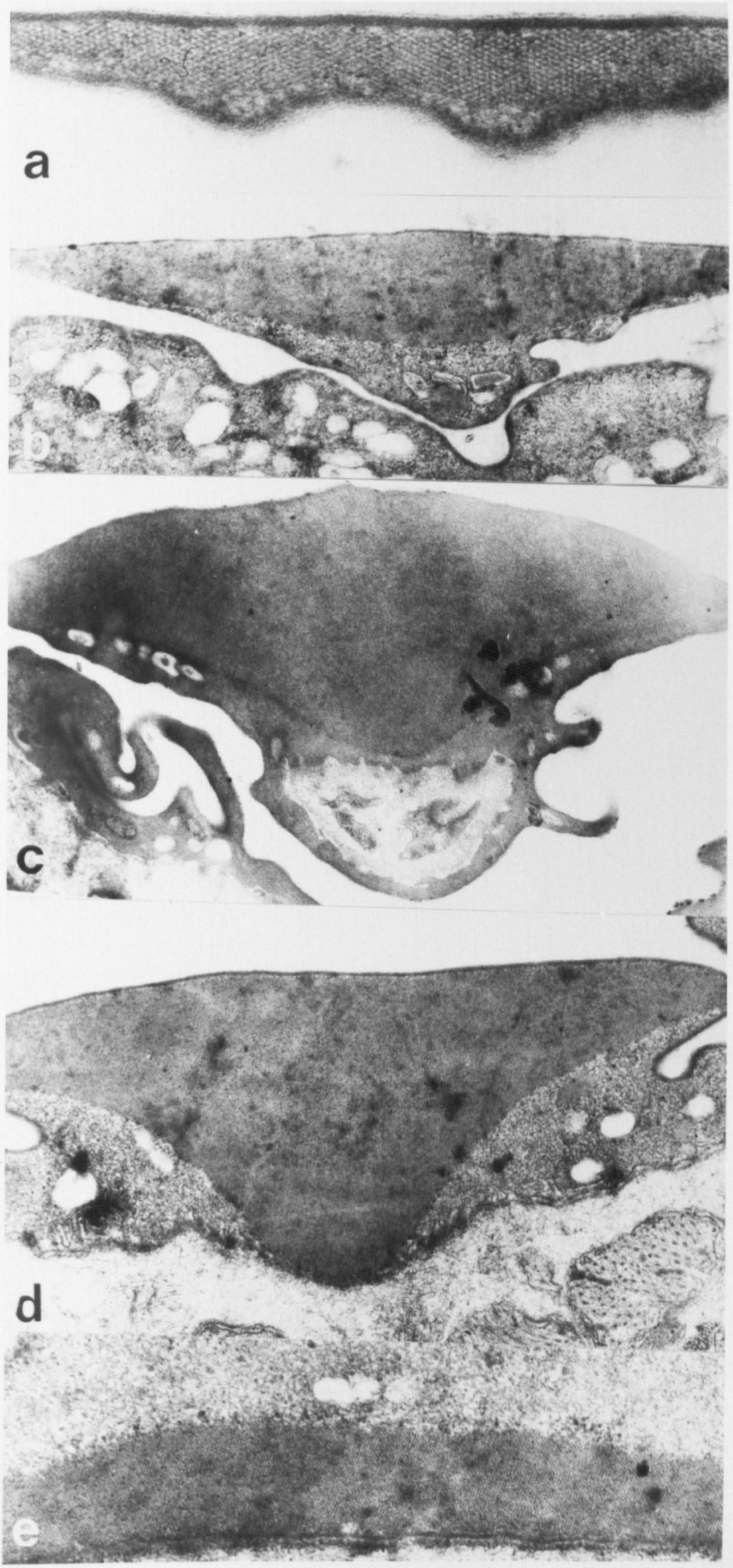
a
b
c
d
e

Plate 41: T.E. micrographs of tegumental spine infrastructure of Type Three cercariae.

a) Spine apex showing trilaminate apical plasma membrane (am) and subjacent dense layer (dl). The spine infrastructure appears composed of electron lucent globular units (gu) in a dense matrix.
Scale bar = 0.1μm.

b) Spine attachment region showing dense zone of spine (dz) and dense basal lamina (bl). The infrastructure appears composed of electron lucent globular units in a dense matrix.
Scale bar = 1 μm.

c) Spine section with striated infrastructure. An electron lucent inclusion (ei) is closely apposed to the spine, and an isthmus of interstitial matrix penetrates adjacent to the spine.
Scale bar = 0.5μm.

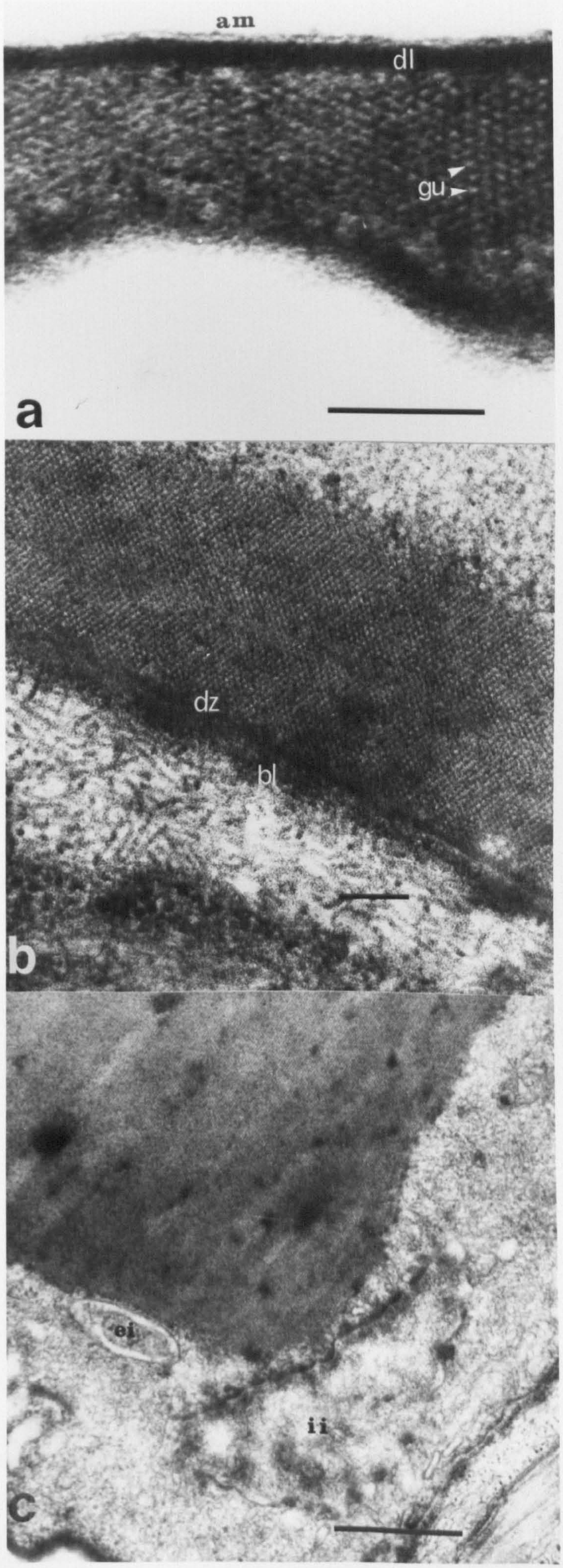
am
dl
gu
a
dz
bl
b
ei
ii
c

Plate 42: S.E. micrographs of adult flukes at the host interface.

a) Mucus surface beneath scale of infected host. The surface is marked with a regular array of spine induced indentations (si).
Scale bar = 10μm.

b) Ventral spines of fluke producing indentations in (a) above.
Scale bar = 3μm.

c) Anterior dorsal surface of fluke (fs) with adjacent fish scale epidermis (ec) displaced.
Scale bar = 10μm.

d) Projecting dorsal (ds) and ventral (vs) spines at the periphery of the adult fluke.
Scale bar = 10μm.

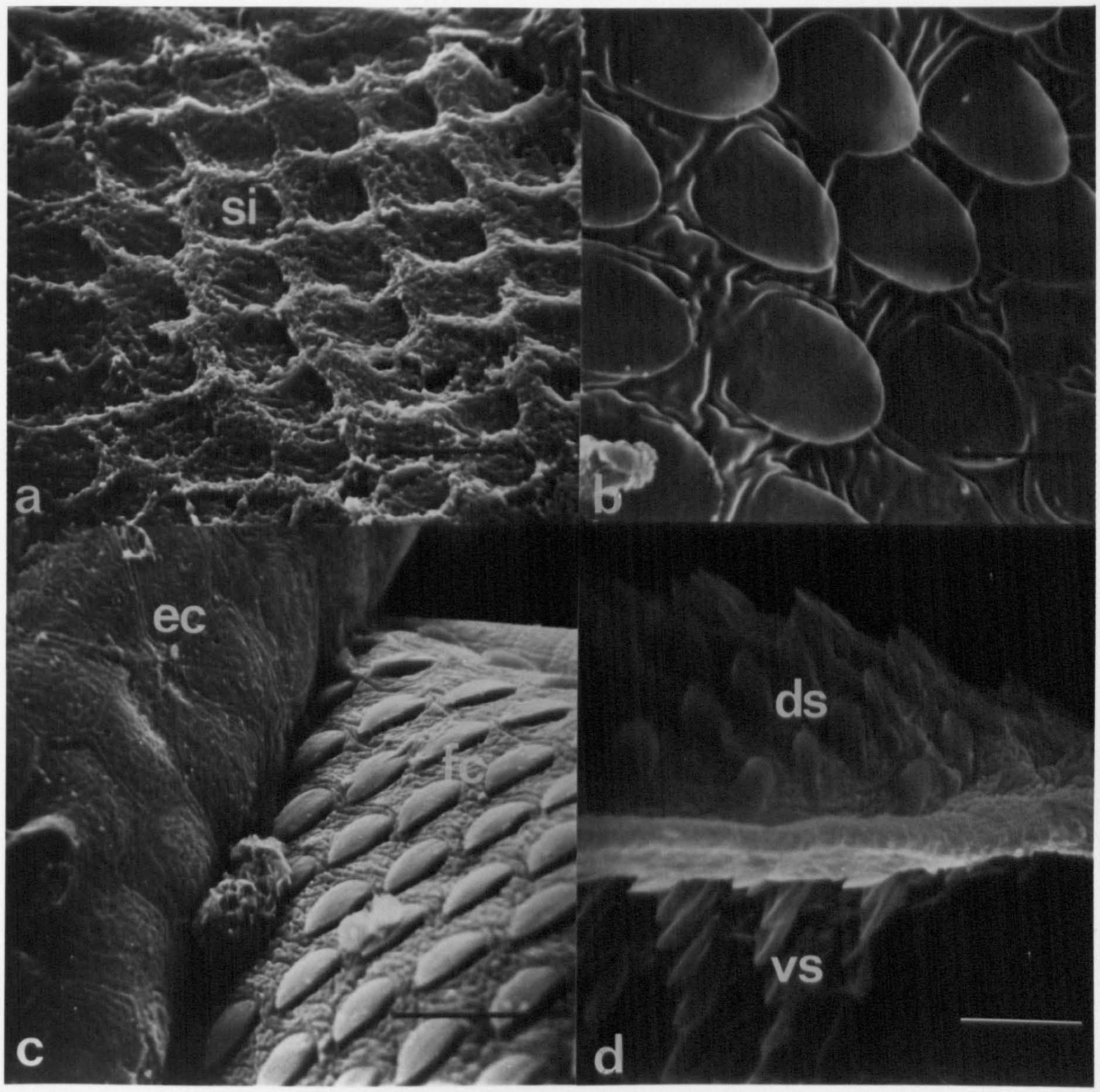
si
a
b
ec
fc
c
ds
vs
d

Plate 43: Microflash photographs of dropping cercariae.

Scale bar = 100μm.

a) In lateral view. The furcae (fu) are symmetrically spread at the distal end of the exposed tail stem (ts). The arm processes (ap) are folded against the reflexed body region (rb).

b) Viewed from above. The furcae (fu) are symmetrically spread.

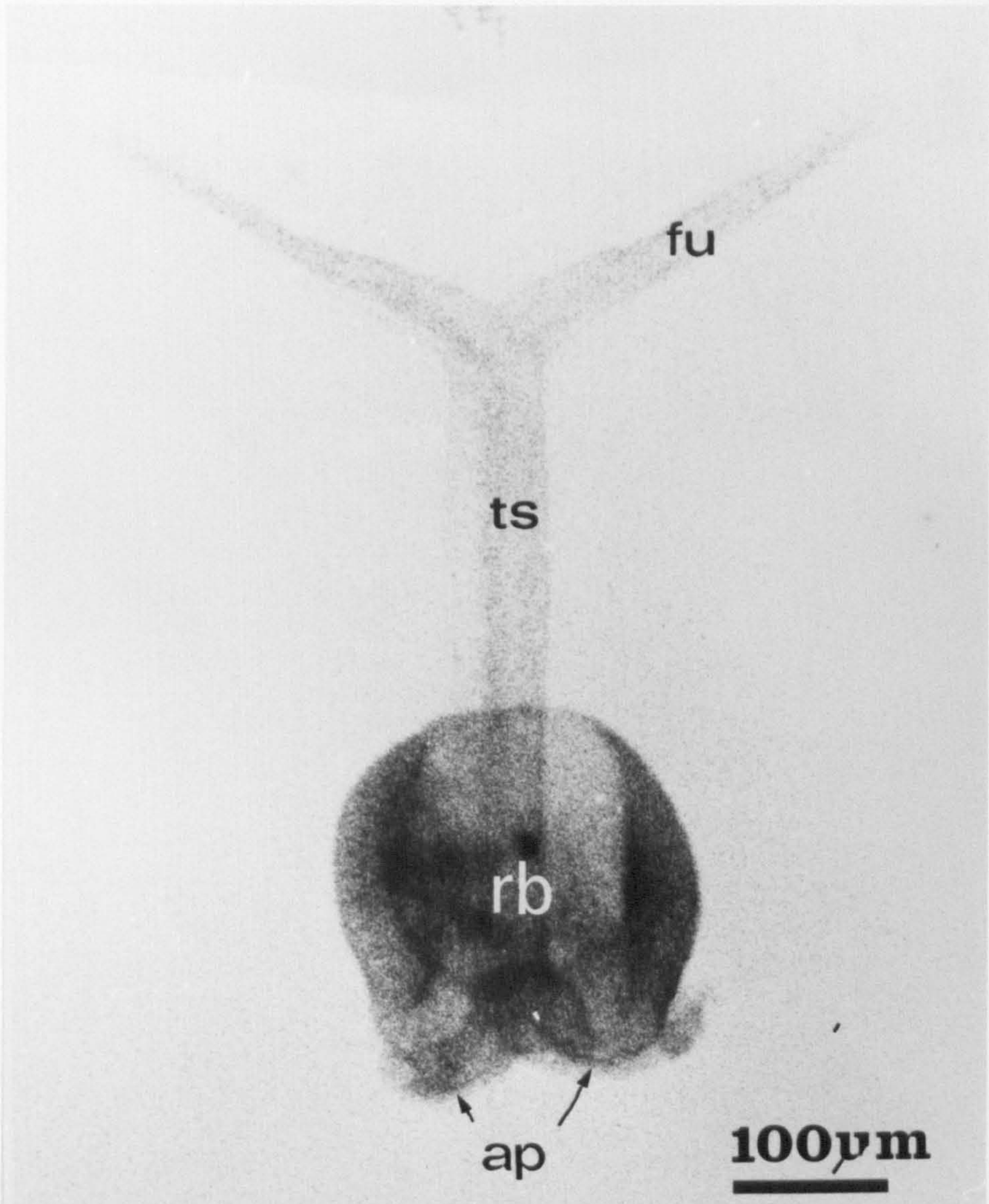
fu
ts
rb
ap
100μm
a

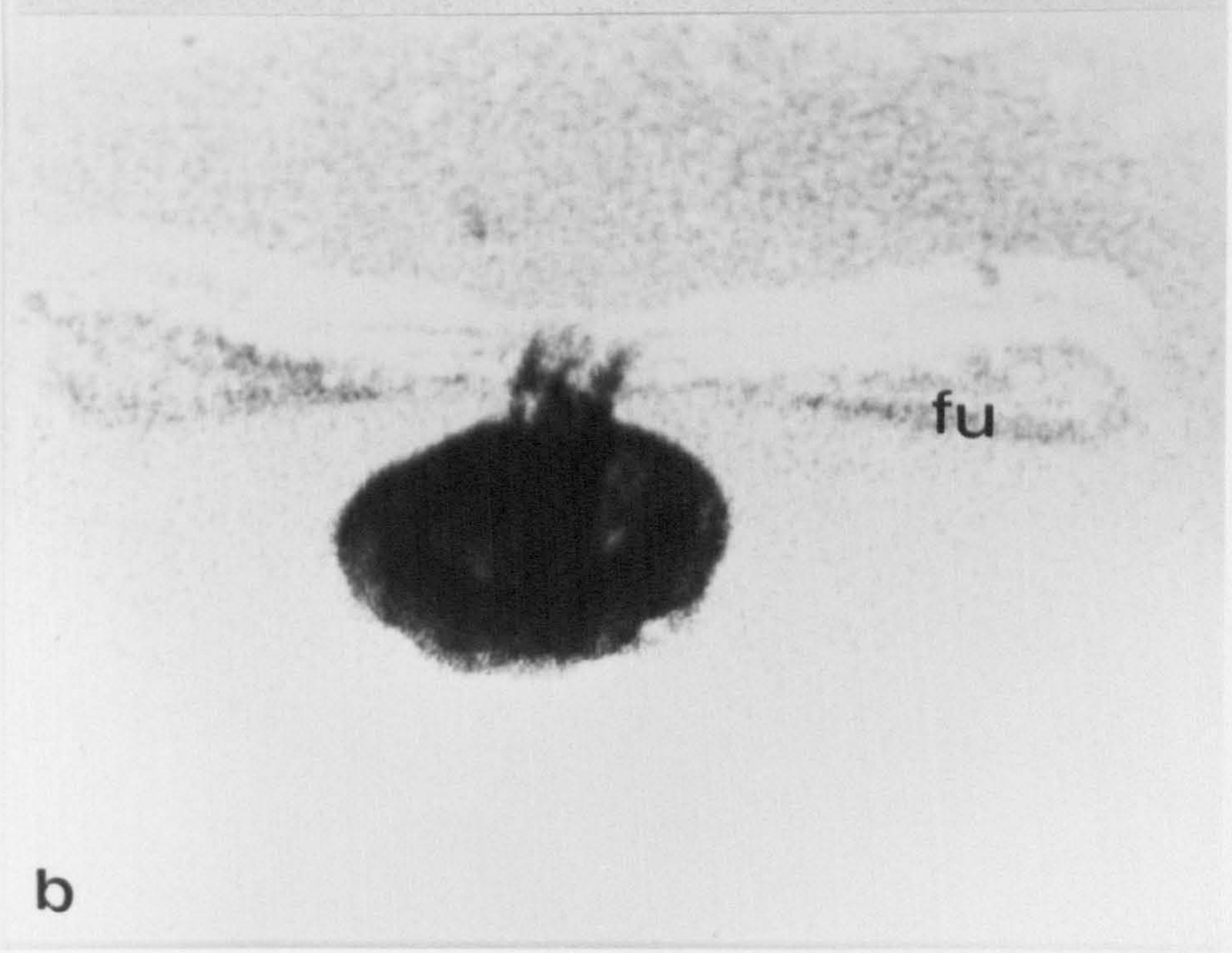
fu
b

Plate 44: Microflash photograhs of swimming and resting cercariae.

Scale bar = 100μm.

a) Swimming. The furca on the right (A) is on the effective stroke and is straight and flattened.

b) Swimming. The furca held vertically (B) is on the recovery stroke and is curled and twisted.

c) Swimming. The furca on the right (C) is on the effective stroke and is reflexed and flattened.

d) The most commonly adopted configuration of the resting cercaria.

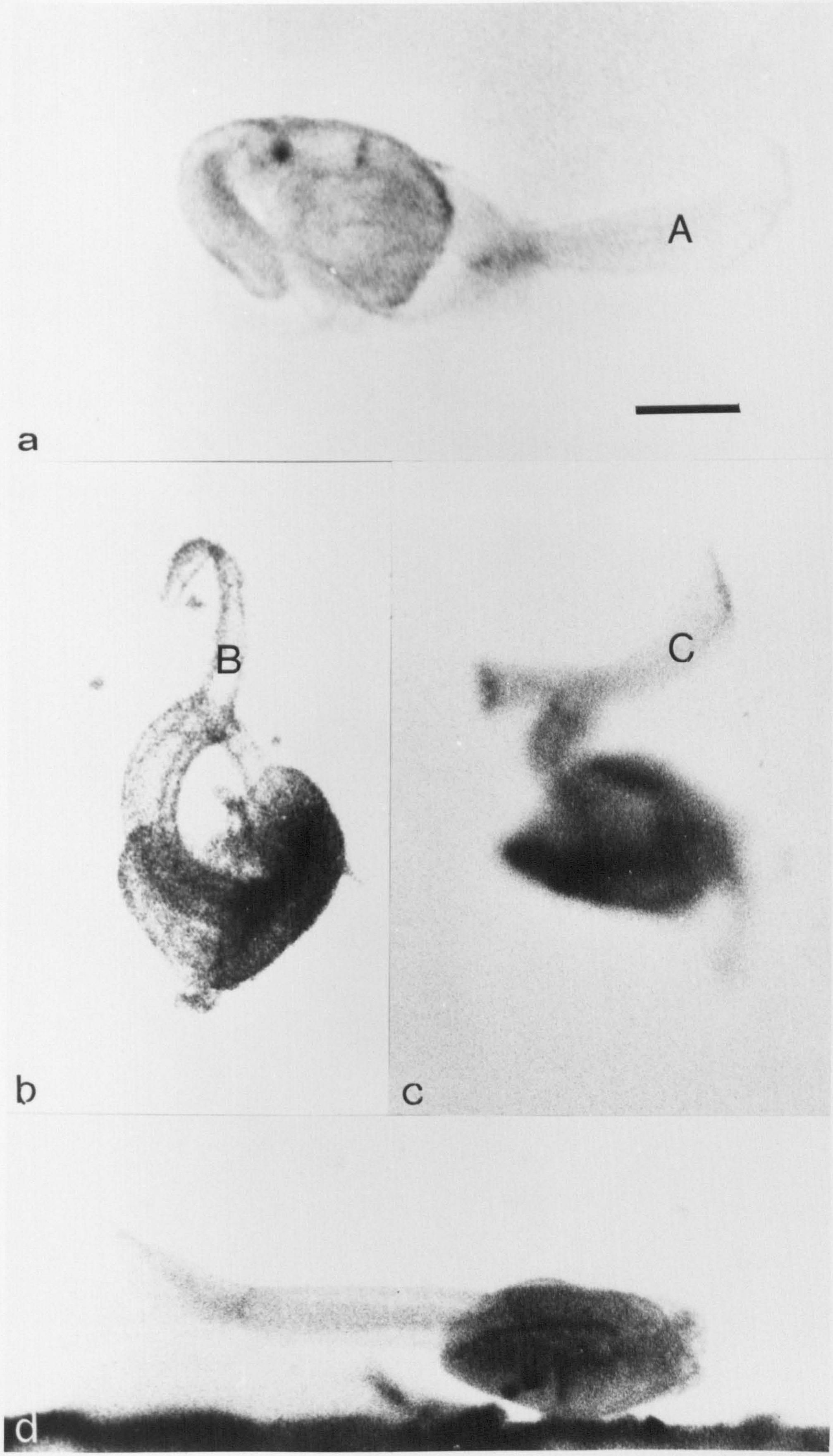
A
a
B
C
b
c
d

Plate 45: Microflash photographs of attaching cercariae.

Scale bar = 100μm.

a) Cercaria attached by the arm processes (ap) to the base of the observation cell.

b) Attached cercaria viewed from above. The body (bd) has extended, the arm processes (ap) remain attached and the tail (ts) is held vertically.

c) Attached cercaria viewed from above. The cercaria has inverted so that the arm processes (ap) now project vertically away from the substrate. The furcae (fu) are closely adpressed.


a
ap

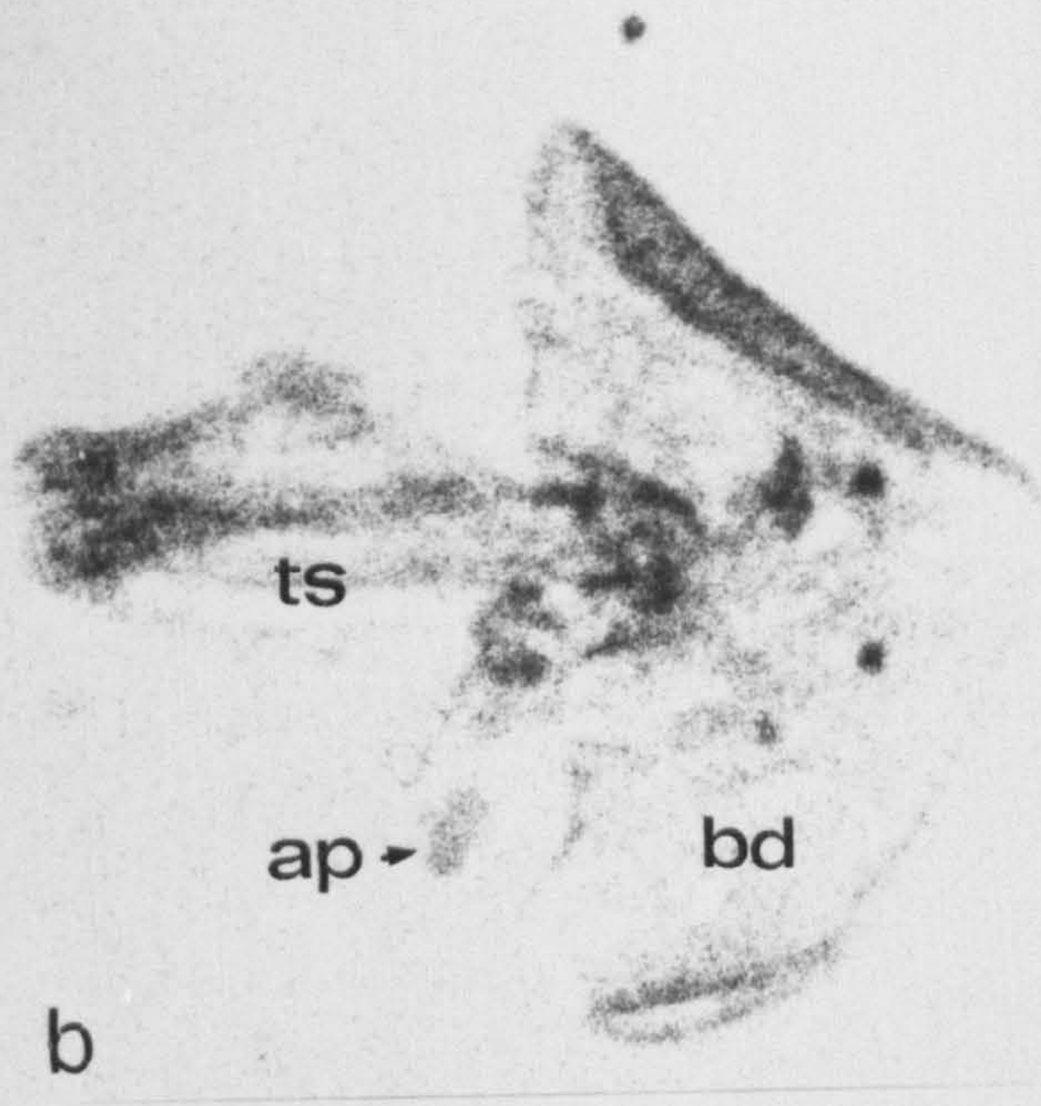
ts
ap
bd
b

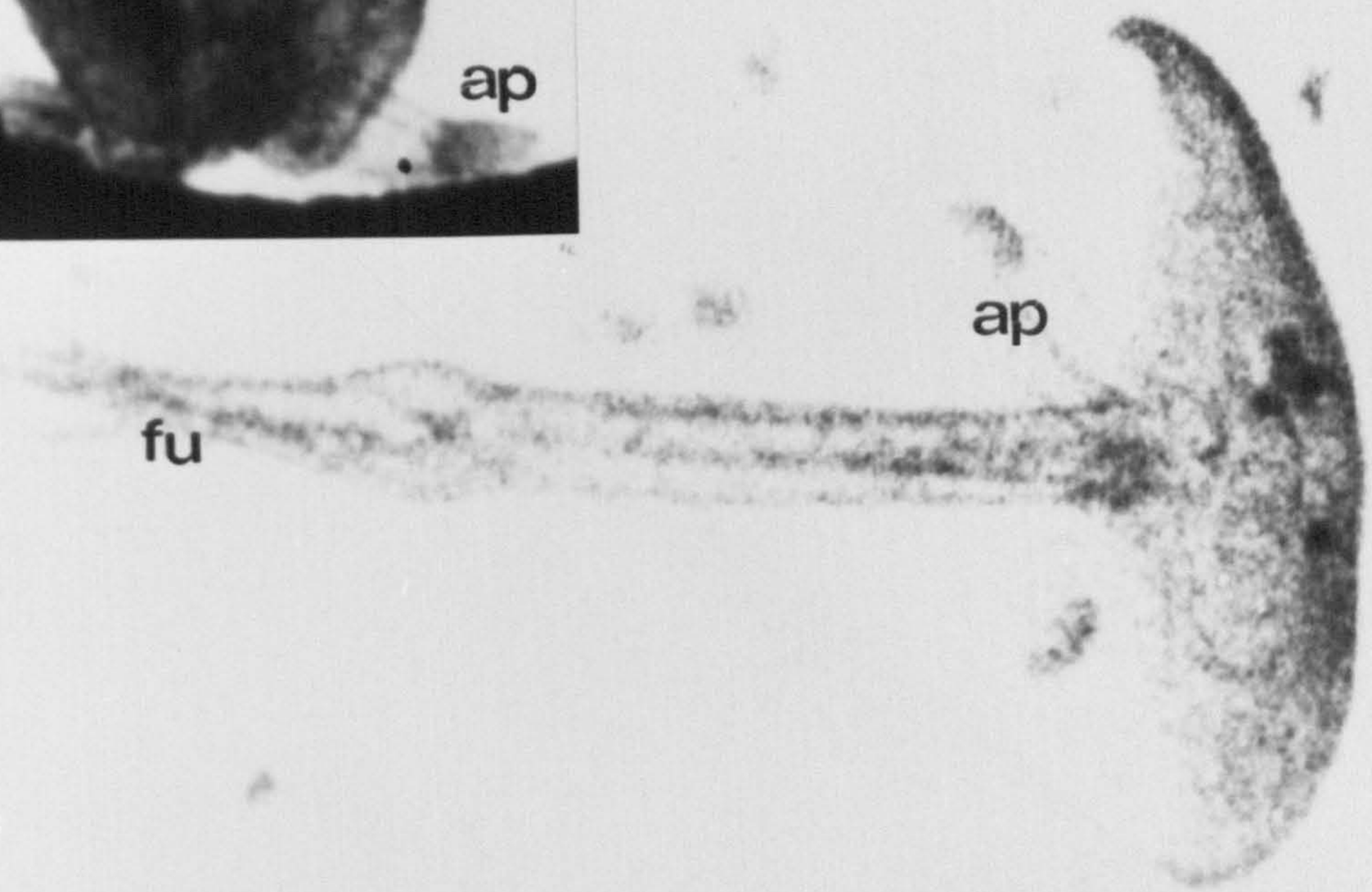
fu
ap
c

Plate 46: Microflash photographs of attached cercaria extending body region.

Scale bar = 100μm.

At (a) the cercaria is recently attached and the body (X) is reflexed about the tail stem. Throughout (b) to (d) the body region is extended.

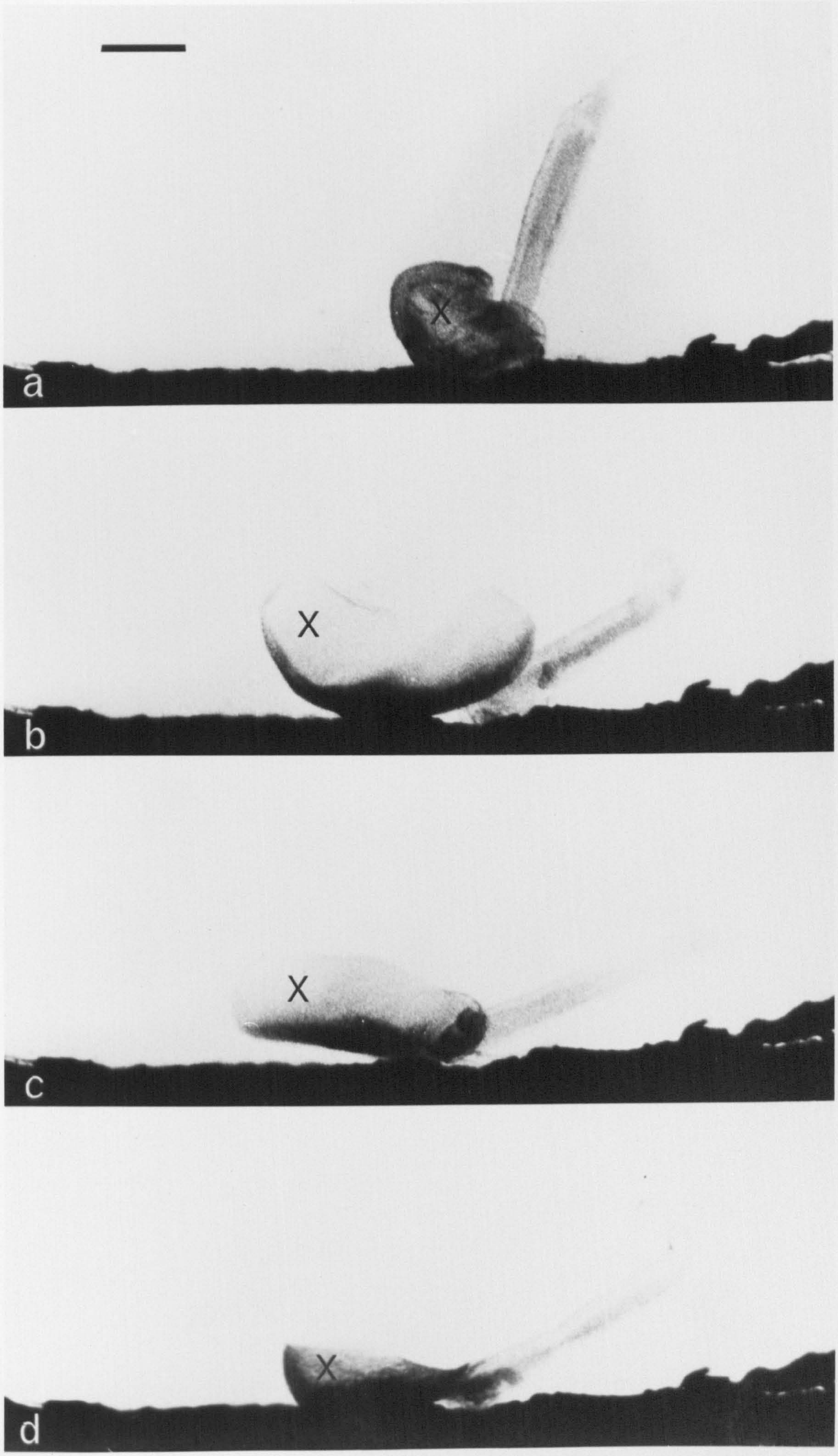
a
X
b
X
C
X
d
X

Plate 47: Highspeed microcinematographic record of swimming sequence A.

A section of swimming sequence A showing the sequential configuration of a swimming cercaria at one msec. intervals. The cercaria is swimming vertically upwards. In frames 7 and 27 respectively the alternate extension of right and left arm processes may be discerned.

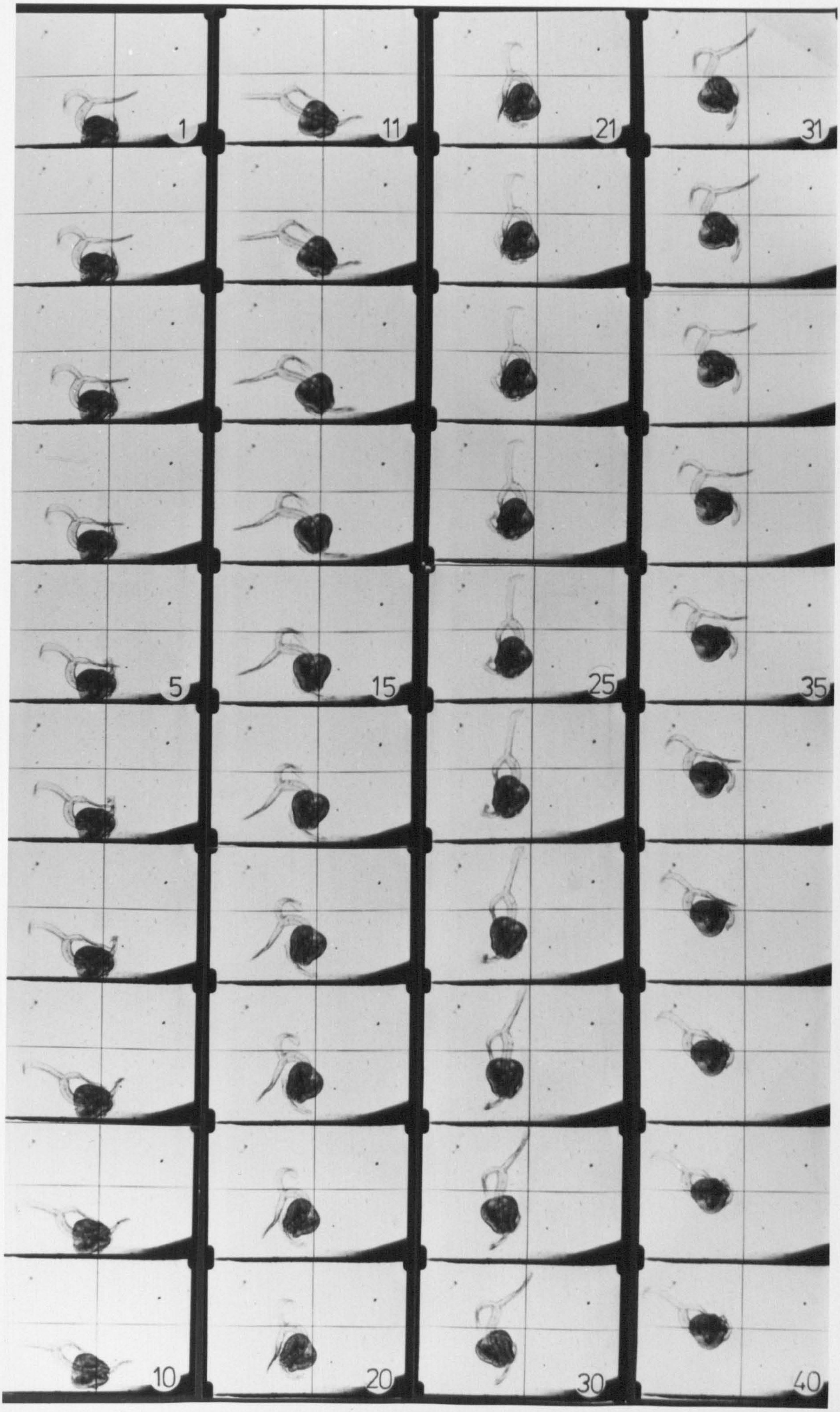
1
11
21
31
5
15
25
35
10
20
30
40

Plate 48: Selected frames of swimming sequence A.

Scale bar = 100μm.

The six prints show the sequential configuration of a swimming cercaria 3 msec. intervals, the numbers referring to the frame numbers in sequence A (Plate 47). The cercaria is swimming vertically upwards.

28

37

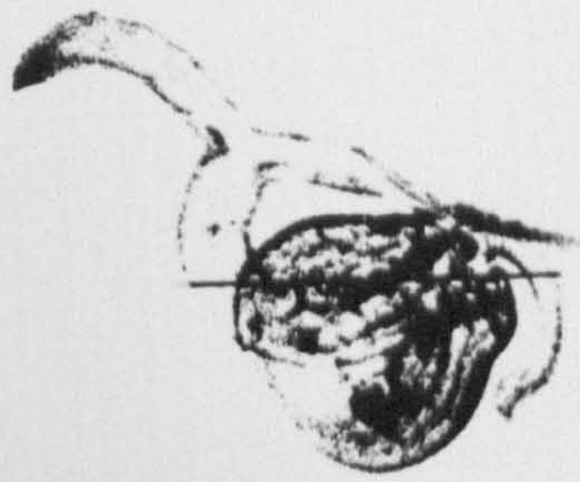

25

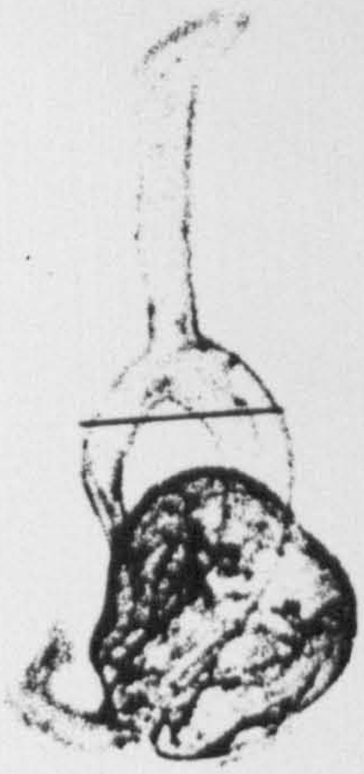

34

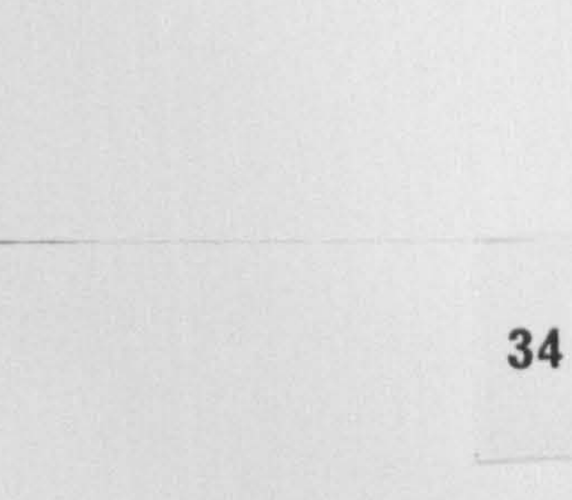

22

31

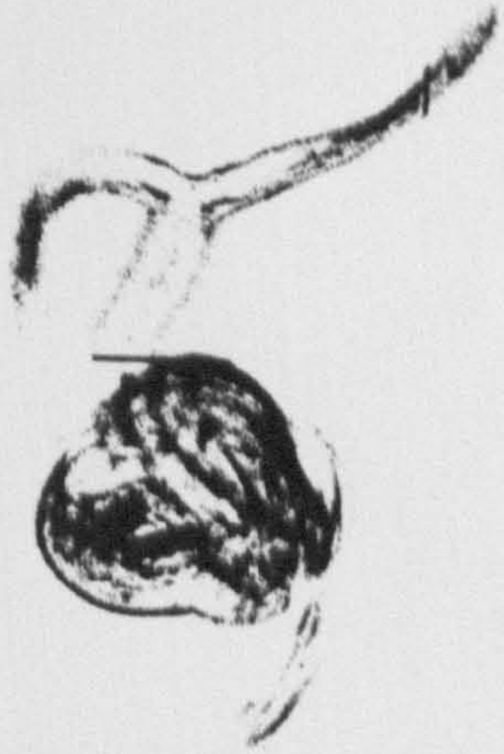

List of Appendices

Appendix 1. Egg development data.

a) Proportion of eggs in assigned stages.

b) Rate of loss of eggs from the developing egg population.

Appendix 2. Data on intramolluscan stages

a) Rediae.

b) Cercariae.

Appendix 3. Procedure to estimate the straight line trajectory of a swimming cercaria.

Appendix 4. Estimation of cercarial volume and viscous resistance to dropping.

4.1 Volume

4.2 Viscous resistance.

Appendix 5. Determination of terminal velocity of dropping cercaria.

Appendix 1: Egg development data

a) Proportion of eggs in assigned stages

TEMP.	DAYS	DEVELOPMENTAL STAGES						
°C	P.C.	0	1	2	3	4	D	M
15	0	0.95					0.03	0.02
	12	0.30	0.60				0.10	0.00
	24	0.05	0.75				0.15	0.05
	36		0.65	0.19			0.13	0.03
	48		0.15	0.60			0.23	0.02
	60			0.55			0.40	0.05
	72			0.48			0.42	0.10
	84			0.40	0.07	0.02	0.43	0.08
	96			0.36	0.17	0.03	0.42	0.02
	108			0.02	0.27	0.05	0.56	0.10
	120				0.05	0.10	0.57	0.28
	132				0.05	0.17	0.53	0.25
	144				0.02	0.07	0.62	0.29
	156						0.72	0.28
20	0	0.96					0.02	0.00
	3	0.15	0.77				0.03	0.05
	6	0.00	0.70	0.12			0.08	0.10
	9	0.03	0.52	0.35	0.02		0.06	0.02
	12		0.03	0.70	0.05		0.12	0.10
	15			0.63	0.10		0.09	0.18
	18			0.58	0.13		0.03	0.26
	21			0.17	0.52		0.05	0.26
	24			0.02	0.72		0.00	0.26
	27		0.02	0.63	0.02	0.02	0.31	
	30			0.35	0.27	0.05	0.33	
	33			0.17	0.30	0.22	0.31	
	36			0.07	0.13	0.53	0.27	
	39			0.02	0.02	0.68	0.28	

TEMP.	DAYS	DEVELOPMENTAL STAGES						
°C	P.C.	0	1	2	3	4	D	M
25	0	0.96		0.02			0.02	
	2		0.94				0.03	0.03
	4		0.05	0.82			0.05	0.08
	6		0.07	0.71		0.02	0.05	0.15
	8		0.08	0.72			0.07	0.13
	10			0.23	0.57		0.03	0.17
	12				0.63		0.10	0.27
	14			0.05	0.58	0.05	0.03	0.29
	16				0.52	0.10	0.08	0.30
	18				0.05	0.45	0.25	0.25
	20					0.10	0.60	0.30
	24					0.01	0.72	0.27
30	0	0.71					0.27	0.02
	2	0.02	0.71		0.02		0.17	0.08
	4		0.03	0.43		0.03	0.34	0.17
	6			0.47	0.05		0.35	0.13
	8			0.05	0.53		0.32	0.10
	10				0.40	0.03	0.38	0.19
	12				0.08	0.27	0.43	0.22
	14				0.05	0.02	0.66	0.27
	19					0.02	0.72	0.26
35	0	0.88	0.02				0.10	
	2	0.75		0.03	0.02		0.13	0.07
	4	0.75		0.03			0.06	0.16
	6	0.58		0.02			0.07	0.33
	8	0.46					0.19	0.35
	10	0.38					0.09	0.53
	18						0.60	0.40

b) Rate of loss of eggs from the developing egg population (μ) per egg per day

10°C		15°C		20°C	
DAYS P.C.		DAYS P.C.		DAYS P.C.	
17.5	0.0022	6	0.0045	1.5	0.0211
59.5	0.0119	18	0.0098	4.5	0.0384
98.0	0.0072	30	-0.0041	7.5	-0.0384
		42	0.0094	10.5	0.0550
		54	0.0258	13.5	0.0221
		66	0.0113	16.5	0.0093
		78	-0.0017	19.5	0.0095
		90	-0.0111	22.5	-0.0233
		102	0.0416	25.5	0.0331
		114	0.0682	28.5	0.0258
		126	-0.0319	31.5	0.0923
		138	0.0745	34.5	0.2848
				37.5	0.5365

25°C		30°C		35°C	
DAYS P.C.		DAYS P.C.		DAYS P.C.	
1	0.0208	1	-0.0274	1	0.0589
3	0.0387	3	0.2128	3	0.0127
5	0.0419	5	-0.0297	5	0.1312
7	0	7	-0.0546	7	0.1328
9	0	9	0.1496	9	0.0955
11	0.1194	11	0.1029		
13	-0.0382	13	0.8047		
15	0.0462	16.5	0.2505		
17	0.1075				
19	0.8047				
22	0.5756				

Appendix 2: Data on intramolluscan stages

a) Rediae; number of intra-redial cercariae (C) and intra-redial rediae (R) per redia. Redial size (S) in arbitrary units

33 days PPI

Replicate 1

S	R	C
121.6	0	0
103.8	40	0
86.5	0	0
69.1	5	0
60.5	0	0
59.5	0	0
57.0	0	0
55.9	2	0
25.3	0	0

Replicate 2

S	R	C
197.4	26	0
115.3	10	0
80.2	4	0
78.8	5	0
78.8	5	0
72.6	2	0
65.0	0	0
59.7	2	0
56.3	0	0
53.5	0	0
52.0	3	0
40.4	0	0
40.2	0	0
39.7	0	0
31.1	0	0
30.3	0	0
28.9	0	0

Replicate 2 (CONT.)

S	R	C
26.8	0	0
26.5	0	0
23.1	0	0
22.6	0	0
20.9	0	0
17.9	0	0

Replicate 3

S	R	C
282.3	19	0
34.3	0	0
31.8	0	0
29.4	0	0
29.4	0	0
29.4	0	0
29.4	0	0
29.0	0	0
27.7	0	0
25.7	0	0
25.6	0	0
24.5	0	0
23.4	0	0
21.1	0	0
20.2	0	0
18.4	0	0
16.7	0	0
16.5	0	0
15.2	0	0
13.6	0	0
10.6	0	0

68 days PPI

Replicate 1

S	R	C
261.1	1	6
259.3	3	0
169.3	4	9
148.2	0	8
130.0	1	8
127.0	0	0
125.2	1	5
103.9	2	5
103.5	1	7
98.2	0	4
97.4	0	6
96.0	1	5
96.0	1	5
95.3	0	8
95.3	0	0
88.2	1	8
76.8	0	3
73.6	1	6
73.6	0	3
63.8	0	0
52.4	0	6
51.7	0	4
49.1	0	0
46.2	0	0
31.8	0	0
27.3	0	0
16.4	0	0
15.1	0	0

Replicate 1 (CONT.)

S	R	C
10.8	0	0
10.3	0	0
10.1	0	0

Replicate 2

S	R	C
120.0	0	9
105.8	0	0
95.3	1	4
77.6	0	4
76.8	1	5
60.4	0	0
57.6	0	3
50.4	0	0
47.0	1	5
28.2	0	0
26.8	0	0
21.7	0	0
19.5	0	0
15.0	0	0
12.6	0	0
12.6	0	0
11.5	0	0
9.9	0	0

Replicate 3

S	R	C
129.8	1	4
108.0	2	6
100.8	0	0
96.0	0	4
96.0	2	4
88.2	0	4
86.4	0	5
77.6	0	7
76.8	1	3
67.2	0	4

Replicate 3 (CONT.)

S	R	C
67.4	0	4
63.8	0	2
63.5	0	6
57.6	0	7
57.6	0	2
57.3	1	4
51.7	0	4
51.7	1	5
45.5	0	2
45.5	0	0
45.5	0	2
40.1	0	0
34.7	0	2
34.6	2	6
21.7	0	0
19.8	0	0
14.4	0	0
14.4	0	0
13.7	0	0
13.0	0	0
10.3	0	0
8.3	0	0

102.5 days PPI

Replicate 1

S	R	C
296.0	0	8
263.4	0	8
197.3	0	8
183.3	0	8
183.3	0	6
180.7	0	7
169.4	0	5
169.4	0	11
169.4	0	5

Replicate 1 (CONT.)

S	R	C
169.4	0	8
140.8	0	6
140.8	0	4
112.9	0	9
112.9	0	0
57.8	0	0
15.9	0	0
14.4	0	0
14.4	0	0
13.0	0	0
13.0	0	0
13.0	0	0
13.0	0	0
11.5	0	0
8.7	0	0
8.7	0	0

Replicate 2

S	R	C
230.2	0	10
230.2	1	8
196.7	0	8
183.3	0	6
141.1	0	5
140.8	5	0
126.9	0	7
117.4	0	6
112.9	4	0
93.9	0	3
93.9	0	6
57.8	0	0
52.0	0	0
28.2	0	0
25.3	0	0
23.8	0	0
23.1	0	0
20.2	0	0

Replicate 2 (CONT.)

S	R	C
19.5	0	0
19.5	0	0
18.0	0	0
17.7	0	0
17.3	0	0
15.2	0	0
15.0	0	0
14.4	0	0
14.4	0	0
14.4	0	0
12.6	0	0
12.6	0	0
11.9	0	0
7.2	0	0

Replicate 3

164.4	1	8
164.4	2	4
155.1	0	6
155.1	0	8
147.8	0	8
147.8	0	8
141.1	0	4
141.1	0	8
126.9	2	8
126.9	4	0
126.9	2	4
126.9	1	5
117.4	1	6
105.5	0	2
84.6	1	4
42.2	0	4
25.3	0	0
22.7	0	0
21.7	1	2
17.3	0	0
16.2	0	0
16.2	0	0

Replicate 3 (CONT.)

S	R	C
14.4	0	0
14.4	0	0
14.4	0	0
13.0	0	0
11.5	0	0
11.5	0	0
10.1	0	0

Replicate 4

470.5	3	6
244.4	0	6
244.4	0	8
225.8	0	8
180.7	1	4
169.4	0	6
141.1	0	6
141.1	0	2
129.0	0	6
126.9	1	4
126.9	0	6
126.9	0	4
112.9	0	6
112.9	0	4
105.5	1	2
105.5	0	4
105.5	0	6
105.5	0	6
93.9	0	7
93.9	0	3
93.9	1	2
84.6	0	5
84.6	2	2
75.3	0	4
70.4	0	3
65.8	2	2
56.4	0	0
29.5	0	0

Replicate 4 (CONT.)

S	R	C
26.0	0	0
26.0	0	0
19.5	0	0
18.0	0	0
18.0	0	0
14.4	0	0
13.0	0	0
13.0	0	0
13.0	0	0
13.0	0	0
13.0	0	0
11.5	0	0
11.5	0	0
11.5	0	0
11.5	0	0
10.8	0	0
10.8	0	0
10.1	0	0
10.1	0	0
10.1	0	0
10.1	0	0

183 days PPI

Replicate 1

170.2	2	6
141.9	0	4
141.9	1	7
132.3	2	4
132.3	0	10
130.0	2	6
127.6	2	4
118.1	0	4
118.1	0	4
118.1	1	7
113.6	0	6
106.2	1	9

Replicate 1 (CONT.)

S	R	C
99.3	0	0
94.5	0	5
94.5	0	2
84.8	0	0
84.8	0	6
82.6	0	10
82.6	0	2
82.6	1	5
75.5	0	2
75.5	0	6
71.0	0	0
42.2	0	0
31.5	0	0
22.6	0	0
22.6	0	0
20.3	0	0
18.8(x3)	0	0
18.2	0	0
17.0	0	0
17.0	0	0
16.6	0	0
16.6	0	0
15.8.	0	0
15.8	0	0
15.0(x5)	0	0
13.6(x3)	0	0
12.1(x7)	0	0
11.2(x3)	0	0
10.6(x3)	0	0
9.0	0	0
9.0	0	0
6.7	0	0

Replicate 2

S	R	C
164.4	1	3
140.4	0	0
117.1	1	4

Replicate 2 (CONT.)

S	R	C
114.9	1	4
114.9	0	4
112.2	0	4
112.2	0	5
112.2	2	5
105.5	0	2
105.5	0	3
98.3	0	0
98.3	0	5
93.6	0	0
93.6	0	5
93.6	0	3
84.6	0	4
84.1	0	0
82.0	0	0
82.0	0	0
82.0	1	3
75.1	0	4
75.1	0	2
75.1	0	6
75.1	0	4
75.1	0	5
70.2(x3)	0	0
60.1	0	0
56.3	0	0
46.9	0	0
46.9	0	0
42.2	0	0
36.1	0	0
36.1	0	0
24.0	0	0
15.1	0	0
13.5	0	0
13.5	0	0
11.2	0	0
9.0	0	0

Replicate 3

S	R	C
180.7	1	6
141.9	0	3
141.9	0	0
141.9	1	4
132.3	2	5
130.0	0	0
130.0	0	4
113.6	0	7
99.3	0	0
94.5	1	2
82.6	0	5
82.6	0	4
82.6	0	4
82.6	0	0
71.0	0	0
71.0	0	2
71.0	0	4
47.6(x3)	0	0
42.2	0	0
37.0	0	0
37.0	0	0
31.5	0	0
31.5	0	0
22.6	0	0
20.3	0	0
18.8	0	0
18.1	0	0
16.6	0	0
16.6	0	0
15.1	0	0
13.6(x3)	0	0
12.3(x5)	0	0
10.6	0	0
10.1	0	0
10.1	0	0

b) Cercariae; numbers in size classes of cercarial length

SIZE CLASS	68 days PPI			102.5 days PPI				183 days PPI		
(μm)	Replicates			Replicates				Replicates		
	1	2	3	1	2	3	4	1	2	3
0- 100	2	0	0	0	0	0	0	0	0	0
100- 200	9	0	8	11	16	23	47	68	36	32
200- 300	0	0	0	31	38	45	21	81	47	73
300- 400	0	0	0	61	39	19	17	35	43	58
400- 500	0	0	0	20	7	0	2	27	31	17
500- 600	0	0	0	9	9	1	5	21	22	19
600- 700	0	0	0	12	7	0	2	8	16	21
700- 800	0	0	0	14	4	0	4	24	25	12
800- 900	0	0	0	9	9	3	1	5	15	18
900-1000	0	0	0	6	5	4	2	37	36	20
1000-1100	0	0	0	16	1	3	0	27	27	11

Appendix 3: Procedure to estimate the straight line trajectory of a swimming cercaria

A sequence of cercarial swimming was filmed at high speed (1000 pps) and each frame of the sequence printed separately at identical magnification. A square was drawn on a sheet of tracing paper and precisely alligned with the frame boundary on the first print of the swimming sequence. A point on the cercaria was selected and the precise position of the point within the frame marked. For present purposes the point selected was the mid-ocelli point, mid-way between the two cercarial ocelli. Using the same sheet of tracing paper the position of the mid-ocelli point relative to the frame boundary was recorded for each print of the swimming sequence. This procedure was followed for the three separate swimming sequences A, B and C.

For each swimming sequence arbitrary axes were drawn within the frame boundary of the traced swimming sequence. The experimental data points were, therefore, in a fixed orientation to the frame and each point could be absolutely defined by its spatial coordinates (x and y) relative to the arbitrary axes.

This approach assumes that movement primarily occurs in two dimensions (x, y), a simplifying assumption that is largely correct. Some movement probably occurs in the third dimension, however, and hence all subsequent conclusions should be considered accurate only to a first approximation.

Appendix Figure 3.1a illustrates some artificial data fitted with a sine wave cycle. Angle θ defines the direction of the mean of the sine wave and is assumed to define the direction of the

straight line trajectory of the data which it mimics. Similarly, the amplitude (a) and the wavelength (λ) of the sine wave and data are assumed to coincide. a and λ are properties of the data, while angle θ is only a property of the data in relation to the specific arbitrary axes imposed upon them.

Fitting a sine wave form to the oscillatory pattern of the mid-ocelli point positions required that estimates be made by inspection of some parameters. The following parameters were estimated in arbitrary axes units (Appendix Figure 3.1a):

w = the period = $2\pi/\lambda$

a = the amplitude

(x_o, y_o) = the origin of the sine cycle

= (x_A, y_A) if at start of cycle

= (x_B, y_B) if at middle of cycle

θ = angle of mean straight line to x axis.

In Appendix Figure 3.1b it can be seen that from simple geometrical principles the equation of the straight line is:

$$y = (x - x_o) \text{ TAN } \theta + y_o$$

and the equation of the normal to the i^{th} data point is:

$$y = (x_i - x)/\text{TAN } \theta + y_i$$

hence the point of intersection of the normal to the straight line:

$$x_N = x_o \text{ SIN}^2 \theta + x_i \text{ COS}^2 \theta + (y_i - y_o) \text{ SIN}\theta \text{ COS}\theta$$

The value of x_N of the i^{th} data point can therefore be determined using the estimated values of θ, x_o and y_o obtained by inspection from the data. It is then possible to estimate

Appendix Figure 3.1: Procedure for fitting sine wave to experimental data (see text).

a) Artificial data fitted with sine wave within arbitrary axes and cine frame.

b) Parameters of the sine wave.

a)

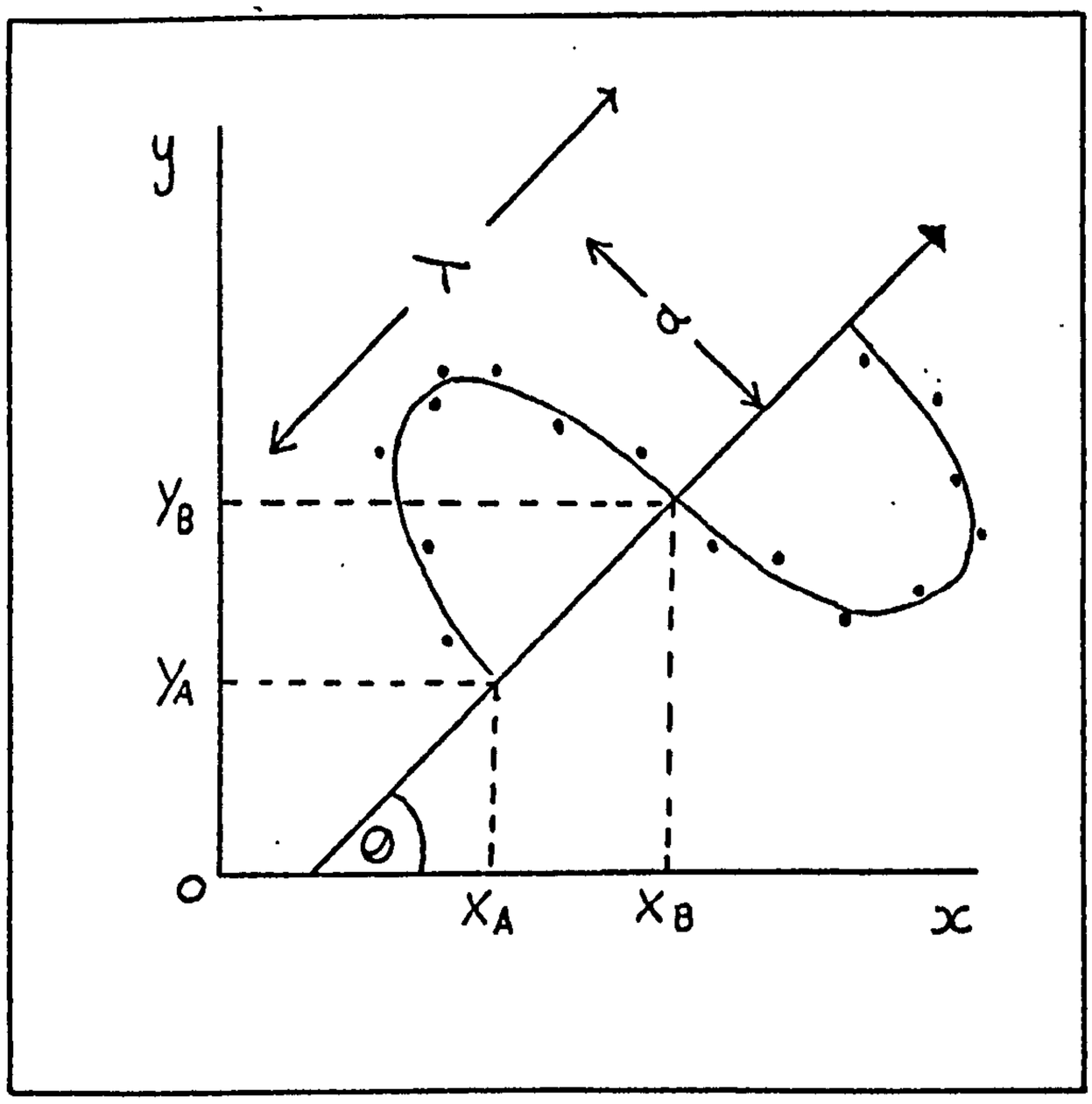

b)

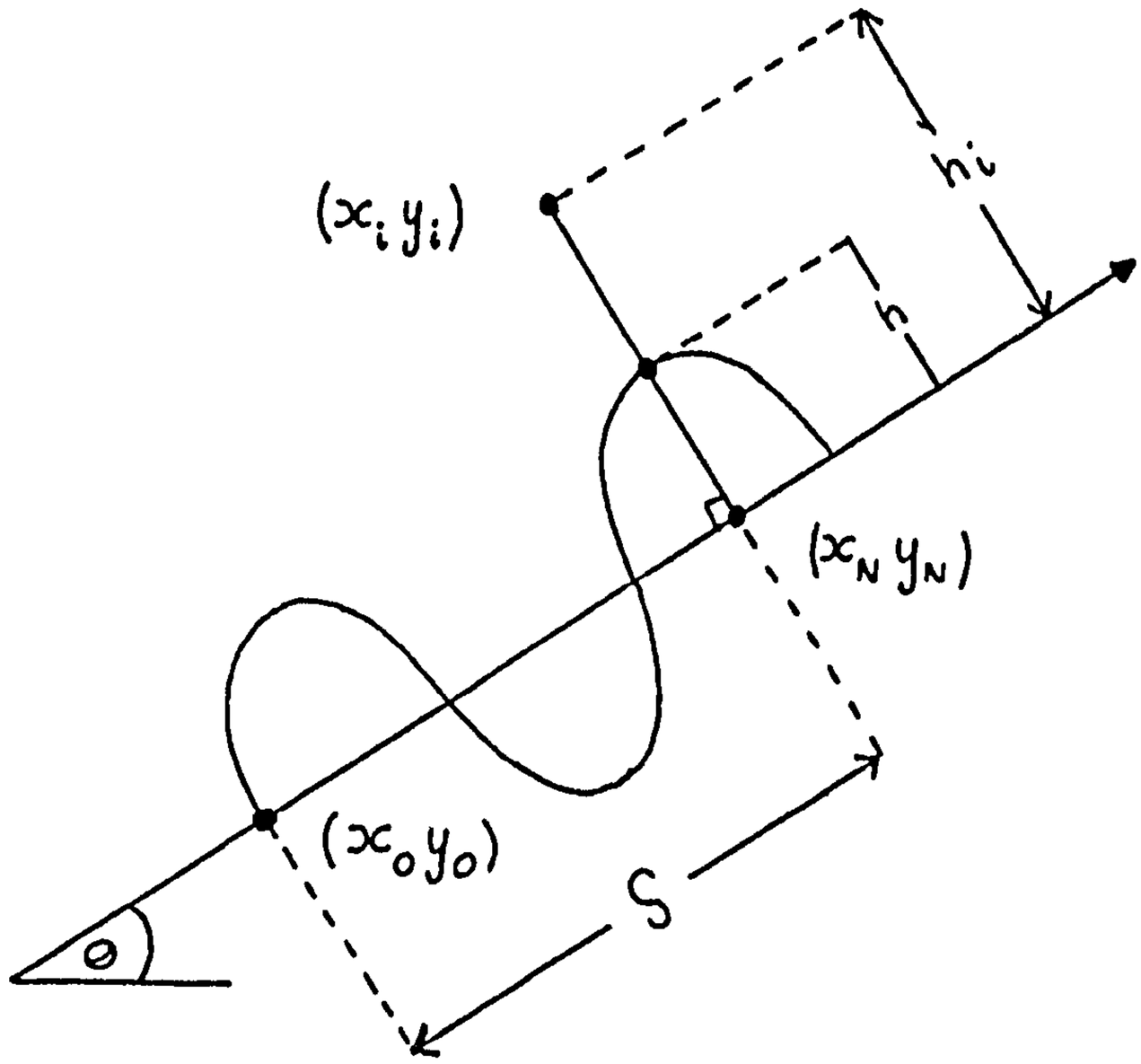

h and h_i (Appendix Figure 3.1b):

$$h = a\ SIN(ws + \phi)$$

where $S = (x_N - x_o)/COS\ \theta$

and $\phi = 0$ if $x_o, y_o = x_A, y_A$

$=$ if $x_o, y_o = x_B, y_B$

$$h_i = (x_N - x_i)/SIN\ \theta$$

Hence the difference, or residual, between the i^{th} data point and the corresponding point on the sine wave generated by the estimated parameters may be determined:

$$\varepsilon_i = h - h_i$$

For the i^{th} data point ε_i is a measure of the variation between the experimental and theoretical data. The sum of squares of residuals (F) of all data points is an inverse measure of the similarity between the experimental and theoretical wave forms. Hence the minimum F value achieved by altering the estimated parameter values indicates the best fit of the sine curve to the data. Minimisation of the sum of squares of residuals required an iterative approach, the F values produced by different substituted parameter values being compared, and hence a computer program was utilised.

The essential sub-programs were as follows:

1) To use initial estimates of parameters (a, w, θ, x_o and y_o) and the experimental data coordinates ($x_1 \ldots x_i \ldots x_n$, $y_1 \ldots y_i \ldots y_n$) to determine the sum of squares of residuals ($F = \sum_{i=1}^{n} \varepsilon_i^2$).

2) To minimise F values by altering the parameter values and comparing the estimated solutions.

Minimisation was achieved using NAG library routine: NAGFLIB:E04FAF: 1310/428: Mk5: Nov 75: Maximising or minimsing a function (adapted from Peckham (1970)).

This library routine finds an approximation to a minimum of the sums of squares of residuals using Peckham's minimsation method. Successful exit from the routine occurs when a number of possible conditions are satisfied. In the present investigation the routine terminated after a relative test on a range of values of F gave a change of less than 10^{-3} in current best point of iteration when the estimated variables were altered by 0.1%.

Appendix Figure 3.2 shows the actual mid-ocelli points, within arbitrary axes, for swimming sequence A. The points are fitted with the theoretical best fit sine wave and the corresponding mean path. Similar results were also obtained for sequences B and C, and the estimated parameter values of the sine waves on exit from the routine are given in Appendix Table 3.1.

APPENDIX TABLE 3.1

Values of sine wave parameters on exit from sine wave fitting routine for swimming sequences A, B and C

PARAMETER	PARAMETER VALUE		
	A	B	C
θ°	33.75	33.62	18.32
a μm	60.56	63.50	61.16
λ μm	308.95	338.07	351.60

Appendix Figure 3.2: Data points within arbitrary axes fitted with sine wave. Data derived from position of mid-ocelli point of swimming cercaria at one msec. intervals from sequence A.

Axes in arbitrary units.

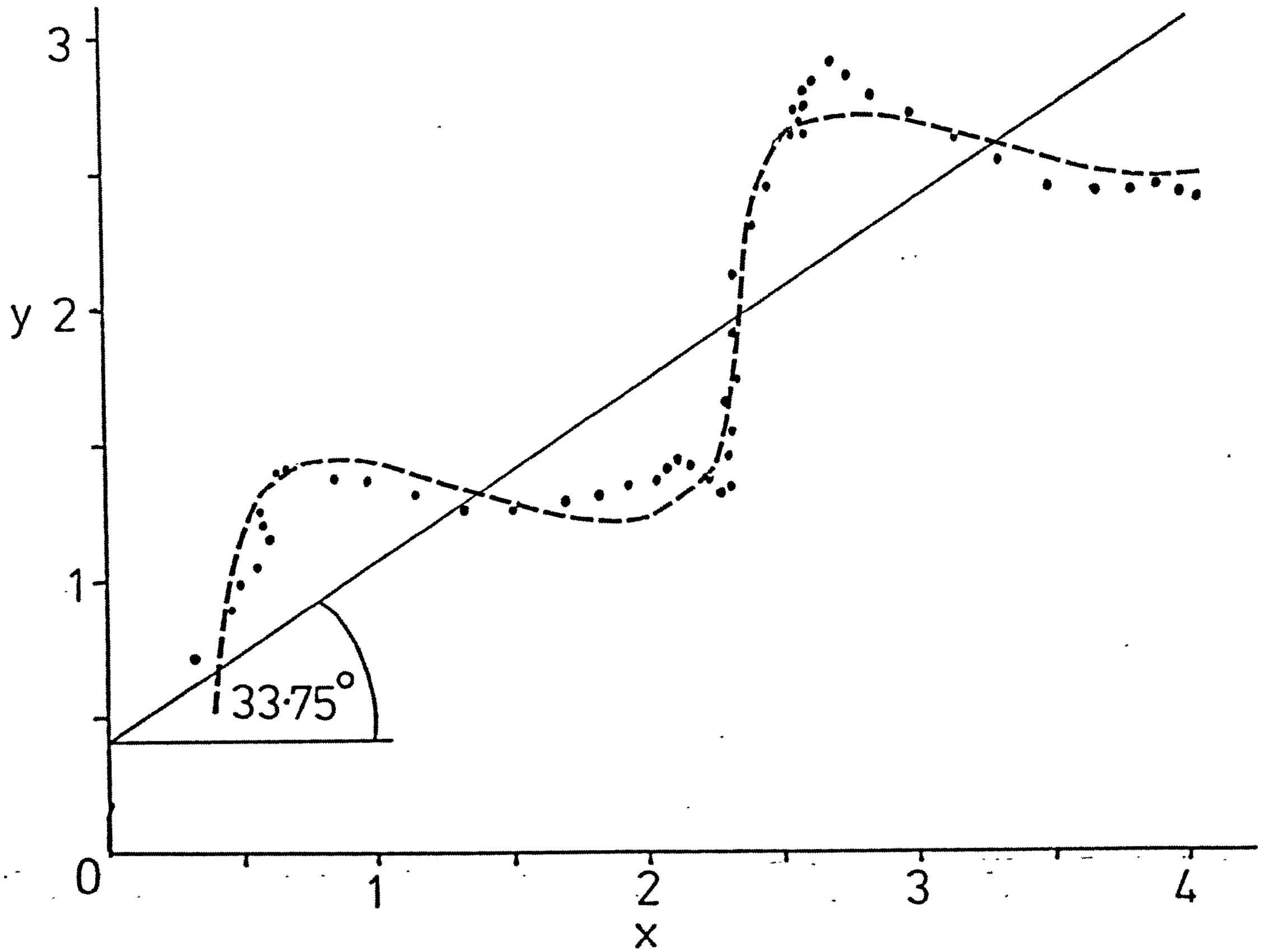
3
y 2
1
0
33·75°
1
2
3
4
x

The amplitude (a) represents the maximum departure of the sine wave from its mean value. In the present context it is also an estimate of the maximum lateral movement of the mid-ocelli point from the trajectory of the cercaria.

The wavelength (λ) represents the length of a single sine wave form along its mean path. In the present context it is also an estimate of the distance moved by the mid-ocelli point along the path of the whole organism during a single complete propulsive cycle.

It is apparent, therefore, that the values of a and λ are biologically generated and comparable between cercariae. The close similarity of the experimental values obtained from the three swimming sequences strengthens reliance on this modelling technique.

The angle subtended by the mean path of the sine wave to the arbitrary x axis (θ) is not comparable between treatments because data from each swimming sequence were separately fitted with different and arbitrary axes. This angle, however, defines the path of each swimming sequence and is the parameter this modelling technique was designed to determine. The mean path of the fitted sine wave is assumed to coincide with the mean path of the experimental data, that is the trajectory of the whole organism. The angle θ therefore defines, within the context of the cine frame, the straight line trajectory of the cercaria in each swimming sequence.

Appendix 4: Estimation of cercarial volume and viscous resistance to dropping

4.1: Volume

Total cercarial volume was determined by summing simple estimates of the volume of the component parts.

a) Body region: estimates of cercarial ventral surface area from Section 11 gave a mean value of 0.171 mm^2. Given a body thickness of 40×10^{-3} mm the total body (V_1) = $\underline{6.84 \times 10^{-3}}$ mm^3.

b) Tail stem: considered to be a cylinder of length 560 μm and diameter 80 μm. Hence tail stem volume

$(V_2) = (40)^2 . 560 \times 10^{-9}$

$= \underline{2.82 \times 10^{-3}}$ mm^3

c) Furcal: consider a single furca to be represented by truncated triangles on the surfaces and triangles on the sides (Appendix Figure 4.1a).

Consider a general section at height z of thickeness d:

Volume of section = 2x. 2y. dz

Given: $x = x_o + z/\cos\phi \ (\tan\delta)$

and $y = y_o - z/\cos\delta \ (\tan\phi)$

Volume of section = $4(x_o + z\ (\tan\delta/\cos\phi)\ )$

$x(y_o - z\ (\tan\phi/\cos\delta)\ )dz$

Therefore volume of furca =

$4(x_o y_o + (t_\delta y_o - t_\phi x_o)z^2/2 - t_\delta\ t_\phi\ z^3/_3)$

Appendix Figure 4.1: Parameters for estimating volume and viscous resistance of furcae. See text for explanation.

a) Schematic representation of a single furca for volume determination.

b) Schematic representation of both furcae considered as single ellipsoid for viscous resistance determination.

a)

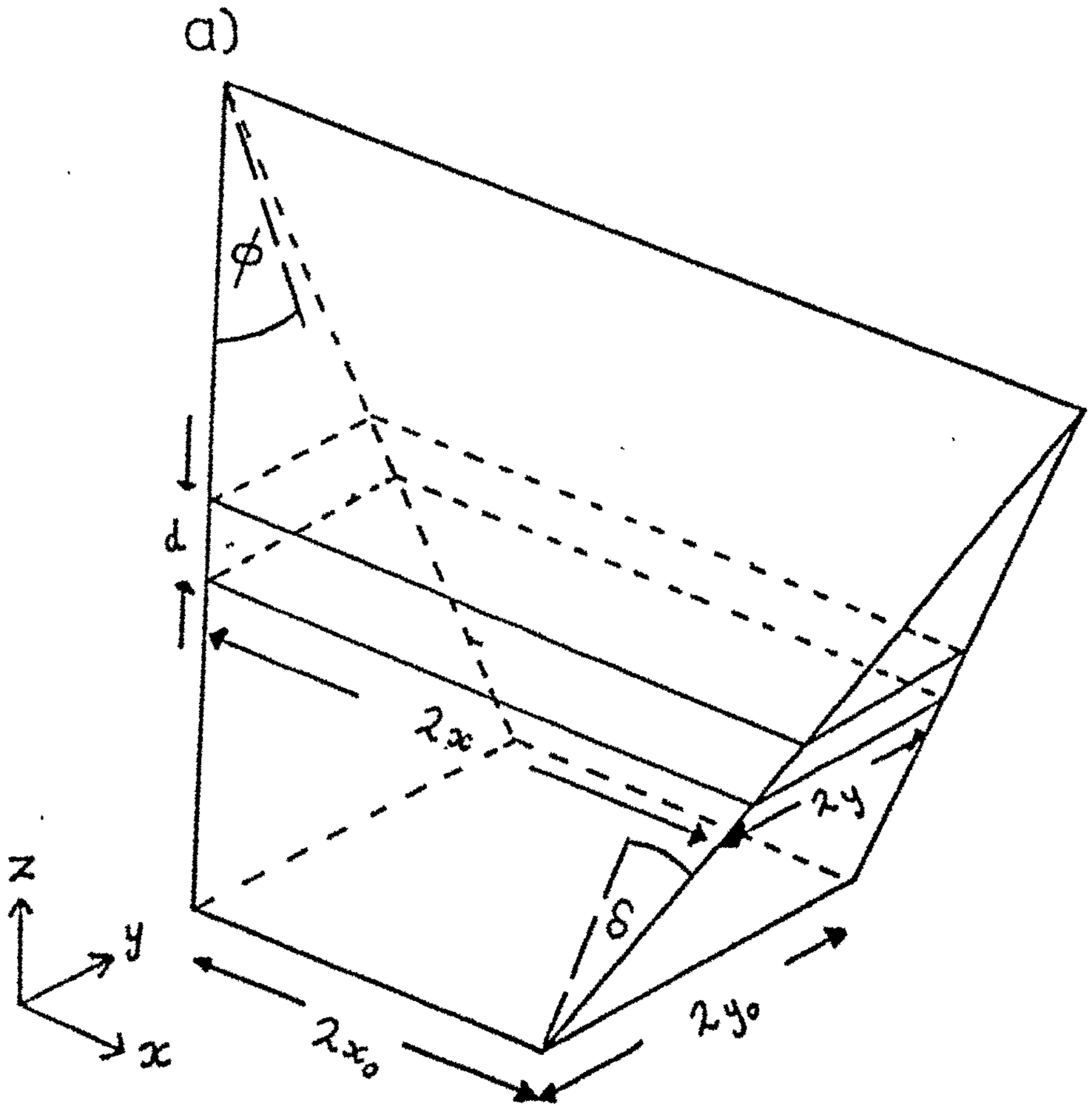

b)

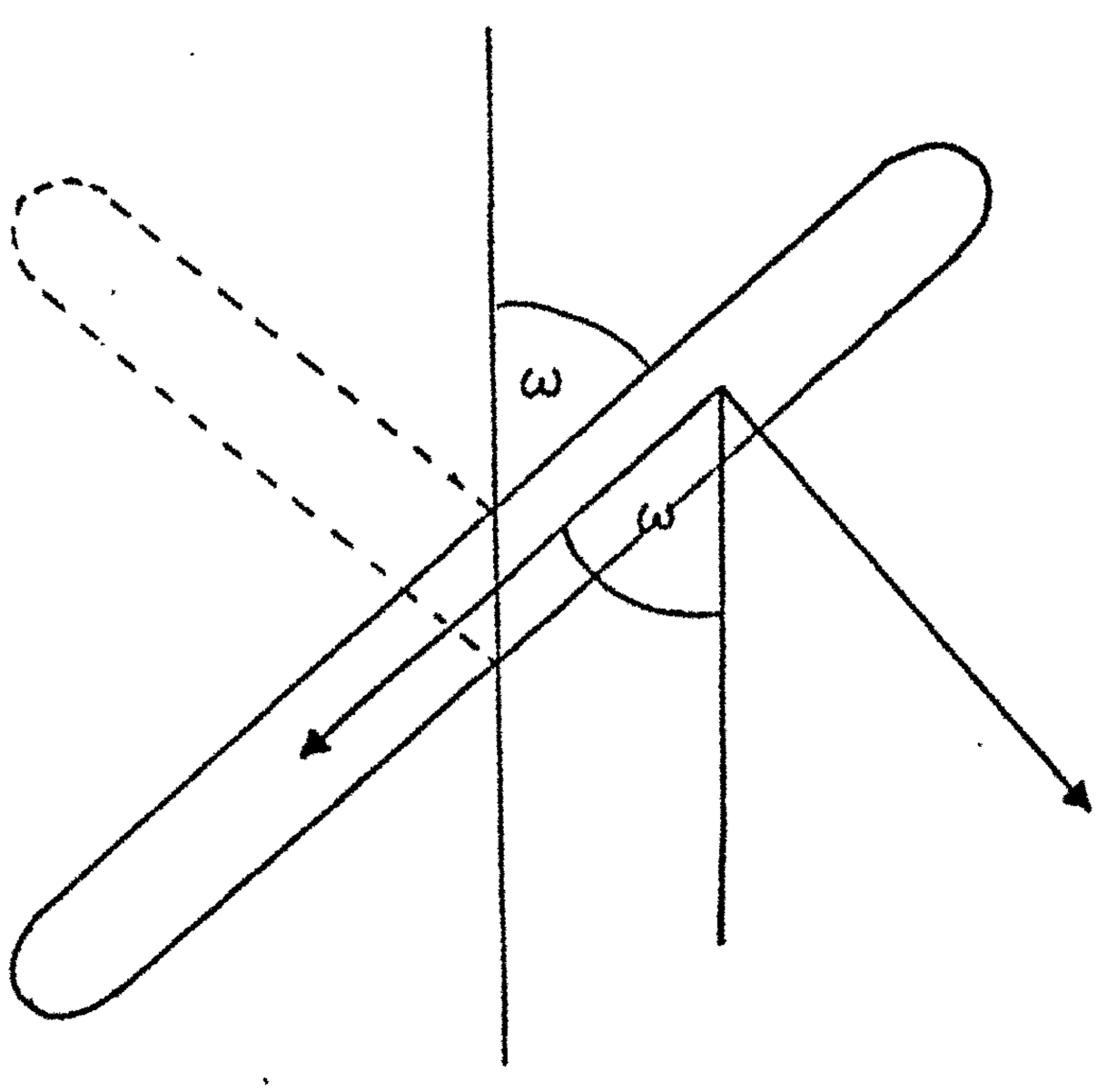

where x_o = ½ base width = 30μm

y_o = ½ base depth = 25μm

z = length = 367μm

Therefore volume of one furca (V_3) = $\underline{0.74 \times 10^{-3}}$ mm^3

From the above estimates of volume (V_1, V_2 and V_3) the total cercarial volumes can be obtained by addition:

Volume of intact cercaria (y_1) = $V_1 + V_2 + 2V_3$

= $\underline{11.14.10^{-3}}$ mm^3

Volume of cercaria with one furca (y_2) = $V_1 + V_2 + V_3$

= $\underline{10.40.10^{-3}}$ mm^3

Volume of cercaria with no furcae (y_3) = $V_1 + V_2$

= $\underline{9.66.10^{-3}}$ mm^3

4.2: Viscous Resistance

Viscous resistance force was estimated separately for each cercarial component.

a) Reflexed body region: this was considered as an ellipsoid with motion parallel to the major axis.

Viscous resistance for an ellipsoid = $6\ \pi\eta Ru$

where η = coefficient of resistance

u = velocity

R = equivalent radius

If motion parallel to major axis:

$$R_{parallel} = (8/3.a)/\left((1/e + 1/e^3).\ln (1 + e/1 - e) - 2/e^2\right)$$

where: a = semi-major axis

$e^2 = (a^2 - b^2)/a^2$

b = semi-minor axis

assume: a = 150μm, b = 100μm (for reflexed body region 300μm long and 200μm wide).

Hence: $e^2 = 0.56$

therefore R parallel $\triangleq$ 110μm

Force due to viscous resistance of reflexed body region

$= \frac{6\pi\eta u\ 110}{}$ N

b) Exposed tail stem: assume a cylinder 275μm long and 40μm radius.

Viscous resistance per unit length of cylinder

$= 2\pi\eta/(\ln(21/r) + 0.5)$

$= 0.32.2\pi\eta$

where: l = length, and r = radius

Force due to viscous resistance of exposed tail stem

$= \frac{2\pi\eta u\ 88}{}$ N

c) Furcae: assume furcae to be ellipsoidal plates. As shown in Appendix Figure 4.1b the two furcae can be considered as a single ellipsoidal plate inclined at an angle w to the vertical.

For ellipsoid representing two furcae the semi-major axis (a) = 367μm, and the semi-minor axis (b) = 40μm (mean length of single furca 367μm, mean depth approximately 40μm).

Hence, as defined above, $e^2 = 0.988$

and Rparallel = 100.7μm

$$\text{Rnormal} = (8/3.a)/(0.5(3/e - 1/e^3).\ln(\frac{1+e}{1-e})+1/e^2)$$

$$= 144\mu\text{m}.$$

Given velocity u acting vertically (Appendix Figure 4.1b), the component of velocity normal to the axis of the ellipsoid = u SIN w, and the component acting parallel = u COS w. Therefore, force normal to axis = C_N u SIN w and force parallel to axis = C_T u SIN w where C_N, C_T represent viscous resistance per unit velocity.

Force acting parallel to velocity u

$= C_N u \text{ SIN}^2 w + C_T u \text{ COS}^2 w$

$= 6\pi\eta u (\text{Rnormal SIN}^2 w + \text{Rparallel COS}^2 w)$

Given an interfurcal angle of 120°, then w = 60°.

Force due to viscous resistance of furcae

$= \underline{6\pi\eta}\ \underline{u\ 133}$ N

Appendix 5: Determination of terminal velocity of dropping cercariae

The terminal velocity of cercariae was determined for cercariae with both furcae intact, one furca removed or both furcae removed.

a) Intact cercaria, terminal dropping velocity = u_1

$$y_1 \times p_D \times g = a_1 + b_1 + c_1$$

where: y_1 = volume intact cercaria = 11.14×10^{-12} m^3

a_1 = viscous resistance due to reflexed body region

= $6 \pi \eta u_1 \ 110 \times 10^{-6}$ N.

b_1 = viscous resistance due to exposed tail stem

= $2 \pi \eta u_1 \ 88 \times 10^{-6}$ N.

c_1 = viscous resistance due to two furcae

= $6 \pi \eta u_1 \ 133 \times 10^{-6}$ N.

$$11.14 \times 10^{-12} . p_D . g = \pi \eta u_1 (660 + 176 + 798) \times 10^{-6}$$

$$u_1 = 11.14 . p_D . g . 10^{-6} / \pi \eta (660 + 176 + 798)$$

$$= 3.01 . 10^{-3} \ ms^{-1}$$

Terminal dropping velocity of intact cercaria = $\underline{3.01 \text{ mm}} \ s^{-1}$

b) Cercaria with one furca, terminal dropping velocity = u_2.

$$y_2 \times p_D \times g = a_2 + b_2 + c_2$$

where: y_2 = volume of cercaria with one furca

= 10.40×10^{-12} m^3

a_2 = viscous resistance due to reflexed body region

= $6 \pi \eta u_2 \ 110 \times 10^{-6}$ N.

b_2 = viscous resistance due to exposed tail stem

= $2 \pi \eta u_2$ 110 x 10^{-6} N.

c_2 = viscous resistance due to single furca

= $6 \pi \eta u_2$ 66.5 x 10^{-6} N.

u_2 = $10.40 . p_D . g . 10^{-6} / \pi \eta$ (660 + 176 + 399)

= $3.72 . 10^{-3}$ ms^{-1}

Terminal dropping velocity of cercaria with one furca

= $\underline{3.72 \text{ mm } s^{-1}}$.

c) Cercaria with no furca, terminal dropping velocity = u_3

$$y_3 \times p_D \times g = a_3 + b_3$$

where: y_3 = volume of cercaria with on furca

= 9.66 X 10^{-12} m^3

a_3 = viscous resistance due to reflexed body region

= $6 \pi \eta u_3$ 110 x 10^{-6} N.

b_3 = viscous resistance due to exposed tail stem

= $2 \pi \eta u_3$ 88 x 10^{-6} N.

u_3 = $9.66 . p_D . g . 10^{-6} / \pi \eta$ (660 + 176)

= $5.11 . 10^{-3}$ ms^{-1}

Terminal dropping velocity of cercaria with no furcae

= $\underline{5.11 \text{ mm } s^{-1}}$.